ELECTRICAL MACHINE DESIGN

McGraw-Hill Book Co. Inc.
PUBLISHERS OF BOOKS FOR
Electrical World ▽ Engineering News-Record
Power ▽ Engineering and Mining Journal-Press
Chemical and Metallurgical Engineering
Electric Railway Journal ▽ Coal Age
American Machinist ▽ Ingenieria Internacional
Electrical Merchandising ▽ BusTransportation
Journal of Electricity and Western Industry
Industrial Engineer

ELECTRICAL MACHINE DESIGN

THE DESIGN AND SPECIFICATION OF DIRECT AND ALTERNATING CURRENT MACHINERY

BY

ALEXANDER GRAY, WHIT. SCH., M. SC.

Professor of Electrical Engineering, Cornell University,
Author of Principles and Practice of Electrical Engineering

REVISED BY

P. M. LINCOLN

Director of the School of Electrical Engineering,
Cornell University

SECOND EDITION

McGRAW-HILL BOOK COMPANY, INC.
NEW YORK: 370 SEVENTH AVENUE
LONDON: 6 & 8 BOUVERIE ST., E. C. 4
1926

Copyright, 1913, 1926, by the
McGraw-Hill Book Company, Inc.

PRINTED IN THE UNITED STATES OF AMERICA

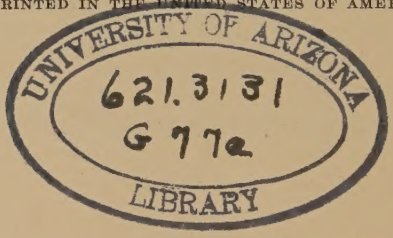

THE MAPLE PRESS COMPANY, YORK, PA.

PREFACE TO SECOND EDITION

The first edition of Prof. Gray's Electrical Machine Design bears the date of 1912. In the fourteen years that have elapsed since that date, much development has occurred in practically all classes of electrical machinery. In direct-current machinery, the commutating pole has become almost universal; it was only just beginning to be used when Gray wrote his first edition. In alternating-current machinery, good inherent regulation was paramount in 1912; today it is considered a minor feature and of little importance. The effect of these changes has been to increase very materially the output that can be secured from a given amount of material both in direct-current and in alternating-current machines.

In this revision, the example machines have been modified so that they represent present-day designs. Also the various curves, tables, photographs, cuts, and other data have been modified so as to represent present-day practice.

Although there has been considerable change in the resulting machines, no change has taken place or can take place in fundamental principles. In his presentation of these fundamental principles and in his methods of analysis Gray was unexcelled. No attempt has been made in this revision to make any modification in the methods of analysis that were so ably put forward by Gray in his first edition.

The reviser wishes to acknowledge his indebtedness both to the General Electric Company of Schenectady and to the Westinghouse Electric and Manufacturing Company of East Pittsburgh for giving freely all data requested on present-day machine designs.

The reviser also wishes to acknowledge his indebtedness to Mr. J. G. Tarboux of Cornell University for assistance in reading proof.

P. M. Lincoln.

Cornell University,
Ithaca, N. Y.
August, 1926.

59538

PREFACE TO FIRST EDITION

The following work was compiled as a course of lectures on Electrical Machine Design delivered at McGill University. Since the design of electrical machinery is as much an art as a science no list of formulæ or collection of data is sufficient to enable one to become a successful designer. There is a certain amount of data, however, sifted from the mass of material on the subject, which every designer finds convenient to compile for ready reference. This work contains data that the author found necessary to tabulate during several years of experience as a designer of electrical apparatus.

A study of design is of the utmost importance to all students, because only by such a study can a knowledge of the limitations of machines be acquired. The machines discussed are those which have become more or less standard, namely, direct-current generators and motors, alternating-current generators, synchronous motors, polyphase induction motors, and transformers; other apparatus seldom offers an electrical problem that is not discussed under one or more of the above headings.

The principle followed throughout the work is to build up the design for the given rating by the use of a few fundamental formulæ and design constants, the meaning and limits of which are discussed thoroughly, and the same procedure has been followed for the several pieces of apparatus.

The author wishes to acknowledge his indebtedness to Mr. B. A. Behrend, under whom he learned the first principles of electrical design and whose influence will be seen throughout the work; to the engineers of the Allis-Chalmers-Bullock Company of Montreal, Canada, and particularly to Mr. Bradley T. McCormick, Mr. G. P. Cole and Mr. H. F. Eilers; to Mr. A. McNaughton of McGill University for criticism of the arrangement of the work and to Mr. A. M. S. Boyd for assistance in the proof-reading.

McGill University,
September 2, 1912.

CONTENTS

SECTION I

DIRECT-CURRENT MACHINERY

CHAPTER I

PAGE

MAGNETIC INDUCTION 1

Lines of Force—Direction of an Electric Current—Magnetic Field Surrounding a Conductor—Magneto Induction—Direction of the Generated E.M.F.—Magnetomotive Force.

CHAPTER II

ARMATURE WINDING 7

Gramme Winding—Re-entrancy—Objections to the Gramme Winding—Drum Winding—E.M.F. Equation—Multipolar Machines—Equalizer Connections—Short-pitch Windings—Multiple Windings—Series Windings—Lap and Wave Windings—"Frog Leg" Equalizers—Shop Instructions—Several Coils in a Slot—Number of Slots—Odd Windings.

CHAPTER III

CONSTRUCTION OF MACHINES 25

Armature—Poles—Yoke—Commutator—Bearings—Slide Rails—Large Machines.

CHAPTER IV

INSULATION 32

Types of Insulation—A.I.E.E. Definitions—Properties Desired—Materials in General Use—Effect of Heat—Grounds and Short-circuits—Puncture Tests—End-connection Insulation—Several Coil Sides in a Slot—Examples of Insulation Specifications—Field-coil Insulation.

CHAPTER V

MAGNETIC CIRCUIT 45

Leakage Factor—Magnetic Areas—Fringing Constant—Flux Densities—Calculation of the No-load Saturation Curve and of the Leakage Factor.

CHAPTER VI

ARMATURE REACTION 57

Armature Reaction—Flux Distribution in the Air-gap—Armature Reaction When the Brushes Are Shifted—Field Distribution in

PAGE

Commutating Pole Machines—Full-load Saturation Curve—Relative Strength of Field and Armature.

CHAPTER VII

DESIGN OF THE MAGNETIC CIRCUIT 68
Field Coil Heating—Size of Field Wire—Length of Field Coils—Weight of Field Coils—Design of the Field System for a Given Armature.

CHAPTER VIII

COMMUTATION (*Resistance Method*) 78
Resistance Commutation—Effect of the Self-induction of the Coils—Current Density in the Brush—Reactance Voltage—Brush-contact Resistance—Energy at the Brush Contact—Reactance Voltage for Full-pitch Multiple, Short-pitch Multiple and Series Windings.

CHAPTER IX

COMMUTATION (*Counter E.M.F. Method*) 92
The Sparking Voltage—Disadvantages of Brush Shifting—Commutating Poles and Their Dimensions—Slots per Pole—Brush Width—Limits of Armature and Field Ampere Turns—Commutating Pole Excitation—Compensating Windings—Saturation—Volts per Bar.

CHAPTER X

EFFICIENCY AND LOSSES 110
Efficiency—Bearing Friction—Brush Friction—Windage Loss—Iron Losses—Additional Losses—Armature Copper Loss—Field Copper Loss—Brush Contact Resistance Loss.

CHAPTER XI

HEATING 122
Temperature Rise—Maximum Safe Temperature A.I.E.E. Rules—Temperature Gradient in the Core—Limiting Values of Flux Density—Heating of Winding—Temperature Gradient in the Conductors—Commutator Heating—Application—Application of the Heating Constants.

CHAPTER XII

PROCEDURE IN ARMATURE DESIGN 133
The Output Equation—Relation between Diameter and Length of the Armature—Magnetic and Electric Loading—Formulæ for Armature Design—Examples of Armature Design.

CHAPTER XIII

MOTOR DESIGNS AND RATINGS 148
Procedure in Design—Ratings for Different Voltages and Speeds—Possible Ratings for a Given Armature.

SECTION II

ALTERNATORS AND SYNCHRONOUS MOTORS

CHAPTER XIV

PAGE

ALTERNATOR WINDINGS 155

Fundamental Diagrams—Y- and Δ-connection—Several Conductors per Slot—Chain, Double-layer and Wave Windings—Several Circuits per Phase.

CHAPTER XV

THE GENERATED ELECTRO-MOTIVE FORCE 173

Form Factor—Wave Form—Harmonics and Methods of Eliminating Them—Y- and Δ- connection—Harmonics Due to Armature Slots—Effect of the Number of Slots on the Voltage—Rating—Effect of the Number of Phases on the Rating—General E.M.F. Equation.

CHAPTER XVI

CONSTRUCTION OF ALTERNATORS 186

Stator—Poles—Field Ring—High-speed Generators—Vertical Shafts.

CHAPTER XVII

INSULATION 194

Definitions—Insulators in Series—Air Films—Thickness of Insulation—Potential Gradient—Time of Application of the Strain—Examples of Alternator Insulation—Volts per Mil.

CHAPTER XVIII

ARMATURE REACTION 208

Armature Fields—Vector Diagram—Full-load Saturation Curves—Synchronous Reactance—Calculation of the Demagnetizing Ampere-turns per Pole and of the Leakage Reactance—End Connection, Slot and Tooth Tip Reactance—Variation of Armature Reactance and Armature Reaction with Power Factor—Full-load Saturation Curves at any Power Factor—Regulation—Effect of Pole Saturation on the Regulation—Relation between the M.M.Fs. of Field and Armature—Single-phase Machines—Comparison between Single-and Polyphase Alternators.

CHAPTER XIX

DESIGN OF THE REVOLVING FIELD SYSTEM 237

Field Excitation—Procedure in Design—Calculation of the Saturation Curves.

CHAPTER XX

LOSSES, EFFICIENCY AND HEATING 247

Bearing Friction—Brush Friction—Windage Loss—Iron Loss—Copper Loss—Eddy-current Losses in the Conductors—Efficiency—Heating—Internal Temperature of High-voltage Machines.

CHAPTER XXI

PAGE

PROCEDURE IN DESIGN 256
The Output Equation—Relation between Diameter and Length of the Armature—Effect of the Number of Poles on this Relation—Variation of Armature Length with a Given Diameter—Windings for Different Voltages—Examples of Alternator Design.

CHAPTER XXII

HIGH-SPEED ALTERNATORS 274
Alternators Built for an Overspeed—Turbo-alternators—Rotor Construction and Stresses—Diameter of Shaft—Critical Speed—Heating of Turbo-alternators—Current on an Instantaneous Short-circuit—Gap Density—Demagnetizing Ampere-turns per Pole—Relation between the M.M.Fs. of Field and Armature—Procedure in the Design of Turbo-alternators—Single-phase Turbo-alternators.

CHAPTER XXIII

SPECIAL PROBLEMS ON ALTERNATORS. 302
Flywheel Design—Design of Dampers—Synchronous Motors for Power Factor Correction—Design of Synchronous Motors—Self-starting Synchronous Motors.

SECTION III

POLYPHASE INDUCTION MOTORS

CHAPTER XXIV

ELEMENTARY THEORY OF OPERATION. 316
Revolving Field—Multipolar Motors—Windings—Rotor Current and Voltage—Starting Torque—Running Conditions—Vector Diagrams.

CHAPTER XXV

GRAPHICAL TREATMENT OF THE INDUCTION MOTOR 329
Current Relations in Rotor and Stator—Revolving Fields of Rotor and Stator—Flux Diagram—Proof of the Circle Law—No-load and Short-circuit Points—Representation of the Losses—Relation between Rotor Loss and Slip—Interpretation of the Circle Diagram.

CHAPTER XXVI

CONSTRUCTION OF THE CIRCLE DIAGRAM FROM TEST RESULTS . . . 339
No Load Saturation Curve—Short-circuit Curve—Construction of the Diagram.

CHAPTER XXVII

CONSTRUCTION OF INDUCTION MOTORS 346
Stator—Rotor.

CHAPTER XXVIII

PAGE
MAGNETIZING CURRENT AND NO-LOAD LOSSES 350
E.M.F. Equation—Magnetizing Current—Friction Loss—Iron Loss—Rotor Slot Design—Calculation of the No-load Losses.

CHAPTER XXIX

LEAKAGE REACTANCE 360
Leakage Fields—Zigzag Reactance—Complete Formula—Belt Leakage—Approximate Formula for Preliminary Design.

CHAPTER XXX

COPPER LOSSES 371
Loss in the Conductors—Loss in the End-connectors.

CHAPTER XXXI

HEATING OF INDUCTION MOTORS 375
Heating and Cooling Curves—Intermittent Ratings—Heating at Starting—Stator and Rotor Heating—Effect of Construction—Enclosed and Semi-enclosed Motors.

CHAPTER XXXII

NOISE AND DEAD POINTS IN INDUCTION MOTORS 385
Windage Noise—Pulsations of the Main Field—Vibration of the Tooth Tips—Variations in the Leakage Field—Dead Points at Starting.

CHAPTER XXXIII

PROCEDURE IN DESIGN 391
The Output Equation—Relation between Diameter and Length of the Stator—Preliminary Design—Detailed Design—Design of Wound Rotor Motors—Variation of the Stator Length with a Given Diameter—Windings for Different Voltages—Examples of Induction Motor Design.

CHAPTER XXXIV

SPECIAL PROBLEMS ON INDUCTION MOTORS 409
Slow-speed Motors—Closed Slots—High-speed Motors—Two-pole Motors—Effect of Variations in Voltage and Frequency on the Operation.

SECTION IV

TRANSFORMERS

CHAPTER XXXV

OPERATION OF TRANSFORMERS 422
No load—Full Load—Short-circuit—Regulation.

CHAPTER XXXVI

CONSTRUCTION OF TRANSFORMERS 428
Distribution Transformers—Distributed Shell Type—Rectangular

PAGE

Core Type—Cruciform Core Type—Simple Shell Type—Large Power Transformers.

CHAPTER XXXVII

MAGNETIZING CURRENT AND IRON LOSS 439
E.M.F. Equation—No-load Losses—Exciting Current.

CHAPTER XXXVIII

LEAKAGE REACTANCE. 445
Core Type with Two Coils per Leg—Core Type with Split Secondary Windings—Shell Type.

CHAPTER XXXIX

TRANSFORMER INSULATION. 449
Transformer Oil—Surface Leakage—Bushings—Coil Insulation—Extra Insulation on the End Turns—Insulation between the Windings and Core.

CHAPTER XL

LOSSES, EFFICIENCY AND HEATING. 461
Iron Loss—Copper Loss—Eddy-current Loss in the Winding—Efficiency—Temperature Gradient in the Oil—Temperature Gradient in Core- and in Shell-type Transformers—Temperature of the Oil—Air-blast Transformers—Water-cooled Transformers—Heating Constants—Effects of Oil Ducts—Maximum Temperature in the Windings—Section of Wire in the Coils.

CHAPTER XLI

PROCEDURE IN DESIGN 475
The Output Equation—Core-type Transformers—Design of a Distributing Transformer—Shell-type Transformers—Design of a 110,000-volt Power Transformer.

CHAPTER XLII

SPECIAL PROBLEMS IN TRANSFORMERS 486
Comparison between Core- and Shell-type Transformers—Three-phase Transformers—Operation on Different Frequencies—Typical.

CHAPTER XLIII

MECHANICAL DESIGN. 496
Fundamental Principles—Yokes—Rotors and Spiders—Commutators—Unbalanced Magnetic Pull—Bearings—Shafts—Pulleys—Brush Holders.

WIRE TABLE. 504

TABLES OF SYMBOLS 507

INDEX. 511

ELECTRICAL MACHINE DESIGN

CHAPTER I

MAGNETIC INDUCTION

1. Lines of Force.—A magnetic field is represented by lines of force. These are continuous lines whose direction at any point is that of the force acting on a north pole placed at the point, therefore, as shown in Fig.1, lines of force always leave a north pole and enter a south pole.

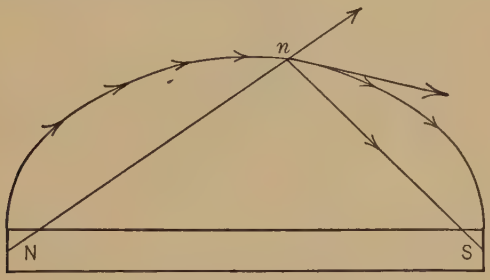

FIG. 1.—Direction of lines of force.

2. Direction of an Electric Current.—P and Q, Fig. 2, are two conductors carrying current. The current is going down in conductor P and coming up in conductor Q. If the direction of

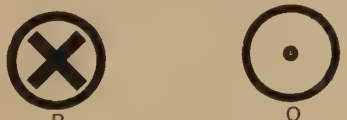

FIG. 2.—Direction of an electric current.

the current be represented by an arrow, then in conductor P the tail of the arrow will be seen and this is represented by a cross; in conductor Q the point of the arrow will be seen and this is represented by a point or dot.

3. Magnetic Field Surrounding a Conductor Which is Carrying Current.—In conductor P, Fig. 3, an electric current is passing downward. It has been found by experiment that in such a case the conductor is surrounded by a whirl of magnetic lines in the direction shown. This direction can be found by the following rule: "If a corkscrew be screwed into the conductor in the direction of the current then the head of the corkscrew will travel in the direction of the lines of force."

4. Magneto Induction.—Faraday's experiments showed that when the magnetic flux threading a coil changes, an e.m.f. is generated in the coil, and that this e.m.f. is proportional to the rate of change of flux in the coil.

FIG. 3.—Magnetic field surrounding a conductor.

The unit of e.m.f. is so chosen that one unit of e.m.f. is generated in a coil of one turn when the rate of change of flux in the coil is one line per second. This is called the c.g.s. unit; the practical unit, called the volt, is 10^8 c.g.s. units.

5. Direction of the Generated E.M.F.—N and S, Fig. 4, are the north and south poles of a magnet, ϕ is the total number of lines of force passing from the north to the south pole, A is a coil of one turn.

When the coil A is moved from position 1, where the number of lines threading the coil is ϕ, to position 2, where the number of lines threading the coil is zero, in a time of t seconds, then the average e.m.f. generated in the coil $= \frac{\phi}{t} 10^{-8}$ volts; or at any instant the e.m.f. $= \frac{d\phi}{dt} 10^{-8}$ volts.

The quantity $\frac{d\phi}{dt}$ is the rate at which conductor xy, Fig. 4, is cutting lines of force, so that the voltage generated by a conductor which is cutting lines of force is equal to

$$(\text{the lines cut per second}) \times 10^{-8}.$$

The direction of this e.m.f. is found by *Fleming's Rule* which states that "If the thumb, forefinger and middle finger of the right hand are all set perpendicular to one another so as to represent three coordinates in space, the thumb pointed in the direction of motion of the conductor relative to the magnetic

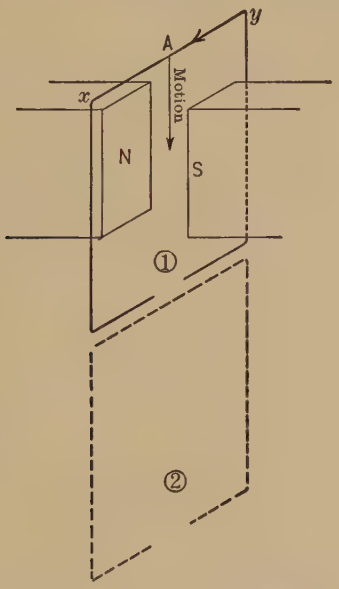

FIG. 4.—Direction of the generated e.m.f.

field, and the forefinger in the direction of the lines of force, then the middle finger will point in the direction in which the generated e.m.f. tends to send the current of electricity."

The direction of the e.m.f. in Fig. 4 is found by Fleming's three-finger rule, and the current due to this e.m.f. is in such a direction as to tend to maintain the flux threading the coil, or, as stated by the very general law known as *Lenz's Law*, "the generated e.m.f. always tends to send a current in such a direction as to oppose the change of flux which produces it." The complete

statement of the e.m.f. equation is, therefore, that the e.m.f. in volts at any instant $= -\frac{d\phi}{dt}10^{-8}$ volts.

6. Magnetomotive Force.—In Fig. 5 the current I passes through the T turns of the coil C which is wound on an iron core, and a magnetic flux ϕ is set up in the magnetic circuit. This flux is found to depend on the number of ampere-turns TI, and, corresponding to Ohm's law for the electric circuit, there is a law for the magnetic circuit—namely, m.m.f. $= \phi R$, where

m.m.f. is the magnetomotive force and depends on TI,
ϕ is the flux threading the magnetic circuit,
R is the reluctance of the magnetic circuit.

The most convenient unit of m.m.f. would have been the ampere-turn, but in order to conform to the definition of potential as used in hydraulic and electric circuits, another unit has to be adopted.

The difference of potential in centimeters between two points in a hydraulic circuit is the work done in ergs in moving unit mass of water from one point to the other, and the difference of magnetic potential (m.m.f.) between two points in a magnetic circuit is the work done in ergs in moving a unit pole from one point to the other.

Let a unit pole, which has 4π lines of force, be moved through the electro-magnet from A to B in a time of t seconds, then an e.m.f. $E = -T \times \frac{4\pi}{t}$ c.g.s. units will be generated between a and b. In order to maintain the current I constant against this e.m.f. an amount of work $= EI$ ergs per second must be done; so that the m.m.f. between A and B

$$= EIt \text{ ergs},$$
$$= \frac{4\pi T}{t} It \text{ ergs},$$
$$= 4\pi TI \text{ ergs when } I \text{ is in c.g.s. units},$$
$$= \frac{4\pi}{10} TI \text{ ergs when } I \text{ is in amperes},$$

therefore the unit of m.m.f. is not the ampere-turn, but is equal to $\frac{4\pi}{10}$ ampere-turns.

It must be understood that this m.m.f. is what might be called the generated m.m.f., thus in the electro-magnet shown

in Fig. 5 the generated m.m.f. is equal to $\frac{4\pi}{10} TI$, but the effective m.m.f. between A and B is equal to this generated m.m.f. minus the m.m.f. necessary to send the magnetic flux round the iron part of the magnetic circuit. Take for example the extreme case shown in Fig. 6, where the core is bent round to form a complete annular ring. The generated m.m.f. between the points A and $B = \frac{4\pi}{10} TI$, but A is the same point as B so that there can be no difference of magnetic potential between them, therefore all the generated m.m.f. is used up in sending the

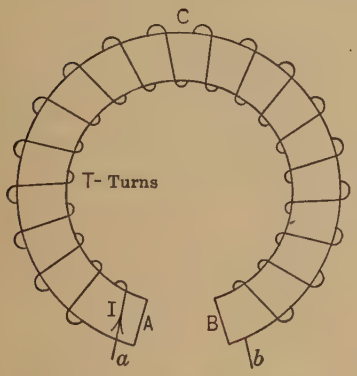

FIG. 5.—Magnetic circuit.

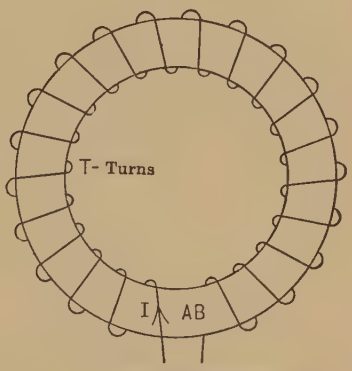

FIG. 6.—Closed magnetic circuit.

flux ϕ through the ring itself. By means of such a ring the magnetic materials used in electrical machinery are tested; the cross-section S of the ring and also the mean length l are known, and for a given generated m.m.f. the flux ϕ can be measured. Then since

$$\text{m.m.f.} = \phi R$$

therefore $\frac{4\pi}{10} TI = \phi \frac{kl}{S} = Bkl$, from which k can be found.

B is the flux density or number of lines per square centimeter,
k is the specific reluctance and $=1$ for air,
l is in centimeters.

For an air path, B, the flux density in lines per square centimeter $= \frac{4\pi}{10} \frac{TI}{l}$, where l is in centimeters. When inch units are

used, so that l is in inches, and the flux density is in lines per square inch, then

$$B, \text{ the flux density in lines per square inch} = 3.2\frac{TI}{l}. \qquad (1)$$

For materials like iron, k, the specific reluctance, is much less than 1, and the value of k varies with the flux density. For practical work the value of k is never plotted; it is more convenient to use curves of the type shown in Fig. 47, page 49, which curves are determined by testing rings of the particular material and plotting B in lines per square inch against $\frac{TI}{l}$, where l is in inches.

CHAPTER II

DIRECT-CURRENT ARMATURE WINDINGS

7. Definition of Armature Winding.—In Fig. 7 the armature A of a generator is revolving in the magnetic field NS in the direction of the arrow. The directions of the e.m.fs. which are generated in the conductors of the armature are found by the three-finger rule and shown in the usual way by crosses and dots. The principal purpose of the armature winding is to connect the armature conductors together in such a way that a desired resultant e.m.f. can be maintained between two points which are connected to an external circuit. The conductors and their interconnections taken together form the winding.

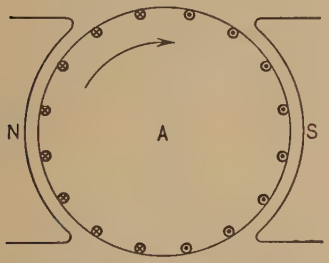

FIG. 7.—Direction of current in a D.-C. generator.

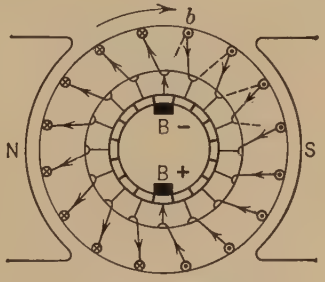

FIG. 8.—Two-pole simplex Gramme winding.

8. Gramme Ring Winding.—This type of winding, which is shown diagrammatically in Fig. 8, was one of the first to be used. Although the winding is now practically obsolete it is mentioned because of its simplicity, and because it shows more clearly than does any other type of winding the meaning of the different terms used in the system of nomenclature.[1]

The two-pole winding shown in Fig. 8 is the simplest type of Gramme winding; it has only two paths between the + and the − brush and is called the *simplex winding* to distinguish it from

[1] The system of nomenclature adopted in this chapter is that of Parshall and Hobart.

the other two fundamental Gramme windings, shown in Figs. 9 and 10. Inspection of these latter figures shows that in each of these cases there are four paths between the + and the − brush, or twice as many as in the case of the simplex winding; for this reason they are called *duplex windings*. There is, however, an essential difference between the two duplex windings and to distinguish between them it is necessary to define the term re-entrancy.

9. Re-entrancy.—If the winding shown in Fig. 8 be followed round the machine starting at any point *b*, it will be found that the winding returns to the starting-point, or is re-entrant, and that before it becomes re-entrant every conductor has been taken in once and only once; such a winding is called a *singly re-entrant winding*.

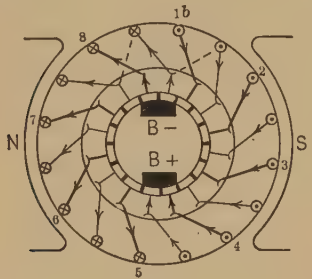

Fig. 9.—Doubly re-entrant duplex winding.

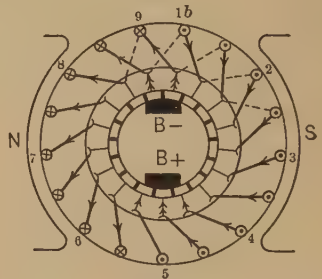

Fig. 10.—Singly re-entrant duplex winding.

If the winding shown in Fig. 9 be followed round the machine starting at any point *b*, it will be found to be re-entrant when only half of the conductors have been taken; in fact the winding is simply two singly re-entrant windings put on the same core, and is called a *doubly re-entrant duplex winding*.

If, on the other hand, the winding shown in Fig. 10 be followed round the machine starting at any point *b*, it will be found that it does not become re-entrant until every conductor has been taken in once and only once; it is therefore a *singly re-entrant duplex winding*.

It is evidently possible to carry this process of increasing the number of paths through the winding much further so as to get multiplex multiply re-entrant, multiplex singly re-entrant, and many other combinations; but such windings are rarely to be found in modern machines, in fact even duplex windings are

seldom used except for large-current low-voltage machines. In such machines the large current entering the brush is divided up and passes through the several paths, so that during commutation the current which is being commutated is only a part of what it would have been had a simplex winding been used. For the case of a singly re-entrant duplex winding this is shown at the positive brush, Fig. 10, where it will be seen that only the current in coil 5, or half of the total current, is being commutated at that instant.

In the case of a duplex winding the brush must be wide enough to cover two segments in order to collect current from all four paths.

10. Objections to the Gramme Winding.—In the case of small machines it is difficult to find space below the core for the return part of the winding without making the diameter of the machine unnecessarily large; while in the case of large machines, where the winding is made of heavy strip copper, it is difficult to remove and replace damaged coils.

The number of coils is twice that required for a machine of the same voltage and with the other type of winding, namely the drum winding.

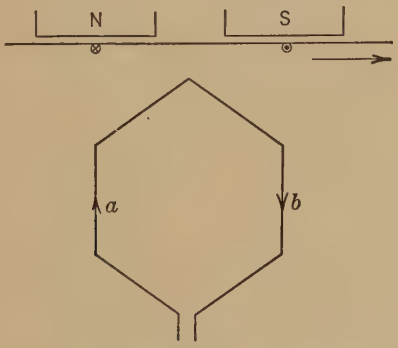

FIG. 11.—Coil for drum winding.

In many cases the active part of a coil is only a small portion of the total coil since the side and return connections do not cut lines of force.

Since the whole winding lies close to the iron of the core the coefficient of self-induction of the coils is large and the machine on that account is liable to spark.

11. Drum Winding.—This winding was developed to overcome the objections to the Gramme winding. In the simplest

case two conductors are joined together to form a coil of the shape shown in Fig. 11. This coil is placed on the machine in such a way that when one side *a* of the coil is under a north pole, the other side *b* is under the adjacent south pole, therefore both sides of the coil are active and the e.m.fs. generated in the two sides act in the same direction round the coil. Since each coil consists of at least two conductors, the total number of conductors for a drum winding must be even.

Fig. 12 shows a two-pole simplex singly re-entrant drum winding with 16 conductors. It might seem that conductors

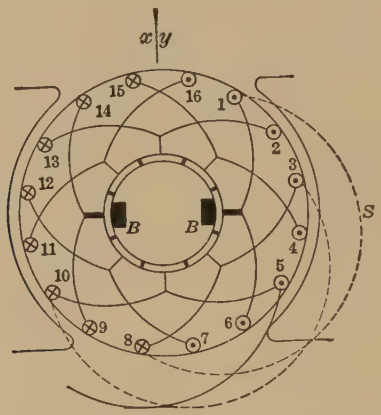

FIG. 12.—Two-pole simplex singly re-entrant drum winding.

which are exactly opposite to one another should be connected in series to form a coil, so that conductor 1 should be connected to conductor 9 and then back to conductor 2, but a few trials will show that in order to get a singly re-entrant winding it is necessary to make the even conductors the returns for the odd. Starting then at conductor 1 the winding goes to the nearest even conductor to that which is exactly opposite, namely conductor 8, then returning back to the south pole the next odd conductor is number 3, which again is connected to conductor 10, and so on; so that the complete winding can be represented by the following table:

$$1^{-}8\_3^{-}10\_5^{-}12\_7^{-}14\_9^{-}16\_11^{-}2\_13^{-}4\_15^{-}6\_1,$$

which shows clearly that the winding is re-entrant, and also that every conductor has been taken in once and only once.

The connections of this winding to the commutator are shown in Fig. 12.

Fig. 13 is another method adopted to show the connections of the same winding and is obtained by splitting Fig. 12 at xy and opening it out on to a plane. This gives what is called the developed winding and shows clearly the shape of the coil which is used. If Fig. 13 be cut out and bent around a drum it will give the best possible representation of a drum winding.

Inspection of Figs. 12 and 13 shows that, just as in the case of the simplex Gramme winding, there are two paths between the + and the − brush.

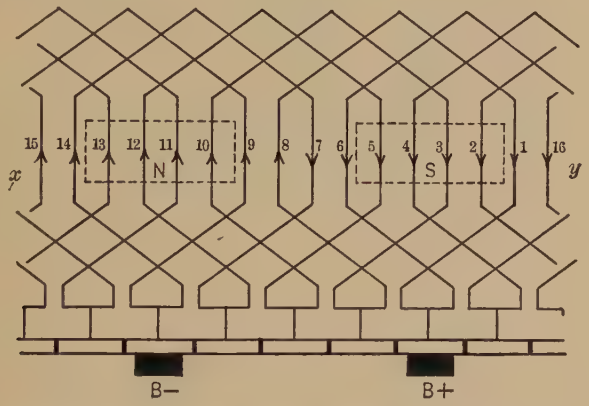

Fig. 13.—Developed two-pole simplex singly re-entrant drum winding.

12. The E.M.F. Equation.—If

ϕ_a is the flux per pole which is cut by the armature conductors,

p is the number of poles,

p_1 is the number of paths through the armature,

Z is the total number of face conductors on the armature surface,

r.p.m. is the speed of the armature in revolutions per minute,

then one conductor cuts $\phi_a p$ lines per revolution

or,

$$\phi_a p \frac{\text{r.p.m.}}{60} \text{ lines in one second.}$$

Since the number of conductors between a+ and a− brush $= \frac{Z}{p_1}$

the e.m.f. between the terminals in volts

$$= \frac{Z}{p_1} \phi_a p \frac{\text{r.p.m.}}{60} 10^{-8} \qquad (2)$$

The number of poles and paths is determined by the designer of the machine.

13. Multipolar Machines.—One of the easiest ways by which to get several paths through the winding is to build multipolar

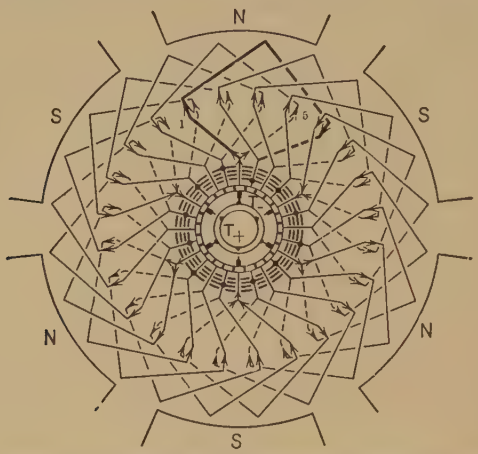

FIG. 14.—Six-pole simplex singly re-entrant multiple drum winding.

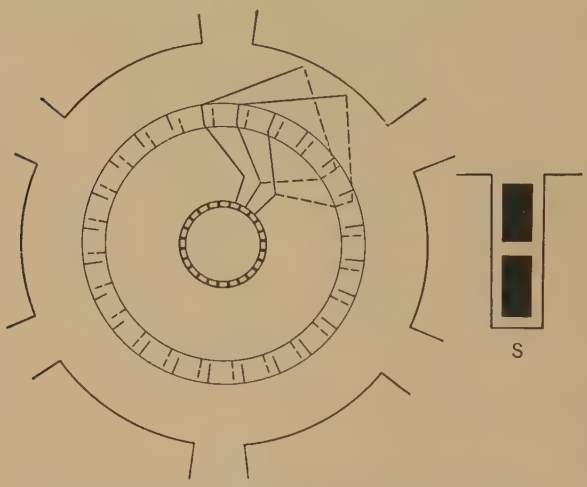

FIG. 15.—Part of a six-pole simplex singly re-entrant multiple drum winding.

machines, thus Fig. 14 shows a six-pole drum winding which has six paths in parallel between the + and the − terminals. There are three + and three − brushes and like brushes are connected together outside of the machine at T_+ and T_-. The

diagram which is used in this case is a slight modification of the developed diagram and gets over the difficulty of splitting the winding. Fig. 14 is rather complicated and will be explained in detail.

Figure 15 shows the armature conductors, the poles and the commutator of the same machine. There are two conductors in each slot so that a section through one of the slots is as shown at *S*, Fig. 15; the winding lies in two layers and is called a *double layer winding*. In Fig. 14 there are 24 slots and 48 conductors; a conductor in the top half of a slot is an odd-numbered conductor and that in the bottom half of a slot is an even-numbered conductor, so that, since the even conductors are the returns for the odd, each coil has one side in the top of one slot and the other side in the bottom of the slot which is one pole pitch further over. The coils are all alike and are made on the same former; a few of the coils are shown in place in Fig. 15, where conductors that are in the top layer are represented by heavy lines while those in the bottom layer are represented by dotted lines.

14. Equalizer Connections.—In the winding shown in Fig. 14 there are six paths in parallel between the + and the − terminals, and it is necessary that the voltages in all six paths be equal, otherwise circulating currents will flow through the machine. In Fig. 16, for example, is shown a case where, due to wear in the bearings, the armature is not central with the poles, and therefore the flux density in the air gap under poles *A* is greater than that in the air gap under poles *B*, so that the conductors under poles *A* will have higher voltages generated in them than those that are under poles *B*, and the voltage between brushes *c* and *d* will be greater than that between brushes *f* and *g*. Since *c* and *f* are connected together, as also are *d* and *g*, a circulating current will flow from *c* to *f*, through the winding to *g*, then to *d* and back through the winding to *c*, as shown diagrammatically at *C*, Fig. 16.

Since the circulating currents pass through the brushes, some of the brushes will have to carry more current than they were designed for, and sparking will result. To prevent the circulating current from having any large value it is necessary to prevent unequal flux distribution in the air gaps under the poles. This can be done by setting up the machine carefully, taking off the outside connections T_+ and T_- between the brushes, and adjusting the thickness of the air gaps under the different poles until

the voltages between + and − brushes are all equal, the machine being fully excited and running at full speed and no load.

It is impossible to eliminate entirely this circulating current, but its effect must be minimized. This is done by providing a low resistance path of copper between the points *c* and *f* and also between *d* and *g*, inside of the brushes, so that the circulating current will pass around this low-resistance path rather than through the brushes. It must be understood that the equalizer connections, as these low-resistance paths are called, do not eliminate the circulating current, but merely prevent it

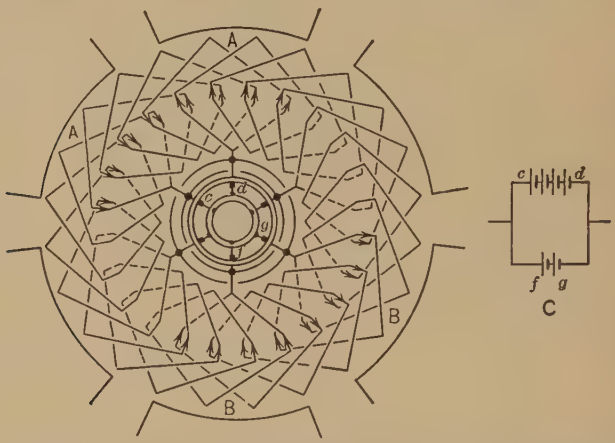

Fig. 16.—Machine with unequal air-gaps to show the action of equalizer connections.

from passing through the brushes. When the armature in Fig. 16 revolves into another position a different set of conductors have to be supplied with equalizers, and in order that the machine may be properly equalized in all positions of the armature, all points which ought to be at the same potential at any instant must be connected together.

Figure 14 is the complete diagram showing all the windings and also the equalizers. It is not necessary to equalize all the coils, because when, as in Fig. 14, the brush is on a coil which is not directly connected to an equalizer, there is still a path of lower resistance than that through the brushes, namely round one turn of the winding and then through the equalizer connection. It is usual in practice to put in about 30 per cent of the maximum possible number of equalizer connections.

The developed diagram corresponding to that of Fig. 14 is shown in Fig. 17; the only change that has been made is that the equalizer connections have been put at the back of the machine where they can be easily got at for repair. When these connections are placed behind the commutator it is impossible to get at them for repair without disconnecting the commutator from the armature winding.

When an armature is supplied with equalizer connections each brush will carry its proper share of the total current, because at

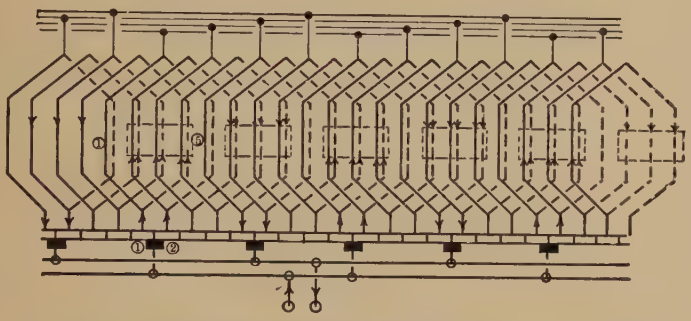

FIG. 17.—Six-pole simplex singly re-entrant drum winding.

one side the brushes are all connected together through the terminal connections and at the other side through the equalizer connections, so that the voltage drop across each brush is the same, and since the brushes are all made of the same material they must have the same current density. A unique method of equalizing a direct-current winding is shown later in this chapter (Art. 19).

15. Short Pitch Windings.—In Fig. 14 the two sides of each coil are exactly one pole pitch apart; such a winding is said to be *full pitch.* In Fig. 18 is shown a winding in which the two sides of each coil are less than one pole pitch apart; such a winding is said to be *short pitch.* Fig. 19 shows the developed diagram for this short-pitch winding at the instant when the coils in the neutral zone are short-circuited. It will be seen that the effective width of the neutral zone has been reduced by the angle α; this disadvantage, however, is compensated for by the fact that the conductors of the coils which are short-circuited at any instant are not in the same slot. This, as shown in Art. 73 page 89, lessens the mutual induction between the short-circuited coils and tends to improve commutation. Shortening the pitch by more than one slot decreases the neutral zone but does not

further decrease the mutual induction, so that there is no advantage in shortening the coil pitch more than one slot, but rather the reverse. Since there are seldom less than 12 slots per pole the effect of the shortening of the pitch on the generated voltage and on the armature reaction can be neglected.

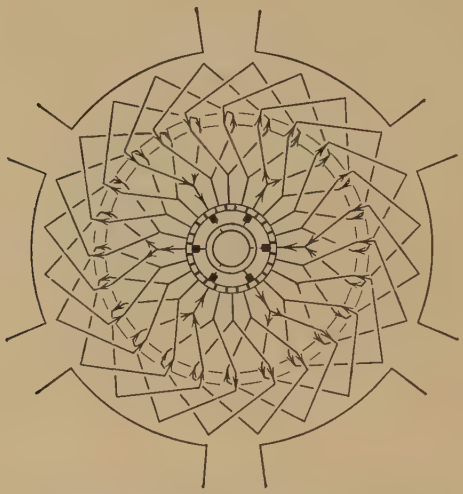

FIG. 18.—Six-pole simplex singly re-entrant short-pitch multiple drum winding.

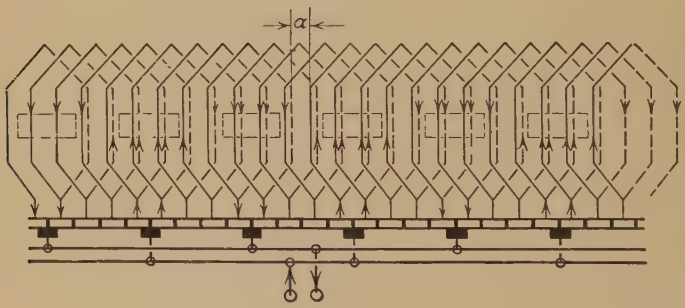

FIG. 19.—Corresponding developed drum winding.

16. Multiple Windings.—The windings shown in Figs. 14 and 18 have the same number of circuits through the armature as there are poles. Had they been duplex windings they would have had twice as many circuits. When the winding has a number of circuits which is a multiple of the number of poles

it is called a *multiple* winding to distinguish it from that described in the next article which is called a *series* winding.

Since windings that are not simplex and singly re-entrant are very rare, these two terms are generally left out, so that, unless it is actually stated to the contrary, all windings are assumed to be simplex singly re-entrant, and the windings shown in Figs. 14 and 18 would be called six-pole multiple drum windings.

FIG. 20.—Six-pole series progressive drum winding.

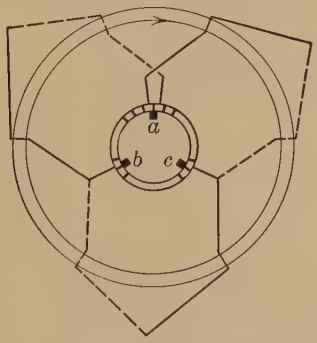

FIG. 21.—Small part of the above winding.

17. Series Windings.—It is possible to wind multipolar machines so that there are only two paths through the armature winding. Such windings are called *series* windings and an example of one is shown in Fig. 20 for a six-pole machine; in Fig. 21 a small portion of the winding is shown to make the complete diagram clearer.

If the winding be followed through, starting from the – brush, it will be seen that there are only two circuits through the armature, and that only two brushes are required. At the instant shown in Fig. 21 the – brush is short-circuiting two commutator segments and in so doing short circuits three coils. Since the points *a*, *b* and *c* are all at the same potential it is possible to put – brushes at each of these points, so that the current will not be collected from one set of brushes but from three; this will allow the use of a commutator of 1/3 of the length of that required when only one set of positive and one set of negative brushes are used. A machine with a series winding will therefore have in most cases the same number of brush sets as there are poles.

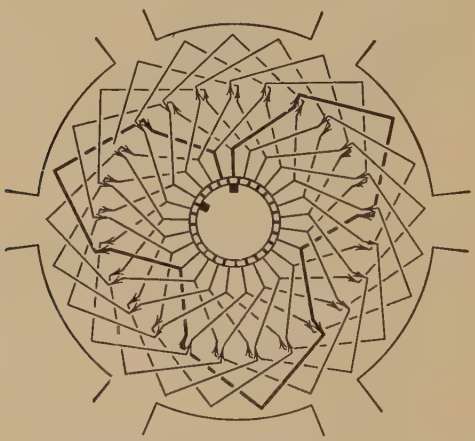

Fig. 22.—Six-pole series retrogressive drum winding.

It may be seen from Fig. 21 that the number of commutator segments must not be a multiple of the number of poles otherwise the winding would close in one turn round the machine; to be singly re-entrant the winding must progress by one commutator segment, as shown in Fig. 20, or retrogress by one commutator segment, as shown in Fig. 22, each time it passes once round the armature, the condition for this is that S, the number of commutator segments, $= k\frac{p}{2} \pm 1$, where k is a whole number and p the number of poles. When the – sign is used the winding is progressive, as in Fig. 20, where the number of commutator

segments is 23, and when the + sign is used the winding is retrogressive, as in Fig. 22, where the number of commutator segments is 25.

The paragraph in Art. 14, page 15, on the division of the total current of the machine, holds to a certain extent for the series winding also; the one side of all the brushes are connected together through the short-circuited coils, as shown in Fig. 21, while the other side of the same brushes are connected together through the terminal connections. It is important to notice, however, that since the number of commutator segments S is not a multiple of $\frac{p}{2}$, the number of pairs of poles, and since the brushes of like polarity are spaced two pole pitches apart, a kind of *selective commutation* will take place; thus when, as shown in Fig. 21, brush a is short-circuiting a set of three coils in series, brush b has just begun to short-circuit an entirely different set of three coils in series and brush c has nearly finished short-circuiting still another set of three coils in series.

The series winding has the great advantage that equalizers are not required, since, as shown in Fig. 21, the winding is already equalized by the coils themselves, so that there can be no circulating current passing through the brushes; further there can

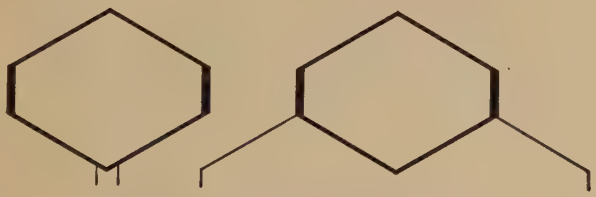

Fig. 23.—Coils with several turns.

be no circulating current in the machine due to such causes as unequal air gaps because each circuit of the winding is made up of conductors in series from under all the poles. On account of this fact, and also because of the property that only two sets of brushes are required, the series winding is used for D.-C. railway motors, because in a four-pole railway motor the two brushes can be set 90 degrees apart so as to have both sets of brushes above the commutator, where they can be easily inspected from the car.

18. Lap and Wave Windings.—From the appearance of the individual coils of the two windings, Figs. 14 and 20, the former is sometimes called a lap winding and the latter a wave winding. It must be understood, however, that each of the coils shown in these diagrams may consist of more than one turn of wire, thus Fig. 23 shows both a lap and a wave coil with several turns per coil, so that the terms *lap* and *wave* apply only to the connections to the commutator and not to the shape of the coil itself; the terms *multiple* and *series* are more generally used.

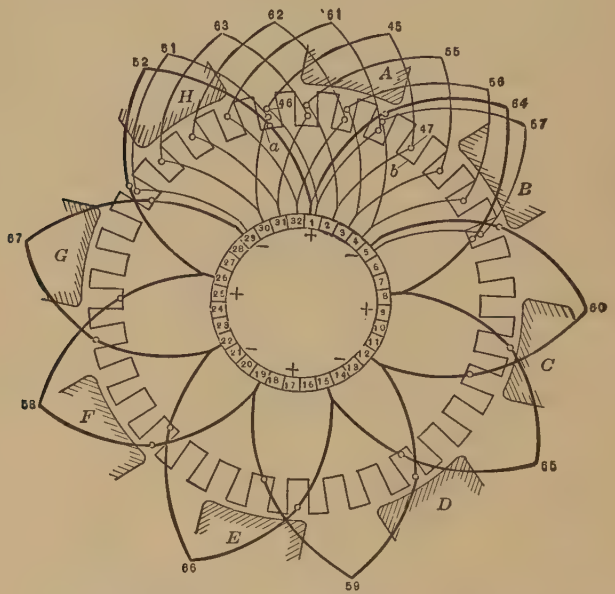

FIG. 24.—Combined lap and wave winding; wave winding forming the cross connections.

19.[1] A unique modification of the method of equalizer connections discussed in Art. 14 has been proposed by W. H. Powell and G. M. Albrecht and has been incorporated into direct-current machines produced by the Allis-Chalmers Company, of Milwaukee, Wis. It consists essentially of combining lap-and-wave windings in the same armature structure. Figure 24 shows a part of the winding for an eight-pole, direct-current machine equalized by this method. Figure 25 shows one complete coil of such a winding and parts of two adjacent coils.

[1] See *Iron and Steel Engineer*, Sept., 1925.

Referring to Fig. 24 and quoting from the paper mentioned in footnote 1:

It will be noted that the group of four lap coils 45, 55, 56, 57, connected to the commutator segments 1 to 5, has connected at its terminals, that is, to segments 1 and 5, the group of four wave coils 52, 58, 59 and 60. There are then between segments 1 and 5, four voltage generating, current carrying, lap wound coils with coil sides under poles *A* and *B*, and also four voltage generating, current carrying, wave wound coils with coil sides under poles *H*, *G*, *F*, *E*, *D*, *C*, *B*, *A*. If all of the poles are of the same magnetic strength, the voltage generated by each circuit will be equal, and as the resistance of the circuits are equal, the currents will be equal. If the magnetic strength of the poles is not equal, the current flowing in the two circuits will be proportional to the voltage generated, which in the lap coils is dependent on one pair of poles, and in the wave coils dependent on the average of all the pairs of poles. In Fig. 24, there are also shown the four lap and wave coils between segments 1 and 29 in which the same conditions obtain as between segments 1 and 5.

On account of the appearance of the coils, this winding has been called by its inventors the "frog leg" winding. Preliminary

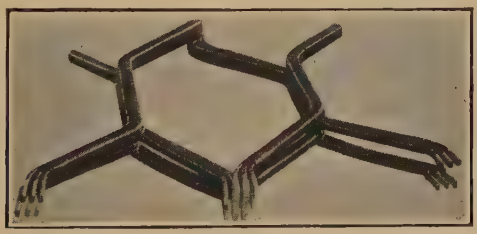

FIG. 25.—Photograph of "frog leg" coil.

tests on this innovation indicate an excellent performance but it has not yet received the test of extended use. Its real value must, of course, rest upon the results of such use.

20. Shop Instructions.—It would be a mistake to send winding diagrams such as those described in this chapter into the shop and expect the men in the winding room to connect up a machine properly from the information given there; the instructions must be given in much simpler form. For a winding such as that shown in Fig. 17 the shop instructions would read: "Put the coil in slots 1 and 5 and the commutator connections in segments 1 and 2," where the position of segment 1 relative to that of slot 1 is fixed by the shape of the end of the coil. All

the coils are made on formers and are exactly alike, so that, having the first coil in place, the workman can go straight ahead and put in the other coils in a similar manner.

In the case of a winding such as that shown in Fig. 20, the instructions would read: "Put the coil in slots 1 and 5 and the commutator connections in segments 1 and 9," where the position of segment 1 relative to that of slot 1 is again fixed by the shape of the coil.

21. Duplex Multipolar Windings.—The multipolar windings discussed so far have all been simplex and single re-entrant. It is evident that both multiple and series windings can be made duplex if necessary; such windings can easily be drawn from the information already given in this chapter and no special discussion of them is necessary.

22. Windings with Several Coil Sides in One Slot.—There are generally more coils than there are slots; Fig. 26 shows part of the winding diagram for a machine which has a multiple winding with four coil sides in each slot and two turns per coil, and Fig. 27 shows part of the winding diagram for a series wound machine also with four coil sides in each slot and two turns per coil. A section through one slot in each case is shown in Fig. 28; there are eight conductors per slot and conductors are numbered similarly in Figs. 27 and 28. In each case there are two commutator segments to a slot since the number of commutator segments is always the same as the number of coils, in fact a coil may be defined as the winding element between two commutator segments.

23. Number of Slots and Odd Windings.—For series or wave windings the number of coils = S, the number of commutator segments, $= k\frac{p}{2} \pm 1$,[1] (k being an interger); the refore the number of coils must alway be odd when $\frac{p}{2}$ (the number of pairs of poles) is even, and even when $\frac{p}{2}$ is odd. Even when the proper number of slots is used, it is not always possible to get a wave winding without some modification. Suppose, for example, that a 110-volt four-pole machine has 49 slots and two conductors per slot, then

[1] This relation is restricted to the singly re-entrant simplex type of wave windings. An inspection of Fig. 24 will indicate that this relationship does not hold when a multiply re-entrant type of wave winding is used such as are that portion of the windings that are of the wave type in that figure.

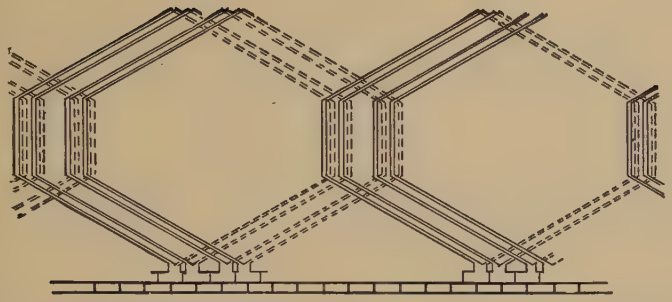

FIG. 26.—Multiple winding with four coil sides per slot and two turns per coil.

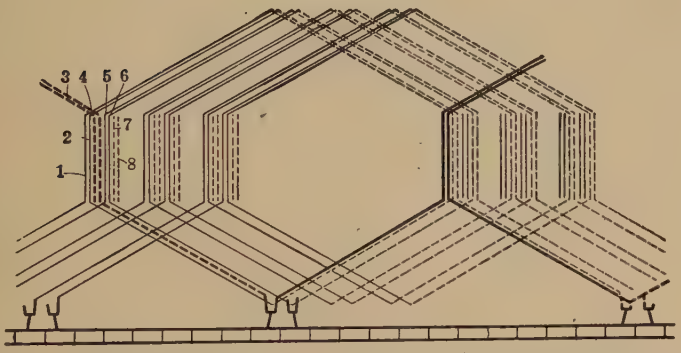

FIG. 27.—Series winding with four coil sides per slot and two turns per coil.

FIG. 28.—Section through one slot of the above windings.

the number of coils $=49 = 24\frac{p}{2} + 1$, which will give a satisfactory winding; when wound for 220 volts the machine requires twice the number of conductors, or four conductors per slot, so that the number of coils $=98 = 49\frac{p}{2} \pm 0$ which will not give a wave winding. In such a case, however, the winding can be made wave by cutting out one coil so that the machine has really 97 coils instead of 98, and has also 97 commutator segments; the extra coil is put into the machine for the sake of appearance but is not connected up, its two ends are taped so as to completely insulate the coil, and it is called a *dead coil.*

When the armature is large in diameter it is built in segments as described in Art. 30, page 29. In such a case it is difficult to get an odd number of slots on the armature; indeed, it can only be done when the number of segments that make up one complete ring of the armature and also the number of slots per segment are both odd numbers; however, for reasons to be discussed under commutation, series or wave windings are seldom found in large machines.

For multiple or lap windings the number of slots must be multiple of half the number of poles if equalizers are to be used; this can be ascertained from Fig. 16, where it is seen that in the case of a six-pole machine the equalizers must each connect together three points on the armature exactly two pole pitches apart from one another. It is found, however, that small four-pole machines with multiple windings run sparklessly without equalizers, and since the only condition that limits a multiple winding without equalizers is that the number of conductors be even, for such small machines the same punching is used as for the machine with the series winding, namely, a punching having an odd number of slots; the number of conductors will be even since the winding is double layer, and has therefore a multiple of two conductors per slot. By the use of the same punching for both multiple and series windings, a smaller stock of standard parts needs to be kept, quicker shipment can be made, and lower selling prices given for small motors, than if different punchings were used. In the case of large machines it is best to make the winding such that equalizers can be used, because the sparking caused by the want of equalizers becomes worse as the number of poles and as the output of the machine increases.

CHAPTER III

CONSTRUCTION OF DIRECT-CURRENT MACHINES

The construction of electrical machinery is really a branch of mechanical engineering but it is one which requires considerable knowledge of electrical phenomena.

Figure 29 shows an exploded view of the type of construction that is generally adopted for D.-C. machines of outputs up to 100 hp. at 600 r.p.m.

24. The Armature.—*M*, the armature core, is built up of laminations of sheet steel 0.014 in. thick; the thinner the laminations the lower the eddy current loss in the core, but sheets thinner than 0.014 in. are flimsy and difficult to handle.

The laminations are insulated from one another by a layer of varnish and are mounted directly on the shaft of the machine and held there by means of a key. Usually these armature punchings are provided with a small notch, called a marking notch, the object of which is to ensure that the burrs on the punchings all lie the same way; it is impossible to punch out slots and holes without burring over the edge, and unless these burrs all lie in the same direction a loose core is produced.

The laminations are punched on the outer periphery with slots which carry the armature coils. The type of slot in general use is the open slot. The other type which is sometimes used is closed or at least partially closed at the top; the coils in this case have to be pushed in from the ends. The open slot has the advantage that the armature coils can be fully insulated before being put into the machine, and that the coils can be taken out, repaired, and replaced, in the case of a breakdown, more easily than if the closed type of slot had been adopted.

The armature core is divided into blocks by means of vent segments, shown at *V*; the object of the vent ducts so produced is to allow free circulation of air through the machine to keep it cool; they divide the core into blocks usually less than 3 in. thick and are approximately $\frac{3}{8}$ in. wide; narrower ducts are not very effective and are easily blocked up, while wider ducts do

not give increased cooling effect and take up space which might be filled with iron.

The vent segments are mounted directly on the shaft, and, along with the laminations of the core, are clamped between two cast-iron end heads which cannot be seen in Fig. 29 because they are hidden by the windings. These end heads carry the coil supports and the ends of the coils projecting beyond the iron laminations M are firmly supported in place by being bound down against them by the band wires B.

25. Poles and Yoke.—The armature revolves in the magnetic field produced by the exciting coils A which are wound on and

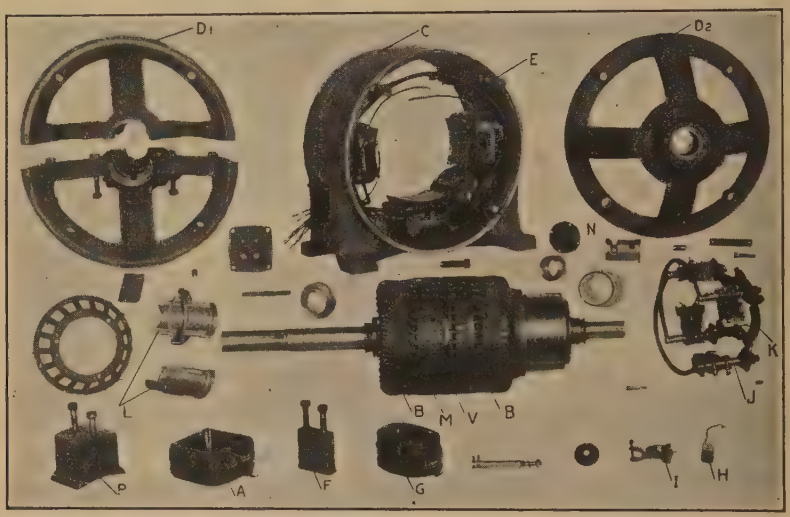

Fig. 29.—Exploded view of a modern D.-C. motor.

insulated from the poles P. The poles P, shown in Fig. 29, are rectangular in cross-section and are made up of laminated iron riveted together. These pole laminations are usually made from sheet steel of approximately 0.025 in. thickness. Formerly, it was quite common to make the poles of D.-C. motors and generators of solid iron of round cross-section. This construction had the merit of using a smaller amount of copper in the field coils but it had the disadvantage of requiring the use of a laminated pole face, usually riveted or bolted to the field core. The purpose of these laminated pole faces was to prevent eddy currents from being set up in the pole face by the armature

teeth, as would be the case if the pole face were solid instead of laminated. The laminated pole construction shown at *P*, Fig. 29, provides the necessary laminated pole face inherently and this construction for poles is almost universal in modern D.-C. generators and motors.

In addition to the main poles *P*, Fig. 29, and their windings *A*, modern D.-C. machines are equipped with auxilliary poles *F* and windings *G*. These are *commutating poles* (formerly called *interpoles*). Their function is to improve commutating conditions and their theory and method of operation is given in succeeding chapters on commutation.

The axial length of the pole is usually made shorter than the axial length of the armature core. This is done to enable the revolving part of the machine to oscillate axially and so prevent the commutator, journals and bearings from wearing in grooves. In order that the armature may oscillate freely it is necessary that the reluctance of the air gap does not change between the two extreme positions, the condition for which is that the armature core be longer or shorter axially than the pole face by the amount to be allowed for oscillation, which is usually $\frac{3}{8}$ in. for motors up to 50 hp. at 900 r.p.m., and $\frac{1}{2}$ in. for larger machines.

The poles are attached to the yoke *C* by means of bolts; the yoke also carries the bearing housings *D* which stiffen the whole machine so that the yoke need not have a section greater than that necessary to carry the flux.

The housings and yoke are clamped together by means of bolts *E* and the construction must be such that the housings are capable of rotation relative to the yoke through 90 or 180 deg. in order that the machine, usually a small motor, may be mounted on the wall or on the ceiling. This rotation of the bearings is necessary in such cases because, since the machines are lubricated by means of oil rings, the oil wells must be always below the shaft.

26. Commutator.—The commutator is built up of segments of hard-drawn copper insulated from one another by mica which varies in thickness from 0.02 to 0.06 in., depending on the diameter of the commutator and the thickness of the segment.

The segments of mica and copper are clamped between two cast-iron V-clamps and insulated therefrom by cones of micanite.

27. Bearings.—The construction of a typical bearing is shown at L and N. This is the oil-ring system of lubrication which is almost universally used in modern machinery. Figure 29 shows a split bearing L used at the pulley end in conjunction with a split housing D_1 and a solid bearing N used at the commutator end in conjunction with the solid housing D_2. On smaller machines, it is usual to make all housings and bearings solid. Screw plugs are located at the bottom of the oil wells in the bearing housings so that old oil may be drained out whenever necessary.

The brushes H with "pig tails" attached for carrying the current, are carried in brush holders I and these are in turn

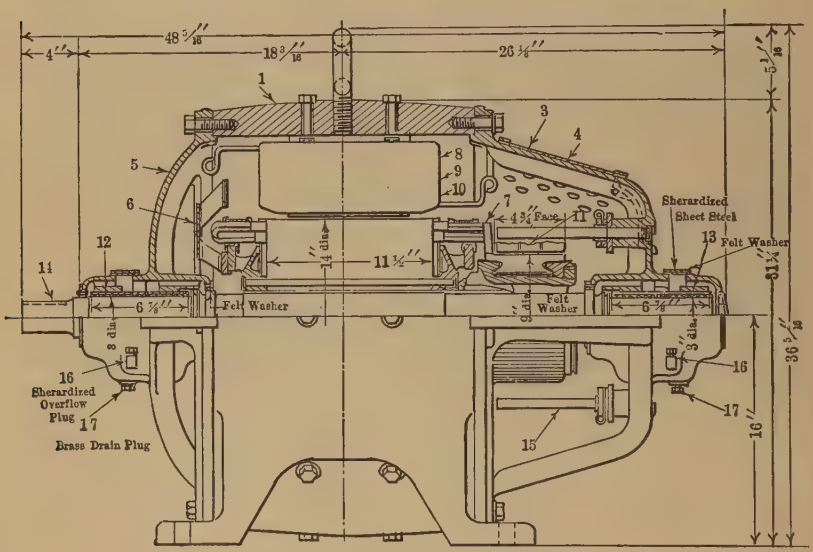

FIG. 30.—Cross section of D.-C. motor.

mounted on brush-holder studs J. The studs are insulated from the rocker arm K, which is usually carried on a turned seat, on the bearing. In the commutating pole type of machines, the proper position of the rocker arm K does not alter with load as it does on the non-commutating pole type. Once the proper position of K is found the rocker arm is clamped in that position and remains there. Sometimes it is dowelled in its proper position.

28. Cross-section.—Figure 30 shows in longitudinal cross-section a small D.-C. machine (about 30 in. outside diameter).

This machine was made by a different company from that shown on Fig. 29. The differences in construction are in minor details only.

29. Slide Rails.—When the machine has to drive or be driven by a belt, arrangements are made so that the entire machine may be mounted on rails; a belt-tightening device is supplied so that the position of the machine on these rails may be adjusted.

30. Large Machines.—The construction of large D.-C. machines differs only in detail from that of the smaller machines already described. Figure 31 shows the front and rear views of a 300-kw. 600-volt D.-C. engine type generator at 200 r.p.m.

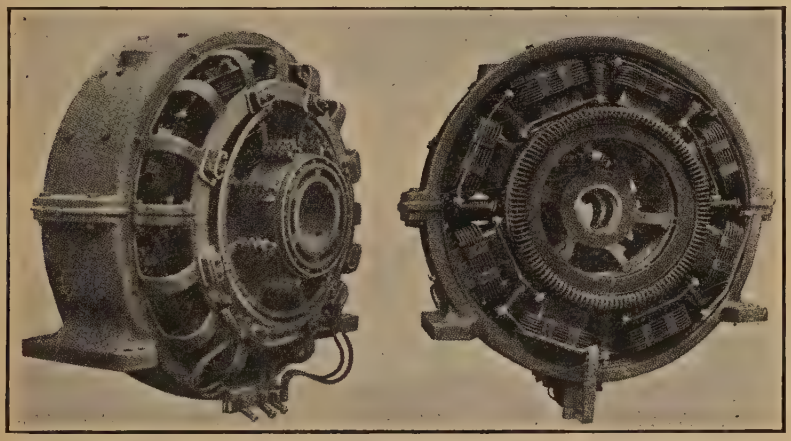

FIG. 31.—Photograph of a typical D.-C. engine type generator.

It will be noted that the machine is equipped with both main and commutating poles as are the smaller machines. In the case of a D.-C. generator (as shown in Fig. 31), the main poles are provided with both shunt and series field coils and the commutating poles, with a series winding. When the armature diameter exceeds 30 in. the punchings for the armature are usually not made in a single ring but from the segments of a circular ring as shown in Fig. 32. These segments are attached by dovetail projections, shown in Fig. 32, to the cast-iron spider shown in the rear view of Fig. 31. Figure 32 shows the shape of a standard armature segment punching and it shows further how one of these standard punchings is provided with ventilating fingers to form a ventilating plate. As indicated in a previous paragraph, one of these ventilating plates is used for not over

2½ in. of solidly stacked laminations. In building up the larger machines, the laminations shown in Fig. 32 are staggered so that alternate segments overlap each other. The ventilating fingers consist of sheet steel on edge. These ventilating plates are used not only interspersed in the core but also at the ends of the core; the end ventilating plates are partly for ventilation but mainly to support the teeth. The pole construction is usually of laminations riveted together as described for the smaller machines.

The shaft, bearings, and base of such a machine are generally supplied by the engine builder. The bearings are similar to those shown in Fig. 29 except that the bushing is generally made of babbitt metal, which is cast and expanded into a cast-iron shell. One oil ring is put in for each 8-in. length of the bearing bushing.

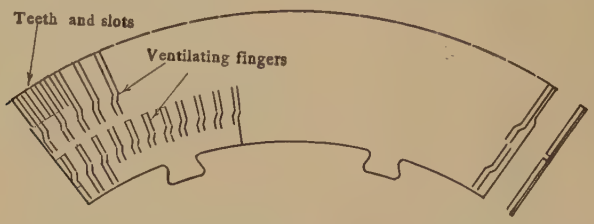

FIG. 32.—Armature segment for a D.-C. generator; showing vent fingers applied.

Since the shaft is supplied by the engine builder it is necessary to support the commutator from the armature spider. The brush rigging must also be supported from the machine in some way and is generally carried from the yoke as shown, in Fig. 31. Brushes of like polarity are joined together by copper rings which carry the total current of the machine to the terminals.

The yoke of a large D.-C. generator is always split so that, should the armature become damaged, one-half of the yoke can be moved away and repairs done without removing the armature.

31. Ventilation.—Figures 33 and 34 show the construction that is provided to secure good ventilation of the shunt field coils and the heavy strap copper windings that are used for the series field and commutating pole windings of modern D.-C. machines. Adjacent turns of the copper strap are separated by an air space so as to allow free circulation of air. A ventilating system such that air is drawn through the machine in an axial direction will therefore carry off heat from both sides of these straps.

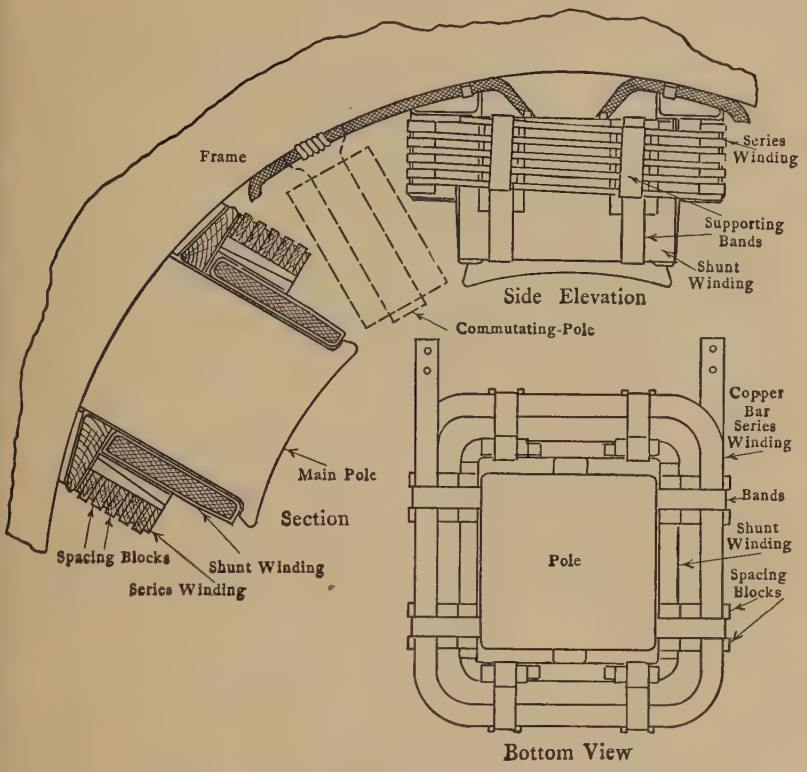

FIG. 33.—Shunt and series fields for D.-C. machine.

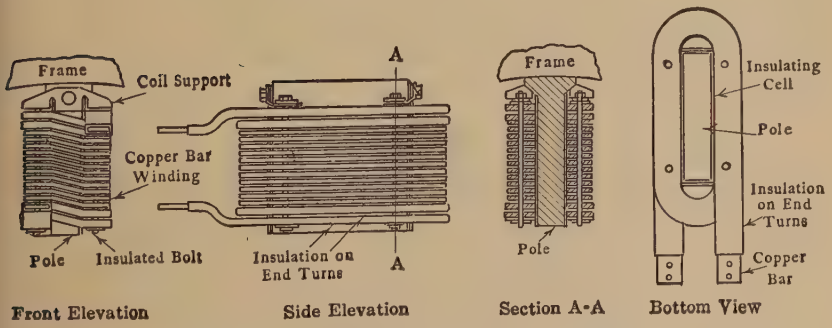

FIG. 34.—Commutating field pole and winding.

CHAPTER IV

INSULATION

32. Types of Insulation Defined.—The standards committee of the American Institute of Electrical Engineers has defined various classes of insulation that are applicable to electrical machinery. There are four classes that are so recognized, defined as follows.

CLASSES OF INSULATION

Class O Insulation Defined.—Class O insulation consists of cotton, silk, paper, and similar organic materials when neither impregnated[1] nor immersed in oil.

Class A Insulation Defined.—Class A insulation consists of cotton, silk, paper, and similar organic materials when impregnated[1] or immersed in oil; also enamel as applied to conductors.

Class B Insulation Defined.—Class B insulation consists of inorganic materials such as mica and asbestos in built-up form, combined with binding substances. If Class A material is used in small quantities in conjunction, for structural purposes only, the combined material may be considered as Class B, provided the electrical and mechanical properties of the insulated windings are not impaired by the application of the temperature permitted for Class B material. (The word "impair" is here used in the sense of causing any change which could disqualify the insulating material for continuous service.)

Class C Insulation Defined.—Class C insulation consists of inorganic materials such as pure mica, porcelain, quartz, etc.

[1] Impregnated cotton, paper or silk.—An insulation is considered to be "impregnated" when a suitable substance replaces the air between its fibers, even if this substance does not completely fill the spaces between the insulated conductors. The impregnating substance, in order to be considered suitable, must have good insulating properties; must entirely cover the fibers and render them adherent to each other and to the conductor; must not produce interstices within itself as a consequence of evaporation of the solvent or through any other cause, must not flow during the operation of the machine at full working load or at the temperature limit specified; must not unduly deteriorate under prolonged action of heat.

Class O insulation is practically never used in electrical machinery, since its properties are so much improved in every way by impregnation, thus making it Class A insulation. Class A insulation is sometimes used and Class B, usually used in the armatures of D.-C. machinery. The insulation usually used consists of the so called "mica wrappers" on the straight or slot portion of the coil and "mica tape" on the end portions. The manner of applying these is given in detail in an insulation specification in Art 42, page 40.

Mica Wrappers.—This is a composite material made by applying mica to paper with an appropriate bond—usually shellac. The paper used is a strong paper, usually 0.004 in. thick. In some types of wrappers this paper thickness is increased to as much as 0.007 in. To this paper is applied mica which has previously been split into thin sheets (about 0.001 in. thick). Several layers of this mica are applied to the paper with a shellac bond between paper and mica and between the several layers of mica. The sheet is then pressed under heat to make the whole as homogeneous as possible. The final thickness of the wrapper is usually from 0.010 to 0.012 in. In special cases where heavier paper is used, the total thickness of the finished wrapper may go up to as much as 0.025 to 0.035 in.

Mica Tape.—This is also a composite material made in very much the same way as above described for the wrappers, the main difference being that a thin "Jap" paper 0.001 in. thick is used for the backing to build on and the thickness of mica is limited to 0.002 to 0.004 in. The sheet of built-up mica is then covered with a top sheet of "Jap" paper. The built-up sheet is then slit into tape of the width required, usually $\frac{3}{4}$ in. The bond used in the manufacture of this sheet that is later slit into tape is of such a nature that the resulting tape is flexible and the mica laminae slip over each other readily when applying the tape.

By weight, the percentage of mica in mica tape is 60 to 70 per cent and in mica wrappers 50 to 60 per cent.

The temperatures that Class A and Class B insulations are expected to withstand are given later in Art. 101.

33. Properties Desired in Insulating Materials.—A good insulator for electrical machinery must have high dielectric strength and high electrical resistance, should be tough and

flexible, and should not be affected by heat, vibration, or other operating conditions.

The material is generally used in sheets and its dielectric strength is measured by placing a sheet of the material between two flat circular electrodes and gradually raising the voltage between these electrodes until the material breaks down. To get consistent results the same electrodes and the same pressure between electrodes should be used for all comparative tests; a size of 2 in. diameter, with the corners rounded to a radius of of 0.2 in. and a pressure of 1.5 lb. per square inch, have been found satisfactory for such tests. The value of the dielectric strength is defined as the highest effective alternating voltage that 1 mil will withstand for 1 min. without breaking down.

The material should be tested over the range of temperature through which it may have to be used, and all the conditions of the test and of the material should be noted; for example, the dielectric strength depends largely on the amount of moisture which the material contains and is generally highest when the material has been baked and the free moisture expelled.

The flexibility is measured by the number of times the material will bend backward and forward through 90 deg. over a sharp corner without the fibers of the material breaking or the dielectric strength becoming seriously lessened. Materials which are quite flexible under ordinary conditions often become brittle when baked so as to expel moisture.

34. Materials in General Use.—For the insulation of windings the choice is limited to the following materials: Micanite, mica, varnished cloth, paper, cotton, various gums and varnishes. Also mica is used in conjunction with paper or cloth to make the composite insulation mentioned above *viz.*, "mica wrappers," "mica tapes" etc.

Cotton tape which is generally 0.006 in. thick and 0.75 in. wide is put on coils in the way shown in Fig. 35, which is called half-lap taping. Such a layer of tape will withstand about 250 volts when dry. When the tape is impregnated with a suitable compound so as to fill up the air spaces between the fibers of the cotton such a half-lap layer will withstand about 1000 volts.

Cotton Covering.—Small wires are insulated by spinning over them a number of layers of cotton floss; the wire generally used for armature and field windings is insulated with two layers of cotton and is called double cotton-covered (d.c.c.) wire. Single

cotton-covered wire is sometimes used for field windings, and for very small wires silk is used instead of cotton because it can be put on in thinner layers. The thickness of the covering varies with the size of the wire which it covers, and its value may be found from the table on page 504. A double layer, with a total thickness for the two layers of 0.007 in., will withstand about 150 volts. When impregnated with a suitable compound it will withstand about 600 volts.

Fig. 35.—Half-lap taping.

Micanite, as used for coil and commutator insulation, is made of thin flakes of mica which are stuck together with a flexible varnish. The resultant sheet is then baked while under pressure to expel any excess of varnish and is afterwards milled to a standard thickness, usually 0.01 or 0.02 in.

It is a very reliable insulator and, if carefully made, is very uniform in quality. It can be bent over a sharp corner without injury because the individual flakes of mica slide over one another. To make this possible the varnish has to be very flexible.

The dielectric strength of micanite is about 800 volts per mil on a 10-mil sample, and is not seriously lessened by heat up to 150° C., but long-continued exposure to a temperature greater than 100° C. causes the sticking varnish to loose its flexibility. Micanite does not absorb moisture readily, but its dielectric strength is reduced by contact with machine oil. Such micanite is the insulation that is used for commutators.

Varnished Cloth.—Cloth which has been treated with varnish is sold under different trade names. Empire cloth for example, is a cambric cloth treated with linseed oil. It is very uniform in quality, has a dielectric strength of about 750 volts per mil on a 10-mil sample, and will bend over a sharp corner without cracking. It must be carefully handled so as to prevent the oil film,

on which the dielectric strength largely depends, from becoming cracked or scraped.

Various Papers.—These go under different trade names, such as fish paper, rope paper, horn fiber, leatheroid, etc. When dry, they have a dielectric strength of about 250 volts per mil on a 10-mil sample. They are chosen principally for toughness and, after having been baked long enough to expel all moisture, should bend over a sharp corner without cracking. The presence of moisture in a paper greatly reduces its dielectric strength and generally increases its flexibility; all papers absorb moisture from the air. It is good practice to mould the paper to the required shape while it is damp, then bake it to expel moisture and impregnate it before it has time to absorb moisture again.

Impregnating Compound.—The compound which has been referred to is usually made with an asphaltum or a paraffin base, which is dissolved in a thinning material. It should have as little chemical action as possible on copper, iron, and insulating materials. It should be fluid when applied; must be used at temperatures below the break-down temperature of cotton, namely 120° C.; should be solid at all temperatures below 100° C., and should not contract in changing from the fluid to the solid state.

Elastic Finishing Varnish.—This is usually an air-drying varnish and is put on the outside of insulated coils. It should be oil-, water-, acid-, and alkali-proof, should dry quickly, and have a hard surface when dry.

35. Thickness of Insulating Materials.—It is not generally advisable to use material which is thicker than 0.02 in., because if there is any flaw in the material that flaw generally goes through the whole thickness, whereas if several thin sheets are used the flaws will rarely overlap; thick sheets also are not so flexible as are thin sheets. For these reasons it is better to use several layers of thin material to give the desired thickness rather than a single layer of thick material. One of the advantages of the mica wrapper and mica tape is that their construction, being several layers thick, avoids the inherent disadvantage of a single layer of material.

36. Effect of Heat and Vibration.—It is not advisable to allow the temperature of the insulating materials mentioned in Art. 34 (except mica) to exceed 85° C. because, while at that temperature the dielectric strength is not much affected, long exposure to

such a temperature makes the materials dry and brittle so that they readily pulverize under vibration. It must be understood that the final test of an insulating material is the way it stands up in service when subjected to wide variations in voltage and temperature and to moisture, vibration, and other operating conditions found in practice.

37. Grounds and Short-circuits.—If one of the conductors an armature winding touch the core, the potential of the core becomes that of the winding at the point of contact, and if the frame (yoke, housings, and base) of the machine be insulated from the ground, a dangerous difference of potential may be established between the frame and the ground. For safety

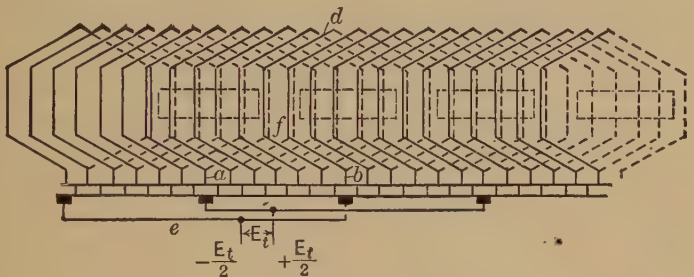

FIG. 36.—Winding with grounds.

it is advisable to ground the frame of the machine, and then the potential of the winding at the point of contact with the core will always be the ground potential.

If the winding be grounded at two points a short-circuit is produced and a large current flows through the short-circuit, this will burn the windings before the circuit-breakers can open and put the machine out of operation.

If, for example, the winding shown in Fig. 36 becomes grounded at the point a, the difference of potential between the point b and the ground changes from $\frac{1}{2}E_t$ to E_t, but no short-circuit is produced unless there exists another ground in the winding at some point d, or in the system at some point e. If the machine were a motor, a short-circuit would open the circuit-breakers, but not before some damage had been done. If the machine were a generator, and a short-circuit took place between points a and d, the circuit-breakers would not open unless power could come over the line from some other source, such as another generator operating in parallel with the machine in question, or

from motors which are driven as generators by the inertia of their load.

38. Slot Insulation and Puncture Test.—As shown in the preceding article, the insulation between the conductors and a core which is grounded may, under certain circumstances, be subjected to a difference of potential equal to the terminal voltage of the machine. Due to operating causes still greater differences of potential are liable to occur. To make sure that there is enough insulation between the conductors and the core, and that this insulation has not been damaged in handling, all new machines are subjected to a puncture test before they are shipped; that is, a high voltage is applied between the conductors and the core for 1 min. If the insulation does not break down during this test it is assumed to be ample. The value of the puncture voltage in accordance with the standards of the A. I. E. E. is, for D.-C. machinery, *twice normal voltage plus* 1000.

39. Insulation of End Connections.—Examination of Fig. 36 will show that the voltage between two end connections which cross one another may be, as at point *f*, almost equal to E_t, the terminal voltage. The end connections must therefore be insulated for this voltage.

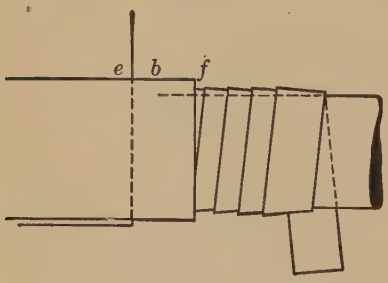

FIG. 37.—Insulation where coil leaves slot.

40. Surface Leakage.—If the end connections had only sufficient insulation to withstand the voltage E_t this insulation would break down during the puncture test due to what is called surface leakage. Figure 37 shows part of a motor winding and the insulation at the point where the winding leaves the slot. The slot insulation is sufficient to withstand the puncture test and is continued beyond the slot for a distance *ef*. When a high voltage is applied between the winding and the core the stress in the air at *b* may be sufficient to ionize it, then the air between *e* and *f* becomes a conductor, the drop of potential between *e* and *f* becomes small, and the voltage across the end-connection insulation at *f*, which equals the puncture voltage minus the drop between *e* and *f*, becomes high. To prevent break-down of the end-connection insulation due to this cause the distance *ef* is made as large as possible without increasing the

total length of the machine to an unreasonable extent and the end-connection insulation is made strong enough to withstand the full puncture voltage but with a lower factor of safety than that used for the slot insulation. Suitable values of *ef*, taken from practice, are given in the following table.

Rated Terminal Voltage of Circuit	Length *ef*., Inches
Up to 600 volts	1
600 to 1,200 volts	1⅛
1,200 to 2,500 volts	1¼
2,500 to 3,500 volts	1½
3,500 to 4,500 volts	1¾
4,500 to 6,600 volts	2¼
6,600 to 11,000 volts	2¾
11,000 to 13,200 volts	3½

The above table covers both D.-C. and A.-C. practice, there being at present no standard D.-C. voltage above 3000 volts.

Fig. 38.

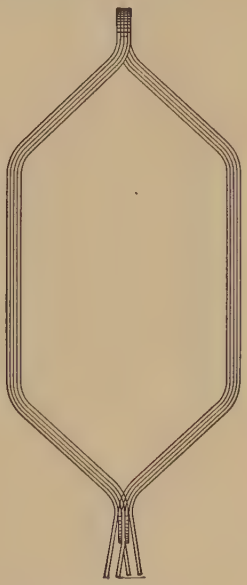

Fig. 39.

Coil for double layer winding with two turns per coil and 8 cond. per slot.

41. Several Coil Sides in One Slot.—Since the voltage between two adjacent commutator segments seldom exceeds 20 volts and is more often of the order of 5 volts, the amount of insulation between adjacent conductors need not be large; thus the conduc-

tors shown are insulated from one another by one layer of tape on each conductor or by a wrapper as indicated in Art. 42 and the group of conductors is then insulated more fully from the core. The completely insulated group of coils is shown in Fig. 38, and Fig. 39 shows the same group of coils before they are insulated.

When the individual coils are made up of a number of turns of d.c.c. round wire it is advisable to put a layer of paper between them, because the cotton covering may become damaged when the coils are squeezed together to get them into the slot. The voltage between adjacent turns of the same coil is so low that the cotton covering on the conductor is ample for insulating purposes.

42. Examples of Armature Insulation.—Modern methods of insulation can be best understood by giving an actual insulation specification. The following is quoted from such an insulation specification of one of the large American manufacturers of electrical apparatus.

INSULATION FOR ROTARY CONVERTER AND D.-C. GENERATOR ARMATURE, SERVICE VOLTAGE—700 OR LESS

Coils formed of bare copper strap.
Diamond type winding.
Mica insulation with cotton tape outside
Insulating Coils:
Conductor Insulation:

First. With one to four conductors inclusive of bare copper strap (widthwise) per coil, tape the *even numbered* conductors with two layers and the *odd numbered* conductors with one layer on parts not covered by wrapper with 0.004 mica tape, half overlapped. Extend the mica tape about $\frac{5}{8}$ in. under the wrapper. Fasten loose ends with one or two turns of 0.0045 cotton tape and liquid glue.

Second. With five or more conductors (widthwise) tape every conductor with 0.0045 mica tape, half overlapping. Apply two layers of tape over the even-numbered conductors on parts not covered by wrapper and one layer over parts covered by wrapper. Apply one layer of tape all around the *odd-numbered* conductors and reinforce between conductors on straight parts in slot with one strip of 0.004 mica tape. Cut these strips about $\frac{1}{32}$ wider than the insulated conductor and lap them over the second taping on the *even-numbered* conductors. Fasten the loose ends of tape on the leads with one or two turns 0.0045 cotton tape and liquid glue. Brush with shellac then assemble.

Wrapping:

Third. For length of wrapper see coil drawing. Wrap coils on straight parts through slots with ($2\frac{1}{2}$) two and one half turns of 0.010-in. thick fish-paper and mica wrapper starting between conductors with one to four con-

ductors per coil inclusive. Do not start wrapper between conductors with five or more conductors per coil. Tape coil ends (diamond portion) with one layer of 0.004 mica tape, half overlapped. Start and end this tape by lapping it about $\frac{5}{8}$ in. over the ends of the wrapper. Where necessary on account of sharp bends around the loop at the rear end of the coil the mica tape may be omitted. Reinforce between the lead or loop and adjacent conductors at rear end with thin splittings of mica, cut to fit the coil. Tape the coils all over with one layer of 0.007 cotton tape, not overlapping over portions of coil embedded in the slot, half overlapping elsewhere. Sew loose ends of tape with strong thread.

Treatments:

Fourth. Singe the tape and treat coils *three* times by dipping in insulating varnish and then baking. Apply this treatment only *once* to portion of coil embedded in slot, but the specified number of times to the end portions.

Gauging:

Fifth. See coil drawing for gauge sizes over insulation. Coils should be pressed in both dimensions where necessary to keep the sizes specified.

Insulation for Cross-connection (unless otherwise specified):

Conductors Insulated Separately.—Insulate individual conductors with two layers of 0.007 cotton tape, half overlapped. Singe the tape and treat connectors *three* times by dipping in insulating varnish and baking.

Conductors Insulated in Groups.—Insulate the odd numbered conductors with one layer and the even numbered conductors with two layers of 0.007 cotton tape, half overlapped.

Assemble conductors as per drawings and bind together with one layer of 0.007 cotton tape, half overlapped. Singe the tape and treat connectors *three* times by dipping in insulating varnish and baking.

Assembling Coils and Cross-connections on Machine:

For method of insulating cross-connections from ground see drawing. Unless the top and bottom portions of the armature coils or cross-connections are substantially separated, insulate between the two layers of winding with spacing pieces or strips of insulating material. See drawing for dimensions and location of this material.

Where the armature coils are connected on the rear end, insulate joints between them and the cross-connections or leads to collector by taping with two layers of 0.007 cotton tape, half-overlapped. Brush the tape with varnish and allow 5 hours to air dry.

Slot Insulation:

Inspect the slots to see that they have been properly filed, corners rounded and free from all dirt or iron fillings. Wind coils in 0.007, or heavier, fish-paper cells, which should extend $\frac{1}{4}$ to $\frac{3}{8}$ in. beyond the iron at each end of the armature. Insert filling strips of treated fullerboard in the slots where necessary to make coils fit tight. Where these strips would exceed $\frac{1}{4}$ in. in thickness, substitute wood strips-treated. Unless otherwise shown on the drawings, place all filling strips depthwise at the bottom of the slot. Fold the fishpaper cells over the top coil and secure the coils in the slot with wedges made in accordance with drawings.

Band Insulation (unless otherwise specified).—Band insulation up to and including $2\frac{3}{4}$ in. in width is to consist of three thicknesses of 0.020 surgical

tape with one thickness of treated 0.015 rope cement paper sandwiched between. Apply a sufficient number of coats of shellac to fill the tape.

Band insulation exceeding 2¾ in. in width is to consist of one thickness of treated 0.030 fullerboard inclosed in a cell of 0.024 friction cloth. Insert one thickness of treated 0.030 fullerboard between the friction cloth and the wire band. Unless otherwise specified on drawings insulate between the bands over the commutator cross-connections or coils (when the coils are banded down to the cross-connections) with sufficient thicknesses of treated fullerboard inclosed in 0.024 friction cloth coil to fill the space.

Insulate segmental bands with three thicknesses of treated 0.030 fullerboard. Butt and break the joints and allow ¼ in. space at all joints for compression.

Leads to Collectors.—Insulate leads to collector when made of copper strap and all joints between armature winding and cross-connections by first brushing with shellac. Wrap leads where supported by metal cleats with three and one-half or more turns of fishpaper and mica. Apply two layers of 0.007 cotton tape, half overlapping. Sew loose ends of tape with strong thread. Brush the first taping with insulating varnish. Apply coats of insulating varnish over the outside taping to thoroughly fill the tape.

Where coils or cross-connections are roped together or to wood or metal blocks or cleats, brush with shellac.

Finish all exposed portions of winding by painting with shellac.

The foregoing is a typical insulation specification for a 600-volt machine. For lower voltages, the slot portion of the insulation is kept the same, but on the end portions, cotton tape may be

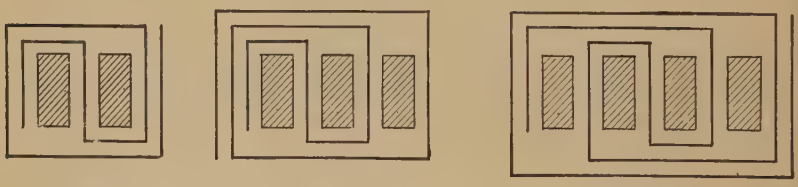

FIG. 40.—Method of interweaving wrapper to insulate contiguous turns in a D.-C. armature coil.

substituted for the mica tape. For higher voltages, mica tape is used on the end portions, practically as above specified but the mica wrapper is increased from two and one-half, to three and one-half or four and one-half or more turns. For marine service or for special heavy-duty service, such as steel mills, the number of dipping and baking treatments may be increased to as many as five on individual coil ends and, in addition several special dipping and baking treatments may be applied to the completely assembled armature and field.

Figure 40 indicates the method of weaving th e wrapper in between the individual turns when there are two, three, or four turns side by side in the slot.

43. Insulation Thickness.—The following table gives the thickness of the insulation used by one of the large manufacturing companies on the slot portion of D.-C. armature coils in their standard product.

Volts	Insulation Thickness to Ground, Inches
0– 500	0.045
500– 800	0.058
800–1500	0.065
1500–3000	0.075

44. Field-coil Insulation.—Two examples of field coil-insulation are shown in Fig. 41. Diagram *A* shows an example of a

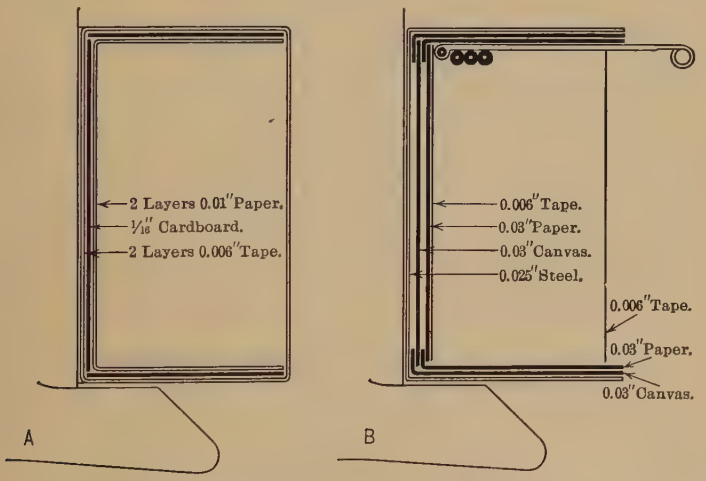

Fig. 41.—Field-coil insulation.

coil which is carried in a cardboard spool while diagram *B* shows on example of a coil which is carried in an insulated metal spool. In both cases the coils, after being wound in the spool and taped up, are baked in a vacuum and then impregnated with compound. This compound is a better insulator than the air which it replaces, it is also a better conductor of heat.

Figure 42 shows the type of coil which is used to a large extent on machines the armature diameter of which is greater than 20 in. The shunt coils are made of d.c.c. wire, wound in layers;

the individual shunt coils are 1 in. thick and are separated by ventilating spaces ½ in. wide. The insulation is carried out entirely by wooden spacing blocks so that there is a large radiating surface, and also little insulation to keep in the heat. The

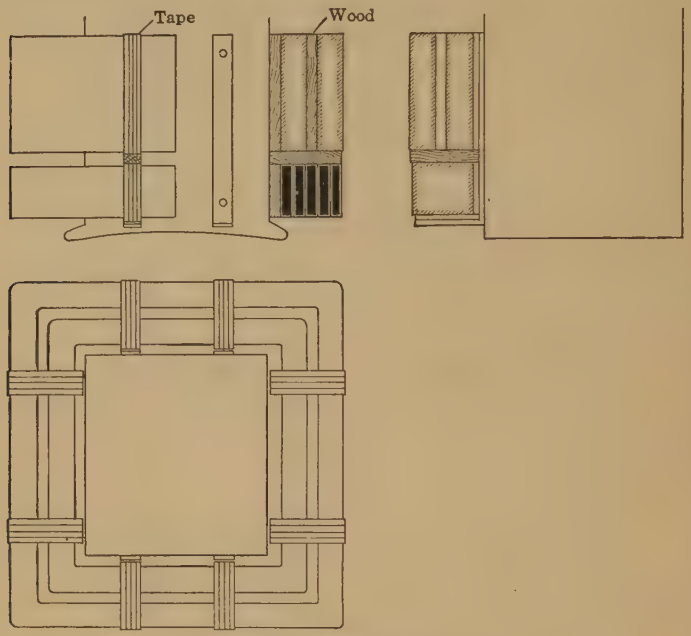

FIG. 42.—Ventilated field coils.

coils are made self-supporting by being impregnated with a solid compound at about 120° C.

The insulation on the individual turns of the series coil when made of wire consists of one layer of cotton tape 0.006 in. thick and half lapped; this coil, when made of strip copper as shown, is not impregnated but is dipped in finishing varnish.

CHAPTER V

THE MAGNETIC CIRCUIT

45. The Magnetic Path.—Figure 43 shows two poles of a multipolar D.-C. generator, each pole of which has an exciting coil of T_f turns through which a current I_f flows. Due to this excitation a magnetic flux is produced and the mean path of this flux is shown by the dotted lines. This magnetic flux consists of two parts, one, ϕ_a, which crosses the air-gap and is therefore cut by the armature conductors, and the other, ϕ_e, which does not cross the air-gap and is called the leakage flux.

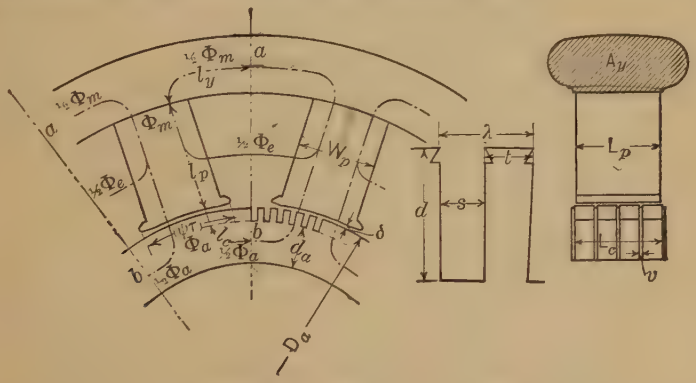

FIG. 43.—The paths of the main and of the leakage fluxes.

46. The Leakage Factor.—The total flux which passes through the yoke and enters the pole $= \phi_m = \phi_a + \phi_e$ and the ratio $\frac{\phi_m}{\phi_a}$ is called the leakage factor and is greater than 1.

47. The Magnetic Areas.—The meanings of the symbols used in this article will be understood by reference to Fig. 43.

D_a = the external diameter of the armature.

p = the number of poles.

τ = the pole pitch $= \frac{\pi D_a}{p}$.

ψ = the per cent enclosure of the pole $= \frac{\text{pole arc}}{\text{pole pitch}}$.

L_c = the axial length of the armature core.

m = the number of vent ducts in the center of the core.
v = the width of each vent duct.
L_g = the gross length of the iron in the core = $L_c - mv$.
L_n = the net length of the iron in the core = $0.9L_g$; it is less than L_g by the amount of the insulation between laminations.
N = the total number of slots in the armature.
λ = the slot pitch.
s = the slot width.
t = the tooth width.
d = the depth of the slot.
d_a = the depth of the armature core below the slot.
W_p = the pole waist.
L_p = the axial length of the pole.

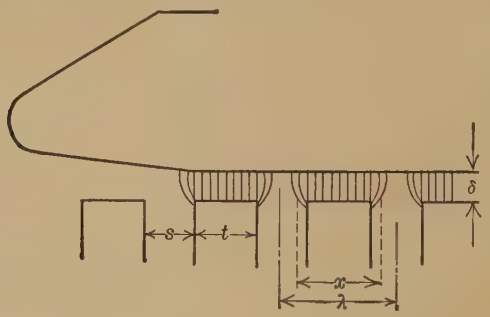

FIG. 44.—Distribution of flux in the air-gap.

Then:

A_g = the apparent gap area per pole = $\psi\tau L_c$.

A_{ag} = the actual gap area per pole = $\frac{A_g}{C}$ where C is a constant greater than 1, called the Carter coefficient. This constant takes into account the effect of the slots in reducing the effective air-gap area.

A_t = the tooth area per pole = $\psi \frac{N}{p} tL_n$; only those teeth which are under the poles are effective.

A_c = the area of the armature core = $d_a L_n$.

A_p = the pole area = $W_p L_p$ when the pole is solid; when built up of laminations the pole area = ($W_p L_p \times$ const.) where the const. is a stacking factor and = 0.95 approximately.

A_y = the yoke area.

48. The Carter Coefficient.[1]—Figure 44 shows the path of the magnetic flux across the air gap. If it were not for the armature slots and vent ducts the air-gap area per pole would be $\psi\tau L_c$

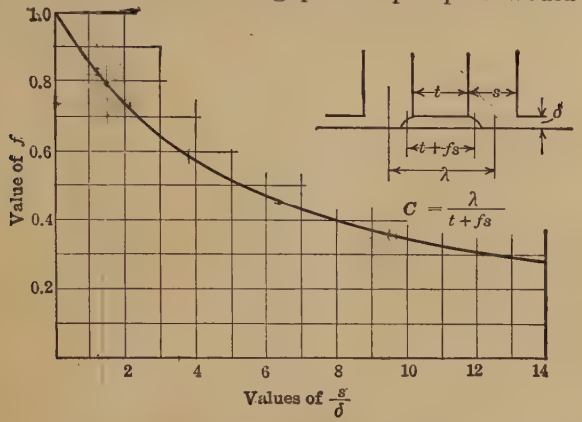

FIG. 45.—The Carter fringing constant.

which is called the apparent gap area. The actual gap area per pole $= \left(\frac{x}{\lambda}\psi\tau L_c\right)$ where $\frac{\lambda}{x}$, Fig. 44, is the Carter coefficient.

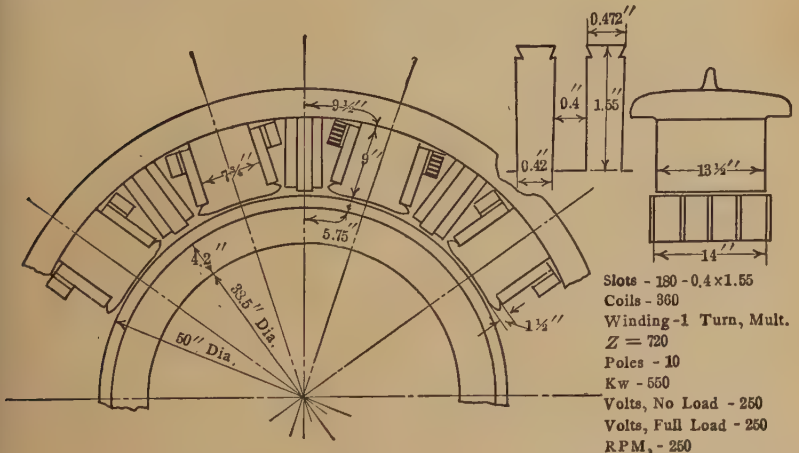

FIG. 46.—Cross section of a 550 kw., 250 r.p.m., 250 volt D.-C. generator.

$x = t + fs$ where f depends on the slot width s and on the air-gap thickness δ, and is got from Fig. 45 for different values of the ratio $\frac{s}{\delta}$; then C, the Carter coefficient $= \frac{\lambda}{x} = \frac{t+fs}{t+fs}$.

[1] *Elec. World and Engineer*, Nov. 30, 1901.

It is required to find the value of the Carter coefficient for the machine drawn to scale in Fig. 46.

$s = 0.40$ in.

$t = 0.472$ in.

$\delta = 0.20$ in.

$\frac{s}{\delta} = 2.0$

$f = 0.73$ from Fig. 45.

$$C = \frac{0.472 + 0.4}{0.472 + 0.73 \times 0.4} = 1.14$$

There is a small amount of fringing at the pole tips which tends to increase the air-gap area, but its effect is counterbalanced by the fact that at the pole tips, δ, the thickness of the air gap is increased.

The Carter coefficient for the vent ducts can be found in the same way as for the slots, but since its value is nearly always = 1 the calculation is seldom made.

49. The Flux Densities.—The flux in the different parts of the magnetic circuit is shown in Fig. 43, then:

B_g = the apparent flux density in the air-gap $= \frac{\phi_a}{A_g}$.

B_{ag} = the actual flux density in the air gap $= CB_g$.

B_t = the apparent flux density in the teeth $= \frac{\phi_a}{A_t}$.

B_c = the flux density in the armature core $= \frac{\phi_a}{2A_c}$.

B_p = the flux density in the pole $= \frac{\phi_m}{A_p}$.

B_y = the flux density in the yoke $= \frac{\phi_m}{2A_y}$.

The flux density in the teeth at normal voltage is generally about 140,000 lines per square inch, and at such densities the permeability of the iron in the teeth becomes comparable with that of air, so that a considerable amount of flux passes down the slots, vent ducts, and the air spaces between the laminations. If the assumption is made that the teeth have no taper, and that the lines of force are parallel both in the teeth and in the air paths, and if

B_{at} = the actual flux density in the teeth.

B_s = the flux density in the air path consisting of the slots, vent ducts, and air spaces between laminations.

B_t = the apparent flux density in the teeth, then

ϕ_a = the total flux per pole entering the armature = $B_t A_t$,

= $B_{at} A_t + B_s A_s$, where A_s is the area of the air path per pole; therefore

$$B_t = B_{at} + B_s\left(\frac{A_s}{A_t}\right).$$

$$= B_{at} + B_s\left(\frac{\lambda L_c - tL_n}{tL_n}\right).$$

For a given number of ampere-turns between the two ends of the slot, assuming the slot to be 1 in. deep,

B_s = 3.2 (ampere-turns); formula 1, page 6.

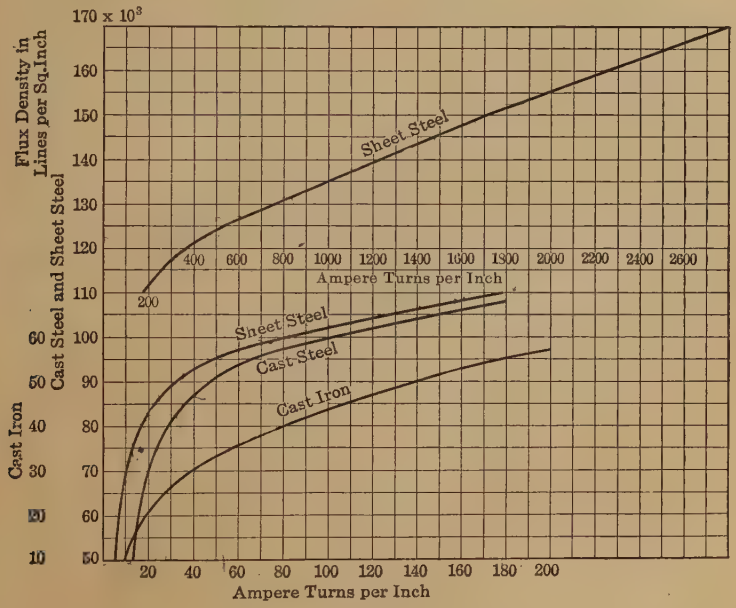

FIG. 47.—Magnetization curves.

B_{at} = the value of flux density corresponding to the given number of ampere turns, found from Fig. 47.

B_t, corresponding to the given number of ampere-turns, is found by substitution in the above formula.

The relation between B_t and B_{at} is plotted in Fig. 48 for different values of the ratio $\frac{\lambda}{t}$ and for the magnetization curve in Fig. 47, the assumption being made that $L_n = 0.8\ L_g$. For example, suppose that in a particular case the width of tooth is

equal to that of the slot so that $\frac{\lambda}{t} = 2$, that the ratio $\frac{L_n}{L_c} = 0.8$, and that the actual flux density in the tooth is 160,000 lines per square inch. Then the ampere-turns necessary to send this flux through 1 in. of the tooth is 2250, from Fig. 47; the flux density in the air path due to 2250 ampere-turns is $3.2 \times 2250 = 7200$ lines per square inch, see formula 1, page 6, and

$$B_{at} = 160{,}000 + 7200\left(\frac{\lambda - 0.8t}{0.8t}\right) \text{ where } \lambda = 2t$$

$$= 170{,}800 \text{ lines per square inch.}$$

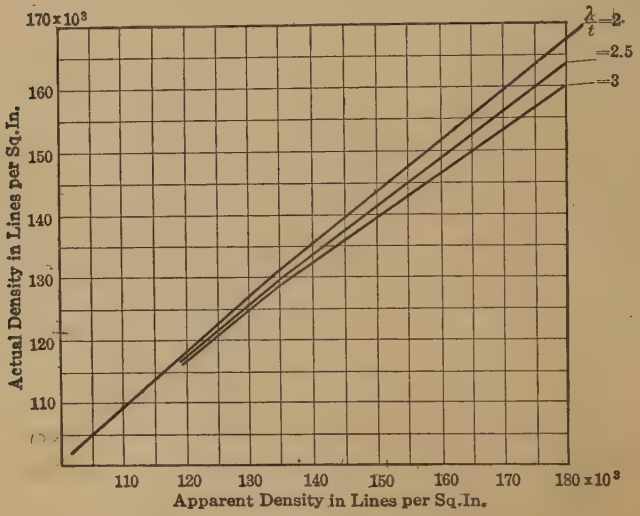

FIG. 48.—Densities in armature teeth.

50. Calculation of the No-load Saturation Curve.—It is required to find the number of ampere-turns necessary to send a certain flux ϕ_a across the air-gap of the machine shown in Fig. 43.

The m.m.f. between points a and b is $T_f I_f$ ampere-turns and this must be equal to $AT_y + AT_p + AT_g + AT_t + AT_c$, where AT_y is the ampere-turns necessary to send the flux $\frac{1}{2}\phi_m$ through the length l_y of the yoke. The value of B_y is known and the corresponding number of ampere-turns required for each inch of the yoke path is found from Fig. 47. This value of ampere-turns per inch multiplied by the length l_y gives the value of AT_y.

AT_p is the ampere-turns necessary to send the flux ϕ_m through the length l_p of the pole and is found in a similar manner.

AT_g is the ampere-turns necessary to send the flux ϕ_a across one air-gap. To find this value it is necessary to find first of all the value of C, the Carter coefficient and then the actual flux density in the air-gap, namely $B_{ag} = CB_g$.

$$B_{ag} \text{ lines per square inch } = 3.2\frac{AT_g}{\delta} \qquad (3)$$

where δ is the air-gap thickness in inches.

AT_t is the ampere-turns necessary to send the flux ϕ_a through the length d of the tooth. The value of B_t, the apparent tooth

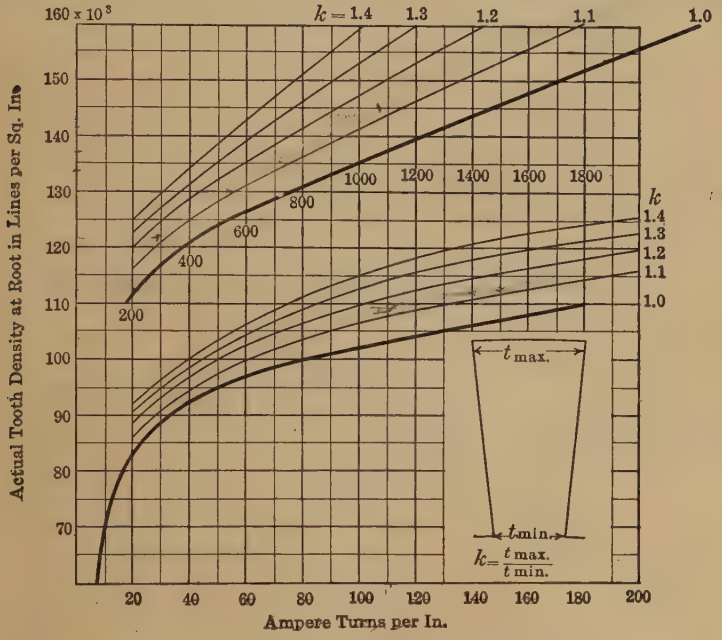

Fig. 49.—Magnetization curves for sheet steel.

density, is readily found, and the value of B_{at}, the actual flux density, can be found by the use of the curves in Fig. 48. The value of ampere-turns per inch corresponding to this actual density can then be taken from Fig. 47. This latter quantity when multiplied by d gives the value of AT_t.

When the teeth are tapered as shown in Fig. 49, so that the flux density is not uniform through the total depth of the tooth, the problem becomes more difficult. It is necessary to divide the tooth length d into a number of small parts, find the average flux density in each of these parts and the corresponding value

of ampere-turns per inch; the average value of these latter quantities multiplied by d gives the value of AT_t. This process is slow, but in Fig. 49 is plotted a series of curves whereby, if the actual flux density at the top and bottom of the tooth is known, the average ampere-turns per inch can be found directly.

AT_c is the ampere-turns necessary to send the flux $\frac{1}{2}\phi_a$ through the length l_c of the core and is found by the use of the curves in Fig. 47.

Example.—Figure 46 shows a dimensioned sketch of a ten-pole, 550 kw., 250-volt, 250-r.p.m. generator; it is required to draw the no-load saturation curve for this machine.

$$E = Z\,\phi_a \frac{\text{r.p.m.}}{60}\,\frac{\text{poles}}{\text{paths}}\,10^{-8} \text{ volts.}$$

Therefore $$\phi_a = \frac{250 \times 60 \times 10 \times 10^8}{720 \times 250 \times 10}$$
$$= 8.35 \times 10^6 \text{ at 250 volts, no-load.}$$

The magnetic areas:

τ = the pole pitch	$= \frac{\pi \times 50}{10} = 15.7$ in.
ψ = the per cent pole enclosure	= 65 per cent.
L_g = the gross iron	= 12.5 in.
L_n = the net iron	= 11.25 in.
λ = the slot pitch	= 0.872 in. at top of slot.
	= 0.82 in. at bottom of slot.
t = the tooth width	= 0.472 in. at top.
	= 0.42 in. at bottom.
A_g = the apparent gap area	$= 0.65 \times 15.7 \times 14. = 143$ sq. in.
C = the Carter coefficient	= 1.14 from Art. 48, page 47.
A_t = the minimum tooth area per pole	$= 0.65 \times {}^{180}\!/_{10} \times 0.42 \times 11.25$
	= 55 sq. in.
A_c = the core area	$= 4.2 \times 11.25 = 47.2$ sq. in.
A_p = the pole area	$= 0.95 \times 7.75 \times 13.5 = 99.4$ sq. in.
A_y = the yoke area	= 61.5 sq. in.

The flux per pole:

ϕ_a = the useful flux per pole	$= 8.35 \times 10^6$
l_f = the leakage factor	= 1.18 (see page 54).
ϕ_m = the total flux per pole	$= 9.85 \times 10^6$

The flux densities:

B_g = the apparent gap density	= 58,500 lines per square inch.
B_t = the apparent tooth density	= 152,000 lines per square inch.
B_{at} = the actual tooth density	= 145,000 lines per square inch, (from Fig. 48).
B_c = the core density	= 88,500 lines per square inch.
B_p = the pole density	= 99,000 lines per square inch.
B_y = the yoke density	= 80,000 lines per square inch.

The magnetic circuit lengths (see Fig. 46):

δ = air-gap clearance = 0.2 in.
d = depth of slot = 1.55 in.
l_c = length of core circuit = 5.75 in.
l_p = length of pole circuit = 9 in.
l_y = length of yoke circuit = 9.5 in.

The excitation:

$A.T._g$ = the gap ampere-turns $= \frac{1.14 \times 58{,}500 \times 0.2}{3.2} = 4240.$

$A.T._t$ = the tooth ampere-turns $= 1080 \times 1.55 = 1680.$

Use curves in Fig. 49 with a tooth taper of 1.125 and a flux density of 145,000 liner per square inch.

$A.T._c$ = the core ampere-turns $= \times 27 \times 5.75 = 155.$
$A.T._p$ = the pole ampere-turns $= 76.5 \times 9 = 690.$
$A.T._y$ = the yoke ampere-turns $= 30.5 \times 9.5 = 290.$

Total ampere-turns for 250 volts at no-load = 7055.

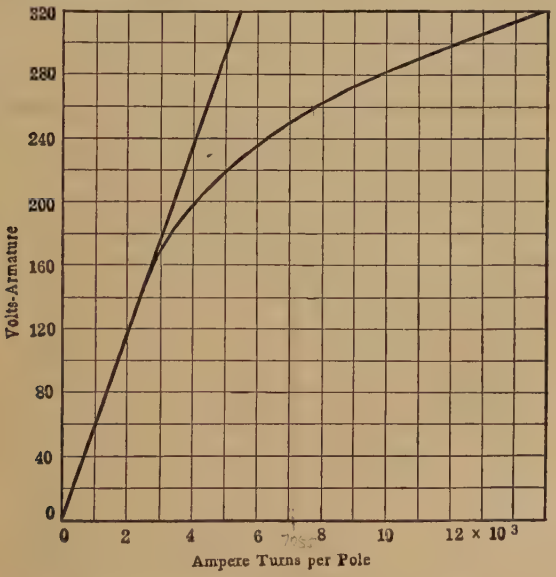

FIG. 50.—No load saturation curve of a 550 kw., 250 volt, 250 r.p.m., D.-C. generator.

In the above calculation two factors have been omitted which would cause the excitation to be slightly larger than that calculated, namely, the excitation required to send the flux across the joint between the pole and the yoke, and also the extra excitation required for the yoke due to the fact that, near the contact surface between the pole and the yoke, the yoke density is high, being equal to that of the pole.

Two other points at different voltages are figured out and the results are tabulated as shown in the following table:

No-load voltage			200		250		300	
Flux per pole			6.7×10^6		8.35×10^6		10×10^6	
Leakage factor			1.18		1.18		1.18	
	Length	Area	Density	*A.T.*	Density	*A.T.*	Density	*A.T.*
Air-gap	0.2	$\frac{143}{1.15}$	46,800	3,400	58,500	4,240	70,000	5,100
Minimum tooth	1.55	55	122,000	.....	152,000	.....	182,000	
			118,000	360	145,000	1,680	168,000	3,100
Air-gap + tooth	.....	.....	.....	3,760	.....	5,920	.....	8,200
Core	5.75	47.2	71,000	60	88,500	155	106,000	750
Pole	7.75	99.4	79,000	140	99,000	690	119,000	2,670
Yoke	9.5	61.5	64,000	160	80,000	290	96,000	550
Total ampere-turns per pole			.....	4,120	.....	7,055	.....	12,170

From these figures the no-load saturation curve in Fig. 50 is plotted.

51. Calculation of the Leakage Factor.[1]—Figure 51 shows part of a machine which has a large number of poles. The total leakage flux per pole $= \phi_e = \phi_{e1} + \phi_{e2} + \phi_{e3} + \phi_{e4}$, where

ϕ_{e1} = the leakage flux in paths 1, between the inner faces of the pole shoes.

ϕ_{e2} = the leakage flux in paths 2, between the flanks of the pole shoes.

ϕ_{e3} = the leakage flux in paths 3, between the inner faces of the poles.

ϕ_{e4} = the leakage flux in paths 4, between the flanks of the poles.

[1] The calculations of leakage factor given in this section take no cognizance of the presence of commutating poles, such are of almost universal application in modern D.-C. machinery. The presence of these commutating poles makes practically no modifidation of the results arrived at in this section, provided the influence of commutating pole in reducing the length of the path for the leakage flux is taken into consideration. At no load (m.m.f. on commutating pole = 0), it is quite obvious that this is the case. Under load, with an appreciable m.m.f. in the commutating pole, while the leakage on one side of main pole is very considerably increased, that on the other side is correspondingly decreased so that the total leakage does not differ materially from what would occur without the commutating pole.

The m.m.f. across paths 1 and 2 $= 2(AT_g + AT_t + AT_c)$
$= 2(AT_{g+t})$, since AT_c can be neglected; therefore, the flux across one path 1

$$= 3.2 \times 2(AT_{g+t}) \frac{L_s h_s}{l_1} \text{ from formula 1, page 6;}$$

$$= 6.4 \times (AT_{g+t}) \frac{L_s h_s}{l_1}$$

and $\phi_{e1} = 13(AT_{g+t}) \frac{L_s h_s}{l_1}$ since there are two paths 1, per pole.

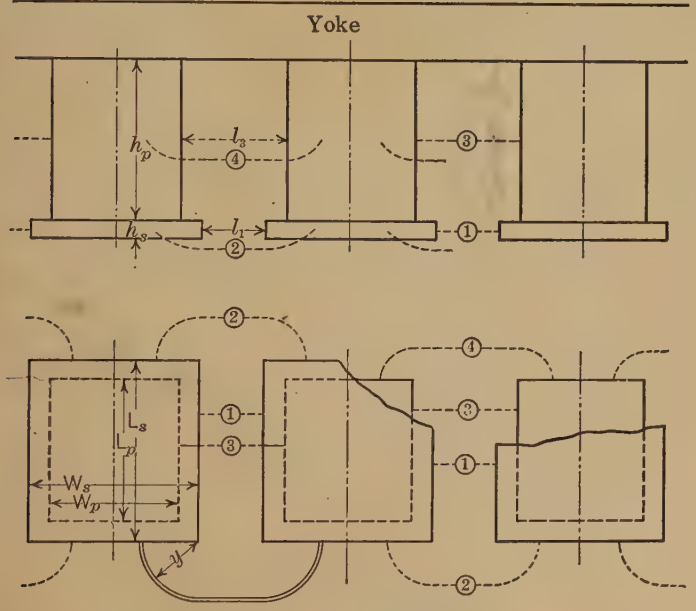

FIG. 51.—The leakage paths.

The flux across one path 2 $= 3.2 \times 2(AT_{g+t}) \int_{\frac{W_s}{2}}^{} \frac{h_s dy}{l_1 + \pi y}$

$$= 6.4 \times (AT_{g+t}) \frac{h_s}{\pi} \log_e \left(\frac{l_1 + \frac{\pi W_s}{2}}{l_1} \right)$$

$$= 4.7(AT_{g+t}) h_s \log_{10} \left(1 + \frac{\pi W_s}{2l_1} \right)$$

and $\phi_{e2} = 19(AT_{g+t}) h_s \log_{10} \left(1 + \frac{\pi W_s}{2l_1} \right)$ since there are four paths 2, per pole.

The m.m.f. across the paths 3 and 4 varies from zero at the bottom of the poles to $2(AT_{g+t})$ at the shoe, and the average value is taken as AT_{g+t} ampere-turns, so that

$$\phi_{e3} = 6.5(AT_{g+t})\frac{L_p h_p}{l_3},$$

and $$\phi_{e4} = 9.5(AT_{g+t})h_p \log_{10}\left(1 + \frac{\pi W_p}{2l_3}\right).$$

Given the complete data on a magnetic circuit, the value of AT_{g+t}, the ampere-turns to send the flux ϕ_a across one gap and tooth, can be found, and then the value of $\phi_e = \phi_{e1} + \phi_{e2} + \phi_{e3} + \phi_{e4}$ can be obtained by substitution in the above formulæ.

$$\text{The leakage factor} = \frac{\phi_a + \phi_e}{\phi_a}$$

It is required to find the leakage factor for the machine shown in Fig. 46.

$h_s = 1.5$ in.
$L_s = 13.5$ in.
$l_1 = 5.5$ in.
$W_s = 10.2$ in.
$h_p = 7.5$ in.
$L_p = 13.5$ in.
$l_3 = 11.25$ in.
$W_p = 7.75$ in.

then $\phi_{e1} = 13(A.T_{g+t})\left(\frac{13.5 \times 1.5}{5.5}\right) = 48(A.T_{g+t})$

$\phi_{e2} = 19(A.T_{g+t})1.5 \log_{10}\left(1 + \frac{\pi \times 10.2}{2 \times 5.5}\right) = 17(A.T_{g+t})$

$\phi_{e3} = 6.5(A.T_{g+t})\left(\frac{13.5 \times 7.5}{11.25}\right) = 58.5(A.T_{g+t}).$

$\phi_{e4} = 9.5(A.T_{g+t})7.5 \log_{10}\left(1 + \frac{\pi \times 7.75}{2 \times 11.25}\right) = 22.5(A.T_{g+t})$

and ϕ_e = the total leakage flux per pole $= 146(A.T_{g+t})$

The value of $A.T_{g+t}$ (from the table in Art. 50).
$= 5920$ ampere-turns.

therefore $\phi_e = 5920 \times 146 = 865{,}000$

and ϕ_a, the flux per pole that crosses the air-gap $= 8.35 \times 10^6$. (Art. 50.)

therefore the leakage factor $= \frac{\phi_a + \phi_e}{\phi a} = \frac{8.35 \times 10^6 + 0.865 \times 10^6}{8.35 \times 10^6} = 1.1.$

For a first approximation the following values of the leakage factor may be used:

Four-pole machines up to 10-in. armature diameter	1.25
Multipolar machines between 10- and 30-in. diameter	1.2
between 30- and 60-in. diameter	1.18
greater than 60-in. diameter	1.15

These values apply to the type of machine shown in Figs. 29, 30, and 31.

CHAPTER VI

ARMATURE REACTION

52. Armature Reaction.—The effect of armature reaction is not materially influenced by the presence of the commutating pole. Our initial analysis will therefore be made on the non-commutating pole design.

In Fig. 52, *A* shows the magnetic field that is produced in the air-gap of a two-pole machine by the m.m.f. of the main exciting coils.

B shows the armature carrying current and the magnetic field produced thereby when the brushes are in the neutral position and the main field is not excited. The m.m.f. between *a* and *b*, called the cross-magnetizing ampere-turns per pair of poles, due to the current I_c in each of the Z conductors $= \frac{1}{2}ZI_c$ ampere-turns, and that between *c* and *d* and also that between *g* and *h* $= \frac{1}{2}\psi ZI_c$ ampere-turns. Half of this latter m.m.f. acts across the path *ce* and the other half across the path *fd* since the reluctances of the paths *ef* and *cd* are so low that they may be neglected. Therefore, the cross-magnetizing effect at each pole tip $= \frac{1}{2}\psi \frac{Z}{p} I_c$ for any number of poles. (4)

C shows the resultant magnetic field when, as under operating conditions, both the main and the armature m.m.fs. exist together. The flux density, compared with the value shown at *A*, is increased at the tips *d* and *g* and decreased at the pole tips *c* and *h*.

A convenient method of showing the flux distribution in the air-gap is shown in diagrams *D*, *E* and *F*, Fig. 52, which are obtained by assuming that the diagrams *A*, *B* and *C* are split at *xy* and opened out on to a plane, and that the flux density at the different points is plotted vertically.

D shows the flux distribution due to the main m.m.f. acting alone.

E shows the flux distribution due to the armature m.m.f. acting alone.

F shows the resultant distribution when both the main and the armature m.m.fs. exist together and is obtained by adding the ordinates of curves *D* and *E*. It is permissible to add these ordinates of flux density together provided that the paths *df* and *gk* do not in the meantime become highly saturated. These paths, however, include the gap and teeth, and the flux density

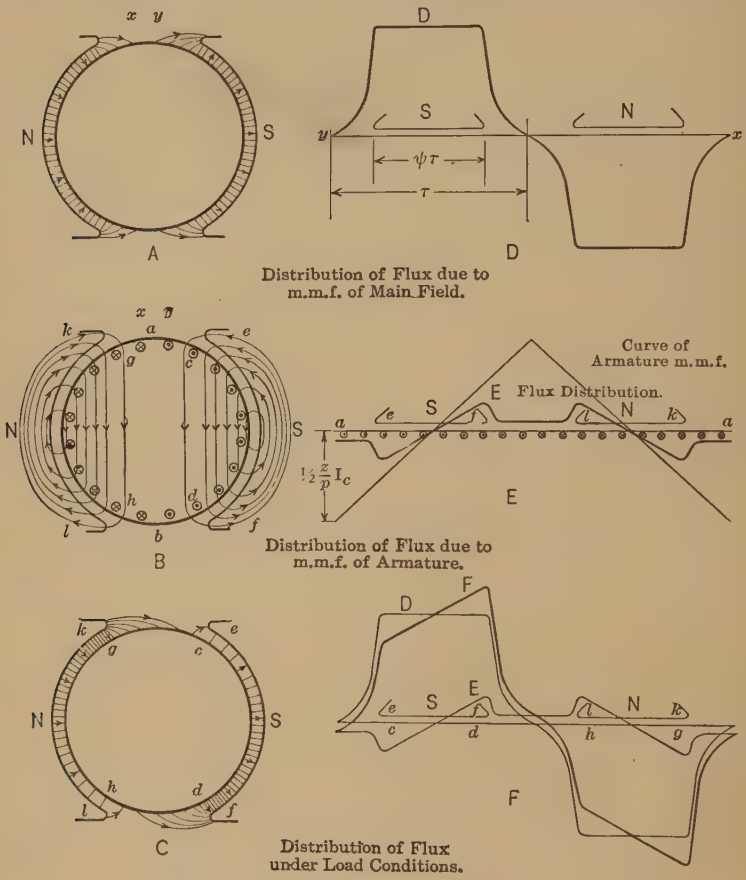

FIG. 52.—Flux distribution curves.

in the teeth due to the main field is about 140,000 lines per square inch at normal voltage, which is well above the point of saturation, so that an increase in m.m.f., such as that at *f* due to the armature m.m.f., will produce an increase in flux density at pole tip *f* of only a small amount; while a decrease in m.m.f. of the same value at pole tip *e* will produce a decrease in flux density

at that pole tip of a much larger amount; thus the total flux per pole will be decreased.

It is usual to consider the effect of armature reaction as being due to a number of lines of force acting in the direction shown in diagram *B*, Fig. 52, and this diagram shows that the same number of lines is added at the one pole tip as is subtracted at the other pole tip. A truer representation is that shown in Fig. 53.

Since the lines of force of armature reaction meet a high reluctance at *d* some of them take the easier path through *hmc*. These latter lines are in the opposite direction to those of the main field and are, therefore, demagnetizing.

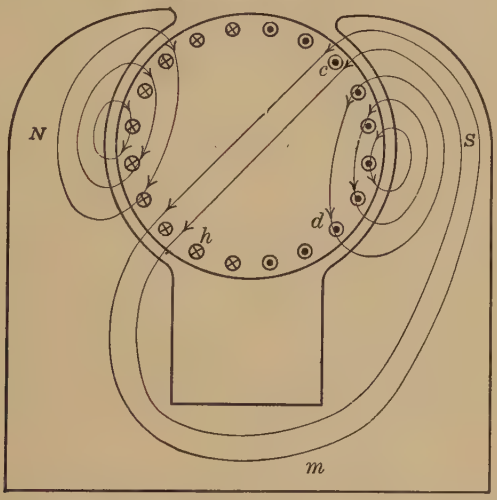

FIG. 53.—Demagnetizing effect of armature reaction with the brushes at the neutral point.

53. Distribution of Flux in the Air-gap at Full Load.[1]—Figure 54 is part of the development of a multipolar machine with p poles, and curve D shows the flux distribution in the air-gap due to the main m.m.f. acting alone. The armature m.m.fs. across df and ce each $= \frac{1}{2}\psi\frac{Z}{p}I_c$ ampere-turns and curve G shows the distribution of the armature m.m.f.

Curve 1, Fig. 55, is the no-load saturation curve of the machine and curve 2 is that part of this saturation curve for the tooth,

[1] The method adopted in this article, is a slight modification of that proposed by S. P. Thompson, Chap. XVII, "Dynamo Electric Machinery," Vol. I.

gap and pole face, so that if *oy* is the ampere-turns per pole required to send the no-load flux through the magnetic circuit

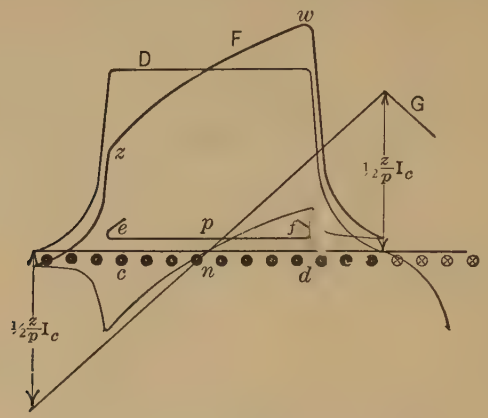

FIG. 54.—Flux distribution at full-load.

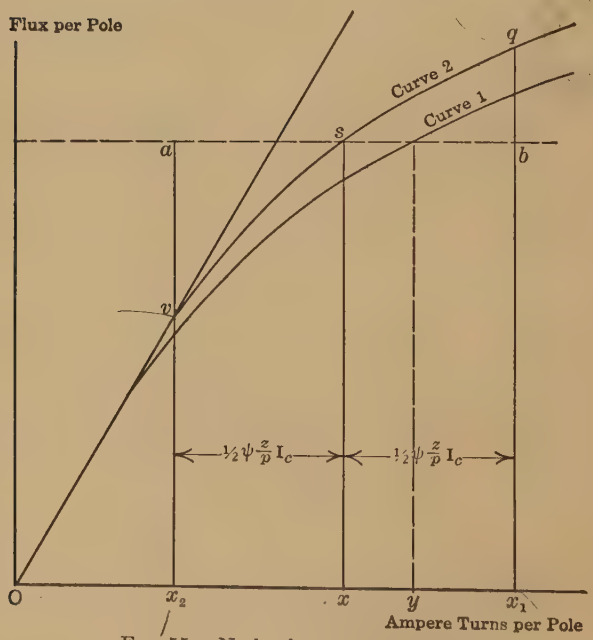

FIG. 55.—No-load saturation curves.

of the machine then *ox* is that necessary to send this same flux through the length of one gap, one tooth and one pole face.

Across np, Fig. 54, the m.m.f. at full-load is the same as at no-load and therefore the flux density in the air-gap at n is unchanged.

Across df the m.m.f. at full-load is no longer ox, Fig. 55, but $= ox_1$, where $xx_1 = \frac{1}{2}\psi\frac{Z}{p}I_c$ = the m.m.f. across df due to the armature; therefore the flux density in the air-gap at d at full-load is increased over its value at no-load in the ratio $\frac{qx_1}{sx}$, Fig. 55, and is so plotted at dw, Fig. 54.

Across ce the m.m.f. at full-load is no longer ox, Fig. 55, but $= ox_2$, where $xx_2 = \frac{1}{2}\psi\frac{Z}{p}I_c$, and therefore the flux density in the air-gap at c at full-load is less than that at no-load in the ratio $\frac{vx_2}{sx}$, Fig. 55, and is so plotted at cz, Fig. 54.

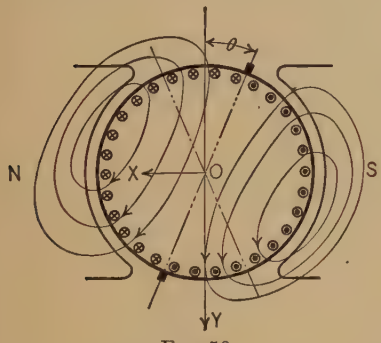

Fig. 56.

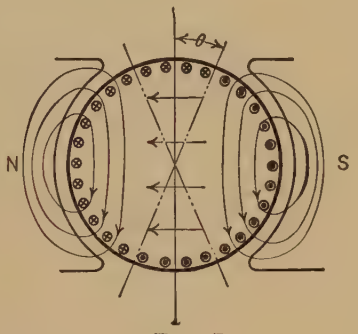

Fig. 57.

Demagnetizing and cross magnetizing effect of the armature.

Thus, in Fig. 54, curve D shows the distribution of the flux in the air-gap at no-load and curve F that at full-load. The total flux per pole is less at full-load than at no-load in the ratio of the area enclosed by curve F to that enclosed by curve D, which ratio is practically the same as area $\frac{x_2vqx_1}{x_2abx_1}$, Fig. 55.

54. Armature Reaction When the Brushes Are Shifted.—In non-commutating pole machines, it is necessary to shift the brushes in order to secure good commutation. This shift of brush position has an effect upon armature reaction that may be analyzed as follows: Figure 56 shows the armature carrying current and the magnetic field produced thereby when the

brushes are shifted through an angle θ so as to improve the commutation. The armature field is no longer at right angles to the main field and the easiest way in which to consider its effect is to assume that it is the resultant of two components, one in the direction OY which is called the cross-magnetizing component, the effect of which has already been discussed, and another in the direction OX which is called the degmanetizing component because it is directly opposed to the main field. Figure 57 shows the armature divided up so as to produce these two components, and it will be seen that the demagnetizing ampere-turns per pair of poles

$$= I_c \frac{Z}{p} \times \frac{2\theta}{180}$$

or the demagnetizing ampere-turns per pole

$$= \frac{1}{2} \frac{Z}{p} \times I_c \times \frac{2\theta}{180} \qquad (5)$$

The angle θ for preliminary calculations is usually taken as 18 electrical degrees so that $\frac{2\theta}{180} = 0.2$.

55. The Full-load Saturation Curve.—It is required to draw this curve for the machine which is drawn to scale in Fig. 46 and to which the following data applies:

Rating: 550 kw., 250 volts, 2200 amperes, 250 r.p.m.
Poles ..... 10.
Coils ..... 360.
Winding ..... one turn, multiple.
Total conductors ..... 720.
Current per conductor ..... 220.
Per cent pole enclosure ..... 65.
Volts drop at full-load across armature and brush contacts ..... = 8.2.

Armature ampere-turns per pole $= \frac{720 \times 220}{2 \times 10} = 7920.$

Cross-magnetizing ampere-turns at each pole tip $= \frac{1}{2} \times \frac{72}{10} \times 0.65 \times 220) = 5150.$

The ampere-turns per pole for gap + teeth = 5920.
The ampere-turns at one pole tip = 5920 + 5150 = 11,070.
The ampere-turns at the other pole tip = 5920 − 5150 = 770.

The flux crossing the air-gap is reduced in the ratio $\left(\frac{\text{area } aefd}{\text{area } abcd}\right)$, Fig. 58, and, due to this reduction in flux, the voltage generated is reduced from 250 to 236 volts.

The terminal voltage is less than the generated voltage of 236 by the amount of the voltage drops through the armature, brushes, commutating pole winding and series field winding.
These voltage drops are as follows:

Armature	=	6.2.
Brush	=	2.
Commutating pole winding	=	1.78.
Series field	=	1.78 (assumed).
Total voltage drop	=	11.76 volts.

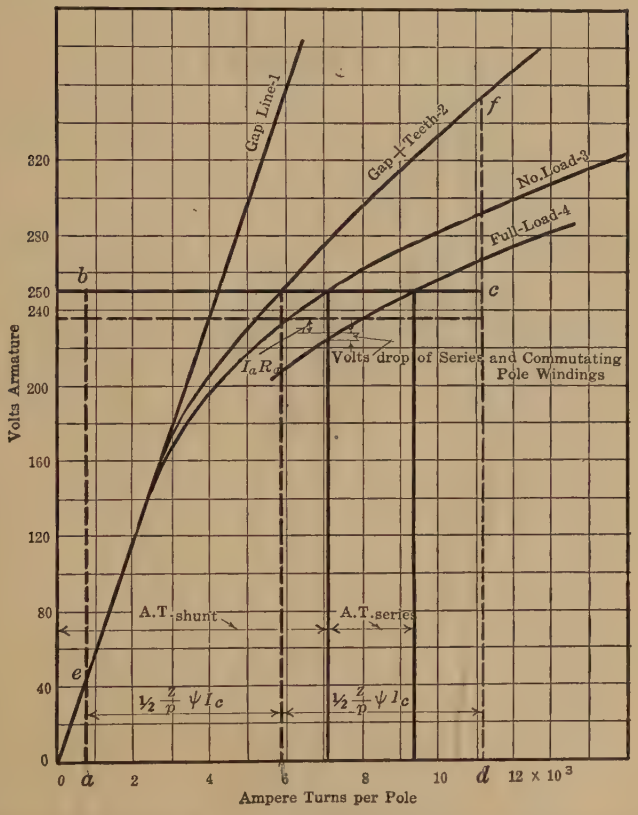

FIG. 58.—Saturation curves of a 550 kw., 250 volt, 250 r.p.m., D.-C. generator.

Since the design of the series field depends on the full-load saturation curve, it is necessary that the volts drop through the series field winding be estimated. As a general rule this drop can be taken equal to the volts drop through the commutating pole winding.

Figure 58 shows the saturation curves at no-load for gap and teeth (Curve 2), the saturation curve including the entire mag-

netic circuit (Curve 3), and the full-load saturation curve (Curve 4), taking into account all I. R. drops as well as the voltage drop due to distortion of the magnetic field.

To obtain the same voltage at full-load as at no-load, an additional m.m.f. must be secured under load and the value of this additional m.m.f. is indicated in Fig. 58. These additional ampere-turns are obtained by a series field winding and in the case shown in Fig. 58, the value of these series ampere-turns at full load is approximately 20 per cent of the ampere-turns to obtain normal voltage at no-load.

In order to get the same flux across the air-gap at full-load as at no-load the field excitation has to be increased over its no-load value so as to counteract the effect of the m.m.f. of the armature. Due to this increase in excitation the leakage flux is increased, so that the leakage factor is greater at full-load that at no-load, and still more excitation is required on account of the resulting increase in the pole and yoke densities. This latter increase in excitation, however, cannot readily be calculated.

56. Field Distribution in Typical Commutating Pole Machine. Figure 59 shows the component and resultant magnetic fluxes in a typical commutating pole machine. In this machine, the main pole enclosure is 66.7 per cent of the pole pitch and the commutating pole enclosure, 11.1 per cent of pole pitch, leaving 11.1 per cent of pole pitch for the air-gaps on either side of the commutating pole. The main air-gap is 0.25 in. and the commutating pole air-gap 0.15 in. The conditions shown in Fig. 59 are for an excitation of the main pole of 6820 ampere-turns; for the commutating pole, of 5480 ampere-turns; and for the armature (maximum value) of 5020 ampere-turns. In Fig. 59, curve *a* shows the magnetic flux that will pass across the air gap, due to the action of the fields alone (both main and commutating pole)—the field m.m.fs. being the values given above. In arriving at this curve, the reluctance in various portions of the gap is not assumed uniform but to be of the value that would obtain when taking into account the tooth saturation due to the passage of the resultant flux *c*. At pole tip *d* the main field m.m.f. and the armature cross-magnetizing m.m.f. are additive, resulting in a total m.m.f. of 6820 ampere-turns (for main field) +3346 ampere-turns (due to armature). The figure 3346 is two-thirds of the maximum armature ampere-turns and is the value of the armature reaction at pole tip *d* since pole enclosure is two-thirds

of the pole pitch. Hence, a total of 10,166 ampere-turns is active at pole tip d to push the flux across the air-gap and teeth. At pole tip e, on the the other hand, armature reaction is opposing the main field and the total m.m.f. is 6820 − 3346 = 3474 ampere-turns to push flux across the gap and teeth at this edge of the pole. At intermediate points, it is obvious that intermediate values of m.m.f. will be available. The higher value of m.m.f. at pole tip d as compared, with pole tip e (ratio of nearly 3 to 1 in the case assumed) results in much higher flux densities at d compared to e and the resulting saturation of teeth gives rise to variation in height of curve a across the pole face. The same effect is taken

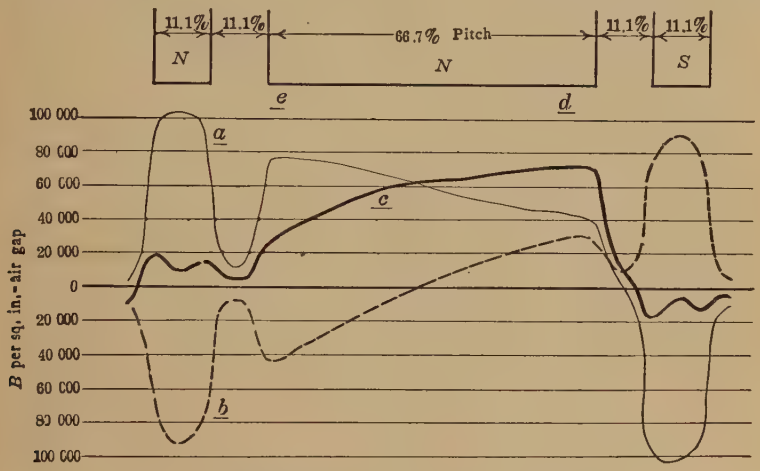

Fig. 59.—Magnetic fluxes in a commutating pole D.-C. machine.

into consideration in arriving at curve b—the flux produced by the armature reaction acting alone.

Since the variation in reluctance is thus taken into account in arriving at the two component curves a and b, the resultant curve c may be obtained at once by adding a and b.

57. Relative Strength of Field and Armature M.M.Fs.—Inspection of Fig. 54 will show that if the armature current be increased to such a value that the cross-magnetizing ampere-turns of the armature at the pole tips, namely $\frac{1}{2}\psi\frac{Z}{p}I_c$ ampere-

turns, becomes equal to the amper-turns for the tooth and gap due to the main field excitation, then the flux density will be zero under the leading[1] pole tip. Since non-commutating pole machines depend upon the fringe of magnetic flux under the leading pole tip for securing satisfactory commutation, it is obvious that there is a more or less definite limit that may be permitted for the quantity $\frac{1}{2}\psi\frac{Z}{p}I_c$ as compared to the total ampere-turns of the main field. Experience with non-commutating pole machines has shown that to secure satisfactory commutating conditions, the m.m.f. of the main field should never become less than 1.7 the m.m.f. of the armature reaction at the pole tip. Since the pole enclosure (ψ) on this type of machine cannot exceed about 0.7 pole pitch, it follows that the ratio

$$\frac{\text{ampere-turns per pole of main field for gap and teeth}}{\text{armature ampere-turns per pole at full load}} \tag{6}$$

should not exceed $1.7 \times \psi = 1.7 \times 0.7 = 1.2$.

This is the limit that is fixed by commutating conditions for the non-commutating pole type of machine.

However, non-commutating pole machines are no longer manufactured for the reason that commutating poles introduce such large economies in material that the non-commutating type cannot compete; so that the above relation is only of academic interest. The reason for the greater economies in the commutating pole type is not far to seek. It is obvious that the output of any machine is fixed by the limiting number of ampere conductors on the armature. The commutating limit that we have just discussed fixes this limit at not greater than 83 per cent of the field ampere-turns per pole. The commutating pole removes this limit and permits us to increase the armature ampere-turns to the point where field distortion begins seriously to limit the useful flux that may be pushed through the armature. It is

[1] By "leading pole tip" is meant the pole tip toward which the coil under commutation is traveling and toward which the brushes are shifted in order to secure good commutation *in the case of a non-commutating pole generator. In case of a motor*, it is the opposite or "trailing pole tip" that is weakened by armature reaction and toward which the brushes must be shifted to get good commutation. In other words, for non-commutating machines, brushes are shifted forward for a generator and backward for a motor—*in both cases* the shift being toward that pole tip which is being weakned by armature reaction.

obvious that this limit begins at the point where the net m.m.f. under the weak pole tip reaches zero, *i.e.* where

$$\frac{1}{2}\psi\frac{Z}{p}I_c = \text{ampere-turns per pole of main field.} \qquad (7)$$

The pole enclosure ψ of commutating pole machines is somewhat less than is available with the non-commutating pole type. Instead of 0.7 it must be reduced to not much over 0.65. The additional interpolar space is necessary to give room for the commutating poles. If we go to the limit fixed by formula (7), the ratio $\frac{\text{ampere-turns per pole for main field for gap + teeth}}{\text{armature ampere-turns per pole at full load}} = 0.65.$

We have seen above that this ratio for non-commutating pole machines = 1.2. If, therefore, we go to the limit on the commutating pole type of machine, we may expect to get some 83 per cent more armature ampere-turns than in the non-commutating pole type. To go to the full limit indicated by formula (7) would be more than is dictated by good practice, but modern designs have increased the armature ampere-turns some 50 to 60 per cent above practice with the non-commutating pole type. The greater economy in material so obtained is the reason for the disappearance of the non-commutating pole types. As a first approximation, the field m.m.f. of a commutating pole machine may be taken = .75 armature ampere turns.

CHAPTER VII

DESIGN OF THE MAGNETIC CIRCUIT

The problem to be solved in this chapter is, given the armature of a machine and also its rating, to design the poles, yoke, and field coils.

58. Field-coil Heating.—Figure 60 shows one of the poles of a typical D.-C. machine with its field coil. The exciting current I_f passes through this coil and gradually raises its temperature until the point is reached where the rate at which heat is dissipated by the coil is equal to the rate at which it is generated in the coil.

The hottest part of the field coil will obviously lie somewhere between the surfaces A and B for the outer coil and between

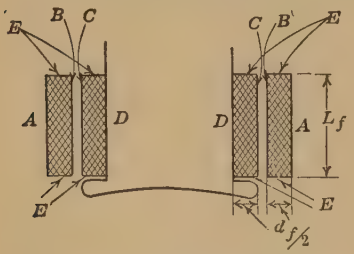

FIG. 60.—Cross section of a typical D.-C. shunt field winding.

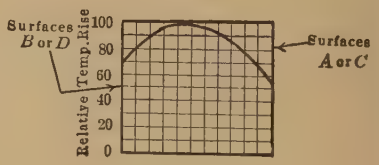

FIG. 61.—Temperature variation inside a typical D.-C. shunt coil winding.

C and D for the inner coil. This follows from the consideration that the heat generated in the interior of the coils must be dissipated from the surfaces and there is necessarily a thermal drop from the interior to the dissipating surfaces. Figure 61 shows the temperature that might be expected in the interior of a field coil. The maximum interior temperature compared to the exterior surface will depend upon the depth of the coil as well as upon its thermal conductivity.

The maximum temperature of the coil limits the amount of current that it can carry without injury, but this temperature is difficult to measure. The external temperature of the coil can be taken by means of a thermometer, and the mean tempera-

ture can be found by the increase in resistance of the coil, since the resistance of copper at any temperature $t = R_t = R_o(1+0.004t)$ where R_o is the resistance at 0° C. and t is in Centigrade degrees.

It is found that the ratio between the maximum and the mean temperature seldom exceeds 1.2, while that between the mean and the external surface temperature varies from about 1.4 to 3. The latter figure is found in some of the early machines whose field coils were covered with tape and rope. When the coil is insulated, as shown in Fig. 41, the ratio of the mean temperature to that of the external surface will be approximately 1.4 if the external surface is left bare except for the d.c.c. on the wire, the whole coil impregnated with compound, and the coil about 1¼ in. thick; the compound is a better conductor of heat than the air which it replaces and is also a better insulator. If two layers

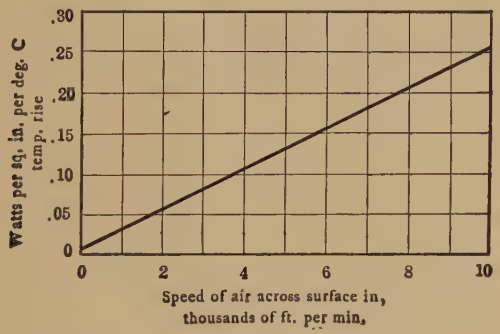

FIG. 62.—Curve of energy loss against air velocity on a flat surface.

of half-lapped tape be put on the external surface of the coil the ratio will increase to about 1.6 and if in addition a layer of cardboard 1/16 in. thick be put on the external surface, as was formerly done to protect the coil, the ratio will exceed 2. These are average figures and may vary considerably since they are affected by the fanning action of the armature, the kind of compound used, the thickness of the insulation on the wire, the radiating power of the poles and yoke on which depends the radiating power of the surfaces B, C, and D.

The heating constants for field coils are figured in many different ways, depending on what is taken for the radiating surface. While it is true that all the surfaces, A, B, C, D, and E of Fig. 60, are active in radiating heat, yet they are not all equally effective,

and for that reason and also for convenience, the radiating surface is taken as the external surface A (Fig. 60).

Heat may escape from any hot body in three ways—by conduction, by radiation, and by convection. Conduction is not present in electrical machinery in sufficient degree to make it worth while to consider; its effect is negligible. For all practical purposes, the same is true of radiation; its effect also may be neglected except at very low air velocities. Convection is the only method of heat escape that need be seriously considered in electrical machinery. The speed of the air relative to the surface has a marked effect on the rate of heat escape by convection. Figure 62 shows the approximate rate of heat escape with various air velocities. This curve takes into account both radiation and convection but, as indicated above, the effect of radiation is almost negligible. It accounts for a part (perhaps 50 per cent) of the heat that escapes at zero air velocity (Fig. 62), and its effect is not influenced by air velocity. The effect of convection increases very nearly in proportion to air velocity as shown in Fig. 62.

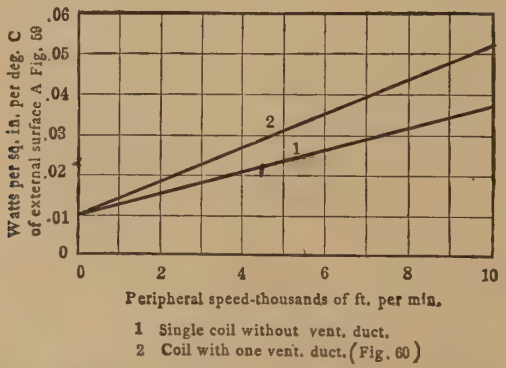

FIG. 63.—Curve of energy loss against peripheral velocity for shunt field coils.

The cooling of electrical machinery depends, therefore, to a marked degree on the velocity that the cooling air can be caused to circulate past the cooling surfaces. It is obvious that this bears almost a direct relation to the peripheral speed of the armature in a D.-C. machine but is necessarily much less than the peripheral speed. Experience has shown that the values of heat dissipation for field coils, given in Fig. 63, are approximately what may be expected with present-day designs of field coils and reasonably efficient blowers.

In applying the values of heat dissipation, as given in Fig. 63, only the *external* surface (surface *A* Fig. 60) is taken as a heat-dissipating surface.

On account of the rapidly increasing internal temperature as the depth of coil increases, present-day practice rarely make this depth greater than 1¼ in. When necessary to put on additional windings, the coil is wound in two or more sections, as shown in Fig. 60.

59. The Size of Wire for Field Coils:

If E_f is the voltage across each field coil,

I_f is the current in the coil,

T_f is the number of turns in the coil,

MT is the length of the mean turn of the coil in inches,

M is the section of the wire used in circular mils,

then the resistance of the coil $= \frac{E_f}{I_f} = \frac{MT \times T_f}{M}$, since the resistance of copper is approximately 1 ohm per circular mil per inch length,

and
$$M = \frac{I_f T_f \times MT}{E_f}, \qquad (8)$$

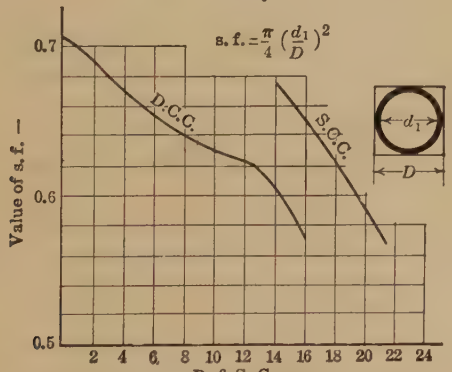

FIG. 64.—Space factor for wire.

so that for a given machine the size of field wire is fixed as soon as the ampere-turns and the voltage per coil are known.

60. The Length L_f of the Field Coil.—The watts radiated from the coil shown in Fig. 60 = external surface × watts per square inch. The total section of copper in the coil $= d_f \times L_f \times sf$ square inch, where *sf*, the space factor of the wire, is the section of the wire divided by the space that the wire takes up in the coil and is got from Fig. 64.

The section of the wire in the coil $= \frac{d_f L_f \times sf}{T_f}$ sq. in.

$$= \frac{d_f \times L_f \times sf \times 1{,}270{,}000}{T_f} \text{ circular mils.}$$

$$= M.$$

The watts loss per coil $= \frac{MT \times T_f}{M} \times I_f^2$ and, substituting for M,

$$= \frac{MT \times T_f^2 \times I_f^2}{d_f \times L_f \times sf \times 1{,}270{,}000}$$

The watts loss per coil also = external surface of coil × watts per square inch.

= external periphery of coil × L_f × watts per square inch.

Therefore, equating these two values together,

$$L^2_f = \frac{\text{mean turn} \times (I_f T_f)^2}{\text{ext. periphery} \times \text{watts per sq. in.} \times d_f \times sf \times 1{,}270{,}000}$$

and $$L_f = \frac{I_f T_f}{1000} \sqrt{\frac{\text{mean turn}}{\text{ext. periphery} \times \text{watts per sq. in.} \times d_f \times sf \times 1.27}} \quad (9)$$

In order to have an idea as to the value of L_f found from the above equation assume the following average values:

sf, the space factor = 0.6.

d_f, the coil depth = 2.0 in. (two sections, each 1 in. deep).

watts per square inch = 0.8.

external periphery = 1.2 × mean turn.

then L_f, the radial length of coil space, $= \frac{I_f T_f}{1200}$ (approximately).

61. Weight and Depth of Field Coils.—The weight of the field coil = 0.32 × $MT \times L_f \times d_f \times sf$ lbs. where 0.32 is the weight of a cubic inch of copper,

and $$L_f = \frac{I_f T_f}{1000} \sqrt{\frac{\text{mean turn}}{\text{ext. periphery} \times \text{watts per sq. in.} \times d_f \times sf \times 1.27}}$$

$$= I_f T_f \frac{\text{a constant}}{\sqrt{d_f}} \text{ (approximately), for a given machine,}$$

therefore the weight of the field coil

$$= 0.32 \times MT \times I_f T_f \times \frac{\text{a constant}}{\sqrt{d_f}} \times d_f \times sf.$$

= a constant $\sqrt{d_f}$ for a given machine.

This may be interpreted as follows: the larger the value of d_f, the shorter the length L_f, the smaller the radiating surface,

and, therefore, the lower the value of permissible loss per coil. Since the section of the field coil wire is fixed, because, as shown in Art. 59, it depends only on the ampere-turns and the voltage per coil, a lower permissible loss can only be obtained by a smaller value of I_f and therefore by a larger value of T_f and a more expensive coil. It would seem then that the thinner the field coil the cheaper the machine, but it must not be overlooked that, as the value of d_f becomes less, and therefore the cost of the field copper decreases, the value of L_f increases and therefore the cost of the poles and yoke also increases. The value of d_f for minimum cost of field system must take this into account and can only be determined by trial.

62. Procedure in the Design of the Field System for a Given Armature.

(1) Find the air-gap clearance as follows:

AT_{g+t}, the ampere-turns per pole for gap and teeth,

$= 0.75$ (armature AT per pole). See Art. 57

From the armature data, AT_t, the ampere-turns per pole for the teeth, can be found:

AT_g, the gap ampere-turns, $= \dfrac{B_g \times C \times \delta}{3.2}$ from formula (3), page 51, from which δ can be found.

(2) Draw the saturation curves.

Before this can be done it is necessary to determine approximately the dimensions of the magnetic circuit, which is done as follows:

It is assumed that the no-load excitation $= 1.25(AT_{g+t})$, and that $L_f = \dfrac{\text{no-load ampere-turns}}{1200}$ (approximately), see Art. 60, page 72. The series field coil is usually placed outside the shunt in modern machines (as indicated in Fig. 31) so that the pole length thus determined does not have to be increased.

The section of the pole is got by assuming that the pole density is 100,000 lines per square inch and that the leakage factor has the value given in the table on page 56; then A_p, the pole area in square inches, $= \dfrac{\phi_a \times l.f.}{100{,}000}$.

The yoke area is found in a similar way by assuming that the yoke density is 75,000 lines per square inch for cast steel and 40,000 lines per square inch for cast iron.

The magnetic circuit may now be drawn in to scale and the saturation curves determined; these may require a slight modification as the work proceeds.

(3) Design the shunt field coil.

Find the no-load excitation from the saturation curve.

Find M the size of field-coil wire from the formula

$$M = \frac{I_f T_f \times MT}{E_f}; \text{ (see Art. 59, page 71).}$$

E_f the volts per coil, $= \dfrac{\text{terminal voltage}}{\text{poles}} \times k$

where k = 0.8 for compound generators; which leaves 20 per cent of the terminal voltage to be absorbed by the field circuit rheostat, so that the shunt excitation may be increased 20 per cent over its normal value should that be desired at any time.

k = 1.0 for shunt motors.

k for shunt generators is determined for each separate case; there should be enough field regulation to allow normal voltage to be maintained from no-load to the desired overload.

L_f is found from the formula

$$L_f = \frac{I_f T_f}{1000} \sqrt{\frac{\text{mean turn}}{\text{ext. periphery} \times \text{watts per sq. in.} \times d_f \times sf \times 1.27}}$$

(see Art. 60, page 72).

T_f is the number of turns of wire of section M that will fill up the space $L_f \times d_f$.

(4) Design the series field coil.

The series excitation at full-load is found from the saturation curves and is the difference between the excitation for the required terminal voltage found from the full-load saturation curve and the no load excitation at the same voltage.

The number of series turns $= \dfrac{\text{series excitation}}{\text{full-load current}}$; this value is generally increased 20 per cent on new designs because of the difficulty in predetermining exactly the full-load saturation curve.

The current density in the series coil and also the value of watts per square inch external surface are 20 per cent greater than in the shunt coils of the same machine, because the series coils are better ventilated than is possible with the shunt coil.

Example.—The armature of a ten-pole, 550-kw., 250-volt no-load, 250-volt full-load, 2200 amperes, 250-r.p.m. generator is shown to scale in Fig. 46; it is required to design the field system, which is not supposed to be given.

1. Find the air-gap clearance.

$$\text{Armature ampere-turns per pole} = \frac{720 \times 220}{2 \times 10} = 7900.$$

Ampere-turns per pole (gap + teeth) $= 0.75 \times 7900 = 5920$.

Ampere-turns per pole for the teeth are found as follows:

$$\phi_a = \frac{250 \times 60 \times 10^8}{720 \times 250} = 8.35 \times 10^6.$$

$$\text{Minimum tooth area per pole} = 0.42 \times {}^{18}\!/_{10} \times 0.65 \times 11.25.$$
$$= 55 \text{ square inches.}$$

$$\text{Maximum tooth density} = \frac{8.35 \times 10^6}{55}.$$
$$= 152{,}000 \text{ lines per square inch (apparent).}$$
$$= 145{,}000 \text{ lines per square inch (actual), (from Fig. 48).}$$

$$\frac{\lambda}{t} = 1.95.$$

$$\text{Tooth taper} = k = \frac{0.472}{0.42} = 1.125.$$

Ampere-turns per pole for the teeth $= 1080 \times 1.55$ (from Fig. 49).
$= 1680.$

Ampere-turns per pole for the gap $= 5920 - 1680.$
$= 4240.$

$$\text{Apparent gap density} = \frac{8.35 \times 10^6}{15.7 \times 0.65 \times 14} =$$
$$= 58{,}500 \text{ lines per square inch.}$$

$$C\delta = \frac{3.2 \times 4240}{58{,}500} = 0.23$$

But $C = \frac{t + s}{t + fs}$, where f depends on the ratio $\frac{s}{\delta}$, (Art. 48); hence the value of C and δ must be obtained by trial solution.

In this case,

$C = 1.14.$

$\delta = 0.2.$

2. Determine the magnetic circuit dimensions.

No-load excitation $= 1.25 \times 5920 = 7400$ ampere-turns (approximately).

$$L_f = \frac{7400}{1200} = 6.16; \text{ make } L_f = 7.5.$$

Leakage factor $= 1.18$ (Art. 51.).

$$\text{The pole area} = \frac{8.35 \times 10^6 \times 1.18}{100{,}000}.$$
$$= 98.5 \text{ sq. in. (approximately).}$$

$$\text{The yoke area} = \frac{8.35 \times 10^6 \times 1.18}{2 \times 80{,}000} = 61.5 \text{ sq. in. (approximately).}$$

From the dimensions found above the magnetic circuit is drawn to scale and the no-load saturation curve can then be determined as outlined in Art. 50.

$C\delta = .388$

3. Design the shunt field coil.

The no-load excitation = 7055 ampere-turns.

E_f, the volts per coil $= \frac{250 \times 0.8}{10} = 20.$

Depth of coil, d_f (assumed) = 1.25.

$M.T.$, the mean turn = 47.5 in.

External periphery of the coil = 52.5 in.

Size of shunt coil wire $= \frac{7055 \times 47.5}{20} = 16{,}600$ circular mils.

Use No. 8 B and S gauge, which has a section of 16,510 circular mils and an overall diameter, when insulated with d.c.c., of 0.14 in., hence make $d_f = 1.26$

Space factor, $sf = 0.64$ (Fig. 64).

$$L_f = \frac{I_f T_f}{1000} \times \sqrt{\frac{\text{mean turn}}{\text{ext. periphery} \times \text{watts per square inch} \times d_f \times sf \times 1.27}}$$ (Art. 60).

Therefore:

$$\text{watts per square inch} = \left(\frac{I_f T_f}{L_f \times 10^3}\right)^2 \frac{M.T.}{\text{ext. periphery} \times d_f \times sf \times 1.27}$$

$$= \frac{7055^2}{7.5^2 \times 10^6} \times \frac{47.5}{52.5 \times 1.26 \times 0.64 \times 1.27} = 0.78.$$

Allowable watts per square inch per degree $C.$ = 0.019 (Fig. 63).

Probable temperature rise of shunt field coils $= \frac{0.78}{0.019} = 41°$ C.

The number of layers of wire in a depth of 1.26 in. $= \frac{1.26}{0.14} = 9.$

The number of turns per layer in a length of 7.5 in. $= \frac{7.5}{0.14} = 53.$

The number of turns per coil $= 9 \times 53 = 477.$

The shunt field current $= {}^{7055}/_{477} = 14.8$ amperes.

The current density in the field coil wire $= \frac{16{,}510}{14.8} = 1115$ circular mils per ampere.

4. Design the series coil.

The excitation at full-load and normal voltage = 9400 ampere-turns.

The shunt excitation at no load and normal voltage = 7055 ampere-turns.

Therefore the series ampere-turns at full load = 2345.

The series turns (assumed) = 3.

The series field current $= {}^{2345}/_{3}$ = 780 amperes.

Connect series field windings in two parallel circuits, hence total series field current = 1560 amperes.

The current in the series shunt = 2200 − 1560 = 640 amperes.

Current density in the series coil $= \frac{1115}{1.2} = 930$ circular miles per ampere.

The size of the series coil wire = 930 × 780.

= 725,000 circular mils.

= 0.57 sq. in.

Width of conductor (assumed) = 1.25 in.

Thickness of conductor = 0.455 in.

Allow ½-in. clearance between shunt field coil and series field coil.
M.T., the mean turn of series coil = 61.5 in.

The resistance of three turns of this conductor $= \frac{61.5 \times 3}{725{,}000} = 0.254 \times 10^{-3}$ ohms.

The volts drop in one series coil = $0.254 \times 10^{-3} \times 780 = 0.199$ volts.
The loss in one series coil = $0.199 \times 780 = 155$ watts.
The permissible watts per degree C. per square inch of external surface = $0.019 \times 1.2 = 0.0228$.
Use ¼-in. spacing blocks between turns of the series field.
Therefore, the length L_f of the series coil = $3(0.455 + 0.25) = 2.12$ in.
External periphery = 66.5 in.
Radiating surface = $66.5 \times 2.12 = 141$ sq. in.

Watts per square inch external surface $= \frac{155}{141} = 1.1$.

Temperature rise of series coil $= \frac{1.1}{0.0228} = 48°$ C.

CHAPTER VIII

COMMUTATION (RESISTANCE METHOD)

The direction of the current in the conductors of a D.-C. machine at any instant is shown in Fig. 65; therefore, as the armature revolves and conductors pass from one side of the neutral line to the other, the current in these conductors must be reversed from a value I_c to a value $-I_c$, where I_c is the current in each conductor.

Figure 67 shows part of a full-pitch double-layer multiple winding with two conductors per slot and with the coils M

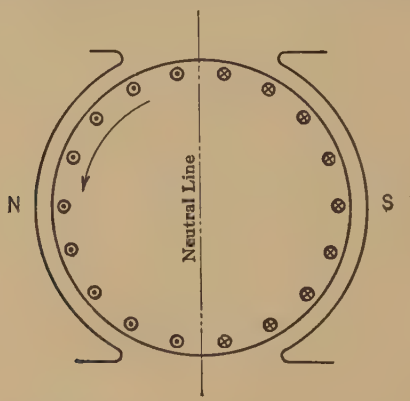

FIG. 65.—Direction of current in a D.-C. armature.

undergoing commutation, and Fig. 66 shows part of the corresponding ring winding. It may be seen from diagrams A and E that the current in coils M is reversed as the armature moves so that the brushes change from commutator segments 1 and 5 to segments 2 and 6.

63. Methods of Commutation.—There are two methods by which commutation may be secured—the resistance method and the counter-e.m.f. method. Before about 1910, practically all D.-C. machines depended on the resistance method to secure commutation; since that date, the counter-e.m.f. method has been employed more and more, until at the present time it is almost universal.

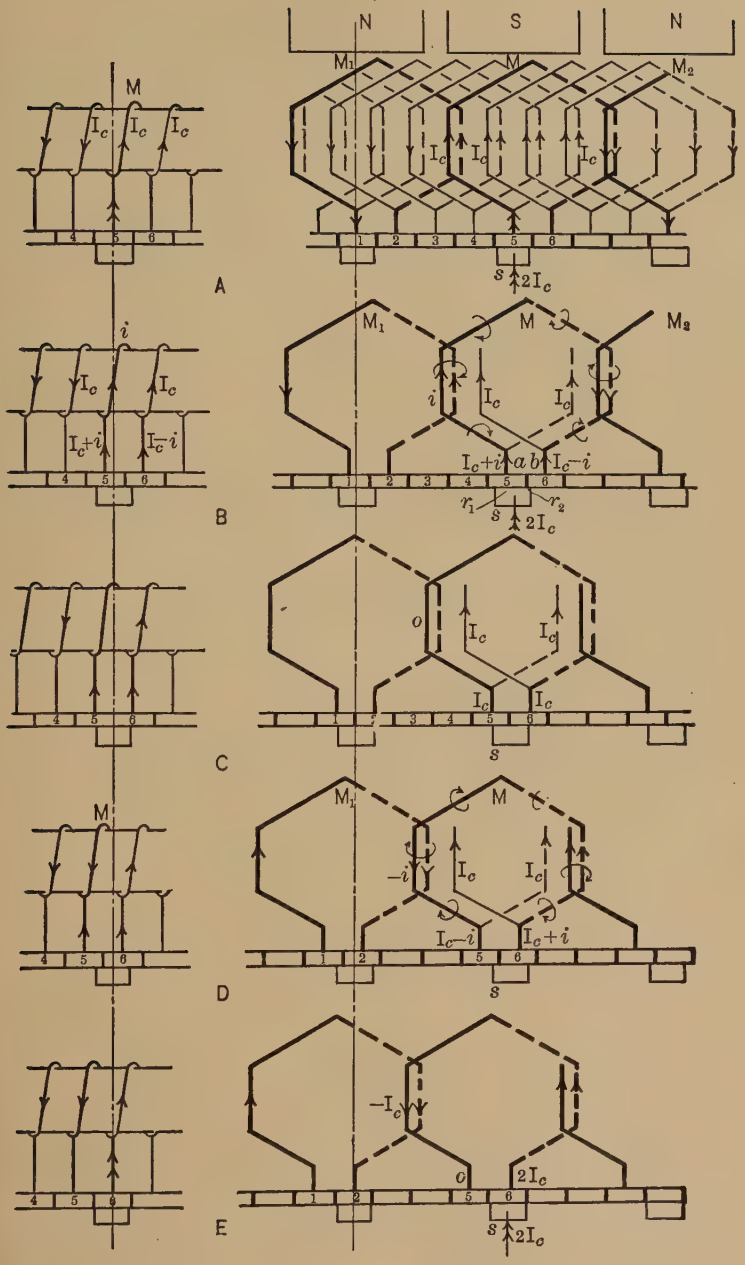

FIG. 66. FIG. 67.

Stages in the process of commutation.

However, in securing a counter-e.m.f., for commutation from a commutating pole, it is impossible, always to generate exactly the proper voltage for perfect commutation and the residual between the theoretically proper voltage and the actual voltage must be taken care of by resistance commutation. It is fitting, therefore, that resistance commutation be considered first.

64. Resistance Commutation.—Let the coils M Fig. 67 be in such a position between the poles N and S that, during commutation, they are not cutting any lines of force due to the m.m.f. of the field and armature, and let the contact resistances r_1 and r_2, diagram B, between the brush and segments 5 and 6, be so large that the effect of the resistance and self-induction of the coils M may be neglected.

In the position shown in diagram B, the contact area between the brush and segment 5 is large while that between the brush and segment 6 is small, and the current $2I_c$, which passes through the brush, divides up into two parts which are proportional to the areas of contact between the brush and segments 5 and 6, respectively, and are equal to $I_c + i$ and $I_c - i$.

In the position shown in diagram C, the two contact areas are equal and there is no tendency for current to flow round the coil M.

In the position shown in diagram D, the contact area between the brush and segment 5 is small while that between the brush and segment 6 is large, and the current $2I_c$ which passes through the brush divides up into two parts as shown in the diagram; the current i in coil M now passes in a direction opposite to that which it had in diagram A. As the contact area with segment 5 decreases, the value of the current i which passes round coil M increases until, at the instant shown in diagram E, this current is equal to $-I_c$.

By this action of the brush the current in the coil M is reversed or commutated while the armature moves through the distance of the brush width, and the variation of current with time is plotted in curve 1, Fig. 68, and follows a straight-line law.

65. Effect of the Self-induction of the Coil.—The resistance of the coil undergoing commutation is generally so low that its effect can be neglected, but the effect of self-induction must be considered.

The current i in the coils M sets up lines of force which link these coils. As this current reverses, the lines of force also

reverse, as shown in diagrams B and D, and the change of flux generates an e.m.f. in each coil M which is generally called its e.m.f. of self-induction. It is important to notice however that part of the flux which links one of the coils, say M, is due to current in the coil M_1 on one side and to current in the coil M_2 on the other side, so that this generated e.m.f. is really an e.m.f. of self- and mutual induction.

The e.m.f. of self- and mutual induction opposes the change of current which produces it, so that at the end of half of the period of commutation the current in the coils M has not become zero but has still the value cd, curves 2, 3 and 4, Fig. 68; these curves show the variation of current with time for different values of the ratio $\frac{RT_c}{L+M}$ where:

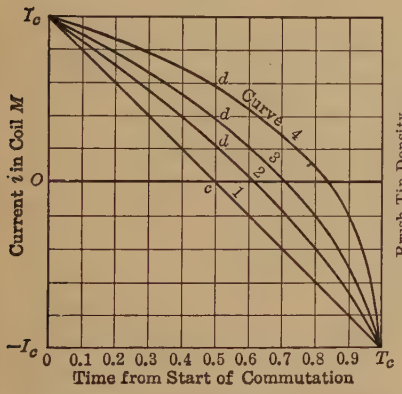

Fig. 68.—Current in the short circuited coil.

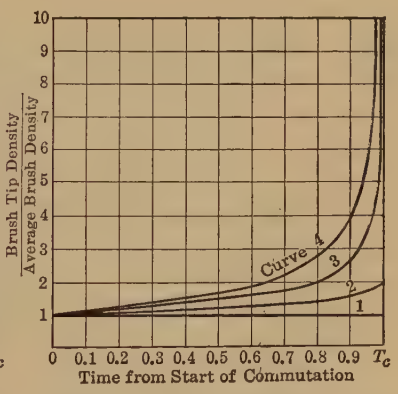

Fig. 69.—Current density at brush tip.

Curve 1.— $\frac{RT_c}{L+M}$ = infinity.

Curve 2.— $\frac{RT_c}{L+M}$ = 2.0.

Curve 3.— $\frac{RT_c}{L+M}$ = 1.0.

Curve 4 — $\frac{RT_c}{L+M}$ = 0.5.

R = the resistance of the total brush contact in ohms,
T_c = the time of commutation in seconds,
L = the coefficient of self-induction of one coil M in henries,
M = the coefficient of mutual induction between coil M and coils M_1 and M_2 in henries.

The equation from which these curves were plotted is derived as follows:

The difference of potential between a and b, diagram B, Fig. 67, $= (I_c + i)r_1 - (I_c - i)r_2$ and this must be equal and opposite to the generated voltage $-(L + M)\frac{di}{dt}$,

or $(I_c + i)r_1 - (I_c - i)r_2 + (L + M)\frac{di}{dt} = 0.$

If now R and T_c have the values already mentioned, and t is the time measured from the start of commutation

then $r_1 = R\left(\frac{T_c}{T_c - t}\right)$,

and $r_2 = R\left(\frac{T_c}{t}\right)$,

therefore $(I_c + i)R\left(\frac{T_c}{T_c - t}\right) + (L + M)\frac{di}{dt} - (I_c - i)R\left(\frac{T_c}{t}\right) = 0,$

and $\frac{di}{dt} = -\left(\frac{RT_c}{L + M}\right)\left(\frac{I_c + i}{T_c - t} - \frac{I_c - i}{t}\right).$

The results from this equation are plotted in Fig. 68 for different values of the ratio $\frac{RT_c}{(L + M)}$.[1]

66. Current Density in the Brush.—By the use of the values of i plotted in Fig. 68 the value of the current $I_c + i$ flowing from the brush to segment 5 can be determined, and from it the current density in the brush tip s at any instant can be obtained. This quantity is plotted against time in Fig. 69, and it will be seen that, for values of $\frac{RT_c}{L + M}$ less than 1, the current density in the brush tip s becomes infinite, and due to the concentration of energy at this tip sparking takes place.

The criterion for sparkless commutation then is that $\frac{RT_c}{L + M}$ be greater than 1, and perfect commutation is defined as such a change of current in the coil being commutated that the current density over the contact surface between the brush and the commutator segment is constant and uniform.

[1] For the solution of this equation see Reid on "Direct Current Commutation," Trans. *A. I. E. E.*, Vol. 24, 1905.

67. Reactance Voltage.—The above criterion for sparkless commutation is used in practice in a slightly different form for

if $\frac{RT_c}{L+M}$ must be greater than 1,

then R must be greater than $\frac{L+M}{T_c}$,

and $2I_cR$ greater than $\frac{2I_c}{T_c}(L+M)$.

This latter quantity is called the average reactance voltage and is the e.m.f. of self- and mutual induction of the coil being commutated on the assumption that the current varies from I_c to $-I_c$ according to a straight-line law. This average reactance voltage then should always be less than $2I_cR$ the voltage drop across one brush contact.

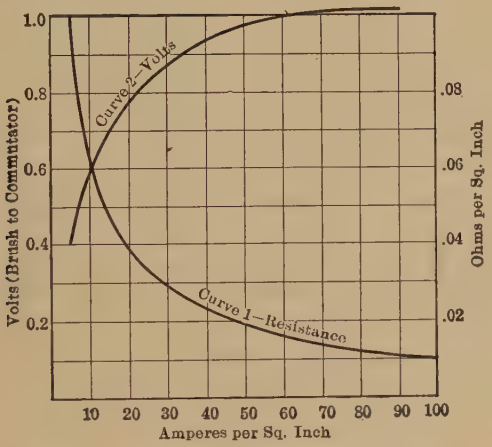

FIG. 70.—Brush-contact resistance curves.

68. Brush Contact Resistance.—Curve 1, Fig. 70 shows the value of the resistance of unit section of brush contact plotted against current density in that contact; the resistance decreases as the current density increases and for higher values than 35 amperes per square inch it varies almost inversely as the current density and the voltage drop across the contact becomes practically constant, as shown in curve 2, Fig. 70.

Such curves of brush resistance are obtained by testing the brushes on a revolving collector ring and allowing sufficient time to elapse between readings to let the conditions become stationary.

It would seem that, by neglecting the effect of the variation of contact resistance with current density, as was done in Art. 65, the results there obtained would be rendered of little practical importance; it is found, however, that the variation in resistance is largely a temperature effect and that at constant temperature the contact resistance does not vary through such extreme limits, also that, due to the thermal conductivity of carbon, the temperature difference between two points on a brush contact is not very great.

Suppose that, having reached the value of 10 amperes per square inch, and the resistance having become stationary at 0.06 ohms per square inch, (see Fig. 70) the current density were suddenly increased to 40 amperes per square inch; the resistance in ohms per square inch would not fall suddenly to 0.023 but would have a value of about 0.06 and this would gradually decrease until, after about 20 min., the resistance would have reached the value of 0.023, the value which it ought to have according to curve 1, Fig. 70. This explains why a machine will stand a considerable overload for a short time without sparking, whereas if the overload be maintained the machine will begin to spark as the brush temperature increases and the contact resistance decreases.

Sparking is cumulative in its effect because slight sparking raises the temperature of the brush contact, which reduces the contact resistance and causes the operation to become worse.

69. Carbon Brushes.—It is impossible in this text to give anything like a complete description of the properties of the various grades of carbon brushes. The coefficient of friction between brush and commutator, the contact drop, the carrying capacity, the specific resistance, and the advisable pressure are all subject to considerable variation, depending upon both the commutating characteristics and upon the particular type of brush selected.

Friction coefficient varies from 0.2 to 0.4; under some special conditions even these limits may be exceeded. The value 0.28 that is given in Chap. X might be taken as a fair average. The character of the brush as well as the condition of the commutator will, however, cause this value to vary over wide limits.

Contact drop between brush and commutator also varies over wide limits, from a minimum of about 0.3 volts to a maximum of about 1.1 volts. With the so-called "metal graphite"

brush the drop goes much lower—to 0.02 volts in some types. These "metal graphite" brushes are, as a rule, used only on slip rings or on very low voltage D.-C. motors—below 25 volts. In resistance commutation, contact resistance is relied upon to prevent sparking; even in counter-e.m.f. commutation, the residual between the e.m.f. set up by the commutating pole and the reactance voltage in the commutated coil must not exceed the contact drop else sparking is apt to occur. Therefore, while contact drop means a necessary loss, it is not an entirely unmixed evil.

Carrying capacity varies from 30 to 60 amperes per square inch. It is the total energy that determines the temperature rise of the brush and this in turn depends on the coefficient of friction, the contact drop, and the specific resistance of the brush. In general, low carrying capacity is coupled with high contact drop and *vice versa;* however, the friction coefficient and the specific resistance of the brush may modify this general relation.

In stationary machines, brush pressure varies from 1¼ to 3 lbs. per square inch. If commutators are not in good condition the pressure may have to be increased. In moving machines, such as railway motors etc., from 3 to 8 lbs. per square inch are used, depending upon motor speed and track condition.

70. Energy at the Brush Contact.—The criterion for sparkless commutation is that the energy at the brush tip, which is proportional to the current density in that tip, shall not become infinite. Also, the average energy at the brush contact is limited as set forth in the preceeding paragraph; with carbon brushes, the contact drop cannot get below about 0.3 volts nor above about 1.1. volts.

The product of amperes per square inch and volts drop across one contact has an average value of 35 watts per square inch. It must be understood that these figures are for machines which operate without sparking and without shifting of the brushes from no-load to 25 per cent. overload, but have not necessarily what was defined, in Art. 66, page 82, as perfect commutation. The better the commutation the more nearly uniform the current density in the brush contact and the higher the average current density that can be used without trouble developing.

71. Calculation of the Reactance Voltage for Machines with Full-pitch Multiple Windings.—Consider first the case where there are T turns per coil and the brush covers only one segment,

as shown in Fig. 71. The winding is of the double-layer type and has two coil sides per slot; a section through one slot is shown at S, Fig. 71, for the case where $T = 6$.

Let ϕ_s be the number of lines of force that circle 1 in. length of the slot part of the coil M for each ampere conductor in the group of conductors that are simultaneously undergoing commutation.

and ϕ_e the number of lines of force that circle 1 in. length of the end connections of the coil M for each ampere conductor in the group of end connections that are simultaneously undergoing commutation.

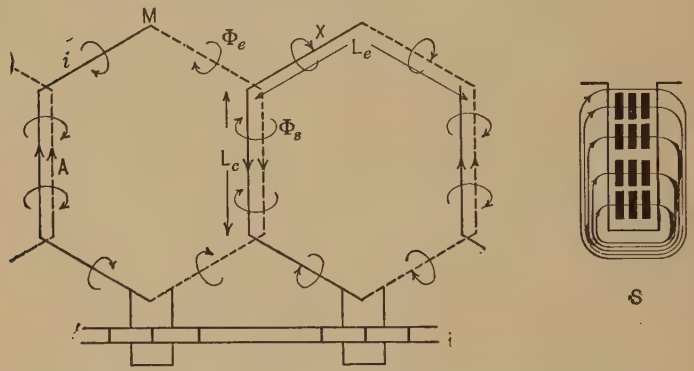

FIG. 71.—Flux circling a full-pitch multiple coil during short-circuit.

In one of the slots A there are $2T$ conductors, each carrying a current i, so that the flux that circles one side of coil $M = \phi_s \times L_c \times 2T \times i$ lines. In one of the groups of end connections, as at X, Fig. 71, there are T conductors, each carrying a current i, so that the flux that circles one group of end connections of length $L_e = \phi_e \times L_e \times T \times i$ lines.

The total flux that circles the coil M due to the current i in the coil $= \phi_c$.

$$= 2Ti(2\phi_s L_c + \phi_e L_e).$$

$$\text{and } (L + M) = \frac{T \times \phi_c}{i} \times 10^{-8} \text{ henry.}$$

$$= 2T^2(2\phi_s L_c + \phi_e L_e) \times 10^{-8} \text{ henry.}$$

T_c, the time of commutation, is the time taken by the commutator to move through the distance of the brush width and is equal to

$$\frac{60}{\text{r.p.m.}} \times \frac{\text{segments covered by the brush}}{\text{total number of commutator segments}},$$

$$= \frac{60}{\text{r.p.m.}} \times \frac{\text{segments covered by the brush}}{S},$$

therefore, when the brush covers only one segment, the average reactance voltage $= \frac{2I_c}{T_c}(L + M)$

$$= 2I_c \frac{(2\phi_s L_c + \phi_e L_e)2T^2 \times \text{r.p.m.} \times S \times 10^{-8}}{60}.$$

72. The Effect of Wide Slots and Brushes.—Neglect for the present the effect of the end connection flux, which is small compared with the slot flux, and compare the four cases shown in Fig. 72.

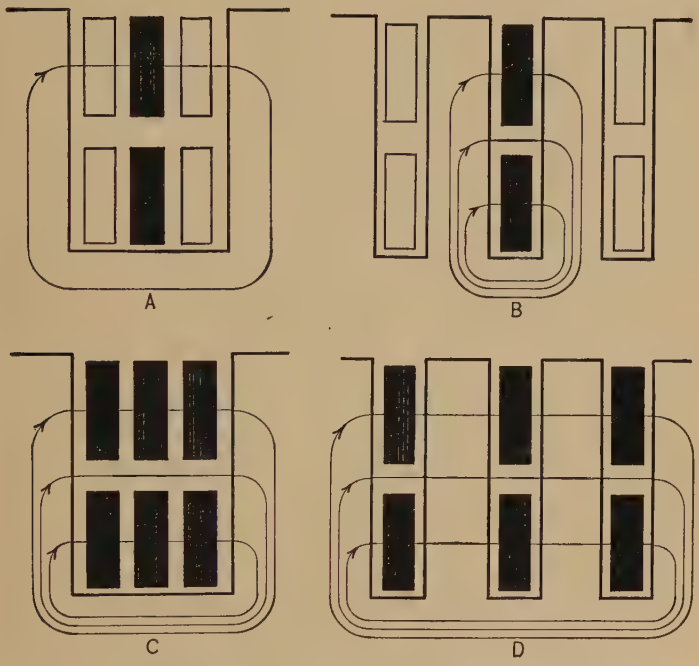

FIG. 72.—Effect of slot and brush width on the reactance voltage.

A shows part of a winding which has 6 coil sides per slot and a brush which covers 1 commutator segment.

B shows part of a winding which has 2 coil sides per slot and a brush which covers 1 commutator segment.

C shows part of a winding which has 6 coil sides per slot and a brush which covers 3 commutator segments.

D shows part of a winding which has 2 coil sides per slot and a brush which covers 3 commutator segments.

The slots in cases *A* and *C* are three times as wide as those in *B* and *D* and the coils shown black are those which are undergoing commutation.

In B the time of commutation is the same as in A, but the flux ϕ_s is three times as large since the reluctance of its path is proportional to the ratio $\frac{\text{slot depth}}{\text{slot width}}$, the reluctance of the iron part of the path being neglected. The reactance voltage is therefore three times as large.

In C the time of commutation is three times as long as in A and the flux ϕ_s also is three times as large since there are three times as many conductors undergoing commutation at the same instant. The reactance voltage is therefore the same in each case.

In D the time of commutation is the same as in C and so also is the flux ϕ_s, since the reluctance of three short paths in series is the same as that of a single path three times as long. The reactance voltage is therefore the same in D as it is in C or A.

From the above discussion the following conclusions can be drawn—namely, that when the brush covers one commutator segment only, the reactance voltage is greater the narrower the slot; compare for example, cases A and B; also that an increase in the brush width has no effect on the reactance voltage as long as the group of conductors simultaneously commutated is not greater than the total number of conductors per slot (compare A and C), but decreases the reactance voltage if the group of conductors simultaneously commutated is greater than the total number of conductors per slot (compare B and D).

The method for determining the brush width is taken up in Art. 81; it is pointed out here, however, that the brush generally covers more than one commutator segment, and under these conditions the case of a very narrow slot with the brush covering one commutator segment, namely case B, Fig. 72, can be neglected; with this restriction the formula for reactance voltage on page 87 can be used for all slot and brush widths.

[1] It has been found experimentally that, for the shape of coil in general use in D.-C. machines and for slots which have the ratio $\frac{\text{slot depth}}{\text{slot width}} = 3.5$, a value which is seldom exceeded in non-commutating machines, the value of ϕ_s may be taken as 10 lines per ampere conductor per inch length of core, and ϕ_e may be taken as 2 lines per ampere conductor per inch length of end connection.

[1] HOBART, "Continuous Current Dynamo Design," page 108.

By substituting the above values in the formula for reactance voltage on page 87, the following result is obtained for the reactance voltage of a full pitch double layer multiple winding namely: Average reactance voltage

$$= \frac{2I_c(2 \times 10 \times L_c + 2 \times L_e) \times 2T^2 \times \text{r.p.m.} \times S \times 10^{-8}}{60},$$

$$= 1.33 \times S \times \text{r.p.m.} \times I_c \times T^2(L_c + 0.1L_e)10^{-8}. \quad (10)$$

73. Short-pitch Multiple Windings.—It was pointed out in Art 15, page 15, that, when a short-pitch winding is used, the conductors of the coils which are short-circuited at any instant are not in the same slot; thus Fig. 73 shows the short-pitch diagram which corresponds to the full-pitch one shown in Fig. 71, and it

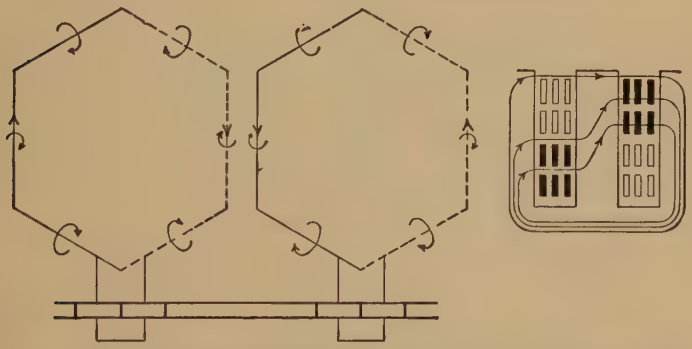

FIG. 73.—Flux circling a short-pitch multiple coil during short-circuit.

will be seen that, while the end connection flux is the same in each case, the slot flux ϕ_s has only half the value for a short-pitch winding that it has for a full-pitch winding so long as the pitch is short enough to prevent the conductors which are short-circuited at any instant from lying in the top and bottom of the same slot.

For a short-pitch double-layer multiple winding the value of the average reactance voltage

$$= 1.33 \times S \times \text{r.p.m.} \times I_c \times T^2 \times \left(\frac{L_c}{2} + 0.1L_e\right) \times 10^{-8}. \quad (11)$$

74. Calculation of the Reactance Voltage for Machines with Series or Two Circuit Windings.—Figure 74, which is a reproduction of Fig. 21, shows that when only one + and one − brush are

used each brush short-circuits $\frac{p}{2}$ coils in series, so that the average reactance voltage in such a case

$$= 1.33 \times S \times \text{r.p.m.} \times I_c \times T^2(L_c + 0.1L_e)10^{-8} \times \frac{p}{2}. \quad (12)$$

When, however, the same number of sets of brushes are used as there are poles, so that brushes are also placed at b and c, there is a short commutation path round one coil which is short-circuited by two brushes at the same potential, in addition to the long path around $\frac{p}{2}$ coils in series and, so far as this short path alone is concerned, the average reactance voltage

$$= 1.33 \times S \times \text{r.p.m.} \times I_c \times T^2(L_c + 0.1L_e)10^{-8}.$$

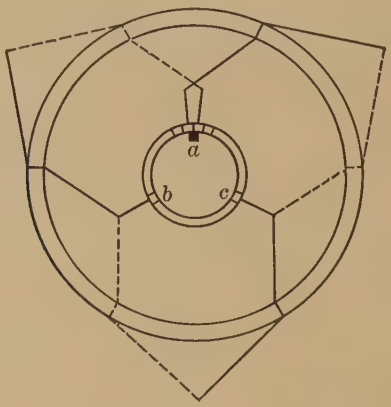

FIG. 74.—Coils in a series winding that are short-circuited by one brush.

The value of the reactance voltage that should be used as a criterion for commutation is somewhere between these two values, and the results are still further complicated by what is known as selective commutation which was described in Art. 17, page 19, so that in practice it is usual to use the former of the two equations, which is pessimistic; the commutation will generally be about 20 per cent better than that indicated by the value of reactance voltage so found.

75. Formulæ for Reactance Voltage.—Collecting together the results obtained in Arts. 72, 73 and 74, the following formulæ are obtained:

The average reactance voltage
$= 1.33 \times S \times \text{r.p.m.} \times I_c \times T^2(L_c + 0.1L_e)10^{-8}$ for full-pitch multiple windings

$= 1.33 \times S \times \text{r.p.m.} \times I_c \times T^2\left(\frac{L_c}{2} + 0.1L_e\right)10^{-8}$ for short-pitch multiple windings

$= 1.33 \times S \times \text{r.p.m.} \times I_c \times T^2 (L_c + 0.1L_e) \frac{p}{2} \times 10^{-8}$ for series windings.

It is pointed out in Art. 110, page 137, that, in order to have an economical machine, the core length L_c should lie between the values (0.9 to 0.6) $\times$ [pole pitch].

The length L_e of the end connections is directly proportional to the pole pitch and = 1.4 (pole pitch) approximately, so that L_e has a value between (1.6 and 2.4) $\times$ [L_c] and an average value = $2L_c$.

Substituting this average value in the above formulæ for reactance voltage the following approximate formula is obtained: The average reactance voltage

$$RV = k \times S \times \text{r.p.m.} \times I_c \times L_c \times T^2 \frac{\text{poles}}{\text{paths}} 10^{-8} \quad (13)$$

where S = the number of commutator segments.
r.p.m. = the speed of the machine in revolutions per minute.
I_c = the current in each armature conductor.
T = the number of turns per coil.
L_c = the frame length in inches.
$\frac{\text{poles}}{\text{paths}}$ = 1 for multiple and = $\frac{p}{2}$ for series windings.
k = 1.6 for series and full-pitch multiple windings.
= 0.93 for short-pitch multiple windings.

CHAPTER IX

COMMUTATION (COUNTER E.M.F. METHOD)

76. The Sparking Voltage.—Down to this point it has been assumed that the coils in which the current is being commutated are in such a position between the poles that, during commutation, they are not cutting any lines of force due to the m.m.f. of the field and the armature. Under these conditions the value of the reactance voltage when sparking begins is called the sparking voltage, and depends on the brush resistance, as shown in Art. 67, page 83.

In practice, the brushes of non-commutating pole machines are generally shifted from the above neutral position in such a direction that the coils which are undergoing commutation are in a magnetic field, and an e.m.f. E_s is generated in them, due to the cutting of this field, which opposes the e.m.f. of self-and mutual-induction and so causes the commutation to be more nearly perfect. In such cases the value of the resultant of this generated voltage and of the reactance voltage, when sparking begins, is called the sparking voltage.

As the load on a machine increases the reactance voltage increases with it, and in order that the commutation may be perfect at all loads the voltage E_s must increase at the same rate; in non-commutating pole machines this can only be the case if the distance the brushes are shifted from the neutral varies with the load.

Suppose that the brushes are in such a position that commutation is perfect at 50 per cent overload, and that they are fixed there; then at no-load there will be no reactance voltage to counteract, but there will be a large generated voltage E_s which will cause a circulating current to flow in the short-circuited coil, and sparking will take place if E_s is larger than the sparking voltage.

Modern D.-C. machines are expected to carry any load from no-load up to 25 per cent overload without sparking and also without shifting of the brushes during operation. To accomplish this result the brushes are shifted from the neutral position,

in such a direction as to help commutation when the machine is loaded, until the machine is about to spark at no-load; the voltage E_s, which is generated in the short-circuit coil, will then be a little less than the sparking voltage. When the machine is

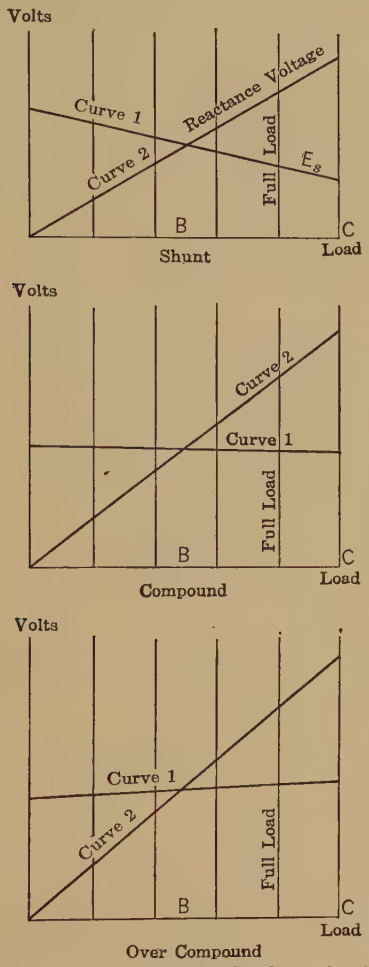

FIG. 75.—Variation of the voltage in the short-circuited coil with load.

carrying 25 per cent overload the reactance voltage will be greater than the generated voltage E_s by an amount which is just a little less than the sparking voltage, and half way between these two points E_s will be equal and opposite to the reactance voltage and the commutation will be perfect.

From the above it would seem that the reactance voltage at 25 per cent overload could have a value equal to about twice the sparking voltage, but in obtaining this result it has been assumed that the generated voltage E_s remains constant at all loads; as a matter of fact, it decreases with increase of load due to the cross-magnetizing effect of the armature, as pointed out in Art. 52, page 57. To prevent this decrease in the value of E_s from becoming too large, the relation between the field and armature strengths is fixed by making the field ampere-turns per pole for gap and tooth greater than 1.2 (the armature ampere-turns per pole) + the demagnetizing ampere-turns per pole).

The diagrams in Fig. 75 show the variation of E_s and of the reactance voltage with load. Curve 1 shows the relation between E_s and the load, and curve 2 shows that between the reactance voltage and load. The brushes are shifted until the value of E_s at no-load is equal to the sparking voltage; at load B the commutation is perfect, and at load C the reactance voltage is greater than E_s by the sparking voltage. These curves show clearly the superiority of the overcompound machine as far as commutation is concerned.

77. Disadvantages of Brush Shifting.—Analysis as well as practice indicates some very decided disadvantages in depending upon brush shifting for securing commutation. These disadvantages may be briefly discussed as follows:

1. The variation of the commutating field with load is exactly opposite from what it should be, thereby limiting the load range within which satisfactory commutation may be secured.

2. The shifting of the brushes gives rise to a demagnetizing component of armature upon the field (see Art. 54, page 61). This requires additional series field excitation to neutralize this demagnetizing effect.

3. The point of commutation at no-load comes in the edge of a strong field where the voltage between bars becomes a maximum very soon after passing under the brush. This causes a tendency to flash over on sudden interruption of load.

78. Commutating Poles.—As has been shown in the preceeding articles, commutation is improved by shifting the brushes under the pole tip which will give an e.m.f. in the coils under commutation which will oppose the e.m.f. of self- and mutual induction in those coils. It is obvious that the same effect may be obtained by leaving the brushes at the neutral point and

moving the commutating field back to them. This is exactly what is done by the commutating pole. Figure 76 shows a four-pole machine equipped with commutating poles. The exciting windings on these poles are in series with the load so that the m.m.f. on these poles is always proportional to the counter m.m.f. of the armature and is made a sufficient amount greater than the armature m.m.f. to produce a flux sufficient to overcome the reactance voltage of armature coils under commutation. Reactance voltage is proportional to load current and so also is the m.m.f. of the commutating pole; theoretically therefore, commutating conditions on commutating pole machines are correct at all loads, from the maximum current in one direc-

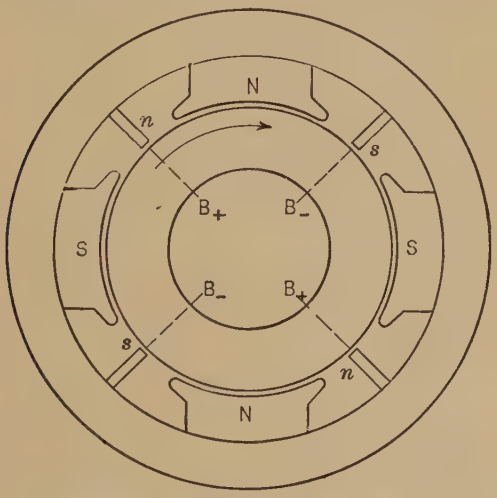

FIG. 76.—Magnetic circuit of a four-pole interpole machine.

tion when the machine acts as a generator to maximum in the other direction, when the same machine acts as a motor. Further, there is no change of brush position for this entire range of load; also the m.m.f. of the commutating pole is always in opposition to that of the armature no matter what the direction of current, provided, of course, that the connections have been properly made.

79. Commutating Pole Dimensions.—Figure 77 shows the approximate dimensions of the interpolar space and how this space is divided between commutating pole and the air spaces between this pole and the two adjacent main poles. The com-

mutating pole is usually tapered as shown and the commutating pole air-gap δ is usually considerably larger than the main pole air-gap.

There are two points to be considered in determining the width of the face of the commutating pole and the air-gap between this face and the armature surface.

1. The magnetic reluctance of the path across air-gap and teeth should be kept as nearly uniform as possible; otherwise a fluctuation will be set up in the magnetic flux passing through the commutating pole, giving rise to undue losses. To accomplish this, the width of the magnetic flux zone under the commutating pole should be adjusted to the commutating pole air-gap and to the width t of the armature teeth (Fig. 77) so that as one tooth is leaving the zone, another is entering.

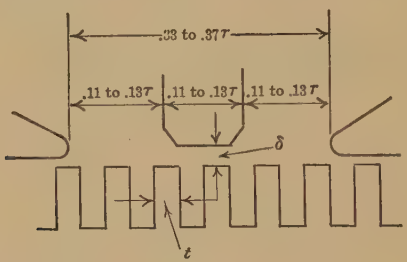

FIG. 77.—Interpolar space and commutating pole.

2. The second consideration is that the magnetic flux zone under the commutating pole that produces the e.m.f. necessary to overcome the reactance voltage should be wide enough to accomplish this purpose. To analyse this problem requires detailed consideration of the number of slots per pole, the width of brush, the commutating pole width, and its air-gap and lastly the matter of shortened pitch in the armature winding. These details will now be considered.

80. Minimum Number of Slots per Pole.—Figure 78 shows three of the stages in the commutation of the current in a machine which has six coil sides per slot. The commutator segments are evenly spaced, while the coils, being in slots, are not. It will be seen that, between the instant when the brush breaks contact with coil A and the instant when it breaks contact with coil C, the slot in which these coils lie has moved through the distance x, and that the magnetic field cannot be uniform for all these

positions. The reactance voltage for all positions (A, B, and C, Fig. 78) is practically uniform but the commutating field from poles N and S is not. When the usual type of "pulled" coil is used and a chording of one slot employed, Fig. 78 indicates the instantaneous position of both sides of a given coil when commutating. While the conductors of one side of the coil (A, B and C, Fig. 78) are under the influence of one commutating pole (pole N, Fig. 78), the other side of the same coil is under the influence of the next adjacent commutating pole (pole S, Fig. 78), and the instantaneous positions are indicated by A', B',

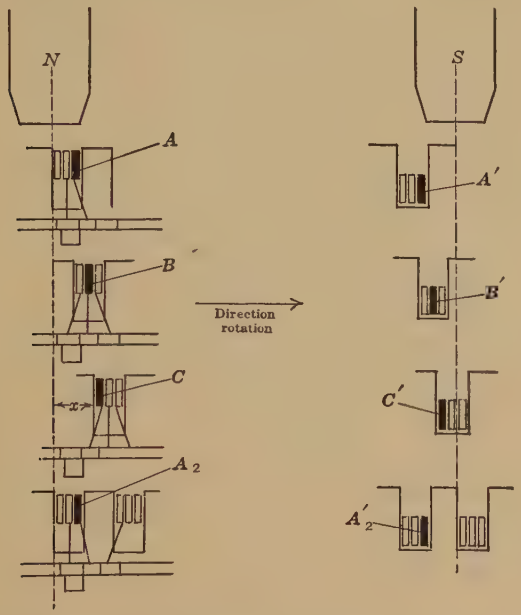

FIG. 78.—Diagram of coil location with respect to commutating pole.

and C'. The total voltage for commutation is the sum of the voltages under pole N and pole S, Fig. 78. Inspection will indicate that the voltage for commutation is not uniform in the three positions AA', BB' and CC'. It is also obvious by inspection that the fewer the number of slots per pole and the greater the number of conductors per slot, the greater will be the departure from uniformity of voltage for commutation that is generated by the commutating poles.

This consideration limits, in practice, the number of slots per pole to not less than the following:

Size	Slots per Pole
5 kw. and under	7 to 8
5 kw. to 50 kw.	9 to 12
50 kw. and above	12 or more

A still further limitation is that above 50 kw. not more than four commutator bars per slot are used and below that size, not more than five.

81. The Brush Width.—It was pointed out in Art. 72, page 87, that the brush width has very little effect on the reactance

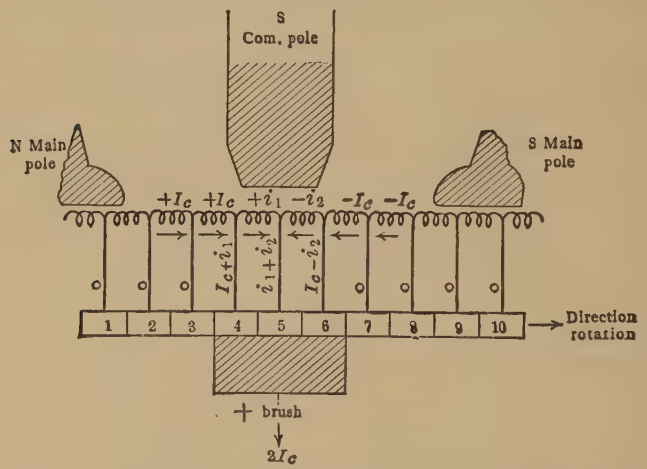

Fig. 79.—Current distribution in brush as influenced by action of commutating pole.

voltage because, while the number of adjacent coils that are simultaneously undergoing commutation increases with the brush width, the time of commutation also increases at the same rate.

Figure 79 shows in diagram the distribution of current over the face of a brush in a typical commutating pole machine. As has been pointed out on previous pages it is obvious that the current in a given armature conductor must change from $+I_c$ to $-I_c$ while the commutator bar to which it is attached is passing under the brush. As was pointed out in the previous chapter, ideal commutation takes place when this change from $+I_c$ to $-I_c$ occurs at a uniform rate while the coil is passing under the brush. Thus, in Fig. 79, if the values i_1 and i_2 are each $= \frac{1}{3}I_c$,

then the current that passes from commutator bar to brush is the same for each of the bars 4, 5, and 6 which are shown in contact with the brush at the instant selected and the current density over the entire brush surface is uniform. Since reactance voltage does not change with slot position, it follows that the flux from the commutating pole which neutralizes this reactance voltage, should also be uniform throughout the range of motion while the coil under commutation is being short-circuited by the brush. If the brush is so wide that a part of this short-circuited zone is outside the zone of the commutating pole field, it is obvious that this additional width of brush will accomplish no good purpose.

Reference to Fig. 77 shows that the width of the commutating pole must be kept down to 11 to 13 per cent (average value 12 per cent) of the pole pitch. The bevelling of the commutating pole is such that the width of the commutating pole face presented to the armature is two-thirds to three-fourths of the pole width; this means that the width of the commutating pole at the armature surface is from 7.3 to 10 per cent of the pole pitch. The comparatively large air-gap of the commutating pole gives a fringe of field at the edges of the commutating pole which increases its zone of activity by some 20 to 40 per cent depending on the air-gap used. As a final result, therefore, we arrive at a width of commutating pole zone that varies from say 9 per cent of pole pitch as a minimum to 15 per cent as a maximum.

As shown above, it does no good to use a brush that is wider than the commutating zone under any conditions. A brush that covers 15 per cent of the commutator circumference is therefore the maximum that could be considered, except possibly on some freak design.

But there are a number of considerations that reduce this value. The most important is probably the influence of the short-pitch winding. The effect of a short-pitch winding is to reduce the effective width of the commutating pole zone by just the amount of the shortening of pitch. The reason for this may be readily seen by inspection of Fig. 78. Here, the winding is assumed to be one slot short of full pitch. As one side of the coil being commutated is leaving the zone of one commutating pole, the other side is entering the zone of the next adjacent commutating pole, and it is obvious, by inspection, that this one slot shortened pitch decreases the commutating zone by one

slot. If we take C_z as the width of the commutating zone at the armature surface, the maximum width of brush is

$$\text{max. width of brush} = C_z \times \frac{\text{commutator diameter}}{\text{armature diameter}}$$

with full-pitch windings. With short-pitch windings (shortened one slot) the brush width becomes

$$(C_z - \lambda)\frac{\text{cummutator diameter}}{\text{armature diameter}}.$$

It has been shown above (Art. 80) that λ has a maximum value of about 14 per cent of pole pitch and that C_z has a minimum of 9 per cent of pole pitch, and it might seem to follow that the brush width would sometimes have a negative value. Values of λ that are as high as 8 to 14 per cent of pole pitch are used

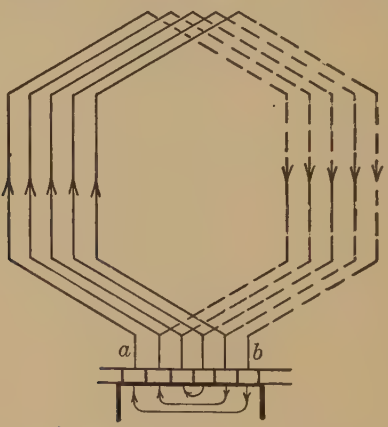

FIG. 80.—Circulating currents at no-load in a wide brush.

only on small machines where wave or series windings are used. In this type of winding an odd number of slots is used and the pitch is shortened only a fraction of a slot. The amount of shortening of pitch usually used is $\frac{\lambda}{p}$, that is, $\frac{1}{4}\lambda$ in a four-pole machine $\frac{1}{6}\lambda$ in a six-pole, etc. The minimum number of slots in which a full slot of chording is used is 12 per pole and usually, it is more than this.

Figure 80 shows another condition that limits the maximum width of brush. If the brush is too wide (Fig. 80 shows a brush six bars wide) there will be a relatively large voltage between the toe of the brush a and its heel b. If there be an unbalance between the reactance voltage in these coils and the counter e.m.f.

for commutation set up by the commutating pole, this unbalanced voltage will be opposed by the resistance of only two carbon to copper contacts (assuming brush resistance and coil resistance = zero) and circulating currents may be set up as indicated. Our previous discussion has shown that a perfect balance for each individual turn is impossible, particularly, when these adjoining turns are in adjacent slots; some circulating current will therefore occur and this circulating current will increase with the width of brush.

Practice has indicated that the brush should not cover more than one slot, unless there is only one commutator bar per slot and then not more than two bars. Practice has further, indicated that the maximum bars covered in small machines (50 kw. or under) should not exceed five and in large machines (over 50 kw.), four.

82. Limit of Armature and Field Ampere-turns per Pole.—Figure 81 shows part of a multipolar machine; the current in the

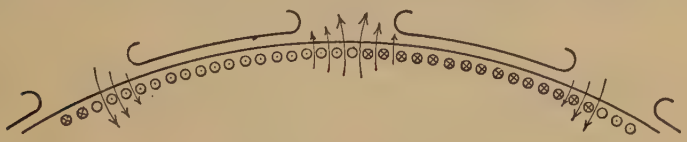

FIG. 81.—Field due to the armature m.m.f.

armature conductors is represented by crosses and dots and the lines of force of armature reaction are also shown. As the number of armature ampere-turns per pole increases the field ampere-turns per pole must also be increased so as to prevent too great a distortion of the main field.

There is, however, one part of the armature field which is not counteracted by the main field, namely, the field out on the end connections; this is stationary in space and therefore cut by the coils which are undergoing commutation. The e.m.f. due to the cutting of this field acts in such a direction as to oppose commutation, and in order to prevent this voltage from having such a value as to cause trouble, it is advisable to limit the number of armature ampere-turns per pole to not over 10,000. This means that the field ampere-turns per pole for gap + teeth for commutating pole machines should not exceed about 7500, in other words the *field ampere-turns per pole for gap + teeth* should be approximately 0.75. armature ampere-turns per pole (see Art. 57, p. 67). When the field ampere-turns per pole exceed this value,

it is more economical to increase the number of poles thereby reducing the ampere-turns per pole to a value less than 7500.

83. Dimensions of Commutating Pole.—The axial length of the commutating pole, L_{ip}, is found as follows: If B_i is the average commutating pole gap density, then the voltage generated in each coil while under the commutating pole

$$= \text{the lines cut per second} \times 10^{-8}$$

$$= 2\,T \times B_i \times L_i \times \pi D_a \times \frac{\text{r.p.m.}}{60} \times 10^{-8}$$

and this should equal the reactance voltage, which, for a chorded winding, the type usually used on interpole machines,

$$= 0.93 \times S \times \text{r.p.m.} \times I_c \times L_c \times T^2 \times 10^{-8} \text{ volts per coil;}$$

therefore, equating these two values together and simplifying,

$$B_i \times L_i = \left(\frac{S \times T \times I_c}{\pi D_a}\right) L_c \times 28$$

$$= \text{ampere-conductors per inch} \times L_c \times 14,$$

and

$$L_i = L_c \left(\frac{\text{ampere-conductors per inch}}{B_i}\right) \times 14.$$

If we assume a value of $B_i = 40{,}000$, and a value of ampere-conductors per inch = 1100 (a value rarely exceeded), the resulting value of L_i is

$$L_i = L_c \frac{1100 \times 14}{40{,}000} = 0.385\, L_c.$$

It is obvious, therefore, that there is considerable latitude in adjusting the number, the length, and the excitation of the commutating poles.

The use of a commutating pole between every pair of main poles is not essential. Reference Fig. 78 will indicate this. This figure shows that while one side of a given coil is under a north commutating pole, the other side is under the next adjacent south pole. The total e.m.f. for commutation is the sum of these two e.m.fs. If we double the flux under one of these poles, the other may be omitted and satisfactory commutating conditions still secured. From the relation between L_i and L_c above indicated it is obvious that this doubling of the flux under the commutating pole may readily be secured by simply doubling the length. There is ample margin so that this may be done. This is frequently resorted to by designers and only half as many commutating poles are used as main poles with a consequent saving in material and labor.

With series or wave-wound armatures when only two sets of brushes are used the designer can go even further and use only a single commutating pole no matter how many main poles the machine may have.

84. Commutating Pole Excitation.—The m.m.f. of the commutating pole must be sufficient to overcome the m.m.f. of the armature and then enough greater to produce the necessary flux for commutation. When using as many commutating poles as main poles, the excitation used on these poles is from 1.2 to 1.4 the armature ampere-turns. When only half the number of commutating poles as main poles is used this m.m.f. is increased to 1.4 to 1.6 the armature m.m.f. The number of turns on the commutating pole is fixed in advance at a value which is large enough and then the final value of commutating pole flux adjusted either by adjusting the air-gap or by shunting down the proportion of armature current that is passed through them.

Example.—Design the commutating pole and its winding for the machine drawn to scale in Fig. 46, and having the following rating:

550 kw., 250 volts, 250 r.p.m., 2200 amperes.

The brush arc	1.036 in.
The slot pitch	0.872 in.
Armature diameter	50 in.
Commutator diameter	35 in.
Armature frame length	14 in.
Ampere conductors per inch (Fig. 94)	1010.
Armature ampere-turns per pole	7900.

$$(C_z - \lambda)\frac{\text{commutator diameter}}{\text{armature diameter}} = 1.036 \text{ (Art. 81).}$$

Hence, the commutating pole zone arc must not be less than,

$$C_z = \left(1.036 \times \frac{\text{armature diameter}}{\text{commutator diameter}}\right) + \lambda = \frac{1.036}{0.7} + 0.872. = 2.352 \text{ in.}$$

To prevent pulsation of the commutating pole field the commutating zone arc should be approximately a multiple of the slot pitch, or $3 \times 0.872 = 2.616$ inches.

Therefore make,

$$C_z = 2.5 \text{ in.}$$

The commutating pole air-gap (assumed) = 0.25 in.

The commutating pole width $= C_z - 2\delta = 2$ in.

Minimum axial commutating pole length,

$$L_i = 0.385 L_c = 5.4 \text{ in. (Art. 83).}$$

Actual axial commutating pole length,

$$L_i = 0.85 L_c = 12 \text{ in.}$$

The average commutating pole gap flux density,

$$B_i = \frac{14 q L_c}{L_i} = \frac{14 \times 1010 \times 14}{12} = 16{,}500 \text{ lines per square inch.}$$

The commutating pole ampere-turns = 7900 × 1.4 = 11,000 (Art. 84).

The number of turns required on each commutating pole =

$$\frac{11{,}000}{\text{full-load current}} = 5.$$

The full-load current is 2200 amperes, and to carry such a large current very heavy copper would be required for the commutating pole winding, hence the winding is divided into two circuits which are connected in parallel, each carrying one half of the total current, namely 1100 amperes.

Therefore, the number of turns per pole = 10.

Current density in commutating pole winding = 930 circular mils per ampere (same as for the series field).

The size of the commutating pole winding = 930 × 1100
= 1,020,000 circular mils.
= 0.8 sq. in.

Width of conductor (assumed) = 1.25 in.

Necessary thickness of conductor = 0.64 in.

M.T., the mean turn of coil = 33 in.

The resistance of 10 turns of this wire $= \frac{33 \times 10}{1{,}020{,}000} = 0.324 \times 10^{-3}$ ohms.

The volts drop in one coil = $0.324 \times 10^{-3} \times 1100 = 0.356$ volts.

The loss in one commutating pole coil = 0.356 × 1100 = 392 watts.

The permissible watts per degree C. per square inch of external surface = 0.0228 (same as for series field coil).

The radial length of coil = 8.5 in. (see Fig. 46).

External periphery of coil = 38 in.

Radiating surface = 38 × 8.5 = 324 sq. in.

Watts per square inch external surface = $^{392}/_{324} = 1.2$.

Temperature rise of commutating pole coil $= \frac{1.2}{0.0228} = 53°$ C.

This temperature rise is not too high for exposed windings (see Art. 101)

85. Compensating Windings.—While the commutating pole gives us a very satisfactory solution of the problem of commutation, it does not prevent field distortion. In fact, the amount of field distortion in commutating pole machines is, in general, much higher on account of the lower ratio

$$\frac{\text{field ampere-turns per pole for gap + teeth}}{\text{armature ampere-turns per pole at full load}}.$$

As had already been set forth, this ratio for non-commutating pole does not usually go below 1.2 and for commutating pole machines it varies from about 0.65 as a minimum to about 1.00 as a maximum. The flux set up across the pole face by the armature m.m.f. is shown in *A*, Fig. 82. If we provide the pole face with another winding, as shown at *B*, Fig. 82, and place this winding in series with the load, it will obviously set up an m.m.f. equal and opposite to that of the armature; this will prevent distortion of the field due to armature reaction. Such pole

face windings are called *compensating windings* and are usually used when the product kw. × r.p.m. reaches a value sufficient to justify the additional expense of these windings. Commutating poles are also used, even when the machine is equipped with compensating winding, but the ampere-turns on these poles is reduced to only about 20 to 30 per cent of the value that would be necessary without such compensating windings. The m.m.f. set up by the compensating windings tends to cause a flux to pass through the commutating poles and hence a reduction in the exictation necessary on these poles when using a compensating winding. Figure 83 shows a machine equipped with such compensating windings.

The value of the product kw. × r.p.m. above which compensating windings are used in approximately 350,000; however, this value is not a hard and fast dividing line. For values greater

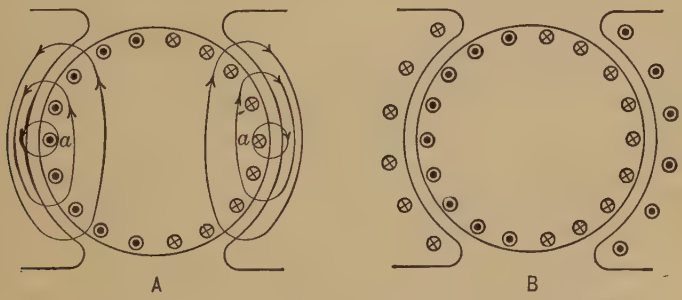

FIG. 82.—Armature field with and without compensating windings.

than this, it is usually more economical to use the compensating winding as well as assuring better performance. Where operating conditions are especially severe, such as frequent reversals of rotation or frequent heavy overloads, the compenasting windings may be used for lower values of kw. × r.p.m.

There is another advantage of the compensating winding that is important. Reference to Fig. 82*A* shows that a cross flux is set up by the armature m.m.f. which may attain a very considerable value. With every load change, the value of this cross flux changes. The maximum value of this cross flux is at *a*, Fig. 82*A*, and variations in the value of this cross flux will set up an e.m.f. in the armature conductors in addition to the normal e.m.f. due to rotation in the field, which will either add to or subtract from this normal e.m.f. depending on whether the load is decreasing or increasing. If the variation in load is sudden, as

with a short-circuit or an interruption of the load current by a circuit-breaker, this additional voltage may become high enough to cause "flashing over." By "flashing over" is meant the bridging of the space from one brush holder to another by an arc. On large high-voltage machines this flashing over may result in serious damage. The use of the compensating winding eliminates this cross flux and reduces materially the tendency of D.-C. machines to flash over.

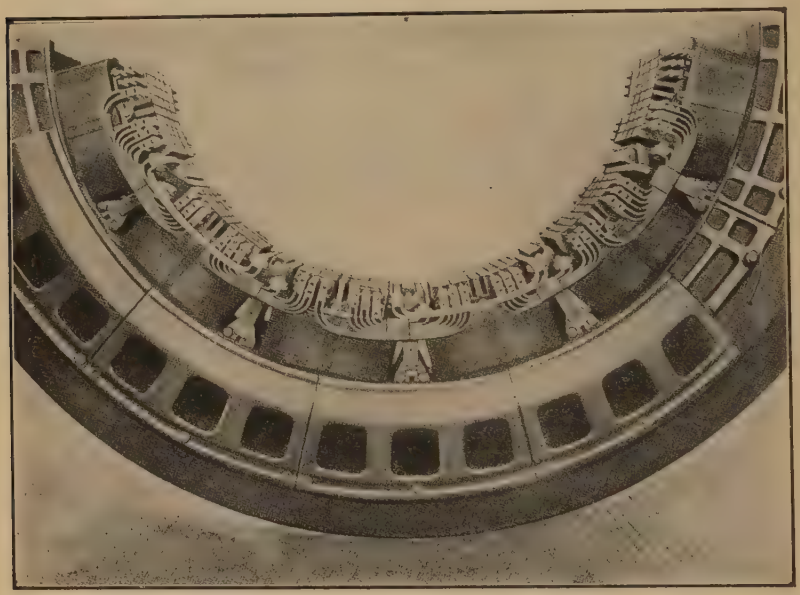

Fig. 83.—Yoke of machine with interpoles and compensating windings.

86. Saturation in Commutating Poles.—In Chap. V is given an analysis of the methods by which magnetic leakage is calculated. It is there shown that the maximum flux in the main pole may be 15 to 25 per cent greater than the useful flux. It is evident that if we apply the same methods of analysis to commutating poles a much higher leakage factor will be found for the commutating pole. Leakage in the commutating poles will, of course, vary with load, and at maximum loads the leakage alone may work the base of the commutating pole to a point up near the saturation of the iron. To reduce this effect to a minimum, the density due to useful flux in the commutating pole is usually kept to a low value (see Art. 83 p. 102). In spite of

this low density of useful flux, saturation often occurs in the commutating pole due to leakage. Saturation will, of course, prevent the useful flux from being proportional to m.m.f. on the commutating pole and sparking may result under heavy loads. To avoid this saturation, the commutating pole is often made tapered so as to have a larger cross-section near its base. Only an analysis of each individual case will tell whether such tapering is necessary.

87. Volts per Bar.—Owing to the absence of perfect functioning of the commutating pole for reasons set forth in Arts. 80 and 86, it has been recognized in practice that there is a limit to the maximum reactance voltage that may be permitted in D.-C. machinery. Since there is a more or less definite relation between reactance voltage and average volts per bar, it follows that there is a limit to the permissible average volts per bar.

The relation between average volts per bar and reactance volts is as follows: The voltage between brushes $= Z\phi_a \frac{\text{r.p.m.}}{60} \times \frac{\text{poles}}{\text{paths}} 10^{-8}$ and the number of commutator segments between brushes is $\frac{S}{p}$ where S is the total number of commutator bars. Therefore, the average voltage between commutator bars

$$= Z\phi_a \frac{\text{r.p.m.}}{60} \times \frac{\text{poles}}{\text{paths}} \times \frac{\text{poles}}{S} 10^{-8}.$$

Since $Z = 2TS$ and $\phi_a = B_g \psi \tau L_c$, the average volts per bar

$$= 2TSB_g\psi\tau L_c \frac{\text{r.p.m.}}{60} \times \frac{\text{poles}}{\text{paths}} \times \frac{\text{poles}}{S} \times 10^{-8}.$$

The reactance voltage $= 0.93 \times S \times \text{r.p.m.} \times I_c \times L_c \times T^2 \times \frac{\text{poles}}{\text{paths}} \times 10^{-8}$ (see Art. 75).

Therefore the ratio $\frac{\text{average volts per bar}}{\text{reactance voltage}}$

$$= \frac{2TSB_g\psi\tau L_c \frac{\text{r.p.m.}}{60} \frac{\text{poles}}{\text{paths}} \frac{\text{poles}}{S} 10^{-8}}{0.93\, S\ \text{r.p.m.}\ I_c L_c\ T^2 \frac{\text{poles}}{\text{paths}} 10^{-8}} =$$

$$= \frac{B_g \psi p \tau}{28 S I_c T} =$$

If we take q as the ampere conductors per inch of periphery of

the armature, then $q = \frac{ZI_c}{\pi D} = \frac{2TSI_c}{\tau p}$ since $Z = 2TS$ and $\pi D = \tau p$. If we substitute this value of q, the ratio

$$\frac{\text{average volts per bar}}{\text{reactance voltage}} = \frac{B_g \psi}{14q} \qquad (14)$$

All of the factors appearing in formula (14) are nearly constant. For commutating pole designs, B_g has a maximum value of about 60,000 for large machines and drops to about 45,000 for small machines, Ψ about 0.65 and q varies from a maximum of about 1100 in large machines (above 1000 kw.) to perhaps 500 in small machines (below 10 kw.)

The ratio $\frac{\text{average volts per bar}}{\text{reactance voltage}}$ varies from about 2.5 for large machines to about 4 for small machines.

It is evident that the ratio $\frac{\text{maximum volts per bar}}{\text{average volts per bar}}$ depends on the field form. At no load when the field is not distorted, the field form will have very nearly the shape of the curve D, Fig. 54. When load is applied, the field flux increases under one pole tip and decreases under the other causing it to become distorted as in F, Fig. 54. The greater the armature current, the greater the field distortion. Curve F, Fig. 54 and curve C, Fig. 59, show approximately the field distortion that may be expected under full load in a non-commutating pole design and a commutating pole design, respectively. In practice, under full-load field distortion the ratio $\frac{\text{maximum volts per bar}}{\text{average volts per bar}}$ varies from about 1.7 to 1.9 averaging 1.8.

When compensating windings are used, the distortion of the field due to armature current is almost entirely eliminated and the field form remains approximately like that shown at D, Fig. 54, under all loads. In compensated machines, therefore, the ratio $\frac{\text{maximum volts per bar}}{\text{average volts per bar}}$ is about 1.40 to 1.50 and does not change materially with load.

In practice the following values of maximum volts per bar, average volts per bar, and reactance voltage are not usually exceeded.

	Maximum Volts per Bar	Average Volts per Bar	Reactance Voltage per Bar
Commutating pole machines (full load)	30	14 to 16	3.5 to 6
Compensated machines (full load)	30	18 to 20	4.5 to 8

The upper limit of reactance voltage per bar applies to large machines (1000 kw. and above) and the lower, to small machines (below 10 kw.) For large very high-speed machines—such as those direct-driven by steam turbines—it may become necessary to exceed the limits of the above table. In such cases extreme care must be taken that the commutating conditions are the best possible that can be secured by design, minimum number of conductors per slot, and a design of commutating pole that will avoid saturation with load to a maximum degree.

CHAPTER X
EFFICIENCY AND LOSSES

88. The Efficiency of a generator $= \frac{\text{output}}{\text{input}} = \frac{\text{output}}{\text{output} + \text{losses}}$ and that of a motor $= \frac{\text{output}}{\text{input}} = \frac{\text{input} - \text{losses}}{\text{input}}$ where the losses are:

a. Mechanical losses—windage, brush, and bearing friction.

b. Iron losses—hysteresis and eddy-current losses.

c. Copper losses in field and armature coils.

d. Commutator contact resistance loss.

e. Load losses.

These various losses may be discussed more in detail as follows:

89. Bearing Friction.—In a high-speed bearing with ring lubrication there is always a film of oil between the shaft and the bushing; bearing friction is therefore an example of fluid friction and the tangential force at the rubbing surface in such a case $= kA_bV_b^n$ lb., where k is a constant which depends on the viscosity of the oil and is found by experiment to be $= 0.036$ for bearings with ring lubrication using light machine oil.

A_b is the projected area of the bearing in square inches = (the bearing diameter d_b in inches $\times$ the bearing length l_b in inches);

V_b is the rubbing velocity of the bearing in feet per minute;

n is found experimentally to vary from 1 for low values of V_b to 0 for very high values and is approximately $= 0.5$ for bearing speeds from 100 to 1000 ft. per minute.

For moderate speed bearings with ring lubrication and with light machine oil the force of friction $= 0.036A_bV_b^{1/2}$ pounds and the friction loss $= 0.036A_bV_b^{3/2}$ ft.-lb. per minute

$$= 0.81d_bl_b\left(\frac{V_b}{100}\right)^{3/2} \text{ watts.} \qquad (15)$$

It is important to notice that this loss is independent of the bearing pressure and is therefore independent of the load.

As the pressure on the bearing increases the thickness of the oil film decreases and at a certain limiting pressure it breaks

down and the bearing seizes. For electrical machinery the bearing pressure $= \frac{\text{bearing load}}{A_b}$, should not exceed 80 lb. per square inch when the machine is carrying full load, such a bearing will carry 100 per cent overload without breakdown.

The bearing loss increases rapidly with the rubbing velocity and after a certain velocity has been reached the bearings are no longer large enough to be self-cooling. For self-cooling bearings the rubbing velocity should not exceed 1000 ft. per minute unless the bearing is specially designed to get rid of the heat, and even this value should only be used for machines which are built so that a large supply of cool air passes continuously over the external surface of the bearing. The bearings of totally enclosed motors, for example, are poorly ventilated and should not be run with a rubbing velocity greater than about 800 ft. per minute.

The thickness of the oil film in a bearing varies inversely as the temperature of the oil, and this temperature should not exceed 70°C. when measured by a thermometer in the oil well

90. Brush Friction.—If

μ is the coefficient of friction,

P the brush pressure in pounds per square inch,

A the total brush-rubbing surface in square inches,

V_r the rubbing velocity in feet per minute,

then the friction loss $= \mu P A V_r$ ft.-lb. per minute.

Approximate values found in practice are:

$\mu = 0.28$ and $P = 2$ lb. per square inch, for which values the

$$\text{friction loss} = 1.25A\frac{V_r}{100} \text{ watts.} \qquad (16)$$

91. Windage Loss.—It is difficult to predetermine this loss but, up to peripheral velocities of 6000 ft. per minute, it is so small that it may be neglected. Figure 84 shows the windage and bearing friction loss of a motor which has an armature diameter of 100 in. and three bearings each 10 by 30 in. The circles show the actual test points and the curve shows the value of the bearing friction loss calculated from the formula, friction loss $= 3 \times 0.81 \times d_b \times l_b\left(\frac{V_b}{100}\right)^{3\frac{1}{2}}$ watts. At a speed of 230 r.p.m. the peripheral velocity of the armature is 6000 ft. per minute, up to which speed the windage loss can be neglected; at higher speeds it becomes large because it is proportional to the (peripheral velocity)^3.

Few electrical machines except turbo generators are run at peripheral speeds greater than 9000 ft. per minute, because the cost increases very rapidly for higher speeds on account of the special construction required to hold the coils against centrifugal force.

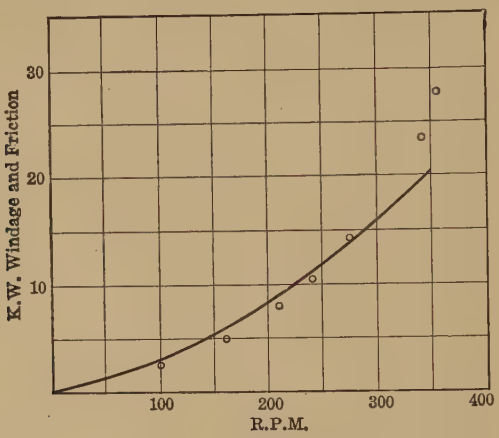

FIG. 84.—Windage and friction loss in a large motor.

92. Iron Losses.—It may be seen from Fig. 85 that the flux in any portion of the armature of a D.-C. machine goes through one cycle while the armature moves through the distance of two

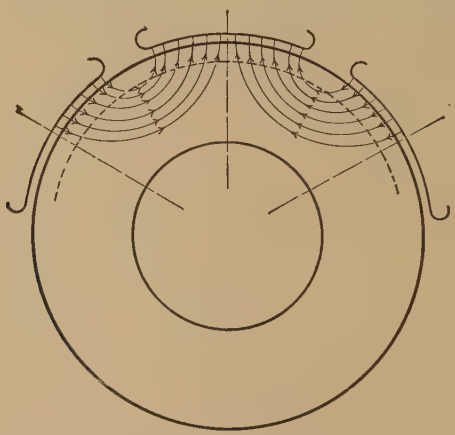

FIG. 85.—Distribution of flux in the armature.

pole pitches; that is, the flux in any portion of the armature passes through $\frac{p}{2}$ cycles per revolution, or through $\frac{p}{2} \times \frac{\text{r.p.m.}}{60}$ cycles per second.

The iron losses consist of the hysteresis loss which $= KB^{1.6}fW$ watts, and the eddy-current loss which $= K_e(Bft)^2W$ watts where K is the hysteresis constant and varies with the grade of iron,

K_e is a constant which is inversely proportional to the electrical resistance of the iron,

B is the maximum flux density in lines per square inch;

f is the frequency in cycles per second,

W is the weight of the iron in pounds,

t is the thickness of the core laminations in inches.

The eddy-current loss can be reduced by the use of iron which has a high electrical resistance. At present, however, most of the grades of very high-resistance iron have a lower permeability than those of lower electrical resistance; they also cost more and are more brittle; machines built with such iron are liable to have the teeth break off due to vibration. The reduction in the total loss by the use of high-resistance iron is not so great as one would expect, because a large part of the loss is due to losses discussed in the next article and these are not greatly affected by the grade of iron used.

The eddy-current loss can be reduced by a reduction in t, the thickness of the laminations; this value is generally about 0.014 in. for frequencies above 40 cycles per second and 0.025 in. below that frequency.

93. Additional Losses.—Besides the ordinary hysteresis and eddy-current loss already mentioned there are additional losses which cannot be calculated, due to the following causes:

(*a*) Loss due to filing of the slots. When the laminations that form the core have been assembled it will be found that in most cases the slots are rough and must be filed smooth in order that the slot insulation may not be cut. This filing burrs the laminations over on one another and provides a low-resistance path through which eddy currents can flow; that is, it tends to defeat the result to be obtained by laminating the core.

(*b*) Losses in the spider and end heads due to the leakage flux which gets into these parts of the machine; these losses may be large because the material is not laminated.

(*c*) Loss due to non-uniform distribution of flux in the armature core. When calculating the value of B_c, the flux density in the core, page 48, it is assumed that the flux is uniformly spread over the core area. This however is not the case and

the actual flux distribution is shown in Fig. 85; the lines of force take the path of least reluctance and therefore crowd in behind the teeth until that part of the core becomes saturated, then they spread further out. Due to this concentration of flux, the core loss, which is approximately proportional to (flux density)^2, is greater than that got by assuming that the flux distribution is uniform through the whole depth of the core.

It is sometimes possible to increase the core depth so as to keep the apparent flux density in the core low and yet make no perceptible reduction in the core loss, because the increased depth of core does not carry its proper share of the flux; for this reason there is seldom much to be gained by making the value of B_c less than 80,000 lines per square inch, which is near the point at which saturation begins and the flux tends to become uniform.

(*d*) Pole-face losses. Figure 44 shows the distribution of flux in the air-gap of a D.-C. machine and, as the armature revolves and the teeth move past the pole face, e.m.fs. will be induced which will cause currents to flow across the pole face. Experiment shows that when solid pole faces are used the loss due to these currents increases very rapidly as the slot opening becomes greater than twice the length of the air-gap; when the slot openings are wider than this the pole face must be laminated.

(*e*) Variation of the iron loss with load. It is shown in Fig. 54 and Fig. 59 that, when the machine is loaded, the flux density is not unifrom in all the teeth under the pole but is higher at one pole tip than at the other. The effect of the increase of flux density in the teeth under one pole tip in increasing the iron loss is greater than the effect of the decrease of flux density in the teeth under the other tip in reducing the iron loss.

(*f*) Eddy-current losses in armature conductors. Some flux from the field passes into the armature by way of the slot instead of the teeth; the proportion that so passes evidently increases as the degree of tooth saturation increases. As this leakage flux in the slot varies, it sets up eddy currents in the armature conductors giving rise to an additional loss. When the field form distorts under load, the maximum value of flux density is thereby increased (as noted in (*e*) above) and the leakage that takes place through the slot is very considerably increased. This in turn causes a larger amount of eddy-current loss in the armature conductors under load than occurs at no load.

Items (*d*), (*e*), and (*f*), above discussed, are all larger under load than at no-load nad are known as "load losses."

94. Calculation of Core Loss.—Due to the additional losses it is impossible to predetermine the total core loss by the use of fundamental formulæ; core loss calculations for new designs are based on the results obtained from tests on similar machines built under the same conditions. Such test results are plotted in Fig. 86 for machines built with ordinary iron of a thickness of 0.014 in., the slots being made with notching dies so that a certain amount of filing has to be done. The curves of Fig. 86 are for the iron alone; to include pole-face losses, about 30 per cent should be added to the values in Fig. 86.

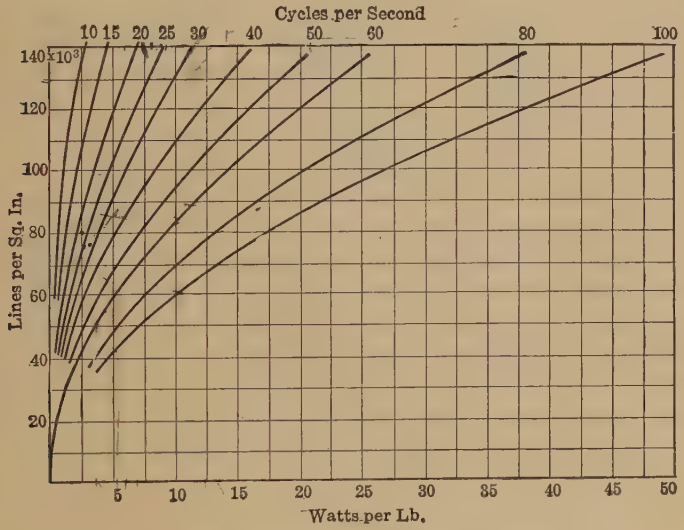

FIG. 86.—Iron loss curves for revolving machinery.

It should be further understood that the values given in Fig. 86 are not to be taken as accurate for all conditions, since the actual loss will depend very largely on the amount of filing of slots. They give fair average values only.

Example of Calculation.—For the machine shown in Fig. 46 the value of B_{at}, the actual flux density in the teeth, and B_c, the average flux density in the core are given in Art. 50.

B_{at} = 145,000 lines per square inch.

B_c = 88,500 lines per square inch.

W_t, the total weight of the armature teeth = 396 lb.

W_c, the total weight of the armature core = 1510 lb.

The frequency = 20.83 cycles per second.
The loss per pound of teeth = 7.5 watts (from Fig. 86).
The loss per pound of the core = 2.5 watts (from Fig. 86).
The total loss = $396 \times 7.5 + 1510 \times 2.5 = 6750$ watts.

95. Armature Copper Loss.—The resistance of copper at the normal operating temperature of an electric machine is approximately 1 ohm per circular mil cross-section per inch length, so that if

Z is the total number of conductors,
L_b is the length of one conductor in inches,
M is the cross-section of each conductor in circular mils,
I_c is the current in each conductor in amperes,

then the resistance of one conductor in ohms $= \frac{L_b}{M}$,

the loss in one conductor in watts $= \frac{L_b}{M} \times I_c^2$,

and the total copper loss in the armature in watts $= Z \frac{L_b}{M} I_c^2$ (15)

The value of L_b =

1.35 (pole pitch) + (armature axial length) + 3 in.

approximately for the type of coil shown in Fig. 39, page 39.

96. Shunt Field Copper Loss.—This loss, which $= E_t I_f$ watts, where E_t is the terminal voltage of the machine and I_f is the current in the shunt coil, is made up of the loss in the field coils and the loss in the field rheostat; the latter for a generator is about 20 per cent of the total shunt field loss.

97. Series Field Copper Loss.—This loss $= I_a^2 R_s$ watts, where R_s is the resistance of the series field in ohms and I_a the total armature current. When a series shunt is used, so that part of the current I_a passes through the series field and the remainder passes through the shunt, the resistance R_s is the combined resistance of the series field and the series shunt in parallel.

98. Brush Contact Resistance Loss.—This loss has already been discussed in Art. 68, page 83, and $= E_b I_a$ watts, where E_b is the voltage drop per pair of brushes and I_a is the armature current. The volts drop per pair of brushes is approximately constant over a wide range of current, as shown in Fig. 70.

99. A. I. E. E. Standard Rules on Efficiency.—The American Institute of Electrical Engineers has through its Standards Committee recommended practices and methods for the determination of the efficiency of D.-C. machinery. The following is

quoted from the report of the A. I. E. E. Standards Committee on D.-C. machines issued in July, 1925:

EFFICIENCY

General

5–350 Efficiency Defined.—The efficiency of a direct-current commutating machine is the ratio of the useful power output to the total power input.

5–351 Methods of Determining Efficiency Recognized.[1]—The following methods of determining efficiency are recognized as standard:

(*a*) *Directly Measured Efficiency.*—The efficiency is obtained from simultaneous measurements of input and output or by an accurate determination of all the component losses.

(*b*) *Conventional Efficiency.*—The efficiency is obtained from the component losses, most of which are accurately determinable and the remainder of which are assigned conventional values; or all of the losses may be determined by conventional methods of test. The efficiency determined in this way is the ratio of the output to the sum of the output and the losses, or of the input minus the losses to the input.

5–352 Method of Determining Efficiency to Be Employed.—Unless otherwise specified the conventional efficiency shall be employed.

Efficiency Determined by Measurement of Input and Output

5–353 Methods of Test.—Efficiency by measurement of input and output shall be determined according to one of the following methods:

(*a*) Input and output are measured simultaneously at the terminals of the machine by means of electrical measuring instruments.

(*b*) The mechanical power is measured by means of brake or dynamometer, the electrical power by means of electrical measuring instruments.

(*c*) The mechanical power is measured by means of a calibrated auxiliary machine, the electrical power by means of electrical measuring instruments.

[1] In other than small machines determinations of efficiencies by (*a*) are impractical unless resort is made to expensive measurements.

The use of the conventional efficiency is recommended. Most of the losses are accurately measurable. Those to which conventional values are assigned are so closely approximated that the percentage of error in the determined efficiency is small. The high efficiency generally attained in electrical machines renders an error in the measurement or estimation of one or more of the losses of much less effect on the efficiency as obtained by the conventional method than would an error of like magnitude in the measurement of the total input and output.

5–354 Measurement of Mechanical Power.—Mechanical power delivered by machines shall be measured at the pulley, gear or coupling, on the rotor shaft, thus excluding the loss of power in the belt or gear friction.

5–355 Normal Conditions for Efficiency Test.

(*a*) *Voltage and Speed.*—The efficiency shall be measured at the rated voltage and speed. In the case of adjustable speed motors the base speed shall be inferred unless otherwise specified.

(*b*) *Load.*—When the efficiency is stated without specific reference to the load conditions, rated load shall be understood and the test made at rated load.

(*c*) *Temperature.*—The efficiency shall be measured at, as nearly as possible, the final temperature attained at operation, for the time specified in the rating, under the conditions of (*a*) and (*b*) above.

5–356 Miscellaneous Losses.

(*a*) *Field-rheostat Losses.*—All losses due to field-rheostats either series or multiple connected shall be included in the determination of the efficiency even when the machine is separately excited.

(*b*) *Ventilating Blower.*—When a blower is supplied as part of a machine set, the power required to drive it shall be charged against the complete unit, but not against the machine alone.

(*c*) *Other Auxiliary Apparatus.*—Auxiliary apparatus, such as a separate exciter for a generator or motor, shall have its losses charged against the plant of which the generator and exciter are a part, and not against the generator. An exception should be noted in the case of turbo-generator sets with direct-connected exciters, in which case the losses in the exciter shall be charged against the generator. The actual energy of excitation and the field-rheostat losses, if any, shall be charged against the generator.

Conventional Efficiency

5–357 Normal Conditions for Efficiency Tests and Calculations.

(*a*) *Voltage and Speed.*—The efficiency shall be determined for the rated voltage and speed. In the case of adjustable speed motors the base speed shall be inferred unless otherwise specified.

(*b*) *Load.*—When the efficiency is stated without specific reference to the load conditions, rated load shall be understood.

(*c*) *Temperature of Reference.*—The efficiency of all apparatus at all loads shall be corrected to a reference temperature of 75° C. but tests may be made at any convenient cooling air temperature preferably not less than 10° C.

5–358 Classification of Losses.—Losses are classified as shown in the following table:

CLASSIFICATION OF LOSSES

Accurately measurable	Approximately measurable or determinable	Indeterminable
No-load core losses including eddy-current losses in conductors at no-load	Brush friction loss	Iron loss due to flux distortion
Load I^2R losses in windings No-load I^2R losses in windings	Brush-contact loss	Eddy-current losses in conductors due to transverse fluxes occasioned by the load currents
	Losses due to windage and to bearing friction	Eddy-current losses in conductors due to tooth saturation resulting from distortion of the main flux
		Tooth-frequency losses due to flux distortion under load
		Short-circuit loss of commutation

5–359 Losses to Be Considered.—Conventional efficiencies shall be based upon the following losses:

(a) I^2R losses in armature and field windings. (Paragraph **5–361.**)

(b) Bearing friction and windage losses. (Paragraph **5–362.**)

(c) Brush friction loss. (Paragraph **5–363.**)

(d) Core loss. (Paragraph **5–364.**)

(e) Brush contact loss. (Paragraph **5–365.**)

(f) Stray load losses. (Paragraph **5–366.**)

(g) Miscellaneous losses. (Paragraph **5–367.**)

5–360 Determination of Losses.—Losses shall be measured, calculated or conventianal taken as specified in paragraphs **5–361** to **5–367** inclusive.

5–361 I²R Losses.—The I^2R losses shall be based upon the current and the measured resistance, corrected to 75 deg. cent.

5–362 Bearing Friction and Windage:

(*a*) *General.*—Drive the machine from an independent motor, the output of which shall be suitably determined. The machine

under test shall have its brushes removed and shall not be excited. This output represents the bearing friction and windage of the machine under test.

(*b*) *Engine-type Generators.*—In the case of engine-type generators, the windage and bearing friction loss is ordinarily very small, amounting to a fraction of one per cent of the output. This loss shall be neglected owing to its small value and the difficulty of measuring it.

5–363 Brush Friction of Commutator and Collector Rings.

(a) Drive the machine from an independent motor, the output of which shall be suitably determined. The brushes shall be in contact with the commutator, but the machine shall not be excited. The difference between the output obtained in the test in paragraph **5–362** and this output shall be taken as the brush friction. The surfaces of the commutator and brushes should be smooth and polished from running when this test is made.

(b) Experience has shown that wide variations are obtained in tests of brush friction made at the factory before the commutator and brushes have received the smooth surfaces that come after continued operation. Conventional values of brush friction, representing average values of many tests, shall be used, as follows:

	Watts per Square Inch of Brush Contact Surface per 1000 Ft. per Minute Peripheral Speed.
Carbon and graphite brushes	8.0 watts
Metal graphite brushes	5.0 watts

In the event that these conventional values are questioned in any case, the brush friction shall be measured as in (a) above.

Where the actual values of the brush friction loss for a given kind of brush for a certain application have been accurately determined these values may be used in similar cases.

5–364 Core Losses.—Drive the machine from an independent motor, the output of which shall be suitably determined. The brushes shall be in contact with the commutator and the machine shall be excited, so as to produce at the terminals a voltage corresponding to the calculated internal voltage for the load under consideration. The difference between the output obtained by this test and that obtained by test under paragraph **5–363** (a) shall be taken as the core loss.

It is also recognized practise to determine the core loss by driving the machine with only one brush on each stud in contact with the commutator and taking the difference of the losses of the machine unexcited and excited as above.

5–365 Brush Contact Loss.—A total drop (of positive and negative brushes) of 2 volts shall be assumed as the standard drop in determining brush-contact loss for carbon and graphite brushes with pigtails attached. A total drop of 3 volts shall be assumed where pigtails are not attached. One-quarter of one volt for each collector ring shall be used at all loads in calculating the brush contact loss for metal-graphite brushes.

5–366 Stray Load Losses.—The stray load losses include the items in the column of the table in paragraph **5–358** headed "Indeterminable." For calculating the conventional efficiencies of direct-current generators and motors stray load losses shall be taken as one per cent of the output except that for motors of 200 h.p. at 575 rev. per min. and smaller, no value has yet been assigned, and for the present stray load losses shall be omitted.

5–367 Miscellaneous Losses.

(*a*) *Field Rheostat Losses.*—All losses due to field rheostats either series or multiple connected shall be included in the determination of the efficiency even when the machine is separately excited.

(*b*) *Ventilating Blower.*—When a separately driven blower supplies air to a machine set the power required to drive it shall be charged against the complete unit but when one or more separately driven blowers supply air through a single duct to two or more machines the power required to drive the blower or blowers shall be charged against the plant or station and not against the machine set.

(c) *Other Auxiliary Apparatus.*—Auxiliary apparatus, such as a separate exciter for a generator or motor, shall have its losses charged against the plant of which the generator and exciter are a part, and not against the generator. An exception should be noted in the case of turbo-generator sets with direct-connected exciters, in which case the losses in the exciter shall be charged against the generator. The actual energy of excitation and the field-rheostat losses, if any, shall be charged against the generator.

5–368 Other Recognized Methods of Determining Losses.

Running Light Method.—The machine is run at no load as a motor and the input measured. This input, after deducting any series I^2R losses, represents the sum of the losses, which shall be regarded as constant, discussed in paragraphs **5–362, 5–363** and **5–364.** The losses at any load may be obtaned by adding to these constant losses the I^2R losses based upon the current and measured resistance, the brush contact losses, the stray losses, and the miscellaneous losses.

CHAPTER XI

HEATING

100. Cause of Temperature Rise.—The losses in an electrical machine are transformed into heat; part of this heat is dissipated by the machine and the remainder, being absorbed, causes the temperature of the machine to increase. The temperature becomes stationary when the heat absorption becomes zero, that is when the point is reached where the rate at which heat is generated in the machine is equal to the rate at which it is dissipated.

101. Maximum Safe Operating Temperature.—The highest temperature at which it is safe to operate D.-C. machinery depends on the type of insulation used; description of types of insulation is covered in Chap. IV.

The A. I. E. E. Standards Committee have carefully considered this matter of the maximum safe operating temperature and their latest (July, 1925) rulings for D.-C. machinery are as follows:

HEATING

Temperature Limitations

5–150 Limiting Temperature Rise for Machines Having Continuous and Short-time Ratings.—The temperature rise of each of the various parts, above the temperature of the cooling medium when tested in accordance with the rating, shall not exceed the values given in the following table. All temperatures shall be determined by the Thermometer Method.

5–152 Machines Having Two Kinds of Insulation.—If different insulating materials are used on various parts of one winding (for instance in the slot and for the end windings) the temperature of each material shall not exceed the limit set for that material.

When insulation consists of layers of materials having different temperature limits (for instance high-temperature limit material adjacent to the copper and lower-temperature limit material adjacent to the iron or to the air) the temperature of each material shall not exceed the limit set for that material.

Item		Type of enclosure	Limiting temperature rise deg. cent.[1]		
			Class O insulation (see art. 32)	Class A insulation (see art. 32)	Class B insulation (see art. 32)
1	Armature windings, wire field windings and all windings other than 2	All types except Totally enclosed	35	50	70
		Totally enclosed	40	55	75
2	Single layer field windings with exposed uninsulated surfaces and bare copper windings	All types except totally enclosed	45	60	80
		Totally enclosed	45	60	80
3	Cores and mechanical parts in contact with or adjacent to insulation	All types except totally enclosed	35	50	70
		Totally enclosed	40	55	75
4	[2] Commutators and collector rings	All types except totally enclosed	50	65	85
		Totally enclosed	50	65	85
5	Miscellaneous parts (such as brush-holders, brushes, pole tips, etc.,) other than those whose temperatures affect the temperature of the insulating material may attain such temperatures as will not be injurious.				

[1] The temperature limits on which the rating of general purpose motors is based are under discussion at the present time and no agreement has yet been reached. In order that work being done in this connection may not be influenced or impeded, the Institute refrains from taking any action at the present time towards revising its Rules for this class of machinery.

[2] These limits for the temperature rise of commutators and collector rings apply where Class O, A or B insulation, respectively, as the case may be, is employed in the commutator, or is adjacent thereto and its life would be affected by the heat from the commutator. It is recognized that the heating of the commutator could correspond to Class B even if the slot insulation were of Class O, on condition that the insulation of connections were not affected by the heating of the commutator.

102. Temperature Gradient in the Core of an Electrical Machine.—Figure 87 shows an iron core built up of laminations that are separated from one another by varnish. In this core there is an alternating magnetic flux and the loss in the core for different flux densities and for different frequencies can be found by the help of curves in Fig. 86, page 115.

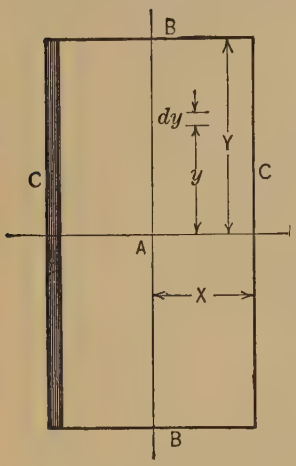

FIG. 87.—The heat paths in an armature core.

The hottest part of the core is at A and the heat in the center of the core has to be conducted to and dissipated by the surfaces B and C.

In order to have an idea as to the relative heat resistances of the paths from A to the surfaces B and C, consider the following propositions:

(a) Assume that all the heat passes in the direction Y, then the watts crossing 1 sq. in. of the core at y = (watts per cubic inch) $\times$ y and since the difference in temperature between two faces a distance dy apart = $\frac{(\text{watts per cubic inch})ydy}{1.1}$ degrees Centigrade, where 1.1 is the thermal conductivity of iron in watts per 1-in. cube per 1° C. difference in temperature,[1] therefore, the difference in temperature between A and surface B

$$= T_{ab} = \int_0^Y \frac{(\text{watts per cubic inch})ydy}{1.1}$$

$$= (\text{watts per cubic inch}) \frac{Y^2}{2.2} \text{ deg. C.}$$

(b) If the heat were all conducted in the direction X then, since the conductivity of a core along the laminations is from forty to one-hundred times as great as that across the laminations and layers of varnish, the difference in temperature between A and surface C would be

$$= T_{ac} = (\text{watts per cubic inch}) \frac{60X^2}{2.2} \text{ deg. C.}$$

[1] The value for thermal conductivity of iron here given is that for the usual grade of iron used in D.-C. machinery. For wrought iron, this value would go up to 1.5 and for high silicon steel, down to 0.4.

(This assumes that the thermal conductivity across the laminations is sixty times that along them—a fair average value.)

Example.—When the frequency is 60 cycles and the flux density is 75,000 lines per square inch then the watts per cubic inch = 2.3 and

$$T_{ab} = 1.04Y^2 \text{ deg. C.}$$
$$T_{ac} = 62.4X^2 \text{ deg. C.}$$

The fact that the conductivity along the laminations is so much better than that across the laminations would indicate that axial ventilation, whereby air is blown across the ends of the laminations, is the most effective. In practice, however, nearly all electrical machines are cooled by means of radial vent ducts, and, in order to discuss intelligently the effect of such ducts, it is necessary to find out the heat resistance between the surfaces *B*, *C*, and the air.

When air is blown across the surface of an iron core at *V* ft. per minute, the watts dissipated per square inch of radiating surface for 1° C. rise of the surface temperature is found by experiment to be $= 0.01 + 0.000025V$[1].

If then, as in case (*a*), all the heat in the core has to be dissipated by surface *B*, the difference in temperature between surface *B* and the air $= T_b$

$$= \frac{\text{watts per square inch on surface } B}{0.01 + 0.000025V}$$
$$= \frac{\text{(watts per cubic inch) } Y}{0.01 + 0.000025V}$$

Similarly in case (*b*), where it is assumed that all the heat is dissipated by surface *C*, the difference in temperature between surface *C* and the air $= T_c$

$$= \frac{\text{(watts per cubic inch) } X}{0.01 + 0.000025V}$$

Where $X = 1.5$ in., and for a value of 1 watt per cubic inch, the following tables show the values of T_{ab}, T_{ac}, T_b and T_c for different values of *Y* and of *Y*.

If all the heat be taken *across* the laminations and dissipated at surfaces *C*, Fig. 87.

[1] This relation for watts dissipated against air velocity is the same as that shown in curve form in Fig. 62. It should not be understood, however, that this relation is rigidly fixed and holds for all conditions. There are many inconsistancies in the known laws governing the escape of heat from hot bodies by forced convection; the relationship here given is the best the writer knows of.

X	Y	V = 1000			V = 10,000		
		T_{ac}	T_c	$T_{ac} + T_c$	T_{ac}	T_c	$T_{ac} + T_c$
1.5	1.5	61.5	43	104.5	61.5	5.8	67.3
1.5	3	61.5	43	104.5	61.5	5.8	67.3
1.5	6	61.5	43	104.5	61.5	5.8	67.3
1.5	12	61.5	43	104.5	61.5	5.8	67.3

If all the heat be taken along the laminations and dissipated at surfaces *B*, Fig. 87.

X	Y	V = 1000			V = 10,000		
		T_{ab}	T_b	$T_{ab} + T_b$	T_{ab}	T_b	$T_{ab} + T_b$
1.5	1.5	1	43	44	1	5.8	6.8
1.5	3	4.1	86	90.1	4.1	11.6	15.7
1.5	6	16.3	172	188.3	16.3	23.2	39.5
1.5	12	65.5	344	409.5	65.5	46.4	111.9

This analysis shows that only with relatively shallow cores is it possible to consider dissipating the heat at the edges of the laminations, unless air velocities become much higher than it is possible to run in ordinary machines. In spite of the much higher thermal resistance across laminations, it is therefore necessary to design so that the heat is conducted across the laminations and dissipated at the ventilating ducts.

In the first table above, if it is desired to reduce internal temperatures, this may be done either by reducing the watts per cubic inch of iron or by reducing the thickness of the iron packages. In the second table, reducing the thickness of the iron packages has no effect and with deep cores proper cooling becomes impossible.

103. Limiting Values of Flux Density.

The peripheral velocity of a machine in feet per minute.

$$= \frac{\pi D_a}{12} \times \text{r.p.m.}$$

$$= \frac{\pi D_a}{p} \times \frac{p}{12} \times \text{r.p.m.}$$

$$= 10 \times \tau \times f \text{ in ft. per minute;} \qquad (18)$$

therefore, for a given frequency, the peripheral velocity of a machine is proportional to its pole pitch.

For a given axial length of core, the longer the pole pitch the greater the flux per pole, and the deeper the core to carry this flux.

Where the peripheral velocity of a machine is low, the core is shallow, the vent ducts have little effect on account of their small radiating surface, and the ventilation is poor; the loss, however, is small because there is not much iron in the core.

Where the peripheral velocity is high the core is deep, the vent ducts are very effective on account of their large radiating surface, and the ventilation is good; the loss, however, is large since much iron is used in the core.

For a given frequency the same flux densities can be used for all peripheral velocities. The following flux densities may be used for D.-C. machines built with iron 0.014 in. thick, the relation between core loss and flux density being as shown in Fig. 86.

Frequency (cycles per second)	Flux density in teeth (lines per square inch)	Flux density in core (lines per square inch)
30	140,000	90,000
40	135,000	75,000
60	130,000	65,000

Core densities higher than 85,000 lines per square inch are seldom used, even for frequencies that are lower than 40 cycles, because at these densities the core becomes saturated and the cost of the extra field copper required to send the flux through a saturated core is greater than the cost of the extra iron required to keep the core density below the saturation point. There is no such objection, however, to high tooth densities because a machine with saturated teeth and a short air-gap is just as effective in preventing field distortion as a machine with unsaturated teeth and a long air-gap (see Art. 57, page 65) and does not require any more excitation.

104. Heating of the End Connections of the Winding.—The end connection heating must be taken up separately from that of the core because the kind of radiating surface is different and also the manner in which it is cooled.

Since the resistance of copper is 1 ohm per circular mil per inch the copper loss in the end connections of one conductor

$$= \frac{L_e}{M} I_c^2 \text{ watts},$$

and the total copper loss in the end connections

$$= Z\frac{L_e}{M}I_c^2 \text{ watts.}$$

The surface by which this loss is dissipated

$$\pi D_a \times 2\lambda_c \text{ sq. in. (see Fig. 88).}$$

$$= \pi D_a \times \frac{L_e}{1.6} \text{ sq. in.}$$

since L_e, as shown in Fig. 88, is approximately equal to $1.6 \times 2\lambda_c$ for standard machines, therefore the watts per square inch

$$= \frac{ZL_e}{M}I_c^2 \times \frac{1.6}{\pi D_a L_e}$$

$$= \frac{\text{ampere conductors per inch}}{\text{circular mils per ampere}} \times \text{a constant.}$$

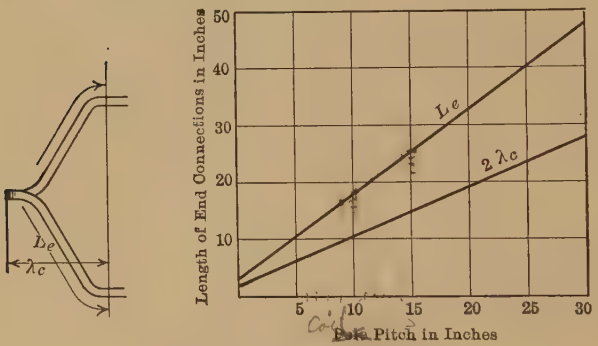

FIG. 88.—Dimensions of coils.

The temperature rise of the end connections is proportional to the watts per square inch of radiating surface, it is therefore proportional to the ratio $\frac{\text{ampere conductors per inch}}{\text{circular mils per ampere}}$ and is found from the curve in Fig. 89.

105. Temperature Gradient in the Copper Conductors.—*ab*, Fig. 90, is a conductor which is carrying current and which is embedded in, and insulated from, the iron core. In order to have some idea of the temperature of the copper in the center of the core, consider the following two propositions:

(*a*) Assume that the slot insulation is much thicker than that on the end connections, then the heat in the embedded portion of the winding has to be conducted along the copper and dissipated at the end connections. It is required to find the difference in temperature between *c* and *a*.

The resistance of copper is 1 ohm per circular mil per inch so that the energy crossing $dx = I_c^2 R_x$

$$= I_c^2 \frac{x}{M}$$

where I_c is the current in the conductor in the slot,
R_x is the resistance of length x of the conductor,
M is the section of the conductor in circular mils,

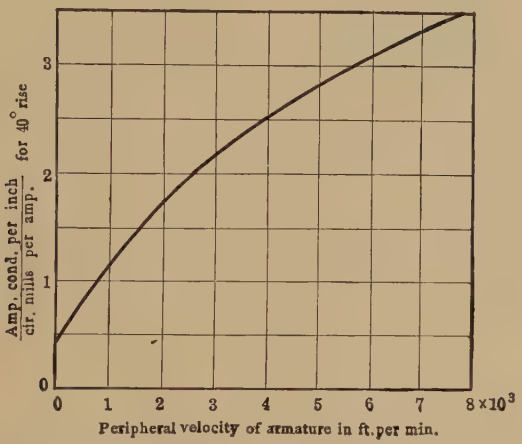

FIG. 89.—Curve of $\frac{\text{ampere conductors loss per inch}}{\text{circular miles per ampere armature.}}$ against peripheral velocity of

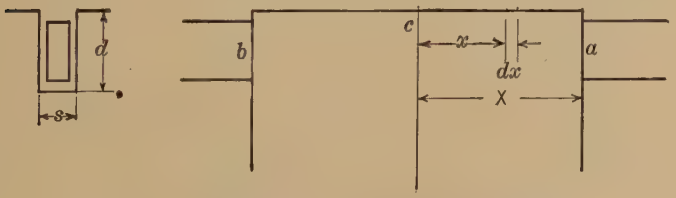

FIG. 90.—Heat paths in an armature conductor.

The difference in temperature between two faces a distance dx apart $= \left(I_c^2 \frac{x}{M}\right)\frac{dx}{A} \times \frac{1}{11.1}$ deg. C.

where A is the section of the conductor in square inches

$$= \frac{M}{1.27 \times 10^6}$$

11.1 is the thermal conductivity of copper in watts per 1 in. cube per 1° C. difference in temperature.

The difference in temperature between the center c and any point X $= \left(I_c^2 \frac{1}{M}\right) \int_0^X \frac{x dx}{A} \times \frac{1}{11.1}$

$$= \frac{I_c^2 \times 1.27 \times 10^6}{M^2} \times \frac{X^2}{2} \times \frac{1}{11.1}$$

$$= \frac{5.7 \times 10^4 \times X^2}{(\text{circular mils per ampere})^2}. \qquad (19)$$

If, for example, the core of the machine is 20 in. long, so that the distance from the center of the core to the end is 10 in., and the circular mils per ampere is 500, then the difference in temperature between the copper at c and that at the end connections = 23° C.

(*b*) Consider now the other case in which it is assumed that the end connections are already so hot that the heat generated in the embedded conductors has to be transmitted through the slot insulation and dissipated by the iron core; it is required to find the difference in temperature between the copper and the surrounding iron.

The copper loss per 1 in. axial length of slot

$$= \frac{\text{conductors per slot} \times I_c^2}{M}$$

$$= \frac{\text{ampere conductors per slot}}{\text{circular mils per ampere}}.$$

If this heat passes through the insulation then the difference in temperature between the inner and outer layers of the insulation

$$= \left(\frac{\text{ampere conductors per slot}}{\text{circular mils per ampere}}\right) \times \frac{\text{thickness of insulation}}{2d + s} \times \frac{1}{0.003}. \qquad (20)$$

where 0.003[1] is the thermal conductivity of ordinary paper and cloth insulation in watts per inch cube per 1° C. difference in temperature, and $2d + s$ is the area of the path per 1 in. axial length of slot.

Take for example the following figures:

Ampere conductors per inch	= 760.
Slot pitch	= 0.88 in.
Ampere conductors per slot	= 760 × 0.88 = 670.
Circular mils per ampere	= 560.
d	= 1.6 in.
s	= 0.43 in.
Thickness of insulation	= 0.07 in., including clearance.

[1] The value of thermal conductivity of insulations varies from 0.002 to 0.004; 0.003 is a fair average value.

Temperature difference between inner and outer layers of insulation

$$= \frac{670}{560} \times \frac{0.07}{3.63} \times \frac{1}{0.003}.$$

$$= 8° \text{ C.}$$

103. Commutator Heating.—The modern D.-C. armature is constructed as shown in Fig. 30; the commutator is smaller in diameter than the armature core, and the commutator necks which join the armature winding to the commutator are separated from one another by air spaces, so that when the armature revolves an air circulation is set up as shown by the arrows in Fig. 91, and cool air is drawn over the commutator surface.

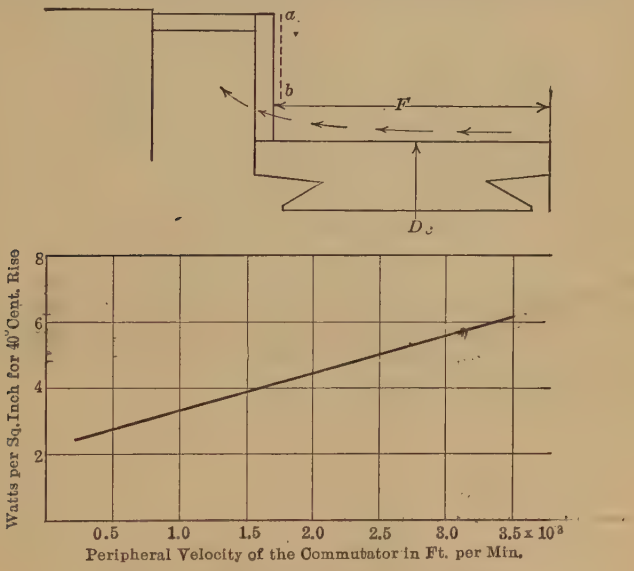

FIG. 91.—Temperature rise of commutators.

The relation between permissible watts per square inch of commutator surface and commutator peripheral velocity, obtained from tests on non-interpole machines, is shown in Fig. 91.

The radiating surface is taken as $\pi D_c F$. It would seem that the radiating surface ought to include that of the commutator necks. It is found, however, that a considerable portion of the commutator neck, such as from a to b, can be closed up without affecting the commutator ventilation or temperature to any great extent; just how much of the surface of the necks should be considered as radiating surface has not yet been determined experimentally.

The heat to be dissipated is assumed to be due to the brush friction and contact resistance losses. There are also losses which cannot be measured, due to poor commutation and to brush chattering. If the commutation is poor and the brushes chatter badly the temperature rise may be higher than that obtained by the use of the curve in Fig. 91, while in cases where the commutation is exceedingly good and where there is no chattering the temperature rise may be lower.

107. Application of Heating Constants.—When designing a new D.-C. machine for a guaranteed temperature rise the core heating is limited by keeping the flux densities below the values given in Art. 103, page 127, and the end connection heating limited by keeping the ratio $\frac{\text{ampere conductors per inch}}{\text{circular mils per ampere}}$ below the values given in Fig. 89, page 129. The approximate increase in temperature of the copper at the center of the core over the temperatures of the iron and of the end connections is found by the use of the formulæ in Art. 105. The design is then compared with designs on similar machines which have already been tested and the densities modified accordingly.

The results of careful tests on similar machines should always take precedence over results obtained from average curves and these curves should always be changing as improvements are made in the methods of ventilation.

CHAPTER XII

PROCEDURE IN DESIGN

108. The Output Equation

$$E = Z\phi_a \frac{\text{r.p.m.}}{60} \times \frac{\text{poles}}{\text{paths}} 10^{-8} \text{ volts (formula (2), page 11).}$$

$$= Z(B_g \psi L_c \tau) \frac{\text{r.p.m.}}{60} \times \frac{\text{poles}}{\text{paths}} 10^{-8} \text{ volts,}$$

and $q = \dfrac{ZI_a}{\text{paths}} \times \dfrac{1}{\pi D_a}$

therefore

$$EI_a = Z(B_g \psi L_c \tau) \frac{\text{r.p.m.}}{60} \times \frac{\text{poles}}{\text{paths}} 10^{-8} \times \frac{q \times \text{paths} \times \pi D_a}{Z}.$$

$$= B_g \times \tau p \times L_c \times \psi \times \text{r.p.m.} \times q \times \pi D_a \times \frac{10^{-8}}{60}.$$

$$= B_g L_c \times \psi \times \frac{\text{r.p.m.}}{60} (\pi D_a)^2 \times 10^{-8} \times q,$$

and

$$D_a^2 L_c = \frac{\text{watts}}{\text{r.p.m.}} \times \frac{60.8 \times 10^{-7}}{B_g \times \psi \times q}. \qquad (21)$$

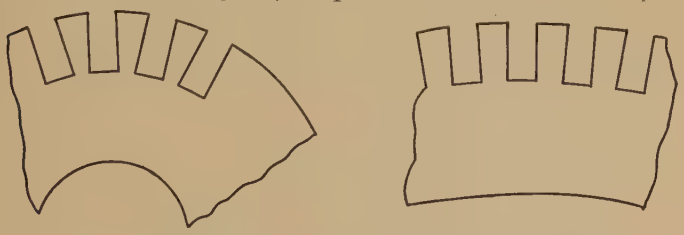

FIG. 92.—Effect of the armature diameter on the tooth taper.

The value of B_g, the apparent average gap density, is limited by the permissible value of B_t, the maximum tooth density, which value, as shown in Art. 103, page 127, is about 140,000 lines per square inch for frequencies up to 30 cycles. That B_g also depends on the diameter of the machine may be seen from Fig. 92; the smaller the diameter the greater the tooth taper and therefore the lower the gap density for a given density at the bottom of the teeth.

Figure 93 shows the relation between B_g and D_a for average machines; in cases where the frequency is greater than 30 cycles per second slightly lower values of B_g must be used.

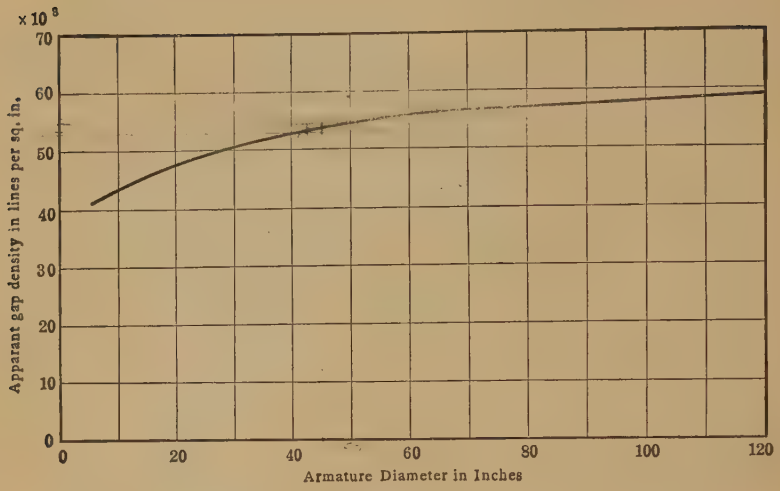

FIG. 93.—Curve of apparent gap density against armature diameter.

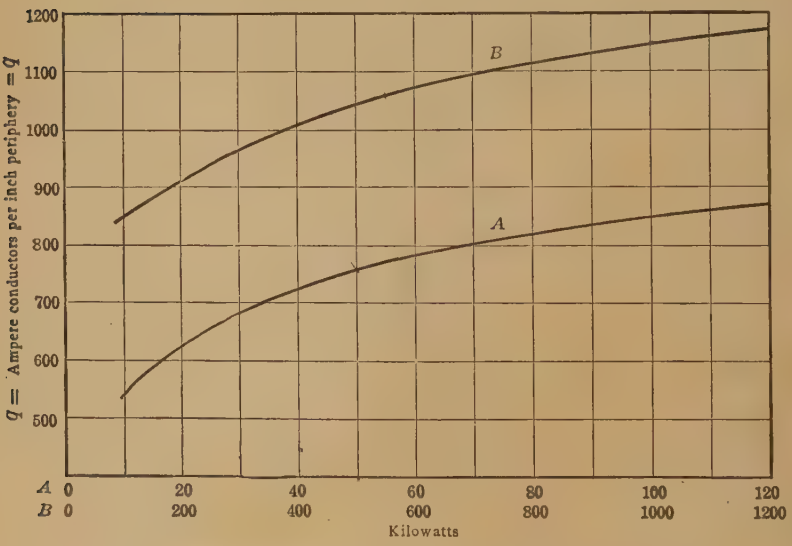

FIG. 94.—Curve of ampere conductors per inch against kilowatts.

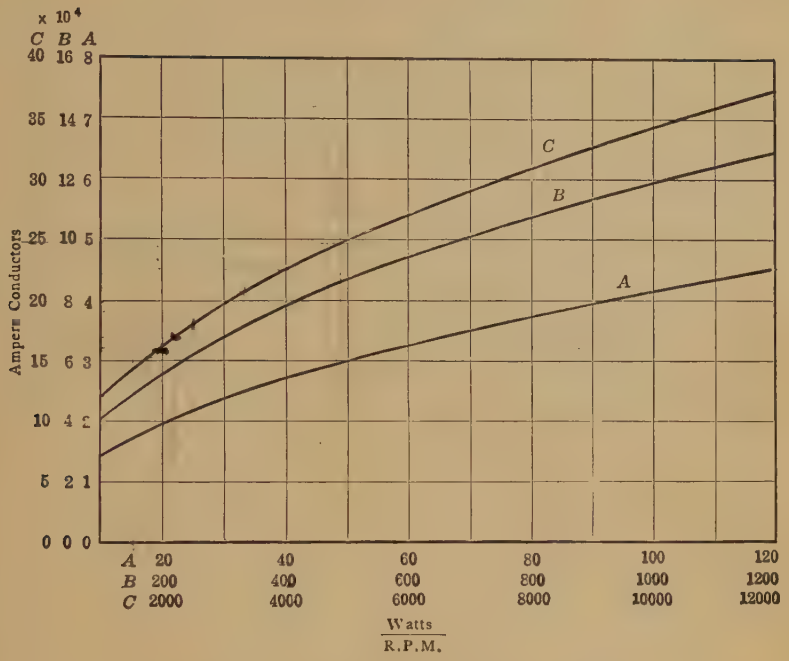

FIG. 95.—Curve of ampere conductors against $\frac{\text{watts}}{\text{r.p.m.}}$.

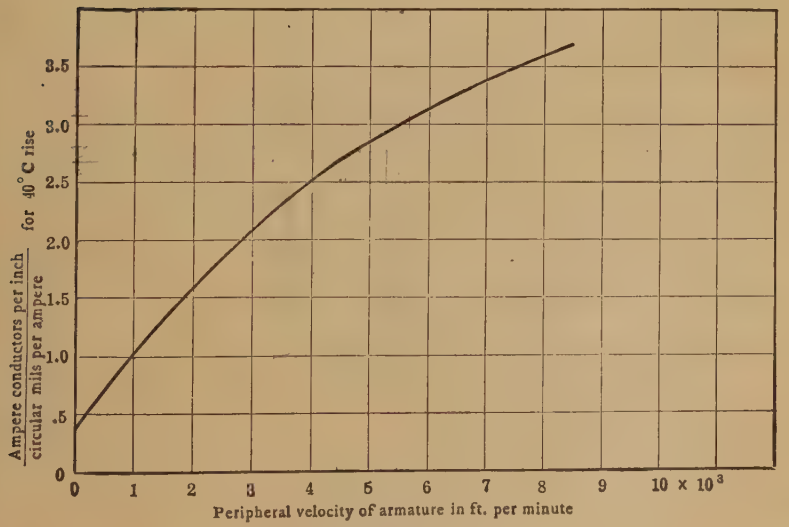

FIG. 96.—Curve of $\frac{\text{ampere conductors per inch}}{\text{circular mils per ampere}}$ against armature velocity.

The value of q, ampere conductors per inch of periphery, in commutating pole machines is limited by heating; except in extreme cases, commutation does not have to be considered. The value of q depends principally on kw. output and the relation between q and kw. for usual designs is plotted in Fig. 94; this curve may be used for preliminary design.

109. The Relation between D_a and L_c.—There is no simple method whereby $D_a^2 L_c$ can be separated into its two components in such a way as to give the best machine. The only satisfactory method is to assume different sets of values of D_a and L_c, work out the design roughly for each case, and choose that which will give good operation at a reasonable cost.

110. Magnetic and Electric Loading.

$$E = Z\phi_a \frac{\text{r.p.m.}}{60} \times \frac{\text{poles}}{\text{paths}} 10^{-8} \text{ volts,}$$

$$\text{therefore } EI_a = \frac{ZI_a}{\text{paths}} \times (\phi_a \times \text{poles}) \frac{\text{r.p.m.}}{60} 10^{-8} \text{ watts,}$$

$$\text{and} \quad \frac{\text{watts}}{\text{r.p.m.}} = \left(\frac{ZI_a}{\text{paths}}\right)(\phi_a \times \text{poles}) \frac{1}{60 \times 10^8}. \tag{22}$$

The term $\frac{ZI_a}{\text{paths}}$ is called the *electric loading* and is the total number of ampere conductors on the periphery of the armature; the larger the value of this quantity the larger the amount of active copper and the smaller the amount of active iron there is in the armature.

The term ($\phi_a \times$ poles) is called the *magnetic loading* and is the total flux entering the armature; the larger its value the larger the amount of active iron and the smaller the amount of active copper there is in the machine.

To get the largest possible output from a given frame both the electric loading and the magnetic loading should be as large as possible.

There is a definite ratio between the magnetic and the electric loading which will give the cheapest machine.

$$\text{The ratio } \frac{\text{magnetic loading}}{\text{electric loading}} = \frac{\phi_a p}{ZI_c}$$

$$= \frac{B_g \psi \tau L_c p}{ZI_c}$$

$$= \frac{B_g \psi L_c}{q}$$

and therefore depends largely on the frame length L_c, which quantity is limited in the following way:

Figure 97 shows one field and one armature coil for a D.-C. machine. A pole of circular section is the most economical so far as the field system is concerned because it has the largest area for the shortest mean turn of field coil. If the pole be rectangular in section then that with a square section has the largest area for the shortest mean turn. It will generally be found that the ratio $\frac{\text{pole pitch}}{\text{frame length}}$ lies between the values 1.1 and 1.7.

The pole pitch is limited by armature reaction; thus in Art. 82 page 101, it was shown that the armature ampere-turns per pole should not exceed 10,000. Further, as pointed out in Art. 57, the

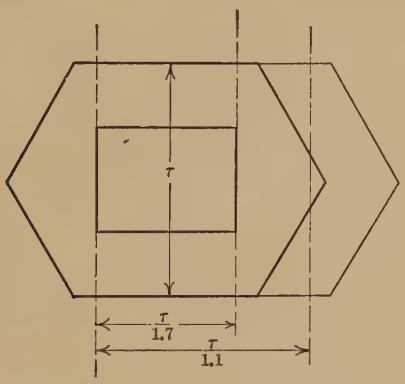

FIG. 97.—Shape of field and armature coils.

ratio $\frac{\text{field ampere-turns per pole (gap + tooth)}}{\text{armature ampere-turns per pole}}$ is seldom less than 0.75. An increase in the armature m.m.f. per pole, therefore, requires a corresponding increase in the m.m.f. of the main field and an increase in the radial length of the poles. Rather than allow the armature ampere-turns per pole to exceed 10,000, it will generally be found economical to increase the number of poles, so that they may not have too great a radial length.

For 10,000 armature ampere-turns per pole, and 1100 ampere conductors per inch, the pole pitch is approximately

$$= \frac{10{,}000 \times 2}{1100}$$

$$= 18.2.$$

L_c therefore, as pointed out above, should not exceed $\frac{18.2}{1.1} = 16.5$ in., except in the special case where the peripheral velocity is already so high that the diameter cannot be increased and the rating can only be obtained by the use of an extra long armature.

If L_c, the frame length = 16.5 in.
B_g, the average gap density = 60,000 lines per square inch.
ψ, the pole enclosure = .65.
q, the ampere conductors per inch = 1100.

then k, the ratio $\frac{\text{magnetic loading}}{\text{electric loading}} = 685$.

For a machine with a small armature diameter the most economical frame length will be less than 16.5 in.; for example, a machine 5 in. in diameter and 16.5 in. long would be more expensive and would give more trouble than one which had the same value of $D_a^2 L_c$, but a diameter of 10 in. and a frame length of $4\frac{1}{8}$ in., so that, since k depends largely on the length L_c its value varies with the diameter of the machine. Now

$$\frac{\text{watts}}{\text{r.p.m.}} = \text{electric loading} \times \text{magnetic loading} \times \frac{1}{60 \times 10^8}$$
$$= k\,(\text{electric loading})^2 \times \text{a constant} \qquad (23)$$

and for each value of $\frac{\text{watts}}{\text{r.p.m.}}$ there is a value of k, and therefore of electric loading (ZI_c), which gives the most economical machine. Figure 95 shows the approximate relation between these two quantities for a line of commutating pole machines, and this curve may be used for preliminary design.

It must be understood, and will be seen from the examples given later, that the value of k may vary over a considerable range without affecting the cost of the machine to any considerable extent. The value of k is also affected by the cost of labor and therefore varies under different conditions of manufacture.

111. Formulæ for Armature Design.

$A - \frac{\text{watts}}{\text{r.p.m.}} = k(\text{electric loading})^2 \times$ a constant (formula (23), page 138), where electric loading $= (ZI_c)$.

$B - D_a^2 L_c = \frac{\text{watts}}{\text{r.p.m.}} \times \frac{60.8 \times 10^7}{B_g \psi q}$. (formula (21), page 133.)

$C - \frac{\text{pole pitch}}{\text{frame length}} = 1.1$ to 1.7. (Art. 110, page 137.)

$D - E = Z\phi_a \frac{\text{r.p.m.}}{60} \times \frac{\text{poles}}{\text{paths}} \times 10^{-8}$. (formula 2, page 11.)

E — Coils $= k\frac{p}{2} \pm 1$ for a series winding. (Art. 23, page 22.)

Slots $= k\frac{p}{2} \pm 1$ for a series winding. (Art. 23, page 22.)

$= k\left(\frac{p}{2}\right)$ for a multiple winding with equalizers (Art. 23, page 22.)

F — Slots per pole should be
at least 9 for small wave-wound armatures.
at least 12 for small lap-wound armatures.
at least 14 for large lap-wound armatures.
(Art. 80, page 96.)

G — Reactance voltage $= k \times S \times$ r.p.m. $\times I_c \times L_c \times T^2 \times \frac{\text{poles}}{\text{paths}} 10^{-8}$ (formula 13, page 91.)

where $k = 1.6$ for series and full-pitch multiple windings;
$= 0.93$ for short-pitch multiple windings.

H — Armature ampere-turns per pole $= \frac{ZI_c}{2p}$ and should be less than 10,000. (Art. 82, page 101.)

J — $\frac{\text{maximum tooth width}}{\text{slot width}} = 1.1$ for large machines;
$= 1.0$ for small machines.
These are approximate values found from practice.

K — Flux density is taken from the following table:

Cycles per second	Tooth density, lines per square inch	Core density, lines per square inch
30	140,000	90,000
40	135,000	75,000
60	130,000	65,000

(Art. 103, page 127.)

L — Commutator dia. $= 0.6$ armature dia. for large machines,
$= 0.75$ armature dia. for small machines.
These are values taken from practice. Except in the case of turbo generators the peripheral velocity of the commutator should not, if possible, exceed 5000 ft. per minute. To keep

below this peripheral velocity it may be necessary to use smaller values for the diameter than those given above.

M – Wearing depth of the commutator, namely, the amount that can be turned off the radius without making the commutator too weak mechanically varies from 0.5 in. on a 5-in. commutator to 1.0 in. on a 50-in. commutator.

N – Brush arc should be as set forth in Art. 81.

P – Watts per square inch brush contact = 35 approximately (Art. 70, page 85.)

Q – Brush friction $= 1.25A\frac{V_r}{100}$ watts (formula (16) page 111.)

112. Preliminary Design.—To simplify the work of preliminary design the necessary formulae and curves are gathered together above and the method of procedure is as follows:

Find the electric loading ZI_c for the given rating, from Fig. 95.

Find $q = \frac{ZI_c}{\pi D_a}$ from Fig. 94.

From these two quantities find D_a the armature diameter.

Tabulate three preliminary designs; one for a diameter 20 per cent larger than that already found and the other 20 per cent smaller.

Find B_g, the apparent gap density, from Fig. 93.

Find L_c, the frame length, from formula B, page 138.

Find p, the number of poles, which should have such a value, that $\frac{\text{pole pitch}}{\text{frame length}}$ lies between the values 1.1 and 1.7. (Art. 110, page 137.)

Find ϕ_a, the flux per pole, $= B_g \psi \tau L_c$ where $\psi = 0.65$ approx.

Find Z, the number of armature face conductors, from formula D.

Choose the smallest diameter machine that will give a ratio $\frac{\text{pole pitch}}{\text{frame length}}$ in accordance with Art. 110.

Find S, the number of commutator segments, from the value of Z and the type of winding used.

Make D_c, the commutator diameter, = (0.6 to 0.75) × (armature diameter) for a first approximation.

Find the commutator length so that the watts per square inch brush contact shall not exceed 35.

Choose between the different designs.

Example.—Determine approximately the dimensions of a D.-C. generator of the following rating:

550 kw., 250 volts, 2200 amperes, 250 r.p.m.

The work is carried out in tabular form as follows (three different diameters are carried through part way for trial):

Ampere conductors	1.68×10^5	(from Fig. 95).		
Ampere conductors per inch	1060	(from Fig. 94).		
Armature diameter	50 in.	40 in.	60 in.	
Apparent gap density	$B_g = 55{,}000$	53,000	56,000	(from Fig. 93).
Frame length	$L_c = 14$ in.	23 in.	9.65 in.	(formula B).
Poles	$p = 10$	6	16	(formula C).
Pole pitch	$\tau = 15.7$ in.	21 in.	11.8 in.	
Flux per pole	$\phi_a = 7.85 \times 10^6$	16.6×10^6	4.15×10^6	
Total face conductors	$Z = 764$	362	1440	(formula D).
Winding	one-turn, multiple, short pitch.			
Commutator segments	$S = 382$	181	720	
Reactance voltage	$R.V. = 2.74$	3.54	2.22	(formula G).
Commutator diameter	$D_c = 35$ in.	28 in.	42 in.	(formula L).
Commutating zone (assumed 0.16τ)	2.5 in.	3.3 in.	1.88 in.	
Slot pitch (assumed 0.05τ)	0.785 in.	1.0 in.	0.58 in.	
Maximum brush arc	1.2 in.	1.6 in.	0.9 in.	
Amperes per square inch brush contact	45	45	45	
Minimum brush length	8.2 in.	10.2 in.	6.8 in.	
$\frac{\text{Magnetic loading}}{\text{Electric loading}} = \frac{\phi_a P}{ZI_c}$	470	750	335	

The second machine, which has an armature diameter of 40 in., has the largest flux per pole and therefore the deepest core and the heaviest yoke. It is the longest machine and therefore the most expensive in core assembly. It has the smallest number of coils and commutator segments and is therefore cheapest in winding and commutator assembly.

The third machine, which has an armature diameter of 60 in., has the smallest flux per pole and therefore the shallowest core and the lightest yoke. It is the shortest machine and therefore the cheapest in core assembly. It has the largest number of coils and commutator segments and is therefore the most expensive in winding and commutator assembly.

The first machine probably costs less than either of the other two; it has also a comparatively low reactance voltage and should commutate satisfactorily.

Before completing the design with the 50-in. diameter it is advisable to design the machine roughly with different numbers of poles in the following way.

Poles	p	8	10	12
Armature diameter		50		
Frame length	L_c	= 14 in.		
Apparent gap density	B_g	= 55,000		
Pole pitch	τ	= 19.65 in.	15.7 in.	13.1 in.
Flux per pole	ϕ_a	= 9.85×10^6	7.85×10^6	6.55×10^6
Total face conductors	Z	= 610	764	916
Winding		one-turn, multiple, short pitch.		
Reactance voltage	$R.V.$	= 2.74	2.74	2.74
Armature ampere turns per pole		10,500	8400	7150
Commutator diameter	D_c	= 35 in.	35 in.	35 in.
Maximum brush arc		1.5 in.	1.2 in.	1.0 in.
Minimum brush length		8.2 in.	8.2 in.	8.2 in.

The first machine is most expensive in material due to the large flux per pole and therefore the deep core and the large section of yoke.

The third machine is most expensive in labor due to the number of coils and commutator segments that are required.

The reactance voltage is the same in each case but the armature ampere-turns per pole is greatest in the first machine and least in the last, so that, so far as commutation is concerned, the last machine is to be preferred, and the first one should not be used if possible.

Armature Design.—Having determined the approximate dimensions of the machine, it is now necessary to design the armature in detail, which is done in tabular form in the following way:

Choose the ten-pole design as the most suitable, then

External diameter of armature	50 in. from preliminary design.
Frame length	14 in. from preliminary design
Center vent ducts	3 × ½ in. wide.
Gross iron in frame length	12.5 in.
Net iron in frame length	11.25 in.
Poles	10
Pole pitch	15.7 in.
Probable flux per pole	7.85×10^6 from preliminary design.
Probable number of conductors	764 from preliminary design.

Winding. One turn, multiple, short pitch.

Total number of slots	180
Conductors per slot	4
Actual number of conductors	720

Coils 360
Commutator segments 360
Reactance voltage 2.6 (formula G)

$$\text{Ampere conductors per inch} = q = \frac{220 \times 720}{\pi \times 50} = 1010$$

Peripheral velocity of armature = 3280 ft. per minute.

$$\frac{\text{Ampere conductor per inch}}{\text{Circular mils per ampere}} = 2.2 \text{ for } 40°\text{C. rise, from Fig. 96.}$$

Circular mils per ampere..... 460
Amperes per conductor at full load 220
Section of conductor = 220 × 460 = 101,000 circular mils.
= 0.0795 sq. in.

$$\text{Slot pitch} = \frac{\pi \times 50}{180} = 0.872 \text{ in.}$$

$$\text{Probable slot width} = \frac{0.872}{2.1} = 0.4 \text{ in. (formula } J\text{).}$$

Determine the dimensions of conductor as follows:

0.4 in. assumed slot width.
0.10 in. width of slot insulation.
0.30 in. available width for copper.

Use strip copper in the slot as shown in Fig. 98. Make the strip 0.13 in. wide.

$$\text{Depth of conductor} = \frac{0.0795}{0.13} = 0.62 \text{ in.}$$

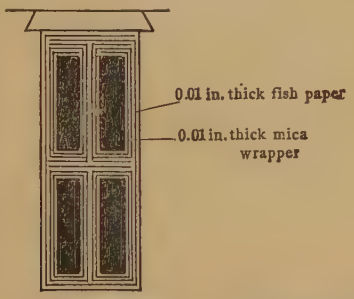

FIG. 98.—Armature coil cross-section.

Slot depth is found as follows:

0.62 depth of each conductor.
0.05 insulation thickness on each coil.

0.67 depth of each insulated coil.
2 number of coils in depth of slot.

1.34 depth of coil space.
0.03 thickness of slot insulation.
0.15 thickness of slot wedge.

1.52 necessary depth of slot; make it 1.55 in. deep.

Diameter at the bottom of the slot = 46.9 in.
Slot pitch at bottom of slot = 0.82 in.
Minimum tooth width = 0.42 in.
Minimum tooth area per pole = $^{18}/_{10} \times 0.65 \times 0.42 \times 11.25 = 55$ sq. in.
Flux per pole with 720 conductors = 8.35×10^6 for 250 volts (formula D).
Maximum tooth density = 152,000 lines per square inch.

This density is not too high, since the frequency of the armature is only about 20 cycles per second.

Note: If the above density had come out too high, it would have been necessary to increase the net frame length.

Flux density in the core, assumed 90,000 lines per square inch.

$$\text{Core area} = \frac{8.35 \times 10^6}{2 \times 90{,}000} = 46.5 \text{ sq. in. (approximately).}$$

$$\text{Core depth} = \frac{\text{core area}}{\text{net iron}} = 4.2 \text{ in.}$$

Internal diameter of armature = 38.5 in.

The above data is now filled in on the armature design sheet shown on page 145 et. seq.

Commutator Design.

Commutator diameter, assume to be 0.7 (armature diameter) = 35 in.
Number of commutator segments = 360.

$$\text{Width of one segment and mica} = \frac{\pi \times 35}{360} = 0.306 \text{ in.}$$

Maximum brush arc = 1.22 in., (formula N).
Use a brush 1 in. thick set at angle of 15°, so that the brush arc = 1.036 in.

Note: For a 15° angle, each inch of brush thickness will cover 1.036 in. on commutator surface.

Segments covered by brush = 3.4.

$$\text{Amperes per set of brushes} = \frac{\text{total current}}{\text{poles}} \times 2 = 440.$$

Probable amperes per square inch of brush contact, 45 assumed.
Necessary brush length = 9.5 in.
Brushes per stud, use 8 brushes, each = 1 in. × 1.25 in.
Actual amperes per square inch of brush contact = 42.5.
Commutator length = 8(1.25 + 0.25) + 1 = 13 in.
Allow 0.25 in. between brushes and 1 in. additional clearance.
Peripheral velocity of commutator = 2300 ft. per minute.
Total brush contact area = 10 × 8 × 1.25 × 1.036 = 103.5 sq. in.
Commutator friction loss..... 2980 watts (formula Q).
Volts drop per pair of brush contacts..... 2.
Contact resistance loss = 2 × 2200 = 4400 watts.

$$\text{Watts per square inch of commutator surface} = \frac{2980 + 4400}{\pi \times 35 \times 13} = 5.17.$$

Allowable watts per square inch of commutator surface for 40°C. temperature rise = 4.8 (see Fig. 91).

$$\text{Probable temperature rise on commutator} = \frac{5.17}{4.8} \times 40 = 43° \text{ C.}$$

Had the temperature rise come out too high, it would have been necessary to have used brushes with lower contact resistance, or else to have increased the commutator radiating surface.

The above data is now filled in on the design sheet shown below.

D. C. Design Sheet

Armature

Ex. dia	50
In. dia	38½
Frame length	14
End ducts	2–½
Center ducts	3–½
Gross iron	12.5
Nett iron	11.25
No. of slots	180
Size of slot	0.4 × 1.55
Cond. per slot	4
Total cond	720
Size of cond	0.13 × 0.62
Coils	360
Turns per coil	1
Type of winding	Multiple
Pitch of winding	Short one slot
Slot pitch	0.872–0.82
Tooth width	0.472–0.42
Tooth/slot	1.18
Core depth	4.2
Pole pitch	15.7
Pole enclos	0.65
Tooth area p. p	55
Core area	46.5
Appar. gap area	143
Perip. Vel	3280

Magnetic Circuit

Flux per pole	8.35×10^6
Leakage Factor	1.18
Density: app. tooth	152,000
act. tooth	145,000
core	88,500
pole	99,000
yoke	80,000
app. gap	58,500
Pole section	99.4
Yoke section	61.5
Weight teeth, pounds	396
core, pounds	1510
Frequency	20.83
Iron loss teeth	2970
core	3780

Magnetic Circuit (*Continued*)

Gap clearance	0.2
Fringing const	1.15
AT. gap	4240
tooth	1680
core	155
yoke	290
pole	690
AT. total	7055

Commutator

Dia	35
Face	13
Bars	360
Bar and mica	0.306
Wearing depth	1
Brush arc	1.036
No. of studs	10
Brushes per stud	$8(1 \times 1\frac{1}{4})$
Perip. vel	2300
Friction watts	2980
Brush drop	2
Current density	42.5
Resist. watts	4400
Watts/surface	5.17
Temp. rise	43
Av. volts per seg	6.95

Arm. Heating and Commut.

Amp. cond./periphery	1010
Circ. Mils/Amp	460
Length of cond	39.25
Copper loss, k. w	13.6
Volts drop, arm. + brush	8.2
Arm. A.T. per pole	7900
ATg+t/arm.AT.p.p	0.75
Reactance volts	2.6
Av. volts per seg./React. volts	2.68

Series Coils

AT. per pole	2345
Turns per coil	5
Current	470
Cir. Mils/Amp	930
Section of wire, sq. in	0.345
Resist. of coil	0.7×10^{-3}
Volts per coil	0.33
Watts/surface	0.89
Rad. surface, sq. in	174
Length of coil	2.625
Size of wire	$2(0.14 \times 1.25)$

Commutating Pole

Amp. turns per pole	11,000
Turns per coil	10
Axial length of pole	12
Pole arc	2
Gap density	16,500
Gap clearance	0.25
Ext. surface of coil	324
Watts/surface	1.2
Loss in coil, watts	392
Size of wire	5(0.128 × 1.25)

Shunt Coils

Volts per coil	20
Mean turn	47.5
Ex. perip	52.5
Size of wire, circ. mils	16,510
Length of coil	7.5
Depth of coil	1.26
Space factor	0.64
Turns per coil	477
Shunt current	14.8
Circ. Mils/Amp	1115
Watts/surface	0.78
Temp. rise	41° C.

Effic. and Losses

Arm. copper loss, watts	13,600
Comm. loss: frict., watts	2980
resist., watts	4400
Excit. loss: shunt, watts	3700
series, watts	1550
com. pole, watts	3920
Iron loss, watts	6750
Load losses, watts	5500
Effic. full load, per cent	92.6
¾	93.0
½	92.4

Rating

KW	550
Volts	250
Amperes	2200
Revs. per min	250
Magnetic/elec. loading	530
Output factor $= \frac{\text{k.w.} \times 10^5}{\text{r.p.m.} \times D_a^2 L_c}$	6.3
Poles	10

CHAPTER XIII

MOTOR DESIGNS AND RATINGS

114. Procedure in Design.—D.-C. motor design is carried out in exactly the same way as is generator design. There is one exception, however, that should be noted and commented upon. In many cases, particularly in high-speed motors, the procedure as laid down in Chap. XII would lead to a two-pole design; two-pole designs are very rarely used in modern motors. The reasons are that, first, the space for entrance of air for ventilation between the shaft and the windings is so limited that it is difficult, sometimes impossible, to secure proper ventilation and, second, the overhang of the end windings is so long that the distance between bearings is unduly great, resulting in so long and flimsy a shaft as to be inadmissible. Reference to Art. 104, Fig. 88, will show that the total overhang of the end windings is approximately equal to the pole pitch and in two-pole designs this leads to an excessive length between bearings. In these high-speed designs where two poles would be dictated by the procedure of Chap. XII, the diameter is usually increased arbitrarily so that four poles may be used; four poles is the minimum that is ordinarily used on modern motors.

Take two specific motor ratings and follow through the designs.

Assume the two following machines:

Motor—30 hp.—900 r.p.m.—120 volts.

Motor—40 hp.—750 r.p.m.—120 volts.

Following the procedure of Chap. XII we may tabulate the design of these two motors as follows:

	30 Hp. 900 Revolutions	40 Hp. 750 Revolutions
Probable efficiency	90 per cent	90 per cent
Full-load current-amperes	208	276
KW. output	25	33.2
Ampere conductors (Fig. 95)	22,000	25,000
Ampere conductors per inch (Fig. 94)	660	700
Armature diameter, inches	10.6	11.4
Gap density (Fig. 93)	44,000	45,000
D^2L (formula *B*, p. 138)	900	1,310
Frame length, inches	8	10

If we apply formula *C*, page 138, we will see that both machines fall between two poles and four poles. For reasons before stated, two poles should not be considered; if four poles are to be used, the diameter should be somewhat increased in order to get a pole that is more nearly square in cross-section.

We will now follow through the designs of these two motors assuming the actual armature diameters that are used by the two large U. S. manufacturing companies. The 30-hp. motor is as designed by manufacturer A and the 40-hp. by manufacturer B.

In passing, it might be observed that undoubtedly a cheaper machine could be produced if the diameters were somewhat decreased from those deduced above and two-pole designs used, but the difficulty in ventilating and the resulting long shaft would make such a course out of the question.

It may also be observed that the actual motors hereinafter tabulated as made by the two large manufacturing companies come within about 6 per cent of having the same D^2L as that deduced above; in one case the D^2L actually used is somewhat higher than the deduced value and in the other case, somewhat lower.

	30 Hp. 900 Revolutions Manufacturer A	40 Hp. 750 Revolutions Manufacturer B
Armature diameter, inches	13	13.5
Internal diameter	5	5.25
Length	5	6.875
End ducts	2 × 0.375	2 × 0.375
Center ducts	1 × 0.375	1 × 0.375
Gross iron, inches	3.875	5.75
Net iron, inches	3.48	5.17
Slots, number	37	41
Conductors per slot	6	6
Slots, size-inches	1.628 × 0.32	1.425 × 0.39
Conductor, size	0.059 × 0.625	0.08 × 0.55
Coils, number	111	123
Turns per coil	1	1
Total conductors	222	246
Winding, (series) in slots	1 and 10	1 and 11
Slot pitch, inches	1.10 maximum 0.826 minimum	1.033 maximum 0.816 minimum
Tooth width	0.78 maximum 0.506 minimum	0.643 maximum 0.426 minimum
$\frac{\text{Maximum tooth width}}{\text{slot width}}$	2.44	1.65

	30 Hp. 900 Revolutions Manufacturer A	40 Hp. 750 Revolutions Manufacturer B
Core depth, inches	4.0	2.7
Pole pitch, inches	10.2	10.6
Per cent enclosure	68.5	57
Minimum tooth area per pole, square inches	11.1	13.01
Core area, square inches	13.9	13.9
Apparent gap area per pole, square inches	35.0	41.7
Densities, iron loss, excitation		
Flux per pole	1.8×10^6	1.95×10^6
Max. tooth density, apparent	162,000	150,000
Maximum tooth density, area actual	157,000	145,000
Core density	65,000	70,000
Apparent gap density	51,500	46,800
Weight teeth, pounds	64.4	64.8
Weight core, pounds	53	97.5
Frequency	30	25
Iron loss, watts	1032	745
Air gap clearance, inches	0.125	0.175
Carter coefficient	1.15	1.12
Ampere-turns, gap	2,320	2,880
Ampere-turns, teeth	1,215	710
Ampere-turns gap, and teeth	3,535	3,590
Ampere-turns-armature per pole	2,910	4,275
$\frac{\text{Field ampere-turns per pole-teeth and gap}}{\text{Armature ampere-turns per pole}}$	1.21	0.84
Total ampere-conductors-armature	23,300	34,200
Ampere conductors per inch	570	805
Circular mils per ampere	448	402
Length of conductor, inches per turn	36	44
Armature copper loss, watts	920	1,870
$\frac{\text{Magnetic loading}}{\text{Electric loading}}$	310	228

There are some points in the two above designs that should be further discussed. Design *A* uses a comparatively high magnetic density, a high m.m.f. in the field and high magnetic loading; this results in an unusually high ratio

$$\frac{\text{field ampere turns per pole-gap and teeth}}{\text{armature ampere turns per pole}}.$$

The high magnetic loading of design *A* leads naturally to a comparatively low electric loading; the value of q in this design (ampere conductors per inch of periphery) is about 15 per cent less than dictated by curve 94. Design *B* on the other hand has a value of q about 15 per cent higher than that dictated by Fig.

94. The ratio $\frac{\text{field ampere-turns per pole-gap and teeth}}{\text{armature ampere-turns per pole}}$ is much nearer the normal that is indicated in Chap. VI. for machine *B* than for machine *A*.

In considering these two designs, it must be borne in mind that the methods of designing used in large companies almost never demand that a design shall be worked out *de novo* as we have in the preceding chapters. These companies have a large range of frames and punchings already available and the designer's problem in general is to meet given requirements using the smallest possible available frame and the minimum length of active material. The relations that have been set forth in Chap. XII will, in general, give the cheapest and best design but there is a wide latitude of departure from some of these relations within which a suitable machine can still be produced. The above table giving the actual designs of two specific machines shows this.

Additional details concerning the design of the commutators in these machines are as follows:

	30 Hp. 900 Revolutions	40 Hp. 750 Revolutions
Commutator	Manufacturer "A"	Manufacturer "B"
Diameter, inches	8.25	9.5
Per cent armature diameter	63.6	70.5
Face length, inches	5.625	7.0
Bars, number	111	123
Width one bar and mica, inches	0.233	0.243
Mica, inches	0.03	0.03
Wearing depth, inches	0.312	0.375
Brush arc, inches	0.625	0.625
Brush studs, number	4	4
Brushes per stud	3	4
Brushes, size	0.625×1.25	0.625×1.25
Amperes per square inch brush contact	45	44
Peripheral velocity, feet per minimum	1940	1860
Friction loss, watts	169	216
Volts per pair of brushes	2	2
Contact resistance loss, watts	416	552
Watts per square inch surface	4	3.68
Probable temperature rise, commutator	41°	36°
Average volts per bar	4.32	3.9
Reactance voltage	1	1.4

The commutator design presents no difficulties. It should be noted in particular that the reactance voltage is low in both these

machines and no trouble from sparking should be anticipated; heating also should be within reasonable bounds.

115. Calculation of Efficiency.—The calculation of efficiency involves the calculation of the individual losses that are enumerated in Chap. X, Art. **88.** The value of most of these losses, as calculated, is given in Art. 114. Those not yet calculated are bearing friction, field copper loss and load losses.

To estimate bearing friction, we must know—or assume—the bearing sizes. In this case, suppose we assume that the bearings are 2.5 × 6 in. for the 30 hp. motor and 2.5 × 8 in. for the 40 hp. The rubbing velocity well then be 5.9 ft. per minute for the 30 hp. and 4.9 ft per min. for the 40 hp. motor; the friction loss will be 350 watts in each case (Art. 89).

The excitation loss may be estimated as follows:

	30-HP. MOTOR	40-HP. MOTOR
Ampere-turns, gap and teeth (p. 73)	3,535	3,590
Total ampere-turns (add 25 per cent)	4,430	4,500
Apparent gap density (from design)	51,500	46,800
Pole density (assumed)	85,000	85,000
Pole area $\left(\frac{51500}{85000} \times \text{gap area}\right)$	21.2	
$\left(\frac{46800}{85000} \times \text{gap area}\right)$		24.0
Pole length (axial)	4.75	6.62
Pole width	4.46	3.62
Pole periphery	18.4	20.5
Depth field winding (assumed)	1.25	1.25
External periphery of field	28.4	30.5
Length mean turn	23.4	25.5
Watts per square inch (Fig. 63), 40° rise	0.76	0.78
Space factor (Fig. 64), approximately	0.65	0.65
Radial length pole (see Art. 60) = $\frac{\text{ampere-turns}}{1000}\sqrt{\frac{\text{length mean turn}}{\text{external periphery} \times \text{watts per square inch} \times df \times sf \times 1.27}}$		
Radial length pole, inches	4.56	4.6
Total excitation loss, watts	407	435

The load losses, according to the A. I. E. E. standards rules set forth in Art. 99, shall be taken at 1 per cent; that is 250 watts for the 30-hp. and 332 for the 40-hp. motor.

The total estimated losses and the resulting estimated efficiency may therefore be tabulated as follows:

	30-HP.	40-HP.
Bearing friction	350	350
Excitation loss	407	435
Iron loss	1,032	745
Armature, copper loss	920	1,870
Commutator friction loss	169	216
Commutator resistance loss	415	552
Load losses	250	332
Total losses	3,543	4,500
Useful output, full load	22,400	29,400
Input, full load	25,943	33,900
Efficiency $= \frac{\text{output}}{\text{input}}$	86.5	86.7

The estimated efficiency that we finally arrive at is in both cases somewhat lower than the assumed efficiency we started with. The estimated efficiency is used to get current and the losses depend partly on this assumed current. The estimated I^2r losses would therefore have to be somewhat increased to get complete accuracy. On the other hand, the iron losses have been estimated on the basis that the magnetic flux is sufficient to produce the entire applied e.m.f. The e.m.f. actually necessary is the applied e.m.f. less the Ir drop in armature and commutating pole windings. This drop is something of the order of 5 per cent in each case which will reduce the iron losses by nearly 10 per cent. These two adjustments in the estimated efficiency will nearly cancel each other thereby leaving the estimated efficiency nearly what we have arrived at.

116. Designing for Other Speeds, Voltages and Out-puts.— In practice, the designer rarely is obliged to design a machine from the beginning particularly in the smaller sizes; he has various diameters of frame, and armature punchings with various numbers of slots. It is the designers task to select the frame diameter, frame length and number of slots that will meet any specific requirements that may be demanded by the prospective user. There is considerable latitude in regard to the electric loading and magnetic loading that may be selected. For a normal machine these values are fixed by Figs. 93, 94, and 95. However, the values given in these curves may be raised or lowered by 10 or even 15 per cent and still obtain a passable machine. If in any case the electric loading is increased, the magnetic loading should be decreased, and *vice versa*.

Suppose, for instance, it were required to design a 30-hp., 120-volt motor to run at 800 r.p.m. instead of 900 r.p.m., as in the

design above tabulated. One method that might be considered would be simply to increase the magnetic density leaving all other proportions the same. However, the apparent magnetic density is already 162,000 maximum in the teeth and 51,500 in the air-gap. To increase this so as to reduce the speed from 900 to 800 r.p.m. would require increasing these densities by about 12 per cent. The magnetic loading on this design is already near the limit and it would be impossible to increase it still further by the required amount. On the other hand, the electric loading is below normal and could be readily increased provided the magnetic loading could be decreased. If another armature punching of a larger number of slots is available, this change could readily be accomplished. Suppose, for instance, another armature punching with 49 slots were available—having approximately the same total slot area as the 37 slot punching. If the same number of turns per slot and the same length of frame were used for the 800-r.p.m. 30-hp. design, as for the 900-r.p.m. this would mean an increase in electric loading in the ratio $^{49}/_{37}$ = 122 per cent. On the other hand, the magnetic loading would be decreased in the ratio $^{37}/_{49} \times {}^{900}/_{800}$ = 85 per cent. The electric loading is already below normal and the magnetic loading above normal, so that this modification would probably give a machine that would be acceptable. Final judgment would have to be based on the results of tests on this frame for ratings, voltages and speed which come as near to the requirements in hand as possible.

CHAPTER XIV

ALTERNATOR WINDINGS

117. Single-phase Fundamental Winding Diagram.—Diagram *A*, Fig. 99, shows the essential parts of a single-phase alternator which has one armature conductor per pole. The direction of motion of the armature conductors relative to the magnetic field is shown by the arrow, and the direction of the generated

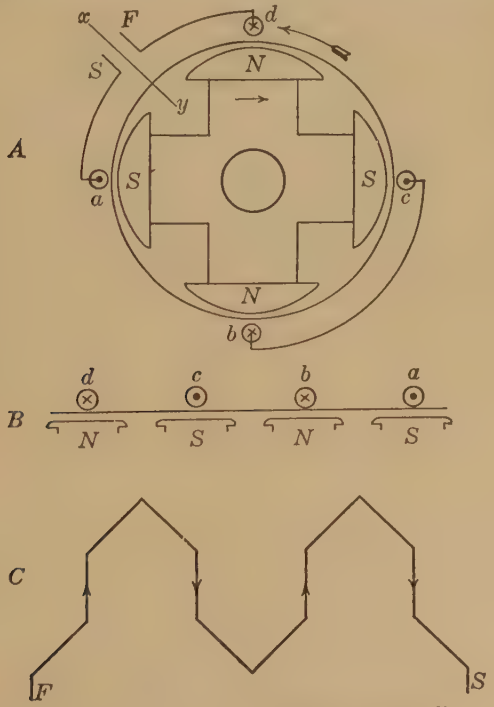

Fig. 99.—Fundamental single-phase winding diagram.

e.m.f. in each conductor is found by Fleming's three-finger rule and is indicated in the usual way by crosses and dots.

The conductors *a*, *b*, *c* and *d* are connected in series so that their voltages add up, and the method of connection is indicated in diagram *A*. Such a connection diagram, however, becomes

exceedingly complicated for the windings that are used in practice and a simpler diagram is that shown at *C*, Fig. 99, which is got by splitting diagram *A* at *xy* and opening it out on to a plane.

Diagram *C* may be called the fundamental single-phase winding diagram because on it all other single-phase diagrams are

FIG. 100.—Fundamental two-phase winding diagram.

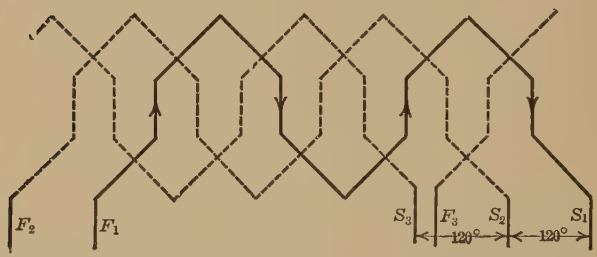

FIG. 101.—Fundamental three-phase winding diagram.

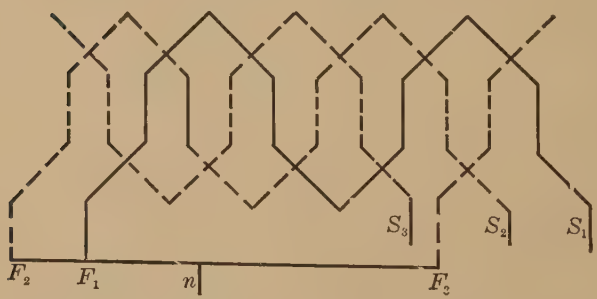

FIG. 102.—Fundamental three-phase Y-connected winding.

based. The letters *S* and *F* stand for the start and finish of the winding, respectively.

118. The Frequency Equation.—The voltage generated in any one conductor goes through one cycle while the conductor

moves relative to the magnetic field through the distance of two pole pitches, so that one cycle of e.m.f. is completed per pair of poles;

$$\text{the cycles completed per revolution} = \frac{p}{2},$$

$$\text{the cycles completed per second} = \frac{p}{2} \times \frac{\text{r.p.m.}}{60}.$$

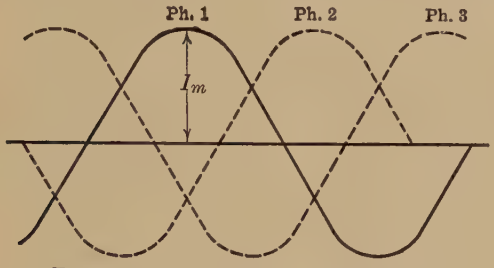

FIG. 103.—Currents in the three phases.

Therefore f, the frequency in cycles per second

$$= \frac{p \times \text{r.p.m.}}{120}. \qquad (23)$$

119. Electrical Degrees.—The e.m.f. wave of an alternator is represented by a harmonic curve and therefore completes one cycle in 2π or 360 deg.; as shown above, the e.m.f. of an alter-

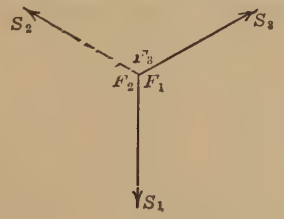

FIG. 104.—Voltage vector diagram for a Y-connected winding.

nator completes one cycle while the armature moves, relative to the poles, through the distance of two pole pitches; it is very convenient to call this distance 360 electrical degrees.

120. Two- and Three-phase Fundamental Winding Diagrams. Figure 100 shows the fundamental winding diagram for a two-phase machine. A two-phase winding consists of two single-phase windings which are spaced 90 electrical degrees apart so that the e.m.fs. generated in them will be out of phase with one another by 90 deg.

Figure 101 shows the fundamental winding diagram for a three-phase machine. A three-phase winding consists of three single-phase windings which are spaced 120 electrical degrees apart so that the e.m.fs. generated in them will be out of phase with one another by 120 deg.

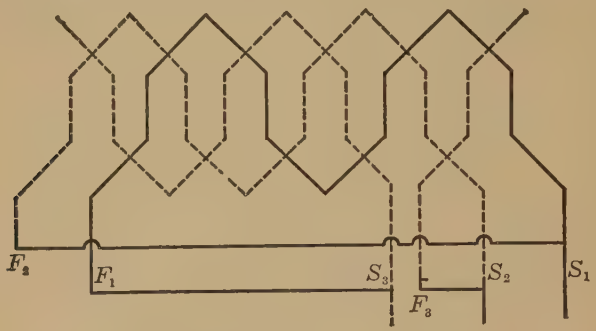

FIG. 105.—Fundamental three-phase Δ-connected winding.

121. Y- and Δ-connection.—It will be seen from Fig. 101 that a three-phase winding requires six leads, two for each phase. It is usual, however, to connect certain of these leads together so that only three have to be brought out from the machine and connected to the load.

Figure 102 shows the Y-connection used for this purpose. The three finishes of the winding are connected together to form a

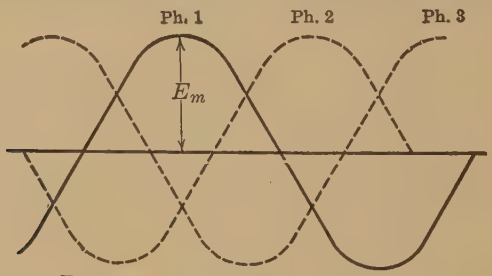

FIG. 106.—E.M.F. in the three phases.

resultant lead n and the current in this lead at any instant is the sum of the currents in the three phases. The current in each of the three phases at any instant may be found from the curves in Fig. 103 from which curves it may be seen that at any instant the sum of the currents in the three phases is zero, so that the lead n may be dispensed with and the machine run with the three leads S_1, S_2 and S_3.

Figure 104 shows the voltage vector diagram for a Y-connected winding, and from the shape of this diagram the connection takes its name.

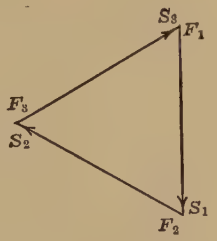

FIG. 107.—Voltage vector diagram for a Δ-connected winding.

Figure 105 shows the Δ-connection. The winding is connected to form a closed circuit according to the following table:

S_1 to F_2
S_2 to F_3
S_3 to F_1

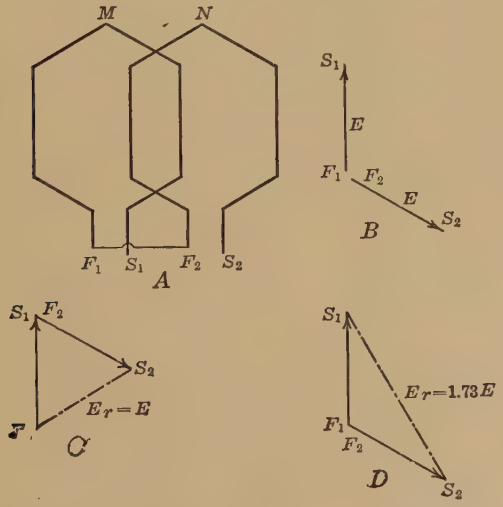

FIG. 108.—Voltage relations in three-phase windings.

It would seem that, since the windings form a closed circuit, the e.m.fs. of the three phases would cause a circulating current to flow in this circuit; however, the three e.m.fs. are 120 deg. out of phase with one another, and an inspection of Fig. 106 will show that the resultant of three such e.m.fs. in series is zero at any instant.

Figure 107 shows the voltage vector diagram for a Δ-connected winding The phase relation of the three voltages is the same as in Fig. 104.

122. Voltage, Current and Power Relations in Y- and Δ-connected Windings.—Let M and N, Fig. 108, represent two phases of a three-phase winding; the voltages generated therein are out of phase with one another by 120 deg. and are represented by vectors in diagram B.

If the phases are connected in series so that F_2 is connected to S_1, then the voltage between F_1 and S_2 = the voltage from F_1 to S_1 + the voltage from F_2 to $S_2 = E_r$, diagram C, and is equal to E, the voltage per phase.

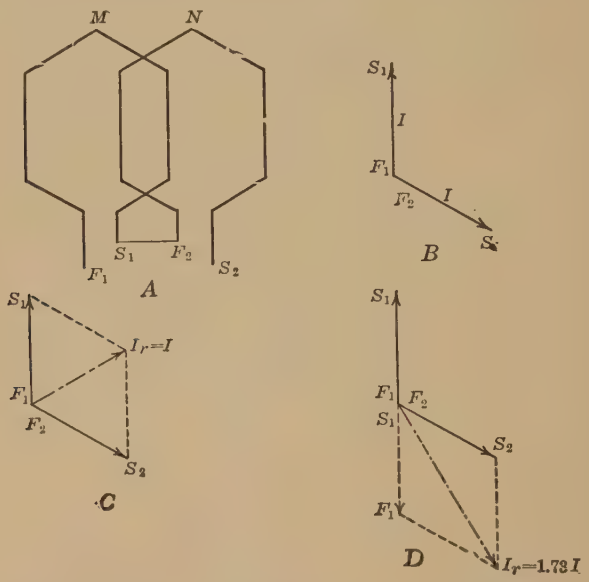

FIG. 109.—Current relations in three-phase windings.

If, however, as in a Y-connected winding, F_2 is connected to F_1, then the voltage between S_1 and S_2 = the voltage from S_1 to F_1 + the voltage from F_2 to $S_2 = E_r$, diagram D, which is equal to 1.73 E.

In a Y-connected machine, therefore, the voltage between terminals is 1.73 times the voltage per phase, while the current in each line is the same as the current per phase.

Let M and N, Fig. 109, represent two phases of a three-phase winding; the currents therein are out of phase with one another by 120 deg. and are represented by vectors in diagram B.

If the two phases are connected in parallel so that F_2 is connected to F_1, then the current in the line connected to F_1F_2 = the current from F_1 to S_1 + the current from F_2 to S_2 = I_r, diagram C, and is equal to I, the current per phase.

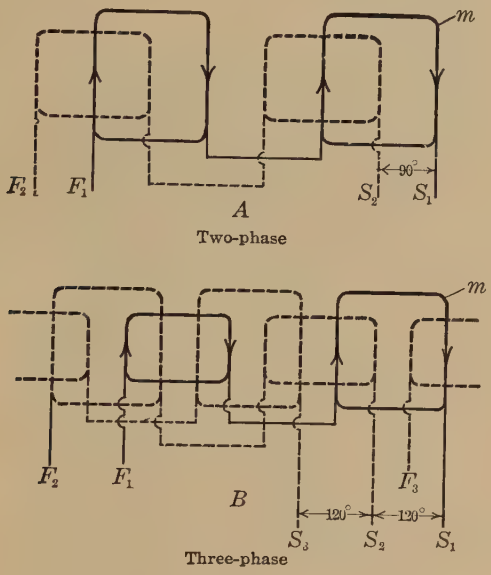

FIG. 110.—Four-pole chain winding.

If, however, as in a Δ-connected winding, S_1 is connected to F_2, then the current in the line connected to S_1F_2 = the current from S_1 to F_1 + the current from F_2 to S_2, which is equal to the current from F_2 to S_2 − the current from F_1 to S_1 = I_r, diagram D, = 1.73I.

In a Δ-connected machine, therefore, the current in each line is 1.73 times the current in each phase, while the voltage between terminals is the same as the voltage per phase.

The power delivered by a three-phase alternator

$= 3\ E\ I \cos \theta,$

$= 1.73\ E_t I_l \cos \theta$ for either Y- or Δ-connected machines

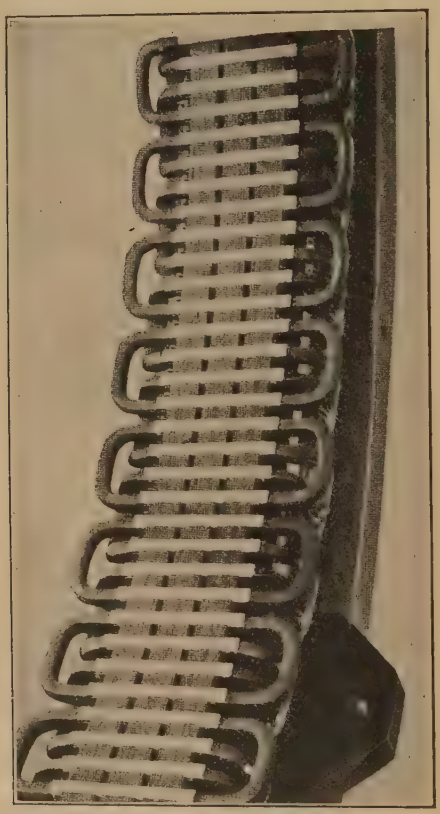

Fig. 111.—Three-phase chain winding with one slot per phase per pole.

where E is the voltage per phase,

I is the current per phase,

E_t is the voltage between terminals,

I_l is the current in each line,

θ is the phase angle between E and I.

123. Windings with Several Conductors per Slot.—When there are more than one conductor per slot, a slight modification must

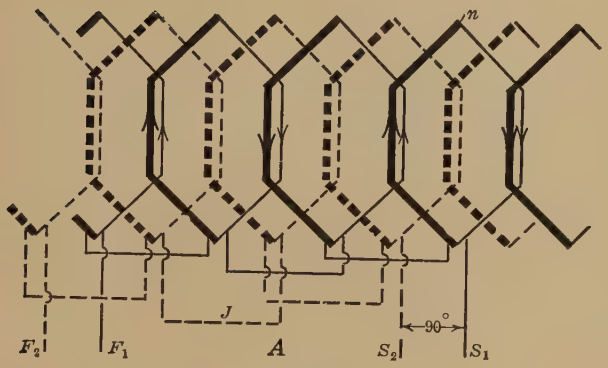

Two phase

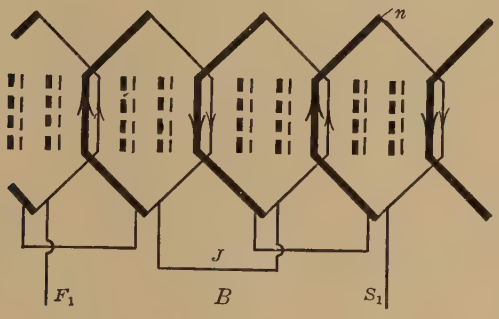

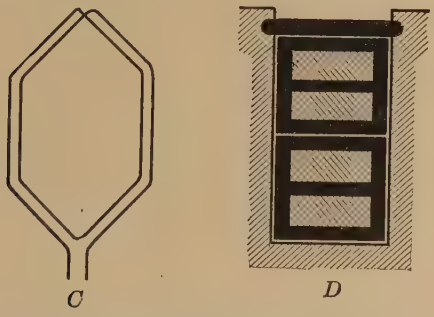

FIG. 112.—Four-pole double-layer winding.

be made on the fundamental winding diagrams. Consider, for example, the case where there are four conductors per slot.

One method of connecting up the winding is shown in Fig. 110, which shows the two- and three-phase diagrams. Each coil *m* consists of four turns of wire as shown in diagram *C*; these wires are insulated from one another and are then insulated in a group from the core so that a section through one slot and coil is as shown in diagram *D*. On account of its appearance this type of winding is called the *Chain Winding*.

Figure 111 shows part of a machine, which is wound according to diagram *B*, Fig. 110; the method whereby one coil is made to jump over the other is clearly shown.

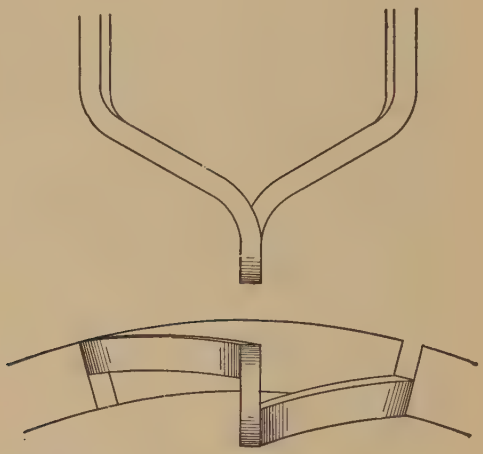

FIG. 113.—Coil for a double-layer winding.

Another method of connecting up the winding is shown in Fig. 112, which shows the two- and three-phase diagrams. Each coil *n* consists of two turns of wire as shown in diagram *C*; these wires are insulated from one another and are also insulated from the core so that a section through one slot and coil is as shown in diagram *D*.

The coils are shaped as shown in Fig. 113; one side of each coil, represented in the winding diagrams by a heavy line, lies in the top of a slot, while the other side, represented by a light line, lies in the bottom of a slot about a pole pitch further over on the armature. The whole winding lies in two layers and is, therefore, called the *Double-layer Winding*.

124. Comparison between Chain and Double-layer Windings.

Chain	Double-layer
The number of conductors per slot may be any number.	The number of conductors per slot must be a multiple of two.
The number of coils is half of the number of slots.	The number of coils is the same as the number of slots.
There are several shapes of coil; therefore, a large outlay is necessary for winding tools, and a large number of spare coils must be kept in case of break-down.	The coils are all alike; therefore, the number of winding tools is a minimum and so also is the number of spare coils that must be kept
The end connections of the winding are separated by large air spaces.	The end connections are all close together and, therefore, more liable to break-down between phases than in the chain winding.

The chain winding is the easier to repair because, in order to get a damaged coil out of a machine, fewer good coils have to be removed than in the case of the doubled-layer winding; this may be seen from the chain winding and the corresponding double-layer winding shown in Figs. 117 and 118.

The chain winding requires the larger initial outlay for tools, but the winding itself is the cheaper because there are not so many coils to be formed and insulated.

The amount of the slot section that is taken up by insulation is less with the chain than with the double-layer winding, as may be seen by comparing diagrams *D*, Figs. 110 and 112.

The chain winding is now obsolete in U. S. practice; it is still used in European practice, perhaps 50 per cent of the European machines being still built of this type.

125. Wave Windings.—The connections from coil to coil, marked *J* in diagram *A*, Fig. 112, and called jumpers, must have the same section as the conductors in the winding. When there are only two conductors per slot, the conductors are large in section and the jumpers become expensive; in such a case the wave winding is generally used because it requires very few jumpers. Such a winding is shown in Fig. 114, which shows the two- and three-phase diagrams.

126. Windings with Several Slots per Phase per Pole.—Modern alternators have seldom less than two slots per phase per pole. The principal advantages of the distributed winding are that the wave form is improved and the total radiating surface of the coils increased; the self-induction of the winding is reduced but that, as shown in Art. 203, page 288, is in some cases a disadvantage.

127. Windings with Several Circuits per Phase.—The windings shown down to this point have all been single-circuit windings, that is, windings in which all the conductors of one phase are connected in series with one another. It is, however, often necessary to use more than one circuit.

Suppose, for example, that a large number of small alternators are to be built for stock; the winding used would be such that by

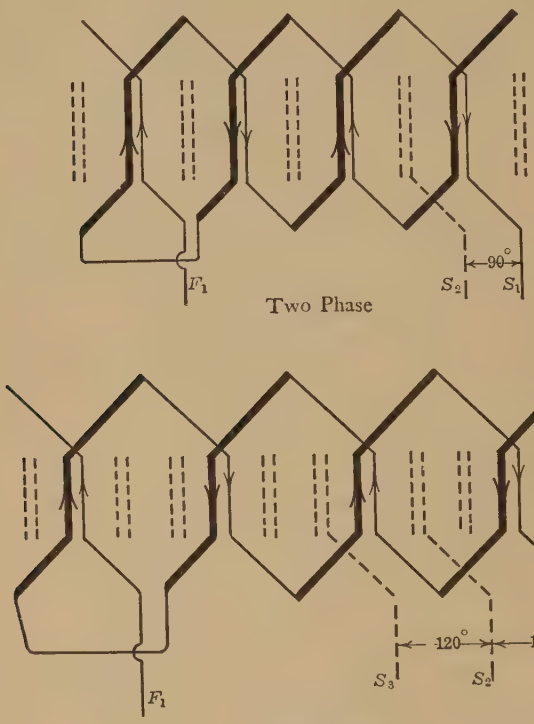

FIG. 114.—Four-pole wave winding.

a slight change in the connections, it could be made suitable for a number of standard voltages.

Figure 115 shows the winding diagram for one phase of an eight-pole three-phase machine with two slots per phase per pole.

Diagram *A* shows a single-circuit connection.

Diagrams *B*, *C* and *D* show possible two-circuit connections.

When a winding is divided up into a number of circuits in parallel, it is necessary, in order to prevent circulating currents,

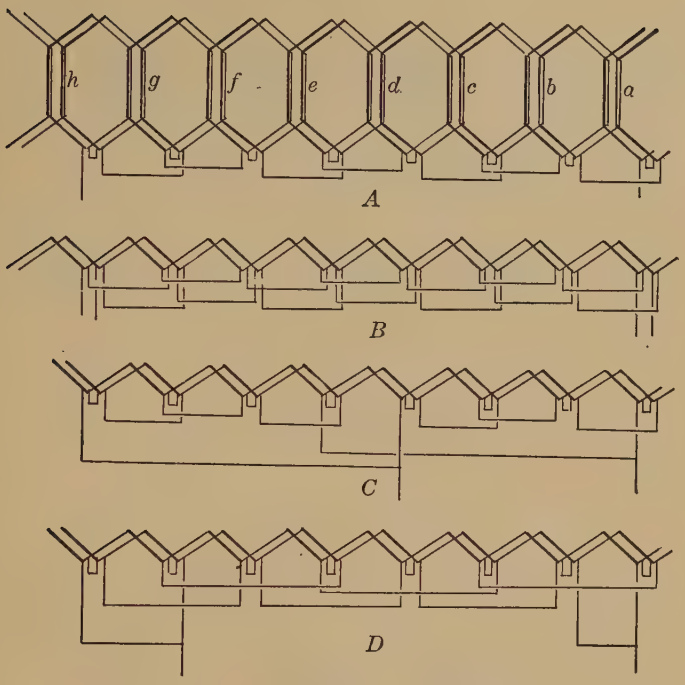

FIG. 115.—Two-circuit windings.

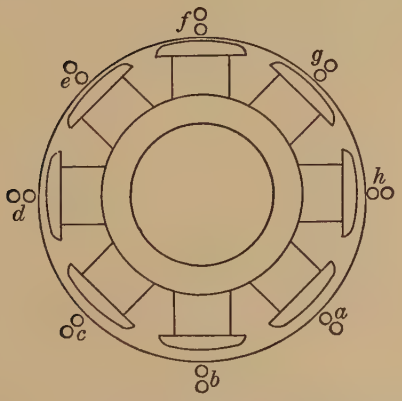

FIG. 116.—Alternator with an eccentric rotor.

that the voltages in the different circuits in parallel be equal to and in phase with one another.

Diagram *B* does not meet this condition because the voltages in the two circuits shown, while of equal value, are out of phase

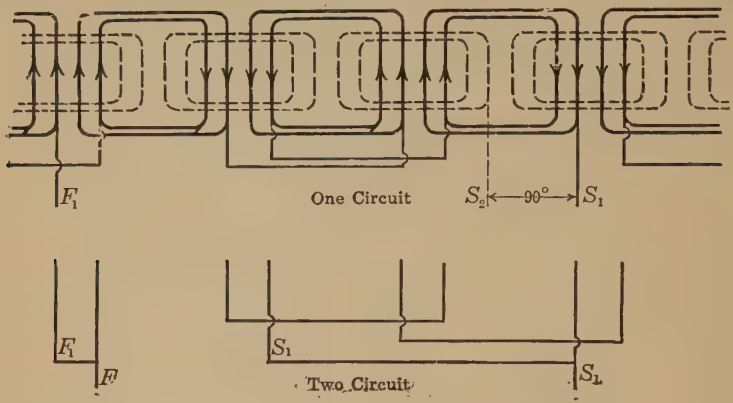

FIG. 117.—Four-pole, two-phase, chain winding with eight slots per pole.

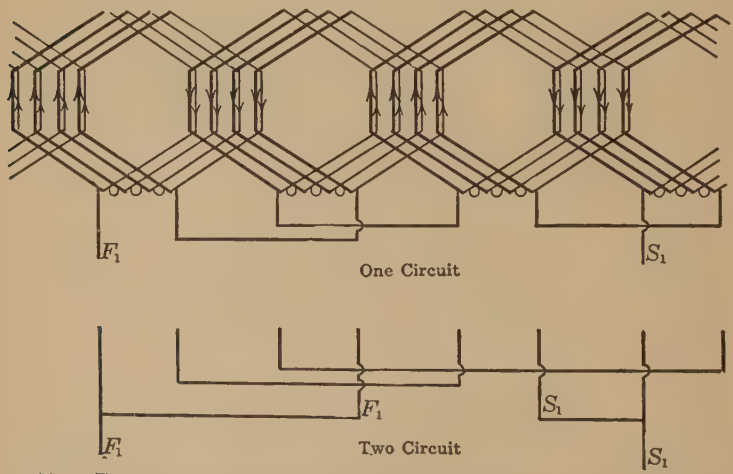

FIG. 118.—Four-pole, two-phase, double-layer winding with eight slots per pole, one phase shown.

with one another by the angle corresponding to one slot pitch, namely, by 30 deg.

The winding shown in diagram *D* is to be preferred to that in diagram *C* for the following reasons. Figure 116 shows an eight-pole machine the field and armature of which are eccentric due to

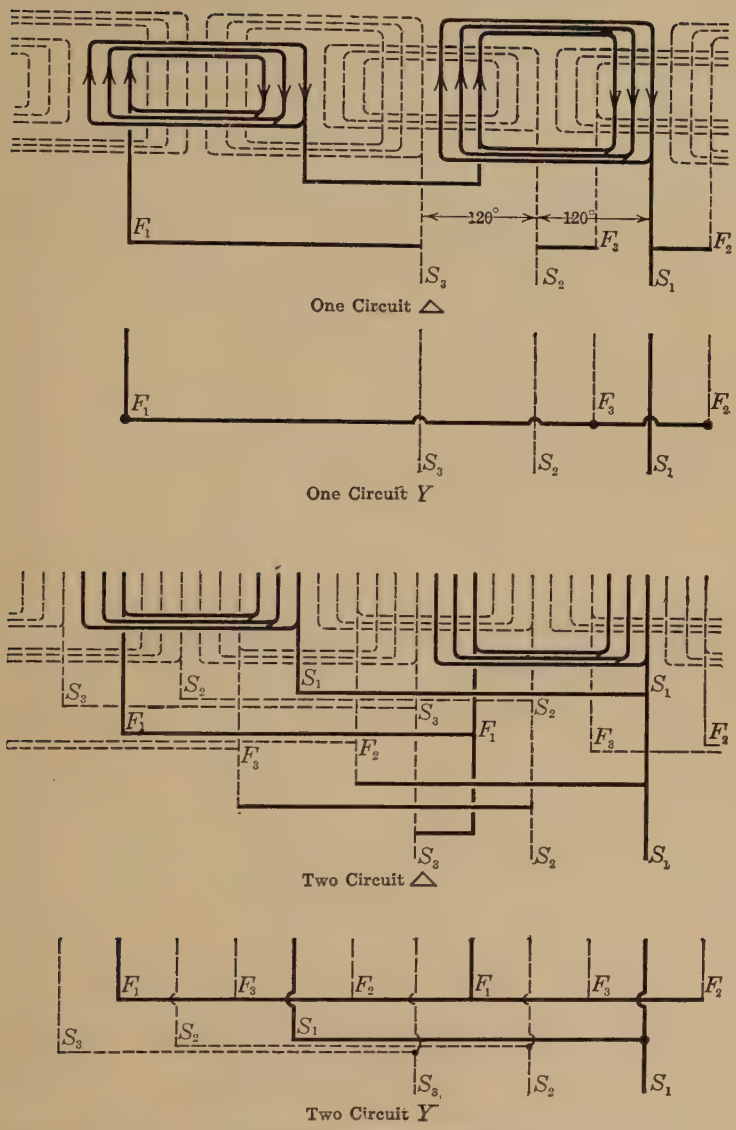

FIG. 119.—Four-pole, three-phase, chain winding with nine slots per pole.

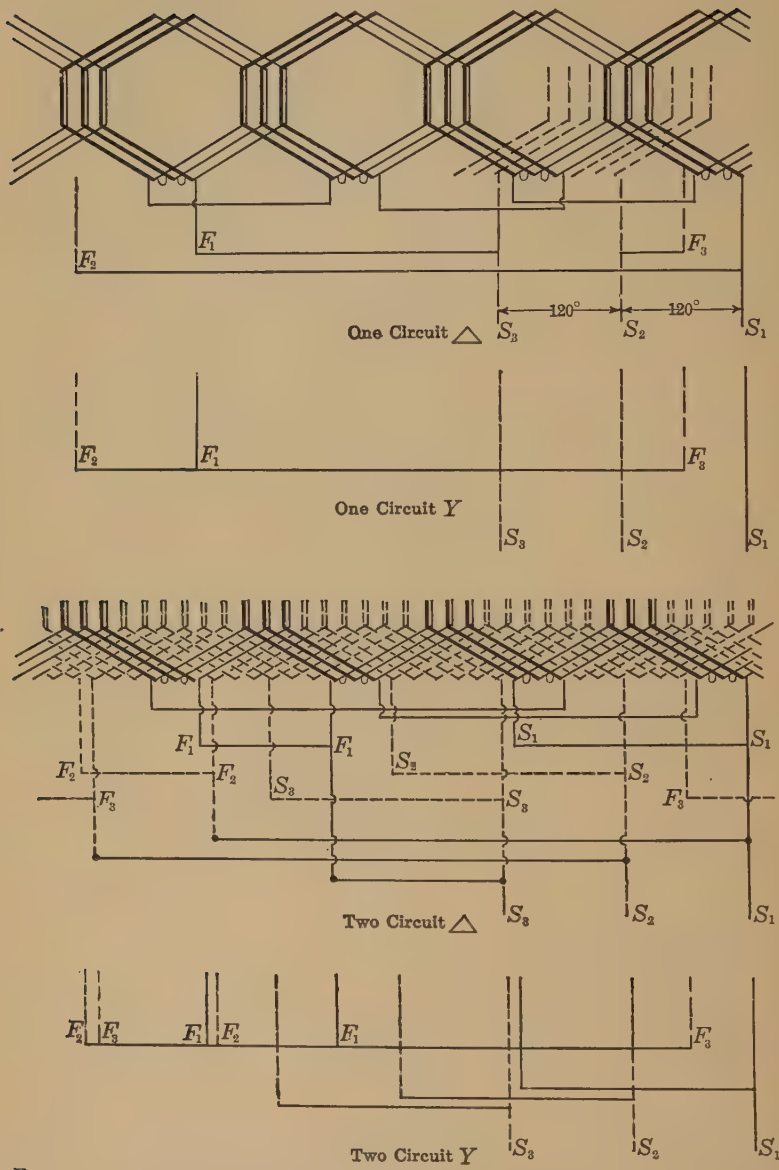

FIG. 120.—Four-pole, three-phase, double-layer winding with nine slots per pole.

poor workmanship in erection. The voltage generated in a circuit made up of conductors in slots *a*, *b*, *c* and *d* is smaller than that generated in a similar circuit wound in slots *e*, *f*, *g* and *h*, so that if these two circuits be put in parallel, a circulating current will flow. Diagram *C*, Fig. 115, shows an example of such a winding.

In diagram *D* the connection is such that each of the two circuits takes in conductors from under all of the poles so that, no matter how different the air-gaps become, the voltages in the two circuits are always equal.

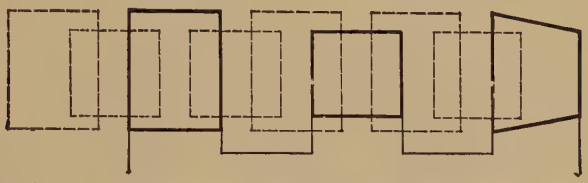

FIG. 121.—Six-pole, three-phase, chain winding with three slots per pole.

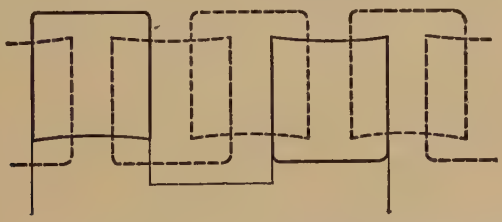

FIG. 122.—Three-phase chain winding with coils all alike.

128. Examples of Winding Diagrams.—Figures 117, 118, 119 and 120 show typical alternator-winding diagrams and should be carefully studied. Many other examples might have been shown but the subject is too wide to take up in greater detail.

When the number of groups of coils is odd in a machine with a chain winding, it is impossible to have the same number of groups of long as of short coils, and one group must be put into the machine the coils of which have one side long and the other side short; such a winding is shown in Fig. 121 for a six-pole machine with three phases, one slot per phase per pole, and one coil per group.

By the use of specially shaped coils, as shown in Fig. 122, it is possible to reduce the number of coil shapes that are required for a chain winding. In the particular case shown the coils are all alike.

In a single-phase machine it is generally advisable, for the reason explained in Art. 137, page 182, to make the winding cover not more than two-thirds of the pole pitch. Such a winding is shown in Fig. 123 for a machine with six slots per pole, of which only four are used.

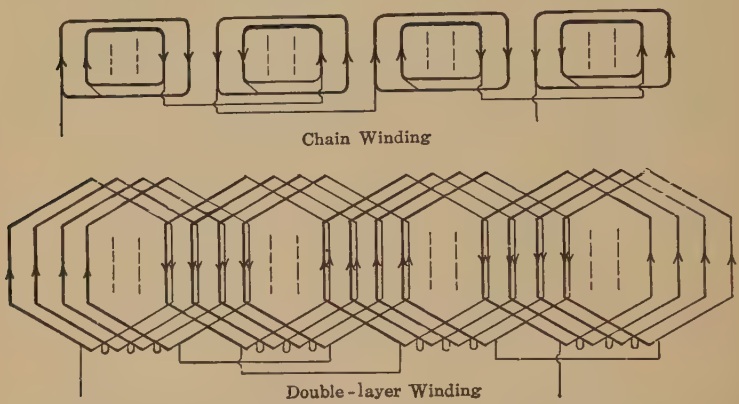

FIG. 123.—Four-pole, single-phase winding with four active slots per pole.

CHAPTER XV

GENERATED ELECTRO-MOTIVE FORCE

129. The Form Factor and the E.M.F. per Conductor.

If ϕ_a is the flux per pole and p the number of poles, then one armature conductor cuts $\phi_a p$ lines of force per revolution

or $$\phi_a p \frac{\text{r.p.m.}}{60} \text{ lines per second}$$

and the average e.m.f. in one conductor $= \phi_a p \frac{\text{r.p.m.}}{60} 10^{-8}$ volts

The form factor of an e.m.f. wave is defined as the ratio

$$\frac{\text{effective voltage}}{\text{average voltage}}$$ and for a sine wave of e.m.f. this value $= \frac{\frac{1}{\sqrt{2}} E_{max}}{\frac{2}{\pi} E_{max}}$

$= 1.11$

The effective e.m.f. per conductor $= \phi_a p \frac{\text{r.p.m.}}{60} 10^{-8} \times$ form factor

$$= 1.11 \, \phi_a p \frac{\text{r.p.m.}}{60} 10^{-8} \text{ for sine wave e.m.f.}$$

$$= 2.22 \, \phi_a f \, 10^{-8} \qquad (24)$$

since f, the frequency $= \frac{p \times \text{r.p.m.}}{120}$

130. The Wave Form.—Figure 124 shows the shape of pole face that is in general use, and curve A shows the distribution of flux in the air-gap under such a pole face. The e.m.f. in a conductor is proportional to the rate of cutting lines of force and has, therefore, a wave form of the same shape as the curve of flux distribution.

Curve A is not a sine wave but can be considered as the resultant of a number of sine waves consisting of a fundamental and harmonics. The frequency and magnitude of these harmonics depend principally on the ratio of pole arc to pole pitch. In Fig. 124 this ratio is 0.65 and the fundamental and harmonics which go to make up the flux distribution curve are shown to scale, higher harmonics than the seventh being neglected.

131. Trouble Due to Harmonics.—The fundamental and harmonics that go to make up an e.m.f. wave act as if each had a separate existence. If the circuit to which this e.m.f. is applied consists of an inductance L in series with a capacity C so that the impedance of the circuit

$$= 2\pi f L - \frac{1}{2\pi f C},$$

then the current in this circuit consists of

a fundamental $= \dfrac{E_1}{2\pi f_1 L - \dfrac{1}{2\pi f_1 C}}$,

and harmonics of the form $\dfrac{E_n}{2\pi f_n L - \dfrac{1}{2\pi f_n C}}$

where E_n is the effective value of the nth harmonic. If, now, f_n has such a value that $2\pi f_n L = \dfrac{1}{2\pi f_n C}$, so that the circuit is in

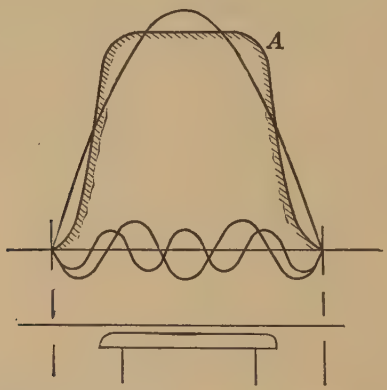

FIG. 124.—E.M.F. wave of an alternator.

resonance at this frequency, then the nth harmonic of current will be infinite, and the nth harmonic of e.m.f. across L and C individually will also be infinite.

The above is an ideal case; in ordinary circuits the current cannot reach infinity on account of the resistance that is always present. Nevertheless, if the circuit is in resonance at the frequency of the fundamental or of any of the harmonics, dangerously high voltages will be produced between different points in the circuit. The constants of a circuit are seldom such as to give trouble at the fundamental frequency; trouble is generally

due to high-frequency harmonics. It is desirable then to eliminate harmonics from the e.m.f. wave of a generator as far as possible, and several of the methods adopted are described below.

132. Shape of Pole Face.—The pole face is sometimes shaped as shown in Fig. 125; that is, the air-gap is varied from a minimum under the center of the pole to a maximum at the pole tip, so

FIG. 125.—Pole face shaped to give a sine wave e.m.f.

as to make the flux distribution curve approximately a sine curve; then the e.m.f. wave from each conductor will be approximately a sine wave.

133. Use of Several Slots per Phase per Pole.—Figure 126 shows part of a three-phase machine which has six slots per pole or two slots per phase per pole. The e.m.f. generated in a con-

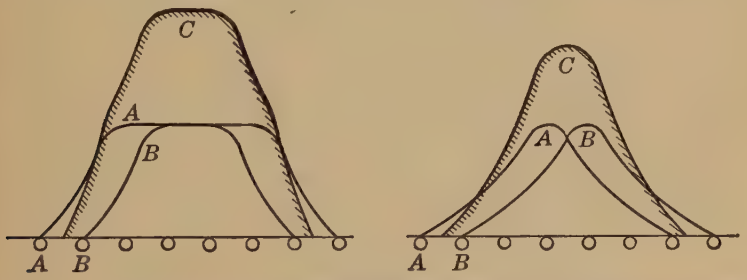

FIG. 126.—E.M.F. wave of a three-phase alternator with two slots per phase per pole.

ductor in slot A is represented at any instant by curve A, and that in a conductor in slot B by curve B, which is out of phase with curve A by the angle corresponding to one slot pitch, or 30 deg

When the conductors in slots A and B are connected in series so that their e.m.fs. add up, the resultant e.m.f. at any instant is given by curve C, which is got by adding together the ordinates of curves A and B. C is more nearly a sine curve than either A or B.

If the fundamental and harmonics that go to make up curves A and B are known, then those which go to make up curve C can be readily found as follows: The fundamental of the resultant

wave C is the vector sum of the fundamentals of A and B, which are θ electrical degrees apart, and the nth harmonic of C is the vector sum of the nth harmonics of A and B which are $(n \times \theta)$ electrical degrees apart. For example, curves A and B, Fig. 127,

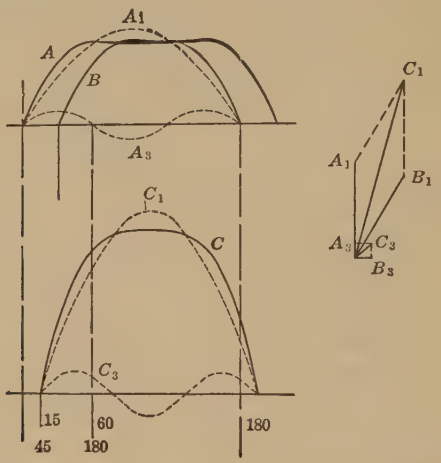

FIG. 127.—The vector diagram for the fundamental and the harmonics.

are 30 deg. out of phase with one another and each consists of a fundamental and a third harmonic as shown. C_1 is the resultant of the fundamentals A_1 and B_1; and C_3, the third harmonic of curve C, is the resultant of the two third harmonics A_3 and B_3.

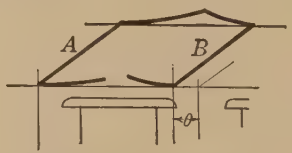

FIG. 128.—Short-pitch coil.

134. Use of Short-pitch Windings.—Figure 128 shows a short-pitch coil. The e.m.f. waves in the conductors A and B are out of phase with one another by θ deg., but each has the same shape as the curve of flux distribution. The problem of finding the resultant e.m.f. wave is, therefore, the same as that discussed in the last article.

If $n\theta$, the phase angle between the nth harmonics of curves A and B, becomes equal to 180 deg., then the corresponding

harmonic is eliminated from the resultant curve C since the two harmonics which go to make it up are equal and opposite. If, for example, there are nine slots per pole and the coil is one slot short, then the angle θ is 20 electrical degrees, and the ninth harmonic is

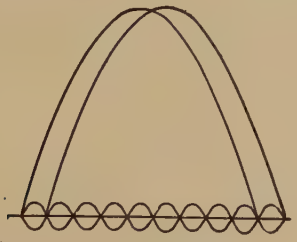

FIG. 129.—Elimination of harmonics from the e.m.f. wave.

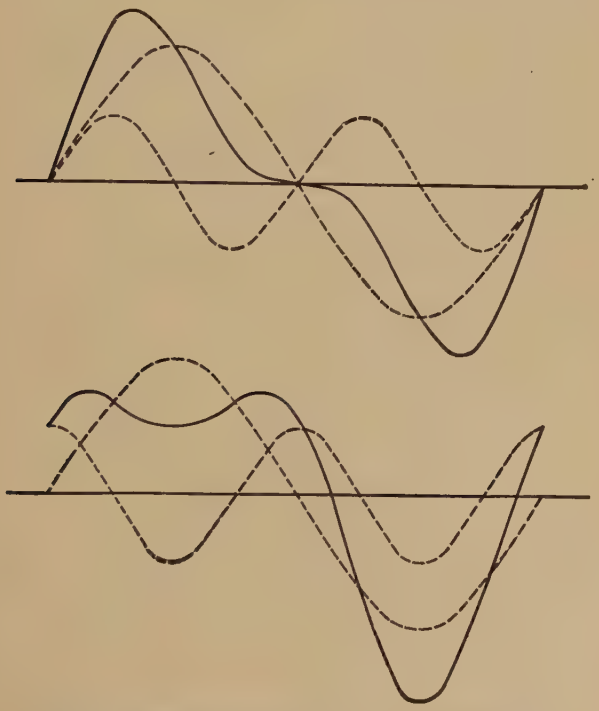

FIG. 130.—Unsymmetrical waves due to even harmonics.

eliminated from the voltage wave of the coil; in general, if the pitch of the coil be shortened by $\frac{1}{n}$ of the pole pitch, then, as shown in Fig. 129, the nth harmonic will be eliminated.

It may be pointed out here that an even harmonic is seldom found in the e.m.f. wave of an alternator, because the resultant of a fundamental and an even harmonic gives an unsymmetrical curve, as shown in Fig. 130, where the resultant curve is made up of a fundamental and a second harmonic. If, then, the e.m.f. wave is symmetrical, it may be assumed that no even harmonics are present.

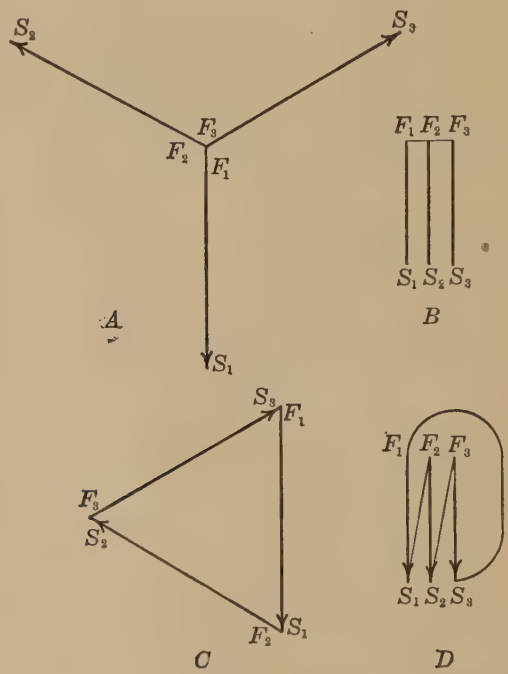

FIG. 131.—Effect of the Y- and Δ-connection on the third harmonic.

135. Effect of the Y- and Δ-connection on the Harmonics. The fundamentals of the three e.m.fs. are 120 deg. out of phase with one another and are represented by vectors in diagram *A*, Fig. 131. The nth harmonics are $(n \times 120)$ deg. out of phase with one another.

When the phases are Y-connected, the terminal F_2 is brought to the potential of terminal F_1 and the resultant fundamental between S_1 and S_2 is represented by the vector S_1S_2 and $= 1.73$ times the fundamental in one phase. In the case of the third harmonic the e.m.fs. are $(3 \times 120) = 360$ deg. out of phase with

one another and are represented by vectors in diagram B; the resultant third harmonic between S_1 and S_2 is zero so that, in a Y-connected alternator, no third harmonic, nor any harmonic which is a multiple of three, is found in the terminal voltage wave.

When the phases are Δ connected, any harmonic in the voltage wave of one phase will also be found in that of the terminal voltage; a greater objection to the use of this connection for alternators is that the harmonics cause circulating currents to flow in the closed circuit produced by the Δ-connection. Diagram C shows the voltage vector diagram for the fundamentals in the e.m.f. wave of each phase; the three vectors are 120 deg. out of phase with one another, and the resultant voltage in the closed circuit due to the fundamentals is zero.

Diagram D shows the voltage vector diagram for the third harmonic in the e.m.f. wave of each phase. The three vectors are 360 deg. out of phase with one another, and the resultant voltage in the closed circuit due to the third harmonics is three times the value of the third harmonic in one phase. A circulating current will flow in the closed circuit, of triple frequency and of a value $= \frac{3E_3}{3z_3}$, where E_3 is the effective value of the third harmonic in each phase and z_3 is the impedance per phase to the third harmonic.

136. Harmonics Produced by Armature Slots.—Figure 132 shows two positions of the pole of an alternator relative to the armature. In position A the air-gap reluctance is a minimum and in position B is a maximum. The flux per pole pulsates, due to this change in reluctance, once in the distance of a slot bitch, or $2a$ times in the distance of two pole pitches, where $a =$ slots per pole, and the e.m.f. generated in each coil by the main field goes through one cycle while the pole moves, relative to the armature, through the distance of two pole pitches; therefore, the frequency of the flux pulsation $= 2af$.

The flux per pole then consists of a constant value ϕ_a, and a superimposed alternating flux which has a frequency of $2a$ times the fundamental frequency of the machine, or at any instant the flux per pole

$$= \phi_p = \phi_a + \phi_1 \cos 2a\theta$$

where $\phi_a + \phi_1$ is the maximum value of the pulsating flux and θ is the angle moved through from position A, Fig. 132, in elec-

trical degrees; therefore, the flux threading coil C, which is a full-pitch coil,

$= \phi_a + \phi_1$ when the coil is in position A

$= [\phi_a + \phi_1 \cos 2a\theta] \cos \theta$ when the coil has moved through θ electric degrees relative to the pole

and the e.m.f. in coil C at any instant

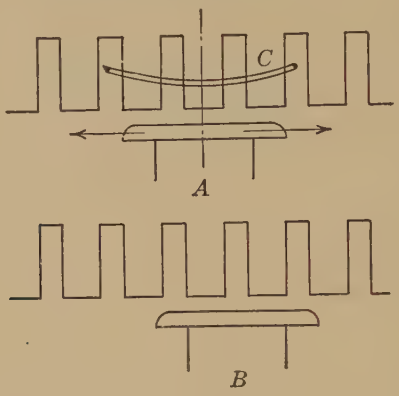

FIG. 132.—Variation of the air-gap reluctance.

$$= -T\frac{d(\phi_a + \phi_1 \cos 2a\theta)\cos\theta}{dt}$$

$$= -T\frac{d(\phi_a + \phi_1 \cos 2a\theta)\cos\theta}{d\theta} \times \frac{d\theta}{dt}$$

$$= -2\pi f[-\sin\theta(\phi_a + \phi_1 \cos 2a\theta) - \cos\theta(2a\phi_1 \sin 2a\theta)]T$$

$$= 2\pi f[\phi_a \sin\theta + \phi_1 \sin\theta \cos 2a\theta + 2a\phi_1 \cos\theta \sin 2a\theta]T$$

$$= 2\pi f[\phi_a \sin\theta + \frac{\phi_1}{2}\{\sin(2a+1)\theta - \sin(2a-1)\theta\} + \frac{2a\phi_1}{2}\{\sin(2a+1)\theta + \sin(2a-1)\theta\}]T$$

$$= 2\pi fT[\phi_a \sin\theta + \frac{\phi_1 + 2a\phi_1}{2}(\sin(2a+1)\theta) + \frac{\phi_1 - 2a\phi_1}{2}(\sin(2a-1)\theta)]$$

so that, due to the variation or the air-gap reluctance as the poles move past the armature slots, two harmonics are produced which have frequencies of $(2a + 1)$ and of $(2a - 1)$ times that of the fundamental, respectively.

A convenient physical interpretation of the above result is as follows: A and B, Fig. 133, are two equal trains of waves which are constant in magnitude, and move in opposite directions at the same speed. The resultant of two such wave trains

superimposed on one another is a series of stationary waves as shown at *C*.

A stationary wave such as that of the alternating magnetic field in the air-gap of an alternator due to a variation in the air-gap reluctance, can, therefore, be exactly represented by two progressive waves of constant value which move in opposite directions through the distance of two pole pitches while the alternating wave goes through one cycle.

Consider both of these waves or fields to exist separately from the main field; then, when the pole moves with the constant

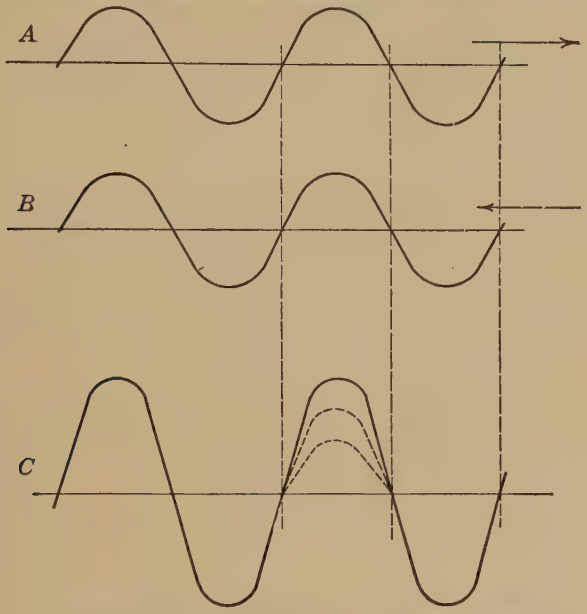

FIG. 133.—Resolution of a stationary wave into two progressive waves.

flux ϕ_a, through a distance y relative to the armature, one of these constant progressive fields moves through a distance $2ay$ relative to the pole, or through a distance $(2a + 1)y$ relative to the armature, while the other moves through a distance $-2ay$ relative to the poles, or through a distance $-(2a - 1)y$ relative to the armature. If, then, the fundamental frequency of the generated e.m.f. is f, the two other fields will generate e.m.fs. of frequencies $= (2a + 1)f$ and $(2a - 1)f$, respectively.

To keep down the value of these harmonics the reluctance of the air-gap under the poles should be made as nearly constant as possible for all positions of the pole relative to the armature

137. Effect of the Number of Slots on the Terminal E.M.F.—Figure 134 shows the winding diagrams for an alternator with six slots per pole and wound for single, two and three phase, respectively, the same punching being used in each case. The e.m.fs. in the conductors in adjacent slots are out of phase with one another by the angle corresponding to one slot pitch $= \frac{180}{6}$ $= 30$ electrical degrees.

In the three-phase winding, the conductors in slots A and B are connected in series so that their voltages act in the same

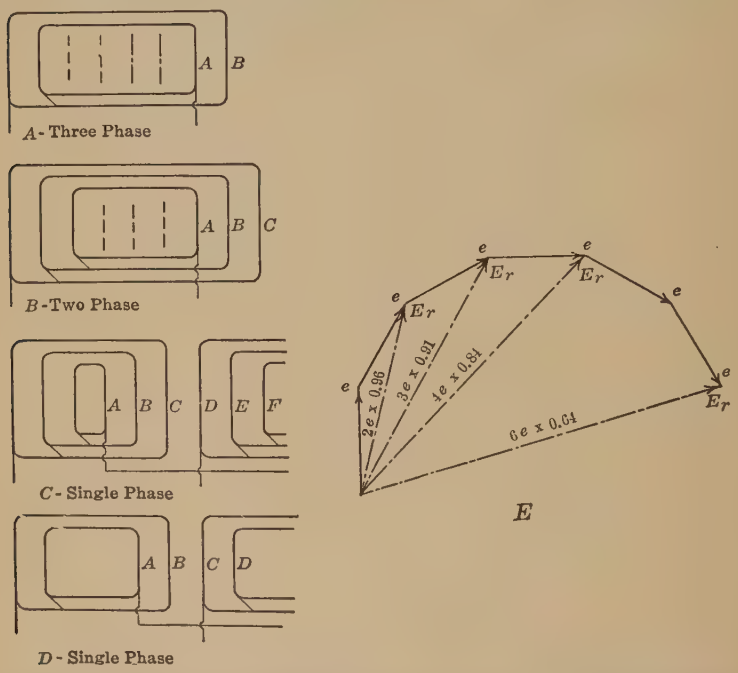

FIG. 134.—Effect of the distribution of the winding on the terminal voltage

direction; the resultant voltage E_r, diagram E, is not equal to $2e$, where e is the voltage per conductor, but is the resultant of two e.m.fs. e which are 30 deg. out of phase with one another and $= 2e \times 0.96$.

In the case of the two-phase winding, the conductors A, B and C are connected so that their voltages add up and the resultant voltage $E_r = 3e \times 0.91$.

In the case of the single-phase winding where all the conductors are used, the resultant voltage $E_r = 6e \times 0.64$, while if

only four of the six slots per pole are used, as shown in diagram *D*, the resultant voltage $E_r = 4e \times 0.84$, which is only 10 per cent lower than that obtained when all six slots are used. A gain of 10 per cent in voltage is not worth the cost of the 50 per cent increase in armature copper that is required, so that single-phase machines are generally wound as shown in diagram *D*.

138. Rating of Alternators.—The maximum voltage that an alternator can give continuously is limited by the permissible value of the flux per pole, and the maximum current is limited by the armature copper loss which, along with the core loss, heats the machine. When the value of volts and amperes is fixed, the kilowatt rating depends only on the power factor of the load. The power factor is a variable quantity, and one over which the builder of the machine has no control, so that an alternator is generally rated by giving the product of volts and amperes which is called the volt-ampere rating, and this quantity divided by 1000 gives the rating in k.v.a. (kilovolt amperes).

139. Effect of the Number of Phases on the Rating.—Consider the four machines whose winding diagrams are shown in Fig. 134, and let the number of conductors per slot be the same in each; then the voltage per phase is given in the following table:

Number of Phases	Voltage per Phase
Single-phase (all slots used)	constant $\times 6e \times 0.64$
Single-phase (two-thirds of slots used)	constant $\times 4e \times 0.84$
Two-phase	constant $\times 3e \times 0.91$
Three-phase	constant $\times 2e \times 0.96$

Since there are the same number of conductors per slot, these conductors have the same section and, therefore, carry the same current I_c; the volt-ampere rating, which equals volts per phase $\times$ current per phase $\times$ number of phases, is given in the following table:

Number of Phases	Volt-ampere Rating	Relative Rating
Single-phase (all slots used)	constant $\times 6e \times 0.64 \times 1 \times I_c$	64
Single-phase (two-thirds of slots used)	constant $\times 4e \times 0.84 \times 1 \times I_c$	56
Two-phase	constant $\times 3e \times 0.91 \times 2 \times I_c$	91
Three-phase	constant $\times 2e \times 0.96 \times 3 \times I_c$	96

In practice the machine is given the same rating for both two- and three-phase windings, although the three-phase machine is the better, and is given approximately 65 per cent of this rating when wound for single-phase operation.

140. The General E.M.F. Equation.—It is shown in Art. 137 that, when the winding of an alternator is distributed, the terminal voltage is less than $Z \times e$

where Z = conductors in series per phase,

e = volts per conductor,

and is equal to kZe where k is the distribution factor and is found from the following table, which is worked up by the method explained in Art. 137:

Slots per Phase per Pole	Distribution Factor	
	Two-phase	Three-phase
1	1.0	1.0
2	0.924	0.966
3	0.911	0.96
4	0.906	0.958
6	0.903	0.956
infinite	0.898	0.955

The single-phase results are not tabulated since they depend on the number of slots that are used by the winding.

When a short pitch is used, as is often done with double-layer windings, then, as shown in Fig. 135, which shows part of a three-phase double-layer winding with three slots per phase per pole, the two adjacent belts A and B are out of phase with one

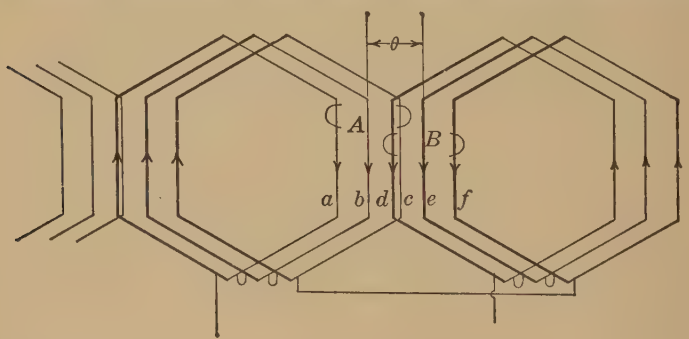

Fig. 135.—Short-pitch winding.

another by θ deg., and, as shown in Fig. 136, the resultant voltage, when these two belts are put in series, is equal to twice the voltage in one belt multiplied by $\cos \frac{\theta}{2}$.

It was shown in Art. 129 that the effective e.m.f. per conductor $= 2.22\phi_a f 10^{-8}$ volts.

If the winding is full pitch and is not distributed, then the voltage per phase $= 2.22Z\phi_a f 10^{-8}$ volts.

If the winding is full pitch and is distributed, the voltage per phase

$$= 2.22kZ\phi_a f10^{-8} \tag{25}$$

and finally, if the winding is short pitch, so that the winding belts are out of phase with one another by θ deg., and is also distributed, then the voltage per phase

$$= 2.22\ kZ\phi_a f10^{-8} \cos \frac{\theta}{2}. \tag{26}$$

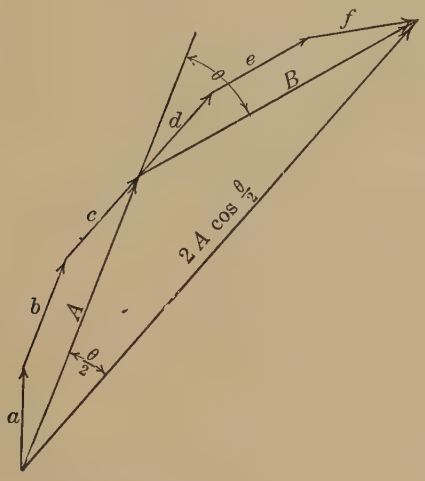

FIG. 136.—Vector diagram for a short-pitch winding.

CHAPTER XVI

CONSTRUCTION OF ALTERNATORS

Figure 137 shows the type of construction that is generally used for horizontal shaft alternators of moderate speed. It shows the revolving field type—as is universal in modern alternators. The type of construction varies, depending on whether shaft is horizontal or vertical and upon the speed of operation.

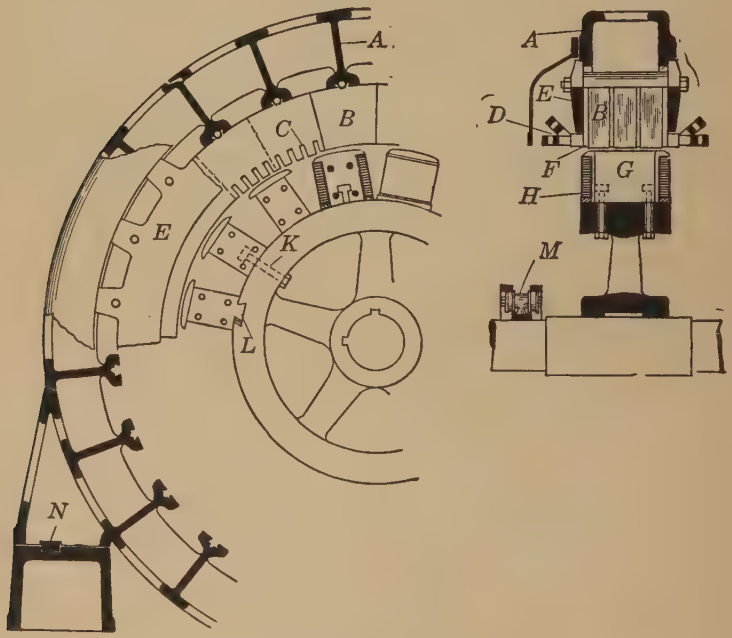

FIG. 137.—Revolving field alternator.

141. The Stator.—In the revolving field type of machine the stator is the armature. In Fig. 137, *B*, the stator core, is built up of laminations of sheet steel 0.014 to 0.0172 in. thick, which are insulated from one another by layers of varnish and are then mounted in a self-supporting cast-iron yoke *A*. These laminations are punched on the inner periphery with slots *C* which carry

the stator coils *D*. The type of slot shown is the open slot; it has the advantage over the closed slot that the coils can be fully insulated before being put into the machine and can also be more easily repaired.

The stator core is divided into blocks by means of vent segments, and the ducts thereby provided allow air to circulate freely through the machine to keep it cool. The vent ducts are spaced $1\frac{1}{2}$ to 3 in. apart and are $\frac{3}{8}$ to $\frac{1}{2}$ in. wide.

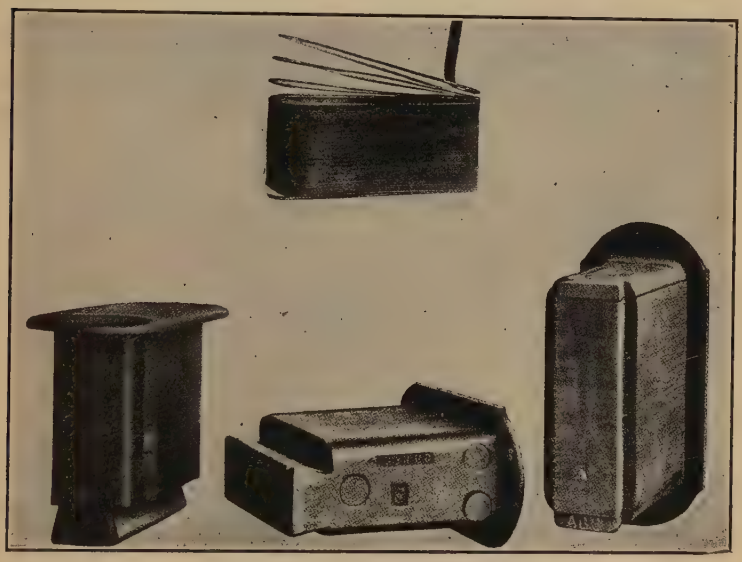

FIG. 138.—Poles and field coil.

The stator laminations and vent segments are clamped between two cast-steel end heads *E*. When the teeth are long, they are supported by strong finger supports placed at *F*, between the end heads and the end punchings of the core.

When the external diameter of the stator core is less than 30 in., the core punching is generally made in a complete ring; when this diameter is greater than 30 in., the core is generally built up in segments which, as shown in Fig. 137, are fixed to the yoke by means of dovetails; the segment of adjacent layers of laminations break joint with one another so as to overlap and produce a solid core.

142. Poles and Field Ring.—Inside of the stator revolves the rotor or revolving field system. The poles *G* carry the exciting

coils H and are excited by direct current from some external source.

The excitation voltage is independent of the terminal voltage of the machine and is generally chosen low, so that for a given

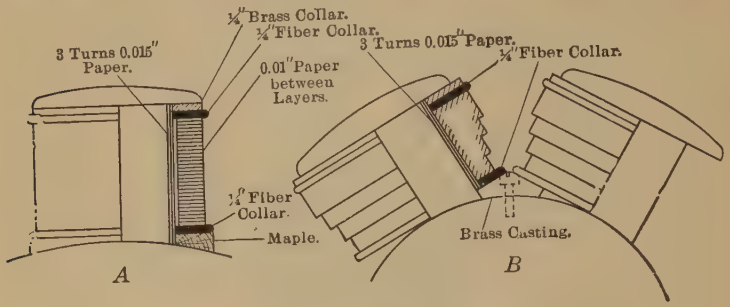

FIG. 139.—Alternator field coils.

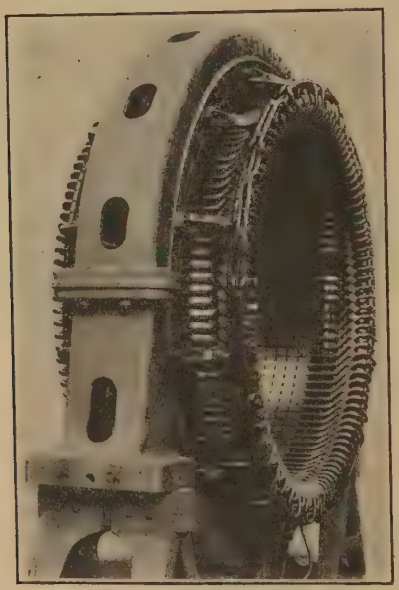

FIG. 140.—Stator of a horizontal shaft moderate speed alternator.

excitation the field current will be comparatively large and the field coils will have few turns.

For the usual excitation voltage of 125 it will generally be possible, except on the smaller machines, to use the type of field winding shown in Fig. 138, which is made by bending strip copper on edge; the layers of strip copper are insulated from one another

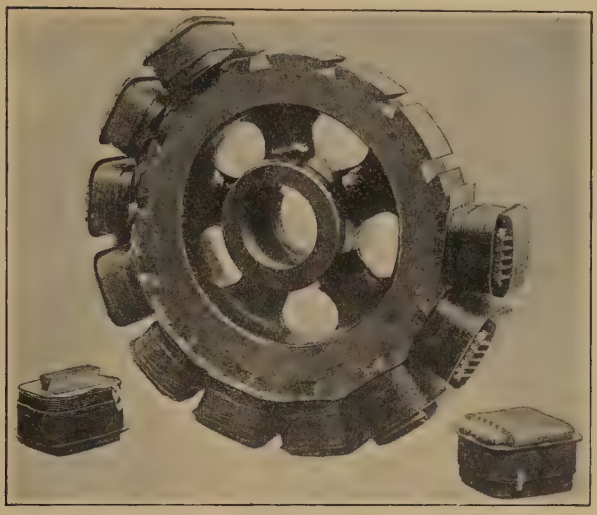

FIG. 141.—Rotor of a horizontal shaft moderate speed alternator.

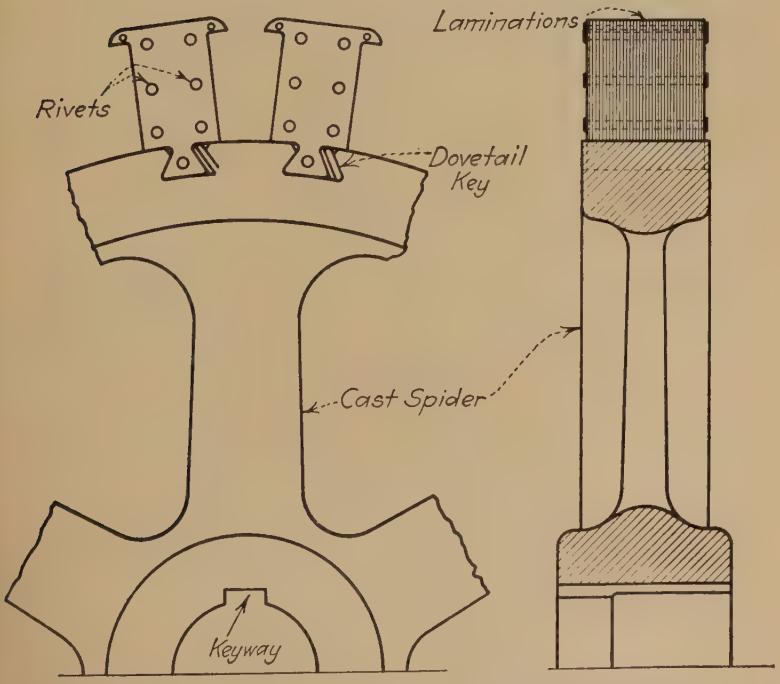

FIG. 142.—Detail of pole fastening in a moderate speed alternator.

by layers of insulation about 0.01 in. thick, and the whole field coil is supported by and insulated from the poles and field ring as shown at *A*, Fig. 139. For small machines the excitation loss is comparatively low, and with an excitation voltage of 125 the section of the wire is too small and the number of turns required too large to allow the use of a strip copper coil; in such cases double cotton-covered square wire is used as shown at *B*, Fig. 139;

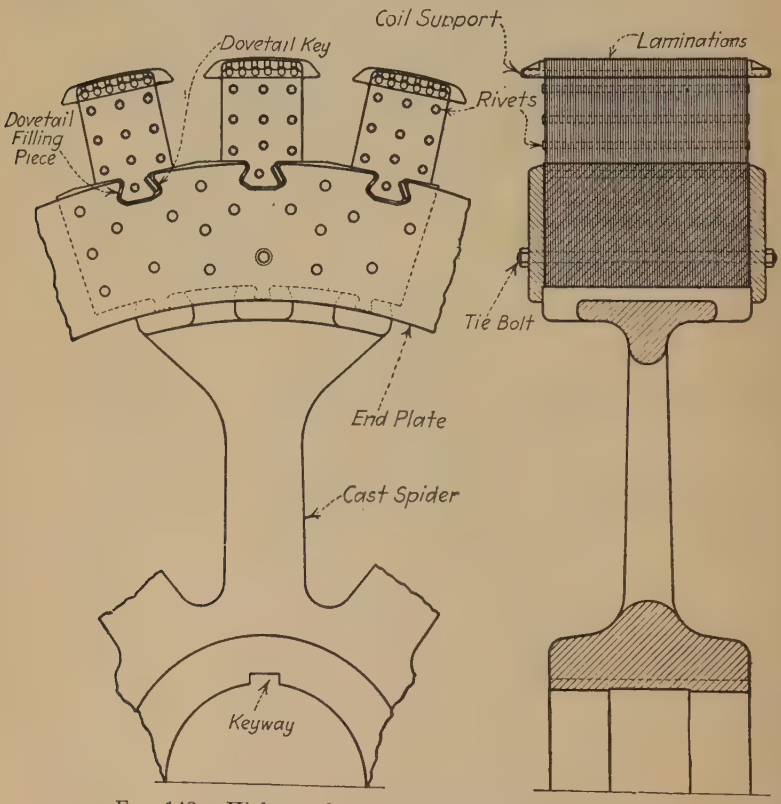

FIG. 143.—High speed rotor with a laminated steel ring.

the coils are tapered so as to allow free circulation of air around them.

Since the number of poles in an alternator is fixed by the speed and the frequency, it rarely happens that this number is such as to allow the use of a pole of circular section; the pole is generally rectangular in section and, as shown in Fig. 138, is built up of punchings of sheet steel 0.025 in. thick which are riveted together between two cast-steel end plates.

The poles are generally attached to the field ring by means of bolts as shown at K, Fig. 137, or by means of dovetails and tapered keys as shown at L; two tapered keys are used which are driven in from opposite ends; the dovetail fastening is the more common.

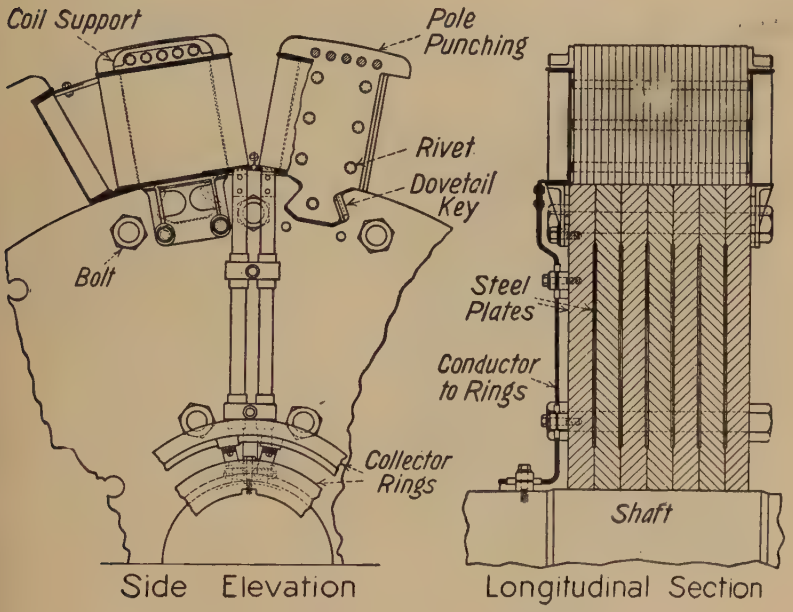

FIG. 144.—High speed rotore rotor with plate steel ring.

The exciting current is led into the revolving field system by means of brushes which bear on cast-iron or cast-brass slip rings; the slip rings are carried by and insulated from the shaft as shown at M; the brushes are generally of so-called "metal graphite" and carry from 100 to 150 amperes per square inch.

The stator of an alternator is seldom split except in the case of very large machines, where it is done for convenience in shipment. In order that the stator windings can be examined and easily repaired, it is advisable to arrange in horizontal shaft machines that the whole stator slide axially on the base, and the key shown at N is for the purpose of keeping the alignment correct.

Figure 140 shows the stator and Fig. 141, the rotor of a typical horizontal shaft alternator of moderate speed.

143. High-speed Generators.—Figure 141 shows the rotor construction when the speed is moderate. In this case the rotor to which the poles are dovetailed is a steel casting. This construction is shown somewhat more in detail in Fig. 142. For higher speeds, where the centrifugal forces are higher, a preferable type of construction is shown in Figs. 143 and 144. Figure 143 shows a rotor construction in which the ring to which the poles are dovetailed is itself of laminated material and is in turn dovetailed to the driving spider. Figure 144 shows a construction suitable for still higher speed, wherein the ring is made up of steel plates. The constructions shown in Figs. 143 and 144 are preferable to that shown in Figs. 137 and 142 because of the certainty of obtaining a ring without flaws and in which there are no initial stresses. Cast rings such as shown in Figs. 137 and 142 can theoretically be relieved of practically all internal stresses by a process of annealing; however, there is no inspection that can be made to insure that these stresses actually have been relieved—short of cutting up the casting. With rolled material, on the other hand, there is a certainty that no internal stresses of serious magnitude will remain after rolling.

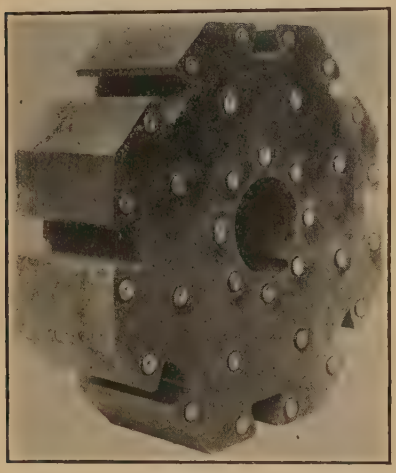

FIG. 145.—Laminated steel body ready to receive poles.

Figure 145 shows the rotor of an eight-pole alternator without shaft or poles. This is of laminated material also.

144. Vertical Shaft Generators.—In many cases, a vertical shaft generator fits into the design of the power plant better than does a horizontal shaft. The general problem of electrical design is not materially changed by use of a vertical shaft; the main difference is the need for a thrust bearing, and this is a mechanical problem rather than electrical. Figure 146 shows the cross-section of a typical vertical shaft generator with direct connected exciter. This is a 8500-k.v.a. machine at 6600 volts, 164 r.p.m. and is typical of modern vertical type construction.

A subsequent chapter (Chap. XXII) deals with the special problems met in the design of high-speed alternators, particularly

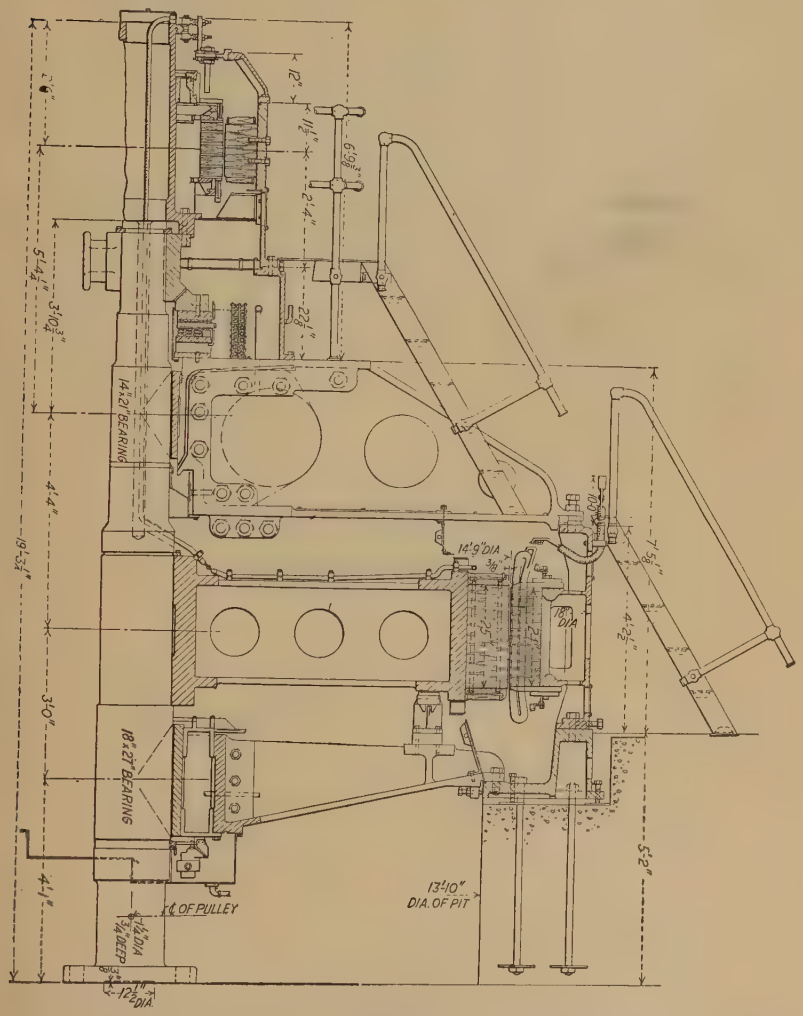

FIG. 146.—Cross section of a vertical shaft alternator with direct connected exciter.

with the turbo-alternator where the speeds are made as high as the materials used will permit.

CHAPTER XVII

INSULATION

The insulation of low-voltage machines has been discussed in Chap. IV and presents no particular difficulty, since insulation which is strong enough mechanically is generally ample for electrical purposes up to 600 volts. For higher voltages, however, the thickness of insulation required to prevent break-down is great compared with that required for mechanical strength and, unless such insulation is carefully designed, trouble is liable to develop.

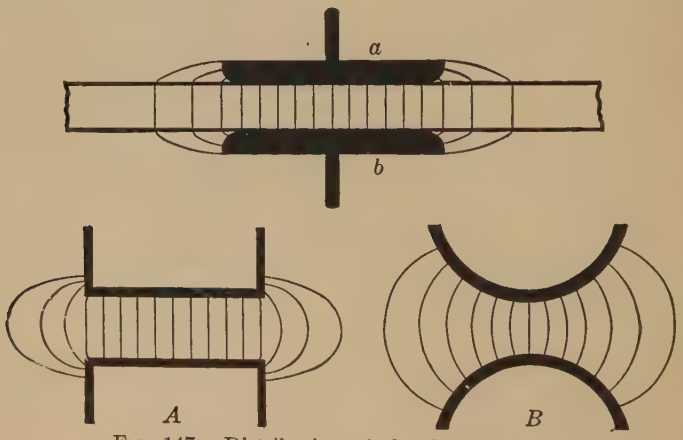

FIG. 147.—Distribution of the dielectric flux.

145. Definitions.—If a difference of electric potential be established between two electrodes *a* and *b*, Fig. 147, which are separated by an insulating material or dielectric, a molecular strain will be set up in the dielectric.

This molecular strain is conveniently represented by lines of dielectric flux, and the number of lines per unit area, which is called the *Dielectric Flux Density*, is taken as a measure of the strain.

When the dielectric flux density reaches a certain critical value, the material is disrupted and loses its insulating properties;

this critical value depends on the nature, thickness and condition of the material.

The distribution of dielectric flux depends largely on the shape of the electrodes, as shown in diagrams *A* and *B*, Fig. 147. When an insulating material of uniform thickness t is placed between two parallel plates and subjected to a voltage E, the dielectric flux density or molecular strain is uniform through the total thickness of the material and is conveniently represented by the ratio $\frac{E}{t}$, the volts per unit thickness. Under such conditions of test, the highest effective alternating voltage that 1 mil (0.001 in.) thickness of the material will withstand for 1 minute is generally called its *Dielectric Strength.*

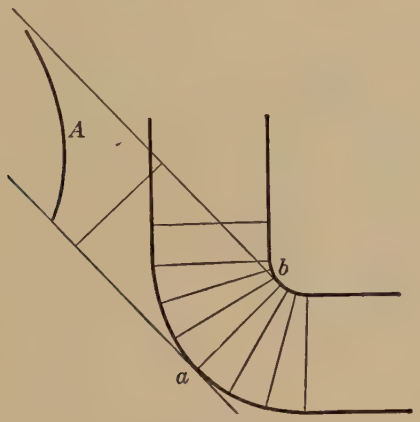

Fig. 148.—Potential gradient at a slot corner.

When the dielectric flux density is not uniform throughout the total thickness of the material, the ratio $\frac{E}{t}$, the volts per unit thickness, has little meaning. In Fig. 148 for example, which shows the dielectric flux distribution at the corner of a slot, it will be seen that the dielectric flux density, or molecular strain, is greatest at the surface of the conductor and decreases as the lines spread out. Under such conditions the strain at any point is conveniently expressed by what is known as the *Potential Gradient* at the point, where this quantity is the volts per unit thickness that would be required to set up the same dielectric flux density as that at the point in question if the material were

of uniform thickness and tested between two parallel plates. The potential gradient across *ab* is given by curve *A*.

146. Insulators in Series.—If an air film be placed between two electrodes and subjected to a difference of potential, a certain dielectric flux density will be produced in the air. If now the air be replaced by mica, a greater dielectric flux density will be produced for the same difference of potential. The *Specific Inductive Capacity* of an insulating material is defined as

$$\frac{\text{the dielectric flux density in the material}}{\text{the dielectric flux density in air}}$$

for the same value of volts per mil.

Figure 149 shows two cases of dielectric subjected to a difference of electric potential between electrodes of the same size and the same distance apart. In *A* the dielectric is air, and in *B* is

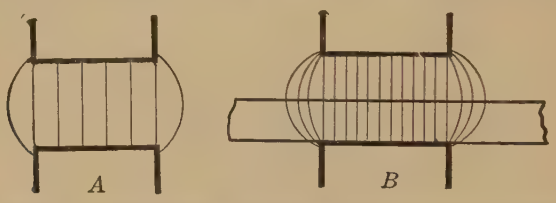

FIG. 149.—Effect of the specific inductive capacity of the dielectric on the dielectric flux density.

made up of air and mica in series. Since the specific inductive capacity of mica is greater than that of the air which it replaces, being about six times air, the dielectric flux density is greater in *B* than in *A* for the same difference of potential between the electrodes, and the air in *B* is subjected to a greater strain than that in *A*, so that it will break down at a lower value of voltage between the terminals, although at the same value of volts per mil.

Since in *B* the two materials, air and mica, are in series, the dielectric flux density is the same in each and, therefore, from the definition of specific inductive capacity,

$$\frac{\text{the volts per mil thickness in the mica}}{\text{the volts per mil thickness in the air}} = \frac{1}{\text{specific inductive capacity of mica}},$$

$$= \frac{1}{6} \text{ (approximately).}$$

The greater the thickness of mica in the total thickness between electrodes the larger will be the dielectric flux density and the

greater, therefore, the value of volts per mil thickness in the air for a given voltage between the electrodes.

147. Effect of Air Films in Insulation.—From the above discussion it will be seen that, should there be an air film in the thickness of a solid dielectric, then, for a perfectly conservative value of volts per mil of total thickness of the dielectric, the volts per mil across the air film may be sufficient to disrupt it if the solid dielectric have a specific inductive capacity greater than one.

When air is disrupted ozone and oxides of nitrogen are formed, these oxidize nearly all the insulators used for electrical machinery except mica and thereby seriously impair their insulating properties.

148. The Design of Insulation.—The voltage that a given insulation will stand depends on:

FIG. 150.—Effect of the voltage on the thickness of the slot insulation.

The thickness of the insulation;
The dielectric strength of the material;
The potential gradient across the material;
The length of time that the voltage is applied.

149. The Thickness of the Insulation.—Figure 150 shows the slot of an alternator insulated in the one case for high voltage and in the other case for low voltage. If the space occupied by insulation could be filled with copper, the output of the machine could be considerably increased, so that the solution of high-voltage insulation problems is not solved economically by indefinitely increasing the thickness of the dielectric with increasing voltage, but by the selection and proper use of the most suitable materials.

150. The Potential Gradient.—Insulating materials break down wherever they are overstressed, and if the stress is not

uniform, they break down first at the point of highest stress; it is therefore, necessary to make a study of the distribution of stress, or of the potential gradient in the material.

Consider the case of the slot corner shown in Fig. 148; the lines of dielectric flux pass radially from the conductor to the side of the slot, so that the dielectric flux density is a maximum at the surface of the conductor and a minimum at the surface of the slot, and the potential gradient curve, if the dielectric is of the same material throughout, is as shown in diagram *A*. The inner layers of the insulation, therefore, carry more than their share of the voltage, and these layers break down long before the stress in the outer layers reaches the break-down point.

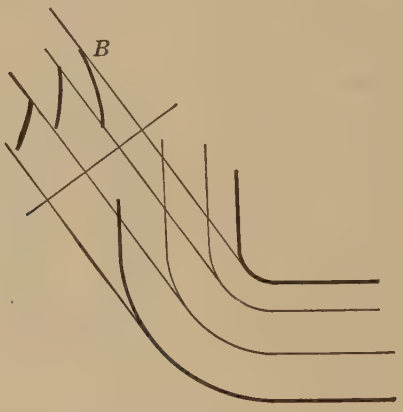

Fig. 151.—Potential gradient with graded insulation.

It is possible to make the outer layers carry their share of the total voltage by grading the insulation in the following way: Materials having different specific inductive capacities are used and put on in layers in such a way that the lower the specific inductive capacity the further away is the material from the conductor. This relieves the strain on the inner layers because, as pointed out in the discussion of insulators in series, the voltage required to send a given dielectric flux through a layer of insulating material is inversely as the specific inductive capacity of the material, so that the higher the specific inductive capacity of the inner layers the lower the voltage drop across these layers and the higher, therefore, the voltage drop across the outer layers. The potential gradient at the corners for such insulation, made up

in three layers, is shown in diagram *B*, Fig. 151. Grading of the insulation would, therefore, tend to equalize the voltage stresses at the corners of the conductors in the slot; but on the flat portions of the conductor, this grading would give an undue stress on the outside layer of insulation. Grading of insulation can be made of use only when the radius of curvature of the conductor is uniform, that is, with a round conductor in a round slot. This form of slot is not applicable to alternators because of the limited conductor area that it would necessitate. It would be impossible to get in the required cross-section of copper conductor and at the same time have sufficient iron cross-section for the necessary magnetic flux. While grading of insulation may be considered for insulated cables, it is not applicable to A.-C. machinery.

The potential gradient can be controlled in many cases by a slight alteration in the shape of the surfaces to be insulated from one another. Figure 152 shows three cases of slot insulation,

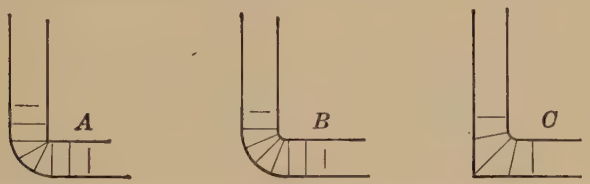

FIG. 152.—Effect of the shape of the surfaces to be insulated on the distribution of dielectric flux.

and it is evident that the potential gradient is more uniform in case *B* than in case *A*, while case *C* is the best of the three because of the extra thickness of the dielectric at the corner; in this last case the insulation generally punctures between the parallel sides of the slot and conductor, and not at the corner.

151. Time of Application of Electric Strain.[1]—That the voltage at which an insulating material will puncture depends on the length of time that this voltage is applied is shown by the curve in Fig. 153. *E* is the maximum voltage that the material will withstand for an infinite length of time without deterioration due to heating and consequent puncture.

If air films are present in the insulation, then a lower voltage than *E* will cause puncture if applied for some time, but the action in this case is a secondary one.

In Art. 146, page 196, it was pointed out that the stress on an air film bedded in a material of specific inductive capacity greater

[1] Fleming and Johnson, *Jour. Inst. Elec. Eng.*, Vol. 47, p. 530.

than one is very high, and that the film may become ruptured and ozone and oxides of nitrogen be produced which attack the other insulation causing deterioration and consequent puncture.

The amount of these gases produced by the rupture of a thin air film is not enough to do much harm unless there is a constant supply of air to the film. When an electrical machine is started up, its coils become heated and, since the gases in the film expand, some of them are expelled. When the machine is shut down, the coils cool off, the gases in the film contract, and a fresh supply of air is drawn in. This action is known as the breathing action of the coils.

Trouble due to this breathing action takes months to develop and usually shows up as a break-down between adjacent turns;

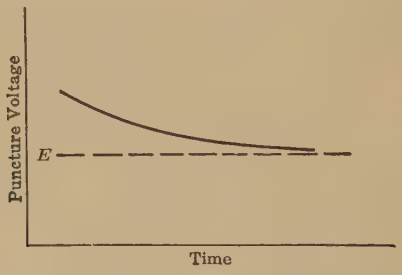

FIG. 153.—Effect of time on the puncture voltage.

the insulation between these turns, having become brittle due to oxidization, readily pulverizes due to vibration. The trouble can be eliminated by constructing the coils so that they contain no air pockets, and in the endeavor to do this various methods have been adopted for impregnating the coils and sealing their ends. The compounds generally used for impregnating purposes are made fluid by heating to a temperature of about 100° C., and in cooling to normal temperatures most of them contract about 10 per cent and this 10 per cent becomes filled with air.

Since, with the present methods of insulating, it may be considered impossible to eliminate all the air pockets from a coil, it is necessary to keep the stress in the air films below that value at which they will rupture. This can be done by increasing the total thickness of the insulation and also by the use of material which has a low specific inductive capacity. It is unfortunate

that mica, which is one of the most reliable of insulators, has a high specific inductive capacity; a good composite insulator can be made up of mica paper, which consists of a layer of mica backed by a layer of paper; the specific inductive capacity of the former is about six, and of the latter is about two, while the combination has a value between these two figures.

Such an insulation is described fully on page 33 and may be expected to withstand about 70 volts per mil indefinitely without trouble due to the break-down of air films. For such insulation, then, the minimum thickness in mils between the conductor and the side of the slot $= \frac{\text{terminal voltage}}{70}$. If the insulation were made up entirely of mica, a greater total thickness would be required on account of the high specific inductive capacity of the mica, while if made up entirely of paper, a smaller total thickness would be required so far as the break-down of the air film is concerned, but paper is not reliable as an insulator when used alone.

152. Design of Slot Insulation.—Slot insulation for A.-C. machinery is very similar to that for D.-C. as described in Chap. VI. The main difference is that the voltages in A.-C. machines are in general much higher than in D.-C., and a thicker insulation is necessary.

The materials in general use are mica built in layers on paper or cloth and used as wrappers or in tape form as described in Chap. IV. Varnished cambric is also used on account of its high dielectric strength and its ability to adhere closely to sharp bends; it is used mostly on the end portions of the coils and on the leads between coils. On this portion of the coil, temperatures can more easily be kept down to the value allowed for class *A* insulation; the temperatures on the slot portion are usually higher and the mica in the wrapper is sufficient to make it class *B* insulation and so available for higher temperatures. (Note: The definitions for these classes of insulation as formulated by the A.I.E.E. are given in Chap. IV, Art. 32, p. 32.)

The temperature rise allowable under the 1925 A.I.E.E. standards rules are slightly different in A.-C. machinery from those for D.-C.; they are as follows:

Item	Description of part	Method of determining temperature	Limiting temperature rise in degrees Centigrade	
			Class *A* insulation	Class *B* insulation
1	Insulated armature windings on machines of 750 k.v.a. and below	Thermometer	50	70
2	Insulated armature windings with two-coil sides per slot on stators of machines above 750 k.v.a.	Embedded detector	60	80
3	Insulated field windings.....	Resistance	..	90
4	Collector rings (the class of insulation refers to insulation affected by heat from the collector rings which insulation is employed in the construction of the collector rings or is adjacent thereto)	Thermometer	65	85
5	Cores or mechanical parts in contact with or adjacent to insulation	Thermometer	50	70
6	Miscellaneous parts (such as brush holders, brushes, pole tips, etc.) other than those whose temperatures affect the temperature of the insulating material may attain such temperature as may not be injurious.			

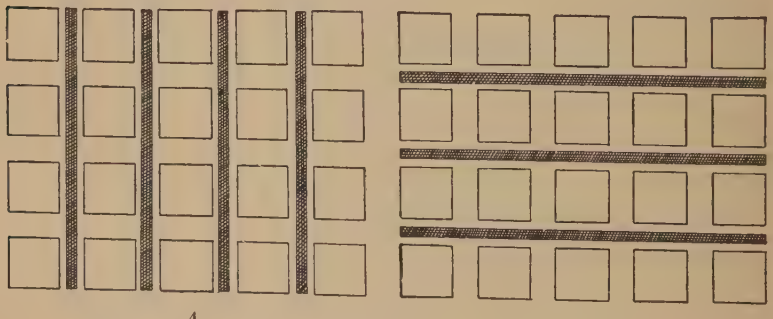

FIG. 154.—Application of shellac paper strips in coil insulation.

The puncture test as recommended by the 1925 A.I.E.E. standards rules is twice rated voltage plus 1000 volts.

Figure 154 shows two ways of applying shellac paper strips for binding coils prior to insulating. These strips are coated with shellac and are used merely as an agency for holding the coil in shape while applying the outside insulation. The conductors are individually insulated to withstand the internal service voltage. End connections between coils or groups of coils should be insulated to withstand full voltage between terminals.

To minimize surface leakage, the slot insulation should be carried beyond the core for the distance set forth in Art. 40, Chap. IV.

153. Insulation between Conductors in Same Slot.—In high-voltage alternators the number of turns per coil is high and the size of wire or ribbons is comparatively small. Figures 155, 156, 157 and 158 show sections through four alternator slots; in Fig. 155 the winding is composed of one layer with six conductors, each composed of four wires in parallel. This method of winding is least expensive and has no cross-overs and is preferred to any of the other types. In Fig. 156 the winding is wound straight up with the distributed cross-overs on the coil end. The conductors are numbered in the order in which they are wound. This coil is more expensive and is confined to smaller sections of wire or ribbon. In Fig. 157 the two layers are wound separately in the order in which they are wound and then assembled, and the starting leads of each layer connected. This form of winding requires additional insulation over the layers to withstand the maximum voltage between layers, and for this reason is often prohibitive owing to the space required for insulation. It is also avoided, if possible, owing to the full voltage of the coil between the starting and finishing leads.

In Fig. 158 the coil is wound as in Fig. 157 except the starting of one layer connects to the finishing of the adjacent layer which halves the voltage between layers. All conductors are insulated with double or triple cotton-covered wire and the coil treated by the vacuum impregnating process or immersed in an insulating varnish and baked in ovens prior to insulating with the slot insulation, consisting of mica and paper insulation on the embedded portion subjected to higher temperatures and treated cambric and cotton tape over the end portion which is ventilated and subjected to lower temperatures. Coils are again immersed several

times in an insulating varnish to resist moisture, oil, dirt, etc.

The insulation on alternators from 220 to 13,200 volts consists of mica and paper wrappers. The number of thicknesses depends

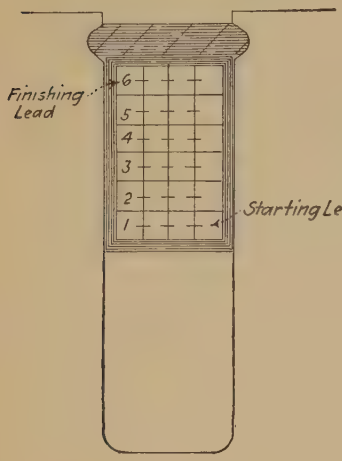

FIG. 155.

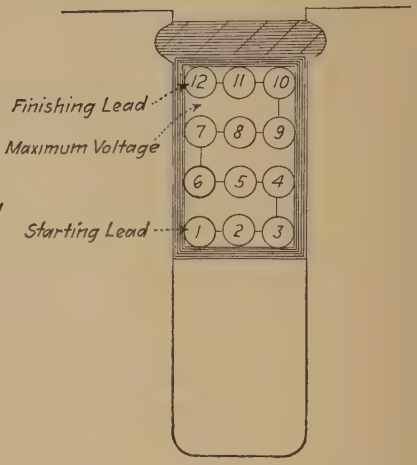

FIG. 156.

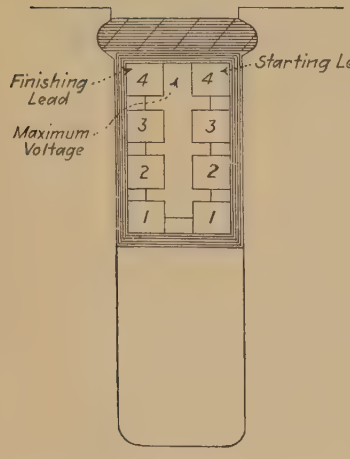

FIG. 157.

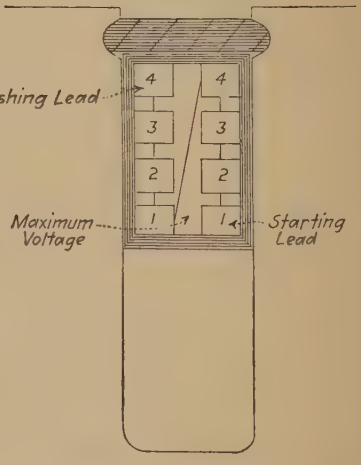

FIG. 158.

FIGS. 155, 156, 157 and 158.—Showing various conductor arrangements within armature coils.

on the voltage. A section through the slot and insulation is shown in Figs. 159 and 160 and the insulation consists of:

(*b*) one layer not lapped 0.0045 thick cotton tape; with heavier sections of copper 0.007 cotton tape is used.

(*e*) Mica and paper wrapper. With voltages under 4000 and capacities under 3000 k.v.a., wrappers are usually applied by hand and held in place by taping with cotton tape. The end tapings of varnished cambric are applied at the same time the slot insulation is, and the coils are again immersed in insulating varnish several times to resist moisture, oil, dirt, etc.

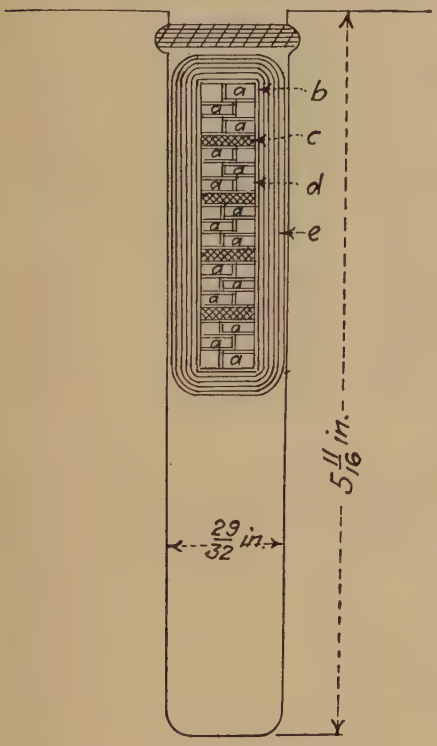

Fig. 159.

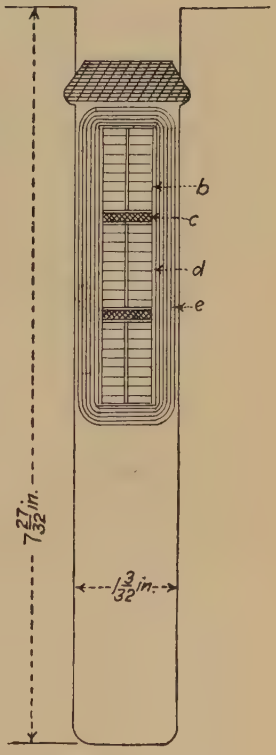

Fig. 160.

Fig. 159.—Cross section through a 11,000 volt alternator armature coil.
Fig. 160.—Cross section through a 13,200 volt alternator armature coil.

With larger alternators and turbo-generators with voltages of 4000 and over, the slot insulation consists of micarta folium. With this method the mica is hand built on thin paper using a shellac bond, very similar to the wrappers for the lower voltages, and applied to the coil by a special wrapping machine under pressure and heat. Then the coil is pressed in cold presses until the shellac has hardened, which renders the insulation firm and solid.

Figure 159 shows the insulation for an 11,000-volt synchronous generator with mica or cotton insulation on separate strands in each conductor and mica insulation over the conductors with mica insulation over the coil. The details of this insulation are:

(*a*) Two coverings of cotton yarn or one layer of 0.004 mica tape on strands. With this arrangement of copper strands all the strands are insulated from each other, although only the (*a*) strands are insulated.

(*b*) One layer of 0.0045 cotton tape binding conductors and two layers of 0.004 mica tape, each layer half lapped with one layer of 0.0045 cotton tape binding the mica.

(*c*) Hard-baked built-up mica 0.02 thick between conductors.

(*d*) One layer of 0.0045 cotton tape binding the coil. The coil is then impregnated in a moisture-resisting compound and pressed prior to receiving the final mica insulation on the slot portion and the varnished cambric on the end portion.

(*e*) Micarta folium insulation. This insulation is first applied as tightly as possible by hand and then placed in a special machine equipped with electrical heating elements which revolve under pressure, softening the bond and tightening the insulation. The wrappers are then pressed in cold presses to required dimensions. The joints between the wrappers and the taping of varnished cambric are sealed with a special compound rendering the joint equal in dielectric strength to the end tapings. The coil ends are then given a number of varnish treatments to render them moisture, oil and dirt resisting.

Figure 160 shows the insulation for an 11,000-volt turbine generator with mica insulation on the separate strands in each conductor and mica insulation over the conductors with mica insulation over the coil. The details of this insulation are:

(*a*) Each strand taped with one layer of 0.004 mica tape, half overlapped.

(*b*) One layer of 0.0045 cotton tape binding conductors with two layers of 0.006 mica tape each layer half lapped with one layer of 0.0045 cotton tape binding the mica.

(*c*) Hard-baked built-up mica 0.02 thick between conductors.

(*d*) One layer of 0.007 cotton tape binding the coil. The coil is then impregnated in a moisture-resisting compound and pressed prior to receiving the final insulation in the slot portion and the varnished cambric on the end portion.

(*e*) Micarta folium insulation. This insulation is first applied as tightly as possible by hand and then placed in a special machine equipped with electrical heating elements which revolve under pressure, softening the bond and tightening the insulation. The wrappers are then pressed in cold presses to required dimensions. The joint between the wrapper and the taping of varnished cambric is sealed with a special compound rendering the joint equal in dielectric strength to the end tapings. The coil ends are then given a number of varnish treatments to render them moisture, oil and dirt resisting.

154. Volts per Mil on Insulation.—In modern A.-C. machinery the thickness of insulation used is approximately that given in Art. 151, *i.e.*, approximately 70 volts per mil referred to the terminal voltage of the machine. For 2200 volts and below, this thickness is somewhat increased for mechanical reasons; a thickness of insulation as dictated above would be so thin as to be liable to mechanical bruising.

CHAPTER XVIII

ARMATURE REACTIONS IN ALTERNATORS

POLYPHASE MACHINES

155. The Armature Fields.—a and b, Fig. 161, are two conductors of one phase of a polyphase alternator. When current flows in these conductors, they become encircled by lines of force. These lines may be divided into two groups; ϕ_r, the lines which pass through the magnetic circuit and whose effect is called *armature reaction*, and ϕ_x, called leakage lines, which do not pass through the magnetic circuit and whose effect is called *armature reactance*.

156. Armature Reaction.—Diagram A, Fig. 162, shows an end view of part of a three-phase alternator which has six slots per pole. The starts of the three windings are spaced 120 electrical degrees apart and are marked S_1, S_2, S_3. The armature moves

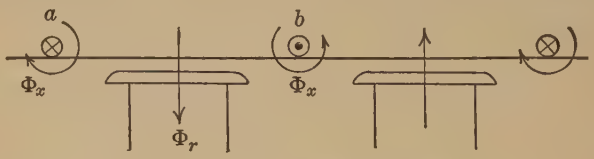

FIG. 161.—The armature fields.

relative to the poles in the direction of the arrow, and the e.m.f. in each phase at any instant is given by the curves in diagram F. In diagram A is shown the relative position of the armature and poles, and also the direction of the e.m.f. in each conductor, at instant 1, diagram F, at which instant the e.m.f. in phase 1 is a maximum.

Let the current be in phase with the generated e.m.f.; then diagram G shows the current in each phase at any instant, and the three diagrams, B, C and D, show the direction of the current in each conductor and also the relative position of the poles and armature at the three instants 1, 2 and 3. It may be seen from these diagrams that the currents in the three phases produce a resultant armature m.m.f. which moves in the same direction as the poles and at the same speed. Since the armature resultant

m.m.f. is added to that of the main field at one pole tip, and subtracted from it at the other tip of the same pole, the resultant effect is cross-magnetizing.

Let the current lag the generated e.m.f. by 90 deg.; then diagram *H* shows the current in each phase at any instant, and diagram *E*

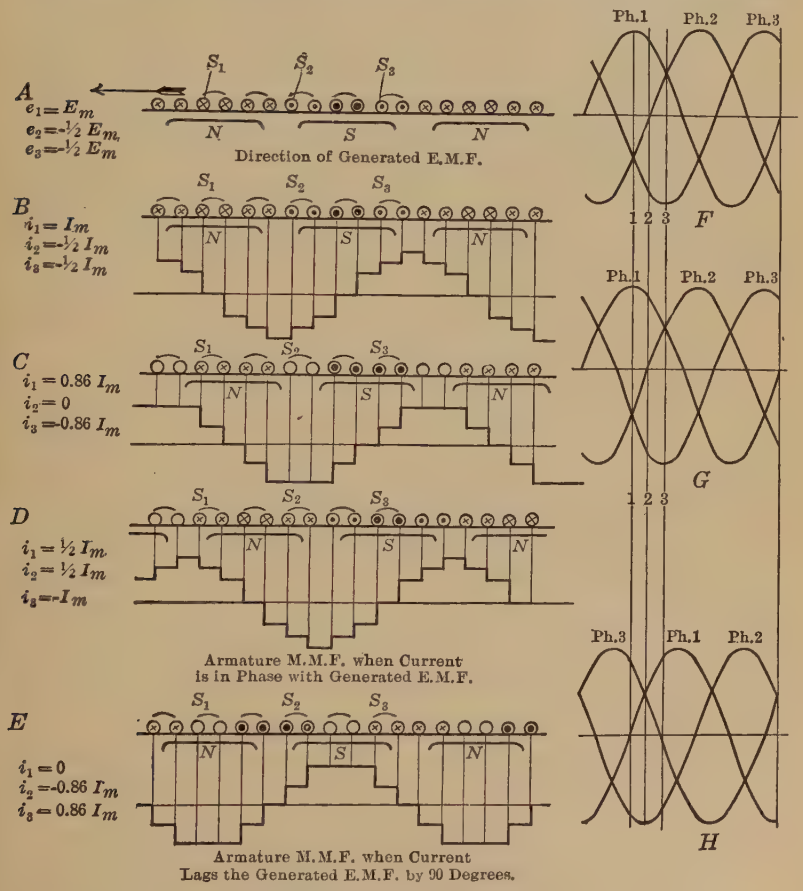

FIG. 162.—The armature m.m.f. of a three-phase alternator.

shows the direction of the current in each conductor and also the relative position of the poles and armature at instant 1. The resultant m.m.f. of the armature has the same value as before and moves at the same speed and in the same direction, but has now a different position relative to the poles and is demagnetizing in effect.

If the current lead the generated e.m.f. by 90 deg., then it can be shown in a similar way that the resultant armature m.m.f. has the same magnitude, speed and direction as before, but is magnetizing in effect.

157. The Alternator Vector Diagram.—On no load the current in the windings of an alternator is zero, and the only m.m.f. which is acting across the air gap is F_0, that due to the main field; F_0 sends a constant flux ϕ_a across the gap. This flux moves relative to the armature surface so that the flux which, due to the m.m.f. F_0, threads the windings of one phase of the armature is alternating and has a maximum value $= \phi_a$.

The voltage generated in a coil lags the flux which threads the coil, and whose change produces the voltage, by 90 deg.; thus, in Fig. 163, the flux threading coil a is a maximum but the voltage

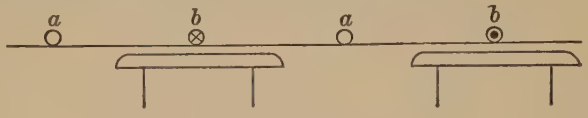

FIG. 163.—The generated e.m.f. in a coil.

in that coil is zero, while the total flux threading the coil b is zero and the voltage in that coil is a maximum; that is, the voltage is in phase with the flux which the coil cuts, but lags the flux which threads the coil by 90 deg.

The vector diagram for one phase of a polyphase alternator is shown in Fig. 164. On no load, F_0, the m.m.f. of the main field referred to the armature produces an alternating flux in the windings of each phase, and E_0, the voltage generated in each phase by that flux, lags F_0 by 90 deg.

When the alternator is loaded, the currents in the armature produce a m.m.f. F_a of armature reaction which, if acting alone, produces a field ϕ_r of constant strength which moves in the same direction and at the same speed as the main field.

In Fig. 162, diagram B, it may be seen that when the current in phase 1 is a maximum, the flux which threads the windings of that phase is also a maximum; in diagram C the current in phase 2 is zero, and the flux which threads the windings of that phase is also zero. In general it may be shown that the flux which, due to the revolving field ϕ_r, threads the winding of one phase of the armature is an alternating flux which has a maximum value $= \phi_r$ and is in phase with the current in that winding.

If the alternator is loaded and I, Fig. 164, is the current per phase, then F_g, the resultant of the m.m.fs. F_0 and F_a, will produce a resultant magnetic flux ϕ_g which is alternating with respect to the armature windings, and E_g, the voltage per phase due to the flux ϕ_g, will lag it by 90 deg.

In addition to the m.m.f. of armature reaction the current in the windings of one phase sets up an alternating magnetic flux ϕ_x which, as shown in Fig. 161, circles these windings but does not link the magnetic circuit; this flux is in phase with the current in the windings and is proportional to that current since its magnetic circuit is not saturated at normal tooth densities.

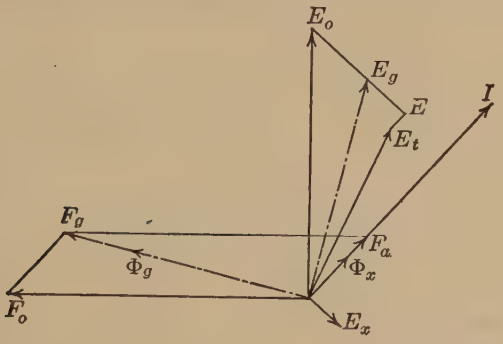

FIG. 164.—The vector diagram for an alternator.

In Fig. 164 F_o is the m.m.f. due to the field excitation referred to one phase of the armature.

E_o is the voltage per phase which would be generated by the flux produced by F_o.

I is the current per phase.

F_a is the m.m.f. of armature reaction referred to one phase of the armature and, as pointed out above, is in phase with I.

F_g is the resultant of the two m.m.fs. F_o and F_a.

ϕ_g is the flux that threads the windings of one phase due to F_g.

E_g is the voltage generated in that phase by ϕ_g.

ϕ_x is the armature leakage flux per phase produced by I.

E_x is the voltage per phase generated by the flux ϕ_x and is called the leakage reactance voltage.

$E_x = IX$ where X is the leakage reactance per phase.

E is the resultant of E_g and E_x.

E_t is the terminal voltage per phase and $= E - IR$ taken as vectors, where R is the effective resistance per phase.

Figure 165 shows the above diagram for the particular case where the power factor is approximately zero and the current lags the generated voltage by 90 deg. In this case the m.m.f. of armature reaction is subtracted directly from that of the main

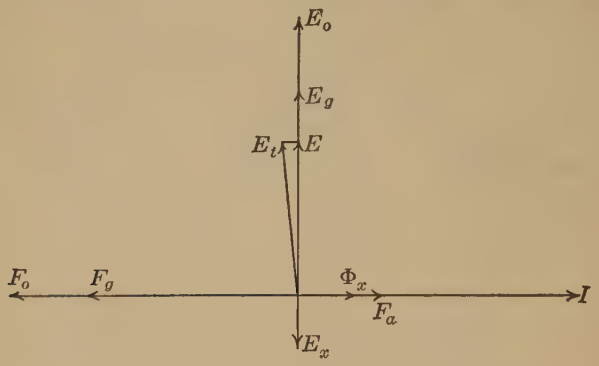

FIG. 165.—The vector diagram for an alternator on zero power factor.

field to give the resultant m.m.f., and the leakage reactance voltage is subtracted directly from the generated voltage E_g to give the terminal voltage. The resistance drop can be neg-

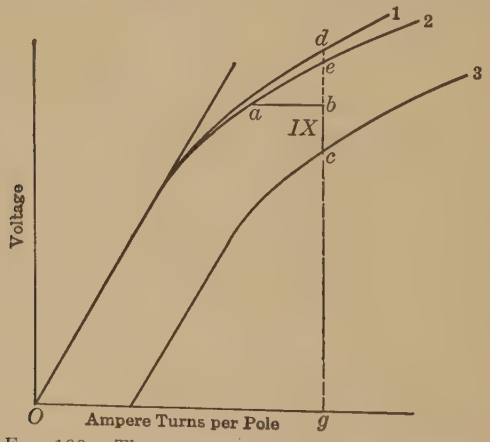

FIG. 166.—The saturation curves of an alternator.

lected in this case since its phase relation is such that it has little effect on the value of the terminal voltage.

158. Full-load Saturation Curve at Zero Power Factor with Lagging Current.—Curve 1, Fig. 166, shows the no-load satura-

tion curve of an alternator. When the machine is loaded, the power factor of the load zero, and the current lagging, the m.m.f. of armature reaction is directly demagnetizing, and to overcome its effect and maintain the flux ϕ_a which crosses the air-gap constant, a number of ampere-turns per pole equal to the armature demagnetizing ampere-turns per pole must be added to the main field excitation. Under these conditions the increase in the field excitation causes the leakage flux ϕ_e, Fig. 167, to increase to the value ϕ_{fe}, where

$$\phi_{fe} = \phi_e\left(\frac{AT_{g+t} + \text{demagnetizing } AT \text{ per pole}}{AT_{g+t}}\right)$$

without increasing the value of ϕ_a, the flux crossing the air-gap.

The leakage factor at no load $= \dfrac{\phi_a + \phi_e}{\phi_a}$ while that for the above load conditions $= \dfrac{\phi_a + \phi_{fe}}{\phi_a}$.

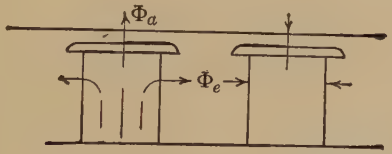

FIG. 167.—The main field and the pole leakage.

Curve 2, Fig. 166, is a new no-load saturation curve which is calculated with the value of the leakage factor corresponding to full load, zero power factor and lagging current.

To maintain the flux crossing the air-gap constant and equal to ϕ_a, a number of ampere-turns per pole, *ab*, equal to the armature demagnetizing ampere-turns per pole, must be added to the value obtained from curve 2.

The terminal voltage is less than that generated due to the flux ϕ_a by IX, the leakage reactance voltage; the resistance drop being neglected on zero power factor since, as shown in Fig. 165, its phase relation is such that it has little effect on the terminal voltage.

The locus of point *c* so found is the full-load saturation curve at zero power factor with lagging current.

159. Synchronous Reactance.—In Fig. 166, *de*, the drop in voltage due to the increase in leakage factor, depends on the demagnetizing effect of the armature, which is proportional to

the load current and, as shown in Fig. 162, varies with the power factor, being zero for unity power factor and a maximum for zero power factor lagging; this drop may, therefore, be considered as part of that due to armature reaction. In Fig. 166, then, the total voltage drop is made up of two parts one, *db*, due to armature reaction, which varies with the slope of curve 1 and, therefore, with the excitation, and the other, *bc*, the armature reactance drop, which is practically constant for all excitations.

Since, for a given excitation, each of these voltage drops is proportional to the current and since, as shown in Fig. 164, they are always in phase with one another, their sum, namely *dc*, Fig. 166 or E_oE, Fig. 164, may be represented by a fictitious reactance voltage called the synchronous reactance voltage and $= I\overline{X}$, where $\overline{X}$ is the synchronous reactance per phase. It may be seen from Fig. 166 that *dc*, and therefore $\overline{X}$, is not constant but decreases as the field excitation and, therefore, the saturation of the magnetic circuit increases.

160. The Demagnetizing Ampere-turns per Pole at Zero Power Factor.—The distribution of the m.m.f. of armature

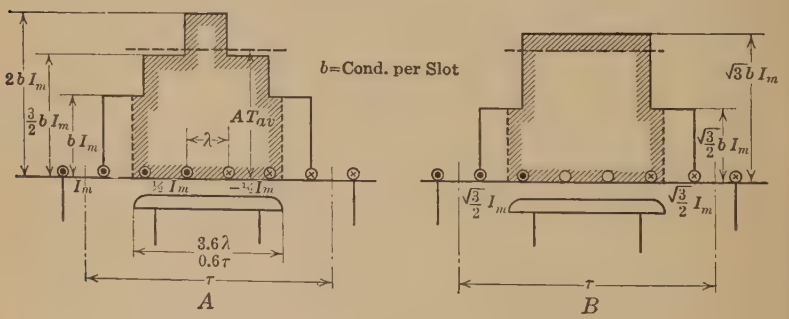

FIG. 168.—Armature m.m.f. on zero power factor.

reaction at two different instants is shown in Fig. 168, for a machine with six slots per pole and *b* conductors per slot. These diagrams are taken directly from Fig. 162 and the relative position of poles and armature shown is that corresponding to zero power factor and lagging current.

The portion of this m.m.f. which is effective in demagnetizing the poles is shown cross hatched; it is required to find AT_{av}, the average value of this cross-hatched part of the curve, for the case where $\psi = 0.6$ and, therefore, the pole covers 3.6 slots.

$$
\begin{aligned}
AT_{av} \times 3.6\lambda &= \text{area of cross-hatched curve, diagram } A \\
&= 2bI_m\lambda + 1.5bI_m \times 2\lambda + 0.6bI_m\lambda \\
&= 5.6bI_m\lambda \\
&= \text{area of cross-hatched curve, diagram } B \\
&= 1.73bI_m \times 3\lambda + 0.866bI_m \times 0.6\lambda \\
&= 5.7bI_m\lambda \\
&= 5.65bI_m\lambda; \text{ an average value from diagrams } A \text{ and } B.
\end{aligned}
$$

$$
\begin{aligned}
\text{Therefore } AT_{av} &= 1.57bI_m \\
&= 2.22bI_c \text{ where } I_c \text{ is the effective current} \\
&= 2.22bI_c \times \left(\frac{\text{slots per pole}}{6}\right), \text{ since there are six slots per pole} \\
&= 0.37 \times \text{conductors per pole} \times I_c. \qquad (27)
\end{aligned}
$$

If the pole enclosure be increased to 0.7, the value at AT_{av} will be reduced to 0.33 × conductors per pole × I_c.

The value can be found in a similar way to the above for any particular value of pole enclosure, number of phases and slots

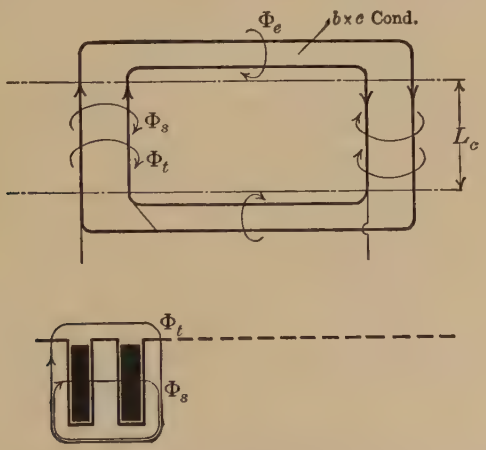

Fig. 169.—The armature leakage fields with a chain winding.

per pole, but the value of AT_{av} is generally taken as 0.35 × conductors per pole × I_c for all polyphase machines; that is, one ampere-turn on the armature (= two ampere conductors) is only about seven-tenths as effective in its demagnetizing effect as one ampere-turn on a salient pole type of field structure. This is because the conductors of the armature are distributed instead of being concentrated as they are on the field poles. On

turbo-generators, the field winding is also distributed (as will be discussed in Chap. XXII), and hence the ratio 0.7 herein deduced for salient pole designs no longer holds. This will be further discussed in Chap. XXII.

161. Calculation of the Leakage Reactance.—Figure 169 shows part of the winding of one phase of a polyphase alternator which has a chain winding.

If ϕ_e = the lines of force that circle 1 in. length of the belt of end connections for each ampere conductor in that belt,

ϕ_s = the lines of force that cross the slots and circle 1 in. length of the phase belt of conductors for each ampere conductor in that belt,

ϕ_t = the lines of force that cross the tooth tips and circle 1 in. length of the phase belt of conductors for each ampere conductor in that belt,

b = conductors per slot,

c = slots per phase per pole,

then the total flux that links the coils shown

$$= \phi_c$$

$$= [\phi_e \times 2L_e + (\phi_s + \phi_t) \times 2L_c]b \times c \times i.$$

The coefficient of self-induction of these coils

$$= \frac{b \times c \times \phi_c}{i} 10^{-8} \text{ henry}$$

$$= b^2c^2[\phi_e \times 2L_e + (\phi_s + \phi_t) \times 2L_c] \times 10^{-8} \text{ henry.}$$

The reactance of these coils in ohms

$$= 2\pi f b^2c^2[\phi_e \times 2L_e + (\phi_s + \phi_t) \times 2L_c] \times 10^{-8}.$$

Since there are $\frac{p}{2}$ of these groups of coils per phase the reactance of one phase in ohms

$$= 2\pi f p b^2c^2[\phi_e L_e + (\phi_s + \phi_t) \times L_c] \times 10^{-8}. \qquad (28)$$

For a double-layer winding a slight modification is required in the above formula.

Figure 170 shows part of the winding of one phase of a polyphase alternator which has a double-layer winding.

The number of turns in the coils shown $= \frac{bc}{2}$.

The total flux that links these coils

$$= \phi_c$$

$$= \phi_e \times 2L_c \times \frac{b \times c}{2} \times i + (\phi_s + \phi_t) \times 2L_c \times b \times c \times i.$$

The coefficient of self-induction of these coils

$$= \frac{b \times c}{2 \times i} \times \phi_c \times 10^{-8} \text{ henry}$$

$$= \frac{b^2 \times c^2}{2}[\phi_e L_e + (\phi_s + \phi_t)2L_c]10^{-8} \text{ henry.}$$

The reactance of these coils in ohms

$$= 2\pi f b^2 c^2 \left[\frac{\phi_e L_e}{2} + (\phi_s + \phi_t)L_c\right]10^{-8}.$$

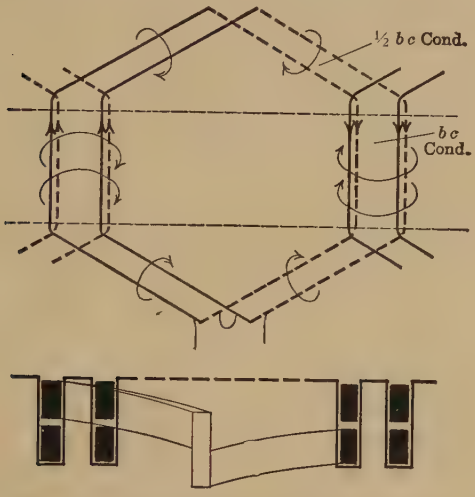

FIG. 170.—The armature leakage fields with a double-layer winding.

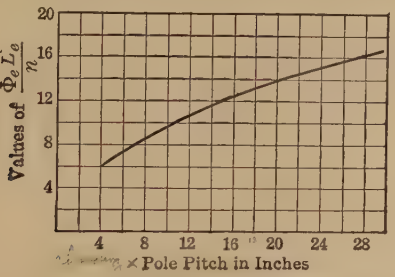

FIG. 171.—The end-connection leakage flux.

Since there are p of these groups of coils per phase, the reactance of one phase

$$= 2\pi f p b^2 c^2 \left[\frac{\phi_e L_e}{2} + (\phi_s + \phi_t)L_c\right] \times 10^{-8}, \qquad (29)$$

which differs from the formula for the chain winding in that the end-connection reactance is reduced to half the value.

The foregoing formulæ for reactance must, of course, be modified when there are two or more parallel paths in the winding. If there are two parallel paths, each path has one-half the reactance as above determined; for three parallel paths, one-third, etc.

162. End-connection Reactance.—ϕ_e depends principally on the length of the end-connection leakage path, namely, the length around the belt of end connections, which, as may be seen from Figs. 169 and 170, is directly proportional to the pole pitch and inversely proportional to the number of the phases, and

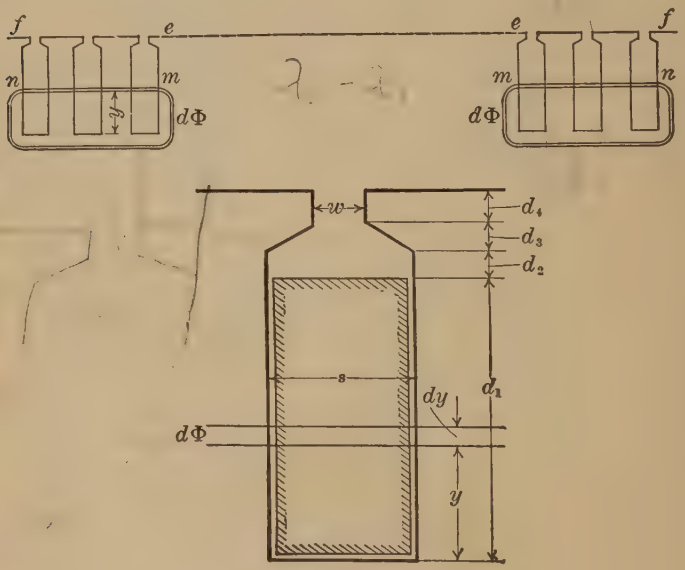

FIG. 172.—The slot leakage flux.

ϕ_e decreases as this length increases, so that $\frac{\phi_e}{n}$ is approximately proportional to $\frac{1}{\text{pole pitch}}$ for any number of phases.

L_e, the length of the end connections, increases with the pole pitch, as may be seen from Figs. 169 and 170, and in Fig. 171 $\frac{\phi_e L_e}{n}$ is plotted against pole pitch from test results.

163. Slot Reactance.—Figure 172 shows part of one phase of an alternator which has a chain winding. The m.m.f. between

m and $n = b \times c \times i \times \frac{y}{d_1}$ ampere-turns; therefore, the leakage flux $d\phi$

$$= \frac{4\pi}{10} \times b \times c \times \frac{y}{d^1} \times i \times \frac{L_c \times dy}{cs} \times 2.54 \text{ all in inch units,}$$

$$= 3.2 \times b \times c \times \frac{y}{d^1} \times i \times \frac{L_c dy}{cs}.$$

The reluctance of the iron part of the leakage path is neglected since it is small compared with that of the air path across the slots.

This flux $d\phi$ links each side of the bc $\frac{y}{d_1}$ turns of the coils shown and the interlinkages per unit current

$$= b \times c \times \frac{y}{d_1} \times \frac{2d\phi}{i}.$$

The coefficient of self-induction of the coils shown, due to the flux which crosses the slots, between the limits $y = o$ and $y = d_1$

$$= \int_o^{d_1} bc \frac{y}{d_1} \times \frac{2d\phi}{i} \times 10^{-8} \text{ henry,}$$

$$= \int_o^{d_1} b^2c^2 \left(\frac{y}{d_1}\right)^2 \times \frac{3.2 \times 2 \times L_c \times dy}{c \times s} \times 10^{-8} \text{ henry,}$$

$$= \frac{b^2c^2 \times 3.2 \times 2L_c}{c \times s} \times \frac{d_1}{3} \times 10^{-8} \text{ henry.}$$

The m.m.f. between e and f, Fig. 172, $= cbi$ ampere-turns; therefore, the leakage flux crossing the slots above the conductors

$$= 3.2cbi \times L_c\left(\frac{d_2}{cs} + \frac{2d_3}{c(s+w)} + \frac{d_4}{cw}\right).$$

The coefficient of self-induction of the coils shown due to this flux

$$= 3.2c^2b^2 \times 2L_c\left(\frac{d_2}{cs} + \frac{2d_3}{c(s+w)} + \frac{d_4}{cw}\right)10^{-8} \text{ henry.}$$

Therefore, the total coefficient of self-induction of the coils shown due to the total slot leakage

$$= 3.2cb^2 \times 2L_c\left(\frac{d_1}{3s} + \frac{d_2}{s} + \frac{2d_3}{(s+w)} + \frac{d_4}{w}\right)10^{-8} \text{ henry,}$$

and the slot reactance of these coils in ohms

$$= 2\pi f \times 3.2cb^2 \times 2L_c\left(\frac{d_1}{3s} + \frac{d_2}{s} + \frac{2d_3}{s+w} + \frac{d_4}{w}\right)10^{-8}.$$

Since there are $\frac{p}{2}$ of these groups of coils per phase the slot reactance per phase

$$= 2\pi f p b^2 c L_c \times 3.2\left(\frac{d_1}{3s} + \frac{d_2}{s} + \frac{2d_3}{s+w} + \frac{d_4}{w}\right)10^{-8},$$

$$= 2\pi f p b^2 c^2 L_c \times \phi_s \times 10^{-8},$$

where $\phi_s = \frac{3.2}{c}\left(\frac{d_1}{3s} + \frac{d_2}{s} + \frac{2d_3}{s+w} + \frac{d_4}{w}\right)$.

164. Tooth-tip Reactance.—*A*, Fig. 173, shows the tooth-tip leakage path round one side of the coils of one phase of a machine which has one slot per phase per pole, when the winding of that phase lies between the poles.

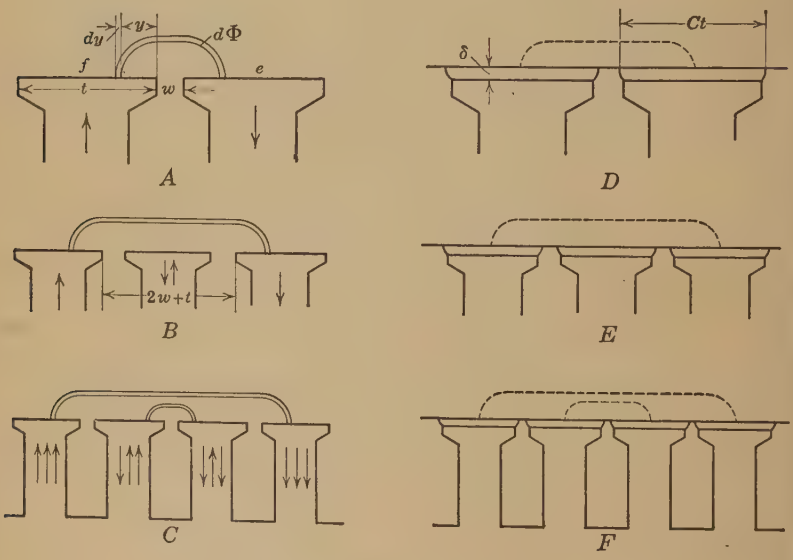

FIG. 173.—Tooth-tip leakage flux.

The m.m.f. between e and $f = bci$ ampere-turns.
Therefore, the leakage flux $d\phi$ per 1 in. length of core

$$= \frac{4\pi}{10} bci \frac{dy}{w + \pi y} \times 2.54 \text{ all in inch units},$$

$$= 3.2bci \frac{dy}{w + \pi y},$$

and the total tooth-tip leakage flux that links one phase belt per 1 in. length of core

$$= 3.2bci \int_0^t \frac{dy}{w + \pi y},$$

$$= 2.35bci \log_{10}\left(1 + \frac{\pi t}{w}\right).$$

Therefore, ϕ_{ta}, the lines of force that cross the tooth tips and circle 1 in. length of the phase belt of conductors for each ampere conductor in that belt, when the belt lies between the poles.

$$= 2.35 \log_{10}\left(1 + \frac{\pi t}{w}\right).$$

B shows the case where there are two slots per phase per pole and it may be seen that in such a case

$$\phi_{ta} = 2.35 \log_{10}\left(1 + \frac{\pi t}{2w + t}\right).$$

C shows the case where there are three slots per phase per pole and it may be seen that in such a case

the flux $2.35 \log_{10}\left(1 + \frac{\pi t}{3w + 2t}\right)$ circles the total belt,

while the flux $\frac{2.35}{3} \log_{10}\left(1 + \frac{\pi t}{w}\right)$ is produced by, and circles one-third of the total belt.

This latter flux is equivalent to a flux $\frac{2.35}{9} \log_{10}\left(1 + \frac{\pi t}{w}\right)$ circling the whole belt.

Therefore, $\phi_{ta} = 2.35 \log_{10}\left(1 + \frac{\pi t}{3w + 2t}\right) + \frac{2.35}{9} \log_{10}\left(1 + \frac{\pi t}{w}\right)$.

D shows the tooth-tip leakage path round the coils of one phase of a machine with one slot per phase per pole, when the winding of that phase lies under the poles. In this case ϕ_{tp}, the lines of force that cross the tooth tips and circle 1 in. length of the phase belt of conductors for each ampere conductor in that belt, when the belt lies under the poles,

$$= 3.2\frac{t \times C}{2\delta}.$$

In the case where there are two slots per phase per pole as shown in *E*

$$\phi_{tp} = 3.2\frac{t \times C}{2\delta}.$$

In the case where there are three slots per phase per pole as shown in F

$$\phi_{tp} = 3.2\frac{t \times C}{2\delta} + \frac{3.2}{9} \times \frac{t \times C}{2\delta}.$$

In Fig. 174 the tooth-tip flux per ampere conductor per inch is approximately

$= \phi_{ta}$ while the conductors are in the belt hk.

$= \phi_{tp}$ while the conductors are in the belt kl.

On zero power factor the current in a conductor is a maximum when the e.m.f. generated in that conductor is zero, that is, when the conductor is between the poles. As the conductor moves relative to the poles the current in the conductor varies

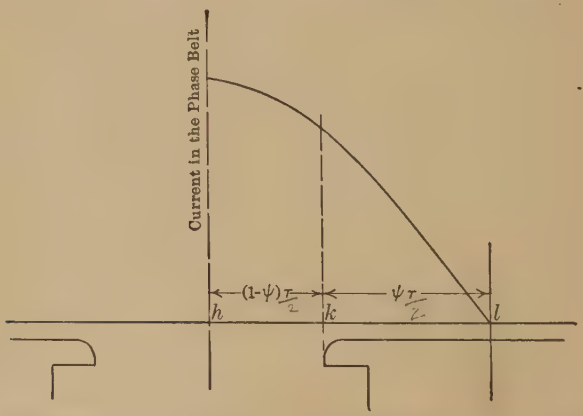

FIG. 174.—Variation of the current in the phase belt at zero power factor with the position of the belt relative to the poles.

according to a sine law as shown in Fig. 174; therefore, since the tooth-tip reactance per phase

$= 2\pi f b^2 c^2 p \phi_{ta} L_c 10^{-8}$ when the conductors are in the belt hk,

and $= 2\pi f b^2 c^2 p \phi_{tp} L_c 10^{-8}$ when the conductors are in the belt kl.

The effective voltage per phase on zero power factor due to tooth-tip leakage

$= 2\pi f b^2 c^2 p \phi_{ta} L_c 10^{-8} \times$ effective current between h and k, while they are in this belt,

and $= 2\pi f b^2 c^2 p \phi_{tp} L_c 10^{-8} \times$ effective current between k and l, while they are in this latter belt,

and from formula (28), page 216, the effective voltage per phase due to tooth-tip leakage

$$= 2\pi f b^2 c^2 p \phi_t L_c 10^{-8} \times I_{eff}.$$

Therefore, ϕ_t is approximately

$$= \left(\frac{1-\psi}{1} \times \frac{\text{effective current in belt } hk}{I_{eff}} \times \phi_{ta} + \psi \frac{\text{effective current in belt } kl}{I_{eff}} \times \phi_{tp}\right).$$

As a general rule, ψ, the pole enclosure $= 0.6$
and for this value $1 - \psi = 0.4$,
effective current in conductors in belt $hk = 0.93\ I_{max}$,
effective current in conductors in belt $kl = 0.5\ I_{max}$.

Therefore, $\phi_t = \phi_{ta} \times 0.4 \times \frac{0.93 I_{max}}{0.71 I_{max}} + \phi_{tp} \times 0.6 \times \frac{0.5\ I_{max}}{0.71 I_{max}}$,

$$= 0.52\phi_{ta} + 0.42\phi_{tp}.$$

165. Final Reactance Formulae.—In the foregoing analysis, it has been assumed that full-pitch windings are used on all armature windings. If short-pitch windings are used, another factor is introduced. It is shown in Art. 140 that the voltage generated in a short-pitch winding is less than that in a full-pitch winding of the same number of turns by the factor $\cos \frac{\theta}{2}$. This same factor enters the expression for reactance, so that the reactance in ohms of one phase of a polyphase generator is

$$= {}^{1}2\pi f b^2 e^2 p(\phi_e L_e + [\phi_s + \phi_t]L_c)10^{-8} \qquad (28a)$$

for chain windings;

$$\longrightarrow = 2\pi f b^2 c^2 p \cos^2 \frac{\theta}{2}\left(\frac{\phi_e L_e}{2} + [\phi_s + \phi_t]L_c\right)10^{-8} \qquad (29)$$

for double-layer windings.

The value of $\phi_e L_e$ may be found from Fig. 171.

$$\phi_s = \frac{3.2}{c}\left(\frac{d_1}{3s} + \frac{d_2}{s} + \frac{2d_3}{s+w} + \frac{d_4}{w}\right).$$

$$\phi_t = 0.52\phi_{ta} + 0.42\phi_{tp}.$$

$$\phi_{ta} = 2.35 \log_{10}\left(1 + \frac{\pi t}{w}\right) \text{ for one slot per phase per pole.}$$

$$= 2.35 \log_{10}\left(1 + \frac{\pi t}{2w + t}\right) \text{ for two slots per phase per pole.}$$

$$= 2.35 \log_{10}\left(1 + \frac{\pi t}{3w + 2t}\right) + \frac{2.35}{9} \log_{10}\left(1 + \frac{\pi t}{w}\right) \text{ for three slots per phase per pole.}$$

[1] Since chain windings can not be other than full pitch, the factor $\cos \frac{\theta}{2}$ does not enter the expression for reactance in chain windings.

$\phi_{tp} = 3.2\dfrac{t \times C}{2 \times \delta}$ for one or two slots per phase per pole.

$= 3.2 \times \dfrac{10}{9} \times \dfrac{t \times C}{2 \times \delta}$ for three slots per phase per pole.

f = frequency in cycles per second.
b = conductors per slot.
c = slots per phase per pole.
p = poles.
n = phases
L_c = frame length in inches.
t = width of tooth at the tip.
C = Carter coefficient found from Fig. 45, page 47.
θ = chording of winding in electrical deg.

Slot dimensions are given in Figs. 172 and 173.

Example of Calculation.—The armature reaction and armature reactance can be checked approximately by the no-load saturation and the short-circuit curves of an alternator. Figure 175 shows the actual test curves on a small alternator which was built as follows:

Poles,	6
Pole enclosure,	0.6
Pole pitch,	10.5 in.
Air-gap clearance,	0.2 in.
Slots per pole,	6
Conductors per slot,	12
Size of slot,	0.75 × 1.75 in., open
Tooth width,	1.0 in.
Carter coefficient,	1.2
Frame length,	6.5 in.
Winding,	double layer, full pitch Y-connected
Turns per field coil,	420
Rating,	65 k.v.a., 600 volts, three phase, 60 cycles.

To send full-load current through the machine on short circuit requires an excitation of 4.8 amperes. Now the power factor during this test is zero since the machine is carrying no load, and the terminal voltage is zero since the machine is short circuited; therefore, m is a point on the full-load saturation curve at zero power factor, the resistance drop being neglected.

The demagnetizing ampere-turns per pole

$= 0.35 \times$ conductors per pole $\times I_c$,

$= 0.35 \times 12 \times 6 \times 62.5$,

$= 1580$ ampere-turns per pole.

The corresponding field current

$$= \frac{\text{demagnetizing ampere-turns per pole}}{\text{field-turns per pole}}.$$

$$= \frac{1580}{420}.$$

$$= 3.75 \text{ amperes.}$$

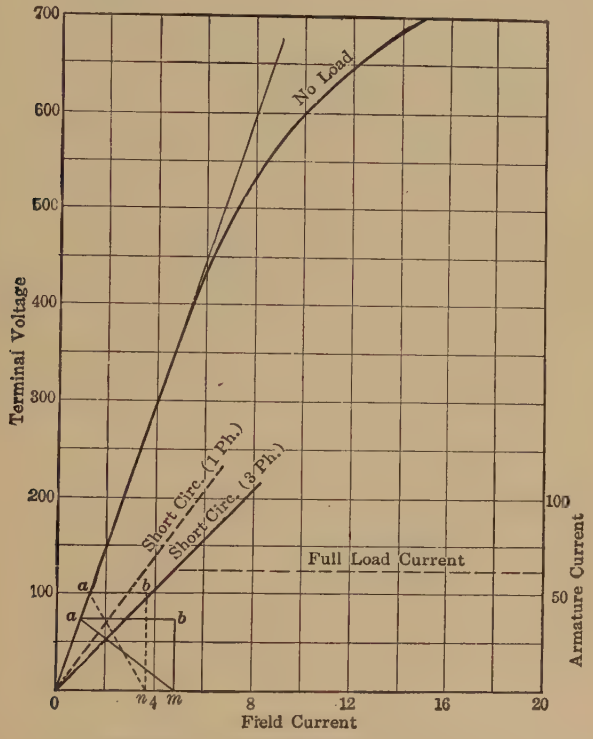

FIG. 175.—No-load saturation and short-circuit curves on a 65-k.v.a. three-phase alternator.

The reactance per phase

$$= 2\pi f b^2 c^2 \cos^2 \frac{\theta}{2} p \left(\frac{\phi_e L_e}{2} + (\phi_s + \phi_t) L_c\right) 10^{-8} \text{ ohms,}$$

where $\frac{\phi_e L_e}{2} = 5 \times n$ from Fig. 171, since the pole pitch = 10.5 in.

$$= 15.$$

$$\phi_s = \frac{3.2}{2}\left(\frac{1.5}{3 \times 0.75} + \frac{0.25}{0.75}\right) = 1.6.$$

$$\phi_{ta} = 2.35 \log \left(1 + \frac{\pi \times 1}{(2 \times 0.75) + 1}\right) = 0.82.$$

$$\phi_{tp} = 3.2 \times \frac{1 \times 1.2}{2 \times 0.2} = 9.6$$

$$\phi_t = 0.52 \times 0.82 + 0.42 \times 9.6 = 4.4:$$

$$\theta = 0°$$

$$\cos^2 \frac{\theta}{2} = 1.$$

Reactance per phase

$= 2 \times \pi \times 60 \times 12^2 \times 2^2 \times 6(15 + (1.6 + 4.4)6.5) \times 10^{-8}$

$= 0.7$ ohm.

The voltage drop per phase $= 0.7 \times 62.5 = 44$ volts,

and the voltage drop at the terminals $= 1.73 \times 44$

$= 76$ volts,

since the winding is Y connected.

These two figures, 3.75 field amperes, 76 terminal volts, are the only ones required for the construction of triangle *abm*, Fig. 175, and it may be seen that the calculated results check the test results very closely.

166. Variation of Armature Reaction and Armature Reactance with Power Factor.—When an alternator is carrying a load

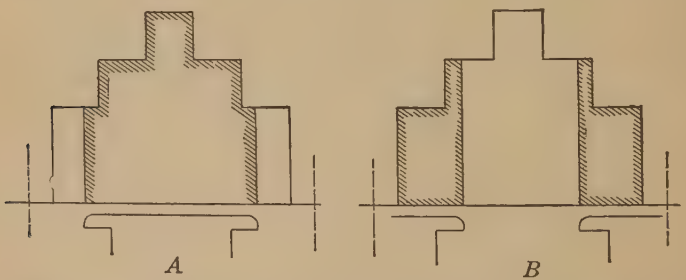

Current lags by 90 degrees. Current is in phase.

FIG. 176.—Effect on the armature reaction of the phase relation between the current and the generated e.m.f.

whose power factor is zero, the current in the conductors reaches a maximum when the conductors are between the poles; the tooth-tip leakage is then a minimum. When, however, the current is in phase with the generated voltage, it reaches a maximum when the conductors are under the center of the poles; the tooth-tip leakage is then a maximum. The voltage drop due to armature reactance, therefore, varies with the power factor and is a maximum when the current is in phase with the generated voltage and a minimum when the current is out of phase with that voltage by 90 deg.

The distribution of the m.m.f. of armature reaction for the same two cases is shown in Fig. 176: diagram *A* shows the distribution when the current lags the generated voltage by 90 deg. and the armature m.m.f. is demagnetizing; diagram *B* shows the distribution when the current is in phase with the generated voltage and the armature m.m.f. is cross magnetizing. It may be seen from these diagrams that AT_{av}, the average value of the part of this m.m.f. which is effective, is a minimum when the current is in phase with the generated voltage and a maximum when the current is out of phase by 90 deg.

The variation of armature reactance and armature reaction with power factor is difficult to calculate and it is usual to assume that any decrease in one of them with a change in power factor is counterbalanced by an increase in the other so that the resultant effect, which is represented by a synchronous reactance, is constant at all power factors, for a given field excitation.

167. Full-load Saturation Curve at Any Power Factor.—Given the no-load saturation curve and also that at full load and zero

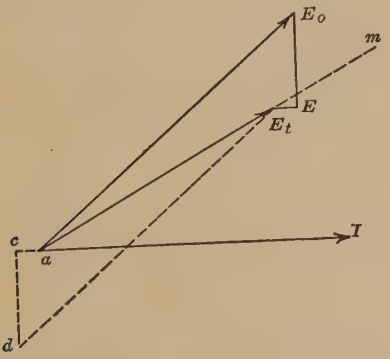

FIG. 177.—Vector diagram for an alternator.

power factor, it is required to draw in the full-load saturation curves for other power factors. The method adopted to determine different points on these curves is shown in Fig. 177, where the diagram shown by heavy lines is taken from Fig. 164.

E_o = the no-load voltage per phase corresponding to the field excitation *og*, Fig. 184, page 237 and = *dg*,

E_oE = the synchronous reactance drop = *dc*, Fig. 184.

E_tE = the resistance drop per phase,

ϕ = the phase angle between E_t and I,

$\cos\phi$ = the power factor of the load.

The construction generally adopted to find E_t is shown by the dotted lines in Fig. 177.

Triangle *acd* is drawn to scale in the proper phase relation with I and equal to triangle EE_oE_t.

Line *am* is set off at an angle ϕ such that cos ϕ is the power factor at which it is desired to find the terminal voltage.

With *d* as center and E_o as radius the line *am* is cut at E_t and the value E_t is then plotted along the ordinate of field excitation for which E_o is the no-load voltage and = *gf*, Fig. 184, for 85 per cent power factor. This gives a point at full load, normal voltage, 85 per cent power factor. To get other points on the 85 per cent power factor full load saturation curve, take any other no-load voltage and with that as a radius cut the line *am* at another point and set off the distance from *a* so obtained against the value of the excitation at no load to give that voltage. This will give another point on the 85 per cent power-factor full load saturation curve. For any other power factor, the angle between *aI* and *am*, Fig. 177, must be made such that its cosine is the power factor.

168. Regulation.—The regulation of an alternator is defined as the per cent increase in voltage when full load is thrown off the machine, the speed and excitation being kept constant, and is equal to

$\frac{ab}{be}$, Fig. 184, at unity power factor,

$\frac{df}{fg}$, Fig. 184, at 85 per cent power factor,

$\frac{hk}{kl}$, Fig. 184, at zero power factor.

169. Effect of Pole Saturation on the Regulation.—A_1 and B_1, Fig. 178, are the no-load saturation curves of two alternators which have armatures that are exactly alike; the field systems differ in that machine A has a smaller air-gap and a greater pole density than has machine B; the excitation is the same for each machine at normal voltage and no load.

A_2 and B_2 are the no-load saturation curves with the full-load leakage factor. The effect of the increase in the leakage factor is the greater in the machine which has the higher pole density.

A_3 and B_3 are the full-load saturation curves at zero power factor; the demagnetizing ampere-turns per pole are the same in each case; the armature reactance drop is slightly greater in the machine with the smaller air-gap clearance.

It may be seen that the machine with the saturated poles is that which has the best regulation; but it is also the machine which takes the largest field excitation on load.

Of two machines that are built to meet the same regulation guarantee, that with the higher pole density is generally the cheaper, because, as shown in Fig. 178, for the same armature reaction and reactance it gives the better regulation, or for the same regulation it can have the greater armature reaction and reactance. If these quantities are increased by increasing the number of armature turns, then, for constant output, the flux per pole must be decreased in the same ratio and the whole

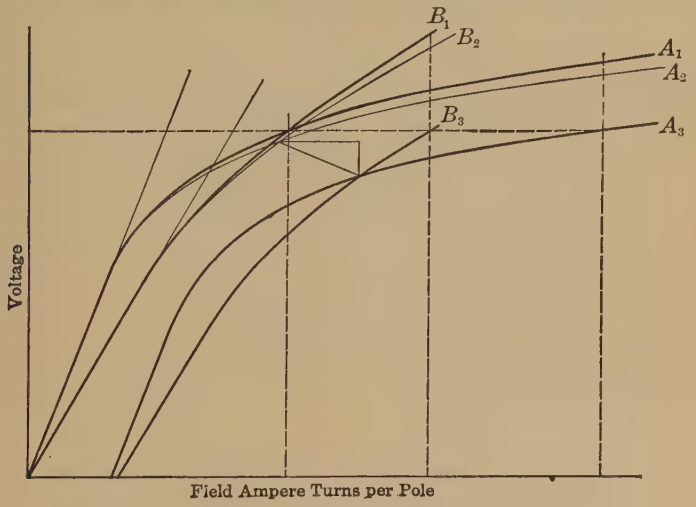

Fig. 178.—Effect of pole saturation on the regulation.

machine may be made smaller. In order to carry an increased number of conductors on a smaller diameter, it is necessary to increase the slot depth.

The pole density is seldom carried above 85,000 lines per square inch at no load and normal voltage, because for higher densities it is difficult to predetermine the saturation curves with sufficient accuracy to insure that there is enough field excitation at the high densities corresponding to normal voltage, full load and zero power factor, since the permeability of the iron used may be lower than was expected.

170. Relation between the M.M.Fs. of Field and Armature.—In Fig. 179, A_1 and B_1 are the no-load saturation curves, A_2 and

B_2 the no-load saturation curves with the full-load leakage factor, A_3 and B_3 the full-load saturation curves at zero power factor, of two machines which are alike in every respect except that the air-gap of machine A is smaller than that of machine B.

It may be seen from these curves that the larger the air-gap and, therefore, the larger the ratio of $\frac{\text{field } AT \text{ per pole}}{\text{armature } AT \text{ per pole}}$, the better is the regulation.

In modern A.-C. generator designs there is no particular attempt to secure good inherent regulation. Suitable voltage regulation

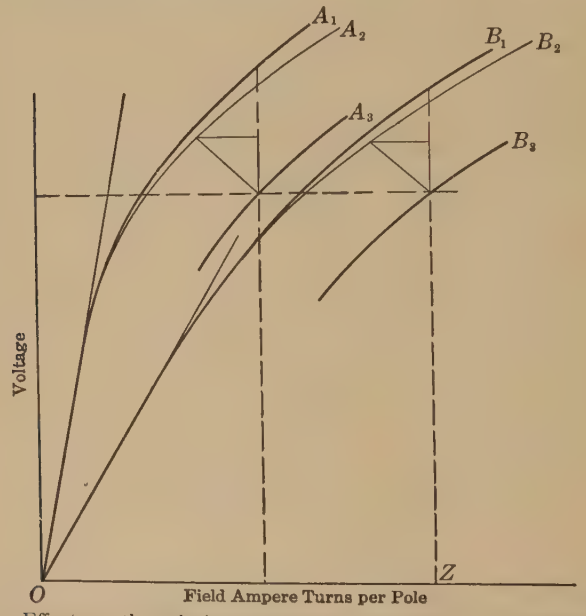

FIG. 179.—Effect on the relative strengths of the field and armature m.m.fs. on the regulation.

may be obtained by means of automatic voltage regulators, of which there are a number available. In present-day practice the maximum field ampere-turns per pole, namely *oz*, Fig. 179, are made from 2.00 to 2.5 times the demagnetizing effect of full-load armature ampere-turns per pole. Since the demagnetizing effect is only about 0.7 the actual armature ampere-turns (see Art. 160), it follows that the maximum field ampere-turns i.e. for zero power factor, full load are from 1.4 to 1.75 times the

armature ampere-turns at full load. For preliminary designs a ratio of 1.75 may be taken as a first approximation.

Such a design admittedly does not give good inherent regulation, but, as indicated above, this may be secured in other ways. Good inherent voltage regulation cannot be divorced from excessive values of current on accidental short-circuit-values of current that may be high enough to damage circuit-breakers as well as other parts of the system that might be affected by excessive currents. Before about 1912, good inherent regulation was usualy demanded by A.-C. generator users, but since that time, regulation has ceased to be a factor.

There is a consideration in very long modern transmission lines of very high voltage that may bring back a demand for good inherent regulation, and that is the use of synchronous machines as condensers on the receiving ends of these long lines. The amount of power that these lines can carry without becoming "unstable" is to some extent a function of the inherent regulation of the synchronous condensers at the receiving ends. The discussion of this matter, however, is one that is outside the bounds of this book.

SINGLE-PHASE MACHINES

171. Armature Reaction in Single-phase Machines.—Consider the conditions at zero power factor; the current lags the e.m.f.

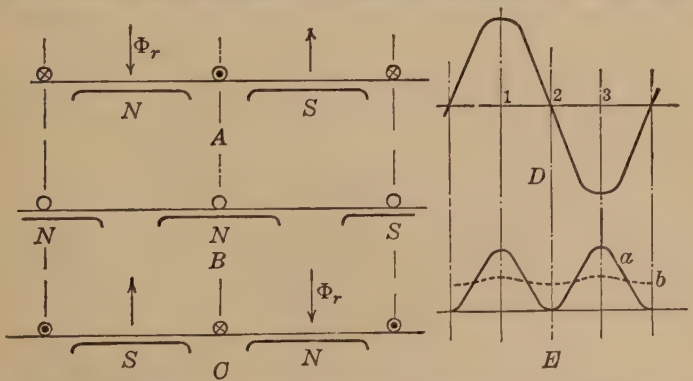

FIG. 180.—Pulsation of the armature field in a single-phase alternator.

by 90 deg. and so reaches a maximum in the conductors when these conductors lie between the poles.

A, *B* and *C*, Fig. 180, show the position of the poles relative to the armature when the current has the values given at instants

1, 2 and 3, diagram *D*. It may be seen that while the current passes through half a cycle and the poles move through one pole pitch, the flux ϕ_r, due to the armature m.m.f., goes through half a cycle relative to the armature coils, while relative to the poles it changes from a maximum in diagram *A* to zero in diagram *B* and back to a maximum in diagram *C*, and so, as shown in curve *a*, diagram *E*, is pulsating relative to the poles with double normal frequency.

The poles are surrounded by the field coils, which are short-circuited through the exciter, and any pulsating flux in the poles induces a current in these coils which, according to Lenz's Laws, tends to wipe out the flux; thus the pulsation becomes dampened out, as shown in curve *b*, diagram *E*. The armature field is, therefore, equivalent in effect to a constant field, which is fixed relative to the poles and has a value of approximately half the maximum value which it would have if the pulsation were not damped out.

Another way to look at the above subject is as follows: the armature field is stationary in space and is alternating. Such a field, as pointed out in Art. 136, page 179, can be exactly represented by two progressive fields of constant value which move in opposite directions through the distance of two pole pitches, while the alternating field goes through one cycle. Consider these two fields to exist separately; then one moves in the same direction and at the same speed as the poles while the other moves at the same speed but in the opposite direction to the poles. The former is, therefore, stationary with regard to the poles and may be treated in exactly the same way as the armature field in a polyphase machine; the latter field revolves at the same speed as the main poles but in the opposite direction and so causes a double-frequency pulsation of flux in these poles, which pulsation induces currents in the field windings that tend to wipe out the flux, so that the effect of this latter field can be neglected in a discussion of armature reaction.

A flux of double frequency in the poles will produce a third harmonic of e.m.f. in the armature, as shown in Art. 136, page 179; a third harmonic of current in the armature will produce a fourth harmonic of flux in the poles and so on; however, high-frequency harmonics in the poles are so well damped out that those higher than the third can be neglected.

The demagnetizing ampere-turns per pole and the leakage reactance are worked out below for a particular case; the method is quite general, but since the result depends on the per cent of the pole pitch that is covered by the winding, no general formula is deduced.

172. The Demagnetizing Ampere-turns per Pole at Zero Power Factor.—Figure 181 shows the distribution of the m.m.f. of armature reaction for a machine with b conductors per slot, and six slots per pole, of which four are used, at the instant when the current has its maximum value.

If the pole arc = 0.6 times the pole pitch, then
the average value of that part of the maximum m.m.f. which is effective $\times$ 3.6λ,

$$= \text{area of cross-hatched curve in Fig. 181,}$$
$$= 2bI_m \times 3\lambda + bI_m \times 0.6\lambda,$$
$$= 6.6bI_m\lambda.$$

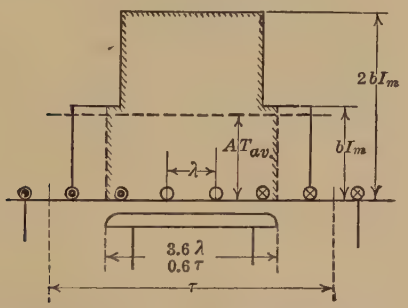

FIG. 181.—The maximum m.m.f. of a single-phase alternator on zero power factor.

The constant field which is fixed relative to the poles, and which is the only one that need be considered in calculations, has a value of half the above maximum value; therefore, the average value of the part of this constant field which is effective = AT_{av} is such that $AT_{av} \times 3.6\lambda = \dfrac{6.6bI_m\lambda}{2}$,

and $AT_{av} = 0.92bI_m$,

$$= 1.3bI_c \text{ where } I_c \text{ is the effective current,}$$
$$= 1.3bI_c \times \frac{\text{effective slots per pole}}{4},$$
$$= 0.32 \times \text{conductors per pole} \times I_c. \qquad (30)$$

173. The Leakage Reactance.—As in the case of the polyphase machine this consists of end-connection, slot and tooth-tip reactance.

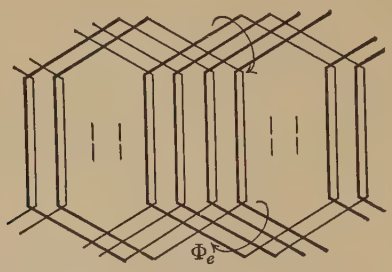

FIG. 182.—The end-connection leakage path in single-phase alternators.

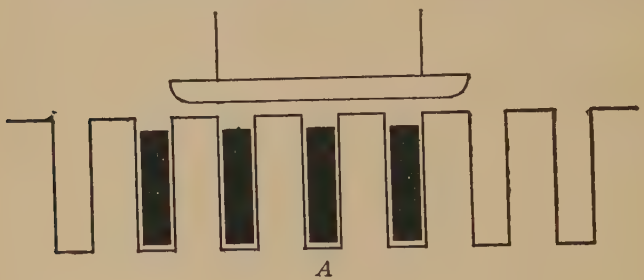

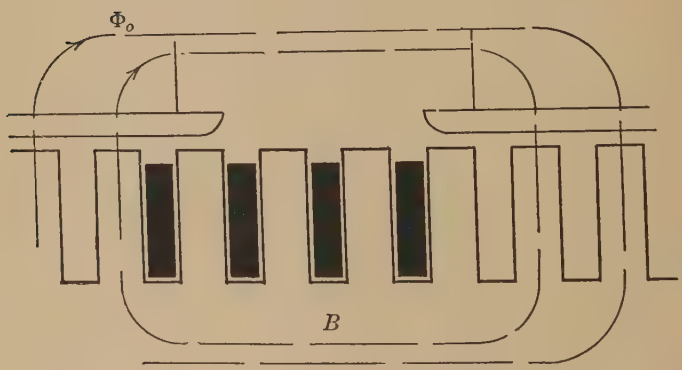

FIG. 183.—The positions of maximum and minimum tooth-tip leakage.

The end-connection reactance $= 2\pi f p b^2 c^2 \left(\cos \frac{\theta}{2}\right)^2 (\phi_e L_e) 10^{-8}$ for a machine with a chain winding and half of this value for a machine with a double-layer winding, where c is the effective number of slots per pole or the number which carry conductors.

$\phi_e L_e$ is found from Fig. 171, but it must be noted that for the type of winding shown in Fig. 182, ϕ_e links the coils of four slots, and the length of the end-connection leakage path is two-thirds of the value which it would have if all the slots were used; the value of $\phi_e L_e$ is, therefore, three-halves times that found from Fig. 171.

$$\text{The slot reactance} = 2\pi f p b^2 c^2 \left(\cos\frac{\theta}{2}\right)^2 L_c \times \phi_s \times 10^{-8}$$

where $\phi_s = \frac{3.2}{c}\left(\frac{d_1}{3s} + \frac{d_2}{s} + \frac{2d_3}{s+w} - \frac{d_4}{w}\right)$; the slot dimensions are given in Fig. 172, page 218, and c is the effective number of slots per pole.

The tooth-tip reactance varies from a maximum, when the conductors are in position A, Fig. 183, to a minimum, when they are in position B. In the former position it may be seen that three only of the slots lie under the pole at any time, while in the latter position it may be assumed that three only of the slots are effective, since the leakage lines ϕ_o which link all the slots have to pass through the field windings and are, therefore, damped out.

An approximate solution for the case of a machine with six slots per pole of which four are used, and which has a pole arc = 0.6 times the pole pitch, is

$$\text{tooth-tip reactance} = 2\pi f b^2 c^2 \left(\cos\frac{\theta}{2}\right)^2 p L_c \times \phi_t \times 10^{-8}$$

where ϕ_t has the value given in Art. 165, page 223, for three slots per phase per pole and c for the assumed conditions = 3.

Example of Calculation.—Figure 175 shows the actual test curves on a small alternator which has six slots per pole of which four are used; the single-phase short-circuit curve is shown dotted.

The demagnetizing ampere-turns per pole

$$= 0.32 \times 12 \times 4 \times 62.5,$$

$$= 960 \text{ ampere-turns per pole.}$$

The corresponding field current

$$= \frac{\text{demagnetizing ampere-turns per pole}}{\text{field-turns per pole}},$$

$$= \frac{960}{420},$$

$$= 2.3 \text{ amp.}$$

The reactance per phase

$$= 2\pi f b^2 c^2 \cos^2\frac{\theta}{2}\, p\left(\frac{\phi_e L_e}{2} + (\phi_s + \phi_t) L_c\right) 10^{-8} \text{ ohms}$$

where these symbols have to be interpreted in the light of the last article.

$\frac{\phi_e L_e}{2}$ = (5 × 1, from Fig. 171) × $\frac{3}{2}$ since, as pointed out in the last article the value found from Fig. 171 has to be increased 50 per cent because four only of the six slots per pole are used.

$$\phi_s = \frac{3.2}{4}\left(\frac{1.5}{3 \times 0.75} + \frac{0.25}{0.75}\right) = 0.8.$$

$$\phi_{ta} = 2.35 \log_{10}\left(1 + \frac{\pi \times 1}{(3 \times 0.75 + (2 \times 1)}\right) + \frac{2.35}{9} \log_{10}\left(1 + \frac{\pi \times 1}{0.75}\right)$$

$$= 0.75.$$

$$\phi_{tp} = 3.2 \times \frac{10}{9} \times \frac{1 \times 1.2}{2 \times 0.2} = 10.7.$$

$$\phi_t = 0.52 \times 0.75 + 0.42 \times 10.7 = 4.9.$$

$$\cos^2 \frac{\theta}{2} = 1$$

Reactance per phase

$$= \{2 \times \pi \times 60 \times 12^2 \times 4^2 \times 6(7.5 + 0.8 \times 6.5)10^{-8}\}$$
$$+ \{2 \times \pi \times 60 \times 12^2 \times 3^2 \times 6(4.9 \times 6.5)10^{-8}\}$$
$$= 1.6 \text{ ohms.}$$

The voltage drop per phase = 1.6 × 62.5,
= 100 volts.

With this value and with the demagnetizing effect = 2.3 amp. the triangle *abn*, shown dotted in Fig. 175, is drawn in and it may be seen that the calculated results check the test results very closely.

174. Regulation of Single-phase and Three-phase Alternators. In the machine whose test results are shown in Fig. 175 the output at full load

= 1.73 × 600 × 62.5 = 65 k.v.a. for the three-phase rating,
= 600 × 62.5 = 37.5 k.v.a. for the single-phase rating,

or the single-phase output is about 60 per cent of the three-phase output. For this ratio, n is a point on the full-load saturation curve of the single-phase machine and m a point on that of the three-phase machine, and, as may be seen, the former machine has the better regulation. For the same regulation in each case the single-phase machine may be given 65 per cent of the three-phase rating.

CHAPTER XIX

DESIGN OF A REVOLVING FIELD SYSTEM

The problem to be solved in this chapter is, given the armature of an alternator and also its rating, to design the whole revolving field system.

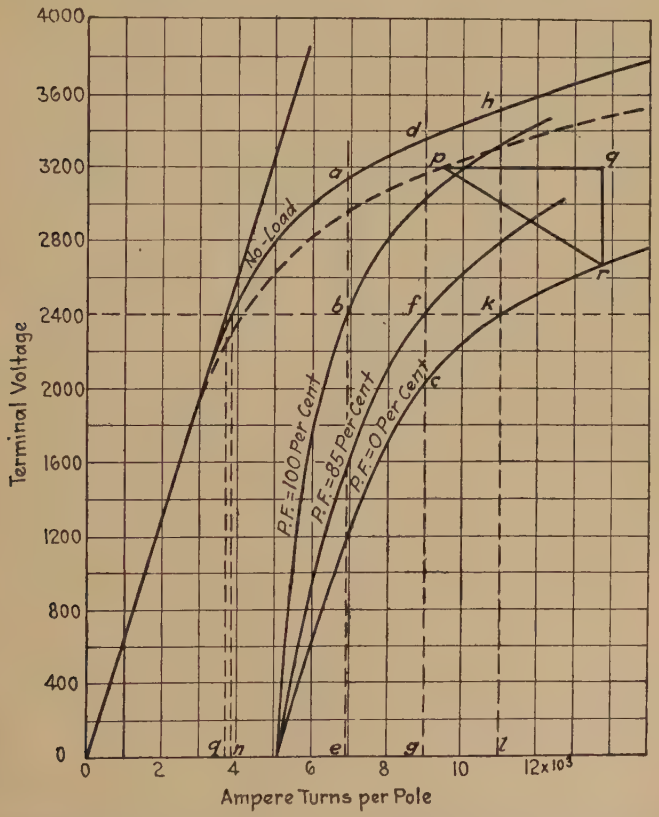

Fig. 184.—Saturation curves for a 937.5-k.v.a., 2400-volt, three-phase, 60-cycle, 600 r.p.m. alternator.

175. Field Excitation.—Figure 184 shows several of the saturation curves of an alternator of the following rating:
937.5 k.v.a. (750 k.w. at 80 per cent power factor), 2400 volts, 600 r.p.m., three phase, 60 cycles.

The excitation required for normal voltage
= *on* at no load,
= *oe* at full load and unity power factor,
= *og* at full load and 85 per cent power factor,
= *ol* at full load and zero factor.

The maximum exciting current $= \frac{\text{exciter voltage}}{\text{hot resistance of field coils}}$ and
the maximum excitation = maximum exciting current × field-turns per pole,
= *ol*.

The radiating surface of the field coils should be large enough to keep the temperature rise with the excitation *og* below that guaranteed, which is generally 50°C. with class *A* and 90°C. with class *B* insulation.

The maximum excitation *ol* should be large enough to enable the alternator to give normal voltage on all loads and power factors to be met in practice. If the maximum excitation is large enough to maintain normal voltage at full load and zero power factor, it will generally be found ample for all ordinary overloads and power factors.

The field resistance should have such a value that the maximum excitation *ol* may be obtained with the normal exciter voltage

176. Procedure in the Design of a Revolving Field System.—(*a*) Find AT_{max}, the maximum excitation = 1.75 (armature AT per pole) for a first approximation, see Art. 170, page 229.

(*b*) Find M, the section of the field coil wire from the formula

$$M = \frac{AT_{max} \times \text{mean turn}}{\text{volts per coil}} \quad \text{(formula (7), page 67)}$$

where the volts per coil $= \frac{\text{exciter voltage}}{\text{poles}}$ and the mean turn is found as follows:

ϕ_a = the flux per pole crossing the gap $= \frac{E \times 10^8}{2.22kZf \cos \frac{\phi}{2}}$

(formula (26) page 185).

lf, the leakage factor, is assumed to be 1.2 for a first approximation.

Pole area $= \frac{\phi_a \times lf}{\text{pole density}}$ where the pole density at normal voltage and frequency and at no load is taken as 85,000 lines per square inch, which is about at the beginning of the bend in

the saturation curve (see Fig. 47). The pole area also = .95 $L_p \times W_p$ (5 per cent being allowed for staking factor).

L_p, the axial length of the pole, is made 0.5 in. shorter than the frame length so that the rotor can oscillate freely. The value of W_p, the pole waist, and of MT, the mean turn of the coil, can then be found approximately.

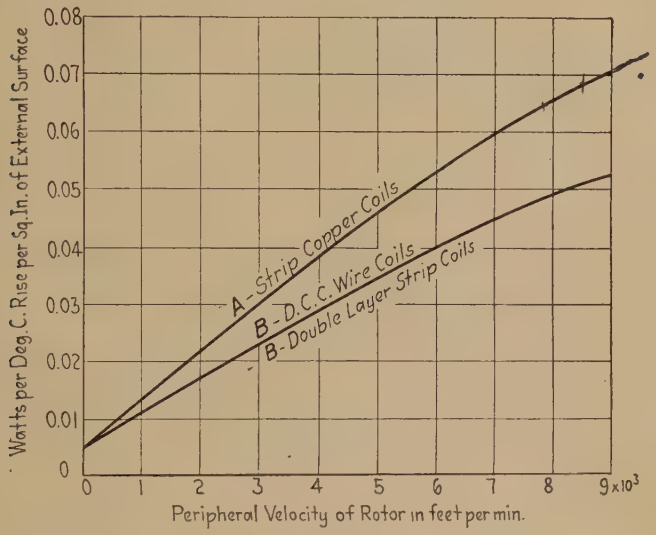

FIG. 185.—Heating curves for the field coils of revolving field alternators.

(*c*) Find L_f, the radial length of the field coil, from the formula

$$L_f = \frac{AT_{max}}{1000} \times \sqrt{\frac{\text{mean turn}}{\text{external periphery} \times \text{watts per square inch} \times d_f \times sf \times 1.27}}$$

(formula (9), page 72), where:

external periphery is found approximately from the pole dimensions;

watts per square inch is found from Fig. 185 which gives approximate heating for field coils on machines similar in construction to that shown in Fig. 137 and with the type of field coil shown in Fig. 141;

d_f, the winding depth, is chosen so as to give the most economical field structure. It was shown in Art. 61, page 72, that the smaller the value of d_f the lower the cost of the field copper but the longer and more expensive the poles. The most

economical depth can be found by trial but the following values may be used as a first approximation:

Pole pitch, inches	Depth of field coil, inches	
	60-cycle	25-cycle
5	1.2	
10	1.5	1.5
15	1.75	2.0
20	....	2.5
30	....	3.0
40	....	3.5

For a given pole pitch the 60-cycle machine runs at a higher peripheral velocity than the 25-cycle machine; it, therefore, requires less radiating surface for the same excitation, and the poles become very short unless the value of d_f is decreased below that which is found best for 25-cycle machines. The above figures are for strip copper field windings; when d.c.c. wire is used, the above depth should be increased about 20 per cent because of the poorer space factor of this type of winding, and the coils should be tapered, if necessary, as shown in Fig. 141. T_f is the number of field-turns that will fill up the space $d_f L_f$, the size of wire being fixed.

177. Calculation of the Saturation Curves.—It is necessary first of all to find the air-gap clearance, which is done as follows: The approximate number of ampere-turns per pole required for the air-gap at no load and normal voltage, namely oq, Fig. 184, $= ol - lq$ and is approximately

$$= AT_{max} - 1.2 \text{ (armature } AT \text{ per pole).}$$

Since the flux per pole and also the dimensions of the machine are given, the apparent gap density and, therefore, the air-gap clearance required, can be found from the formulæ

$$\text{Apparent gap density} = \frac{\text{flux per pole crossing the gap}}{\tau \times \psi \times L_c}.$$

$$\text{Air-gap ampere-turns} = \frac{\text{apparent gap density}}{3.2} \times \delta \times C \text{ (formula (3), page 51).}$$

The magnetic circuit is now drawn in to scale and the leakage factor and the no-load saturation curves calculated by the method explained in Arts. 50 and 51, page 50.

The leakage factor at full load and zero power factor

$= 1 + m\left(\frac{AT_{g+t} + \text{demagnetizing } AT \text{ per pole}}{AT_{g+t}}\right)$ (Art. 158, page 212), where m is the no-load leakage factor, minus 1 and the demagnetizing AT per pole $= 0.35 \times$ conductors per pole $\times I_c$.

A new no-load saturation curve is calculated using the above full-load leakage factor and plotted as shown in the dotted curve in Fig. 184.

The reactance per phase is determined from the formulæ on page 223, and the triangle *pqr* and the full-load saturation curve at zero power factor are then drawn in.

The full-load saturation curves at other power factors are calculated by the use of the diagram shown in Fig. 177, and from these curves the regulation at the different power factors is determined.

Example of Field Calculation.—The armature data of a 937.5-k.v.a. (750 kw. at 80 per cent power factor) 2400-volt, 600-r.p.m. 60-cycle alternator are as follows:

Poles	12.
Internal diameter	42.5 in.
Pole pitch	11.12 in.
Frame length	12.5 in.
Center vent ducts	$5 \times \frac{3}{8}$ in.
Slots per pole, number	9, open type.
Slot dimensions	0.43×2.35 in.
Conductors per slot	12.
Connection	2 parallel Y.
Exciter voltage	125.
Armature amperes full load	226.

It is required to design the revolving field system:

The armature ampere-turns per pole

$$= \text{slots per pole} \times \frac{\text{conductors per slot}}{2} \times I_c$$

$$= 9 \times \frac{12}{2} \times \frac{226}{2} = 6100 \text{ ampere-turns.}$$

AT_{max} = the maximum excitation $= 1.75 \times 6100 = 10{,}700$ (see Art. 170) (approximately).

E = the voltage per phase = $\frac{2400}{1.73}$ (since connection is Y) = 1380.

ϕ_a = flux per pole = $\frac{1380 \times 10^8}{2.22 \times 0.96 \times \frac{9 \times 12}{3 \times 2} \times 12 \times 60.}$ (see Art. 140) = 5×10^6.

lf = field leakage factor, assumed to be = 1.2.

Pole area = $\frac{5 \times 10^6 \times 1.2}{85{,}000} = 70.6$ (approximately).

L_p = axial length of the field pole is made 0.5 in. shorter than the frame length and = 12 in.

W_p = pole waist = $\frac{70.6}{0.95 \times 12} = 6.2$ in.

d_f = depth of field-coil winding, from Art. 176, should be about 1.5 in. (table on p. 238). However, to obtain adequate ventilating space the field winding is tapered and made partly of strap copper 0.625 in. wide and the remainder of 1.125 strap. MT = length mean turn = $2(12 + 6.2) + \pi \times 2.3 = 43.6$ in. The factor 2.3 allows for the width of strap and also for the necessary insulation between pole and field winding.

External periphery of field coil = 45 in. (approximately).

M = section of field copper = $\frac{10{,}700 \times 43.6}{10.4} = 45{,}000$ circular mils (see Art. 59, p. 71).

45,000 circular mils = 0.0354 sq. in. = $\begin{cases} 0.625 \times 0.057 \\ 1.125 \times 0.032 \end{cases}$

Section actually used = $\begin{cases} 0.625 \times 0.063. \\ 1.125 \times 0.04. \end{cases}$

This increased section of field copper allows ample margain for obtaining more than the calculated 10,700 ampere-turns on field if necessary without exceeding the normal 125 exciter volts.

Watts per square inch for 90°C. temperature rise = $0.057 \times 90 = 5.13$ (see Fig. 185, p. 239).

sf = space factor = about 0.75 if asbestos or mica of approximately 15 mils be used between turns.

L_f = radial length of field coil =

$$\frac{10{,}700}{1000} \sqrt{\frac{43.6}{45 \times 5.13 \times 1 \times 0.75 \times 1.27}}$$

= 4.75 in. (see Art. 176).

Using the calculated value of copper conductor and 15-mil insulation between turns, this space would be filled by 23 turns of 0.625- × 0.057-in. strap and 65 turns of 1.125 × 0.032. However, a larger cross-section of field copper than the calculated value was actually used, and the total height of the pole occupied by windings was made 5.4 in.

T_f = number of turns field winding per pole = 88.

Maximum exciting current = $\frac{AT_{max}}{T_f} = \frac{10{,}700}{88} = 122$ amperes.

Maximum exciter output = 15.3 kw. including rheostat.

= 1.63 per cent of normal volt-ampere rating.

ATg = air-gap ampere-turns per pole at normal voltage and no load.

= $AT_{max} - 1.2$ armature AT per pole (see Art. 177).

= $10{,}700 - 1.2 \times 6100 = 3400$.

ψ = pole enclosure is taken as 0.74.

Bg = apparent gap density = $\frac{5.0 \times 10^6}{11.12 \times 0.74 \times 12} = 50{,}500.$

$\delta \times C = \frac{3400 \times 3.2}{50{,}500} = 0.216.$

C = Carter coefficient = 1.12 (from Fig. 45 page 47).

δ = air-gap in inches = $\frac{0.216}{1.12} = 0.192$ in. (0.2 in. taken).

Calculation of the leakage factor (see Art. 51, p. 54). In Fig. 186 $h_s = 1.2$ in.

$L_s = 12.0$ in.

$l_1 = 2.9$ in.

$W_s = 8.25$ in.

$h_p = 5.4$ in.

$L_p = 12.0$ in.

$l_3 = 2.8$.

$W_p = 6.2$.

$\phi_e = \phi_{e1}\,\phi_{e2} + \phi_{e3} + \phi_{e4}$.

$$\phi_{e1} = 13(AT_{g+t})\frac{L_s h_s}{l_1} = AT_{g+t}\frac{13 \times 12.0 \times 1.2}{2.9} = 64.7(AT_{g+t})$$

$$\phi_{e2} = 19(AT_{g+t})h_s \log_{10}\left(1 + \frac{\pi W_s}{2l_1}\right) = (AT_{g+t}) \times 19 \times 1.2 \times \log_{10}\left(1 + \frac{3.14 \times 8.25}{2 \times 2.9}\right) = 16.0(AT_{g+t})$$

$$\phi_{e3} = 6.5(AT_{g+t})\frac{L_p h_p}{l_3} = (AT_{g+t})\frac{6.5 \times 12.0 \times 5.4}{2.8}$$
$$= 150(AT_{g+t}).$$

$$\phi_{e4} = 9.5(AT_{g+t})h_p \log_{10}\left(1 + \frac{\pi W_p}{2l_3}\right).$$
$$= (AT_{g+t}) \times 9.5 \times 5.4 \times \log_{10}\left(1 + \frac{3.14 \times 6.2}{2 \times 2.8}\right)$$
$$= 31.7(AT_{g+t}).$$

$$\phi_e = 262.4(AT_{g+t}).$$

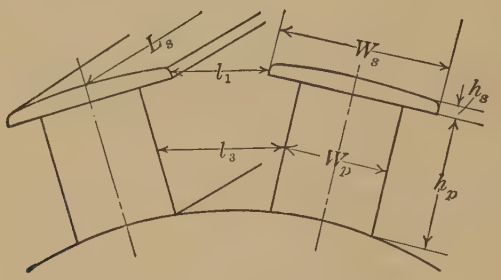

FIG. 186.—The pole dimensions.

Without serious error we may assume that the ampere-turns for the gap are equal to the ampere-turns for both gap and teeth; the tooth density is generally low enough to justify this assumption. As determined above, the gap ampere-turns in this case are 3400. Therefore, $\phi_e = 262.4 \times 3400 = 892{,}000$ and the no-load leakage factor $= \dfrac{5.0 \times 10^6 + 892{,}000}{5.0 \times 10^6}, = 1.17.$

The full-load leakage factor at zero power factor $= 1 + 0.17 \times \left(\dfrac{3400 + 9 \times 12 \times 113 \times 0.35}{3400}\right) = 1 + 0.17 \times 2.26 = 1.38$ (see Art. 177).

The magnetic areas are:

τ = pole pitch	= 11.12 in.
ψ = pole enclosure (per cent)	= 74.
L_g = gross iron	= 10.625 in.
L_n = net iron	= 9.6 in.
A_g = apparent gap area	= 98.0 sq. in.
C = Carter coefficient	= 1.12.
A_t = minimum tooth area per pole	= 51.0 sq. in.

Three points on the no-load saturation curve may now be calculated; these calculations may be tabulated as follows:

No-load voltage			2400		2700		3000	
Flux per pole			5×10^6		5.62×10^6		6.25×10^6	
Leakage factor			1.2		1.2		1.2	
	Length	Area	Density	AT	Density	AT	Density	AT
Air-gap	0.2	$\frac{98}{1.12}$	50,500	3660	56,800	4120	63,000	4580
Teeth	2.35	51	98,000	115	110,000	260	122,500	600
Pole	5.5	70.6	85,000	120	95,600	280	106,000	770
Total ampere-turns per pole			.....	3895	.....	4660	.....	5950

To get the figures for the no-load saturation curve with the full-load leakage factor, it is necessary to recalculate the excitation for the poles, using a leakage factor of 1.38; the air-gap and teeth are not affected.

Leakage factor = 1.38

Pole	5.5	70.6	97,000	330	109,000	940	121,000	2100
Total ampere-turns per pole			.....	4105	.....	5320	.....	7280

From the former set of values the no-load saturation curve in Fig. 184 is plotted and from the latter set the dotted curve, which is the no-load saturation curve with the full-load leakage factor is plotted.

In the above calculation the core and revolving field ring have been neglected since the flux density is very low in the case of the core to keep down the temperature of the iron and in the case of the field ring to give the necessary mechanical strength and rigidity.

The reactance per phase is found by the method shown in Arts. 162, 163 and 164 page 218, as follows:

$$\frac{\phi_e L_e}{2} = 5.2 \times 3 \text{ (from Fig. 171)} = 15.6.$$

$$\phi_s = \frac{3.2}{3}\left(\frac{2.1}{3 \times 0.43} + \frac{0.25}{0.43}\right) = 2.36 \text{ (from Art. 163).}$$

$$\phi_{ta} = 2.35 \log_{10}\left(1 + \frac{\pi \times 0.8}{3 \times 0.43 + 2 \times 0.8}\right) + \frac{2.35}{9}\log_{10}\left(1 + \frac{\pi \times 0.8}{0.43}\right) = 0.86 \text{ (from Art. 164).}$$

$$\phi_{tp} = 3.2 \times \frac{10}{9} \times \frac{0.8 \times 1.12}{2 \times 0.2} = 7.96 \text{ (from Art. 164).}$$

$$\phi_t = 0.52 \times 0.86 + 0.42 \times 7.96 = 3.8 \text{ (from Art. 164).}$$

Reactance per phase per circuit in ohms (Art. 165).

$$= 2 \times \pi \times 60 \times \overline{12}^2 \times 3^2 \times \frac{12}{2} (15.6 + [2.36 + 3.8]12.5)10^{-8} = 2.7 \text{ ohms.}$$

Equivalent reactance per phase = 1.35 ohms.

The voltage drop per phase = $1.35 \times 226 = 305$ volts.

The voltage drop at the terminals = 1.73×305
= 528 volts since the winding is YY connected
= 22 per cent of normal voltage.

The demagnetizing ampere-turns per pole = $0.35 \times 9 \times 12 \times \frac{226}{2}$, = 4280

and the corresponding field current = $\frac{4280}{\text{field-turns per pole}}$
= 48.6 amp.

The full-load saturation curve at zero power factor lagging may now be drawn in and is shown in Fig. 184

The curves at power factor = 1.00 and power factor = 0.85 are also shown in Fig. 184. From these curves the regulation may be determined and is

31 per cent at power factor = 100.
40 per cent at power factor = 0.85.
46 per cent at power factor = 0.0.

CHAPTER XX

LOSSES, EFFICIENCY AND HEATING

Many of the losses in an alternator are similar to and are figured out in the same way as those in a D.-C. machine.

Losses may be itemized in the same way as in D. C. machines; the itemized losses on D.-C. machinery as given in Chap. X are applicable to A.-C. machinery also.

178. Bearing Friction Loss $= 0.81dl\left(\frac{V_b}{100}\right)^{\frac{3}{2}}$ watts

where d = the bearing diameter in inches,

l = the bearing length in inches,

V_6 = the rubbing velocity of the bearing in feet per minute

This is the same result as arrived at in Chap. X for D.-C. machinery.

179. Brush Friction.—This loss is small since there are few brushes and the rubbing velocity is low;

the loss $= 1.25\,A\,\frac{V_r}{100}$ watts

where A is the total brush-rubbing surface in square inches,

V_r is the rubbing velocity in feet per minute.

This also is the same as for D.-C. machinery; it is negligible in A.-C. machinery.

180. Windage Loss.—Except in the turbo-generator, windage losses are usually negligible. They vary with the cube of velocity through the air and it is, therefore, only when peripheral speeds become very high that they become appreciable. Further comment will be given this item in a subsequent chapter on high-speed alternators.

181. Iron or Core Losses.—As in the case of the D.-C. machine, these include the hysteresis and eddy-current losses; additional core loss is due to filing, to leakage flux in the yoke and end heads, and to non-uniform distribution of flux in the core; losses in the pole face. It is exceedingly difficult to take into consideration all of the factors that affect iron losses; the amount filing of slots, the insulation between laminæ, the number and width of ventilating ducts, the distribution of flux in the core, the grade of

iron employed, etc. all have an important bearing on iron loss. The loss curves given in Fig. 86 may be taken as a basis for calculation, but the results given therein should be multiplied by the following factors to make them applicable to A.-C. machine designs; even then, there is apt to be a very considerable departure in the losses of the actual machine from the calculated results. The best guide to iron loss is a test on a similar machine built up under similar conditions. The following table gives factors to apply to the curves of Fig. 86 for a first approximation:

	Factors by which to multiply value in curves, Fig. 86	
	Core	Teeth
Mill-annealed sheet steel (usually used in A.-C. machinery) 0.0172 in. thick	0.7	4.5
2¼ per cent silicon sheet steel (used in special cases) 0.014 in. thick	0.55	3.

There are two reasons to account for the very much higher values of the above factor for the teeth as compared to the core:

(*a*) The armature core is interrupted every 1½ to 3 in. of its length by ventilating ducts; the field structure, on the other hand, is continuous. Hence a part of the field flux enters the teeth from the sides. The eddy currents that are set up in the iron are, therefore, very much, increased and this increase occurs in the teeth only.

(*b*) Whatever filing is done is in the slots, and hence there is a much better path for eddy currents within a package of iron in the tooth portion of the magnetic circuit than in any other part.

182. Excitation Loss.—As shown in Fig. 184, field excitation and, therefore, excitation losses vary with power factor. This loss is the product of the field amperes by the exciter voltage; losses in the field rheostat, if used, are to be included in obtaining efficiency according to the 1925 A.I.E.E. standards rules.

183. Armature Copper Loss.

The resistance of one conductor $= \frac{L_b}{M}$ ohms,

and the loss in one conductor $= \frac{L_b I_c^2}{M}$ watts,

where L_b is the length of one conductor in inches,
I_c is the current in each conductor,
M is the section of each conductor in circular mils.

$$\text{The total armature copper loss} = Z_c \frac{L_b I_c^2}{M} \text{ watts} \qquad (31)$$

where Z_c is the total number of conductors.

In addition to the above copper loss there are eddy-current losses in the conductors which losses may be large and cause trouble due to heating unless care is taken properly to laminate the conductors.

Figure 187 shows the flux distribution in the slots and air-gap of an alternator. The flux entering a slot changes from a maximum in position A to zero in position B, and this change of flux causes eddy currents to flow in the conductors in the direction

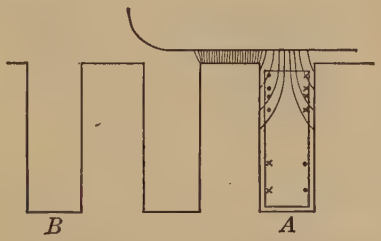

FIG. 187.—Flux in an armature slot.

indicated by crosses and dots. To prevent these eddy currents from having a large value, it is necessary to laminate the conductors both vertically and horizontally. This flux seldom gets beyond half the depth of the slot, so that it is not important to laminate conductors which lie in the bottom of the slot.

The loss due to these eddy currents is a constant loss, being present at no load as well as at full load, and is, therefore, measured with the core losses.

Of much greater importance are the eddy currents produced by the armature leakage flux. Figure 188 shows the leakage flux crossing an alternator slot due to the current in the conductors. This flux is alternating and, therefore, sets up eddy currents, the direction of which is indicated at one instant by crosses and dots. To prevent these eddy currents from having a large value it is necessary to laminate the conductors horizontally.

The m.m.f. tending to send this leakage flux across the slot at mn is due to the current in the conductors which lie below mn; therefore, the leakage flux density is zero at the bottom of the

slot and a maximum at the top of the slot; it is, therefore, more important to laminate the conductors in the top of the slot than those in the bottom.

The loss due to leakage flux is a load loss since the leakage flux which produces it is proportional to the current in the conductors. The following example will show how large it may become.

Consider the case of the double-layer winding shown in Fig. 188; the flux $d\phi = 3.2\left(bI_c \times \frac{y}{d}\right) \times \frac{L_c dy}{s}$

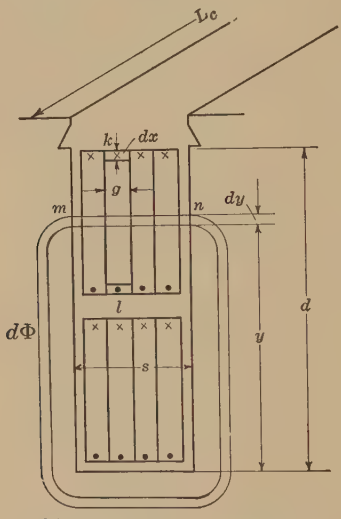

FIG. 188.—Eddy currents due to armature slot leakage.

and ϕ, the flux crossing the upper layer of conductors

$$= 3.2bI_cL_c \int_{d/2}^{d} \frac{y \times dy}{d \times s},$$

$$= 3.2bI_cL_c \times \frac{3d}{8s},$$

$$= 1.2\, bI_cL_c \frac{d}{s},$$

ϕ_m, the maximum flux crossing the upper layer of conductors

$$= 1.2bI_mL_c \times \frac{d}{s},$$

$$= 1.7\, bI_cL_c \times \frac{d}{s}.$$

Consider a loop kl of width g and thickness dx, the effective e.m.f. in this loop due to the flux which crosses the conductors

$$= 4.44\,\phi_m f\,10^{-8} \text{ volts.}$$

The resistance of this loop

$$= \frac{1 \times 2L_c}{g \times dx \times 1.27 \times 10^6} \text{ ohms.}$$

The eddy current in the loop

$$= \frac{\text{effective e.m.f.}}{\text{resistance}},$$

$$= \frac{4.44 \times \left(1.7 \times bI_cL_c \times \frac{d}{s}\right) \times f \times 10^{-8}}{\frac{2L_c}{g \times dx \times 1.27 \times 10^6}},$$

$$= 4.8 \times 10^{-2} \times bI_c \times \frac{d}{s} \times f \times g \times dx \text{ amp.},$$

and the current density in the loop

$$= \frac{\text{current}}{g \times dx}$$

$$= 4.8 \times 10^{-2} \times bI_c \times \frac{d}{s} \times f \text{ amp. per square inch.}$$

The normal current density in one of the top conductors

$$= \frac{I_c \times 2}{g \times d} \text{ amp. per square inch (approximately),}$$

and the ratio

$$\frac{\text{current density at the edge of conductor due to slot leakage}}{\text{normal current density}}$$

$$= 2.4 \times 10^{-2} \times d^2 \times f \times \frac{b \times g}{s}.$$

To take a particular example

$$f = 60 \text{ cycles},$$

$$\frac{b}{2}g = 0.7s,$$

$$d = 2 \text{ in.},$$

and the above ratio = 8.

The eddy currents, however, tend to wipe out the flux which produces them so that the above result is greatly exaggerated.[1]

It is evident, however, that a solid conductor will give rise to undue loss on account of these eddy currents. Present-day practice is to laminate the conductor copper so as to avoid these eddy currents.

[1] For an accurate solution of this problem, see Field, *Proceedings* Am. Inst. Elec. Eng., Vol. 24, p. 765.

The Brown-Boveri Company have devised a very ingenious composite armature conductor which is composed of strands each of which makes one complete spiral around the slot it occupies; the e.m.f. which sets up the eddy currents is, therefore, neutralized in each individual strand in this conductor.

184. The Efficiency.—For an alternating current generator

$$\text{the efficiency} = \frac{\text{output in kilowatts}}{\text{output in kilowatts} + \text{losses in kilowatts}}$$

where the losses are:

Windage, bearing and brush friction;

Excitation loss;

iron losses;

Armature copper loss (neglecting eddy-current loss);

Load losses, which are principally the eddy-current losses in the conductors.

These load losses are determined in the following way:

The alternator is run at normal speed with the armature short-circuited through an ammeter; it is then excited with sufficient field to circulate full-load current through the armature and under these conditions the input into the driving motor is measured; the field is then taken off the machine, the armature open circuited, and the power taken by the driving motor again measured; the difference between the two readings is called the short-circuit core loss and includes:

The armature I^2R loss;

The eddy-current loss in the armature conductors due to leakage flux;

The small iron loss due to the flux in the core.

It is recommended in the standardization rules of the American Institute of Electrical Engineers that the load losses be taken as the short-circuit losses less I^2R loss and friction and windage losses, when the test is made in the manner above described.

185. Heating.—The temperature rise of the stator of a revolving field alternator is limited in the same way as that of the armature of a D.-C. machine.

For stator cores, built with iron of the same grade as used in D.-C. machines and of a thickness = 0.014 in., the following flux densities may be used for a machine whose temperature rise at normal load must not exceed 60° C.

Frequency	Maximum Tooth Density in Lines per Square Inch	Maximum Core Density in Lines per Square Inch
60 cycles	90,000	60,000
25 cycles	105,000	72,000

The end-connection heating is limited by keeping the value of the ratio $\frac{\text{ampere conductors per inch}}{\text{circular mils per ampere}}$ below that given in Fig. 189; the curve applies to revolving field open-type machines.

The stator heating is affected by that of the rotor because the air which cools the stator passes over the rotor surface, during which time it is heated; the hotter the rotor the hotter the air which is blown on to the stator and the greater the temperature rise of the stator above that of the air in the power house.

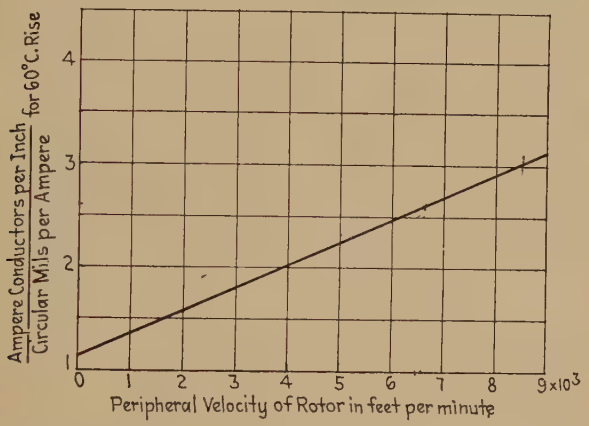

FIG. 189.—Heating curves for stator end connections of revolving field alternators.

The ventilation of the power house has a good deal to do with the temperature rise of the machines operating therein. In the case of belt-driven units the belt keeps the air in the power house circulating; the flywheel of a direct-connected engine type of machine has the same effect. In the case of water-wheel units, however, the circulation of the air in the power house has generally to be brought about by the machines themselves and, unless they are built with fans, so as to prevent the air which has passed through the machines and has thereby become heated from being sucked in again, they will often get hot even although liberally designed. Such machines sometimes stand over a pit and it will often be found that, if this pit is connected by a duct to the external air, the temperature rise of the machine above that of the air in the power house will be reduced.

186. Internal Temperature in High-voltage Machines.—It was pointed out in Art. 105, page 128, that the difference in

temperature between the copper in the center of a machine and that on the end connections, if all the heat in the copper is conducted axially along the conductors

$$= \frac{5.7 \times 10^4 \times \left(\frac{L_c}{2}\right)^2}{(\text{circular mils per ampere})^2} \text{ degrees Centigrade}$$

while if all the heat is conducted through the slot insulation the difference in temperature between the copper and the iron

$$= \frac{\text{ampere conductors per slot}}{\text{circular mils per ampere}} \times \frac{\text{thickness of insulation}}{2d + s} \times \frac{1}{0.003} \text{ degree Centigrade.}$$

That the results of these formulæ require careful consideration in the case of high-voltage machines of considerable length is shown by the following example:

Assume a turbo-alternator 15,000 k.v.a., 11,000 volts, two poles, 25 cycles, 1500 r.p.m. The dimensions of such a machine will be approximately as follows:

Full-load amperes	788.
Frame length	60. in.
Insulation thickness	0.2 in.
Diameter, internal	49.5 in.
Number slots	54.
Slot pitch	2.88 in.
Slot width	1.15 in.
Slot depth	5.6 in.
Ampere conductors per inch periphery	1090.
Circular mils per ampere	810.
Ampere conductors per slot	3150.

The difference in temperature between the copper in the center of the armature and that on the end connection, if all the heat is conducted along the copper,

$$= \frac{5.7 \times 10{,}000 \times 30^2}{810^2} = 78°\text{C.}$$

If, however, all the heat is conducted through the insulation to the iron of the armature, the difference in temperature between copper and iron

$$= \frac{3150 \times 0.2}{810 \times 12.35 \times 0.003} = 21°\text{C.}$$

From this analysis it is evident that most of the internal copper heat must be conducted through the slot insulation into the iron

of the armature and there dissipated along with the iron losses in the core and teeth. However, some heat is conducted into the end windings and there dissipated. This fact coupled with the long end extensions of turbo-alternator armature windings makes so much heat to be dissipated therein that the ratio $\frac{\text{ampere conductors per inch}}{\text{circular mils per ampere}}$, as given in Fig. 189, is made considerably lower for turbo-alternators than there indicated.

CHAPTER XXI

PROCEDURE IN DESIGN

187. The Output Equation.

$E = 2.22kZ\phi_a f \times 10^{-8}$(formula (25), page 185).

$$= 2.12 \times Z \times (B_g \psi\tau \times L_c) \times \frac{p \times \text{r.p.m.}}{120} \times 10^{-8}$$

taking $k = 0.96$, and $q = \frac{nZI_c}{\pi D_a}$.

Therefore nEI = the output in volt-amperes,

$$= n \times 2.12ZB_g\psi\tau L_c \times \frac{p \times \text{r.p.m.}}{120} \times 10^{-8} \times \frac{\pi D_a q}{nZ},$$

$$= \frac{2.12 \times \pi^2 \times 10^{-8}}{120} \times B_g\psi L_c \text{ r.p.m. } qD_{a2},$$

$$\text{and } D^2{}_a L_c = \frac{\text{volt-amperes}}{\text{r.p.m.}} \times \frac{5.7 \times 10^8}{B_g\psi q}. \qquad (32)$$

The value of B_g, the apparent gap density, is limited by the permissible value of B_t, the maximum stator tooth density which, as pointed out in Art. 185, page 252, is approximately

90,000 lines per square inch at 60 cycles
105,000 lines per square inch at 25 cycles

for open-slot machines.

Now $\phi_a = B_t\psi\tau L_n \times \frac{t}{\lambda}$

and also $= B_g\psi\tau L_c$

Therefore, $B_g = B_t \times \frac{t}{\lambda} \times \frac{L_n}{L_c}$.

The ratio $\frac{L_n}{L_c}$ is approximately equal to 0.75 taking the vent ducts and the insulation between the laminations into account. The ratio $\frac{\lambda}{t}$ varies with the slot pitch. Suppose, for example, that in a given alternator the number of slots is halved; since the same total number of conductors is required in each case, the total space required for copper remains constant, but the space required for slot insulation is approximately proportional to the number of slots, since its thickness is unchanged, so that

when the number of slots is halved, each slot may be less than twice the width of the original one; the ratio $\frac{\text{tooth}}{\text{slot}}$, therefore, increases as the slot pitch increases.

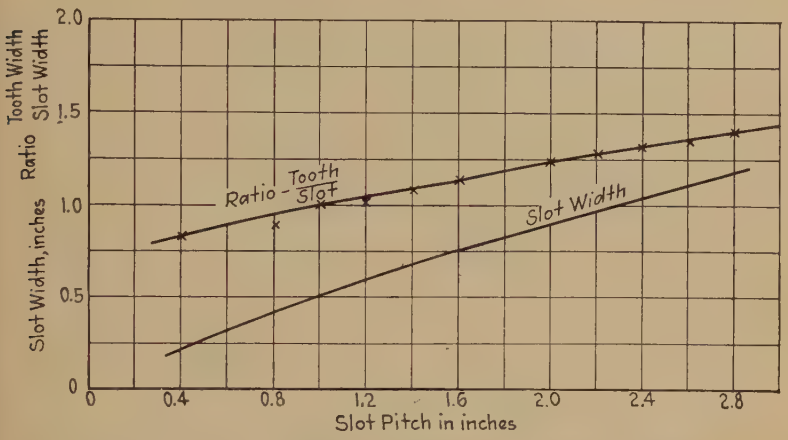

FIG. 190.—Curve to obtain slot dimensions for preliminary design.

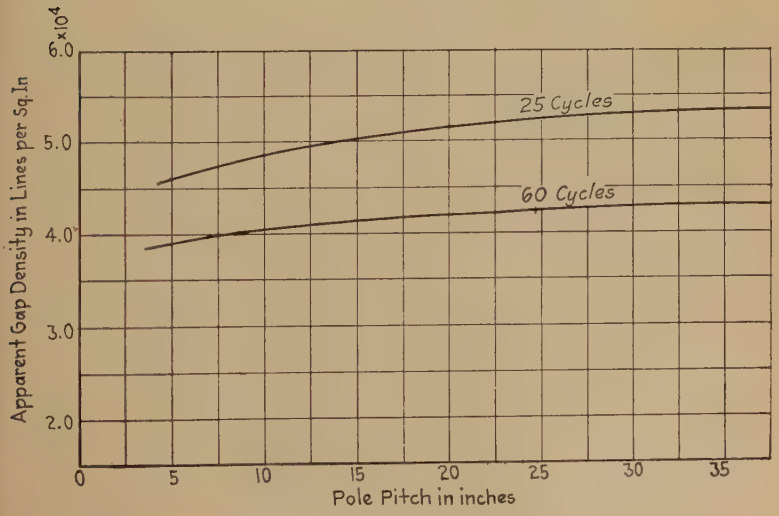

FIG. 191.—Curve for magnetic density for preliminary design.

The slot pitch is seldom made greater than 2.0 in. because the section of the copper in a coil for such a slot is large compared with the radiating surface of the coil and it becomes difficult to

keep the windings cool. Furthermore, the ampere-turns in a single slot become unduly large, thereby exaggerating the eddy currents, as analyzed in Art. 183.

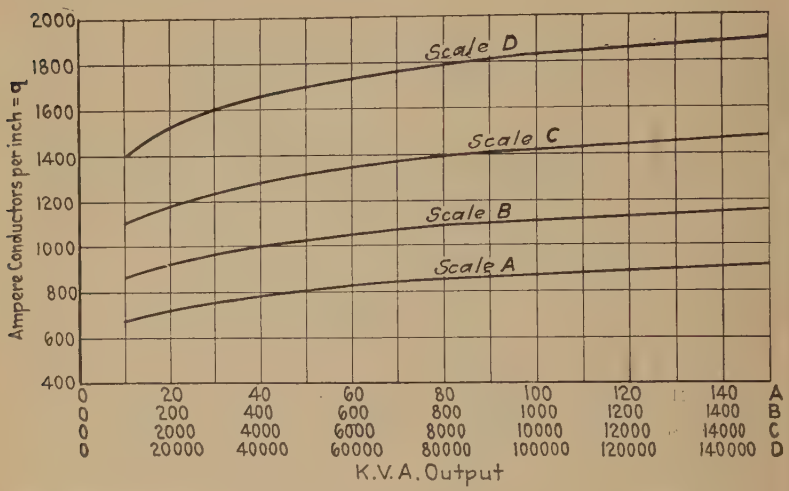

FIG. 192.—Curve to obtain ampere conductors per inch of periphery for preliminary design.

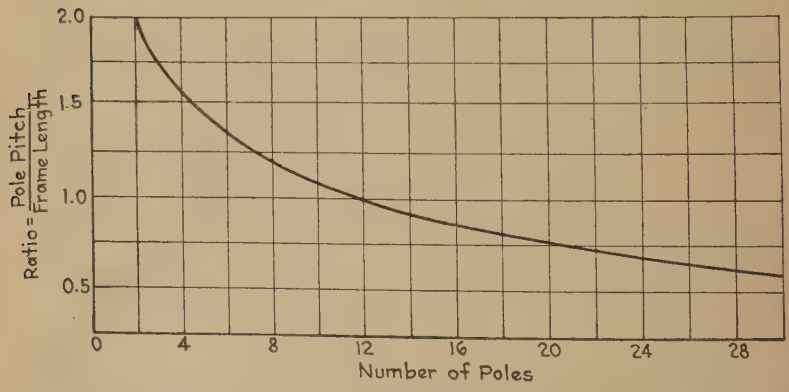

FIG. 193.—Curve to obtain ratio $\frac{\text{Pole pitch}}{\text{Frame length}}$ for preliminary design.

Figure 190, which shows the relation between $\frac{\text{tooth}}{\text{slot}}$ and slot pitch found in practice for open slot machines, may be used in preliminary design.

B_g is found from the formula given above and is plotted against pole pitch in Fig. 191, a reasonable value for the slot pitch being assumed.

The value of B_g for alternators is considerably less than that found for D.-C. machines because of the lower tooth density in the former type of machine due to the fact that its armature is stationary while that of the D.-C- machine is revolving. For a given output and speed, therefore, the value of $D^2{}_a L_c$ is greater for alternators than for D.-C. machines.

The value of q is limited by heating. The values of q given in Fig. 192 may be used as a first approximation in preliminary design. Since heating is what limits the value of q, larger values than permitted by Fig. 192 may be used in machines of high peripheral velocity, while with low peripheral velocities they may have to be decreased.

188. The Relation between D_a and L_c.—There is no simple method whereby $D_a{}^2 L_c$ can be separated into its two components so as to give the best machine. In the case of the D.-C.machine the ratio between the magnetic and the electric loading was used in order to determine D_a and L_c, and then the number of poles was chosen so as to give an economical shape of coil.

The number of poles in an alternator is fixed by the speed and the frequency, and the diameter and length of the machine should be chosen so as to give an economical shape of coil. If, for example, the number of poles on a given diameter be increased, the pole pitch will be reduced, the field coil will become more and more flattened out, and a point will finally be reached at which it would be more economical to increase the diameter and shorten the length of the machine than to keep the diameter constant. For salient pole alternators the ratio $\frac{\text{frame length}}{\text{pole pitch}}$ should not exceed 3; otherwise it becomes difficult, if not impossible, to secure adequate ventilation.

189. Effect of the Number of Poles on the Ratio $\frac{\text{Pole Pitch}}{\text{Frame Length}}$.

Figure 194 shows part of two machines which are duplicates of one another so far as the pole unit is concerned; that is, they have the same pole pitch, air-gap, armature ampere-turns per pole and field ampere-turns per pole; but the total number of poles is small in machine A and large in machine B. It may be seen that in the former machine there is not room for the field coils

because of the large angle between the poles. In order to get the field coils on to the poles, it is necessary to increase the diameter of the machine without increasing the radial length of the field coil, that is, without increasing the armature ampere-turns per pole, on which this length principally depends, so that the same number of armature ampere-turns per pole must now be put on a larger pole pitch and the value of q, the ampere conductors per inch, thereby reduced. Although the diameter of the

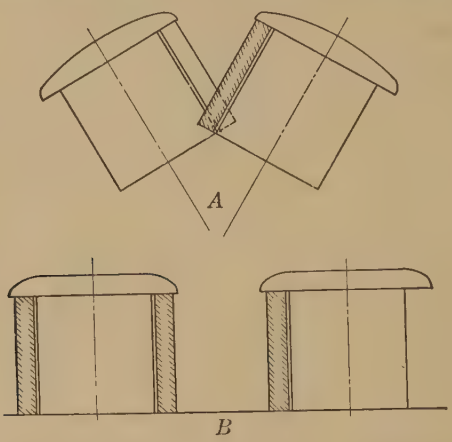

FIG. 194.—Effect of the number of poles on the length of field coils.

machine is increased, the flux per pole must be kept constant, otherwise the pole waist will increase; the pole arc will generally be unchanged and the ratio $\frac{\text{pole arc}}{\text{pole pitch}}$ will decrease as the diameter is increased, and in four- and six-pole machines will have a value of about 0.7.

The above difficulty, due to a small number of poles, is more apparent in machines of low than in those of high frequency, because in the former the output per pole is generally larger; for example

a 400-k.v.a., 514-r.p.m., 60-cycle machine has 14 poles and an output of 28.5 k.v.a. per pole;

a 400-k.v.a. 500-r.p.m., 25-cycle machine has 6 poles and an output of 67 k.v.a. per pole;

a six-pole, 60-cycle alternator with an output of 67 k.v.a. per pole would have a rating of 400 k.v.a. at 1200 r.p.m., which would be as difficult to build as the above 25-cycle machine.

The value of q in Fig. 192 applies to machines which have more than 10 poles; for machines with four poles this value should be reduced 30 per cent for a first approximation, and for a machine with six poles should be reduced about 20 per cent.

Figure 193 shows the value of the ratio $\frac{\text{pole pitch}}{\text{frame length}}$ generally found in revolving field machines when the diameter is not limited by peripheral velocity, and may be used in preliminary design; the reason for the increase in the ratio as the number of poles decreases has been pointed out above.

190. Procedure in Design.

$D_a^2 L_c = \frac{\text{volt-amperes}}{\text{r.p.m.}} \frac{5.7 \times 10^8}{B_g \psi q}$ (formula (32), page 256)

and $\frac{\text{pole pitch}}{\text{frame length}}$ = a constant (found from Fig. 193, page 258);

therefore $L_c = \frac{\text{pole pitch}}{\text{a constant}}$,

$= \frac{\pi \times D_a}{p \times \text{a constant}}$,

and $D_a^3 = \frac{\text{volt-amperes}}{\text{r.p.m.}} \times \frac{5.7 \times 10^8 \times p \times \text{a constant}}{\pi \times B_g \times \psi \times q}$; (33)

from which D_a may be found approximately, since

B_g can be found approximately from Fig. 191,

q can be found from Fig. 192,

ψ is assumed to be = 0.7 for a first approximation,

the constant = the ratio $\frac{\text{pole pitch}}{\text{frame length}}$ (from Fig. 193).

Tabulate three preliminary designs, one for a diameter 20 per cent larger than that already found and the other 20 per cent smaller.

Find the probable total number of conductors = $\frac{q \times \pi D_a}{I_c}$ and assume that the winding to be used is single circuit, and Y connected if three phase, so that I_c = the full-load line current.

Find the number of slots; there should be at least two slots per pole per phase in order to get the advantages of the distributed winding (see Art. 133, page 175), but the slot pith should not exceed 2.00 in.; (Art. 187, page 257).

Find the conductors per slot = $\frac{\text{probable total conductors}}{\text{number of slots}}$; take the nearest number that will give a suitable winding.

Find the corresponding total number of conductors.

Find ϕ_a from the formula, $(E) = 2.22\,kZ\phi_a f \cos\frac{\theta}{2}10^{-8}$ (formula (25), page 185).

Find the actual frame length as follows:

slot pitch $= \dfrac{\pi \times D_a}{\text{total slots}}$;

divide this into $s + t$ by the use of Fig. 190, page 257;

the minimum tooth area required $= \dfrac{\phi_a}{\text{maximum tooth density}}$,

where the maximum tooth density = 90,000 lines per square inch for 60 cycles,
105,000 lines per square inch for 25 cycles,

the tooth area per pole = slots per pole $\times\ \psi \times t \times L_n$, from which L_n can be found.

$$L_g = \frac{L_n}{0.9}.$$

$L_c = L_g +$ (the center vent ducts), where these ducts are $\frac{3}{8}$ in. wide and are spaced 1.5 to 2 in. apart.

Find δ, the air-gap clearance, as follows:

$$B_g = \frac{\phi_a}{\tau \times \psi \times L_c}.$$

$$\delta C = \frac{AT_g \times 3.2}{B_g}.$$

where AT_g is taken as 1.2 (armature ampere-turns per pole) for a first approximation (see Art. 177).

The field is now designed roughly, as explained in Art. 176, page 238, and the machine drawn out to scale, after which the saturation curves are calculated, drawn in, and the regulation determined.

Example.—Determine approximately the dimensions of an alternator of the following rating: 937.5 k.v.a. (750 kw. at 80 per cent power factor), 2400 volts, 60 cycles, 226 amperes, 600 r.p.m., 12 poles, three phase. The work may be carried out as follows in tabular form:

Apparent gap density	B_g	= 42,000 (approximate, Fig. 191).
Ampere conductors per inch	g	= 1100 (Fig. 192).
Per cent pole enclosure	ψ	= 70 (assumed).
$\frac{\text{Pole pitch}}{\text{Frame length}}$ = a constant		1 (Fig. 193).
Number poles for 60 cycles, 600 r.p.m.		= 12.
Armature diameter	D_a	= 47 in. (formula (33), p. 261).

Tabulate results on this machine together with two others, one approximately 20 per cent smaller in diameter and the other 20 per cent larger.

Armature diameter	D_a = 39 in.	47 in.	56 in.
Total conductors probable	Z_c = 595	716	855
Pole pitch	τ = 10.2 in.	12.3 in.	14.7 in.
Slots per pole	6	6	9
Total slots	72	72	108
Conductors per slot	8	10	8
Connection	Y	Y	Y
Total conductors (actual)	576	720	864
Amount of chording	1 slot	1 slot	2 slots
Flux per pole (formula (26))	ϕ_a = 5.64 × 10^6	4.5 × 10^6	3.82 × 10^6
Slot pitch	λ = 1.7 in.	2.05 in.	1.63 in.
Slot width	s = 0.82 in.	0.93 in.	0.80 in.
Minimum tooth width	t = 0.88 in.	1.12 in.	0.83 in.
Tooth area per pole required	62.7 sq. in.	50 sq. in.	42.5 sq. in.
Net axial length iron	L_n = 16.9 in.	10.6 in.	8.15 in.
Gross length	L_g = 18.8 in.	11.6 in.	9.1 in.
Center vent ducts	8 × ⅜ in.	5 × ⅜ in.	4 × ⅜ in.
Frame length	L_c = 21.8 in.	13.5 in.	10.6 in.
Apparent gap density	B_g = 36,200	38,800	35,000
Armature AT per pole	5420	6780	8130
AT_g (assumed 0.6 armature AT)	3250	4070	4880
δC	0.29	0.336	0.445
Field System			
Maximum AT per pole (Art. 170)	9500	11,850	14,250
Leakage factor, full load, assumed	1.3	1.3	1.3
Pole area required	86.2 sq. in.	68.8 sq. in.	58.3 sq. in.
Axial length of pole	L_p = 21.3 in.	13.0 in.	10.1 in.
Pole waist	W_p = 4.1 in.	5.3 in.	5.8 in.
Depth of field coil	1.5 in.	1.5 in.	1.75 in.
Mean turn	58.0 in.	43.8 in.	39.6 in.
External periphery	61.0 in.	46.8 in.	43.0 in.
Exciter voltage	125	125	125
Section field copper	M = 45,500 c.m.	42,500 c.m.	50,500 c.m.
	1.5 × 0.024	1.5 × 0.022	1.75 × 0.023
Watts per square inch 60°C. rise (Fig. 185)	3.2	3.8	4.2
Space factor	s_f = 0.75	0.75	0.75
Radial length field coil for 60°C. rise	L_f = 3.7	4.2	4.4

The three machines are now drawn in to scale as shown in Fig 195.

The 39-in. machine is expensive in core assembly while the 56-in. machine is expensive in inactive material, such as the material in the yoke.

So far as operation is concerned, there is little to choose between the machines. The armature ampere-turns per pole is the same fraction of the field ampere-turns per pole in each case, the voltage drop due to armature reactance is also about the same for each design. In the 39-in. machine the air-gap is small and the length L_c is large, which tend to make the reactance large, but there are only 8 conductors per slot, whereas in the 56-in. machine, while

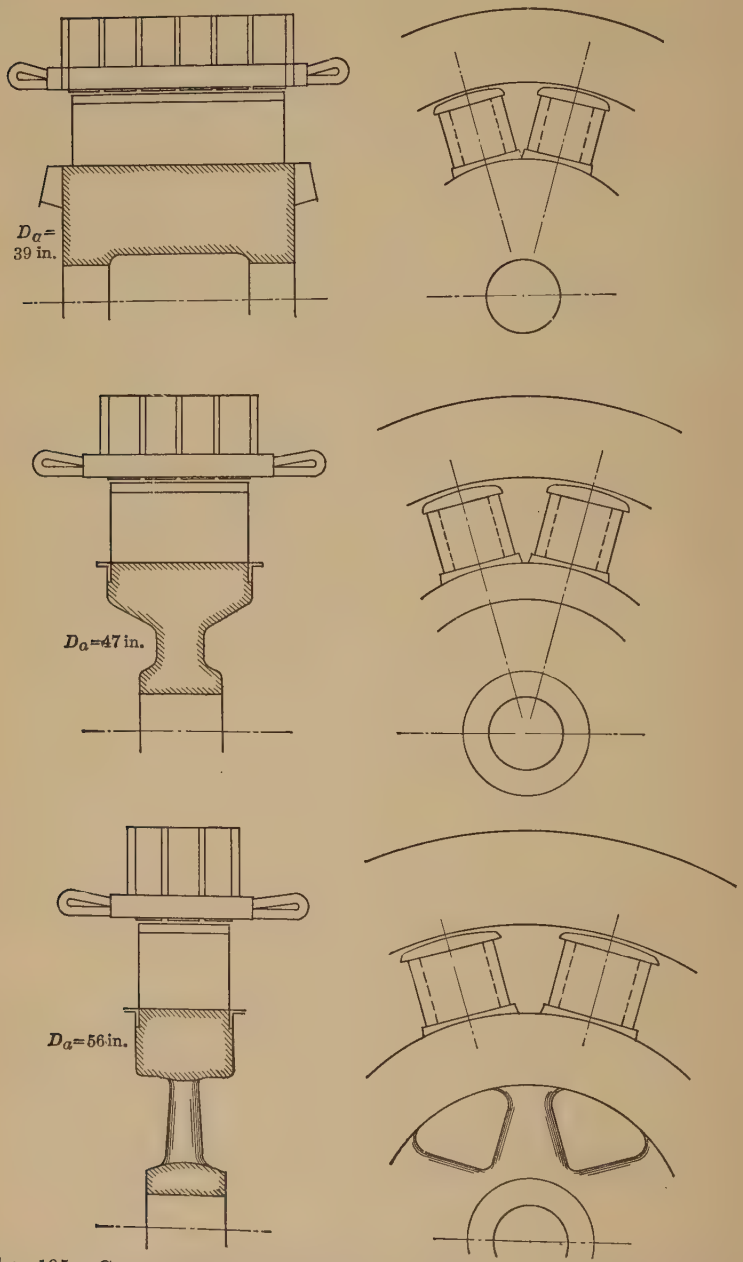

FIG. 195.—Comparative designs for a 937.5-k.v.a., 60-cycle, 600-r.p.m alternator.

the air-gap is larger and the frame length shorter, the number of conductors per slot is eight but it has nine slots per pole instead of six.

The 39-in. machine is rather long for its diameter and might be somewhat difficult to ventilate. The ratio $\frac{\text{pole pitch}}{\text{frame length}}$ is still far within the limit set in Art. 188, but the peripheral speed is somewhat low to secure good ventilation. On the other hand, the 47- and the 56-in. machines require an undue amount of inactive material, as pointed out above. The performance of any of these machines would undoubtedly be satisfactory, and our problem is to select the one that is most economical to build. Any diameter between 39 and 56 in. is satisfactory; in our particular case it so happens that one of the large electrical manufacturing companies has a design for this rating on a diameter of 42.5 in. The details of this design are as follows: rating, 937.5 k.v.a. (750 kw. at 80 per cent power factor), 2400 volts, three phase, 60 cycle, 226 amperes, 12 pole, 600 r.p.m.

Armature diameter	42.5 in.
Ampere-conductor per inch, (Fig. 192)	1100.
Per cent pole enclosure	74.
$\frac{\text{Pole pitch}}{\text{Frame length}}$	1.0.
Total conductors $\left(\frac{1100 \times 42.5 \times \pi}{226}\right)$ probable	654.
Pole pitch $\left(\frac{42.5 \times \pi}{12}\right)$	11.12 in.
Slots per pole	9.
Total slots (9×12)	108.
Conductors per slot	6.
Connection (make 12 conductors per slot instead of 6 and so divide conductors more completely; make two Y's in parallel)	YY.
Total conductors, actual	1296.
Voltage per phase $\frac{2400}{1.73}$	1380.
Flux per pole	5.02×10^6.
Slot pitch $\left(\frac{42.5 \times \pi}{108}\right)$	1.23 in.
Slot width (Fig. 190) (slot width actually made 0.43 in.)	0.52 in.
Minimum tooth width	0.8 in.
Tooth area per pole required ($B_t = 90{,}000$)	55.8 sq. in.
Net axial length of iron	10.4 in.
Gross axial length of iron	11.5 in.

Center vent ducts	$5 \times \frac{3}{8}$ in.
Frame length (frame length was actually made 12.5 in., thereby increasing tooth density to about 103,000)	13.4 in.
Apparent gap density	48,500.
Armature AT per pole $\left(108 \times \frac{226}{2 \times 2}\right)$	6100.
AT_g (assumed = 0.6 armature AT)	3660.
δC	0.242.
Field System	
Maximum AT per pole (1.75 × armature AT)	10,700.
Leakage factor, assumed	1.2
Pole area required (B_p = 85,000)	70.6 sq. in.
Axial length of pole, gross	12 in.
Axial length of pole, net	11.4 in.
Pole waist	6.2 in.
Depth of field coil (Art. 176)	1.5 in.

As noted in Art. 177, the actual depth of field coil used was reduced below that indicated in Art. 176 so as to allow better ventilation of the field coils. The field winding actually used was tapered, 23 turns being made of copper strap 0.625 in. wide and 65 turns of 1.125-in. strap.

Mean turn	43.6 in.
External periphery	46 in.
Exciter voltage	125.
Section of field conductor (Art. 54)	38,500 cir. mils.

This gives the cross-section of copper that is necessary to give the maximum field ampere-turns with not more than 125 volts applied. As actually built, the field copper was increased about 15 per cent over the figure determined above, thereby permitting the maximum excitation to be secured at about 110 volts exciter voltage; in other words, more margin was allowed in the design of the field. The field as actually built was wound with 23 turns of copper strap, 0.562 × 0.066 in. and 65 turns of 1.125 × 0.033 in. = 47,200 cir. mils.

Watts per square inch 60° C. rise (Fig. 185)	3.4.
Space factor (assumed)	0.75.
Radial length of field (Art. 176)	5.0 in.
$\frac{\text{Ampere conductors per inch}}{\text{Circular mils per ampere}}$ (Fig. 189)	2.6.
Circular mils per ampere	425.
Amperes per conductor at full load	113.
Section of conductor	48,000 c.m. 0.0376 sq. in.

Slot width	0.43 in.
Thickness slot insulation at 40 volts per mil (see Art. 154)	0.060 in.
Thickness conductor insulation, say	0.008 in.
Width of slot available for copper $= 0.43 - 2(0.06 + 0.008)$	0.294 in.

To reduce eddy currents, wind coils two wide and three deep to get the six conductors required in each coil side; make width of each conductor 0.14 in.; make depth 0.27 in.; hence total cross-section = 0.0378 sq. in., or practically the value determined above.

Slot depth is determined as follows:

Six conductors, 0.27 in. each	1.62 in.
Slot insulation, 4×0.06	0.24 in.
Conductor insulation, 12×0.008	0.096 in.
Total for two coil sides	1.956 in.
Allow for wedge and insulation	0.394 in.
Slot depth	2.350 in.

Flux density in core 60,000 (Art. 185).

$$\text{Core area} = \frac{\phi_a}{2 \times 60{,}000} = 41.8 \text{ sq. in.}$$

$$\text{Core depth} = \frac{\text{core area}}{\text{net iron}} = 4 \text{ in.}$$

External diameter = 56 in.

Most manufacturing companies provide themselves with blank forms on which design data may be entered. Such forms usually provide for information such as is given in the foregoing tabulations so that designs may be readily compared.

191. Field Design.—This may be carried out as indicated in Chap. XIX where the field system of the 42.5-in. internal diameter machine tabulated above is designed completely, the saturation curves determined and drawn in Fig. 184, and the regulation found.

192. Variation of Length on a Given Diameter.—As indicated in Art. 190, an acceptable 937.5-k v.a. machine can be built on any diameter from 39 to 56 in., and perhaps even wider limits of diameter variation. Conversly, considerable variation of output may be secured on a given diameter of frame by varying the length of active material. This method of construction is widely used by the manufacturing companies so as to reduce to a minimum the dies and other tools that are necessary in the process of manufacture. A very material saving in die and other tool

cost can be brought about by providing for a series of frame diameters in which the rating with the greatest length of active material in a given diameter will overlap or adjoin the rating of the shortest length of active material in the next larger diameter; the rating in the shortest length of active material will overlap or adjoin the rating of the longest active material in the next smaller diameter. Thus, a reasonable provision for dies and tools can be made to cover any rating that may be called for.

Let us see how this works out on the 42.5-in. diameter frame, the details of which we have given above; suppose we increase and also decrease the length of active material by 50 per cent. What rating will result? The essential items of such designs may be tabulated as follows, the middle tabulation being that of the 937.5-k.v.a. machine given above:

Armature diameter	42.5 in.	42.5 in.	42.5 in.
Net axial length of iron	7.0 in.	10.4 in.	15.6 in.
Gross axial length of iron	7.8 in.	11.5 in.	17.3 in.
Center vent ducts	3 × ⅜ in.	5 × ⅜ in.	8 × ⅜ in.
Frame length	8.9 in.	13.4 in.	20.3 in.
Total number slots	108	108	108
Conductors per slot	18	12	8
Connection	YY	YY	YY
Size of conductor	0.14 × 0.18 in.	0.14 × 0.27 in.	0.14 × 0.405 in.
Ampere conductors per inch	1100	1100	1100
Circular mils per ampere	425	425	425
Armature AT per pole	6100	6100	6100
Amperes per conductor	75	113	170
Terminal voltage per phase	2400	2400	2400
Output in k.v.a	625	937.5	1400

The above machines are discussed under the following heads:

Conductors per Slot.—Since the intention is to use the same armature punching, the number of slots is fixed, and for the same flux density in the different machines the flux per pole must be directly proportional to the net iron. Now the voltage per conductor is proportional to the flux per pole, so that, for the same terminal voltage, the number of conductors in series per phase must be inversely as the flux per pole and, therefore, inversely as the net iron in the frame length.

Size of Conductor.—For the same total copper section, this is inversely proportional to the number of conductors per slot and, therefore, directly proportional to the net iron in the frame length.

Current Rating.—For the same current density in the conductors the current in each conductor must be proportional to the conductor section and, therefore, to the net iron in the frame length.

Output.—For the same voltage in each case the output in k.v.a. is proportional to the current and, therefore, to the net iron in the frame length.

Air-gap Clearance.—The current per conductor is inversely as the number of conductors per slot, so that the ampere conductors per slot is the same in each case, and the armature ampere-turns per pole, which $= \frac{\text{ampere conductors per slot}}{2} \times$ slots per pole, is independent of the frame length; the maximum excitation and the air-gap clearance are, therefore, also independent of the length of the frame.

Regulation.—The demagnetizing ampere-turns per pole

$$= 0.35 \times \text{conductors per pole} \times I_c$$

and since I_c is inversely proportional to the number of conductors per slot, the demagnetizing ampere-turns per pole is independent of the frame length.

The armature reactance drop

$$= 2\pi f p b^2 c^2 \cos^2 \frac{\theta}{2} \left(\frac{\phi_e L_e}{2} + (\phi_s + \phi_t) L_c \right) 10^{-8} \times I_c$$

where $\frac{\phi_e L_e}{2}$ is independent of frame length since it depends on

the pole pitch, which is constant,

ϕ_s is the same in each case since the slots are unchanged,

ϕ_t is the same in each case since the teeth and air-gap are unchanged.

The armature reactance drop is, therefore, proportional to (conductors per slot)$^2 \times$ current $\times (A + BL_c)$

or to (conductors per slot) $(A + BL_c)$

or to $\frac{(A + BL_c)}{L_c}$, where A and B are constants,

so that the longer the machine the lower is its reactance drop and the better the regulation, other things being unchanged.

The pole leakage flux consists of flank leakage which is constant and pole-face leakage which is proportional to the frame length; ϕ_a, the flux per pole, is directly proportional to the frame length; the leakage factor $= \frac{\phi_a + \phi_e}{\phi_a} = \frac{C + DL_c}{FL_c}$ where C, D and F are

constants and so is smallest for the longest machine that is built on a given diameter.

A machine cannot be lengthened indefinitely, however, because a point is finally reached at which it becomes impossible to cool the center of the core without a considerable modification in the type of construction and the addition of fans, and still further, as the length increases the pole section departs more and more from the square section.

193. Windings for Different Voltages and Phases.—Let us assume that we wish to adapt the 937.5-k.v.a. generator above detailed to other voltages and phases. What modification in windings is necessary? Suppose, for instance, that we wish to change this machine to meet the following ratings. What changes become necessary?

600 volts, three-phase, 60 cycles,
2400 volts, two-phase, 60 cycles.

To Find the Conductors per Slot.

$$E = 2.22 k Z \phi_a f \cos\frac{\theta}{2} 10^{-8}$$

$$= \text{a constant} \times k \times \text{conductors per slot} \times \frac{\text{slots}}{\text{phases}}$$

$$= \text{a constant} \times k \times \frac{\text{conductors per slot}}{\text{phases}} \text{ for a given frame and frequency.}$$

For the machine in question $k = 0.96$ for a three-phase winding

$$\text{and the constant} = \frac{\text{volts per phase} \times \text{phases}}{k \times \text{conductors per slot}}$$

$$= \frac{\frac{2400}{1.73} \times 3}{0.96 \times 12}$$

$$= 360.$$

For the 600-volt, three-phase winding

$$\text{conductors per slot} = \frac{\text{volts per phase} \times \text{phases}}{k \times \text{a constant}}$$

$$= \frac{600 \times 3}{0.96 \times 360}$$

$= 5.2$, or say 5, if 600 is the voltage per phase, that is if the winding is Δ connected

and

$$= \frac{\frac{600}{1.73} \times 3}{0.96 \times 360}$$

$= 3.0$ if $\frac{600}{1.73}$ is the voltage per phase, that is if the winding is Y connected.

The Y-connected winding is the better of the two because with such a connection any third harmonic in the e.m.f. wave is eliminated, whereas in the case of a Δ-connected winding the third harmonics cause a circulating current to flow in the closed circuit of the delta.

Since the winding is double layer, the number of conductors per slot must be a multiple of two, so that the winding actually used will have six conductors per slot and will be connected four circuits in parallel.

For the 2400-volt, two-phase winding, it will be noted at once that the nine slots per pole that are used in the three-phase winding cannot be divided by two so as to be suitable for a two-phase winding. It is preferable to use a number of slots that is suitable for both two and three phases; that is, a number of slots per pole that is divisible by six. In that event, it is suitable, for either two-phase or three-phase winding as may be desired. Any even number of slots would be suitable for a two-phase winding, but to obtain a satisfactory wave form, not less than 6 slots per pole should be used, and 12 slots per pole would be preferable from this standpoint. Either six or 12 slots per pole would be suitable for both two phase and for three phase; more than 12 would be undesirable because the coils get so narrow as to be flimsy. Once having chosen the number of slots to be used, the winding for two phase, 2400 volts may be worked out by methods similar to those outlined above.

Reference to the table in Art. 140 will show that the distribution factor for two-phase winding, with a given number of slots per pole, is less than for a three-phase winding. This difference in the value of the distribution factor leads theoretically to a slightly lower rating when a given machine is wound for two phase than when wound for three phase. This theoretical difference is approximately 6 per cent; it is usually disregarded and the same ratings are used whether the winding is two or three phase.

194. Typical 100-k.v.a. Generator with Field Coils of D.C.C. Wire.—The following is a preliminary design for a 100-k.v.a., 2400-volt, three-phase, 24-ampere, 60-cycle, 1200-r.p.m., six-pole A.-C. generator:

Apparent gap density (Fig. 191)	$B_g = 41{,}000$
Ampere conductors per inch (Fig. 192)	$q = 860.$
Per cent pole enclosure (assumed)	$\psi = 68.$
$\frac{\text{Pole pitch}}{\text{Frame length}}$ = a constant (Fig. 193)	1.35.
D_a (formula (33))	17.4 in.

While the diameter and ratio $\frac{\text{pole pitch}}{\text{frame length}}$ hereby found would undoubtedly make an acceptable machine, the foregoing discussion indicates that these values may vary over quite wide limits and still obtain an acceptable design. The dimensions of an actual machine being made by one of the large manufacturing companies are available, and these two last items, as well as the remainder of the design, are now tabulated as actually made by this company.

$\frac{\text{Pole pitch}}{\text{Frame length}}$	1.99.
Armature diameter	19 in.
Total conductors, probable (Art. 190)	2140.
Pole pitch	9.95 in.
Slots per pole, number	12.
Total slots, number	72.
Conductors per slot	30.
Connection	Y.
Total conductors, actual	2160.
Chording armature coils	1 slot.
Flux per pole	1.52×10^8.
Slot pitch	0.83 in.
Slot width	0.43 in.
Minimum tooth width	0.40 in.
Net axial length of iron	4 in.
Gross axial length iron	4.25 in.
Center vent ducts	$2 \times \frac{3}{8}$ in.
Frame length	5 in.
Apparent gap density	44,800.
Maximum tooth density	115,000.
Armature AT per pole	4320.
AT gap	2410.
δC	0.176 in.
Field System	
Maximum AT per pole (1.5 × armature AT per pole)	6480.
No-load leakage factor	1.11.
Pole area	18.6 sq. in.
Pole waist	3.38 in.
Depth of field coil	1.5 in.
Mean turn	25.0 in.

External periphery	29.0 in.
Exciter voltage	125.
Section of field wire	11,100 cir. mils.
Watts per square inch	1.19.
Radial length of field coils	4.5 in.

The field coil as designed with a uniform thickness of 1.5 in. is shown dotted in Fig. 196, the actual shape of coil used is shown by heavy lines.

There are some points in which the design as tabulated above departs considerably from the design that would be arrived at by

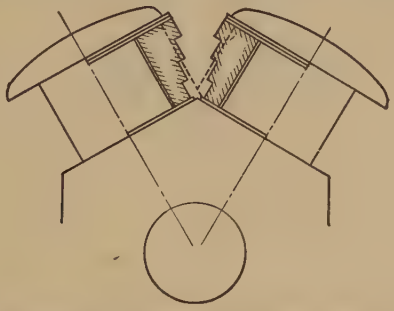

FIG. 196—Field system of a 75-k.v.a., 60-cycle, 1200-r.p.m. alternator.

following the procedure set forth in the first part of this chapter. The tooth density used is some 25 per cent in excess of that recommended in Art. 185; also, the gap density is considerably higher than that given in Fig. 191. This results in much higher iron losses than in a design as dictated in the first part of this chapter, but this is a very small machine for an alternator and, therefore, has a relatively large radiating surface, and some liberties may be justified.

CHAPTER XXII

HIGH-SPEED ALTERNATORS

195. Alternators Built for an Overspeed.—A typical example of such a machine is an alternator which is direct connected to a water wheel.

The peripheral velocity of a water wheel is less than the velocity of the operating water; if the load on such a machine be suddenly removed, and the governor does not operate rapidly enough, then the machine will accelerate until it runs with a peripheral velocity which is approximately equal to the velocity of the water and is from 50 to 100 per cent above normal, depending on the type of wheel used.

An alternator which is direct connected to a water wheel must have a diameter small enough to allow the machine to run at the above overspeed without the stresses due to centrifugal force becoming dangerous. When this diameter has been reached, the output for a given speed can be increased only by increasing the length of the machine, and after a certain length has been reached it becomes impossible to keep the center of the machine cool without the use of special methods of ventilation.

Example.—Determine approximately the dimensions of an alternator of the following rating:
2750 k.v.a., 2400 volts, three phase, 660 amperes, 60 cycles, 600 r.p.m.; the machine has to run at an overspeed of 75 per cent.

If the design were carried out in the usual way, then the following would be the result.

Apparent gap density	$B_g = 43{,}000.$
Ampere conductance per inch	$q = 1220.$
Per cent enclosure	$\psi = 70.$
$\frac{\text{Pole pitch}}{\text{Frame length}}$ = a constant	$= 1.00.$
Poles	$p = 12.$
Armature diameter	$D_a = 65$ in.

With this diameter, the peripheral velocity at 600 r.p.m. would be 10,200 ft. per minute, and the peripheral velocity at,

say, 75 per cent overspeed would be 17,850 ft. per minute. With the type of construction shown in Fig. 197, a safe and comparatively cheap machine can be built with this peripheral velocity.

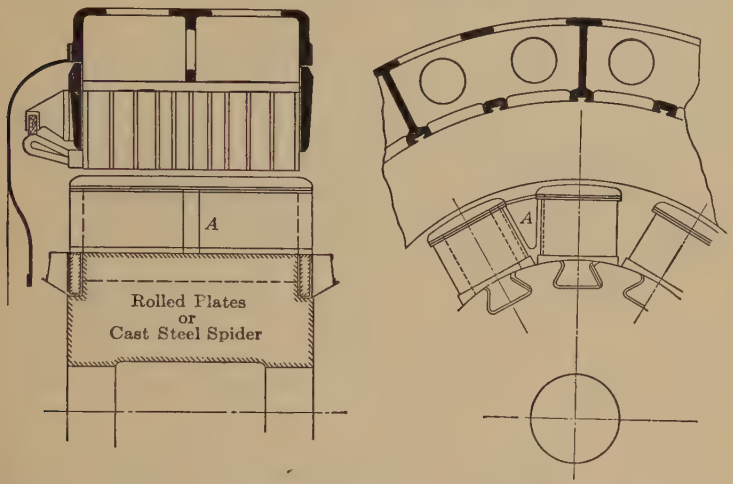

FIG. 197.—Outline of a 2750-k.v.a., 600-r.p.m., 60-cycle, water-wheel driven alternator, to run at 75 per cent overspeed.

The design may now be continued as follows:

Armature diameter	65 in.
Total conductors (probable)	378.
Pole pitch	τ = 17 in.
Slots per pole	9.
Total slots	108.
Conductors per slot	3.5.
(Use fourteen conductors per slot and connect four circuits in parallel.)	
Total conductors (actual)	378.
Amount of chording armature coils	3 slots.
Flux per pole	8.9×10^6.
Slot pitch	1.89 in.
Slot width	0.63 in.
Tooth width	1.26 in.
Tooth area required per pole	98.9 sq. in.
Net axial length of iron	12.5 in.
Gross length of iron	13.9 in.
Center-vent ducts	$8 \times \frac{3}{8}$ in.
Frame length	16.9 in.

The remainder of the design is carried out in the usual way and the machine is then drawn to scale as shown in Fig. 197, which shows the kind of ventilation required to keep the center

of the machine cool. Fans are placed at the ends of the rotor to create an air pressure and so force air out across the back of the punchings and also through the vent ducts. Coil retainers are put at A to prevent the rotor coils from bulging out due to centrifugal force.

196. Turbo-alternators.—Alternators which are direct connected to steam tubines run at a high speed and have, therefore, few poles, even for large ratings. It was pointed out in Art. 189, page 259, that when the number of poles is small, it becomes difficult to find space for the necessary field copper, but that this difficulty could be overcome by increasing the diameter of the machine and lowering the value of q, the ampere conductors per inch.

In the case of the turbo-alternator, the diameter cannot be increased beyond the value at which the stresses in the machine due to centrifugal force reach their safe limit, and some other method of solving the difficulty must be found.

The answer that has been found satisfactory for modern steam turbine-driven alternators is to use an insulation on the field coils that will withstand high temperatures. As indicated in Art. 152, the temperature rise in field windings provided with class B insulation is 90° C. according to the standards established by the A.I.E.E. The use of a field winding capable of operating with a temperature rise of 90° C., and of a rotor construction that is described in the following article, has resulted in a satisfactory structure.

197. Rotor Construction for Turbo-alternators.—Due to the high velocities required in turbo-alternators, the centrifugal forces in such a structure are very high; for instance, a weight of 1 lb. revolving at 1800 r.p.m. with a peripheral speed of 26,000 ft. per minute is acted on by a centrifugal force of over 2500 lbs. It is therefore necessary to adopt a type of construction which is capable of resisting very high centrifugal forces. The type of construction shown in Figs. 198 and 199 is the type now universally used for turbo-alternator rotors except that for the through shaft therein shown there is now substituted a construction in which the body of the rotor (the part carrying the exciting windings) is either of solid-forged steel with no center hole for a shaft, or is made up of rolled-steel plates about 2 in. thick rabbited together. The shaft is either forged on, in the former type of construction, or consists of a forging ending in a flange of

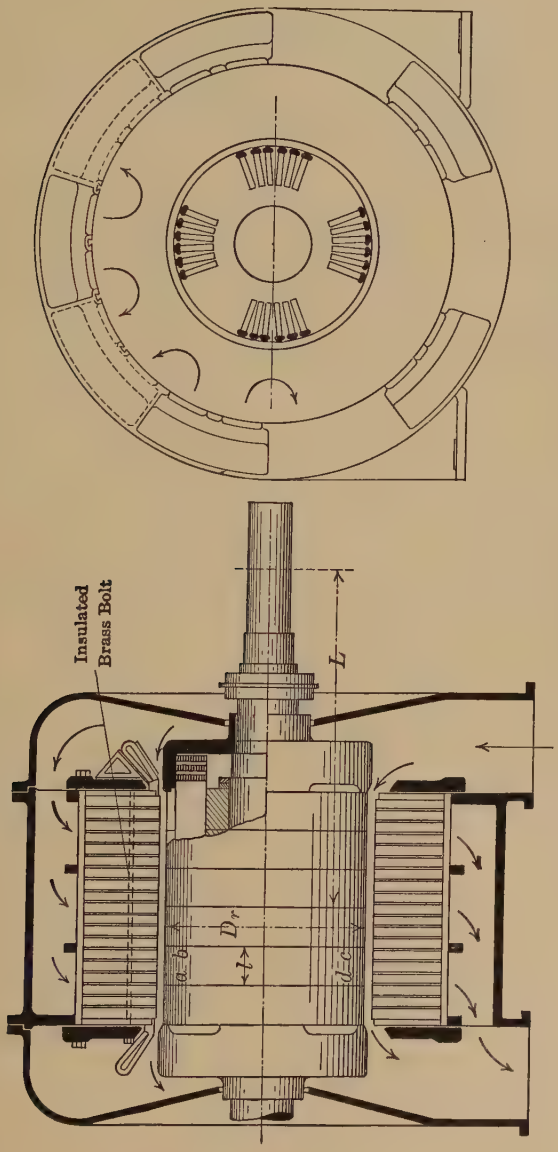

FIG. 198.—Outline of a 5000-kw., 1800-r.p.m., 60-cycle turbo-alternator.

the same diameter as the rolled plates, in the latter type. In the latter type of construction, through bolts hold the shaft flanges to the body of the rotor as well as hold together the individual body plates. In both types, the slots for the field windings are milled out, as shown in Figs. 198 and 199. Figure 200 shows the body of a turbo-rotor using rolled-steel plates about 2 in. thick rabbited together for the body of the rotor, and the shaft flanges bolted on at each end.

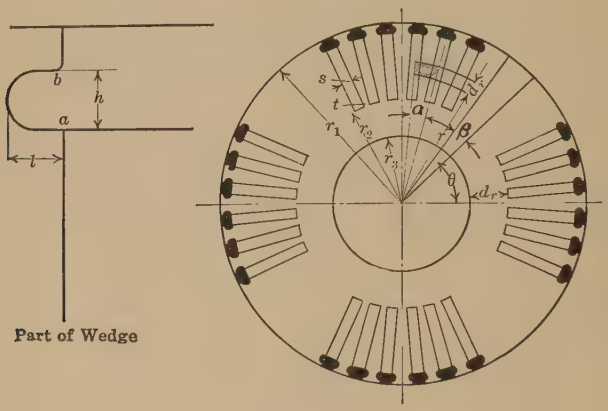

FIG. 199.

198. Stresses in Turbo-rotors.—The electrical and mechanical design of a turbo-rotor must be carried out together, because the space available for field copper cannot be determined until the section of steel below the rotor coils, required for mechanical strength, has been fixed. The most important of the stresses in the type of rotor shown in Fig. 198 are determined approximately as follows:

Stress at the Bottom of a Rotor Tooth.—Assume that one tooth carries the centrifugal force due to its own weight and to that of the contents of one slot, and also that the total weight of copper, insulation and wedge in a slot is the same as that of an equal volume of steel.

Consider 1 in. in axial length of the rotor; then in Fig. 199, where all the dimensions are in inches:

$dw = 2\pi r \frac{\alpha}{360} \times dr \times 0.28$ lb. = weight of the cross-hatched piece,

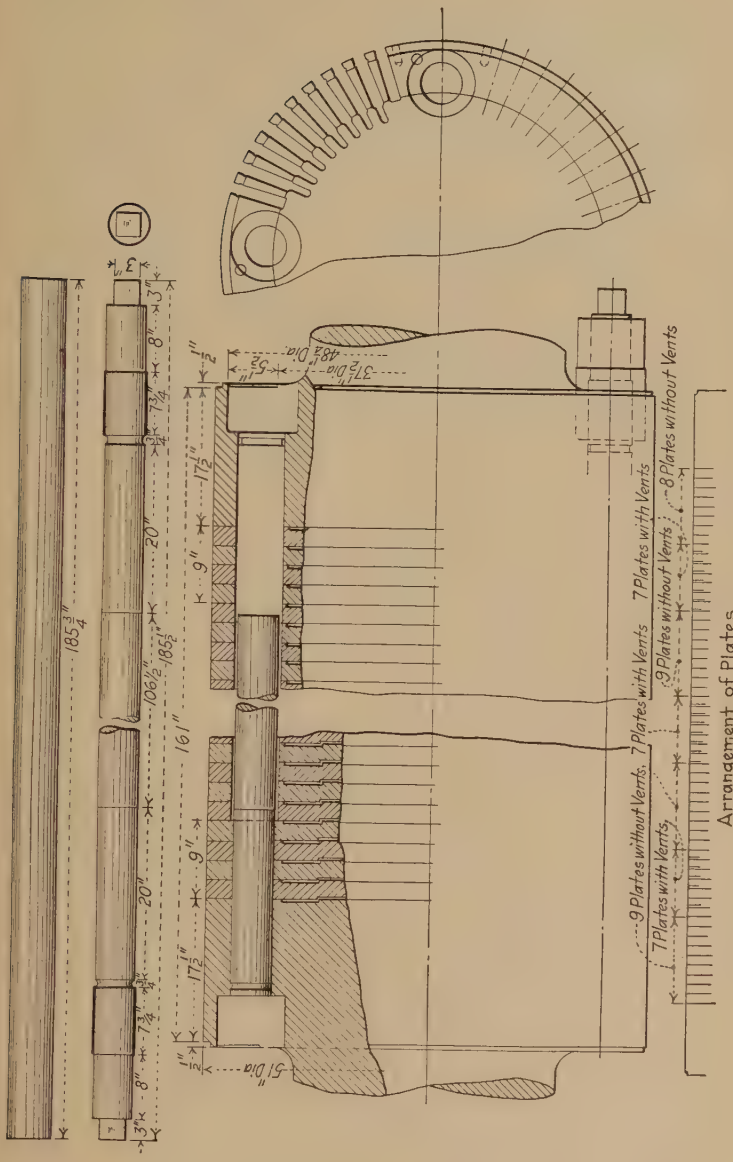

FIG. 200.—Turbo-rotor construction—made up of rolled steel plates rabbited together.

$v = \frac{2\pi r}{12} \times \frac{\text{r.p.m.}}{60}$ = the peripheral velocity of this piece;

the centrifugal force due to $dw = \frac{dw \times v^2 \times 12}{g \times r}$;

the total centrifugal force carried by a rotor tooth

$$= \int_r^{r_1} 2\pi r \frac{\alpha}{360} \times dr \times 0.28 \times \left(\frac{2\pi r}{12} \times \frac{\text{r.p.m.}}{60}\right)^2 \times \frac{12}{g \times r};$$

$$= \frac{(r_1^3 - r_2^3)\text{r.p.m.}^2 \times \alpha}{21.5 \times 10^6} \text{ lb.}$$

the stress at the bottom of a rotor tooth $= \frac{\text{centrifugal force}}{t}$;

$$= \frac{(r_1^3 - r_2^3)\text{r.p.m.}^2}{21.5 \times 10^6 \times t} \times \frac{(t + s) \times 360}{2\pi r_2}. \qquad (34)$$

Stress in the Disc.—The centrifugal force of the section of the rotor enclosed in the angle $\beta = \frac{(r_1^3 - r_3^3)\text{r.p.m.}^2\beta}{21.5 \times 10^6}$ lb.;

the vertical component of this force

$$= \frac{(r_1^3 - r_3^3)\text{r.p.m.}^2\beta}{21.5 \times 10^6} \sin\theta;$$

the total vertical component due to half the rotor

$$= \frac{(r_1^3 - r_3^3)\text{r.p.m.}^2 \times 180}{21.5 \times 10^6} \times \text{average value of } \sin\theta,$$

$$= \frac{(r_1^3 - r_3^3)\text{r.p.m.}^2}{1.9 \times 10^5} \text{ lb.};$$

the stress in the section $d_r = \frac{(r_1^3 - r_3^3)\text{r.p.m.}^2}{3.8 \times d_r \times 10^5}$. (35)

When there is no through shaft used, as is the case in modern construction, d_r becomes equal to r_2 and r_3 becomes zero.

Stress in the Wedge.—The total force acting upward on the wedge is the centrifugal force of the contents of the slot

$$= \int_{r_2}^{r_1} s \times dr \times 0.3 \times \left(\frac{2\pi r}{12} \times \frac{\text{r.p.m.}}{60}\right)^2 \times \frac{12}{g \times r};$$

$$= \frac{(r_1^2 - r_2^2) \times s \times \text{r.p.m.}^2}{2.3 \times 10^5};$$

$$= P;$$

the stress at section ab due to shear $= \frac{P}{2 \times h} = S$;

the stress at point b due to bending $= \frac{P \times l}{4} \frac{6}{h^2} = B$;

the maximum stress in the wedge $= \frac{B}{2} + \sqrt{\frac{B^2}{4} + S^2}$.

199. Diameter of the Shaft.—Every shaft deflects due to the weight which it carries so that as it revolves it is bent to and fro once in a revolution. If the speed at which the shaft revolves is such that the frequency of this bending is the same as the natural frequency of vibration of the shaft laterally between its bearings, then the equilibrium becomes unstable, the vibration excessive, and the shaft liable to break unless very stiff. The speed at which this takes place is called the critical speed and should not be within 20 per cent of the actual running speed.

The critical speed for turbo-rotors in r.p.m. = a constant $\times \sqrt{\frac{EI}{ML^3}}$ where E = Young's modulus for the shaft material = about 30,000,000 for steel;

I = the moment of inertia of the shaft section about a diameter $= \frac{\pi}{64} d_s^4$;

M = the mass of the revolving part $= \frac{\text{weight of rotor}}{g}$;

$2L$ = the distance between the bearings (see Fig. 198).

the constant[1] = 75 for turbo-rotors, if inch and pound units are used.

Therefore the critical speed $= 100 \times d_s^2 \sqrt{\frac{28 \times 10^6}{\text{rotor weight} \times L^3}}$. (36)

If, instead of vibrating as a whole, the shaft vibrates in two halves with a node in the middle, then the frequency of this harmonic is got by substituting for L in the above equation the value $\frac{L}{2}$ and is equal to

= the fundamental frequency $\times 2^{3/2}$;

= 2.8 times the fundamental frequency.

It is found in practice that this harmonic has a value which varies from about 2.4 to 2.6 times the fundamental frequency.

The deflection of the shaft is generally limited to 5 per cent of the air-gap clearance so that there shall not be any trouble due to magnetic unbalancing, therefore

$$\text{deflection} = \frac{W \times (2L)^3}{48EI} = 0.05\delta \text{ in.}$$

where W = the weight of the rotor + the unbalanced magnetic pull in pounds (see Art. 331).

[1] BEHREND, *Elec. Rev.*, N. Y., 1904, p. 375.

In modern turbo-generators, the structure of the rotating element is not a simple shaft of circular cross-section, as has been assumed in the foregoing; in obtaining the critical speeds and the deflection, the character of this structure must be analyzed, and suitable values used for I in the equations derived above.

The stress in the shaft is determined as follows:

M_b, the bending moment at the center of the shaft $= \frac{WL}{2}$ in.-lb.

M_t, the twisting moment $= \frac{\text{watts input}}{746} \times \frac{33{,}000}{2\pi \text{r.p.m.}} \times 12,$

$$= \frac{\text{watts input}}{\text{r.p.m.}} \times 85 \text{ in.-lb.}$$

M_e, the equivalent bending moment $= M_b + \frac{\sqrt{M^2_b + M^2_t}}{2},$

$$= \text{stress} \times \frac{\pi}{32} d_s{}^3. \qquad (37)$$

200. Heating of Turbo-rotors.—The assumption made in the following discussion is that all the heat generated in the part $abcd$ of the rotor, Fig. 198, is dissipated from the surface $\pi D_r l$, so that each part of the rotor gets rid of its own heat and there is no conduction axially along the winding.

The difference in temperature between the rotor copper and the air which enters the machine

= the difference in temperature from copper to iron,

+ the difference in temperature between the iron and the air at the rotor surface,

+ the difference in temperature between the air at the rotor surface and that entering the machine, which value may be taken as 15° C.

It was shown in Art. 105, page 128, that in any slot the difference in temperature between the copper and the iron

$$= \frac{\text{ampere conductors per slot}}{\text{circular mils per ampere}} \times \frac{\text{thickness of insulation}}{2d + s} \times \frac{1}{0.003},$$

$$= \frac{\text{ampere conductors per pole} \times 33}{\text{slots per pole} \times \text{circular mils per ampere}} \times \frac{1}{2d},$$

taking the thickness of slot insulation and the slot clearance to be 0.1 in. and neglecting s for the case of strip copper laid flat in

the slot, because the heat will not travel down through the layers of insulation.

The difference in temperature between the rotor surface and the air surrounding it is found as follows:

The resistance of a conductor of M cir. mils section, l in. long

$$= \frac{l}{M} \text{ ohm.}$$

The loss in this conductor $= \frac{lI_c^2}{M}$ watts.

The total loss in section *abcd* (Fig. 198) $= \frac{lI_c^2}{M} \times$ conductors per slot $\times$ slots per pole $\times$ poles $= \frac{\text{ampere conductors per pole}}{\text{circular mils per ampere}} \times p \times l.$

The watts per square inch of radiating surface

$$= \frac{\text{ampere conductors per pole}}{\text{circular mils per ampere}} \times \frac{p \times l}{\pi D_r l},$$

$$= \frac{\text{ampere conductors per pole}}{\text{circular mils per ampere}} \times \frac{1}{\tau}.$$

The temperature rise of this surface *abcd*, Fig. 198, above the air may be obtained from the formula given in Art. 101—*viz.*: watts per square inch per degree Centigrade $= 0.01 + 0.025V$ where V is the peripheral velocity in thousands of feet per minute. Transposing this relation

$$\text{temperature rise in degrees Centigrade} = \frac{\text{watts per square inch}}{0.01 + 0.025V}$$

$$= \frac{\text{ampere conductors per pole}}{\text{circular mils per ampere} \times \tau \times (0.01 + 0.025V)}.$$

The temperature rise of the rotor copper above the air entering the machine may therefore be taken as

$$= \frac{\text{ampere conductors per pole}}{\text{circular mils per ampere}} \left(\frac{1}{\text{pole pitch} \times (0.01 + 0.025V)} + \frac{33}{\text{slots per pole } (2d)} \right) + 15,$$

and for the allowable temperature rise of 90° C. (A.I.E.E. standard), the circular mils per ampere

$$= \frac{\text{ampere conductors per pole}}{75} \left(\frac{1}{\text{pole pitch} \times (0.01 + 0.025V)} + \frac{33}{\text{slots per pole } (2d).} \right). \quad (38)$$

201. Heating of Turbo-stators.—Compared to its output, the radiating surfaces of a turbo-alternator are small, and forced ventilation is essential. In the earlier designs of such machines,

fans were attached to the rotor for the purpose of circulating the necessary air. The limitations in design were such that the fans were not very effective and, in present-day practice, the fan for circulating the ventilating air is usually a separate piece of equipment driven by a separate motor. Also it is now becoming more and more common to use an entirely enclosed air system, spraying the air with water before it enters the alternator, thus not only cooling it but washing out all particles of dust and other solid matter. The desirability of doing this may be realized when the amount of air necessary for cooling is calculated.

If, in a machine which is cooled by forced ventilation,

t_i = the temperature of the air at the inlet in degrees Centigrade,

t_o = the average temperature of the air at the outlet in degrees Centigrade, then each pound of air passing through the machine per minute takes with it $0.238(t_o - t_i)$ lb. calories per minute

$$\text{or } 7.5(t_o - t_i) \text{ watts,}$$

and each cubic foot of air per minute takes

$$0.536(t_o - t_i) \text{ watts,}$$

since the specific heat of air at constant pressure = 0.238 and the volume of 1 lb. of air is approximately 14 cu. ft.

If 100 cu. ft. of air per minute are supplied for each kilowatt loss in the machine, then the average rise in temperature of the air will be 19° C.

For a generator that weighs 15 lb. per kilovolt-ampere, and has an efficiency of 97 per cent, the amount of air that will be drawn through for cooling—allowing for 15° C. rise in the cooling air—will be the generator's own weight of air every 55 min. This indicates the large quantity of air that is necessary for generator cooling.

The losses in air friction that occur in circulating this amount of air are considerable. In fact, they are large enough to lead designers to consider the feasibility of using hydrogen instead of air for cooling purposes. Hydrogen has a specific heat of 3.4—fourteen times that of air—and a specific gravity of about 0.07—air being 1. Thus, hydrogen is very much better as a cooling medium than is air; the amount of power required for circulating hydrogen for a given amount of cooling is only about 10 per cent of what would be required with air. Of much greater importance

is the fact that, if hydrogen cooling could be used, heat could be dissipated from the machine much more readily, and a considerably higher rating could be secured for a given weight of machine than is now possible with air cooling. The use of a completely closed system for the cooling medium in our modern turbo-generators renders the idea of using hydrogen for cooling less chimerical than might seem at first thought. While the idea has not yet been put into actual operation (1926), it is receiving serious consideration.

When air is blown across the surface of an iron core at V thousand feet per minute, the watts dissipated per square inch per degree Centigrade rise of that surface is $0.01 + 0.025V$ (see Art. 101). It is not generally advisable to use air velocities higher than 6000 to 8000 ft. per minute because of the losses in air friction that take place at these high velocities. For an air velocity of 8000 ft. per minute, the watts per square inch dissipated for a 1° C. rise are 0.21.

The watts of iron loss per square inch of vent duct surface = watts per cubic inch of iron $\times X$ (Fig. 87, p. 124).

For 1½-in. thick packages of iron, an air velocity of 8000 ft. per minute and a difference in temperature between iron and air of 10° C., the

watts per cubic inch of iron $= 0.21 \times 10 \times 0.75 = 1.575$

and the watts per pound of iron $= \dfrac{1.575}{0.28} = 5.63$ (there being 0.28 lb. of iron per cubic inch) which according to Fig. 86 gives a flux density of

63,000 lines per square inch at 60 cycles,

and 102,000 lines per square inch at 25 cycles.

As a matter of fact the iron loss in turbo-generators is not much over (See Art. 181) 0.7 times the value found from the curves in Fig. 86 because the bulk of this loss is in the core behind the teeth and is therefore not affected by filing of the slots; the pole face loss in a turbo-generator is also small because the air-gap is long and so prevents tufting of the flux.

In a long machine like a turbo-generator most of the heat due to stator copper loss has to be conducted through the slot insulation and dissipated from the sides of the vent ducts, and this counteracts the effect of the reduced core loss so far as core heating is concerned. For a new machine the following values of flux density should not be exceeded unless there is considerable information obtained from tests on other machines which would justify the use of higher values.

Frequency	Maximum Tooth Density, Lines per Square Inch	Maximum Core Density, Lines per Square Inch
25 cycles	120,000	90,000
60 cycles	110,000	80,000

for silicon steel 0.014 in. thick.

202. Stator Ventilation.—Figure 201 shows the methods of ventilation used in modern turbo-alternators. *A* in Fig. 201 shows the method of ventilation that was formerly used; all of the air for ventilating the stator was forced into the air-gap from the ends and thence passed radially through the vent ducts in the stator. This method answered very satisfactorily for ratings up to 15,000 to 20,000 k.v.a. When larger ratings were attempted, the area of the air-gap was not sufficient to admit the necessary quantity of air to carry away the heat. It must be borne in mind that the peripheral speed of rotors is up to a point where a consideration of centrifugal forces will not permit further increase in diameter and the only way of securing the larger outputs that were demanded was to lengthen the machine. It is obvious that this lengthening cannot be carried on indefinitely without reaching a point where it is impossible to pass all the necessary air for ventilation through the air-gap from the two ends, only. The answer to this difficulty is found in diagrams *B* and *C*, Fig. 201. The stator is divided into sections for ventilating purposes, and as many multiple paths as may be necessary may be secured. With these multiple paths, the cross-section of the air-gap no longer is the determining factor in dictating the amount of air that can be passed through a generator. So far as ventilating is concerned, therefore, the length of a generator may be increased indefinitely and still secure satisfactory results.

Figure 201*A* shows a modern turbo-generator ventilating layout using a self-contained blower and a radiator type of air cooler.

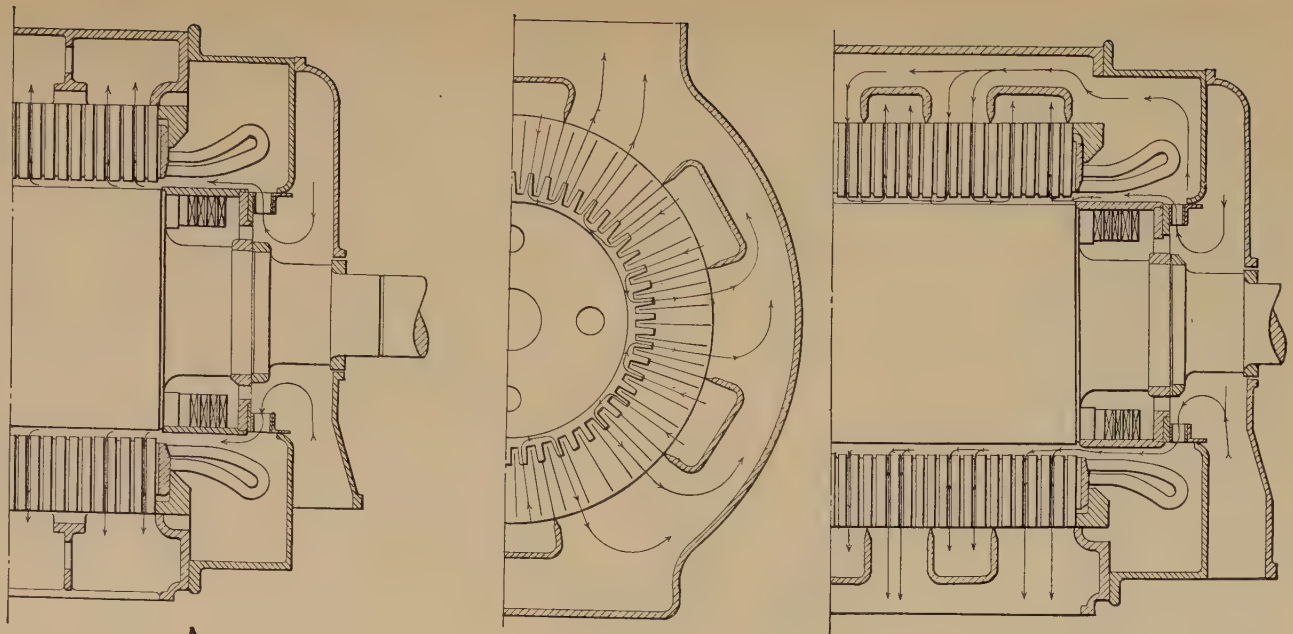

FIG. 201.—Diagram showing various methods for ventilation of turbo-generator stators.

203. Short-circuits.—When an alternator running at normal speed is short-circuited and the field excitation gradually increased, the current which flows for any field excitation can be found from a short-circuit curve such as that in Fig. 175, page 225, and at the excitation for normal voltage and no load the armature current on short-circuit will for modern generators seldom exceed 1.25 times full-load current.

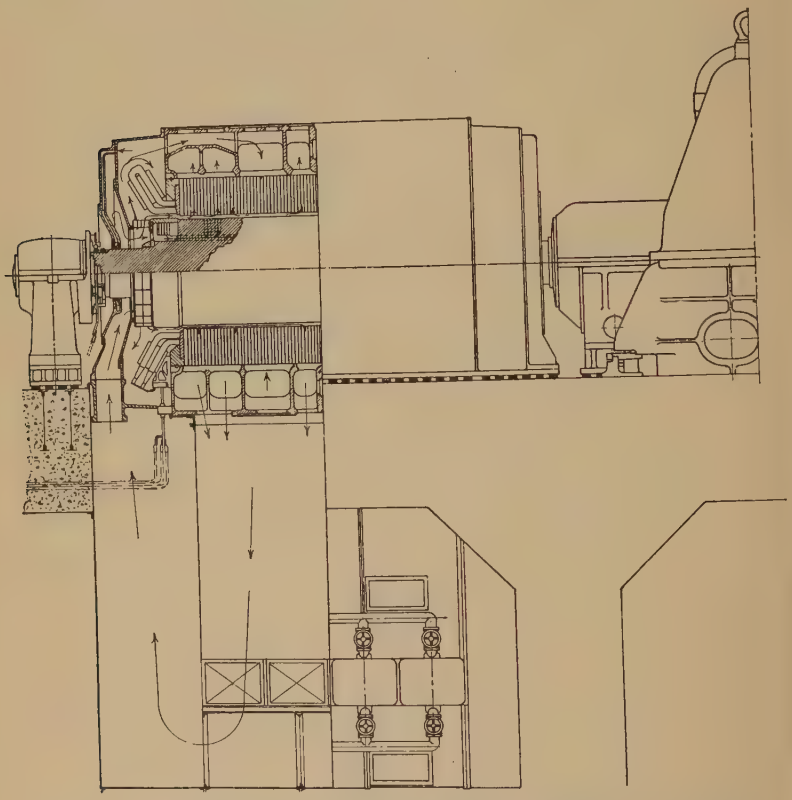

FIG. 201*A*.—Ventilating system for a turbo-alternator consisting of a self contained blower and radiator type air cooler.

The terminal voltage and the power factor are both zero on short-circuit, and the voltage drop, as shown in diagram *A*, Fig. 202, is made up of the drop E_oE_g due to armature reaction, and of the armature reaction drop IX.

When an alternator, running at normal speed, no load and excited for normal voltage, is suddenly short-circuited, the arma-

ture current increases and tends to demagnetize the poles. Now the flux in the poles cannot change suddenly because the poles are surrounded by the field coils, which are short-circuited through the exciter, as well as by a squirrel-cage winding—in many modern generators—recessed into the faces of the poles so that any decrease in the flux in the poles causes a current to flow round the field coils or in the squirrel-cage amortisseur winding in such a direction as to maintain the flux. The armature reaction is therefore not instantaneous in action and at the first instant after the short-circuit the current in the armature is limited only by the armature reaction. The operation of an alternator on a sudden short-circuit is shown in diagram *B*, Fig. 202.

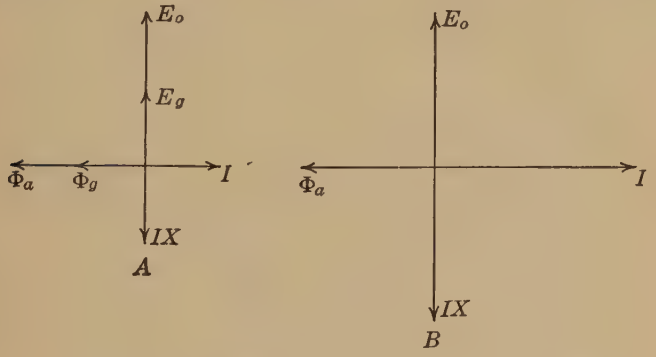

Fig. 202.—Vector diagram for an alternator on short-circuit.

The maximum value of the current depends on the value of the voltage at the instant of the short-circuit; in Fig. 203, curve 1 gives the value of the generated e.m.f. at any instant, and curve 2, the value of the reactance voltage at any instant during the first few cycles after the short-circuit; the terminal voltage is zero, the armature reaction is dampened out by the field winding, or the amortisseur winding, and the reactance voltage is equal and opposite to the generated e.m.f.

The reactance voltage is produced by the change in the short-circuit current and, according to Lenz's Law, acts in such a direction as to oppose this change. If then, as in diagram *A*, Fig. 203, the short-circuit takes place at the instant *a*, when the generated voltage is a maximum, then between *a* and *b* the reactance voltage is negative and must therefore be opposing a growth of current, while between *b* and *c* the reactance voltage

is positive and must be opposing a decay of current. At the instant of short-circuit the current is zero, and curve 3 is the current curve which meets these conditions.

If, as in diagram *B*, Fig. 203, the short-circuit takes place at the instant *f*, when the generated voltage is zero, then between

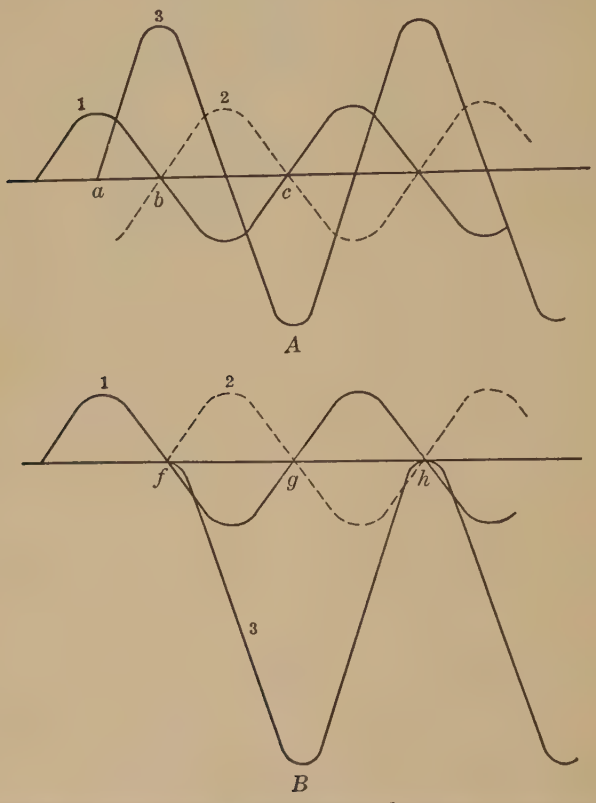

Fig. 203.—Effect on the value of the current of the point of the e.m.f. wave at which the short circuit occurs.

f and *g* the reactance voltage is positive and must therefore be opposing a decay of current, while between *g* and *h* the reactance voltage is negative and must be opposing a growth of current. At the instant of short-circuit, the current is zero and curve 3 is that current curve which meets these conditions.

Neglecting the leakage reactance of the rotor, the current in the case represented by diagram *A*, Fig. 203, has an effective

value $= \frac{\text{generated voltage per phase}}{\text{reactance per phase}}$, while in the case represented by diagram B the maximum current is twice as large.

204. Probable Value of the Current on an Instantaneous Short-circuit.—It was shown in the last article that the effective current under the most favorable conditions

$= \frac{\text{generated voltage per phase}}{\text{reactance per phase}}$, and therefore

$$\frac{\text{current on instantaneous short-circuit}}{\text{full-load current}} = \frac{\text{generated voltage}}{\text{reactance voltage}}.$$

The generated voltage per phase

$= 2.22 \times k \times \cos\frac{\theta}{2} Z\phi_a f 10^{-8}$ (formula (26), page 185);

$= 2.12(bcp) \times \cos\frac{\theta}{2}(B_g \psi \tau L_c) f 10^{-8}$ taking $k = 0.96$;

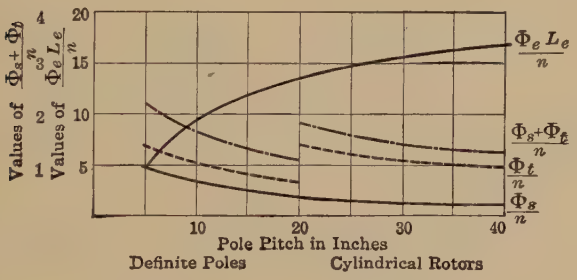

FIG. 204.—Values of the leakage fluxes.

the reactance voltage per phase

$= 2\pi f b^2 c^2 p[\phi_e L_e + (\phi_s + \phi_t)L_c]10^{-8} \times I$ for a chain winding (formula (28a), page)223;

$= 2\pi f b^2 c^2 \cos^2\frac{\theta}{2} p\left[\frac{\phi_e L_e}{2} + (\phi_s + \phi_t)L_c\right]10^{-8} \times I$ for a double-layer winding (formula (29), page 223).

Where $\frac{\phi_e L_e}{n}$ varies with the pole pitch as shown in Fig. 204, $\frac{\phi_s}{n} = \frac{3.2}{cn}\left[\frac{d_1}{3s} + \frac{d_2}{s} + \frac{2d_3}{s+w} + \frac{d_4}{w}\right]$, and since $c \times n \times s$, the total slot width per pole, is proportional to the pole pitch, therefore $\frac{\phi_s}{n}$ is approximately inversely proportional to the pole pitch;

$\phi_t = 0.42\ \phi_{tp} = 1.34\dfrac{Ct}{2\delta}$ for machines with definite pole rotors, neglecting the value of ϕ_{ta},

$= 3.2\dfrac{Ct}{2\delta}$ for machines with cylindrical rotors, the type generally used for turbo-generators. In order that the regulation of the machine may have a reasonable value, δ, the air-gap, is fixed by the value of the armature ampere-turns per pole and is approximately proportional to the pole pitch; therefore ϕ_t is approximately inversely proportional to the pole pitch.

The ratio $\dfrac{\text{reactance voltage}}{\text{generated voltage}} = \dfrac{3q}{B_g\psi}\left[\dfrac{\phi_e L_e}{nL_c} + \dfrac{\phi_s + \phi_t}{n}\right]$ for a chain winding $= \dfrac{3q}{B_g\psi}\cos\dfrac{\theta}{2}\left[\dfrac{\phi_e L_e}{2nL_c} + \dfrac{\phi_s + \phi_t}{n}\right]$ for a double-layer winding,

where $\dfrac{\phi_s + \phi_t}{n} = \dfrac{\text{a constant}}{\text{pole pitch}}$ for a given number of phases. (39)

The values of ϕ_s and ϕ_t are plotted in Fig. 204 for average machines which have not less than two slots per phase per pole nor a larger slot pitch than 2.0 in., and for machines with open slots and laminated rotors.

Example.—Determine, approximately, the ratio $\dfrac{\text{reactance voltage}}{\text{generated voltage}}$ for the 937.5-k.v.a. machine detailed in Chap. XXI. This machine had the following dimensions:

Normal output in kilovolt-ampere	937.5.
Normal voltage	2400.
Number of phases	3.
Current per phase	226.
R.p.m.	600.
Frequency	60.
θ = chording factor	0
Internal diameter armature	42.5.
Pole pitch	11.12 in.
Frame length	12.5 in.
Average gap density	48,500.
Per cent pole enclosure	74.
Ampere conductors per inch	1100.
Winding	Double layer, Y-connected.

$$\frac{\text{Reactance voltage}}{\text{Generated voltage}} = \frac{3 \times 1100}{48{,}500 \times 0.74}\left(\frac{10}{2 \times 12.5} + 1.5\right) = 0.174.$$

That is, this machine would give an instantaneous short-circuit current of $5\frac{3}{4}$ normal full-load current, if short-circuited at such a point in its voltage

wave as to give the minimum short-circuit value and double this value at the maximum.

When a solid pole face is used, as in most turbo-alternators with cylindrical rotors, the value of ϕ_t will be lower than that found from Fig. 204, because the flux will be prevented from entering the pole face by eddy currents which it produces therein; this tends to make the short-circuit current larger than the value found from formula (39).

Down to this point the effect of the leakage reactance of the rotor winding has been neglected. As shown in Fig. 167, page 213, the total flux per pole $= \phi_m = \phi_a + \phi_e$ and this remains constant during the first few cycles after an instantaneous short-circuit. In order that ϕ_m remain constant, a current must flow in the rotor winding in such a direction as to oppose the demagnetizing effect of the armature reaction. This current is large, so that the m.m.f. between the poles and, therefore, the leakage flux ϕ_e is much larger immediately after a sudden short-circuit than at no load.

If ϕ_{eo} = the pole leakage flux at no load

and ϕ_{es} = the pole leakage flux immediately after a short-circuit,

then the generated voltage in the machine, which is produced by the flux ϕ_a, is less immediately after a short-circuit than it was immediately before in the ratio $\frac{\phi_m - \phi_{es}}{\phi_m - \phi_{eo}}$, and this tends to make the short-circuit current smaller than the value found from formula (39).

To reduce the ratio $\frac{\text{current on instantaneous short circuit}}{\text{full-load current}}$ it is necessary as shown in formula (39):

To increase the value of q, the ampere conductors per inch; this will at the same time cheapen the machine but will cause its regulation to be poorer.

Use a chain rather than a double-layer winding so as to increase the end-connection reactance.

Use deep, narrow and closed slots so as to increase the slot reactance.

Use as small a pole pitch as possible until the point is reached at which the term $\frac{\phi_e L_e}{nL_c}$ becomes of more importance than the term $\frac{\phi_s + \phi_t}{n}$.

Use a laminated rotor if possible.

Use a cylindrical rotor rather than one of the definite pole type, because of the larger value of ϕ_t, as may be seen from Fig. 204. All the above changes are made to increase the reactance of the machine and, therefore, tend to make the regulation poor.

The value of the instantaneous short-circuit current can be reduced by making the pole leakage factor large, and this will not affect the regulation seriously if the pole pieces are unsaturated at normal voltage.

205. Supports for Stator End Connections.—The large current due to an instantaneous short-circuit takes several seconds to get down to the value which it would have on a gradual short-circuit, and during this time the force of attraction between adjacent conductors of the same phase is very large and tends

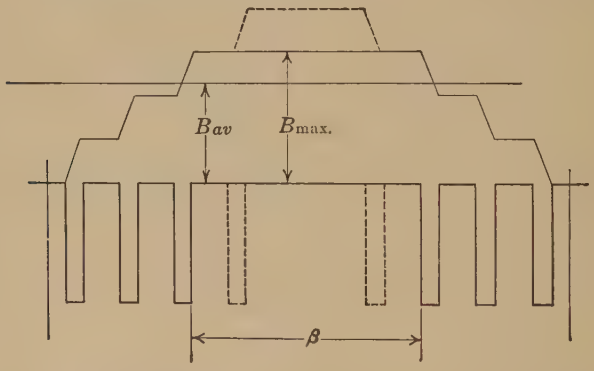

FIG. 205.—Flux distribution in the air gap of a turbo-alternator.

to bunch the end connections of each phase together. The force between the groups of end connections of adjacent phases is also very large and, when the currents in these phases are in opposite directions, this force tends to separate the phase groups of end connections. To prevent any movement of the coils due to this effect it is necessary to brace them thoroughly in some such way as that shown in Fig. 198.

206. The Gap Density.—For the type of rotor shown in Fig. 198, the distribution of flux in the air-gap is given by the heavy line curve in Fig. 205; if two more slots per pole are added, as shown dotted in Fig. 205, the flux will be increased by the amount enclosed by the dotted curve and, for a considerable increase in rotor copper and rotor loss, only a small increase in the flux per

pole will be obtained. The angle β is therefore seldom made less than 30 electrical degrees, and for this value the maximum gap density = the average gap density $\times$ 1.5, approximately.

The maximum gap density depends on the permissible value of the maximum tooth density, since

$$B_{g\ max} = B_{t\ max} \times \frac{L_n}{L_c} \times \frac{t}{\lambda};$$

the blocks of iron in the core are about 1.5 in. thick, the vent ducts 0.375 in. wide and the stacking factor = 0.9;
therefore

$$\frac{L_n}{L_c} = 0.72,$$

an average value for $\frac{\lambda}{t} = 1.75$ for turbos, since the slot pitch is generally large,
and $B_{t\ max}$ = 110,000 lines per square inch for 60 cycles,
= 120,000 lines per square inch for 25 cycles;
therefore

$B_{g max}$ = 45,300 lines per square inch for 60 cycles,
= 49,400 lines per square inch for 25 cycles.

207. The Demagnetizing Ampere-turns per Pole at Zero Power Factor.—The distribution of the m.m.f. of armature reaction at two different instants is shown in Fig. 168, page 214, for a machine with six slots per pole and b conductors per slot. In the case of a definite pole machine, the portion of this diagram which is cross-hatched is effective in demagnetizing the poles, whereas in the type of machine with a cylindrical rotor the whole armature m.m.f. is effective, and for this case

$AT_{av} \times 6\lambda$ = area of diagram A,
$= 2bI_m\lambda + 1.5bI_m \times 2\lambda + bI_m \times 2\lambda,$
$= 7bI_m\lambda,$
= area of diagram B,
$= 1.73bI_m \times 3\lambda + 0.866bI_m \times 2\lambda,$
$= 6.92bI_m\lambda,$
$= 6.96bI_m\lambda$ the average value from diagrams A and B.

Therefore $AT_{av} = 1.16bI_m,$
$= 1.64bI_c$ where I_c is the effective current per conductor,
$= 1.64bI_c\left(\frac{\text{(slots per pole)}}{6}\right),$
= 0.275 $\times$ conductors per pole $\times$ I_c

The maximum m.m.f. of the field windings is that at the center of the poles and is equal to the ampere-turns per pole.

The average m.m.f. when β, Fig. 205, is 30 electrical degrees

$$= \frac{\text{maximum m.m.f.}}{1.5} \text{ (approximately)},$$

$$= \frac{\text{the ampere-turns per pole}}{1.5}.$$

Therefore the ampere-turns per pole required on the field to overcome the demagnetizing effect of the armature

$$= 1.5 \times 0.275 \times \text{conductors per pole} \times I_c,$$

$$= 0.41 \times \text{conductors per pole} \times I_c. \qquad (40)$$

208. Relation between the Ampere-turns per Pole on Field and Armature.—For definite pole machines the value of the ampere-turns for the gap on no load and normal voltage

$= AT_g$,

= 1.2 times the armature ampere-turns per pole for a first approximation (see Art. 177, page 240).

It may be seen by a comparison of formulæ 27 and 40, pages 215 and 296, that, for a machine with a cylindrical rotor, a somewhat larger number of field ampere-turns are required to overcome the demagnetizing effect of the armature than for a definite pole machine; and further, it will be seen from the example in Art. 209 that the air-gap of a turbo-alternator is very long and the number of ampere-turns used up in sending the flux through the poles is, therefore, very small compared with that required for the gap, so that the saturation curve does not bend over and the advantage of a saturated pole, pointed out in Art. 169, page 228, cannot readily be obtained. The regulation of turbo-generators is, in general, therefore, not quite so good as in a salient pole generator. On the other hand, turbo-generators are usually of much larger capacity than those with salient poles and, therefore, there is not the need for good, inherent regulation since a given change in load is a smaller proportion of the generator rating; further, it is not good practice to design very large generators with good inherent regulation because of the large current they will deliver on instantaneous short-circuit. It is, therefore, usual to design large turbo-alternators with a somewhat stronger armature compared to the field than in salient pole machines. For a first approximation, the following relation may be used for turbo-alternators:

AT for gap = 0.75 armature AT at full load.

209. Procedure in Turbo Design.—The method of working up the preliminary design of a turbo-alternator may best be illustrated by an example.

Make a preliminary design for a 25,000-k.v.a., 13,200-volt, three-phase, 60-cycle, 1800-r.p.m., 4-pole, 1095-ampere generator.

Peripheral speed rotor..... 24,000 ft. per minute assumed.
Rotor diameter..... $D_r = 51$ in.
Rotor pole pitch..... $\tau = 40$ in.
Ampere conductors per inch (Fig. 192)..... $q = 1560$.

Armature AT per pole $= \frac{q\tau}{2}$..... $= 31{,}200$.

$AT_g = 0.75$ armature AT for first approximation..... 23,400.

Probable value of $C\delta = \frac{3.2 \times AT_g}{B_{g\ max}}$..... $= 1.65$ in.

$C = 1$ for so large a gap. Make air-gap... $= 1.5$ in.
Internal diameter stator..... $Da = 54$ in.

Total conductors (probable)..... $Z_c = \frac{q \times \pi \times D_a}{I_c} = 242.$

Stator pole pitch..... $\tau = 42.3$ in.
Slots per pole..... 18.
Total slots..... 72.
Conductors per slot..... 3.
Total conductors (actual)..... $Z_c = 216$.
Armature resistance at 75° C..... 0.0265 ohm.

(Three conductors per slot will not wind into a two-layer winding; so use six conductors per slot—two circuits in parallel.)

Chording of winding..... $\frac{2}{3}$ pitch.
Flux per pole..... $\phi_a = 86.5 \times 10^6$.
Stator slot pitch..... $\lambda = 2.36$ in.
Slot width..... $s = 1.06$ in.
Tooth width..... $t = 1.30$ in.

Tooth area per pole required $= \frac{\phi_a}{B_{tav}} = \frac{\phi_a}{\frac{B_{t\ max}}{1.5}} = 1350$ sq. in.

Net length iron in core..... $L_n = 58.2$ in.
Gross length iron in core..... $L_g = 65.0$ in.
Center-vent ducts..... $60 \times \frac{3}{8}$ in. $= 22.5$ in.
Frame length..... 87.5 in.
(Was made 90 in.)

The machine may be drawn approximately to scale and the distance between bearings determined; this distance is approximately 210 in.

Rotor Design.

Probable rotor weight $= 0.7854 \times 51^2 \times 90 \times 0.28 \times 1.5 = 77{,}000$ lb.
The factor 1.5 is used to take account of end connections, field coil retainers, shaft extensions, etc (actual weight = 81,000 lb.).

Shaft diameter in bearings ..... 14 in.
Rotor deflection due to its own weight ..... 0.0071 in.
Length of each bearing ..... 24 in.
Critical speeds ..... First —2230, Second—8000 } approximately.
Normal running speed is therefore safely below first critical speed.
Length rotor body ..... 91.0 in.
Rotor slot pitch ..... 2.81 in.
Rotor slot width ..... 1.219 in.
Rotor slot depth ..... 7.0 in.
Rotor tooth width, maximum ..... 1.591 in.
Rotor tooth width, minimum ..... 0.821 in.
Number rotor slots, total ..... 40.
Depth wedge in rotor slots ..... 1.25 in.
Rotor conductors per slot ..... 22.5.
Total rotor conductors ..... 900.
Total rotor turns ..... 450.
Conductor size ..... 2 of 0.109 × 1.0 in
Exciter voltage ..... 250.
Field resistance—75° C ..... 0.434 ohm.
Armature ampere-turns per pole (full load) 29,600
Maximum field ampere-turns per pole ..... 47,300 (= 1.6 × armature AT per pole)
Length mean turn (field) ..... 270 in.

Stator Core Design.

Conductors per slot ..... 6.
Ampere conductors per inch (actual) ..... 1400.
Ampere conductors per slot ..... 3175.
Circular mils per ampere ..... 877.
Circular mils per conductor ..... $877 \times \frac{1095}{2} = 480{,}000.$

Conductor made up of 18 copper straps (2 wide and 9 deep), each strap 0.258 × 0.081 in. (0.081 in. dimension being depthwise).

Wedge for retaining armature winding sunk 1 in. to increase armature reactance.

Calculated losses are as follows:

	Kilowatts
Bearing losses	40.
Windage losses	400.
Iron losses	210.
Armature copper loss	45.
Load loss	120.
Field loss	80.
Total losses	895.

This gives the following efficiency (80 per cent power factor):

Per cent load	40	60	80	100
Per cent efficiency	91.3	93.8	95.0	95.7

Figure 206 shows the cross-section of one end of a turbo-generator of the same internal diameter as the one detailed above. It shows some of the ventilating air ducts, ventilation being of the multiple radial type, the air flowing axially in the air-gap. This is the type of ventilation shown in *C* of Fig. 201.

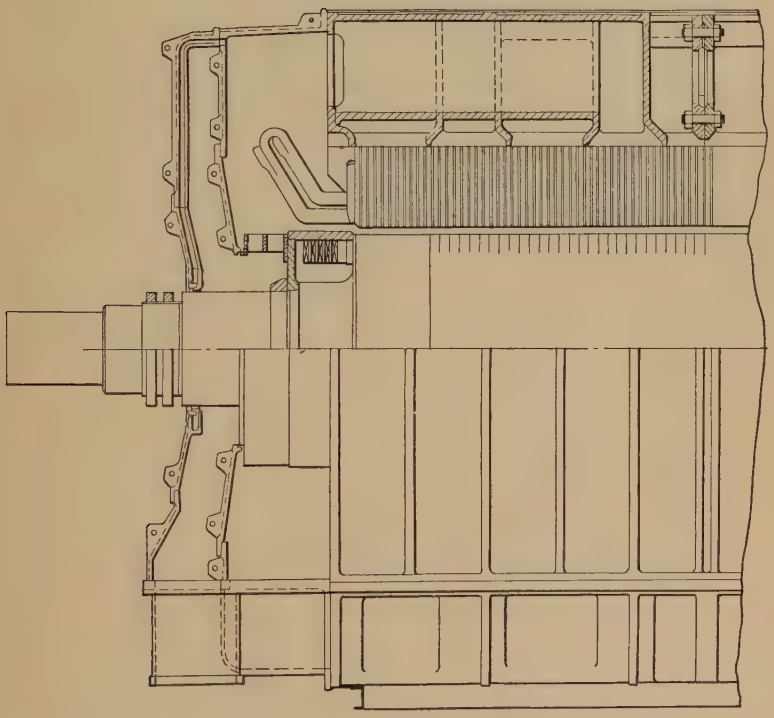

FIG. 206.—Cross-section through a modern turbo-generator.

Figure 207 shows the saturation curves—no load and full load, zero power factor—of the turbo-generator above detailed; also, the short-circuit characteristics.

210. Single-phase Turbo-generators.—In the design of this type of machine a new difficulty presents itself. It was shown in Art. 171, page 231, that the armature reaction in a single-phase alternator is pulsating and causes a double-frequency pulsation of flux in the poles, and, therefore, a large eddy current and hysteresis loss therein.

These pulsations are damped out somewhat by the eddy currents, but an eddy-current path in iron is a high-resistance path, and the eddy-current loss is, therefore, large. In order to damp out the flux pulsations with a minimum loss, it has been found necessary to surround the rotor with a squirrel-cage winding of copper in which eddy currents will be induced tending to wipe out the pulsating effect of armature reaction,

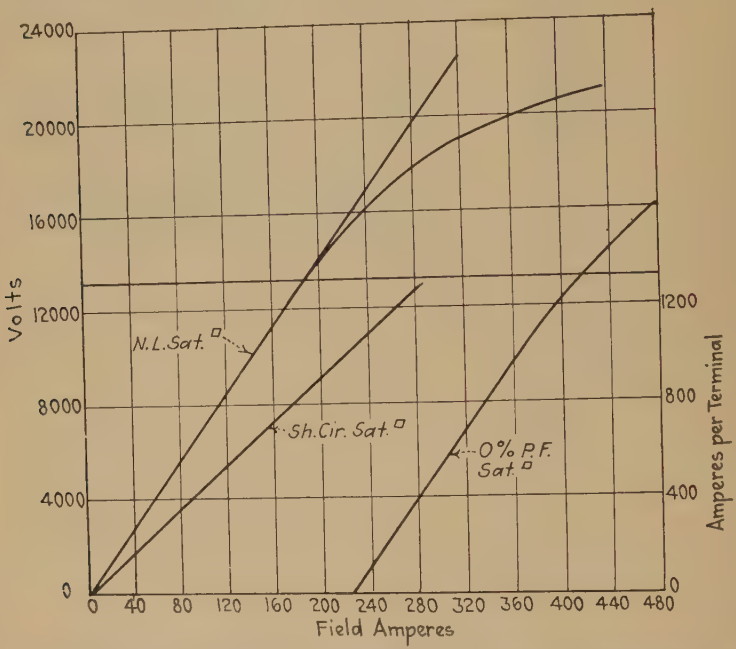

FIG. 207.—Saturation curves for a 25,000-k.v.a., 13,200-volt, three-phase, 60-cycle, 1800-r.p.m., four-pole, 1095-ampere full-load, turbo-generator.

and since the resistance of this squirrel cage can be made low its loss can be small. A suitable squirrel cage may be made by using copper for the slot wedges shown in Fig. 199, dovetailing similar wedges into the pole face, and connecting them all together at the ends by copper rings.

The following figures[1] show how necessary these dampers are: A 1000-k.v.a., two-pole, 25-cycle turbo-alternator was tested three phase; one phase was then opened and the machine run with two phases in series, which gave a single-phase winding with two-thirds of the total conductors (see Fig. 199, page 278). The

[1] Waters, *Trans.* A. I. E. E., Vol. 29, p. 1069.

same flux per pole and the same current per conductor were used in each case with the following result:

Heat Runs on Full-load

Three-phase No Dampers	Single-phase No Dampers	Single-phase with Dampers	
31	122	37	Temperature rise in degrees Centigrade

In the three-phase machine the armature reaction is constant in value and revolves at the same speed and in the same direction as the poles so that dampers are not required.

The pulsating field of armature reaction, as pointed out in Art. 171, page 231, is equivalent to two revolving fields, one of which revolves in the same direction and at the same speed as the poles, while the other, which causes the trouble, revolves at the same speed but in the opposite direction. The e.m.f. induced in an eddy-current path depends on the rate at which the lines of force of this latter field are cut and has a large value in a high-speed turbo-alternator but causes little trouble in moderate-speed machines.

CHAPTER XXIII

SPECIAL PROBLEMS ON ALTERNATORS

211. Flywheel Design for Engine-driven Alternators.—When two alternators are operating properly in parallel the currents flow as shown in diagram *A*, Fig. 208, and the operation is represented by diagram *B*. The e.m.fs. *P* and *Q* are equal and opposite with

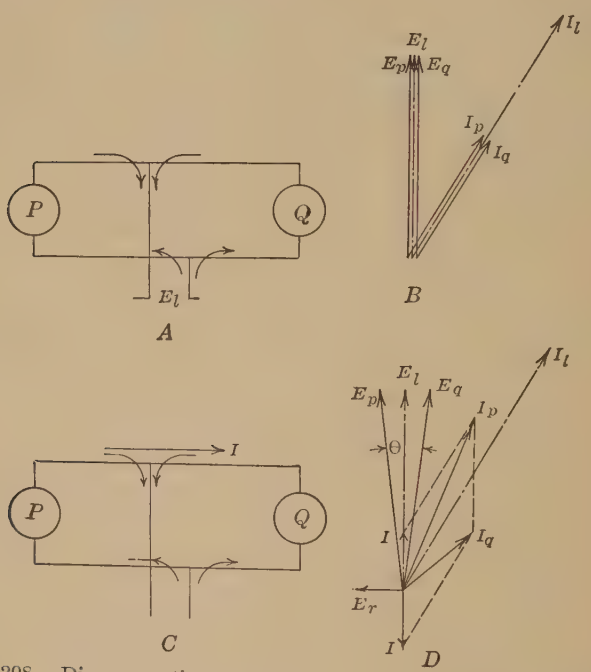

FIG. 208.—Diagrammatic representation of two alternators in parallel.

respect to the closed circuit consisting of the two armatures and the lines connecting them, and there is, therefore, no current circulating between the machines.

Should one of the machines, say *Q*, slow down for an instant, the currents will flow as shown in diagram *C*, and the operation is

represented by diagram D when machine Q lags behind machine P by θ electrical degrees. The two e.m.fs. are no longer opposed to one another and there is a resultant e.m.f. E_r which sends a circulating current round the closed circuit. While this circulating current has no separate existence, because it combines with the current which each machine supplies to the load to give the resultant current in the machine, yet it is convenient to consider its effect separately.

This circulating current $= \dfrac{E_r}{\bar{X}_p + \bar{X}_q}$ and lags E_r by 90 deg.,

where $\bar{X}_p$ = the synchronous reactance of machine P;

$\bar{X}_q$ = the synchronous reactance of machine Q;

the resistances of the armatures and the resistance and reactance of the line are all small compared with the above reactances and so can be neglected. It may be seen from diagram C that this circulating current is in the same direction as the e.m.f. in P; it therefore acts as an additional load on that machine and causes it to slow down; being opposed to the e.m.f. in Q, it, therefore, lightens the load on that machine and causes it to speed up; therefore, the two machines tend to come together, until they are in the position shown in diagram B, where the machines are in step and the circulating current is zero. Due, however, to the inertia of the machines, they will swing beyond the position of no circulating current which current will then be reversed and tend to pull the machines together again. The frequency of this swinging will be that of the natural vibration of the machines; the swinging will gradually die down due to the damping effect of eddy currents in the pole faces, field coils and dampers.

If one of the machines is direct connected to an engine whose torque is pulsating, forced oscillations will be impressed on the machine; if their period of vibration is within 20 per cent of the natural period of vibration, cumulative oscillation will take place and the machines be thrown out of step unless they are powerfully damped. It is, therefore, of extreme importance to study the natural period of vibration of alternators.

212. Two Like Machines Equally Excited.—When swinging takes place between two such machines, they move in opposite directions with the same frequency, so that if Fig. 209 shows the vector diagram of the two machines referred to the closed circuit, then

θ = the angle of displacement between the two machines;

$\alpha = \frac{\theta}{2}$ = the angle of displacement of one machine from the position of zero circulating current or mean position.

$E_r = 2E \sin \frac{\theta}{2}$,

I, the circulating current $= \frac{E_r}{2X}$ where X is the synchronous reactance of each machine,

$$= \frac{2E \sin \frac{\theta}{2}}{2X},$$

$$= I_{sc} \sin \frac{\theta}{2},$$

where I_{sc} is the short-circuit current at the excitation required at no load for voltage E and may be found from a short-circuit curve such as that in Fig. 211. I_{sc} for machines of modern design ranges from about 0.8 to 1.25 times normal full-load current.

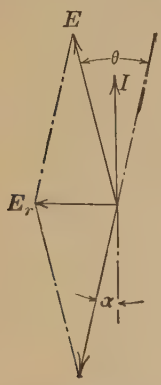

FIG. 209.—Vector diagram for two like machines in parallel.

The synchronizing power, or power transferred from one machine to the other, in watts

$= nEI \cos \frac{\theta}{2}$;

$= nE\left(I_{sc} \sin \frac{\theta}{2}\right) \cos \frac{\theta}{2}$;

$= nEI_{sc} \frac{\sin \theta}{2}$;

$= nEI_{sc} \frac{\theta}{2}$ for small oscillations, where θ is the angular displacement between the machines in electrical radians;

$= nEI_{sc}\alpha$ where α is the angular displacement of one machine from its mean position in electrical radians;

$= nEI_{sc}\, \alpha \frac{p}{2}$ where α is the same angular displacement in mechanical radians.

The torque corresponding to the above power transfer

$$= n\left(EI_{sc}\alpha\frac{p}{2}\right) \times \frac{33{,}000}{746 \times 2 \times \pi \times \text{r.p.m.}} \text{ lb. at 1 ft. radius,}$$

$$= nEI_{sc}\frac{p}{\text{r.p.m.}} \times 3.5\alpha,$$
$$= K\alpha;$$

that is to say, the torque is directly proportional to the displacement and therefore the equation for the small displacements is

$$K\alpha = \frac{Wr^2}{g}\frac{d^2\alpha}{dt^2},$$

from which the time of oscillation in seconds

$$= 2\pi\sqrt{\frac{Wr^2}{g \times K}},$$
$$= 2\pi\sqrt{\frac{Wr^2 \times \text{r.p.m.}}{g \times nEI_{sc} \times p \times 3.5}},$$
$$= \sqrt{\frac{Wr^2 \times \text{r.p.m.}}{\text{watts} \times k_1 \times p \times 2.9}}, \qquad (41)$$

where Wr^2 = the moment of inertia of one machine in pound-feet^2,

r.p.m. = the speed of the machine in revolutions per minute,

watts = the normal output of the machine at unity power factor,

k_1 = the ratio $\frac{\text{short-circuit current}}{\text{full-load current}}$ at the excitation corresponding to voltage E at no load,

p = the number of poles.

213. One Small Machine in Parallel with Several Large Units. In this case, if the small machine is driven by an engine, it will swing about its mean position but will not be able to make the large units with which it is in parallel swing in the opposite direction, so that if Fig. 210 shows the vector diagram of the two machines referred to the closed circuit then

α = the angle of displacement between the small machine and the others with which it is in parallel, and is also the angle of displacement of the small machine from its mean position,

$$E_r = 2E \sin\frac{\alpha}{2},$$

I, the circulating current $= \frac{E_r}{\overline{X}}$ where $\overline{X}$ is the synchronous reactance of the small machine; the reactance of all the other machines in parallel is very small compared with this value and may be neglected,

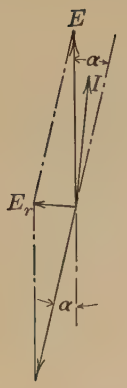

FIG. 210.—Vector diagram for a small machine in parallel with a large station.

$$I = \frac{2E \sin \frac{\alpha}{2}}{\bar{X}},$$

$$= 2I_{sc} \sin \frac{\alpha}{2}$$

the synchronizing power in watts,

$$= nEI \cos \frac{\alpha}{2},$$

$$= nE \times 2I_{sc} \sin \frac{\alpha}{2} \cos \frac{\alpha}{2},$$

$$= nEI_{sc} \times 2 \times \frac{\sin \alpha}{2},$$

$$= nEI_{sc}\alpha;$$

this is the same value as that obtained for two like machines so that the time of oscillation will be the same as for two like machines.

Example.[1]—Cross compound engines running at 83 r.p.m., with a flywheel effect of 8.5×10^6 lb.-ft.^{2}, driving three-phase alternators of 2100-k.v.a. output at 50 cycles, were found to hunt with the periodicity of the revolution. The short-circuit current of the machine for different excitations varied between 2.3 and 3.3. times full-load current.

In such a case there is an impulse impressed on the system every stroke or four impulses per revolution; if any one of these impulses differs in magnitude from the others, due to unequal steam distribution, there will also be a forced oscillation with the periodicity of the revolution.

For the machine in question the time of one cycle of natural

$$\text{frequency} = \sqrt{\frac{8.5 \times 10^6 \times 83}{2100 \times 1000 \times \left[\begin{matrix}2.3\\3.3\end{matrix}\right] \times 72 \text{ poles} \times 2.9}},$$

$$= 0.7 \text{ to } 0.84 \text{ sec.}$$

The number of forced oscillations per minute due to unequal steam distribution is 83, and the corresponding period of vibration is, therefore, $= {}^{60}\!/_{83} = 0.72$ sec., which corresponds very closely with that of the natural frequency. It was found possible to maintain parallel operation long enough to allow tests to be made by carefully equalizing the steam distribution so as to eliminate this low-frequency forced oscillation.

[1] Rosenberg, *Jour. of the Inst. of Elect. Eng.*, Vol. 42, p. 549.

It is advisable to design the flywheel so that the natural frequency of vibration of the machine is lower than that of the lowest forced oscillation; this will sometimes require the use of an enormous wheel; as, for example, in the case of alternators

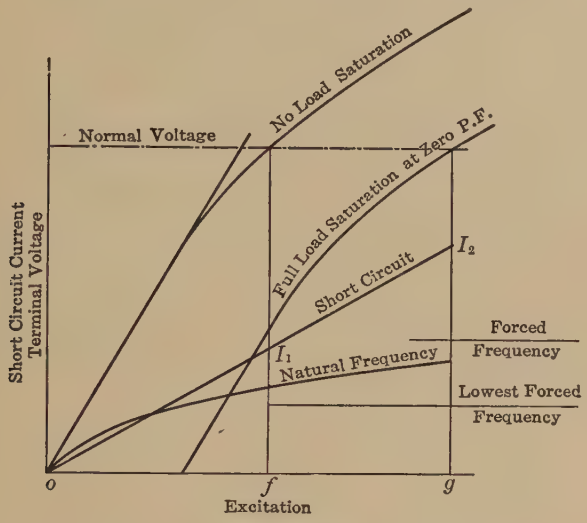

FIG. 211.—Variation of the natural frequency of oscillation with excitation.

operating in parallel and driven by large slow-speed gas engines. Gas engines are generally of the four-cycle type; that is, there is an explosion once in two revolutions. If the engine is of the four-cycle, double-acting, cross-tandem type there are four

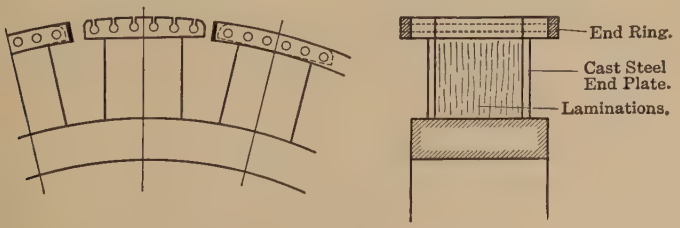

FIG. 212.—Alternator dampers.

explosions to the revolution and the forced frequencies in such a case are:

One impulse every two revolutions due to an unequal distribution of gas making one explosion always more powerful than the others; this is not a desirable condition of operation but one that must be provided for.

One impulse per revolution due to the want of perfect balance of the reciprocating parts.

One impulse per quarter revolution due to the four explosions in each revolution.

In order that the natural frequency of oscillation of the alternator be below the frequency of the lowest impulse, a very heavy and expensive flywheel is required, so that the wheel is often made with a moment of inertia of such a value that, over the whole range of operation, the natural frequency of the alternator is more than 20 per cent higher than that of the lowest impulse and more than 20 per cent lower than that of the impulse of next higher frequency. For example, in Fig. 211 the excitation during operation may vary from *of* to *og* and the value of the short-circuit current from I_1 to I_2. The natural frequency of oscillation is directly proportional to the square root of the short-circuit current, and for the value of W^2r chosen is not within 20 per cent of the frequency of either of the two lowest impulses for any excitation between *of* and *og*.

214. Use of Dampers.—For gas-engine-driven alternators powerful dampers are supplied because the applied torque varies so much during each revolution. The type of damper

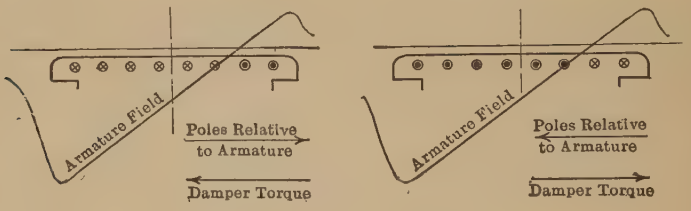

FIG. 213.—Operation of dampers.

shown in Fig. 212 is that generally used; it consists of a complete squirrel cage around the machine and acts as follows:

The damper rods are embedded in the pole face and so do not cut the main field; therefore any damping effect is due to cutting of the armature field. If the armature field revolves at synchronous speed with a uniform angular velocity, then, due to the impulses of the engine, the poles oscillate about the position of uniform angular velocity and cut this field. The curve in Fig. 213 shows the distribution of the armature field; the poles move relative to it in the direction of the arrow, and e.m.fs. are

induced in the rotor bars in the direction shown by the dots and crosses. The frequency of these e.m.fs. is that of the oscillation of the machine and is of the order of two cycles per second, so that the reactance of the damper bars can be neglected compared with their resistance if the slots in which they lie are open at the top as shown in Fig. 212. The currents in the bars are, therefore, in phase with the e.m.fs. and so are also represented by the same crosses and dots; it may be seen that the direction of these currents is such that the force exerted on them by the armature field tends to prevent the relative motion of the armature and the damper rods.

The e.m.f. in a damper rod at any instant $= B_{ga} \times L_c \times V_c \times 10^{-8}$ volts.

Where B_{ga} = the gap density at that part of the field which is being cut at the particular instant,

L_c = the frame length,

V_c = the velocity of the damper rod relative to the armature field in inches per second,

the average value of $V_c = \dfrac{\text{displacement from mean position}}{\text{time of } \frac{1}{4} \text{ cycle}}$,

$$= \frac{\beta \times \tau}{180} \times 4f_n,$$

where β = the maximum displacement of the poles, in electrical degrees, from the position of uniform angular velocity

and f_n = the frequency of oscillation;

therefore the effective voltage in a damper rod is approximately

$$= 1.1 \times B_{ga} \times L_c \times \frac{\beta \times \tau}{180} \times 4f_n \times 10^{-8} \text{ volts.}$$

The resistance of a damper rod of copper $= \dfrac{L_c}{M}$ ohms,

the effective current in a damper rod

$$= B_{ga} \times \frac{\beta \times \tau}{180} \times 4.4f_n \times M \times 10^{-8},$$

the current density in circular mils per ampere

$$= \frac{10^8 \times 180}{B_{ga} \times \beta \times \tau \times 4.4f_n}.$$

The damping effect depends on the value of the total damper current, which, for a given machine, depends on the number of damper rods and on their section. If the section of these rods be increased, they will carry a larger current and will have a greater damping effect; and the angle of swing will be

reduced so that the larger this section the lower the current density because of the reduction in the value of β.

It is of interest to know the order of magnitude of this current density; for example, assume that

B_{ga} = 25,000 lines per square inch,

$\beta = \pm 5$ electrical degrees which will give a circulating current of about 25 per cent of full-load current,

τ = 10 in., for which the peripheral velocity is 6000 ft. per minute at 60 cycles,

f_n = two cycles per second;

$$\text{then the current density} = \frac{10^8 \times 180}{25{,}000 \times 5 \times 10 \times 4.4 \times 2}$$

$$= 1640 \text{ cir. mils per ampere.}$$

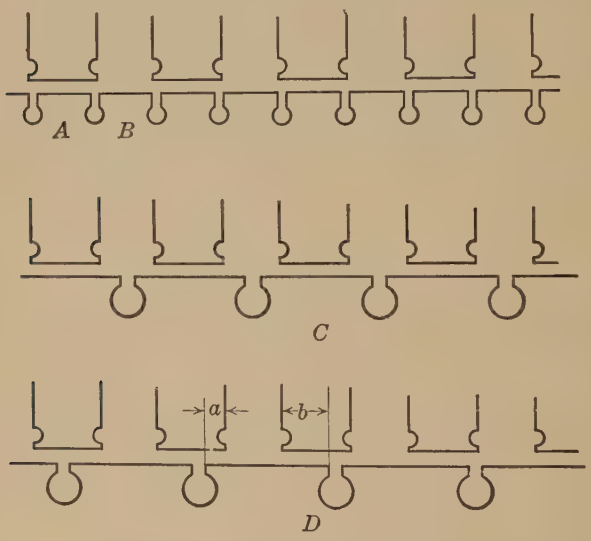

FIG. 214.—Spacing of dampers.

This value is pessimistic in that it neglects the resistance of the end connectors.

It was pointed out above that the damping effect depends on the total damper section. For gas-engine alternators it is usual to put into the dampers about 25 per cent of the section of copper that is put into the stator and then, if the damping is not sufficient, or if the dampers get too hot, to look for the cause of the trouble in the governor, flywheel or load on the system; a pulsating load is equivalent as far as hunting is concerned to a pulsating torque in the engine.

One cause of damper heating must be carefully guarded against. If the dampers are spaced as in Fig. 214, then, when in position A, the flux threading between two adjacent dampers is large, while in position B this flux is small, so that every time a stator tooth is passed, the flux threading between two damper rods goes through one cycle and the frequency of the current which the induced e.m.f. sends round the closed circuit = the number of stator slots × the revolutions per second. This current is not a damping current and is liable to cause excessive heating and, to prevent the flux pulsation which produces it, the distance between damper rods should be a multiple of the stator slot pitch, as shown at C.

215. Synchronous Motors for Power-factor Correction.—Consider a synchronous motor running with constant load and

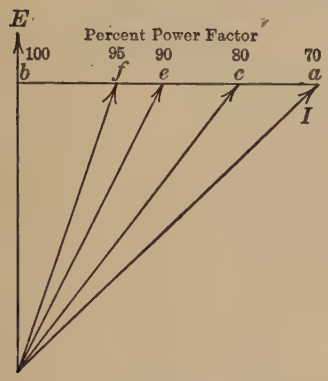

Fig. 215.—Size of motor for power-factor correction.

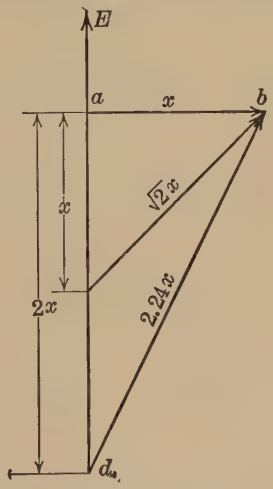

Fig. 216.—Size of motor for power-factor correction.

constant applied voltage. If the field excitation of the motor be increased, its back e.m.f. tends to increase, but this cannot increase much because the applied voltage is constant; so that a demagnetizing current must flow in the motor armature to counteract the effect of the increased field excitation; this current must be wattless because the load is constant and to be demagnetizing it must lag the back generated e.m.f. of the motor and, therefore, lead the applied e.m.f. of the generator.

If, on the other hand, the field excitation of the motor be decreased, its back e.m.f. tends to diminish and a wattless and

magnetizing current must flow in the motor armature; to be magnetizing this current must lead the back generated e.m.f. of the motor and, therefore, lag the applied e.m.f. of the generator.

The size of motor required for a given power-factor correction may be found from a diagram such as Fig. 215 where E is the voltage of the power station I, the total station current per phase, lags E by θ deg., and the power factor is 70 per cent.

To raise the power factor of this station to 100 per cent, the synchronous motor must draw a leading current = ab and the motor input must be $= \frac{n \times E \times ab}{1000}$ k.v.a., if the motor is running light and the efficiency is 100 per cent.

It may be seen from Fig. 215 that to raise the power factor of the system from

70 to 80 per cent requires a wattless current ac per phase,
70 to 90 per cent requires a wattless current ae per phase,
70 to 95 per cent requires a wattless current af per phase,
70 to 100 per cent requires a wattless current ab per phase.

The improvement in power factor from 95 to 100 per cent is, therefore, obtained at a considerable cost.

When synchronous motors are used for power-factor correction it is advisable to arrange that some of the load on the system is carried by these machines; for example, if ab, Fig. 216, is the wattless current per phase required for power-factor correction, then in order to carry a mechanical load of the same value in k.v.a. the rating of the motor would not be doubled but increased by only 41 per cent; or for the case shown by triangle abd, with an increase in current of 12 per cent over the value required for the mechanical load a power-factor correction effect of 50 per cent may be obtained.

216. Design of Synchronous Motors.—Diagram A, Fig. 217, shows some of the saturation curves of an alternator taken at constant current and varying power factor. If this machine were used as a synchronous motor then

for the maximum power-factor correction effect the power factor of the motor would be zero and the excitation = of;
for zero power-factor correction effect the power factor of the motor would be 100 per cent and the excitation = og;
for 80 per cent load and 60 per cent power-factor correction effect the excitation would be = oh.

Synchronous motors are generally high-speed machines and have, therefore, few poles, so that, as pointed out in Art. 189, page 259, they will be troubled with field heating if designed in the same way as synchronous generators, because for power-factor correction work they are operated with large excitation.

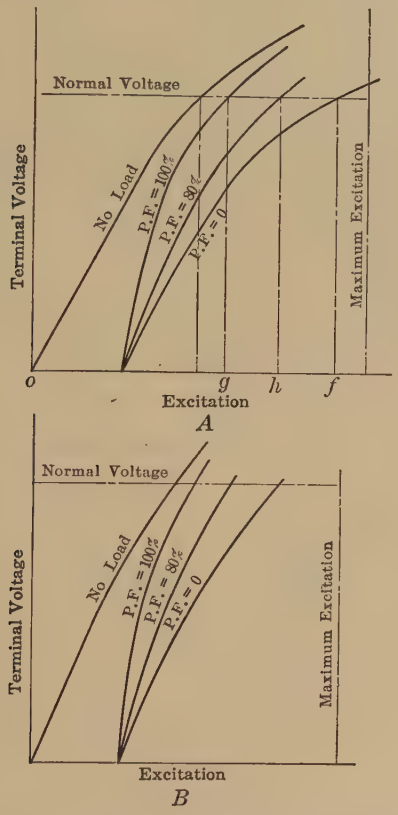

FIG. 217.—Saturation curves of an alternator.

Since the flywheel effect of a synchronous motor is generally small, no extra flywheel being supplied, its natural frequency of vibration will generally be comparatively high and the machine therefore liable to be set in violent oscillation by some of the forced frequencies on the system; for that reason synchronous motors are generally supplied with dampers.

217. Self-starting Synchronous Motors.—These are polyphase machines which are used for motor generator sets and for driving apparatus which requires a small starting torque, when a special

starting motor is not desired. They are built exactly like gas-engine alternators and consist of a standard synchronous motor supplied with a squirrel-cage winding on the poles. The method whereby this squirrel cage is calculated so as to meet the required starting conditions will be understood after a study of the induction motor; the following points of importance, however, must be noted here:

Polyphase currents in the armature winding produce a revolving field which tends to pull the squirrel cage round with it. In order that e.m.fs. may be induced in the squirrel cage by the revolving field the flux must enter the poles; therefore the poles should be laminated and, during the starting period, the field coils should be open-circuited.

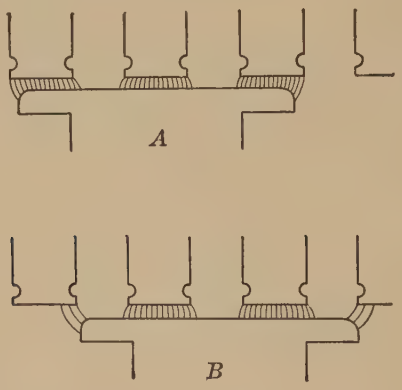

Fig. 218.—Effect of the pole arc on the air-gap reluctance.

The pole enclosure must be such that the air-gap under the pole has a constant reluctance for all positions of the pole relative to the armature. If the pole were made as shown in Fig. 218, then in position A the air-gap reluctance would be a minimum and in position B would be a maximum; in such a case the machine would lock in position A and would require a large force to move it out of this locking position.

In Art. 272 on the induction motor, it is shown that if the rotor slot pitch is a multiple of that of the stator, locking will take place due to the leakage fields, and that in order to prevent this locking, the rotor slot pitch must differ from that of the stator. It was pointed out in Art. 214 that to prevent useless circulating currents, the rotor slot pitch should be a multiple of that of the

stator, so that a compromise must be made and the rods spaced as shown in diagram *D*, Fig. 214, where t_r, the rotor tooth, is made equal to the stator slot pitch, for which value it will be found that the air-gap reluctance under a rotor tooth, which is proportional to $a + b$, is constant in all positions of the rotor.

Since the frequency of the flux which, due to the revolving field, passes through the poles, is very high at starting, being equal to the frequency of the applied e.m.f., there will be high voltages generated in the field coils because the number of turns per coil is large, so that for self-starting synchronous motors the excitation voltage should be as low as possible so as to keep down the number of turns per pole and the field coils must be better insulated than for ordinary synchronous machines; in the case of machines with a large total flux it is sometimes advisable to supply a break-up switch which will open up the field circuit in several places at starting so that the starting e.m.fs. in the different poles will not add up. When the motor is nearly up to speed, the field circuit is closed and a small excitation applied which tends to bring the motor into synchronism and insures that it comes into step with the proper polarity.

CHAPTER XXIV

A.-C. INDUCTION MOTORS

ELEMENTARY THEORY OF OPERATION

218. The Revolving Field.—*P*, Fig. 219, shows the essential parts of a two-pole, two-phase induction motor. The stator or stationary part carries two windings *M* and *N* spaced 90 electrical degrees apart. These windings are connected to a two-phase alternator and the currents which flow at any instant in the coils *M* and *N* are given by the curves in diagram *Q*; at instant *A*, for example, the current in phase 1 = $+I_m$ while that in phase 2 = zero.

The windings of each phase are marked *S* and *F* at the terminals and these letters stand for start and finish, respectively; a + current is one that goes in at *S*, and a − current one that goes in at *F*.

The resultant magnetic field produced by the windings *M* and *N* at instants *A*, *B*, *C* and *D* is shown in diagram *R* from which it may be seen that, although the windings are stationary, a revolving field is produced which is of constant strength and which moves through the distance of two pole pitches while the current in one phase passes through one cycle.

To reverse the direction of rotation of this field it is necessary to reverse the connections of one phase.

P, Fig. 220, shows the winding for a two-pole, three-phase motor; *M*, *N* and *Q*, the windings of the three phases, are spaced 120 electrical degrees apart. These windings are connected to a three-phase alternator and the currents which flow at any instant in the coils *M*, *N* and *Q* are given by the curves in diagram *R*.

The resultant magnetic field that is produced by the windings at instants *A*, *B*, *C* and *D* is shown in diagram *S* from which it may be seen that, just as in the case of the two-phase machine, a revolving field is produced which is of constant strength and which moves through the distance of two pole pitches while the current in one phase passes through one cycle.

To reverse the direction of rotation of this field it is necessary to interchange the connections of two of the phases; for example, to connect phase 2 of the motor to phase 3 of the alternator and phase 3 of the motor to phase 2 of the alternator.

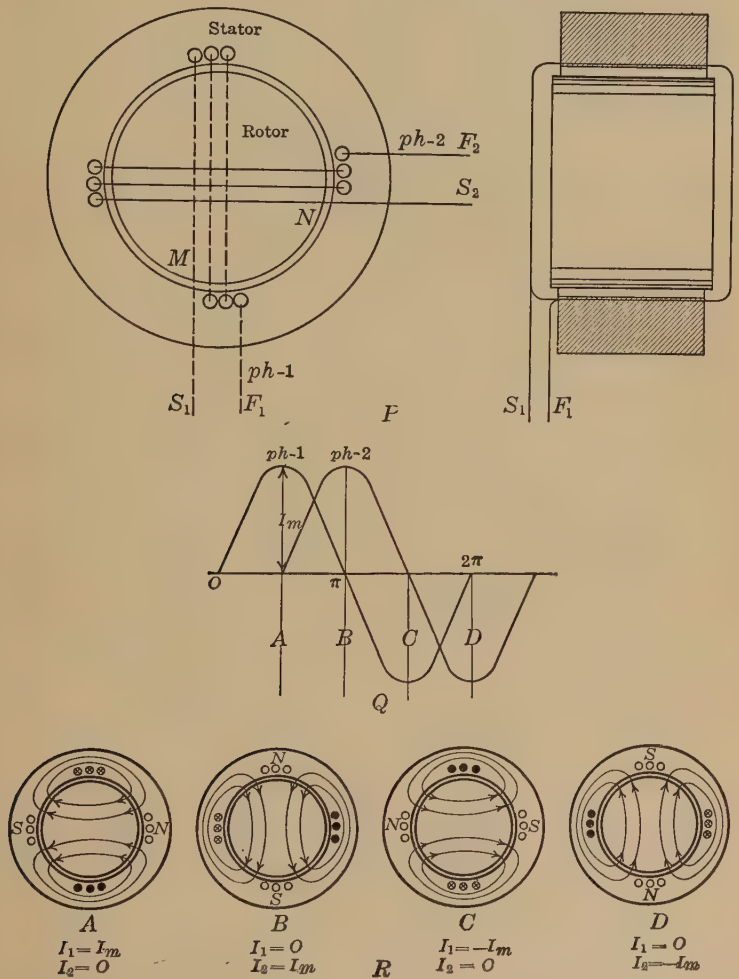

FIG. 219.—The revolving field of a two-pole, two-phase, induction motor.

219. Multipolar Motors.—Figure 221 shows the winding for a four-pole, two-phase motor and also the resultant magnetic field at the instants *A* and *B*, Fig. 219. The field moves through the

distance of ½ (pole pitch) while the current in one phase passes through ¼ (cycle).

Figure 221 shows the winding for a four-pole, three-phase motor and also the resultant magnetic field at the instants *A* and

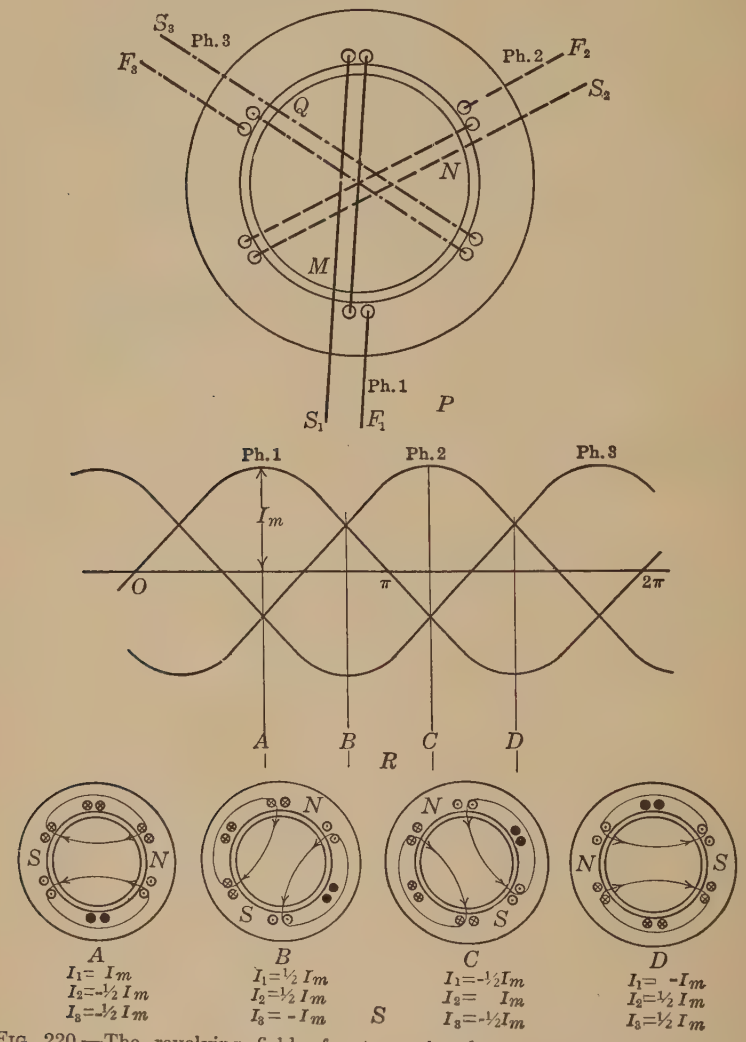

FIG. 220.—The revolving field of a two-pole, three-phase, induction motor.

B, Fig. 220. In this case the field moves through the distance of ⅓ (pole pitch) while the current in one phase passes through ⅙ (cycle).

In general the field moves through the distance of two pole pitches or through $\frac{2}{p}$ of a revolution while the current in one phase passes through one cycle; therefore, the speed of the revolving field $= \frac{2}{p} \times f$ revolutions per second,

$$= \frac{120 \times f}{p} \text{ revolutions per minute.} \qquad (42)$$

This is called the synchronous speed.

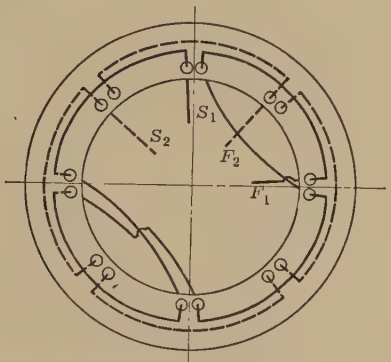

Diagrammatic Representation of a 4 Pole 2 Phase Induction Motor

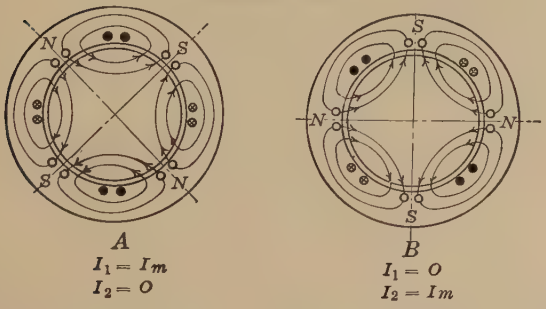

FIG. 221.—The revolving field of a four-pole, two-phase, induction motor.

220. Induction Motor Windings.—The conditions to be fulfilled by these windings are that the phases should be wound alike, should have the same number of turns, and should be spaced 90 electrical degrees apart in the case of a two-phase winding and 120 electrical degrees apart in the case of a three-phase winding.

The above are the conditions that have to be fulfilled by alternator windings so that the diagrams developed in Chap. XIV apply to induction motors as well as to alternators.

Figure 223 shows an actual stator with its windings arranged in phase belts. The ends of the coils are bent back so that the rotating part of the machine, called the rotor, can readily be put in position.

The type of rotor which is in most general use is shown in Fig. 224 and is called the squirrel-cage type. It consists of an iron core slotted to carry the rotor bars; these bars are jointed together at the ends so as to form a closed winding. Various

Diagrammatic Representation of a 4 Pole 3 Phase Induction Motor

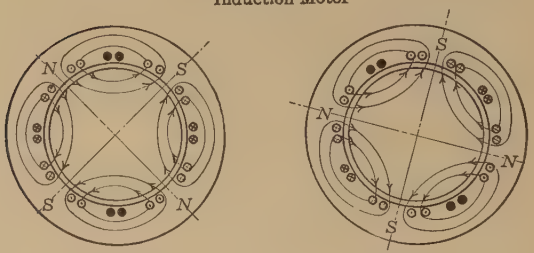

FIG. 222.—The revolving field of a four-pole, three-phase, induction motor.

methods are used to join the bars to the end rings; in some of the earlier designs a bolted connection was made between bar and ring using a spring washer to maintain a suitable pressure between bar and ring. In later designs these joints are usually welded; in some designs both end rings and rotor bars are made by using molten metal—either aluminum or copper—and casting it into the slots and forming the end rings with the same metal in the same operation.

It is customary, also, to vary the specific resistance of the material of the bars and end rings, using a material with low specific resistance, such as copper, where a high torque at standstill is not required, and a material with a relatively higher specific resistance, such as brass, when a high torque at standstill is required.

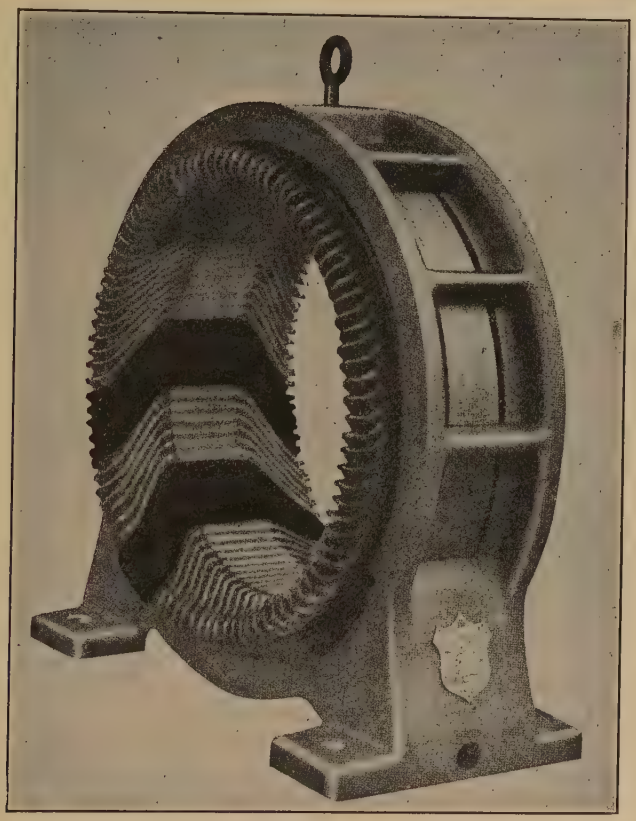

FIG. 223.—Stator of an induction motor.

221. Rotor Voltage and Current at Standstill.—The actions and reactions of the stator and rotor will be taken up later; it is necessary, however, to point out here that, since the applied voltage per phase is constant, the back voltage per phase must be approximately constant at all loads. This back voltage is produced by the revolving field; therefore, the actions and reac-

tions of the stator and rotor must be such as to keep the revolving field approximately constant at all loads.

Let the revolving field be represented by a revolving north and south pole as shown in diagram *A*, Fig. 225, and then for convenience let this figure be split at *xy* and opened out on to a plane; the result will be diagram *B*, of which a plan is shown in diagram *D*.

The distribution of flux on the rotor surface due to the revolving field is given by the curve in diagram *B* at a certain instant. The field is moving in the direction of the arrow; it therefore

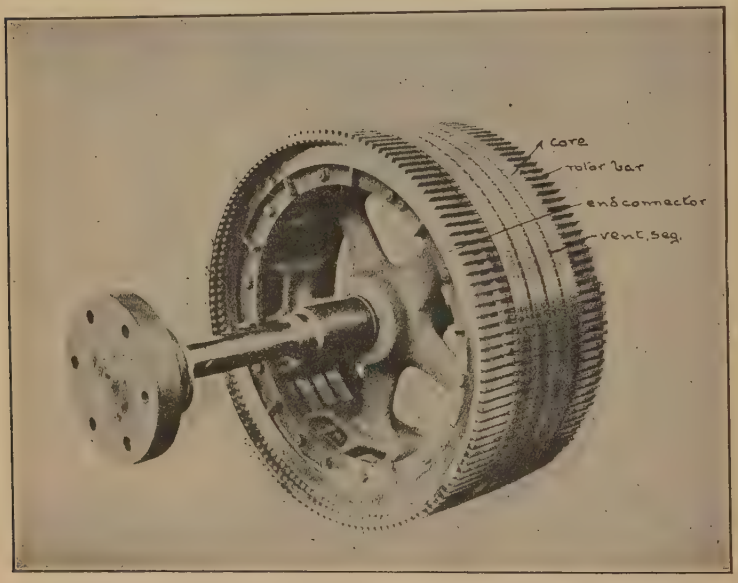

Fig. 224.—Squirrel-cage rotor.

cuts the rotor bars and generates in them, e.m.fs. which are shown in magnitude at the same instant in diagram *D*. Since the rotor circuit is closed, these e.m.fs. will cause currents to flow in the rotor bars.

The frequency of the e.m.fs. in the rotor bars at standstill $= \frac{p \times \text{syn. r.p.m.}}{120}$ cycles per second = the frequency of the stator applied e.m.f., so that the frequency of the rotor currents is high, and the reactance of the rotor, which is proportional to this frequency, is large compared with its resistance; the rotor

current therefore lags considerably behind the rotor voltage as shown by the curve in diagram *D* and also by crosses and dots in diagram *C*. The value of this curent at standstill

$$= \frac{\text{rotor voltage at standstill}}{\text{rotor impedance at standstill}},$$

and this is usually 5.5 about times the full-load rotor current.

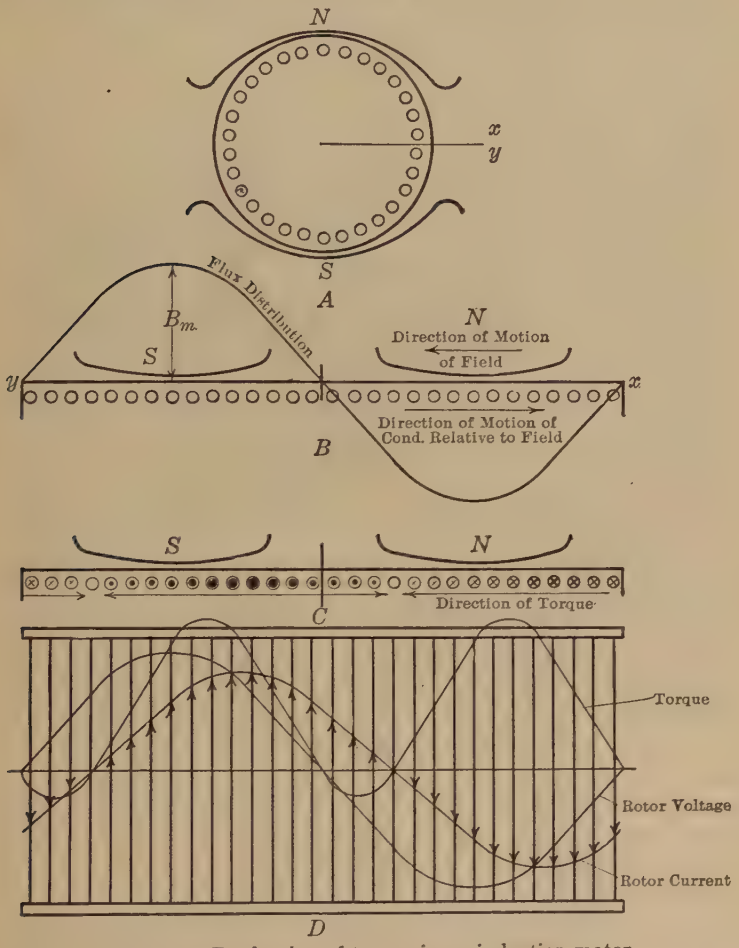

Fig. 225.—Production of torque in an induction motor.

222. Starting Torque.—As shown in diagrams *C* and *D* the rotor bars are carrying current and are in a magnetic field so that a force is exerted tending to move them; this force when multiplied by the radius of the rotor gives the torque. The relative torque

at different points on the rotor surface is given by the curve in diagram *D*, which is got by multiplying the value of flux density at different points on the rotor surface by the value of the current in the rotor bar at these points. It may be seen from this curve, and also from diagram *C*, that at some points on the rotor surface the torque is in one direction and at other points is in the opposite direction so that the resultant torque is quite small. As a rule the starting torque of a squirrel-cage motor is about 1.5 times full-load torque when the rotor current is about 5.5 times

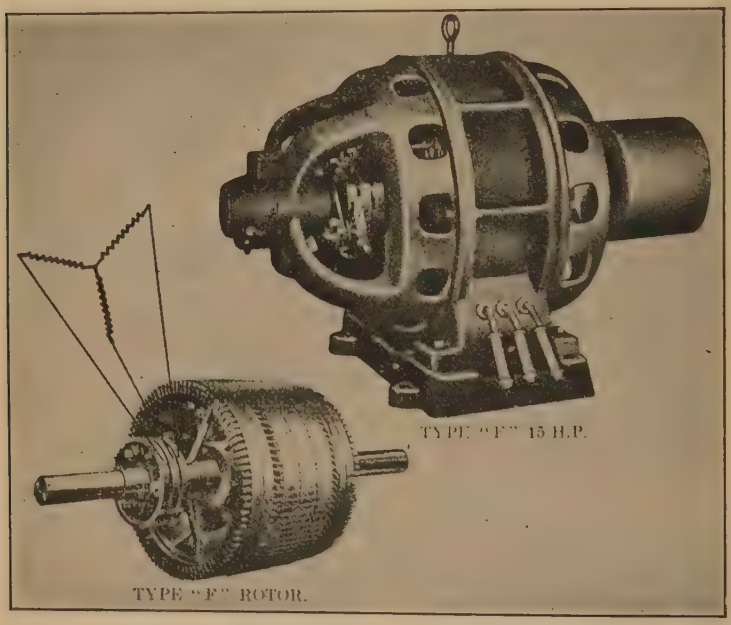

FIG. 226.—Wound rotor type of induction motor.

the full-load rotor current. Diagram *C* shows that the resultant torque is in such a direction as to tend to make the rotor follow up the revolving field.

The starting torque can be increased for a given current if that current be brought more in phase with the voltage; this can readily be seen from the curves in Fig. 225. The angle of lag of the rotor current can be decreased by increasing the rotor resistance, and sufficient resistance is generally put in the rotor circuit to bring the current down to its full-load value; the angle of lag is then so small that full-load torque is developed.

When a motor is running under load, a large rotor resistance is undesirable because it causes large loss, low efficiency and excessive heating. To get over this difficulty the wound rotor motor was developed. This type of motor has the same kind of a stator as that used for the squirrel-cage machine, but its rotor is as shown in Fig. 226; the rotor bars are connected together to form a winding, but this winding is not closed on itself as in the squirrel-cage machine; it is left open at three points which are connected to three slip rings, and the winding is closed outside of the machine through resistances which can be adjusted. The winding is finally short-circuited at the slip rings when the motor is up to speed. In this way it is possible

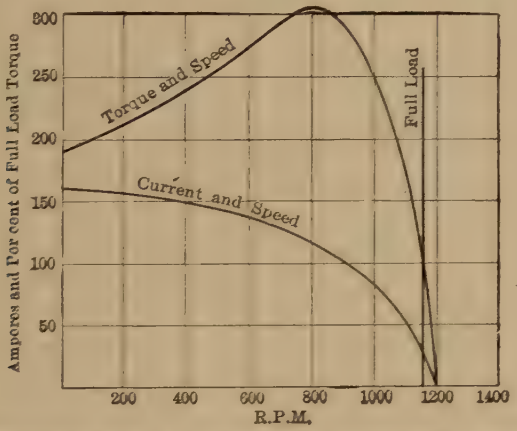

FIG. 227.—Characteristics of a 25-hp., 440-volt, three-phase, 60-cycle, 1200-syn. r.p.m. induction motor.

to have the advantage of high rotor resistance for starting and low rotor resistance when the motor is running at full speed.

223. Running Conditions.—It was pointed out in the last article that the resultant torque is in such a direction as to make the rotor follow up the revolving field. When the motor is not carrying any load, the rotor will revolve at practically synchronous speed, that is, at the speed of the revolving field. If the motor is then loaded, it will slow down and slip through the revolving field, the rotor bars will cut lines of force, the e.m.fs. generated in these bars will cause currents to flow in them and a torque will be produced. The rotor will slow up until the point is reached at which the torque developed by the rotor is equal to the torque exerted by the load.

The ratio $\frac{\text{syn. r.p.m.} - \text{r.p.m. of rotor}}{\text{syn. r.p.m.}}$ is called the per cent slip and is represented by the symbol s; its value at full load is generally about 4 per cent.

As the load is increased, the rotor drops in speed and the slip, rotor current, frequency and lag of rotor current all increase. The torque developed by the rotor tends to increase due to the increase in rotor current and to decrease due to the increase in current lag. Up to a certain point, called the break-down point or point of maximum torque, the effect of the current is greater than that of the current lag; beyond that point the effect of the current lag is the greater, so that after the break-down point is passed, the torque actually decreases even although the current is increasing.

The relation between speed, torque, and current is shown in Fig. 227 for a 25-hp., 440-volt, three-phase, 60-cycle, 1200-syn. r.p.m. induction motor.

224. Vector Diagram at No Load.—At no load a motor runs at almost synchronous speed so that the slip, rotor voltage and rotor current may be taken equal to zero for all practical purposes.

Consider the winding S_1F_1 of one phase of the stator as shown in Fig. 219 or 220. The voltage E_1 applied to this phase causes a current I_0, called the magnetizing current, to flow in the winding. This current, along with the magnetizing currents in the other phases, produces a revolving field ϕ_f of constant strength.

While the revolving field ϕ_f is of constant strength, the flux ϕ_g which threads the winding S_1F_1 is an alternating flux and is a maximum and $= \phi_f$ when the magnetizing current in the winding S_1F_1 is a maximum; this can be ascertained by examination of diagram R, Fig. 219, and of diagram S, Fig. 220, so that the flux which threads the winding S_1F_1 is in phase with the magnetizing current I_0 in that winding.

The alternating flux ϕ_g generates an alternating e.m.f. E_{1b} called the back e.m.f. in the winding S_1F_1, and this voltage lags the flux ϕ_g by 90 deg. To overcome this back e.m.f. the applied e.m.f. must have a component which is equal and opposite to E_{1b} at every instant; the other component of the applied e.m.f. must be large enough to send a current I_0 through the impedance of the winding.

In Fig. 228

I_0 is the magnetizing current in one phase,
ϕ_g is the flux per pole threading that phase,
E_{1b} is the back e.m.f. in that phase of the stator and lags ϕ_g which produces it by 90 deg.,
E_{11} is the component of the applied e.m.f. which is equal and opposite to E_{1b},
I_0Z_1 is the component of the applied e.m.f. which is required to send the current I_0 through the stator impedance Z_1,
E_1 is the applied voltage per phase and is the resultant of E_{11} and I_0Z_1.

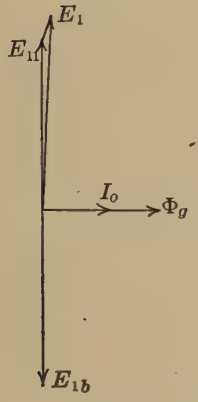

Fig. 228.—No-load vector diagram.

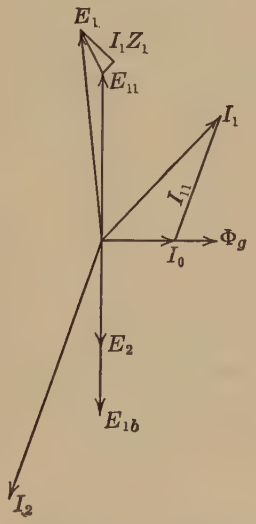

Fig. 229.—Vector diagram at full-load.

225. Vector Diagram at Full Load.—At full load the speed of the rotor = r.p.m.$_2$ = $(1 - s)$r.p.m.$_1$, and the speed of the revolving field relative to the rotor surface = s(r.p.m.$_1$), so that the frequency of the e.m.f. which is generated in the rotor winding by the revolving field = $\dfrac{s(\text{r.p.m.}_1) \times p}{120} = sf_1$.

The flux ϕ_g threads the rotor coils and generates in each phase of the rotor winding a voltage E_2 which lags ϕ_g by 90 deg. This voltage causes a current $I_2 = \dfrac{E_2}{Z_2}$ to flow in the closed rotor circuit; I_2 lags the voltage E_2 by an angle whose tangent = $\dfrac{sX_2}{R_2}$,

where Z_2 is the rotor impedance at full load,
X_2 is the rotor reactance per phase at standstill,
R_2 is the rotor resistance per phase,
s, the per cent slip, is approximately = 4 per cent.

With this value of s the angle of lag of the rotor current at full load seldom exceeds 20 deg.

In Fig. 229

I_0 is the magnetizing current, which has the same value as in Fig. 228,

ϕ_g is the flux per pole threading one phase of both rotor and stator windings,

E_{1b} is the back e.m.f. of the stator,

E_2 is the e.m.f. generated in one phase of the rotor by flux ϕ_g,

I_2 is the current in that phase,

E_{11} is the component of the applied e.m.f. which is equal and opposite to E_{1b}.

Now E_1, the applied voltage, is constant and is the resultant of E_{11} and I_1Z_1; this latter quantity is comparatively small even at full load, so that it may be assumed that E_{11} has the same value at full load as at no load and therefore E_{1b}, which is equal and opposite to E_{11} and ϕ_g which produces E_{1b}, are approximately constant at all loads, so that the resultant magnetizing effect of the stator and rotor currents must be equal to the magnetizing effect of the current I_o. The stator current may therefore be divided into two components, one of which I_{11} has a m.m.f. equal and opposite to that of the rotor current I_2; the other component of stator current must be I_o, because this is the necessary condition for a constant value of ϕ_g and of E_{1b}; therefore, in Fig. 229, I_{11} is a component of primary current whose m.m.f. is equal and opposite to that of I_2.

I_1 is the primary current and is the resultant of I_2 and I_{11}.

E_1 is the applied voltage and is the resultant of E_{11} and I_1Z_1.

CHAPTER XXV

GRAPHICAL TREATMENT OF THE INDUCTION MOTOR

226. Current Relations in Rotor and Stator.—It is shown in Art. 225 that the m.m.f. of the rotor opposes that of the stator, and that the resultant m.m.f., namely, that of the magnetizing current, is just sufficient to produce the constant revolving field ϕ_f.

Figure 230 shows the position of the windings of one phase of both rotor and stator, and also the direction of the currents in these windings, at the instant that the rotor and stator m.m.fs. are

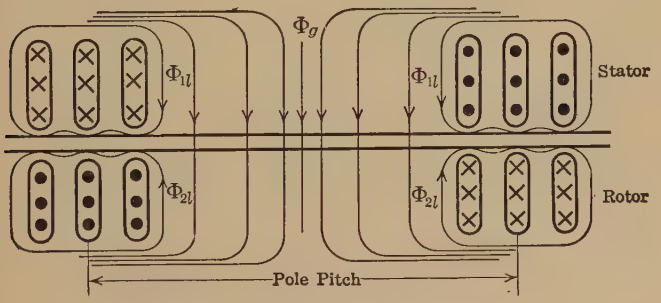

FIG. 230.—The magnetic fields in an induction motor.

directly opposing one another. As the rotor revolves relative to the stator there will be positions on either side of that shown in Fig. 230, in which the rotor and stator m.m.fs. do not quite oppose one another; two such positions are shown in Fig. 231; this overlapping of the phases is called the *belt effect* and is discussed more fully in Chap. XXIX.

Due to the revolving field ϕ_f an alternating flux ϕ_g threads one phase of both rotor and stator windings. It is shown in Fig. 230 that, in addition to the flux ϕ_g which crosses the air-gap, there is a leakage flux ϕ_{1l} which links the stator coils but does not cross the air-gap; ϕ_{1l} is proportional to the current I_1 which produces it. There is also a leakage flux ϕ_{2l} which links the rotor

coils but does not cross the air-gap; ϕ_{2l} is proportional to the current I_2 which produces it.

227. The Stator and Rotor Revolving Fields.

If f_1 = the frequency of the stator current,

s = the per cent slip,

r.p.m.$_1$ = the synchronous speed,

then f_2, the frequency of the rotor current = sf_1 (see Art. 225) and $(1 - s)$r.p.m.$_1$ = the rotor speed.

The stator current acting alone produces a field which revolves at synchronous speed, namely r.p.m.$_1$; the rotor current acting

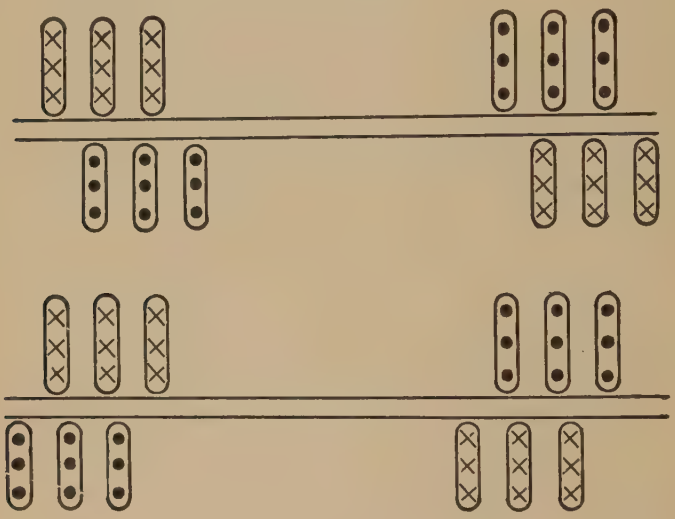

FIG. 231.—Overlapping of the phases.

alone produces a field which revolves at a speed of s(r.p.m.$_1$) relative to the rotor surface, or at s(r.p.m.$_1$) + $(1 - s)$r.p.m.$_1$ = r.p.m.$_1$ relative to the stator surface; that is, the two fields revolve at the same speed in space and so can be represented on the same diagram.

228. The Voltage and Current Diagram.—Figure 234 shows the voltage and current relations in an induction motor.

E_1 = the voltage per phase applied to the stator windings,

I_1 = the stator current per phase, and lags E_1 by θ deg.; the locus of I_1 is a circle.

229. The Flux Diagram.—Consider the stator current acting alone; then in Fig. 232:

ϕ_1 = the flux per pole threading one phase of the stator and, as pointed out in Art. 224, page 326, is in phase with I_1,

ϕ_{1l} = the stator leakage flux per phase per pole (see Fig. 230),

ϕ_{1g} = that part of ϕ_1 which crosses the gap and threads one phase of the rotor = $v_1\phi_1$.

Consider the rotor current I_2 acting alone; then

ϕ_2 = the flux per pole threading one phase of the rotor,

ϕ_{2l} = the rotor leakage flux per phase per pole,

ϕ_{2g} = that part of ϕ_2 which crosses the gap and threads one phase of the stator = $v_2\phi_2$.

Under load conditions, when both I_1 and I_2 are acting,

ϕ_{1s} = the actual flux per pole threading one phase of the stator,

ϕ_{2r} = the actual flux per pole threading one phase of the rotor,

ϕ_g = the actual flux per pole in the gap between rotor and stator,

E_{1b} = the stator e.m.f. per phase generated by ϕ_{1s} and consists of two components:

E_{1g} generated by the flux ϕ_g,

$E_{1l} = I_1X_1$, generated by the flux ϕ_{1l};

E_{2g} = the rotor e.m.f. per phase generated by ϕ_g. This e.m.f. sends a current I_2 through the rotor winding which produces the leakage flux ϕ_{2l} and generates the e.m.f. $E_{2l} = I_2X_2$ in that winding.

E_{2g}, therefore, consists of two components, namely, E_{2r} to overcome the resistance per phase, and a voltage equal and opposite to E_{2l} to overcome the reactance per phase.

Since E_{2r} is in phase with I_2 and therefore with ϕ_2, the angle aoh = angle oab = 90 deg.

The applied voltage must be equal and opposite to E_{1b} if the stator resistance per phase and therefore the voltage I_1R_1 is sufficiently small to be neglected. Since E_1 is constant, therefore E_{1b}, and the flux ϕ_{1s} which produces E_{1b}, must be constant in magnitude.

230. Geometrical Proof of the Circle Law.—In Fig. 232 draw dk perpendicular to fd so as to cut the line of produced at k.

In triangles aob and fdk,

$$\text{angle } oab = \text{angle } fdk = 90 \text{ deg.}$$
$$\text{angle } oba = \text{angle } dfk;$$

therefore,

$$\frac{fk}{ob} = \frac{fd}{ab} = \frac{fd}{ac-cb} = \frac{fd}{oh-cb}$$

and

$$fk = \frac{ob \times fd}{oh - cb},$$

$$= \frac{(v_1 \times of)(v_2 \times oh)}{oh(1 - v_1 v_2)},$$

$$= \frac{of(v_1 v_2)}{1 - v_1 v_2},$$

= a constant, since v_1, v_2 and of are all constant.

Since fk is constant and angle fdk is an angle of 90 deg., the locus of d, or of ϕ_1, is a circle whose center is on the line ok and whose diameter $= fk$.

If the magnetic circuit be not saturated, and this is the case at the actual flux densities due to ϕ_{1s} and ϕ_{2r}, the actual fluxes

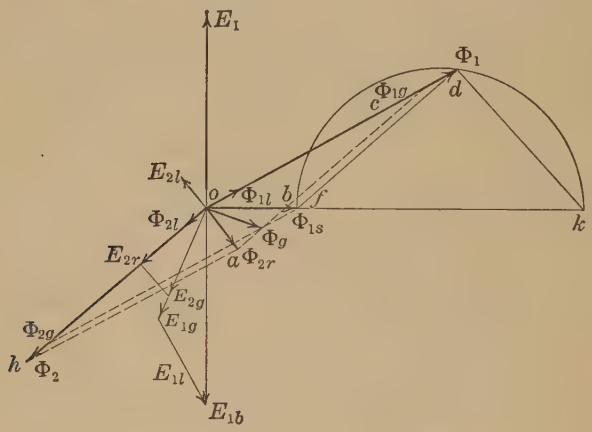

FIG. 232.—Voltage and flux diagram.

in the machine, then Fig. 232 may be transformed into Fig. 233, which is a m.m.f. and voltage diagram, by making $n_1 b_1 c_1 I_1$ proportional to ϕ_1 and $n_2 b_2 c_2 I_2$ proportional to ϕ_2.

Figure 233 may be transformed into a voltage and current diagram as shown in Fig. 234, and in this form, with a slight modification, it is generally used.

231. Special Cases.—1. The motor is running without load and, therefore, at synchronous speed, so that the rotor e.m.f. and the rotor current are zero. Under these conditions Fig. 234 becomes Fig. 235.

2. The motor is at standstill and the rotor resistance is assumed to be zero. Under these conditions Figs. 232 and 234 give Fig.

237. Since R_2 is zero, therefore E_{2r} and ϕ_{2r} are both zero, and E_{2g} must be equal and opposite to E_{2l} and therefore equal to I_2X_2.

Now $E_{1b} = E_{1g} + E_{1l}$,

$= E_{1g} + I_1X_1$,

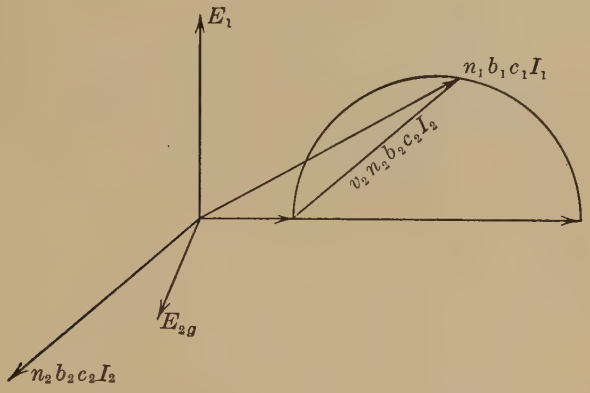

FIG. 233.—Voltage and m.m.f. diagram.

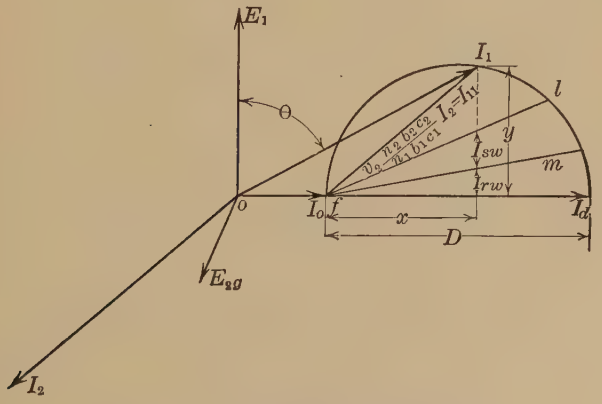

FIG. 234.—Voltage and current diagram.

and $\dfrac{E_{1g}}{E_{2g}} = \dfrac{b_1c_1}{b_2c_2}$ since they are produced by the same flux ϕ_g;

therefore $E_1 = E_{2g}\left(\dfrac{b_1c_1}{b_2c_2}\right) + I_1X_1$,

$= I_2X_2 \times \left(\dfrac{b_1c_1}{b_2c_2}\right) + I_1X_1$,

$$= I_1 X_2 \times \frac{n_1}{n_2}\left(\frac{b_1 c_1}{b_2 c_2}\right)^2 + I_1 X_1,$$

$$= I_1\left[X_1 + \frac{n_1}{n_2}\left(\frac{b_1 c_1}{b_2 c_2}\right)^2 X_2\right]. \qquad (43)$$

The value of I_1 in this case is I_d, the maximum current, Fig. 234.

232. Representation of the Losses on the Circle Diagram.—The losses in an induction motor are:

Constant losses { Mechanical losses—windage and friction loss. / Iron or core loss—hysteresis and eddy-current loss.

Variable losses { Stator copper loss. / Rotor copper loss. / Load losses.

FIG. 235.

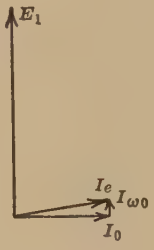

FIG. 236.

No-load conditions.

Constant Losses.—As a motor is loaded, the rotor drops in speed, and the slip and therefore the frequency of the flux in the rotor core increase. Due to the drop in speed, the windage and friction loss decrease, and due to the increase in frequency of the rotor flux, the iron loss in the rotor core increases, so that it is reasonable to assume that the sum of these two losses is constant at all speeds.

To overcome the constant loss, a stator current I_{wo} is required, in phase with the applied voltage and of such a value that $n_1 E_1 I_{wo}$ = the constant loss in watts. To take account of this in the circle diagram the no-load conditions have to be changed from those of Fig. 235 to those of Fig. 236.

Variable Losses.—These are $n_1 I^2{}_1 R_1$ and $n_2 I^2{}_2 R_2$.

In Fig. 234 the stator current $= I_1$ and the corresponding rotor current $= I_2 = I_{11} \times \frac{1}{v_2} \times \frac{n_1 b_1 c_1}{n_2 b_2 c_2}$.

The Rotor Copper Loss.—This loss $= n_2 I^2_2 R_2$ watts,

$$= n_2 I^2_{11} \left(\frac{1}{v_2} \times \frac{n_1 b_1 c_1}{n_2 b_2 c_2}\right)^2 R_2,$$

$$= I^2_{11} \times \text{a constant.}$$

Now $I^2_{11} = x^2 + y^2$ (Fig. 234),

$= x^2 + x(D - x)$,

$= xD$; where D is a constant.

Therefore the rotor loss $= x$(a constant).

To allow for the rotor loss on the circle diagram take any stator current I_1, find the corresponding rotor current I_2 and the rotor copper loss $n_2 I^2_2 R_2$ in watts; set up from the base line oI_d a current I_{rw} as shown in Fig. 234, in phase with E_1, such

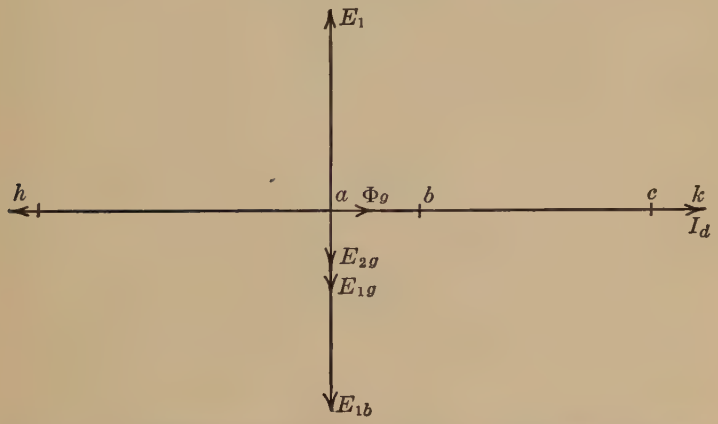

Fig. 237.—Conditions at standstill with zero rotor and stator resistance.

that $n_1 E_1 I_{rw}$ = the rotor copper loss in watts. Draw a straight line through I_o and I_{rw}. The vertical distance from the base to this line is proportional to x and is a measure of the rotor loss.

The Stator Copper Loss.—This loss $= n_1 I^2_1 R_1$ watts. I^2_1 is assumed to be $= I^2_o + I^2_{11}$; the error due to this assumption is comparatively small. The part of the copper loss $n_1 I^2_o R_1$ is added to the constant losses; the other part $n_1 I^2_{11} R_1$ is proportional to x just as in the case of the rotor loss.

To allow for the stator loss on the circle diagram take any stator current I_1; find the corresponding stator copper loss $n_1 I^2_1 R_1$ in watts; set up from the line fm, Fig. 234, a current I_{sw} in phase with E_1, such that $n_1 E_1 I_{sw}$ = the stator copper loss in watts. Draw a straight line through I_o and I_{sw}.

Load Losses.—These consist of various eddy-current losses which cannot be accurately predetermined and which are made as small as possible by careful design; they are usually allowed for by increasing the variable losses by a certain percentage found from tests on similar machines.

233. Relation between Rotor Loss and Slip.—Let the curve in Fig. 238 represent the distribution of the actual rotor revolving field ϕ_r corresponding to the alternating flux ϕ_{2r}, Fig. 232.

The e.m.f. generated in a rotor conductor by this flux

$$= 2.22\ \phi_r f_2\ 10^{-8} \text{ volts},$$

$$= 2.22 \left(B_{rm} \frac{2}{\pi} \tau L_c\right) (sf_1) 10^{-8} \text{ volts},$$

and is in phase with the flux density.

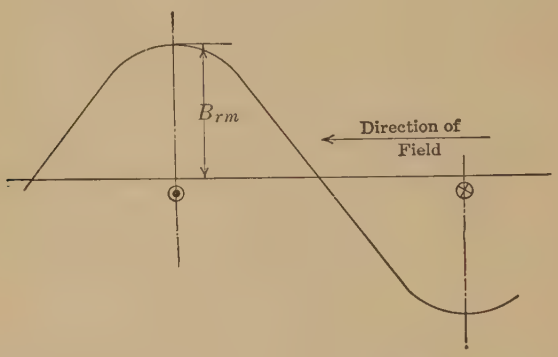

Fig. 238.—Torque on a rotor conductor.

It is shown in Fig. 232 that I_2 is in phase with the voltage E_{2r} so that the loss per conductor

$$= E_{2r} \times I_2 \text{ watts},$$

$$= 2.22\ B_{rm} \frac{2}{\pi} \tau L_c s f_1 I_2 10^{-8} \text{ watts}.$$

Since I_2 is in phase with E_{2r}, it is also in phase with the flux density so that the average force on a rotor conductor

$$= B_{reff} \frac{I_2}{10} \times L_c \text{ dynes, where } B_r \text{ and } L_c \text{ are in centimeter units,}$$

and the work done by this conductor in ergs is therefore

$$= B_{reff} \times \frac{I_2}{10} \times L_c \times \text{conductor velocity in centimeters per second,}$$

$$= \frac{B_{rm}}{\sqrt{2}} \frac{I_2}{10} \times L_c \times \pi \text{ (rotor diameter} \times \text{revolutions per second)},$$

$$= \frac{B_{rm}}{\sqrt{2}} \frac{I_2}{10} \times L_c \times p\tau \times \frac{2(1 - s)f_1}{p},$$

or in watts

$$= \frac{B_{rm}}{\sqrt{2}} \frac{I_2}{10} \times L_c \times \tau \times (1 - s)f_1 \times 2 \times 10^{-7}.$$

Therefore, $\frac{\text{rotor loss}}{\text{rotor output}} = \frac{s}{1 - s}$

and $\frac{\text{rotor input}}{\text{rotor output}} = \frac{1}{1 - s}$,

$$= \frac{\text{synchronous speed}}{\text{actual speed}}.$$

234. The Final Form of the Circle Diagram.—Figure 239 shows the form in which the circle diagram is generally used.

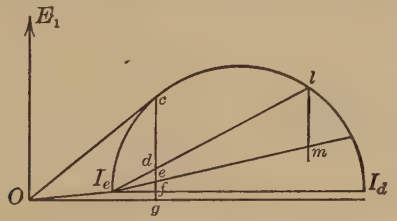

FIG. 239.—The circle diagram.

For a stator current $I_1 = oc$ = full-load current,
gc = the power component of the primary current,
fg = that part of gc required to overcome the constant losses,
ef = that part of gc required to overcome the stator copper loss,
de = that part of gc required to overcome the rotor copper loss,
cd = that part of gc required to overcome the mechanical load,

$\frac{cg}{oc}$ = the power factor,

$\frac{cd}{cg}$ = the efficiency,

$\frac{dc}{ce} = \frac{\text{rotor output}}{\text{rotor input}} = \frac{\text{actual speed}}{\text{synchronous speed}}$,

$\frac{de}{ce} = \frac{\text{rotor loss}}{\text{rotor input}} = s$ = per cent slip,

the horsepower output $= \frac{n_1 E_1 (dc)}{746}$,

the corresponding torque, $T = \frac{n_1 E_1(dc)}{746} \times \frac{33{,}000}{2\pi \text{ r.p.m.}_2}$ lb. at 1 ft. radius.

At synchronous speed this same torque would produce

$$\frac{T \times 2\pi \text{ r.p.m.}_1}{33{,}000} \text{ hp.}$$

$$= \frac{n_1 E_1(ce)}{746} \text{ hp.; this is called the}$$

Synchronous Horsepower due to full-load torque.

At standstill the synchronous horsepower due to the starting torque $= \frac{n_1 E_1(lm)}{746} = \frac{\text{the rotor copper loss in watts}}{746}$.

The maximum horsepower output of the motor

$$= \frac{n_1 E_1(\text{maximum value of } dc)}{746}.$$

The maximum torque is that which gives a synchronous horsepower $= \frac{n_1 E_1 \text{ (maximum value of } ce)}{746}$.

The use of this circle diagram is shown by an example which is worked out fully in the next chapter.

CHAPTER XXVI

CONSTRUCTION OF THE CIRCLE DIAGRAM FROM TESTS

The no-load saturation and the short-circuit tests are those that are usually made on an induction motor in order to determine its characteristics.

235. The No-load Saturation Curve.—The figures necessary for the construction of this curve are got by running the motor at normal frequency and without load. Starting at 50 per cent above normal voltage, the voltage is gradually reduced until the motor begins to drop in speed, and simultaneous readings are taken of voltage, current and total watts input.

The results of such a test on a 75-hp., 440-volt, three-phase, 60-cycle, eight-pole, Y-connected motor are given below.

No-load Saturation

E_t Terminal volts	I_l Line current	P Watts input
555	35	2940
520	31.4	2650
482	28.0	2350
435	24.5	2100
390	21.4	1860
347	18.4	1650
294	15.4	1450
254	13.5	1300
205	11.4	1150
162	9.6	1060
111	8.1	960

In Fig. 240:

The relation between E_t and I_l is shown in curve 1.

The relation between E_t and P is shown in curve 2.

The straight line, curve 3, shows the relation between E_t and that part of the exciting current which is required to send the

magnetic flux across the air-gap; this curve is calculated by the method explained in Chap. XXVIII.

At normal voltage the exciting current is 25 amperes; the magnetizing current required to send the magnetic flux across the air-gap is 22.5 amperes and the ratio $\frac{25}{22.5} = 1.11 = Ko$, which is called the iron factor, or saturation factor.

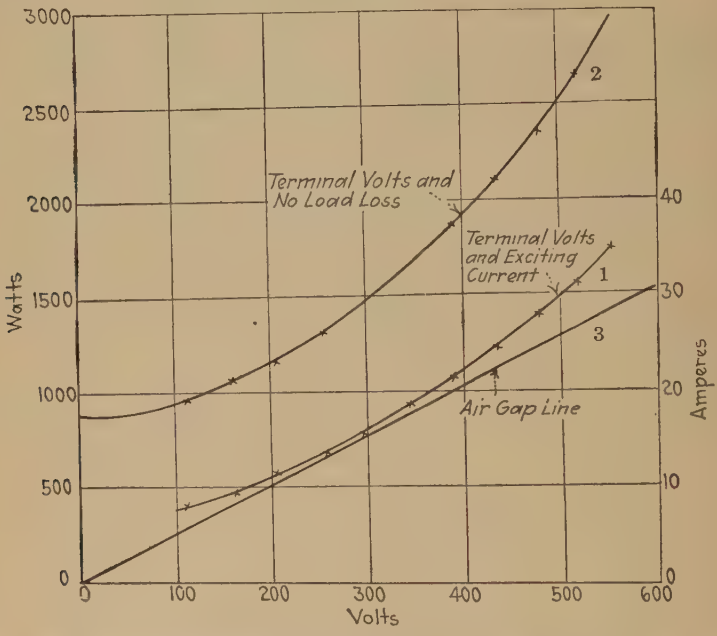

FIG. 240.—No load saturation on a 75-hp. 440-volt, three-phase, 60-cycle, 900-r.p.m. syn. speed, 8-pole induction motor.

Curve 1 is not tangent to curve 3 because, in addition to the true magnetizing current, the exciting current contains the power component I_{wo} which is required to overcome the losses P. I_{wo} is quite large at low voltages; for example, at 111 volts,

$I_e = 8.1$ amperes

$P = 960$ watts

$$I_{wo} = \frac{960}{1.73 \times 111} = 4.97 \text{ amperes}$$

$$I_o = \sqrt{8.1^2 - 4.97^2} = 6.43 \text{ amperes} = \text{the true magnetizing current.}$$

The difference between I_o and I_e is comparatively small at normal voltage; for example, at 440 volts,

I_e = 25.0 amperes

P = 2120 watts

$$I_{wo} = \frac{2120}{1.73 \times 440} = 2.78 \text{ amperes}$$

$$I_o = \sqrt{25^2 - 2.78^2} = 24.8 \text{ amperes.}$$

P contains the windage and friction loss, the core loss, and the small stator copper loss due to the current I_e. If curve 2 be produced so as to cut the axis as shown, then the watts loss at zero voltage = 800 watts must be the windage and friction loss, since the flux, and therefore the core loss, is zero and the stator copper loss can be neglected.

236. The Short-circuit Curve.—This curve shows the relation between stator voltage and current, the rotor being at standstill. The data necessary for its construction are obtained by blocking the rotor so that it cannot revolve, and applying voltage to the stator windings at normal frequency; the rotor is sometimes held by means of a prony brake so that readings of starting torque may also be taken. The applied voltage is gradually raised from zero to a value that will send about twice full-load current through the motor, and simultaneous readings are taken of voltage, current, total watts input and torque.

The results of such a test on a 75-hp. motor on which the foregoing saturation test was made are given below:

SHORT-CIRCUIT

E_t terminal volts	I_{sc} line current	P watts input	I_{wsc}	T torque in pounds at 1-ft. radius	$\frac{T}{E_t}$
205	200	3000	84	155	0.76
186	178	2400	74	122	0.66
164	155	1820	64	94	0.58
150	138	1420	55	71	0.48
127	118	990	44.5	51	0.40
111	95	680	36	35	0.31
93	78	440	27	23	0.25
74	63	270	21.6	14	0.20
53	45	140	15.0	7	0.13
35	29	60	9.7		

$$\text{On short-circuit } I_{sc} = \frac{E_t}{X_1 + X_2\left(\frac{b_1 c_1}{b_2 c_2}\right)^2 \frac{n_1}{n_2}}$$

(formula (43), page 334),

so that theoretically the relation between E_t and I_{sc} in the table on page 341 should be represented by a straight line. The actual

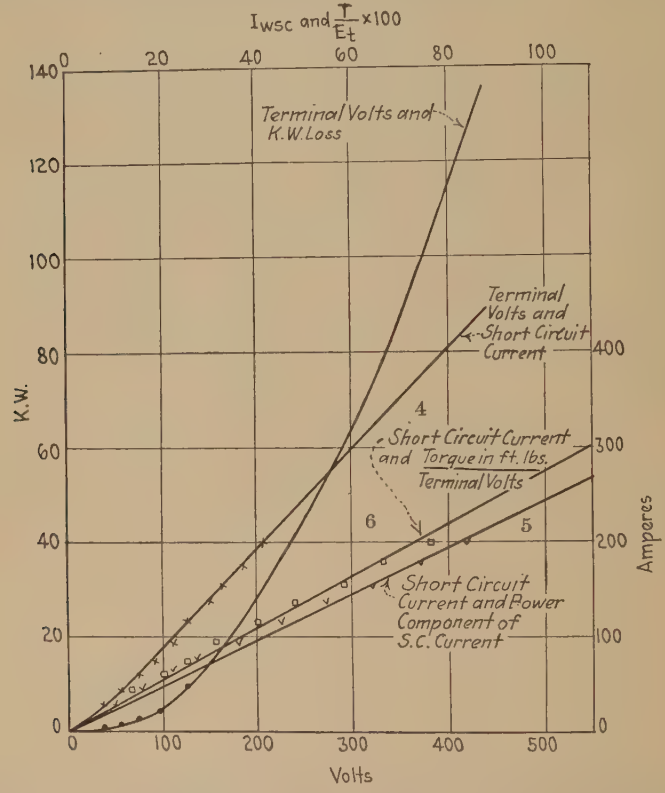

FIG. 241.—Locked saturation on a 75-hp., 440-volt, three-phase, 60-cycle, 900-r.p.m. syn. speed, 8-pole induction motor.

relation is shown in curve 4, Fig. 241; the curve gradually bends away from the straight line due to the gradual saturation of the iron part of the leakage path.

The watts input on short-circuit $= 1.73 E_t I_{wsc}$; it is also $= kI_{sc}^2$, because it is all expended in copper loss, and since E_t is proportional to I_{sc}, (see curve 4), therefore I_{wsc} also is proportional to I_{sc} and the relation is plotted, for the tests in the table on page 341, in curve 5.

In Art. 234, it was shown that the starting torque is proportional to $n_2 I^2_2 R_2$, the rotor copper loss, where I_2 is the rotor current on short-circuit, and since I_2 is proportional to I_{sc} which is proportional to E_t, therefore $\frac{\text{starting torque}}{E_t}$ is proportional to I_{sc} and the relation is plotted, for the tests in the table on page 341, in curve 6.

Curves 4, 5 and 6 are produced as shown, so that the probable values at normal voltage of I_{sc}, I_{wsc} and $\frac{\text{torque}}{\text{volts}}$ may be determined; at 440 volts $I_{sc} = 445$ amperes. $I_{wsc} = 180$ amperes.

$$\frac{\text{Torque in pound-feet}}{\text{Volts}} = 1.6.$$

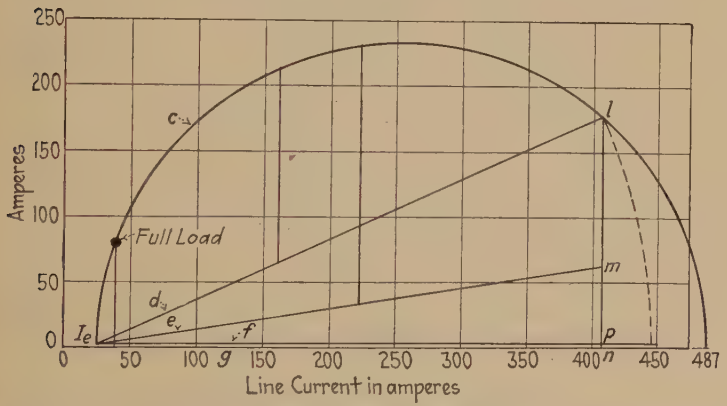

FIG. 242.—Circle diagram for a 75-hp. 440-volt, three-phase, 60-cycle, 900-r.p.m. syn. speed, 8-pole induction motor.

Torque in pounds at 1-ft. radius $= 1.6 \times 440 = 705.$

Torque in synchronous horsepower $=$

$$\frac{705 \times 2\pi \times 900}{33{,}000} = 120.$$

237. Construction of the Circle Diagram.—The results obtained from the curves in Figs. 240 and 241 are to be used in order to construct the circle diagram, Fig. 242, from which the characteristics of the motor will be determined.

1. Locate the short-circuit point. With o as center and radius $I_{sc} = 445$ amperes describe the arc of a circle; of the total current I_{sc} the power component $I_{wsc} = 180$ amperes. These two values of current give l, the short-circuit point.

2. Locate the no-load point. At 440 volts the exciting current

$= I_e = 25$ amperes and the value of P at the same voltage $=$ 2120 watts, so that the power component of the exciting current $= \dfrac{2120}{1.73 \times 440} = 2.78$ amperes. These two values of current give the point I_e, the no-load point.

3. Draw the circle. The circle must pass through the two points l and I_e and must have its center on the constant loss line.

4. Find the stator and rotor copper losses. Of the total copper loss represented by lp, the part mp represents the stator copper loss, and is determined as follows: The resistance of the stator winding from terminal to neutral, measured by direct current $=$ 0.080 ohm, so that the stator copper loss on short-circuit $=$ $445^2 \times 0.080 \times 3 = 47{,}000$ watts, and the corresponding power component of current $= \dfrac{47{,}000}{1.73 \times 440} = 73.3$ amperes $= mp$.

For any stator current oc
the constant loss $= pn \times 1.73 \times 440$ watts.
the stator copper loss $= fe \times 1.73 \times 440$ watts.
the rotor copper loss $= de \times 1.73 \times 440$ watts.
the mechanical output $= cd \times 1.73 \times 440$ watts.

These values are all to be measured from the point c on the circle, vertically to the straight lines d, e, f and g.

238. To Find the Characteristics at Full Load.—The full load $= 75$ hp. and the value of cd corresponding to this output $= \dfrac{75 \times 746}{1.73 \times 440} = 73.3$ amperes; the point c on the circle is then found to suit and the following values scaled off:

$ce = 77.5$ amperes,
$cg = 82.4$ amperes,
$oc = 91.0$ amperes,

from which the efficiency $= \dfrac{cd}{cg} = \dfrac{73.3}{82.4} = 89.0$ per cent,

the power factor $= \dfrac{cg}{oc} = \dfrac{82.4}{91} = 90.5$ per cent,

the slip $= \dfrac{de}{ce} = \dfrac{4.17}{77.5} = 5.37$ per cent.

The actual speed $=$ synchronous speed $-$ slip $= 900(1 - 0.0537) = 900 \times 0.9463 = 852$ r.p.m.

The maximum value of $cd = 149$ amperes so that the maximum horsepower $= \dfrac{149 \times 1.73 \times 440}{746} = 152.$

The maximum value of ce = 197 amperes so that the maximum torque in synchronous horsepower = $\frac{197 \times 1.73 \times 440}{746}$ = 202 = about 2.7 times full-load torque.

The value of ml = 116 amperes so that the starting torque in synchronous horsepower = $\frac{116 \times 1.73 \times 440}{746}$ = 119 or about 1.59 times full-load torque, which checks closely with the value found by brake readings.

In plotting test results it is advisable to plot line current and terminal volts rather than current per phase and voltage per phase, because then the diagram becomes independent of the connection, since three-phase power = 1.73 $E_l I_l$ for either Y- or Δ-connection, and two-phase power = $2E_l I_l$ for either star or ring connection.

CHAPTER XXVII

CONSTRUCTION OF INDUCTION MOTORS

239. Figure 243 shows the type of construction that is generally adopted for motors up to 200 hp. at 600 r.p.m. The particular machine shown is a squirrel-cage motor.

240. The Stator.—*B*, the stator core, is built up of laminations of sheet steel 0.014 in. thick which are separated from one

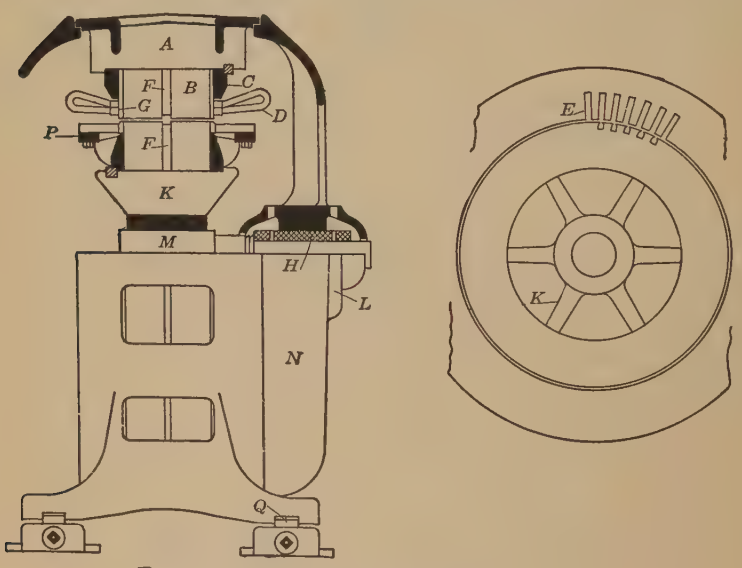

FIG. 243.—Small squirrel-cage induction motor.

another by layers of varnish and have slots *E* punched on their inner periphery to carry the stator coils *D*.

Two kinds of slot are in general use and both are shown in Fig. 244. The partially closed slot is used for all rotors and has the advantage that it causes only a small reduction in the air-gap area; the open slot is generally used for stators because the stator coils are subject to comparatively high voltages, and the open-slot construction allows the coils to be fully insulated

before they are put into the machine; it also allows the coils to be easily and quickly repaired in case of break-down.

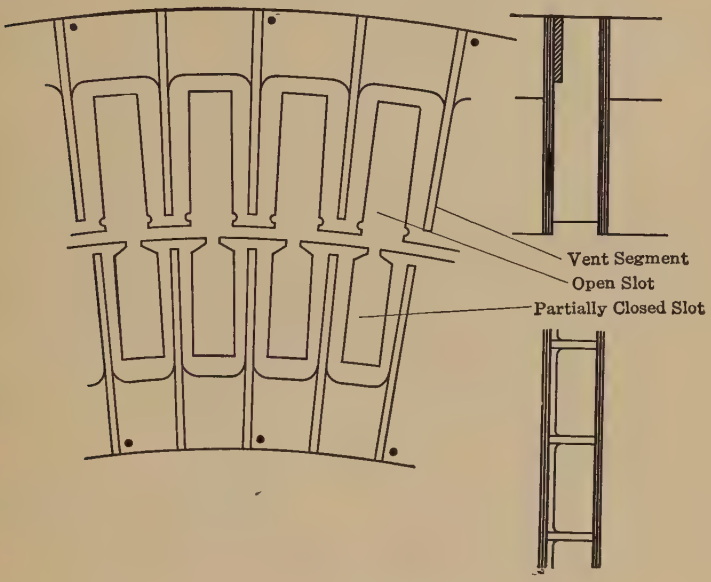

Fig. 244.—Slots and vent segments.

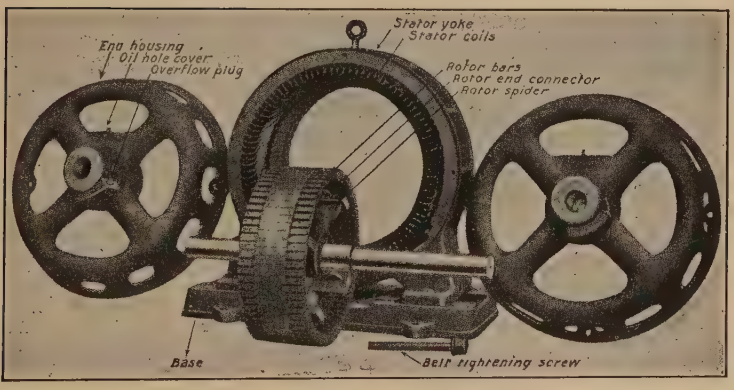

Fig. 245.—Parts of an Allis Chalmers Bullock squirrel-cage induction motor

The core is built up with ventilating segments spaced about 3 in. apart; one segment is shown at *F*, Fig. 243, and in greater detail in Fig. 244, and consists of a light brass casting which is riveted to the adjacent lamination of the core; the lamination

for this purpose is usually made of 0.025-in. steel. The laminations are clamped tightly between two cast-iron end heads C, and in order to prevent the core from spreading out on the inner periphery, tooth supports G, of strong brass, are often placed between the end heads and the core.

The stator yoke A carries the stator core and the bearing housings N. When the motor has to be mounted on a wall, or on a ceiling, the housings N must be rotated through 90 or 180 deg., respectively; this is necessary because ring oiling is always used for motor bearings, and the oil well L must always be below the shaft. The bearing housings help to stiffen the whole machine and allow the use of a fairly light yoke. The shape of the housings, as may be seen from Fig. 245, is such that it is a simple matter to close the openings between the arms with perforated sheet metal so as to form a *semi-enclosed motor*, or all the openings in the machine with sheet metal so as to form a *totally enclosed motor*.

241. The Rotor.—The rotor core also is built up of laminations of sheet steel, which are usually 0.025 in. thick; the use of such thick sheets is permissible because the frequency of the magnetic flux in the rotor is low and the rotor core loss is small.

The core with its vent ducts is clamped between two end heads and mounted on a spider K, Fig. 243. In the case of squirrel-cage rotors the depth of the rotor slot is usually so small that a tooth support is not required.

The rotor bars are carried in partially closed slots and are connected together at the ends by rings P called end connectors; these rings are usually supported on fan blades which are carried by the end heads.

The shaft M is extra stiff because the clearance between the stator and rotor is very small, and the bearings H are extra large so as to give a reasonably long life to the wearing surface.

The whole machine is carried on slide rails Q, which are rigidly fixed to the foundation, and by sliding the motor along the rails the belt may be tightened or slackened. Slide rails are not used for geared or direct connected motors.

242. Large Motors.—Figure 246 shows the type of construction for large motors. Pedestal bearings are used, so that the yoke has to be extra stiff in order to be self-supporting. The stator coils are tied to a wooden coil support ring R, which is carried by brackets attached to the end heads; coil supports

should be used even on small motors if the coils are flimsy and liable to move due to vibration.

Both squirrel-cage and wound-rotor constructions are shown in Fig. 246, and it may be seen that the same spider U can be used in either case; the two rotors differ in the number and size

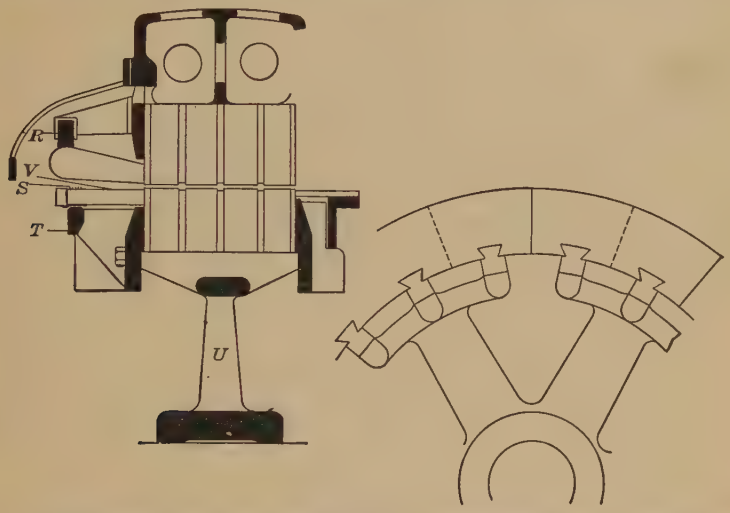

FIG. 246.—Large induction motor; both squirrel-cage and wound-rotor construction shown.

of slots and in the shape of the end head. S is a band of steel wire used to bind down the rotor coils of the wound-rotor machine on to the coil support T which is carried by the end heads; this coil support acts as a fan and helps to keep the machine cool. When the rotor diameter is greater than 30 in., the rotor core is generally built up of segments which are carried by dovetails on the rotor spider.

CHAPTER XXVIII

MAGNETIZING CURRENT AND NO-LOAD LOSSES

243. The E.M.F. Equation.—The revolving field generates e.m.fs. in the stator windings which are equal and opposite to those applied; therefore, as shown in Art. 140, page 185,

$$E = 2.22\, kZ\phi_a f 10^{-8} \cos\frac{\theta}{2} \text{ volts},$$

where E = the voltage per phase,
k = the distribution factor from the table on page 184,
Z = the conductors in series per phase,
ϕ_a = the flux per pole of the revolving field,
f = the frequency of the applied e.m.f.,
θ = chording of stator coils in electrical degrees,

so that, if the winding of an induction motor and also its operating voltage and frequency are known, the value of the revolving field can be found from the above equation.

244. The Magnetizing Current.—Diagram A, Fig. 247, shows an end view of part of the stator of a three-phase induction motor which has twelve slots per pole. The starts of the windings of the three phases are spaced 120 electrical degrees apart and are marked S_1, S_2 and S_3.

Diagram B shows the value of the current in each phase at any instant.

Diagram C shows the direction of the current in each conductor at the instant F and the corresponding distribution of m.m.f.

Diagram D shows the direction of the current in each conductor at the instant G and the corresponding distribution of m.m.f.

It will be seen that the revolving field is not quite constant in value but varies between the two limits shown in diagrams C and D. The average m.m.f., AT_{av}, is found as follows:

$$
\begin{aligned}
AT_{av} \times 12\lambda &= \text{area of curve in diagram } C \\
&= 4.0\ bI_m \times \lambda \\
&\quad 3.5\ bI_m \times 2\lambda \\
&\quad 3.0\ bI_m \times 2\lambda \\
&\quad 2.5\ bI_m \times 2\lambda \\
&\quad 2.0\ bI_m \times 2\lambda \\
&\quad 1.0\ bI_m \times 2\lambda \\
&\quad \overline{\qquad\qquad} \\
&\quad 28\ bI_m\lambda
\end{aligned}
$$

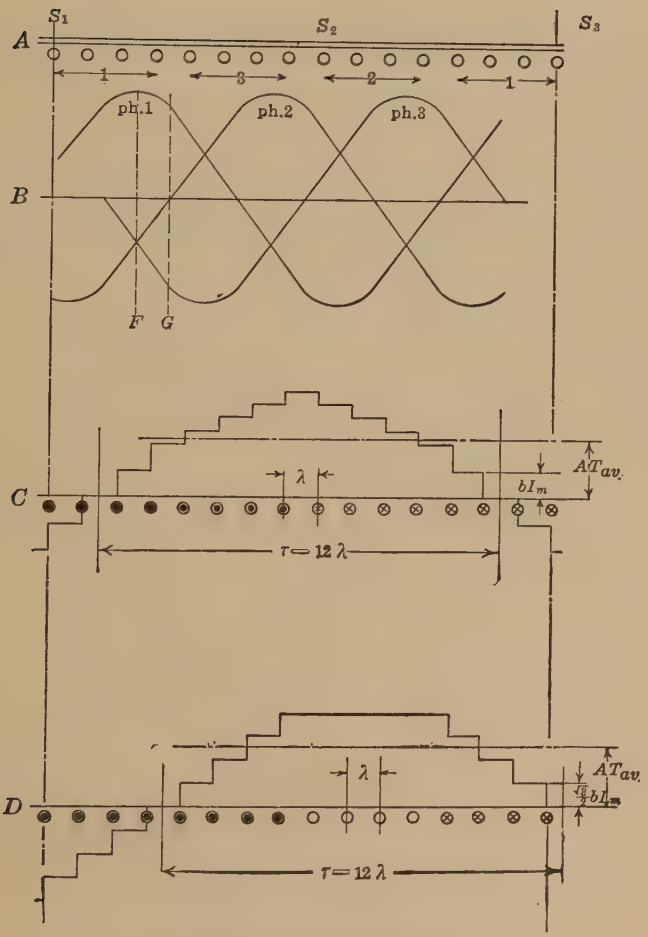

FIG. 247.—The revolving field.

Also $AT_{av} \times 12\lambda$ = area of curve in diagram D

$$= 4.0 \times 0.866\, bI_m \times 5\lambda$$
$$3.0 \times 0.866\, bI_m \times 2\lambda$$
$$2.0 \times 0.866\, bI_m \times 2\lambda$$
$$1.0 \times 0.866\, bI_m \times 2\lambda$$

$$27.7\, bI_m\lambda$$

Therefore, taking the mean of these two values,

$$AT_{av} \times 12\lambda = 27.85\, bI_m\lambda$$

and $$AT_{av} = 2.32\, bI_m,$$

$$= 2.32 \times \left(\frac{\text{slots per pole}}{12}\right) \times b \times \sqrt{2}I_c$$

since there are 12 slots per pole,

$$= 0.273 \left(\text{conductors per pole} \times \cos\frac{\theta}{2}\right)I_c.$$

The value of AT_{av} can be found in a similar way for any number of slots per pole and for both two- and three-phase windings and varies slightly from the above figure for different cases, but in general the value of AT_{av} used for all polyphase windings $= 0.273 \left(\text{conductors per pole} \times \cos\frac{\theta}{2}\right)I_c$.

The relation between the flux per pole and the magnetizing current per phase is found from the formula

$$\phi_a = 3.2\frac{AT_{av}}{\delta}\frac{\tau L_g}{C},$$

$$= 0.87 \left(\text{conductors per pole} \times \cos\frac{\theta}{2}\right)I_c \frac{\tau L_g}{\delta C},$$

$$\text{or } I_o = \frac{1}{0.87\left(\text{conductors per pole} \times \cos\frac{\theta}{2}\right)} \times \frac{\phi_a}{\tau L_g} \times \delta C, \quad (44)$$

where I_o = the magnetizing current per phase (effective value),

ϕ_a = the flux per pole of the revolving field,

τ = the pole pitch in inches,

L_g = the axial length of air-gap in inches and is used instead of L_c because, on account of the small air-gap, there is little fringing into the vent ducts,

δ = the air-gap clearance in inches

C = the Carter coefficient (see Fig. 45, p. 47),

θ = chording in electrical degrees.

To allow for the m.m.f. required to send the flux through the iron part of the magnetic circuit, the value of current found from

the last formula has to be multiplied by a factor which is found from the results of similar machines that have already been tested; where no such information is available the factor is taken as 1.15.

245. No-load Losses.—These losses are similar to and are figured out in the same way as the no-load losses in a D.-C. machine.

$$\textbf{Bearing Friction Loss} = 0.81dl\left(\frac{V_b}{100}\right)^{3/2} \text{ watts,}$$

where d = the bearing diameter in inches,
l = the bearing length in inches,
V_b = the rubbing velocity of the bearing in feet per minute.

Brush Friction.—This loss is found only in wound-rotor motors; it is very small, and $= 1.25A\frac{V_r}{100}$ watts,

where A is the total brush rubbing surface in square inches,
V_r is the rubbing velocity in feet per minute.

Windage Loss.—This loss cannot readily be separated out from the bearing friction loss so that its value is not known; it is generally so small that it can be neglected.

The Iron Loss.—The iron loss in the induction motor is made up of several parts each due to a different cause, as follows:

a. Loss in the core and teeth due to the fundamental line frequency. The frequency in the stator is the line frequency, and the frequency in the rotor is the rotor slip times the line frequency. This last is usually very low, and not calculated unless the rotor is of the wound-rotor type, and will operate for long periods at speeds much below normal speed.

b. Loss in the surface of the teeth in the air-gap.

This loss is caused by the variation in air-gap density under the tooth and under the slot opening. The frequency is very high (1000 to 1500 cycles per second) and the volume affected is a thin layer of the tooth face.[1]

As shown by Spooner and Kinnard this loss may be calculated as follows:

$$W_s = 0.69 \times K_{Bag} \times K_{ft} \times K_q \times K_\lambda \times \pi \times D \times l, \qquad (44a)$$

where W_s = surface loss in watts,
K_{Bag} = a factor depending on magnetic density,
K_{ft} = a factor depending on frequency,

[1] See Spooner and Kinnard, *Trans.* A. I. E. E., February, 1924.

K_q = a factor depending on ratio, $\frac{\text{slot width,}}{\text{air-gap}}$

K_λ = a factor depending on slot pitch,

D = internal stator diameter in inches,

L_c = frame length in inches.

The values of K_{Bag}, K_{ft}, K_q and K_λ may be taken from Fig. 248.

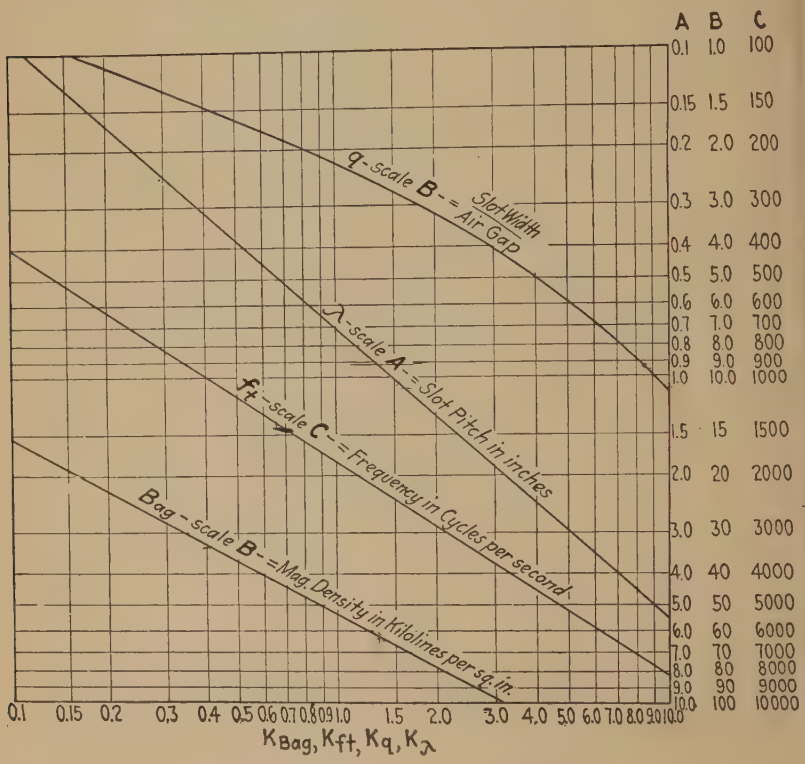
A
B
C
q-scale B- = Slot Width / Air Gap
λ-scale A- = Slot Pitch in inches
ft-scale C- = Frequency in Cycles per second
Bag-scale B- = Mag. Density in Kilolines per sq. in.
0.1 0.15 0.2 0.3 0.4 0.5 0.6 0.7 0.8 0.9 1.0 1.5 2.0 3.0 4.0 5.0 6.0 7.0 8.0 9.0 10.0
KBag, Kft, Kq, Kλ

FIG. 248.—Curves for the value of K_{Bag}, K_{ft}, K_q and $K\lambda$ in formula (44*a*).

c. Tooth pulsation loss. The frequency is high. The volume affected is the tooth volume and is caused by the variation in tooth density when two teeth are opposite each other and when one tooth is opposite a slot.[1]

Other losses which cannot be separated from the above very easily are:

Losses due to filing the slots (usually very small unless too much filing is done).

[1] See Spooner, *Trans.* A. I. E. E., February, 1924.

Losses due to stray fluxes in end plates and end bells. (These are not, as a rule, of much importance in the usual construction where these parts do not come too close to the windings.)

Losses due to non-uniform flux distribution in the core. (This is not usually a large loss and can be neglected in most cases.)

The line frequency loss is found by using curves for the iron used at the line frequency. The volume considered is the stator core and stator teeth.

The surface loss is figured for both stator and rotor after the curves found by Mr. Spooner, A. I. E. E., February, 1924, and quoted above. This loss is usually very small when the opposing

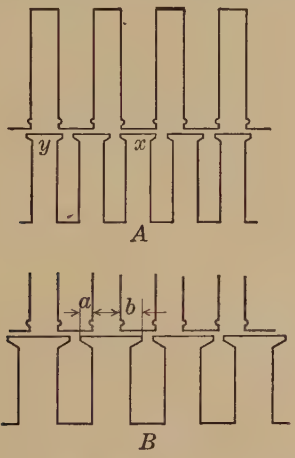

FIG. 249.—Flux pulsation in the rotor teeth.

members have partially closed slots, but is an important part of the losses when the slots are open.

Figure 249 indicates the nature and cause of the tooth pulsation loss mentioned in *c* above. In diagram *A* of Fig. 249, it is obvious that the flux passing through tooth x is greater than through tooth y; the reluctance of the magnetic circuit at x is a minimum, and at y a maximum. Hence, there is a pulsation of the magnetic densities in both rotor teeth and stator teeth of a frequency equal to the number of teeth in rotor or stator times the revolutions per second.

246. Rotor Slot Design.—To make the pulsation loss a minimum, the reluctance of the air-gap under each tooth should remain constant. This can be accomplished by the use of totally closed slots for both rotor and stator; even partially closed slots

will give approximately this result if the slits at the top of the slots be made narrow.

When open slots are used in the stator, the size of rotor tooth, which makes the pulsation loss a minimum, is found in the following way: The rotor slot is made partially closed and the rotor tooth is made equal to the stator slot pitch as shown in *B*, Fig. 249, where it will be seen that the pulsation of flux in a rotor

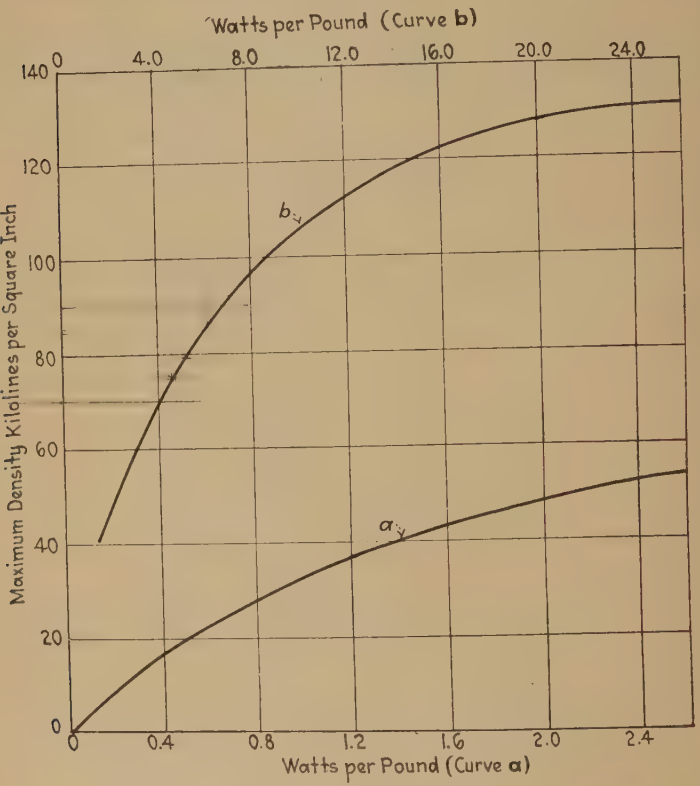

FIG. 250.—Curve of iron loss for use in induction-motor design.

tooth is zero because the area of air-gap under a rotor tooth $= a + b =$ a constant. The pulsation of flux in the stator teeth is small because the rotor slots are almost closed and the fringing makes them equivalent to totally closed slots so far as pulsation is concerned.

247. Calculation of the Iron Loss.—The loss in the stator core and teeth due to the line frequency is similar to that in a trans-

former, except that, due to the strains in the teeth and core from punching the small sections, the loss is approximately 75 per cent greater than the same iron used in a transformer.

Figure 250 shows the iron loss curve for 60 cycles, and for other frequencies the loss can be taken as proportional to the 1.3 power of the frequency.

The surface losses can be calculated as indicated above.

The tooth pulsation losses can be calculated as shown in Mr. Spooner's article in the *A. I. E. E. Journal*, February, 1924, or these losses can be avoided by using the proportions as given in Art. 246.

248. Calculation of Magnetizing Current, Iron Losses and Bearing Friction.—Assume a 75-hp. 440-volt, three-phase, 60-cycle, 900-r.p.m. synchronous-speed, 8-pole induction motor of the following dimensions; calculate magnetizing current and losses.

	Stator	Rotor
External diameter	25 in.	18.94 in.
Internal diameter	19. in.	15.5 in.
Frame length	6.375 in.	6.375 in.
Vent ducts	$1 \times \frac{3}{8}$ in.	$1 \times \frac{3}{8}$ in.
Gross iron	6 in.	6 in.
Net iron	5.4 in.	5.4 in.
Slots, number	96	79
Slots, size	0.32×1.55 in.	0.45×0.4 in.
Conductors per slot, number	12	1
Conductors per slot, size	0.091×0.204 in.	0.4×0.35 in.
Coil pitch—in slots 1×10	67.5 electrical degrees	
Connection	YY	squirrel cage
Air-gap clearance	0.033 in.	

A stator and a rotor slot are shown to scale in Fig. 254.

Voltage per phase (since connection is Y) is $\frac{440}{1.73} = 254$.

Flux per pole, (Art. 243) is found as follows,

$$E = 2.22\, kZf\, \phi_a \cos\frac{\theta}{2}\, 10^{-8},$$

$$254 = 2.22 \times 0.958 \times \left(\frac{96 \times 12}{3 \times 2}\right) \times 60 \times \phi_a \times 0.924 \times 10^{-8},$$

from which $\phi_a = 1.115 \times 10^6$.

C_1, the stator Carter coefficient, is found as follows:

$$\frac{s}{\delta} = 9.7, f(\text{from Art. 48}) = 0.35, C_1 = \frac{0.302 + 0.32}{0.302 + 0.32 \times 0.35} = 1.51.$$

C_2, the rotor Carter coefficient, is found as follows:

$$\frac{s}{\delta} = 2.1, f\ (\text{Art. 48}) = 0.72, C_2 = \frac{0.68 + 0.07}{0.68 + 0.07 \times 0.72} = 1.03.$$

The pole pitch $= \frac{\pi \times 19}{8} = 7.48$ in.

The magnetizing current $= \frac{1}{0.87\left(\text{conductors per pole} \times \cos\frac{\theta}{2}\right)} \times \frac{\phi_a}{\tau L_g}$

$\times \delta C, = \frac{1}{0.87 \times (6 \times 12 \times 0.924)} \times \frac{1.115 \times 10^6}{7.48 \times 6} \times 0.033 \times 1.51 \times 1.03,$

$= 22.2$ amperes for air-gap alone; this has to be increased by 15 per cent to allow for the iron part of the magnetic circuit. Therefore, the magnetizing current

$= 22.2 \times 1.15 = 25.5$ amperes.

The Flux Densities.—Figure 251 shows the flux distribution in a four-pole induction motor.

The average stator tooth density $= \frac{\text{flux per pole}}{\text{tooth area per pole}}$ and

Fig. 251.—Flux distribution in a four-pole induction motor.

the maximum tooth density, namely, that at point A

$= \text{average tooth density} \times \frac{\pi}{2} = \frac{\text{flux per pole}}{\text{tooth area per pole}} \times \frac{\pi}{2}.$

The tooth area per pole taken one-third of the slot depth from the air-gap = teeth per pole $\times$ tooth width $\times$ net iron.

$= 12 \times 0.335 \times 5.6 = 22.6$ sq. in.

The maximum tooth density $= \frac{1{,}115{,}000}{22.6} \times \frac{\pi}{2} = 77.500$ lines per square inch.

The volume of the stator teeth $= 1.55 \times 22.6 \times 8$

$= 280$ cu. in., or a weight of 73 lb.

The loss per pound from curve 250 is 5 watts, which gives a stator tooth loss of 365 watts.

The core area = core depth × net iron,
= 1.45 × 5.6 = 8.1 sq. in.

The maximum core density at *B*, Fig. 251,

$$= \frac{\phi_a}{2 \times \text{core area}} = \frac{1{,}115{,}000}{2 \times 8.1} = 69{,}000 \text{ lines per square inch.}$$

The volume of the stator core = area × mean circumference,
= 8.1 × π × 23.55 = 600 cu. in. or a weight of 156 lb.

The loss per pound from curve 250 is 4 watts, which gives a stator core loss of 624 watts.

The surface losses as calculated from Art. 245 =

$$W_s = 0.69 K_{Bag} \times K_{ft} \times K_q \times K_\lambda \times \pi DL$$

In this case $B_{ag} = \frac{1{,}115{,}000 \times 8}{\pi \times 19 \times 6} \times \frac{\pi}{2} = 39{,}000$

$$f_t = \frac{96 \times 2}{8} \times 60 = 1440$$

$$q = \frac{0.32}{0.033} = 9.7$$

$$\lambda = 0.622$$

$$W_s = 0.69 \times 0.55 \times 0.6 \times 9 \times 0.88 \times \pi \times 19 \times 6 = 650 \text{ watts.}$$

The face of the rotor tooth is 0.672 inch wide, and the stator pitch is 0.622 inch. These are nearly the same, and the rotor face is wider than the stator pitch, which are favorable conditions in regard to tooth pulsation losses. In this case, none of these losses will be assumed.

The total iron loss is then:

Stator teeth	365 watts.
Stator core	624 watts.
Surface loss	650 watts.
Tooth pulsation	0
Total iron losses	1639 watts.

Friction and Windage.

Size of bearings = 3 × 9 in.

The loss in each bearing $= 0.81 dl \left(\frac{V_b}{100}\right)^{3\frac{1}{2}}$ watts.

V_b = the rubbing velocity which, at 900 r.p.m., is 700 ft. per minute.

The loss in two bearings = $2 \times 0.81 \times 3 \times 9 \times (7)^{3\frac{1}{2}} = 810$ watts.

CHAPTER XXIX

LEAKAGE REACTANCE

249. Necessity for an Accurate Formula.—To calculate the reactance voltage of the coils undergoing commutation in a D.-C. machine an approximate formula is used. A more accurate formula is of little extra value because commutation depends on so many other things such as brush contacts, shape of pole tips, etc., about the effect of which comparatively little is known.

In the case of an alternator 20 per cent error in the calculation of the armature reactance has comparatively little effect on the value of the regulation determined by calculation since the reactance drop is only a part of the total voltage drop, the remainder being due principally to armature reaction.

In the case of an induction motor, however, the maximum current I_d, and therefore the starting torque and the overload capacity, depend entirely on the leakage reactance, as shown in formula (43), page 334, so that it is necessary to develop a formula which will give this reactance accurately.

250. The Leakage Fields.—The leakage in an induction motor consists of the end connection and the slot leakage, which are also found in alternators, and the leakage ϕ_z, Fig. 252, which links the conductors and passes zigzag along the air-gap.

Except for the end-connection leakage these fluxes have no separate existence but form part of the total flux in the machine; since, however, the magnetic circuit of an induction motor is not saturated, their effect may be considered separately.

251. Reactance Formula.—If

ϕ_e = the lines of force that circle 1 in. length of the belt of end connections for each ampere conductor in that belt,

ϕ_s = the lines of force that cross the slots and circle 1 in. length of the phase belt of conductors for each ampere conductor in that belt,

ϕ_z = the lines of force that zigzag along the air-gap and circle 1 in. length of the phase belt of conductors for each ampere conductor in that belt,

then, just as in the case of the alternator, the stator reactance per phase in ohms

$$= 2\pi f b^2 c^2 \left(\cos\frac{\theta}{2}\right)^2 p\left[\frac{\phi_e L_e}{2} + (\phi_s + \phi_z)L_g\right]10^{-8} \text{ for a double-layer winding;}$$

because of its lower reactance the double-layer winding is almost universally used for induction-motor work.

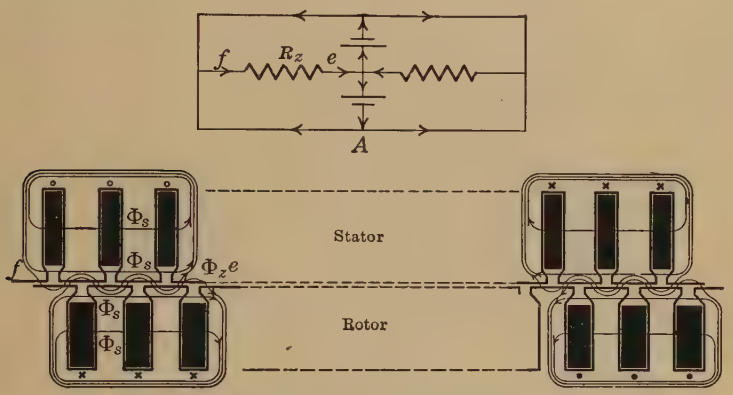

FIG. 252.—The leakage fields.

252. Zigzag Reactance.[1]—Figure 252 shows part of the winding of one phase of the stator and the corresponding part of the rotor winding of a three-phase induction motor. It was shown in Art. 226, page 329, that the m.m.f. of the rotor is opposed to and practically equal to that of the stator, so that the direction of the currents in the conductors is as shown by the crosses and dots at the bottom of the slots, and a peculiar magnetic circuit is produced of which the electrical equivalent is shown in diagram *A*, Fig. 252.

The m.m.f. between *e* and *f* = *bci* ampere-turns, therefore the flux along one path $R_z = \dfrac{3.2bci}{R_z}$

where R_z is proportional to the reluctance of one of the zigzag paths.

In order to find R_z it is assumed for simplicity that there are the same number of stator as of rotor slots so that $\lambda_1 = \lambda_2 = \lambda$; also that

t_1 = the width of the stator tooth and its magnetic fringe,

t_2 = the width of the rotor tooth and its magnetic fringe,

[1] Adams, *Trans.* A. I. E. E., Vol. 24, p. 327.

so that $\frac{\lambda_1}{t_1} = C_1$, the Carter coefficient for the stator,

$\frac{\lambda_2}{t_2} = C_2$, the Carter coefficient for the rotor,

y_1 (Fig. 253) $= \frac{t_2}{2} + x - \frac{s_1}{2} = m + x,$

$y_2 \quad = \frac{t_2}{2} - x - \frac{s_1}{2} = m - x,$

then $\frac{1}{R_z} = \frac{L_g}{c\left(\frac{\delta}{y_1} + \frac{\delta}{y_2}\right)},$

$$= \frac{L_g}{c\left(\frac{\delta}{m+x} + \frac{\delta}{m-x}\right)},$$

$$= L_g \frac{m^2 - x^2}{2cm\delta}.$$

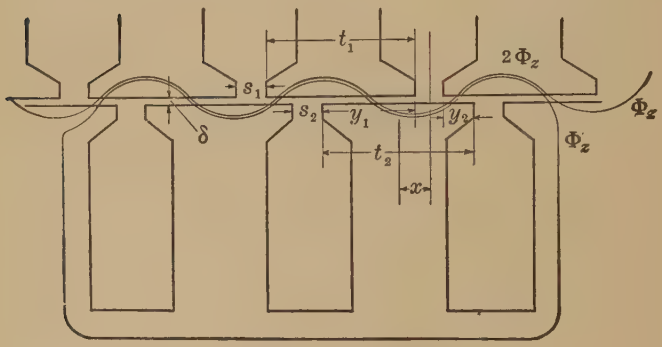

FIG. 253.—Zigzag leakage.

This value varies over the range of half a slot pitch between a maximum when x is zero and zero when $x = \frac{t_2}{2} - \frac{s_1}{2} = m$

and the average value of $\frac{1}{R_z} = \frac{2}{\lambda}\int_o^m L_g \frac{(m^2 - x^2)}{2cm\delta} dx,$

$$= \frac{2}{\lambda}\left(\frac{2}{3} \times \frac{L_g m^2}{2c\delta}\right),$$

$$= \frac{4L_g}{6c\delta\lambda}\left(\frac{t_2}{2} - \frac{s_1}{2}\right)^2,$$

$$= \frac{L_g}{6c\delta\lambda}(t_2 - \lambda + t_1)^2,$$

$$= \frac{L_g\lambda}{6c\delta}\left(\frac{t_2}{\lambda} - 1 + \frac{t_1}{\lambda}\right)^2,$$

$$= \frac{L_g\lambda}{6c\delta}\left(\frac{1}{C_1} + \frac{1}{C_2} - 1\right)^2.$$

Therefore, the leakage flux along one path R_z

$$= 3.2bci\frac{L_g\lambda}{6c\delta}\left(\frac{1}{C_1} + \frac{1}{C_2} - 1\right)^2$$

and ϕ_z the lines per ampere conductor per 1-in. length of stator or rotor

$$= 3.2\frac{\lambda}{6c\delta}\left(\frac{1}{C_1} + \frac{1}{C_2} - 1\right)^2 \times \frac{1}{2}$$

$$= 0.26\frac{\lambda}{\delta c}\left(\frac{1}{C_1} + \frac{1}{C_2} - 1\right)^2,$$

since half the lines link the stator coils and the other half link the rotor coils.

253. Final Formula for Reactance.—For double-layer windings the stator reactance per phase

$$= 2\pi f_1 b_1{}^2 c_1{}^2\left(\cos\frac{\theta}{2}\right)^2 p\left[\frac{\phi_e L_e}{2} + (\phi_s + \phi_z)L_g\right]10^{-8},$$

the rotor reactance per phase

$$= 2\pi f_2 b_2{}^2 c_2{}^2\left(\cos\frac{\theta}{2}\right)^2 p\left[\frac{\phi_e L_e}{2} + (\phi_s + \phi_z)L_g\right]10^{-8},$$

the maximum current per phase

$$= I_d = \frac{\text{volts per phase,}}{X_1 + X_2\left(\frac{b_1c_1}{b_2c_2}\right)^2\frac{n_1}{n_2}},$$

$$= \frac{E}{X_{eq}},$$

where X_{eq} is the equivalent reactance per phase and

$$= 2\pi f_1 b_1{}^2 c_1{}^2\left(\cos\frac{\theta}{2}\right)^2 p^2 n_1\left[\frac{\phi_e L_e}{2n_1p} + \left(\frac{\phi_s + \phi_z}{n_1p}\right)L_g + \frac{\phi_e L_e}{2n_2p} + \left(\frac{\phi_s + \phi_z}{n_2p}\right)L_g\right]10^{-8},$$

$$= 2\pi f_1 b_1{}^2 c_1{}^2 p^2\left(\cos\frac{\theta}{2}\right)^2 n_1\left[\frac{\phi_e L_e}{2n_1p} + \left(\frac{\phi_s+\phi_z}{n_1p} + \frac{\phi_s+\phi_z}{n_2p}\right)L_g\right]10^{-8}, \quad (45)$$

where $\frac{\phi_s + \phi_z}{n_1p} = \frac{1}{n_1c_1p}\left[3.2\left(\frac{d_1}{3s} + \frac{d_2}{s} + \frac{2d_3}{s+w} + \frac{d_4}{w}\right) + 0.26\frac{\lambda_1}{\delta}\left(\frac{1}{C_1} + \frac{1}{C_2} - 1\right)^2\right],$

$$\text{and } \frac{\phi_s + \phi_z}{n_2 p} = \frac{1}{n_2 c_2 p}\left[3.2\left(\frac{d_1}{3s} + \frac{d_2}{s} + \frac{2d_3}{s+w} + \frac{d_4}{w}\right) + 0.26\frac{\lambda_2}{\delta}\left(\frac{1}{C_1} + \frac{1}{C_2} - 1\right)^2\right],$$

The end-connection reactance in formula (45) is the equivalent reactance of both rotor and stator. For squirrel-cage motors the end-connection reactance of the rotor may be neglected and the curve for $\frac{\phi_e L_e}{n}$ in Fig. 256 used directly. For wound-rotor motors, on the other hand, it might seem at first that this value should be doubled, but it must be remembered that the m.m.fs. of rotor and stator are opposing and the leakage flux has to get through the space V, Fig. 246, between the two layers of windings, so that the closer together these windings are the more restricted is the space V and the smaller the leakage flux; for ordinary motors it is satisfactory to use the value for $\frac{\phi_e L_e}{n}$ in Fig. 256 and increase it by 35 per cent.

Example of Calculation.—Find the maximum current I_d for the following machine.

Rating.—75 hp., 440 volts, three phase, 60 cycle, 900 syn. r.p.m. The construction of the machine is as follows:

	Stator	Rotor
External diameter	25 in.	18.94 in.
Internal diameter	19 in.	15.5 in.
Frame length	6.375 in.	6.375 in.
Vent ducts	1 × ⅜ in.	1 × ⅜ in.
Gross iron	6 in.	6 in.
Slots, number	96	79
Slots, size	0.32 in. × 1.55 in.	0.45 in. × 0.4 in.
Conductors per slot, number	12	1
Conductors per slot, size	0.091 in. × 0.204 in.	0.4 in. × 0.35 in.
Connection	YY	Squirrel cage
Coil pitch	67.5°	
Winding	Double layer	
Air-gap clearance	0.033 in.	

A stator and a rotor slot are shown to scale in Fig. 254.

The calculation is carried out in the following way:

pole pitch = 7.5 in.

$\frac{\phi_e L_e}{2n}$ = 4.3 (from Fig. 256).

λ_1 = 0.622.

C_1 = 1.51.

C_2 = 1.03.

$$\frac{\phi_s + \phi_z}{n_1 p} = \frac{1}{96}\left[3.2\left(\frac{1.35}{3 \times 0.32} + \frac{0.2}{0.32}\right) + 0.26\frac{0.622}{0.03}\left(\frac{1}{1.5} + \frac{1}{1.03} - 1\right)^2\right],$$

$$= \frac{1}{96}[6.3 + 2.1] \text{ for the stator.}$$

$$\lambda_2 = 0.76.$$

$$\frac{\phi_s + \phi_z}{n_2 p} = \frac{1}{79}\left[3.2\left(\frac{0.40}{3 \times 0.45} + \frac{2 \times 0.07}{0.45 + 0.07} + \frac{0.03}{0.07}\right) + 0.26\frac{0.76}{0.03}\left(\frac{1}{1.52} + \frac{1}{1.03} - 1\right)^2\right],$$

$$= \frac{1}{79}[3.2 + 2.6] \text{ for the rotor.}$$

$$X_{eq} = 2 \times \pi \times 60 \times 6^2 \times 4^2 \times 8^2 \times 0.924^2 \times 3\left[\frac{4.3}{8} + \left(\frac{8.4}{96} + \frac{5.8}{79}\right) \times 6\right] 10^{-8},$$

$$= 0.541 \text{ ohm.}$$

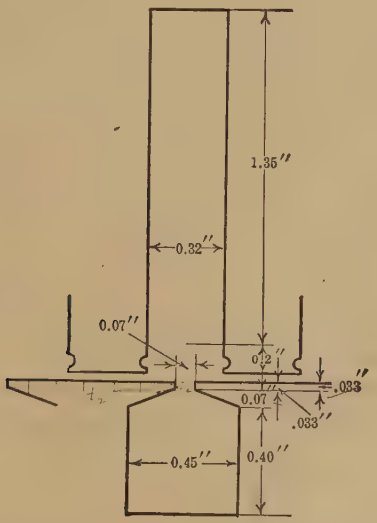

FIG. 254.—Stator and rotor slot for a 75-hp., 900-syn. r.p.m. induction motor.

The voltage per phase $= \frac{440}{1.73} = 254$, since the connection is Y. If the stator and rotor resistances were zero, the current at standstill, often called the ideal locked current, would be $\frac{254}{0.541}$ = 470 amperes. When the stator and rotor resistances are added vectorially to X, the locked current will be decreased slightly below 470.

254. Belt Leakage.[1]—In addition to the end connection, slot and zigzag leakage, there is another which enters into the reactance formula for a wound-rotor motor, namely, the belt leakage.

In developing the formula on page 363 it was assumed that the m.m.f. of the rotor was equal and opposite to that of the stator at every instant. This cannot be the case in a wound-

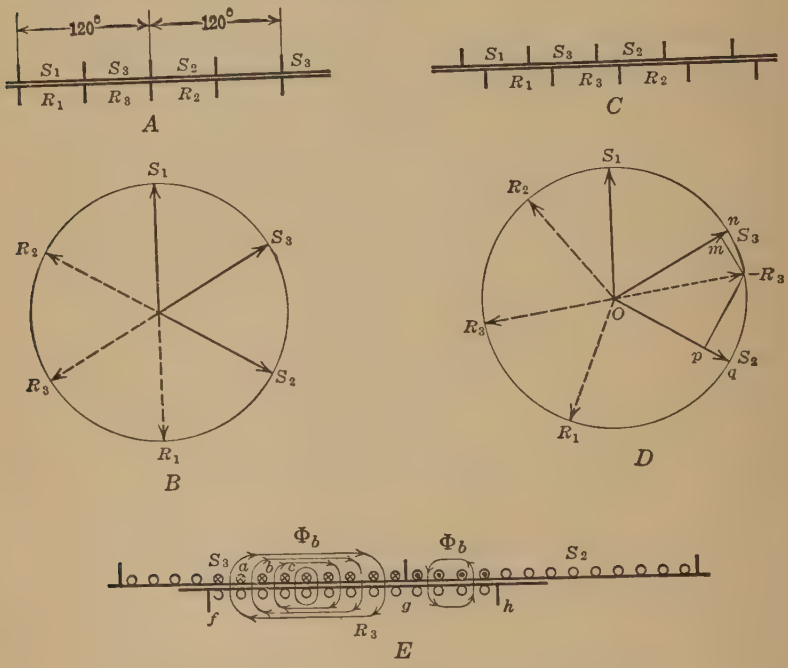

Fig. 255.—Belt leakage in three-phase machines.

rotor machine because, as shown in Fig. 231, the winding is arranged in phase belts and the stator and rotor belts sometimes overlap one another.

When the stator and rotor are in the relative position shown in diagram *A*, Fig. 255, the currents in the stator phase belts are exactly opposed by those in the rotor phase belts. The starts of the windings of the three phases are spaced 120 electrical degrees apart, and it may be seen from diagram *A* that the currents in the three stator belts S_1, S_2 and S_3, and also in the three

[1] Adams, *Trans.* of International Electrical Congress, 1904, Vol. 1, p. 706.

rotor belts R_1, R_2 and R_3 are out of phase with one another by 60 deg.; they are represented by vectors in diagram B.

When the stator and rotor are in the relative position shown in diagram C, the currents in the belts have the phase relation shown in diagram D.

Part of diagram C is shown to a large scale in diagram E, where it may be seen that belt R_3 overlaps belt S_3 by a distance fg, and belt S_2 by a distance gh.

In the belt fg the current in the stator conductors is S_3, diagram D, and that in the rotor conductors is R_3, of which the component om opposes the stator current; mn, the remaining part of the stator current, is not opposed by an equivalent rotor current and is represented by crosses in diagram E.

In the belt gh, the current in the stator conductors is S_2, diagram D, and that in the rotor conductors is R_3, of which the component op opposes the stator current; pq, the remaining part of the stator current, is not opposed by an equivalent rotor current and is represented by dots in diagram E.

The currents represented by crosses and dots in diagram E set up the flux ϕ_b, which is in phase with the current in the belt which it links and is therefore the same in effect as a leakage flux; it is called the belt leakage. ϕ_b varies through one cycle while the rotor moves, relative to the stator, through the distance of one-phase belt, and this belt flux is the cause of the variation in short-circuit current with constant applied voltage that is found in wound-rotor motors, when the rotor is moved relative to the stator.

The belt flux per ampere conductor in the phase belt and per inch axial length of core depends on the reluctance of the belt-leakage path and is directly proportional to the pole pitch, is inversely proportional to the air-gap clearance and to the Carter fringing constant, and is the greater the smaller the number of phases and therefore the wider the phase belt, so that the average value of the belt leakage that circles 1 in. length of the phase belt per ampere conductor in that belt,

$$= \text{a constant} \times \frac{\tau}{\delta \times C}$$

and the average belt reactance per phase which must be added to formula (45), page 363, in the case of wound-rotor motors

$$= 2\pi f b^2 c^2 p^2 \left(\cos \frac{\theta}{2}\right)^2 n L_g 10^{-8} \left(\text{a constant} \times \frac{\text{pole pitch}}{p \times \delta \times C}\right). \quad (46)$$

In addition to varying with the number of phases, the constant depends on the number of slots per phase per pole because, as shown in diagram *E*, the belt flux which links conductors *a* and *b* is smaller than if these conductors were concentrated in slot *c*. The value of the constant, which is found theoretically, is given in the following table:

Stator Slots per Pole	Two-phase Motors	Three-phase Motors
6	0.0052×3	0.00107×3
12	$\times 1.5$	$\times 1.5$
18	$\times 1.25$	$\times 1.25$
24	$\times 1.15$	$\times 1.15$
30	$\times 1.10$	$\times 1.1$
Infinity	$\times 1.0$	$\times 1.0$

For motors which have two-phase stators and three-phase rotors a mean value should be used.

255. Approximate Values for the Leakage Reactance.—For a machine with a double-layer winding the equivalent reactance per phase

$$= 2\pi f b_1^2 c_1^2 \left(\cos\frac{\theta}{2}\right)^2 p n_1 \left[\frac{\phi_e L_e}{2n_1} + \left(\frac{\phi_s + \phi_z}{n_1} + \frac{\phi_s + \phi_z}{n_2}\right) L_g\right] 10^{-8}$$

from formula (45), page 363, where

$\frac{\phi_e L_e}{2n_1}$ varies with the pole pitch as shown in Fig. 256.

$\frac{\phi_s}{n} = \frac{3.2}{cn}\left(\frac{d_1}{3s} + \frac{d_2}{s} + \frac{2d_3}{s+w} + \frac{d_4}{w}\right)$, and since $c \times n \times s$, the total slot width per pole, is proportional to the pole pitch, therefore $\frac{\phi_s}{n}$ is approximately inversely proportional to the pole pitch.

$\frac{\phi_z}{n} = \frac{1}{nc} \times 0.26 \frac{\lambda}{\delta}\left(\frac{1}{C_1} + \frac{1}{C_2} - 1\right)^2$; the ratio $\frac{\lambda}{\delta}$ is approximately constant, the maximum value being limited by humming as shown in Art. 271, page 387, and that being the case the Carter fringing constants C_1 and C_2 are also approximately constant. The number of slots per pole $= n \times c$ is approximately proportional to the pole pitch, therefore $\frac{\phi_z}{n}$ is approximately inversely proportional to pole pitch.

The reactance per phase then

$$= 2\pi f b^2 c^2 \left(\cos\frac{\theta}{2}\right)^2 p n (K_1 + K_2 L_g) 10^{-8}, \qquad (47)$$

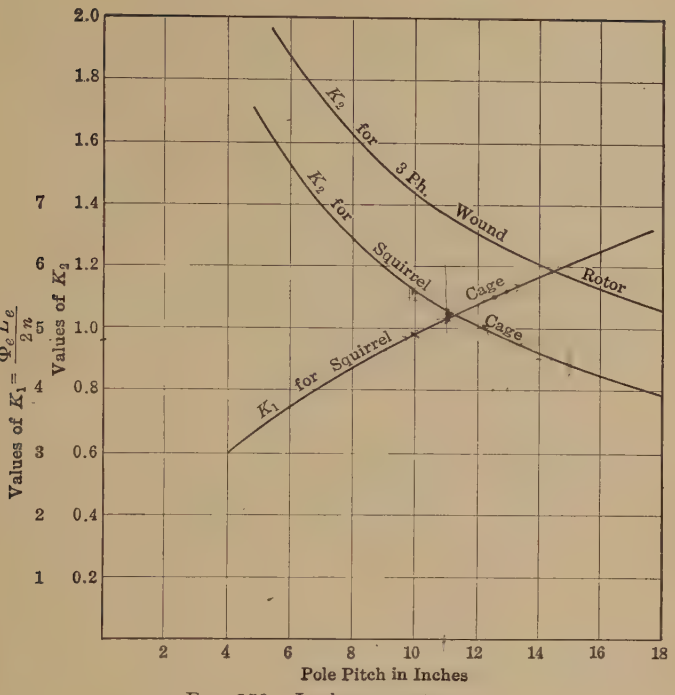

FIG. 256.—Leakage constants.

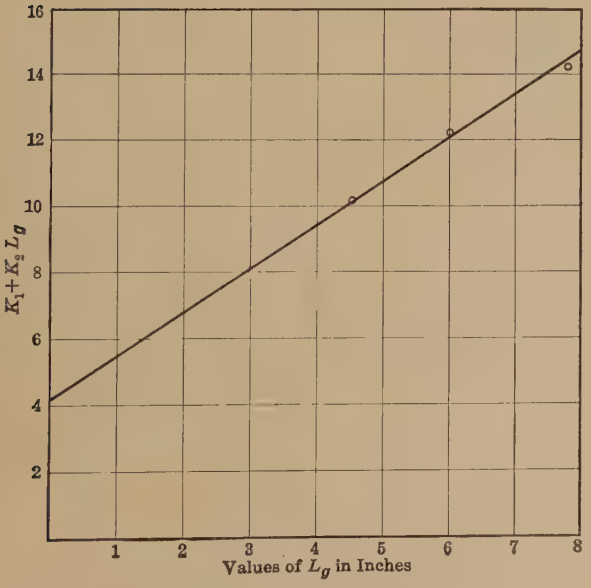

FIG. 257.—Variation of the leakage flux with frame length.

where K_1 and K_2 are plotted in Fig. 256, against pole pitch, from the results of tests on a large number of machines with open stator slots, partially closed rotor slots, and double-layer windings. The reason for the large value for wound-rotor motors compared with that for squirrel-cage machines is that in the former there is the additional end-connection leakage of the rotor, the belt leakage, and the larger rotor-slot leakage due to the deep slots required to accommodate the rotor conductors and insulation.

The method whereby these constants were determined may be understood from the following example.

Three machines were built as follows:

	A	B	C
Terminal voltage	440	440	440
Phases	3	3	3
Cycles	60	60	60
Poles	8	8	8
Stator internal diameter	19 in.	19 in.	19 in.
Pole pitch	7.5 in.	7.5 in.	7.5 in.
Gross iron	4.5 in.	6 in.	7.75 in.
Slots per pole	12	12	12
Conductors per slot	8	6	8
Coil pitch	all full pitch		
Connection	Y	Y	Δ
Maximum current I_d from test	270	400	575

The results are worked up as follows:

Voltage per phase	254	254	440
Current per phase	270	400	334
Reactance per phase	0.94	0.63	1.32
$K_1 + K_2 L_g$	10.2	12.2	14.2

These results are plotted against the values of L_g in Fig. 257 from which it may be seen that K_1, the part which is independent of the frame length, = 4.2 while K_2 = 1.30; these values check closely with the curves in Fig. 256.

CHAPTER XXX

THE COPPER LOSSES

256. Copper Losses in Stator Conductors.

Let L_{b1} = length of one stator conductor in inches,
I_{c1} = current per conductor,
M_1 = area of each conductor in circular mils,
n = number of phases.

Since copper at 75° C. has approximately 1 ohm resistance for each circular mil per inch length, resistance of one phase of motor

$$R_1 = \frac{L_{b1} \times \text{total number of stator conductors}}{M_1 \times n},$$

stator copper loss $= I^2_{c1}Rn =$

$$\frac{I^2_{c1} \times L_{b1} \times \text{total number stator conductors}}{M_1}. \qquad (48)$$

257. Copper Losses in Rotor Conductors.—The rotor resistance may be best dealt with by converting it into terms of the stator; this may be done by considering the motor as a transformer and using the ratio of stator to the rotor conductors.

The total *effective* conductors on the stator per phase

$$= \frac{\text{total stator conductors} \times \cos\frac{\theta}{2} \times k}{n},$$

where θ = chording factor of stator coils in electrical degrees,
k = distribution factor,
n = number of phases.

The total effective conductors on a squirrel-cage rotor is N_2; therefore, to convert the rotor resistance into terms of the stator resistance, the actual rotor resistance must be multiplied by the factor

$$\left(\frac{\text{total stator conductors} \times \cos\frac{\theta}{2} \times k}{N_2}\right)^2. \qquad (49)$$

The resistance of the squirrel-cage rotor bars

$$= \frac{L_{b2} \times N_2 \times K_b}{M_{b2}},$$

where L_{b2} = length of rotor bars between rings in inches,
N_2 = number of rotor bars,
K_b = $\frac{\text{specific resistance of bar material}}{\text{specific resistance of copper}}$,
M_{b2} = cross-section of rotor bars in circular mils.

The loss in the bars is, therefore,

$$= \frac{I^2_{c2} \times L_{b2} \times N_2 \times K_b}{M_{b2}}. \qquad (50)$$

Rotor Ring Losses.—Figure 258 shows the distribution of current in part of the rotor of a squirrel-cage motor. The *effective* current in each rotor bar = I_{c2} and the *maximum* current = $I_{c2}\sqrt{2}$. The maximum current in the rotor rings at A, Fig. 258, assuming the current in all bars at its maximum value:

$$= \frac{I_{c2}\sqrt{2}N_2}{2p} \text{ where } p = \text{number of poles.}$$

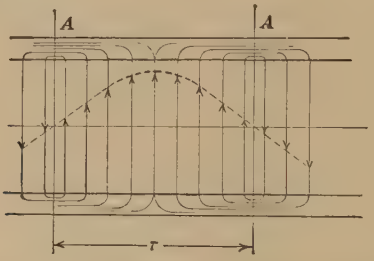

FIG. 258.—Current distribution in the rotor end connectors.

But the current in the rotor bars is not all of this maximum value, but the value varies in accordance with a sine law; hence the maximum value of the rotor current at A, Fig. 258,

$$= \frac{I_{c2}\sqrt{2}N_2}{2p} \times \frac{2}{\pi}$$

and the effective or r.m.s. value of the current at A

$$= \frac{\sqrt{2}}{2} \times \frac{I_{c2}\sqrt{2}N_2}{2p} \times \frac{2}{\pi} = \frac{I_{c2}N_2}{\pi p}.$$

The resistance of one rotor ring

$$= \frac{\pi D_r K_r}{M_r},$$

where D_r = diameter of end ring in inches.
K_r = $\frac{\text{specific resistance of ring material}}{\text{specific resistance of copper}}$.
M_r = cross-section of ring in circular mils.

The loss in the two rings, therefore,

$$= \left(\frac{I_{c2}N_2}{\pi p}\right)^2 \times \frac{2\pi D_r K_r}{M_r} \text{ watts.} \qquad (51)$$

The total rotor copper loss

$$= I^2_{c2}N_2{}^2\left(\frac{L_{b2}K_b}{M_{b2}N_2} + \frac{2D_rK_r}{\pi p^2 M_r}\right).$$

The total rotor resistance

$$= N_2{}^2\left(\frac{L_{b2}K_b}{M_{b2}N_2} + \frac{2D_rK_r}{\pi p^2 M_r}\right).$$

The total rotor resistance converted to terms of the stator

$$= N_2{}^2\left(\frac{L_{b2}K_b}{M_{b2}N_2} + \frac{2D_rK_r}{\pi p^2 M_r}\right) \times \left(\frac{\text{total stator conductors} \times \cos\frac{\theta}{2} \times k}{N_2}\right)^2$$

$$= \left(\frac{L_{b2}K_b}{M_{b2}N_2} + \frac{2D_rK_r}{\pi p^2 M_r}\right) \times \left(\text{total stator conductors} \times \cos\frac{\theta}{2} \times k\right)^2.$$

The effective rotor resistance *per phase* converted to terms of the stator $= R_e$,

$$= \frac{\left(\text{total stator conductors} \times \cos\frac{\theta}{2} \times k\right)^2}{n} \times \left(\frac{L_{b2}K_b}{M_{b2}N_2} + \frac{2D_rK_r}{\pi p^2 M_r}\right). \qquad (52)$$

In addition to the above copper losses there are eddy-current losses in the conductors due to the leakage flux which crosses the slot horizontally, as described in Art. 183, page 248. To prevent these losses from having a large value it is necessary to laminate the conductors horizontally.

When the rotor is running at full speed the eddy-current loss in the rotor bars is small, because the rotor frequency is low; even at standstill, when the rotor frequency is the same as that of the stator, the eddy-current loss in the rotor bars is still low because the conductors are not very deep.

Such eddy-current loss at standstill causes an increase in the starting torque without a sacrifice of the running efficiency, since the frequency is low and the eddy-current loss negligible at full-load speed. A number of patents have been take out on different methods of exaggerating this eddy-current loss in the rotor, but motors built under these patents have not come into general use.

Example of Copper Loss Calculation.—A 75-hp., 440-volt, three-phase, 60-cycle, 900-r.p.m. synchronous speed, eight-pole induction has the following dimensions:

	Stator	Rotor
External diameter	25 in.	18.94 in.
Internal diameter	19 in.	15.5 in.
Frame length	6.375 in.	6.375 in.
Slots, number	96	79
Slots, size	0.32 × 1.55 in.	0.45 × 0.4 in.
Conductors per slot	12	1
Conductors, size	0.091 × 0.204 = 2.36 × 10^4 c.m.	0.4 × 0.35 = 1.79 × 10^5 c.m.
Connection	YY	Squirrel cage
Coil span	¾ pitch	
Area end ring		1.595 × 10^6 c.m.
Diameter end ring = D_r		17.5 in.
Specific resistance end ring		8.33 × copper

L_{b1} = length of stator conductor,
= 0.75 × 15 (Fig. 88) + 6.37 = 17.7 in.
L_{b2} = length of rotor conductor,
= 6.375 + 4.12 = 10.5 in.
(Approximately 2 in. added at each end of rotor.)

Stator resistance per phase

$$= \frac{17.7 \times 96 \times 12}{2 \times 2 \times 3 \times 2.34 \times 10^4} = 0.072 \text{ ohm.}$$

The rotor resistance per phase converted into equivalent stator resistance = R_e (formula (52)),

$$= \frac{(96 \times 6 \times 0.924 \times 0.958)^2}{3} \times \left[\frac{10.5}{1.79 \times 10^5 \times 79} + \frac{2 \times 17.5 \times 8.33}{3.14 \times 8^2 \times 1.59 \times 10^6}\right],$$

= 0.142 ohm.

The total resistance for calculating copper losses is therefore 0.072 + 0.142 = 0.214 ohm per phase. The total copper losses may readily be calculated at any desired load and are equal to I^2R_{eq}.

For instance, the full-load current of the 75-hp. motor above detailed is 91 amperes; the total full-load copper loss both stator and rotor is, therefore, $91^2 \times 0.214 = 1770$ watts.

CHAPTER XXXI

HEATING OF INDUCTION MOTORS

258. Heating and Cooling Curves.—The losses in an electrical machine are transformed into heat; part of this heat is dissipated by the machine and the remainder, being absorbed, causes the temperature of the machine to increase. The temperature becomes stationary when the heat absorption becomes zero, that is, when the point is reached where the rate at which heat is generated in the machine is equal to the rate at which it is dissipated by the machine.

The rate at which heat is dissipated by any machine depends on θ, the difference between the temperature of the machine

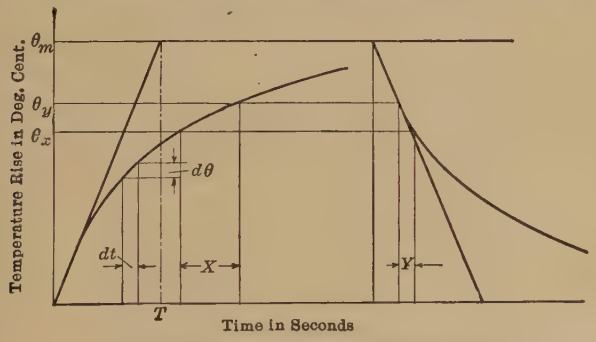

FIG. 259.—Heating and cooling curves.

and that of the surrounding air. During the first interval after a machine has been started up, θ is small; very little of the generated heat is dissipated; therefore a large part is absorbed and the temperature rises rapidly. As the temperature increases, that part of the heat which is dissipated increases; therefore the part which is absorbed decreases and the temperature rises more slowly. The relation between temperature rise and time is shown in Fig. 259. The equation to this curve is derived as follows:

In a given machine let $d\theta$ be the increase in temperature in the time dt.

The heat generated during this time $= Q \times dt$ lb. calories
where $Q = 0.53$ (kw. loss).
The heat absorbed by the machine $= W \times s \times d\theta$ lb. calories
where W is the weight of the active part of the machine in pounds
and s, its specific heat $= 0.1$ approximately.
The heat dissipated $= A(a + bV)\theta \times dt$ lb. calories
where A is the radiating surface of the machine,
V is the peripheral velocity,
a and b are constants.
The heat generated = the heat dissipated + the heat absorbed, or

$$Qdt = A(a + bV)\theta dt + Wsd\theta,$$

and the temperature rise is a maximum and $= \theta_m$ when the heat absorbed is zero or when

$$Qdt = A(a + bV)\theta_m dt.$$

Therefore

$$A(a + bV)\theta_m dt = A(a + bV)\theta dt + Wsd\theta$$

and

$$\int_o^t dt = \int_o^y \frac{Wsd\theta}{A(a + bV)(\theta_m - \theta)},$$

from which

$$t = -\frac{Ws}{A(a + bV)}(\log_e (\theta_m - \theta) - \log_e \theta_m),$$

$$= \frac{Ws}{A(a + bV)} \log_e \frac{\theta_m}{\theta_m - \theta},$$

and

$$\frac{\theta_m}{\theta_m - \theta} = e^{\frac{t(A(a + bV))}{Ws}}.$$

Therefore

$$\theta = \theta_m\left(1 - e^{\frac{-t(A(a + bV)}{Ws}}\right),$$

$$= \theta_m\left(1 - e^{-\frac{t}{T}}\right), \tag{53}$$

where

$$T = \frac{Ws}{A(a + bV)},$$

$$= \frac{Ws\theta_m}{A(a + bV)\theta_m},$$

$$= \frac{Ws\theta_m}{Q},$$

or

$$QT = Ws\theta_m. \tag{54}$$

Therefore T is the time that would be taken to raise the temperature of the machine θ_m deg. if all the heat were absorbed.

The cooling curve is the reciprocal of the heating curve and its equation is derived as follows:

If the temperature falls $d\theta$ deg. in dt sec., then
the heat dissipated $= -W \times s \times d\theta = A(a + bV)\theta \times dt.$

Therefore $$dt = -\frac{Ws}{A(a + bV)} \frac{d\theta}{\theta},$$

or $$\int_o^t dt = -\int_{\theta_m}^{\theta} T \frac{d\theta}{\theta},$$

and $$t = -T \log \frac{\theta}{\theta_m},$$

from which $$\theta = \theta_m e^{-\frac{t}{T}}. \qquad (55)$$

If the motor is standing still while cooling, the temperature drops much more slowly, as shown in Fig. 260.

Consider the following example: An induction motor is run at full load and the final temperature rise = 45° C.
The current density in the stator conductors = 480 cir. mils per ampere.
The iron loss at no load and normal voltage = 1000 watts.
The weight of iron in the stator = 115 lb.
The iron loss per pound = 8.7 watts.
It is required to find the time constant T.

The resistance of a copper wire L in. long and M cir. mils section

$$= \frac{L}{M} \text{ ohms.}$$

The loss in this wire due to a current I

$$= \frac{LI^2}{M} \text{ watts,}$$

$$= \frac{LI^2}{M} \times 5.3 \times 10^{-4} \text{ lb. calories per second.}$$

The weight of this wire $= L \times M \times 2.5 \times 10^{-7}$ lb.
The specific heat of copper = 0.09.

Since $$QT = Ws\theta_m,$$

therefore $$\frac{LI^2}{M} \times 5.3 \times 10^{-4} \times T =$$

$$L \times M \times 2.5 \times 10^{-7} \times 0.09 \times \theta_m$$

and $$\frac{\theta_m}{T} = \frac{2.3 \times 10^4}{(\text{circular mils per ampere})^2} \text{ deg. Cent. rise per second.}$$

In the given problem $M = 480$ and $\theta_m = 45°$ C.
Therefore T for the coils $= 450$ sec.

Consider now the iron loss:

The loss per pound of iron $= P$ watts,

$= P \times 5.3 \times 10^{-4}$ lb. calories per second.

The specific heat of iron $= 0.1$ approximately.

Since $QT = Ws\theta_m$,

therefore $P \times 5.3 \times 10^{-4} \times T = 1 \times 0.1 \times \theta_m$

and $$\frac{\theta_m}{T} = \frac{P}{190} \text{ deg. C. rise per second.}$$

In the given problem $P = 8.7$ watts per pound and $\theta_m = 45°$ C. Therefore T for the iron of the stator $= 1000$ sec.

For the value of T found for the copper, and for $\theta_m = 47°$ C., the relation between temperature and time is plotted in Fig.

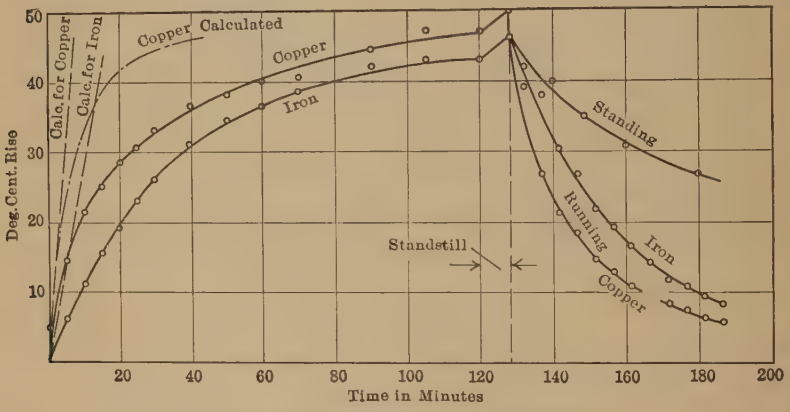

FIG. 260.—Heating and cooling curves.

260, and it will be seen that the calculated curve differs considerably from that found from test.

The actual temperature rise in a given time is less than that calculated because:

a. It has been assumed that all the iron loss is in the stator whereas a portion of it which cannot readily be separated out is due to rotor pulsation loss.

b. Part of the heat developed in the active part of the machine is conducted to and absorbed by the frame.

c. The temperature of the copper rises more rapidly than that of the iron and there is a transfer of heat which tends to bring them to the same temperature.

d. The thermal capacity of the insulation has been neglected.

529. Time to Reach the Final Temperature.—Due to the chances of error pointed out above, it is difficult to predetermine the rate of increase of temperature.

It may be seen from formula (53) that the larger the value of T, which is called the time constant, the smaller is the rate of increase of temperature. T is the time that would be taken to raise the temperature of the machine to its final value if all the heat were absorbed, so that the lower the copper and iron densities the larger the value of T and the smaller the rate of increase of temperature.

Slow-speed machines have poor ventilation and therefore low copper densities so that for such machines the rate of increase of temperature is comparatively small.

Low-frequency machines, in which the flux density in the core is limited by permeability rather than by the iron loss, have the loss per pound of iron low and the rate of increase of temperature comparatively small.

The current density in the field coils of D.-C. machines is usually of the order of 1200 cir. mils per ampere so that such coils heat up slowly.

260. Intermittent Ratings.—Suppose that a motor is operating on a continuous cycle, X sec. loaded and Y sec. without load; the final temperature will vary, during each cycle, between θ_x and θ_y, Fig. 259, where these temperatures are such that the temperature increase in time X is equal to the temperature decrease in time Y. Under such conditions of service therefore θ_y, the highest temperature, is lower than θ_m, the maximum temperature which would be obtained on continuous operation under load. For such service, therefore, a motor may have higher copper and iron densities than it would have if designed for the same load but for continuous operation.

261. Heating of Squirrel-cage Motors at Starting.—The loss in a squirrel-cage rotor at starting is very large and equals the full-load output of the machine $\times$ the per cent of full-load torque required to start the load. Thus, if a 20-hp. squirrel-cage motor has to develop full-load torque at starting, the rotor loss under these conditions must be 20 hp. This loss, in the form of heat, has to be absorbed by the rotor copper, and the temperature rises rapidly unless there is sufficient body of copper to absorb this heat during the starting period.

The stator current also is large at starting; an average squirrel-cage motor with normal voltage applied to the terminals develops about 1.5 times full-load torque and takes about 5.5 times full-load current; when started on reduced voltage it develops full-load torque with about 4.5 times full-load current, since the starting torque is proportional to the rotor loss and therefore to the square of the current.

As shown in Art. 258, the temperature rise when the heat is all absorbed may be found from the following formulæ.

$$\text{Degrees Centigrade rise per second} = \frac{2.3 \times 10^4}{(\text{circular mils per amp.})^2} \text{ for copper wire}$$

$$= \frac{\text{watts per pound}}{190} \text{ for iron bodies}$$

$$= \frac{\text{watts per pound}}{170} \text{ for copper bodies.}$$

An average value for the circular mils per ampere at full load is 500, for both rotor and stator. The starting current in the motor for full-load torque is about 4.5 times full-load current, the corresponding value of circular mils per ampere is 110, and the temperature rise 1.9° C. per second.

The proper weight of end connector to be used in any particular case depends on the starting torque required and the time needed to bring the motor up to full speed. For motors from 5 to 100 hp., the loss per pound of end connector is generally taken about 1 kw. and, corresponding to this loss, the temperature rise of the end connectors

$$= \frac{1000}{170},$$

$$= 6° \text{ C. per second approximately.}$$

262. Stator Heating.—The temperature rise of the stator of an induction motor is fixed in the same way as that of the armature of a D.-C. machine.

For induction motors built with such a grade of iron that the iron loss curves are as shown in Fig. 250, the following flux densities may be used for a machine whose temperature rise at normal load must not exceed 40° C.

Frequency	Maximum Tooth Density in Lines per Square Inch	Maximum Core Density in Lines per Square Inch
60 cycles	85,000 to 95,000	65,000 to 90,000
25 cycles	100,000	85,000 to 100,000

These figures represent standard practice for machines with open stator slots and partially closed rotor slots when the rotor slot is designed as pointed out in Art. 246, page 355, for minimum pulsation loss. When both stator and rotor slots are partially closed, these densities may safely be increased 15 per cent.

The end-connection heating is limited by keeping the value of the ratio $\frac{\text{ampere conductors per inch}}{\text{circular mils per ampere}}$ below that given in Fig. 261, which curve applies to wound-rotor motors, and to squirrel-cage motors with less than 4 per cent slip, of the type shown in Figs. 243 and 246.

263. Rotor Heating.—At full load and normal speed the frequency of the flux in the rotor is very low so that comparatively high flux densities may be used. The rotor tooth density is not carried above 120,000 lines per square inch if possible, because, for greater values, the m.m.f. required to send the flux through these teeth becomes large and causes the power factor to be low; for the same reason the rotor core density is seldom carried above the point of saturation, namely about 85,000 lines per square inch. So far as heating is concerned the rotor core loss is so small that it may be neglected.

The rotor copper loss is limited by making the ratio $\frac{\text{ampere conductors per inch}}{\text{circular mils per ampere}}$ the same for the rotor as for the stator, and then, if the motor is of the squirrel-cage type, any additional rotor resistance that is required to give the necessary starting torque is put in the end connectors, which are easily cooled.

Since the rotor ventilation is better than that of the stator, because it is revolving, the rotor temperature is generally lower than that of the stator and is not calculated.

264. Effect of Rotor Loss on Stator Heating.—The heating of the rotor causes the air which blows on the stator to be hotter than the surrounding air. The heating curve in Fig. 261 applies to squirrel-cage motors with about 4 per cent slip or 4 per cent rotor loss, and for the type of construction shown in Figs. 243 and 246. When greater rotor loss than this is required, as in the case of squirrel-cage motors for operating certain classes of cement machinery, then the air blowing on the stator will be hotter than usual and the stator temperature will be higher than the value got from Fig. 261. On account of this extra

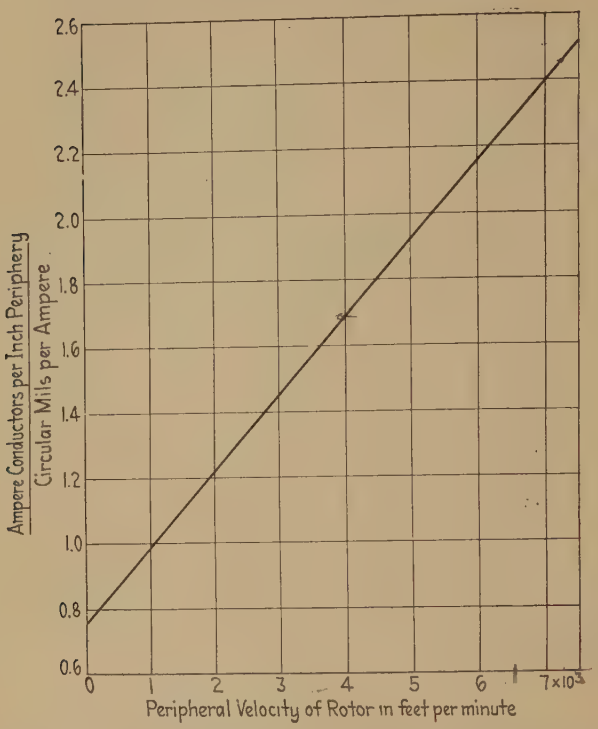

FIG. 261.—Curve for determination of conductor size for preliminary design of induction motors.

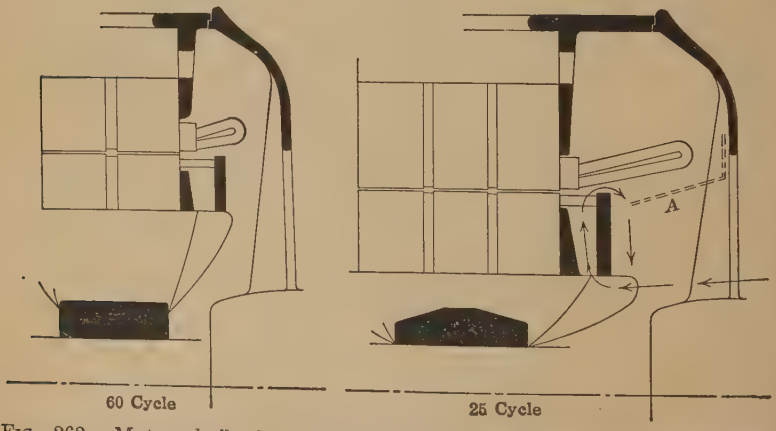

FIG. 262.—Motors built for the same output and speed but for different frequencies.

rotor loss such high torque squirrel-cage motors are built on frames that are about 20 per cent larger than standard.

265. Effect of Construction on Heating.—Figure 262 shows the relative proportions of a 25-cycle and of a 60-cycle motor of the same horsepower and speed and therefore with the same size of bearings. In the case of the 25-cycle machine, the bearing blocks up the air inlet, and in such a case the temperature rise should be figured conservatively until the first machine has been tested and accurate data obtained. Another objection to the 25-cycle motor is that the coils stick out a considerable distance from the iron of the core and there is a tendency for the cooling air to circulate as shown by the arrows and not to pass out of the machine; in such a case it may be necessary to put in a baffle, as indicated by the dotted line *A*, to deflect the air stream in the proper direction.

266. Heating of Enclosed Motors.—Experiment shows that in the case of a totally enclosed motor the temperature rise of the coils and core of the machine is proportional to the total loss (neglecting bearing friction) and is independent of the distribution of this loss, is inversely proportional to the external radiating surface and depends on the peripheral velocity of the rotor.

267. Heating of Semi-enclosed Motors.—When the openings in the frame of a motor are blocked up with perforated sheet metal the machine is said to be semi-enclosed. The perforated metal acts as a baffle, prevents the free circulation of air through the machine, and causes the temperature to rise, on an average, about 25 per cent higher than it would for the same machine operating at the same load but as an open motor.

The effect of enclosing a motor may be seen from the following table which gives the results of a series of heat runs made on a motor similar to that shown in Fig. 243 and constructed as follows:

Internal diameter of stator	20 in.
Frame length	5.5 in.
Peripheral velocity of rotor	4730 ft. per minute.
Stator copper loss	0.77 kw.
Rotor copper loss	0.9 kw.
Iron loss	0.77 kw.
Total loss	2.44 kw.
External radiating surface	3260 sq. in.

Parts of motor	Open motor	Opening in housings closed with perforated sheet metal $\frac{3}{8}$-in. holes on $\frac{5}{8}$-in. centers	Openings in housings closed with sheet metal	Openings in housings closed with sheet metal
		Yoke openings open	Yoke openings open	Yoke openings closed
Stator coils	18.5	22	46	74
Stator iron	18.5	20	48	71
Rotor conductors	15	21	46	71
Rotor ring	14	21	44	69
Rotor iron	14	20	41	61
Oil in bearings	14	24	39	57
Outside of yoke	....	..	30	

The temperature rise is given in degrees Centigrade.

The first machine of a new type that is built is generally very liberally designed, and the copper and iron densities are low. If this machine runs cool in test, it may get a higher rating than that for which it was originally built, and, based on the results of the tests on this machine, the next is designed more closely. Electrical design is not an exact science but is always changing to suit the requirements of the customer, the accumulating experience of the designer and the competition of other manufacturers.

CHAPTER XXXII

NOISE AND DEAD POINTS IN INDUCTION MOTORS

268. Noise Due to Windage.—Figure 263 shows the standard construction used for induction motors. As the rotor revolves, air currents are set up in the direction shown by the arrows, and it may be seen from diagram *A* that a puff of air will pass through the stator, between the stator coils, every time a rotor tooth comes opposite a stator tooth, so that the machine acts as a siren.

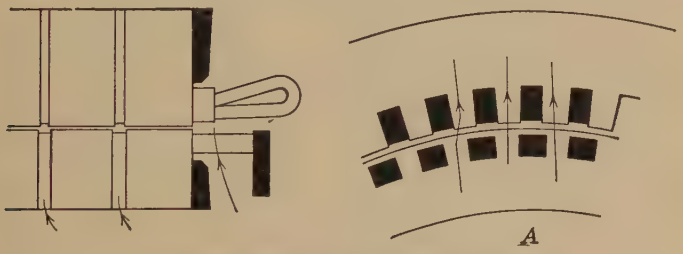

FIG. 263.—Windage in induction motors.

The intensity of the note emitted depends on the peripheral velocity of the rotor, while its pitch or frequency

$$= \text{the number of puffs per second,}$$

$$= \text{the number of rotor slots} \times \text{revolutions per second,}$$

$$= \frac{\text{peripheral velocity of rotor in feet per minute}}{5 \times \text{rotor slot pitch in inches.}}. \quad (56)$$

The higher the pitch of the note the more objectionable it becomes, and a note with a frequency greater than 1560 cycles per second, which is the high G of a soprano, is very objectionable if loud and long sustained. For a peripheral velocity of 8000 ft. per minute and a rotor slot pitch of 1 in., the frequency of the windage note is 1600 cycles per second.

Noise due to windage can be lowered in intensity by blocking up the rotor vent ducts; if the motor then runs hot due to poor ventilation, some other method of cooling must be adopted, such as blowing air across the external surface of the punchings, or the motor may be totally enclosed and cooled by forced

ventilation. The intensity of the note can be greatly reduced by staggering the vent ducts as shown in Fig. 264, and since the air-gap clearance is large in high-speed machines, which are the only ones that are noisy due to windage, the ventilation of such machines will not be seriously affected. It should also be noted that for high-speed machines a large number of narrow ducts will give quieter operation than a smaller number of wide ducts, because the velocity of the air through each duct will be reduced.

269. Noise Due to Pulsations of the Main Flux.—In Fig. 249 page 355, *A* shows part of a machine which has a large number of rotor slots. The flux in a rotor tooth pulsates from a maximum, when the tooth is in position *x*, to a minimum when the tooth is in position *y*, and the frequency of this pulsation is equal to the number of stator teeth × revolutions per second. This

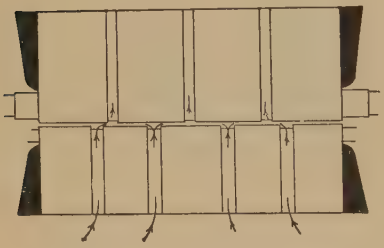

FIG. 264.—Motor with staggered vent ducts.

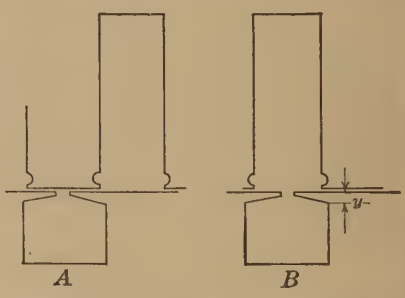

FIG. 265.—Variation of the force of magnetic attraction on the rotor tooth tips.

pulsation of flux causes a noise which varies in intensity with the voltage. To minimize this noise the machine should be designed so as to have a minimum pulsation loss, the condition for which, as shown in Art. 246, page 355, is that the rotor tooth shall be equal to the stator slot pitch, and the rotor slit shall be narrow. The noise due to pulsation of the main flux may be minimized by stacking the rotor tightly.

270. Noise Due to Vibration of the Rotor Tooth Tips.—Figure 265 shows several of the slots of the stator and rotor of an induction motor. When the rotor tips are in the position shown at *A*, there is a force of attraction between the stator tooth and the rotor tooth tip, while in position *B* this force is zero; the rotor tooth tip will therefore be set in vibration with a frequency equal to the number of stator teeth × revolutions per second. This

noise cannot be minimized by making the core tight and must be provided against by having the root y sufficiently thick to prevent bending and by the use of a moderate air-gap clearance. Noise due to this cause is rarely found in conservatively designed machines; it has been found in machines which are built with a small air-gap so as to lower the magnetizing current, and those built with a very thin rotor tooth tip so as to lower the reactance.

271. Noise Due to Leakage Flux.—The principal cause of noise in induction motors is the variation in the reluctance of the zigzag leakage path. When the stator and rotor slots are in the relative position shown in *B*, Fig. 265, the zigzag leakage flux is a minimum, and when in the relative position shown in *A*, is a maximum, so that there is a pulsation of flux in the tooth tips and two notes are emitted which have frequencies equal to the number of rotor slots $\times$ revolutions per second and the number of stator slots $\times$ revolutions per second, respectively.

To insure that the noise thus produced will not be objectionable, it is necessary to make the variation in the zigzag leakage flux a minimum, and the most satisfactory way to do this is to make the zigzag leakage as small as possible. This leakage flux is directly proportional to the ampere conductors per slot and inversely proportional to the air-gap clearance, and it has been found from experience that in order to prevent excessive noise up to 25 per cent overload the ratio

$$\frac{\text{ampere conductors per slot at full load}}{\text{air-gap clearance in inches}}$$

should not exceed 14×10^3 for machines with open stator and partially closed rotor slots, or 12×10^3 for machines with partially closed slots for both stator and rotor.

It is also found that, as the frequencies of the two notes produced by zigzag leakage approach one another in value, the noise becomes more and more objectionable, and that, for even lower values of the ratio

$$\frac{\text{ampere conductors per slot at full load}}{\text{air-gap clearance in inches}}$$

than those given above, the noise will be objectionable if the number of rotor slots is within 20 per cent of the number of stator slots.

The cause of the noise in any given case can readily be determined. Run the motor on normal voltage and no load and, if it is noisy, the trouble is due to windage, pulsation of the main field or weak rotor tooth tips; then open the circuit, and if the

motor is still noisy the trouble is due to windage. If the motor is quiet on no load but noisy when loaded, the trouble is due to the zigzag leakage flux.

272. Dead Points at Starting.—It was shown in Art. 234, page 337, that the starting torque in synchronous horsepower is equal to the rotor loss at starting. If the rotor is not properly designed, this torque may not all be available.

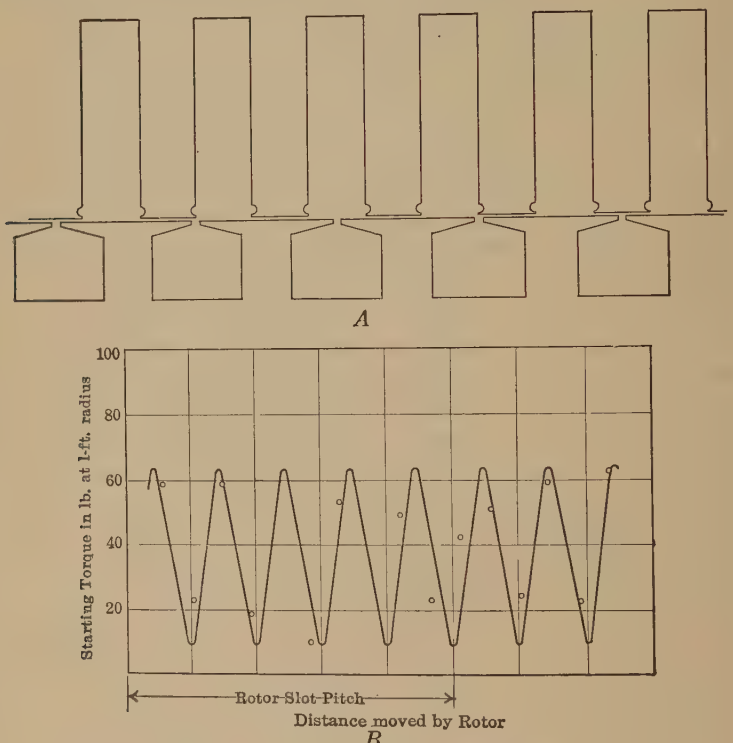

FIG. 266.—Variation in the starting torque.

In the case of a squirrel-cage motor at standstill, the applied voltage is low and the main flux therefore small, but the starting current is several times full-load current and therefore the zigzag leakage flux is large. This flux is a maximum when the stator and rotor slots have the relative position shown in diagram *A*, Fig. 265, and a minimum when they have the position shown in *B*, so that there is a tendency for the rotor to lock in position *A*, the position of minimum reluctance. If the force tending to

rotate the rotor is less than that tending to hold the rotor locked, then the rotor will not start up.

A, Fig. 266, shows several slots of a machine which has five stator slots for every four rotor slots, so that when the available torque is a minimum, every fourth rotor slot is in the locked position. Diagram *B* shows the result of a test made on this machine, the torque being measured by a brake for different positions of the rotor relative to the stator; it may be seen that there are five positions of minimum torque in the distance of a rotor slot pitch.

In order that the variation in starting torque may be a minimum, it is necessary to make the number of locking points small. If the number of rotor slots is equal to the number of stator slots, then, when the starting torque is a minimum, each rotor slot will be in the locked position; if there are four rotor to every five stator slots, then the number of locking points will be one-fourth of the total number of rotor slots; if the number of rotor and of stator slots are prime to one another, then only one rotor slot can be in the locked position at any instant and the best conditions for starting are obtained. It has been found by experience that the starting torque for a squirrel-cage motor will be practically constant, if not more than one-sixth of the total number of rotor slots are in the locked position at any instant.

Wound-rotor motors have a regular phase winding and, in order that this winding may be balanced, the number of rotor slots as well as the number of stator slots must be a multiple of the number of poles and of the number of phases; the ratio $\frac{\text{stator slots}}{\text{rotor slots}}$ must therefore $= \frac{\text{stator slots per phase per pole}}{\text{rotor slots per phase per pole}}$ and, since the number of rotor slots per phase per pole is often three or four, it might be expected that such machines would not have good starting torque because of dead points. This is not the case however because, at starting, wound-rotor motors have a large resistance in the rotor circuit, and full-load torque tending to cause rotation is obtained with full-load current; therefore the zigzag leakage at starting is much smaller than in squirrel-cage machines and the force tending to cause locking is small.

If a wound-rotor motor be taken which has not more than 30 per cent of the rotor slots in the locking position at any instant, and full voltage be applied to the stator while the rotor circuit is open, then the main flux will have its normal value; it will be

found that the rotor can readily be rotated by hand, which shows that dead points are not, as generally stated, due to variations in the reluctance of the air-gap to the main field. If now this same motor be short-circuited at the rotor terminals, so that it is equivalent to a squirrel-cage motor with low rotor resistance, it will be found impossible in most cases to get the motor to start up even without load, because of the locking effect of the leakage flux. If resistance be inserted in the rotor circuit, it will be found that, as the rotor resistance increases, the variation in the starting torque becomes less and less, and that when this resistance is such that full-load torque is developed with normal voltage and full-load current, the variation in starting torque due to leakage flux is so small that it can be neglected.

Dead points can be very greatly minimized by skewing the rotor slots. This method of construction is almost universally used in modern induction motors. The effect of this skewing is to prevent magnetic locking along the whole length of a slot—when the construction is such as to get magnetic locking—but at only one point along the length of the slot. The amount of skewing is usually one slot. This does not prevent the magnetic locking but distributes its effect so that it is greatly minimized.

CHAPTER XXXIII

PROCEDURE IN DESIGN

273. The Output Equation.

$$E = 2.22kZ\phi_a f 10^{-8} \cos\frac{\theta}{2} \text{ volts (see p. 350)},$$

$$= 2.22\ kZ(B_g \tau L_g)\left(\frac{p \times \text{r.p.m.}}{120}\right) 10^{-8} \cos\frac{\theta}{2} \text{ volts},$$

$$= \frac{2.22k10^{-8}}{120} ZB_g \pi D_a L_g \times \text{r.p.m.} \times \cos\frac{\theta}{2} \text{ volts},$$

$$\text{and } q = \frac{nZI}{\pi D_a}.$$

$$\text{Therefore } nEI = n\left[\left(\frac{2.22k10^{-8}}{120}\right) ZB_g \pi D_a L_g \text{ r.p.m.} \times \cos\frac{\theta}{2}\right]\left(\frac{\pi D_a q}{nZ}\right),$$

$$\text{and} \qquad \text{hp.} = \frac{nEI}{746} \cos\phi \times \eta,$$

$$= 2.35 \times 10^{-12} B_g q \cos\phi \times \eta \times \text{r.p.m.} \times \cos\frac{\theta}{2} \times D_a^2 L_g,$$

taking $k = 0.96$,

$$\text{from which } D_a^2 L_g = \frac{\text{hp.}}{\text{r.p.m.}} \frac{10^{12}}{2.35 \times B_g q \cos\phi \times \cos\frac{\theta}{2}\eta}. \qquad (57)$$

The value of B_g, the apparent average gap density, is limited by the permissible value of B_t, the maximum stator tooth density, since

$$B_g = B_t \times \frac{L_n}{L_g} \times \frac{t_1}{\lambda_1} \times \frac{2}{\pi},$$

where the iron insulation factor $= \frac{L_n}{L_g} = 0.93$,

the permissible value of B_t = 85,000 lines per square inch for 60 cycles,
= 100,000 lines per square inch for 25 cycles,

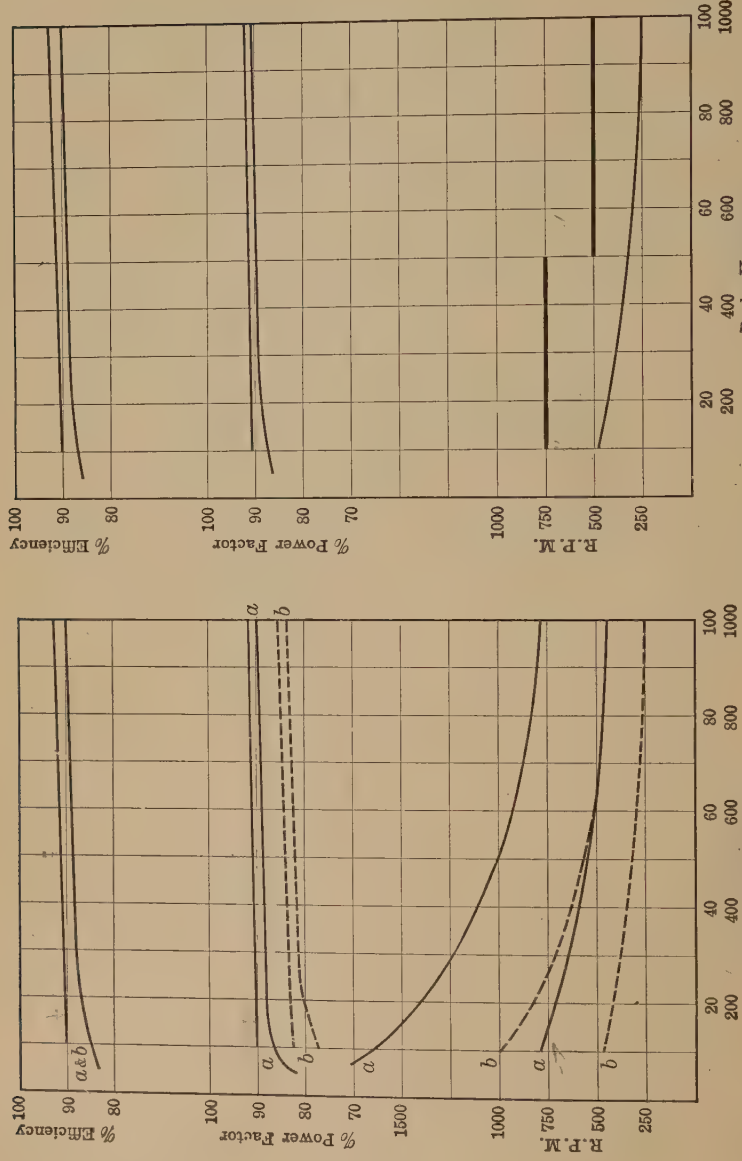

FIG. 267.—Power factor and efficiency curves for induction motors with open stator slots and partially closed rotor slots.

and $\frac{\lambda_1}{t_1} = 2.0$ approximately, being slightly larger for machines of small pole pitch. Therefore, for machines with a pole pitch greater than 7 in.,

B_g = 26,000 lines per square inch for 60 cycles, approximately.
= 29,000 lines per square inch for 25 cycles, approximately.

The Values of cos ϕ and η.—The values that may be expected from a line of 60-cycle motors with open stator slots and partially closed rotor slots are given in Fig. 267, diagram *A*, and corresponding curves for a line of 25-cycle motors are given in diagram B.

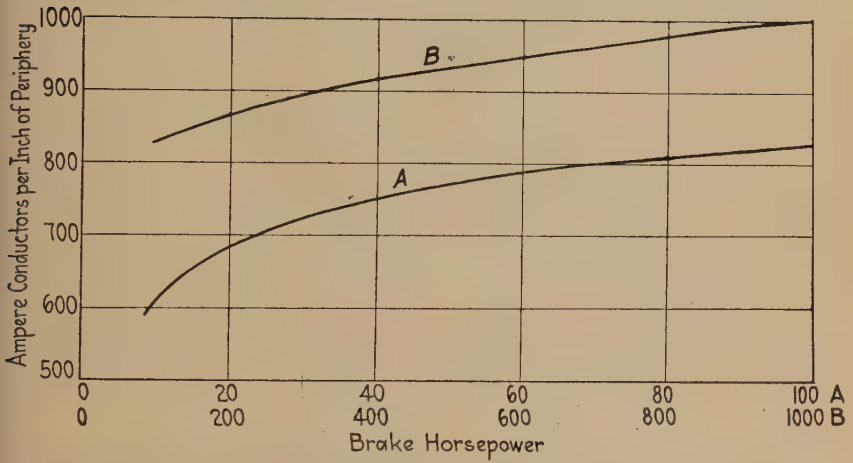

FIG. 268.—Curve to determine amphere conductors per inch of periphery for use in preliminary design of induction motors.

Two power factor curves *a* and *b* are given for the 60-cycle machines; these correspond to the two speed curves *a* and *b*. The power factor increases very slowly for speeds above *a* but drops very rapidly for speeds below *b*.

The power factor and efficiency can be improved by the use of partially closed slots for both stator and rotor.

274. The Relation between D_a and L_g.—There is no simple method whereby $D_a^2 L_g$ can be separated into its two components in such a way as to give the best machine. The only satisfactory method is to assume different sets of values, work out the design roughly for each case, and pick out that which will give good operation at a reasonable cost.

To simplify this work the following equations are developed.

I_o = the magnetizing current per phase

$$= \frac{1}{0.87 \times \text{conductors per pole} \times \cos\frac{\theta}{2}} \times \frac{\phi_a}{\tau L_g} \times \delta \times C \times 1.15 \text{ (Art. 244)}.$$

Assuming $\cos\frac{\theta}{2} = 0.92$ (a fair average value),

$$I_o = \frac{2.16}{\text{conductors per pole}} \times B_g \times \delta,$$

taking C = 1.5, an average value for machines with open stator slots and partially closed rotor slots.

Therefore $\frac{I_o}{I}$ = the per cent magnetizing current,

$$= \frac{2.16}{\text{conductors per pole} \times I} \times B_g \times \delta,$$

$$= 2.16\frac{B_g}{q} \times \frac{\delta}{\tau}. \qquad (58)$$

The minimum permissible air-gap clearance is fixed by mechanical considerations and should increase as the diameter, frame length and peripheral velocity increase, its value should not be smaller than that given by the following empirical formula:

$$\delta = 0.005 + 0.00035D_a + 0.001L_g + 0.003V, \qquad (59)$$

where δ = the air-gap clearance in inches,

D_a = the stator internal diameter in inches,

L_g = the gross iron in the frame length in inches,

V = the peripheral velocity of the rotor in thousands of feet per minute.

The ratio $\frac{I_d}{I}$ is found as follows:

$$I_d = \frac{E}{X_{eq}},$$

where $E = 2.22kZ\phi_a f \cos\frac{\theta}{2} 10^{-8}$ volts (formula (26)), page 185,

$$= 2.22kZ(B_g\tau L_g)f \cos\frac{\theta}{2} 10^{-8} \text{ volts},$$

and $X_{eq} = 2\pi f b^2 c^2 \left(\cos\frac{\theta}{2}\right)^2 pn(K_1 + K_2 L_g)10^{-8}$ ohms (formula (47)), page 368,

$$= 2\pi f Z^2 \left(\cos\frac{\theta}{2}\right)^2 n\left(\frac{K_1 + K_2 L_g}{p}\right) 10^{-8} \text{ ohms}.$$

$$\text{Therefore } \frac{I_d}{I} = \frac{2.22 \times 0.96}{0.92 \times 2\pi} \times \frac{B_g \tau L_g}{nZI} \times \frac{p}{(K_1 + K_2 L_g)},$$

$$\left(\text{again taking } \cos\frac{\theta}{2} = .92 \text{ and } k = .96\right)$$

$$= 0.366 \times \frac{B_g}{q} \times \frac{L_g}{K_1 + K_2 L_g}. \qquad (60)$$

The Value of q.—From formulæ (57), (58) and (60) it may be seen that the larger the value of q the smaller the value of $D_a^2 L_g$, the smaller the per cent magnetizing current, and the smaller the circle diameter and therefore the overload capacity. Since the copper heating depends on the ratio $\frac{\text{ampere conductors per inch}}{\text{circular mils. per ampere}}$, the larger the value of q, the greater the amount of copper

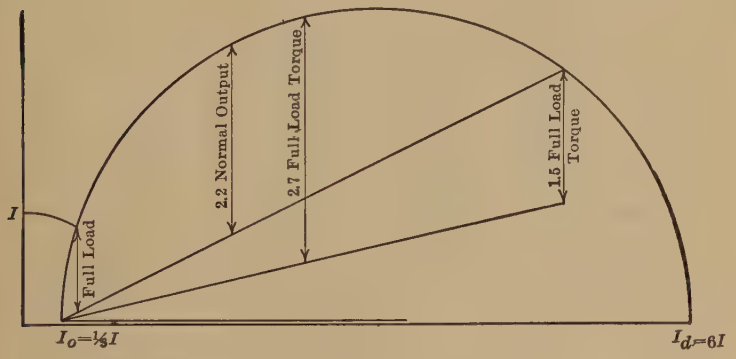

FIG. 269.—Circle diagram for an average induction motor.

required to keep the temperature rise within reasonable limits and therefore the deeper the slots and the larger the slot reactance. Figure 268 gives average values of q for both 25- and 60-cycle induction motors and this curve may be used for a first approximation.

275. Desirable Values for I_o and I_d.—Figure 269 shows the circle diagram for a reasonably good induction motor:

The power factor at full load.....	90 per cent.
The starting torque.....	1.5 times full-load torque.
The maximum torque.....	2.7 times full-load torque.
The maximum output.....	2.2 times full load.

To obtain such characteristics, the magnetizing current should not exceed one-third of full-load current, nor should the maximum current I_d be less than six times full-load current.

276. Example of Preliminary Design.—To simplify the work the necessary formulæ are gathered together below.

$$D_a^2 L_g = \frac{\text{hp.}}{\text{r.p.m.}} \times \frac{10^{12}}{2.35 B_g q \cos\phi \times \cos\frac{\theta}{2}\eta},$$

$$\frac{I_o}{I} = 2.16 \frac{B_g}{q} \times \frac{\delta}{\tau},$$

$$\frac{I_d}{I} = 0.366 \times \frac{B_g}{q} \times \frac{L_g}{K_1 + K_2 L_g},$$

where D_a = the internal diameter of the stator in inches,

L_g = the axial length of the gross iron in inches,

B_g is taken as ~~26,000~~ for 60 cycles,

29,000 for 25 cycles,

q is found from Fig. 268,

$\cos\phi$ and η are found from Fig. 267,

$$\delta = 0.005 + 0.00035 D_a + 0.001 L_g + 0.003 V,$$

where V = the peripheral velocity of the rotor in thousands of feet per minute.

K_1 and $K_2 L_g$ are found by the use of the curves in Fig. 256.

The work is carried out in tabular form as shown below, where the figures are given for a 75-hp., 60-cycle, 900-r.p.m. motor.

PRELIMINARY DESIGN SHEET

75 hp., squirrel cage, 60 cycles, 900 r.p.m.

B_g = 25,000, q = 820, $\cos\phi$ = 89 per cent, η = 89 per cent, $D_a^2 L_g$ = 2180

D_a	L_g	τ	V	δ	$K_1 + K_2 L_g$	$\frac{I_o}{I}$	$\frac{I_d}{I}$
15	9.5	5.9	3.5	0.03	3.7 + 14.6 = 18.3	0.365	5.3
17	7.5	6.7	4.0	0.03	4.0 + 10.8 = 14.8	0.32	5.2
19	6.0	7.5	4.5	0.031	4.3 + 8.1 = 12.4	0.30	5.0
21	5.0	8.2	4.9	0.032	4.5 + 6.4 = 10.9	0.28	4.7
23	4.0	9.0	5.4	0.033	4.7 + 4.8 = 9.5	0.26	4.35

So far as operation is concerned the 19-in. diameter machine is probably the best all-round machine. The 15-in. machine has the largest magnetizing current and therefore the lowest power factor while the 23-in. machine has the smallest circle diameter and therefore the smallest overload capacity.

The shop conditions must be known before the costs of the above machines can be intelligently compared. The cost of yoke, spider and housings is greatest for the 23-in. machine, and

the cost of assembling the cores is greatest for the 15-in. machine; the total cost is probably least for the 19-in. machine, but will not vary very much over the range of machines shown.

277. Detailed Design.—The work of completing the 75-hp., 60-cycle, 900-r.p.m. design is carried out in tabular form for the 440-volt, three-phase rating as follows:

STATOR DESIGN

Poles $= \frac{f \times 120}{\text{r.p.m.}}$	8.
Internal diameter of stator	19 in. from preliminary design.
Gross iron	6 in. from preliminary design.
Vent ducts	1 − 0.375 in.
Net iron = 0.93 × gross iron	5.58 in.
Pole pitch	7.46 in.
Slots per pole	12, to be suitable for two and three phase.
if chosen	6, the machine would be noisy (see Art. 271).
if chosen	18, the slots would be very narrow.
Slot pitch $= \frac{\text{pole pitch}}{\text{slots per pole}}$	0.622 in.
Slot width	0.311 = half the slot pitch for a first approximation.
Ampere conductors per inch	820 from preliminary design.
Ampere conductors per slot	510 = ampere conductors per inch × slot pitch.
Full-load current	92 amperes taking $\cos \phi = 0.89$ and $\eta = 0.89$.
Conductors per slot	$5.55 = \frac{\text{ampere conductors per slot}}{\text{full-load current}}$

To obtain the *effective* ampere conductors the actual ampere conductors considered in the foregoing discussion must be multiplied by $\cos \frac{\theta}{2}$, where θ is the stator chording factor; thus, the 5.55 conductors per slot arrived at above may be increased to 6 by using a value of $\cos \frac{\theta}{2} = 0.924$ or a coil span of three-quarters full pitch.

Connection—YY

Y, because the current has been assumed equal to line current, and two circuits in parallel, because with only 6 conductors per slot, each conductor would be too stiff to wind easily and would tend to tear the insulation when being connected to the adjacent coils.

$\frac{\text{Ampere conductors per inch}}{\text{Circular mils per ampere}}$ ..... 1.6 from Fig. 261.

Circular mils per ampere ..... 510 required.

Circular mils per conductor ..... $510 \times \frac{\text{full-load current}}{2}$

$= 510 \times \frac{92}{2} = 23{,}400.$

Size of conductor ..... 0.0185 sq. in.

Size of slot and section of conductor are worked out in tabular form thus:

0.311 in. = assumed slot width.
0.064 in. = width of slot insulation.
0.04 in. = necessary clearance.
0.207 in. = available width for copper and insulation on conductors.

Use copper strip 0.204 in. wide insulated with double cotton covering and change the slot width to 0.32 for a second approximation; therefore the size of conductor = 0.091 × 0.204 in.

0.091 in. = depth of each conductor.
0.015 in. = thickness of the cotton covering.
0.106 in. = depth of each conductor and its insulation.
0.636 in. = depth of six conductors and their insulation.
0.084 in. = depth of slot insulation on each coil.
0.720 in. = depth of insulated coil.
1.440 in. = depth of two insulated coils.
0.1 in. = thickness of stick in top of slot.
1.54 in. = necessary depth of slot.

Before fixing the slot depth, the windings for all the probable ratings to be built on this frame should be worked out and the slot made deep enough for the worst. In this case a suitable slot depth is 1.55 in.

Voltage per phase $= \frac{440}{1.73} = 254$, since the connection is Y.

Flux per pole 1.115×10^6 from formula (26) page 185:

Tooth width at one-third tooth length from air-gap = 0.335 in taking slot width = 0.32 in.

Tooth area per pole $= 0.335 \times \frac{96}{8} \times 5.6 = 22.6$ sq. in.

Maximum tooth density $= \frac{\text{flux per pole}}{\text{tooth area per pole}} \times \frac{\pi}{2}$,

$= \frac{1.115 \times 10^6}{22.6} \times \frac{3.14}{2} = 77{,}500.$

Had the density come out too high, it would have been necessary to have increased the length of the machine or decreased the slot width.

Maximum core density = 68,000 assumed,

$= \frac{\text{flux per pole}}{2 \times \text{core depth} \times \text{net iro}}$

Core depth $= \frac{1.115 \times 10^6}{2 \times 68{,}000 \times 5.6} = 1.47$ in.; use 1.45 in. to get an even figure and thus make external diameter = 25 in.

ROTOR DESIGN

Air-gap clearance..... 0.033 in. from preliminary design.
External diameter..... 18.934 in.
Gross iron..... 6 in.
Vent ducts..... $1 - \frac{3}{8}$ in.—same as stator.
Net iron..... 5.58 in. $= 6 \times 0.93$.
Number of slots..... $\frac{\text{stator slots}}{1.2}$ for quiet operation, Art. 271, p. 387.

With this number = 80 there would be 5 rotor slots for every 6 stator slots and the starting torque would not be uniform (see Art. 272, p. 388); use therefore 79 slots.

Rotor current per conductor at full load

$$= I_{11} \text{ (Fig. 234)} \times \frac{\text{total stator conductors}}{\text{total rotor conductors}}$$

where I_{11} is taken equal to $0.85 \times I$ for a first approximation, a value which must be checked after the data for the circle diagram has been calculated and the circle drawn;

$$= 0.85 \times 92 \times \frac{96 \times 6}{79},$$

$$= 570 \text{ amperes.}$$

Ampere conductors per inch $= \frac{570 \times 79}{\pi \times 19},$

$$= 755.$$

$\frac{\text{Ampere conductors per inch}}{\text{Circular mils per ampere}}$ = 2.2 approximately, 35 per cent higher than stator.

Circular mils per ampere = 342 desired.
Size of conductor = 342×570
= 195,000 cir. mils,
= 0.15 sq. in. approximately.

Size of slot must be chosen so that the flux density at the bottom of the rotor tooth shall not exceed 120,000 lines per square inch and the work is carried out as follows:

Assumed copper section.....	0.2 in.×0.75 in.	0.3 in.×0.5 in.	0.4 in.×0.35 in
Slot section to allow for insulation and clearance.....	0.25 in.×0.8 in.	0.35 in.×0.55 in.	0.45 in.×0.4 in.
Rotor diameter at bottom of slot.....	17.134 in.	17.634 in.	17.934 in.
Minimum slot pitch.....	0.68 in.	0.70 in.	0.72 in.
Minimum rotor tooth.....	0.43 in.	0.35 in.	0.27 in.
Minimum tooth area per pole.....	23.7 sq. in.	19.2 sq. in.	14.9 sq. in.
Flux per pole.....	1.115×10^6	1.115×10^6	1.115×10^6
Maximum tooth density; lines per square inch.....	74,000	91,000	118,000

The wider and shallower the slot, the lower is the rotor reactance so that the last of the three is chosen, namely, 0.45×0.4 in.

A starting torque of approximately 1.5 × full-load torque is desired, so that the rotor loss at start will have to be $1.5 \times 75 \times 0.746$ or 84 kw. This will consist of loss in both rotor bars and rotor end rings. The locked current will be approximately 90 per cent of the value found in Chap. XXIX

with reactance only, or $0.90 \times 470 = 425$ amperes. This means that the equivalent rotor resistance must be $\frac{84{,}000}{3 \times 425} = 0.155$ ohm per phase to give the required starting torque. The ratio of turns is $\frac{576 \times 0.924 \times 0.96}{79} = 6.48$ and the actual total resistance of bars and end rings must be $3 \times 0.155 \times \frac{1}{(6.48)^2} = 0.0110$ ohm.

The resistance of the bars, assuming them to be of copper, is $\frac{10.5 \times 79}{0.14 \times 1.00 \times 1.27 \times 10^6} = 0.00493$ ohm since there are 1.27×10^6 cir. mils in 1 sq. in. The resistance of the rings must make up the difference or 0.00607 ohm.

This ring resistance is $\frac{0.00607}{0.011} = 55$ per cent of the total and so the loss at start in the rings will be 55 per cent of the total 84 kw. assumed or 46 kw.

At 1 kw. per pound, the weight of each ring must be 23 lb., which, with 17.5 in. diameter gives a section of 1.3 sq. in. Substituting this in the equation for ring resistance with all values known except specific resistance of ring material,

$$R \text{ ring} = \frac{N_2^2}{\pi^2 p^2} \times \frac{2\pi D_r \times K_r}{M_r}$$

$$0.00607 = \frac{79^2}{\pi^2 \times 64} \times \frac{2\pi \times 17.5 \times K_r}{1.3 \times 1.27 \times 10^6}$$

$$K_r = 9.2$$

Standard alloy of 12 per cent conductivity with a section of 1.25 sq. in. will be used. The design is now complete and the data should be gathered in convenient form on a design sheet similar to that on page 402.

278. Design of a Wound-rotor Machine.—It is desired to design a rotor of the wound type for the 75-hp., 440-volt, three-phase, 60-cycle, 900-r.p.m. motor of which the stator data are tabulated on page 402.

The work is carried out in a similar way to that adopted for the squirrel-cage design.

Air-gap clearance	0.033 in. the same as for the squirrel-cage motor.
External diameter	18.934 in.
Gross iron	6 in.
Vent ducts	$1 - \frac{3}{8}$ in.
Net iron	5.58 in.
Number of slots	$\frac{\text{stator slots}}{1.2}$ for quiet operation. 80; use 72 or 9 slots per pole.
Conductors per slot	2, assumed; this number gives the simplest winding.
Current per conductor at full load	$0.85 \times 92 \times \frac{96 \times 6}{72 \times 2} = 312$ amperes.

Terminal voltage at standstill..... $440 \times \frac{72 \times 2}{96 \times 6 \times 0.924} = 119.$

The brushes and slip rings will be cheaper and more easily cooled if the winding is made with 4 conductors per slot, Y-connected; then

Current per conductor at full load.. 156 amperes.
Terminal voltage at standstill..... 238.
Ampere conductors per inch..... 820.
$\frac{\text{Ampere conductors per inch}}{\text{Circular mils per ampere}}$ ..... 1.6, the same as for the stator.
Circular mils per ampere desired.... 510.
Size of conductor..... $510 \times 156 = 79{,}500$ cir. mils $= 0.062$ sq. in.
Size of slot is found in the same way as for the squirrel-cage machine and that chosen in this case..... 0.42 in. × 1.35 in.
Size of conductor..... 0.125 × 0.50 in. arranged 2 wide and 2 deep
The magnetizing current..... 25 amperes, the same as for the squirrel-cage machine.
The iron loss..... 1640 watts.
The bearing friction loss..... 810 watts.

The maximum stator current is worked out in a similar way to that for the squirrel-cage machine, see Art. 253, page 363; thus for a wound-rotor machine the reactance per phase

$$= 2\pi f b^2 c^2 p^2 \left(\cos\frac{\theta}{2}\right)^2 n\left[\frac{\phi_e L_e}{2n_1 p} \times \frac{4}{3} + \left(\frac{\phi_s + \phi_z}{n_1 p} + \frac{\phi_s + \phi_z}{n_2 p} + \frac{\text{constant} \times \tau}{p \times \delta \times C_1 C_2}\right) L_g\right] 10^{-8},$$

where $\tau = 7.5$ in.,

$\frac{\phi_e L_e}{2n_1} = 4.3$ (from Fig. 256),

$\lambda_1 = 0.622$ in.

$\delta = 0.033$ in.,

$C_1 = 1.51$,

$C_2 = 1.03$,

$$\frac{\phi_s + \phi_z}{n_1 p} = \frac{1}{96}\left[3.2\left(\frac{1.3}{3 \times 0.32} + \frac{0.2}{0.32}\right) + 0.26 \times \frac{0.622}{0.033}\left(\frac{1}{1.51} + \frac{1}{1.03} - 1\right)^2\right],$$

$$= \frac{1}{96}[6.3 + 1.9] = \frac{1}{96} \times 8.2,$$

$\lambda_2 = 0.83$,

$$\frac{\phi_s + \phi_z}{n_2 p} = \frac{1}{72}\left[3.2\left(\frac{1.2}{3 \times 0.42} + \frac{0.1}{0.42} + \frac{2 \times 0.07}{0.42 + 0.1} + \frac{0.03}{0.1}\right) + 0.26 \times \frac{0.83}{0.033}\left(\frac{1}{1.51} + \frac{1}{1.03} - 1\right)^2\right],$$

$$= \frac{1}{72}(5.6 + 2.55) = \frac{1}{72} \times 8.15,$$

constant = 1.5 × 0.00107 (from p. 368),

$$X_{eq} = 2\pi \times 60 \times 6^2 \times 4^2 \times 8^2 \times 0.924^2 \times 3\left[\frac{4.3}{8} \times \frac{4}{3} + \left(\frac{8.2}{96} + \frac{8.1}{72} + 0.00107 \times 1.5 \times \frac{7.48}{8 \times 0.033 \times 1.51}\right) \times 6\right] \times 10^{-8},$$

$$= 0.355 \times [0.72 + (0.086 + 0.112 + 0.029) \times 6] \times 10^{-8},$$

$$= 0.74.$$

$$\text{Voltage} = \frac{440}{1.73} = 254.$$

Maximum current per phase $= \frac{254}{0.74} = 343$ amperes as against 470 for the squirrel-cage motor.

279. Induction-motor Design Sheet.—All dimensions in inch units.

	Stator	Squirrel Cage	Wound Rotor
External diameter	25	18.934	18.934
Internal diameter	19	15.5	13.5
Frame length	6.375	6.375	6.375
End ducts	none	none	none
Center ducts	1 − 0.375	1 − 0.375	1 − 0.375
Gross iron	6	6	6
Net iron	5.58	5.58	5.58
Slots, number	96	79	72
size	0.32 × 1.55	0.45 × 0.4	0.42 × 1.35
Conductors per slot, number	12	1	4
size	0.091 × 0.204	0.4 × 0.35	0.125 × 0.50
Winding-type	double-layer	squirrel-cage	double-layer
Winding connection	YY		Y
Minimum slot pitch	0.622	0.72	0.73
Minimum tooth width	0.302	0.27	0.31
Core depth	1.45	1.22	1.37
Pole pitch	7.46		
Minimum tooth area per pole	19.6	14.4	15
Core area	8.7	7.3	8.2
Apparent gap area per pole	45		
Flux per pole	1.115×10^6	1.115×10^6	1.115×10^6
Maximum tooth density	79,000	119,000	99,000
Maximum core density	68,000	82,000	73,000
Ampere conductors per inch	820	755	820
Circular mils per ampere	510	400	510
Length of conductors	17.7	10.5	19
Section of each end connector		1.25 sq. in.	
Resistance factor		8.3	
Maximum ring loss		46 kw.	
Apparent gap density	25,000		
Air-gap clearance	0.033		
Carter coefficient	1.51	1.03	1.03

	Stator	Squirrel Cage	Wound Rotor
Magnetizing current, gap	22.2		
total	25.5		
$K_1 + K_2L_g$	12	....	16.75 stator
Reactance per phase	0.54	....	0.74 stator
Maximum line current I_d	470	2880	345 stator
Rating			
Horsepower	75		
Terminal voltage	440		
Amperes, full load	92	575	158
Phases	3		
Frequency	60		
Synchronous r.p.m	900		
Poles	8		

280. Design of a 25-cycle Motor.—It is required to design a motor of the following rating: 75 hp., 440 volts, three phase, 25 cycle, 750 r.p.m., squirrel cage.

Preliminary Design Sheet

$B_g = 29{,}000$; $q = 820$; $\cos \phi = 90$ per cent; $\eta = 89$ per cent; $D_a^2L_g = 2200$

D_a	L_g	τ	V	δ	$K_1 + K_2L_g$	$\frac{I_o}{I}$	$\frac{I_d}{I}$
13	13	10.2	2.55	0.30	5.0 + 14.4 = 19.4	0.24	8.0
15	9.75	11.8	2.95	0.29	5.4 + 10.0 = 15.4	0.21	7.5
17	7.6	13.3	3.34	0.28	5.7 + 7.2 = 12.9	0.17	7.1
19	6.1	14.9	3.74	0.29	6.0 + 5.4 = 11.4	0.16	6.4
21	5.0	16.5	4.12	0.30	6.4 + 4.2 = 10.6	0.15	5.7

Any one of these machines would be satisfactory as far as magnetizing current and overload capacity are concerned. The 13-in. machine, however, is long and difficult to ventilate properly so that it need not be considered. Of the others, the machine with the smallest diameter will generally be the cheapest so that the choice lies between the 15- and the 17-in. machine; there will be very little difference in cost between the two, but the 17-in. machine will be the easier to ventilate properly and will have the better appearance.

Detailed Design for the 17-in. Machine.—Since the per cent magnetizing current is small, it will be advisable to increase the air-gap over the minimum value of 0.029 in.; it may be taken = 0.04 in. without making the magnetizing current too large or the power factor at full load too low.

Poles	4.
Internal diameter of stator	17 in.
Gross iron	7.5 in.
Vent ducts	2–0.5 in.
Net iron	7.0 in.
Slots per pole	12 or 18.
slot pitch	1.12 in. 0.74 in.
ampere conductors per slot	920 610
$\frac{\text{ampere conductors per slot}}{\text{air-gap clearance}}$	23×10^3 15×10^3.
	Noisy Quiet (see Art. 271 p. 387).
Slots per pole	18, suitable for both two- and three-phase.
Pole pitch	13.4 in.
Slot pitch	0.74 in.
Slot width	0.375 in.
Ampere conductors per inch	820 from preliminary design.
Ampere conductors per slot	610.
Full-load current	91 amperes
Conductors per slot	6.7 if Y connected
	11.5 if Δ connected: this may be increased to 12 per slot if span of coil is made five-sixths full pitch; $\cos \frac{5 \times 90}{6} = \cos 75° = 0.966$
$\frac{\text{Ampere conductors per inch}}{\text{Circular mils per ampere}}$ (Fig. 261)	1.3.
Circular mils per ampere	625.
Amperes per conductor	52 for Δ-connected winding.
Circular mils per conductor	32,500
Section of conductor	0.0255 sq. inches = 0.102 × 0.258 in.
Size of slot	0.375 × 1.75 in.
Flux per pole	2.97×10^6
Volts per phase	440 (Δ connected)
Minimum tooth width	0.365 in.
Minimum tooth area per pole	46.0 sq. in.
Maximum tooth density	98,000.

The rotor of this machine may be designed by the same method as used in the 60-cycle design in Art. 277; the probable number of slots = 59.

281. Variation in the Length of a Machine for a Given Diameter.—In order to save on the original outlay for the tools required to build a line of induction motors, it is advisable to design at least two or three lengths of machine for each diameter. In the case of small factories, where the total output is not very large, three different frame lengths may be used for each diameter.

The principal dimensions of three squirrel-cage machines built on a 19-in. diameter for eight poles, 60 cycles and 900 r.p.m. are tabulated below.

External diameter of stator	25 in.	25 in.	25 in.
Internal diameter of stator.	19 in.	19 in.	19 in.
Frame length	4.5 in.	6.375 in.	8.125 in.
Center ducts	none	1–0.375 in	1–0.375 in.
Gross iron	4.5 in.	6 in.	7.75 in.
Net iron	4.2 in.	5.6 in.	7.2 in.
Slots	96	96	96
Size of slot	0.32 in. × 1.55 in.	0.32 in. × 1.55 in.	0.32 in. × 1.55 in.
Conductor per slot	8	12	8
Stator coil span	¾ pitch	¾ pitch	¾ pitch
Size of conductors	0.129 × 0.204	0.091 × 0.204	0.129 × 0.204
Connection	Y	YY	Δ
Ampere conductors per inch	780	820	850
Circular mils per ampere	520	510	465
Amperes per conductor	64	46	71.6
Amperes per terminal	64	92	123
Terminal voltage	440	440	440
Phases	3	3	3
Output	50 hp.	75 hp.	100 hp.
Air-gap clearance	0.033 in.	0.033 in.	0.0033 in.
Magnetizing current	19 amperes	25 amperes	32 amperes
K_1 actual (see Fig. 257, p. 369)	4.30	4.30	4.30
K_2L_g actual	5.90	7.90	9.90
Reactance per phase in ohms	0.78	0.53	1.08
Maximum current in line	320 amperes	470 amperes	710 amperes
Magnetizing current	30 per cent	27 per cent	26 per cent
Maximum current	5.0 full load	5.1 full load	5.8 full load

The above machines are discussed under the following heads:

Conductors per Slot.—Since the same stator punchings are used in each case, the number of slots is fixed, and for the same flux density in the different machines the flux per pole must be directly proportional to the net iron. Now the voltage per conductor is proportional to the flux per pole, so that the number of conductors in series, for the same voltage per phase, must be inversely proportional to the flux per pole and therefore inversely proportional to the net iron in the frame length.

Size of Conductor.—This is inversely proportional to the number of conductors per slot for the same total copper section per slot.

Current Rating.—For the same current density in the conductors, the current in each conductor must be proportional to the conductor section. If the connection is Y, the current rating is the same as the current per conductor; if the connection is Δ, the current rating $= 1.73$ times the current per conductor.

Output.—For the same total section of copper, the output of the machine is proportional to the net iron in the frame length, because output = a constant $\times$ phases $\times$ volts per phase $\times$ current per phase,

$$= \text{a constant} \times n \times Z\phi_a \times I_c,$$
$$= \text{a constant} \times nZI_c \times \phi_a,$$
$$= \text{a constant} \times \text{total copper section} \times L_n.$$

$$\text{Magnetizing Current} = \frac{1}{0.87 \times \text{conductors per pole} \times \cos\frac{\theta}{2}} \times$$

$B_g \times \delta \times C$, and since B_g, δ, $\cos\frac{\theta}{2}$ and C are all constant, the magnetizing current is inversely proportional to the number of conductors per pole and therefore to the number of conductors per slot.

Maximum Current.—The leakage flux per phase is made up of two parts, the end-connection leakage which is independent of the frame length, and the slot and zigzag leakages which are directly proportional to the frame length. The reactance per

$$\text{phase} = 2\pi f b^2 c^2 \left(\cos\frac{\theta}{2}\right)^2 pn(K_1 + K_2 L_g)10^{-8}$$
$$= \text{a constant} \times b^2(K_1 + K_2 L_g)$$

for machines built with the same punchings and same coil span.

From the data in the table it may be seen that, so far as magnetizing current and overload capacity are concerned, the longest machine is the best; but a machine cannot be lengthened indefinitely because a point is finally reached at which it becomes impossible to cool the center of the core properly, without considerable modification in the type of construction. Even before this point is reached, it will generally be found economical to increase the diameter rather than keep on increasing the length, because, since the output is proportional to $D_a^2 L_g$, an increase in diameter of 10 per cent is equivalent to an increase in frame length of 22 per cent.

282. Windings for Different Voltages.—The stator of a 50-hp., 440-volt, three-phase, 64-ampere, 60-cycle, 900-r.p.m. induction motor is constructed as follows:

Internal diameter of stator	19 in.
Frame length	4.5 in.
Slots, number	96.
Slots, size	0.32 × 1.55 in.
Conductors per slot, number	8.
size	0.129 × 0.204.
Connection	Y.

It is required to design windings for the following voltages:
220 volts, three phase, 60 cycles,
550 volts, three phase, 60 cycles,
250 volts, three phase, 60 cycles,
550 volts, two phase, 60 cycles.

Conductors per Slot.

$$E = 2.22kZ \cos\frac{\theta}{2}\,\phi_a f 10^{-8} \text{ volts},$$

$$= \text{a constant} \times k \times \frac{\text{conductors per slot}}{\text{phases}} \times \cos\frac{\theta}{2} \text{ for a given}$$

frame and frequency.

For the machine in question $k = 0.958$ for three-phase windings,
$= 0.903$ for two-phase windings,

$$\text{and the constant} = \frac{\text{volts per phase} \times \text{phases},}{k \times \text{conductors per slot} \times \cos\frac{\theta}{2}},$$

$$= \frac{\frac{440}{1.73} \times 3,}{0.956 \times 8 \times \text{chord factor for three-phase Y.}}$$

$$= 99.4 \div \text{chord factor for three-phase Y.}$$

The windings for the different voltages may be tabulated thus:

Terminal voltage	Phases	Volts per phase	Conductors per slot times chord factor	Stator coil span	Chord factor	Conductors per slot	Connection
440	3	254	7.39	¾ pitch	0.924	8	Y
220	3	127	3.69	¾ pitch	0.924	4	YY
550	3	320	9.24	¾ pitch	0.924	10	Y
250	3	144 Y	4.2	7/12 pitch	0.79	5	?
		250 Δ	7.28	¾ pitch	0.924	8	Δ
550	2	550	11.3	¾ pitch	0.924	12	series

Size of Conductor.—This must be chosen so that the stator copper loss and copper heating are the same for each voltage; that this may be the case it is necessary to keep the ratio

$\frac{\text{ampere conductors per inch}}{\text{circular mils per ampere}}$ constant. The work is carried out in tabular form thus:

Terminal voltage	Phases	Current per terminal	Current per conductor	Conductors per slot	Connection	Ampere conductors per inch	Circular mils per ampere	Conductor size
440	3	64	64	8	Y	825	525	0.129 × 0.204
220	3	128	64	8	YY	825	525	0.129 × 0.204
550	3	51	51	10	Y	820	520	0.102 × 0.204
250	3	113	65	8	Δ	835	515	0.129 × 0.204
550	2	44	44	12	series	850	530	0.091 × 0.204

The rotor winding is the same for all stator voltages and phases, because the only connection between the stator and rotor is the flux in the air-gap, and this is kept constant by the use of the proper number of stator conductors per slot. It is therefore possible to build motors for stock, complete except for the stator winding, which winding can be specified when the voltage and number of phases on which the machine will operate are known.

It must not be imagined that the designs which have been worked out in this chapter are the only ones that could have been used. Electrical design is very flexible, and different values for flux density and ampere conductors per inch might have been used to give a satisfactory machine, and perhaps a cheaper one.

When one design for a given rating is worked out completely, the designer has to go over it and try the effect of changing the different quantities until he is satisfied that, for the shop in which machines of his design will be built, the final design will give the most satisfactory machine both as regards manufacturing cost and reliability when in service.

CHAPTER XXXIV

SPECIAL PROBLEMS IN INDUCTION MOTOR DESIGN

283. Slow-speed Motors.

Since $\frac{I_o}{I} = 2.16\frac{B_g\delta}{q\tau}$ (formula (58), p. 394)

and $\frac{I_d}{I} = 0.366\frac{B_gL_g}{q(K_1 + K_2L_g)}$ (formula (60), p. 395),

therefore $\frac{I_d}{I_o} = \text{a constant}\ \frac{\tau L_g}{\delta(K_1 + K_2L_g)}$ (61)

and the ratio $\frac{I_d}{I_o}$ depends largely on the ratio $\frac{\tau}{\delta}$.

In moderate-speed machines $\frac{I_d}{I_o} = \frac{\text{6 full-load current}}{\text{0.33 full-load current}} = 18.$ In high-speed machines the dimensions are small and the peripheral velocity high, so that the ratio $\frac{\tau}{\delta}$ is generally large, since the value of τ is directly proportional to the peripheral velocity and the value of δ increases with the dimensions of the machine. Such machines therefore have a large value of I_d and a large overload capacity; they have also a small value of I_o and a high power factor.

In the case of slow-speed machines, the dimensions are large so as to get the necessary radiating surface, and the peripheral velocity is generally low because of the large number of poles. Because of the small pole pitch the ratio $\frac{I_d}{I_o}$ is small, and the characteristics of the machine are small overload capacity, large magnetizing current and low power factor.

Compare, for example, the preliminary designs for machines of 300-hp. output, 60 cycles and 720 and 300 r.p.m., respectively.

Horsepower	300	300
Frequency	60	60
R.p.m.	720	300
B_g	23,000	23,000
q	730	730
cos ϕ, assumed	91 per cent	84 per cent

η assumed	91 per cent	90 per cent
$D_a^2L_g$	12,700	33,500
D_a	36 in.	65 in.
L_g	10 in.	8 in.
τ	11.3 in.	8.5 in.
V in thousands of feet per minute	6.8	5.1
δ	0.048 in.	0.051 in.
K_1	5.3	4.5
K_2L_g	10.5	10
$K_1 + K_2L_g$	15.8	14.5
$\frac{I_o}{I}$	0.275	0.39
$\frac{I_d}{I}$	6.7	5.9

These two machines are shown to scale in Fig. 270.

The above figures show that, the higher the speed for a given horsepower, the smaller is the magnetizing current and the larger the overload capacity; this is a characteristic property which cannot be changed except by the use of air-gaps on the slow-speed machines which are not large enough for mechanical purposes.

For slow-speed motors the use of 25 cycles offers considerable advantage over the use of 60 cycles because, for the same r.p.m., the number of poles is the smaller in the case of the 25-cycle motor and therefore the pole pitch and the ratio $\frac{I_d}{I_o}$ are the larger. Compare for example the preliminary designs for machines of 300 hp. at 300 r.p.m., for 25- and 60-cycle operation, respectively.

Horsepower	300	300
Frequency	60	25
R.p.m.	300	300
Poles	24	10
B_g	23,000	27,000
q	730	730
cos ϕ, assumed	84 per cent	90 per cent
η, assumed	90 per cent	90 per cent
$D_a^2L_g$	33,500	26,500
D_a	65 in.	46 in.
L_g	8 in.	12.5 in.
τ	8.5 in.	14.5 in.
V, in thousands of feet per minute	5.1	3.6
δ	0.051 in.	0.045 in.
K_1	4.5	5.9
K_2L_g	10	11.3

$K_1 + K_2 L_g$	14.5	17.2
$\frac{I_o}{I}$	0.39	0.235
$\frac{I_d}{I}$	5.9	9.0

When most of the motors that are to be used are slow-speed machines, that is, they lie below the speed curve *b* in Fig. 267, then 25-cycle apparatus will have a comparatively high power factor and overload capacity, while for 60-cycle apparatus these will be low.

284. Closed-slot Machines.—By the use of closed slots for both stator and rotor the characteristics of slow-speed machines can be considerably improved. The only objection to the use of closed slots for the stator is that the windings are difficult to repair in case of break-down. There is not the same objection to their use for the rotor because, in the case of the squirrel-cage machine, there is only one conductor per slot and this is put in from the end, while in the case of the wound-rotor machine the winding can be chosen with two or four conductors per slot which can be formed to shape at one end, the slot part and one end insulated, and the other end bent to shape and insulated after the conductor has been pushed into place. There is no connection between the stator applied voltage and the rotor voltage at standstill; this latter voltage can be kept low by the use of a small number of rotor conductors per slot. When the machine is up to speed and the rotor short-circuited, the voltage between the rotor windings and the core is very low and the chance of break-down small.

By the use of closed slots the air-gap area is increased, and the magnetizing current decreased for the same winding, the slot leakage and zigzag leakage are increased and the overload capacity reduced; as a rule the increase in leakage is not as large as the decrease in magnetizing current.

The following table shows comparative designs for a 300-hp., 440-volt, three-phase, 60-cycle, 300-r.p.m. motor; the one design has open stator slots and the other closed stator slots; the rotor is of the squirrel-cage type in each case and has closed slots. The designs need not be worked through carefully, but it is necessary to understand the conclusions tabulated at the end of the design sheet.

Inch Units Are Used	A Open-slot Stator	B Closed-slot Stator	A Rotor	B Rotor
External diameter	72	63	64.9	56.9
Internal diameter	65	57	61	53
Frame length	9.5	11	9.5	11
End ducts	2–0.5	2–0.5	none	none
Center ducts	2–0.5	2–0.5	2–0.5	2–0.5
Gross iron	8.5	10	8.5	10
Net iron	7.6	9	7.6	9
Slots, number	288	288	220	220
size	0.35 × 1.5	0.31 × 1.6	0.55 × 0.45	0.45 × 0.45
Conductors per slot, number	2	2	1	1
size	0.23 × 0.5	0.2 × 0.5	0.5 × 0.4	0.4 × 0.4
Winding, type	double layer	double layer	squirrel cage	squirrel cage
connection	Δ	YY		
Minimum slot pitch	0.71	0.62	0.91	0.8
Minimum tooth width	0.36	0.31	0.36	0.35
Core depth	2	1.4	1.4	1.4
Pole pitch	8.5	7.45		
Minimum tooth area per pole	33	33.5	25	29
Core area	15.2	12.6	10.6	12.6
Apparent gap area per pole	72.5	74.5		
Flux per pole	1.8×10^6	2.08×10^6	1.8×10^6	2.08×10^6
Maximum tooth density	85,000	97,000	113,000	113,000
Maximum core density	59,000	82,000	85,000	83,000
Ampere conductors per inch	660	640	520	510
Circular mils per ampere	630	640	520	490
Apparent gap density	25,000	28,000		
Air-gap clearance	0.05	0.05		
Carter coefficient	1.4	1.04	1.02	1.02
Magnetizing current, gap	145, terminal	140, terminal		
total	175	168		
K_1	4.5	4.2		
K_2L_g	10.2	16.4		
Maximum line current, I_s	3000	2800		
Horsepower	300	300		
Terminal voltage	440	440		
Amperes, full load	400	400	485	415
Phases	3	3		
Frequency	60	60		
Synchronous r.p.m.	300	300		
Poles	24	24		

Reactance per phase =

$$2\pi f b^2 c^2 p^2 \left(\cos\frac{\theta}{2}\right) n\left[\frac{\phi_e L_e}{2n_1 p} + \left(\frac{\phi_s+\phi_z}{n_1 p} + \frac{\phi_s+\phi_z}{n_2 p}\right) L_g\right] 10^{-8}$$

where for machine A

$$\frac{\phi_e L_e}{2n_1} = 4.5,$$

$$\frac{\phi_s+\phi_z}{n_1 p} = \frac{1}{288}\left[3.2\left(\frac{1.3}{3\times 0.35}+\frac{0.2}{0.35}\right)+0.26\frac{0.71}{0.05}\left(\frac{1}{1.4}+\frac{1}{1.02}-1\right)^2\right] = \frac{7.56}{288},$$

$$\frac{\phi_s+\phi_z}{n_2 p} = \frac{1}{220}\left[3.2\left(\frac{0.45}{3\times 0.55}+\frac{2\times 0.07}{0.55+0.07}+\frac{0.03}{0.07}\right)+ 0.26\times\frac{0.93}{0.05}\left(\frac{1}{1.4}+\frac{1}{1.02}=-1\right)^2\right] = \frac{5.25}{220}.$$

Taking $\theta = 180$ deg.

Reactance per phase $= 2\pi \times 60 \times 2^2 \times 4^2 \times 24^2 \times 3\left[\frac{4.5}{24} + \left(\frac{7.56}{288} + \frac{5.25}{220}\right)8.5\right]10^{-8}$,

$= 0.256$.

Voltage per phase $= 440$ for Δ-connection.

Maximum current per phase $= \frac{440}{0.256}$,

$= 1720$ amperes.

Maximum line current $= 1720 \times 1.73$,

$= 3000$ amperes.

For machine B

$$\frac{\phi_e L_e}{2n} = 4.2,$$

$$\frac{\phi_s + \phi_z}{n_1 p} = \frac{1}{288}\left[3.2\left(\frac{1.5}{3 \times 0.31} + \frac{2 \times 0.07}{0.31 + 0.1} + \frac{0.03}{0.1}\right) + 0.26\frac{0.62}{0.05}\left(\frac{1}{1.04} + \frac{1}{1.02} - 1\right)^2\right] = \frac{10.5}{288},$$

$$\frac{\phi_s + \phi_z}{n_2 p} = \frac{1}{220}\left[3.2\left(\frac{0.45}{3 \times 0.45} + \frac{2 \times 0.07}{0.45 + 0.07} + \frac{0.03}{0.07}\right) + 0.26\frac{0.81}{0.05}\left(\frac{1}{1.04} + \frac{1}{1.02} - 1\right)^2\right] = \frac{7.0}{220}.$$

Taking $b = 180$ deg.

Reactance per phase $= 2\pi \times 60 \times 1^2 \times 4^2 \times 24^2 \times 3\left[\frac{4.2}{24} + \left(\frac{10.5}{288} + \frac{7.0}{220}\right)10\right]10^{-8}$,

$= 0.09$.

Voltage per phase $= \frac{440}{1.73} = 254$ for a Y-connection.

Maximum current per phase $= \frac{254}{0.09}$,

$= 2800$,

$=$ maximum line current.

The points of importance in the above designs are:

	Open Slot	Closed Slot
Flux density, stator teeth	85,000	97,000
Flux density, stator core	59,000	82,000
Core depth	2.0 in.	1.4 in.
Carter coefficient	1.4	1.04
Conductors per slot	$2\Delta = 1.16Y$	$2YY = 1Y$
Internal diameter of stator	65 in.	57 in.
Flux per pole	1.8×10^6	2.08×10^6
Magnetizing current	175 amperes	168 amperes
$K_2 L_g$	10.2	16.4
Maximum current	3000	2800

When closed slots are used, the flux density may be high, since the pulsation loss is almost entirely eliminated.

The value of the Carter fringing coefficient is decreased and therefore the magnetizing current is reduced for the same winding or, as in the above machines, the number of conductors is reduced for the same magnetizing current.

Because of the reduction in the number of conductors the stator internal diameter is decreased for the same value of q, the ampere conductors per inch.

Because of the reduced number of conductors the reactance of the winding is decreased, and because of the increase in the slot and the zigzag leakage, due to the closing of the slot, the reactance is increased.

The final result is that the closed-slot machine is smaller and cheaper than the open-slot machine, especially if, as in Europe, the cost of winding labor is cheap; it has the same characteristics as the open-slot machine.

If the closed-slot machine were made on the same diameter as the open-slot machine, it would have the better characteristics.

285. High-speed Motors.—The number of speeds in the useful range for small belted motors is smaller for 25 than for 60 cycles, as may be seen from the following table:

Poles	Revolutions per minute	
	60 cycles	25 cycles
2	3600	1500
4	1800	750
6	1200	500
8	900	375
10	720	300

For that reason, and also because they are cheaper than 25-cycle motors of the same speed, 60-cycle motors should be used where most of the driven machines are moderate-speed belted machines.

Compare, for example, the preliminary design for a 300-hp., 60-cycle, 720-r.p.m. machine with that for a 300-hp., 25-cycle, 750-r.p.m. machine.

Horsepower	300	300
Frequency	60	25
R.p.m.	720	750
Poles	10	4

B_g	23,000	27,000
q	730	730
cos ϕ, assumed	91 per cent	92 per cent
η, assumed	91 per cent	91 per cent
$D^2_a L_g$	12,700	10,300
D_a	36 in.	27 in.
L_g	10 in.	14 in.
τ	11.3 in.	21 in.
V, in thousands of feet per minute	6.8	5.3
δ	0.048 in.	0.045 in.
K_1	5.3	7
$K_2 L_g$	10.5	10.2
$K_1 + K_2 L_g$	15.8	17.2
$\frac{I_o}{I}$	0.275	0.16
$\frac{I_d}{I}$	6.7	10.2

These two machines are shown to scale in Fig. 270.

Since the magnetizing current of the 25-cycle machine is so small, it will be advisable to increase the air-gap clearance and thereby have less chance of mechanical trouble.

Because the 25-cycle machine has the smaller diameter, it must not be imagined that it is the cheaper machine. It has the smaller number of poles, the larger flux per pole and, therefore, the deeper core. Due to the large pole pitch the end connections are long, and due to the lower peripheral velocity and the greater difficulty in cooling the long machine, a large section of copper and deep slots are necessary. These facts are shown by the following table:

Horsepower	300	300
R.p.m.	720	750
Poles	10	4
Pole pitch	11.3 in.	21 in.
Gross iron	10 in.	14 in.
Flux per pole $= B_g \tau L_g$	2.6×10^6	8.0×10^6
Stator core density, assumed	65,000	85,000
Necessary core area	20 sq. in.	47 sq. in.
Core depth	2.25 in.	3.75 in.
Rotor core density, assumed	85,000	85,000
Necessary core area	15 sq. in.	47 sq. in.
Core depth	1.7 in.	3.75 in.
Length of stator conductor	30 in.	48 in. from Fig. 88.

A section through the two machines is shown to scale in Fig. 270, from which it may be seen that the 25-cycle motor has the

larger amount of material in it, and will probably be the more expensive machine.

In the case of large high-speed motors, such as those for direct connection to centrifugal pumps or for motor generator sets, care must be taken in the design to insure that the machines will be quiet in operation.

Consider, for example, the design of a direct connected wound-rotor motor of the following rating: 1000 hp., 60 cycles, 900 r.p.m.

PRELIMINARY DESIGN SHEET

$B_g = 24{,}000$, $q = 800$, $\cos \phi = 92$ per cent, $\eta = 92$ per cent, $D_a^2 L_g = 29{,}000$

D_a	L_g	τ	V	δ	$K_1 + K_2 L_g$	$\frac{I_o}{I}$	$\frac{I_d}{I}$
32	28.5	12.6	7.55	0.067	7.5 + 36 = 43.5	0.33	6.6
36	22.5	14.1	8.45	0.065	7.7 + 27 = 34.7	0.28	6.6
40	18.0	15.7	9.40	0.065	8.3 + 20.5 = 28.8	0.26	6.3
44	15.0	17.2	10.3	0.066	8.6 + 17 = 25.6	0.24	6.0

When using the curves in Fig. 256 to determine K_1 and K_2, it should be noted that, for wound-rotor machines, the values of K_1 found from the curve must be multiplied by four-thirds, and the values of K_2 must be taken from the upper curve.

In order that the noise of the machine be not objectionable at no load, the peripheral velocity should, if possible, be less than 8000 ft. per minute and the pitch of the windage note should be kept below 1400 cycles per second. The number of rotor slots per pole to satisfy this latter condition may be found from formula (56), page 385, namely:

frequency of windage note = rotor slots $\times$ revolutions per second
= 1440 if 12 slots per pole are used.

For quiet operation at full load, the number of slots per pole for the stator should exceed that for the rotor by about 20 per cent (see Art. 271, p. 387).

For machines with 15 slots per pole, the values of the stator slot pitch $= \frac{\pi D_a}{8 \times 15}$, of the ampere conductors per slot $= q \times \lambda$, and of the ratio $\frac{\text{ampere conductors per slot}}{\text{air-gap clearance}}$ on which the noise at full load largely depends, are given in the following table:

D_a	λ_1	Ampere conductors per slot	δ	Ampere conductors per slot / δ
32	0.84	670	0.067	10.0
36	0.94	750	0.065	11.5
40	1.05	840	0.065	12.8
44	1.15	920	0.066	13.8

The last of these machines is close to the noise limit, and the first is too long to ventilate properly, so that the choice lies between a machine of 36-in. and one of 40-in. diameter. If the designer has been troubled with noisy machines, he will probably choose that with the smaller diameter, because it will have the lower peripheral velocity, and, therefore, the lower intensity of windage note. If he is satisfied, from experience with other high-speed machines which have been built and tested, that the 40-in. motor will not be noisy, then it will probably be chosen because it is shorter and easier to ventilate.

The rating of 1000 hp. is about the highest that can safely be built at 900 r.p.m. with the open type of construction, since a machine of larger diameter is liable to give trouble due to noise, and a longer machine is liable to get hot at the centre of the core. A larger diameter and a higher peripheral velocity may be used if the motor is partially enclosed, so as to muffle the noise, and then cooled by forced ventilation.

286. Two-pole Motors.—Since, for induction motors operating on 25 cycles, there is no available speed between 1500 and 750 r.p.m., the former speed is largely used for motors that are direct connected to centrifugal pumps, and would also be largely used for small belted motors were it not that the cost of a 1500-r.p.m. motor is seldom less than that of a 750-r.p.m. machine of the same horsepower.

Consider, for example, comparative designs for a 300-hp., 25-cycle induction motor at 1500 and at 750 r.p.m., respectively.

Horsepower	300	300
R.p.m.	750	1500
Poles	4	2
B_g	27,000	27,000
q	730	730
cos ϕ, assumed	92	93

η, assumed	91	90
$D_a^2L_g$	10,300	5100
D_a	27 in.	18 in.
L_g	14 in.	16 in.
τ	21 in.	28 in.
V, in thousands of feet per minute	5.3	7.0
δ	0.045 in.	0.048 in.
K_1	7	8
K_2L_g	10.2	9.3
$K_1 + K_2L_g$	17.2	17.3
$\frac{I_e}{I}$	0.16	0.13
$\frac{I_d}{I}$	10.2	11.5
Flux per pole	8.0×10^6	12.0×10^6
Core density; lines per square inch	85,000	85,000
Core area	47 sq. in.	71 sq. in.
Core depth	3.75 in.	5 in.
Length of stator conductor	48 in.	62 in.

Some idea as to the relative proportions of these two machines may be obtained from Fig. 270.

When full-pitch windings are used for induction-motor stators, the revolving field consists of a fundamental and harmonics. If there is a pronounced nth harmonic, the resultant revolving field may be considered as the resultant of a fundamental which revolves at synchronous speed, and of a harmonic which revolves at n times synchronous speed; if these fields move in the same direction the resultant torque curve will be curve 3, Fig. 271, which is made up of curves 1 and 2, due to the fundamental and the harmonic, respectively. One of the characteristics of the two-pole motor, and particularly of the two-pole, 25-cycle motor, is its large pole pitch and consequent large overload capacity, so that for such machines, when of the squirrel-cage type and designed with small slip in order to obtain high efficiency, the overload torque ab of the harmonic may become comparable with the normal torque of the fundamental, and in such a case the motor will run at a speed m, which is approximately $\frac{1}{n}$th of synchronous speed, and is called a sub-synchronous speed.

This sub-synchronous locking speed may be eliminated by the use of a high-resistance rotor, which raises the part cd of curve 1 without affecting the overload torque; an extreme case of a high-resistance rotor is a rotor of the wound type. Another way

to eliminate these locking speeds is to eliminate the harmonics by the use of a short-pitch winding in the stator. As shown in Art. 137 page 182, a shortening of the pitch of an alternator winding by $\frac{1}{n}$th of the full pitch will eliminate the nth harmonic. Similarly, a shortening of the span of the coils in an induction motor winding by $\frac{1}{n}$th of the pitch will eliminate all effects of

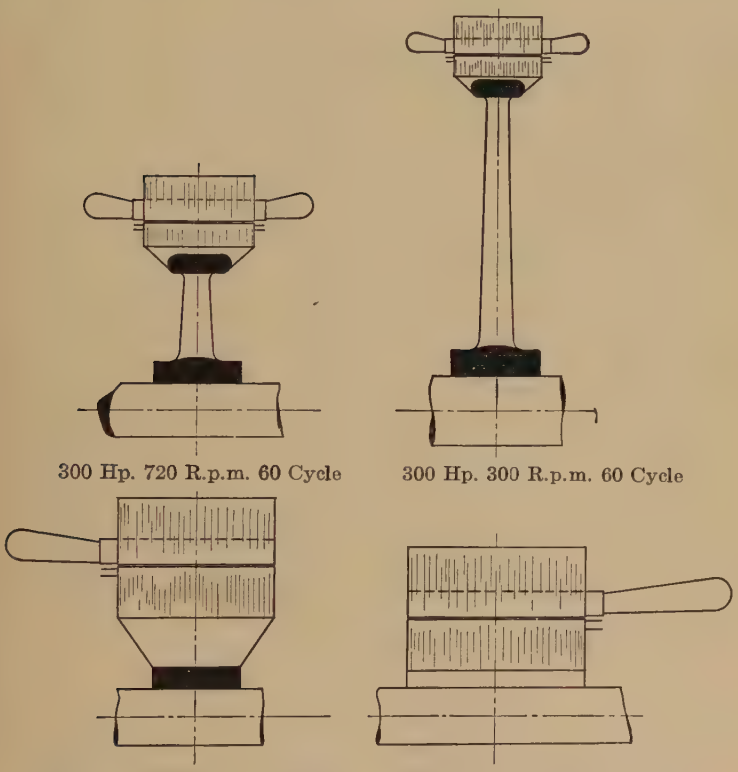

FIG. 270.—300 hp. induction motors for different speeds and frequencies.

the nth harmonic on that machine. Furthermore, there are other advantages in a short-pitch winding for an induction motor. The main advantage is that the length of the end connections of the coils is reduced. The length of these end connections is proportional to the span of the coil; with a coil span of two-thirds full pitch, for instance, the length of the end

connections is only two-thirds of what it would be if a full-pitch winding were used. Thus, there is a saving in copper losses by shortening the coil span. A still greater advantage is the possibility of shortening the distance between bearings because of the shortened overhang of the end connections. This is of particular importance in high-speed motors where the pole pitch is large.

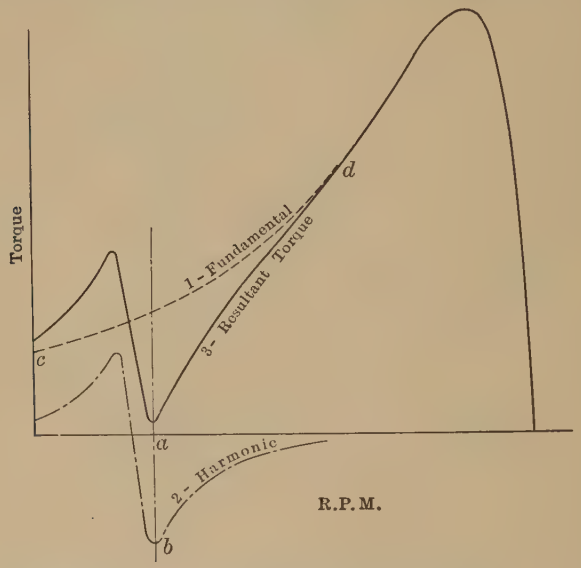

FIG. 271.—Speed torque curve for a motor with harmonics in the wave of flux distribution.

287. Effect of Variations in Voltage and Frequency on the Operation.—For a given machine

$$E = \text{a constant} \times \phi_a \times f,$$
$$I_o = \text{a constant} \times \phi_a,$$
$$X_{eq} = \text{a constant} \times f,$$
$$I_d = \frac{E}{X_{eq}} = \text{a constant} \times \phi_a.$$

If the voltage applied to the motor terminals is reduced, the value of ϕ_a, the flux per pole, will be reduced, and therefore,
I_o will be reduced and the power factor improved;
I_d will be reduced and the overload capacity decreased.
The flux density will be reduced, the current will be increased for the same output, and the result will probably be increased heating and a liability to pull out of step.

If the voltage be increased, the value of the flux per pole will be increased and therefore,

I_o will be increased and the power factor decreased;

I_d will be increased and so also will be the overload capacity.

The flux density will be increased, but the current will be reduced for the same rating; this may result in increased or in decreased heating depending on whether the iron loss or the copper loss is the greater at normal voltage.

If the frequency of the applied voltage be reduced, the voltage being unchanged, then the flux per pole will be increased and so also will be the magnetizing current and the overload capacity. The core loss and copper loss will be practically unchanged, but the heating will be increased due to the reduction in speed.

If the frequency be increased, the voltage being unchanged, then the flux per pole will be reduced and so also will be the magnetizing current and the overload capacity. The core loss and copper loss will be unchanged and the heating reduced because of the increase in speed, but the rating of the motor cannot be increased because of the reduced overload capacity.

If the voltage and frequency both increase or decrease together, then, for a change of 10 per cent, the characteristics of the machine are not changed; thus it is possible to sell 440-volt 60-cycle motors for operation on 400 volts and 50 cycles, with the same guarantee in each case except that of heating; the temperature will increase due to the increase in current and to the decrease in speed.

CHAPTER XXXV

TRANSFORMERS

OPERATION OF TRANSFORMERS

288. No-load Conditions.—Figure 272 shows a transformer diagrammatically; the two windings, which have T_1 and T_2 turns, respectively, are wound on an iron core C.

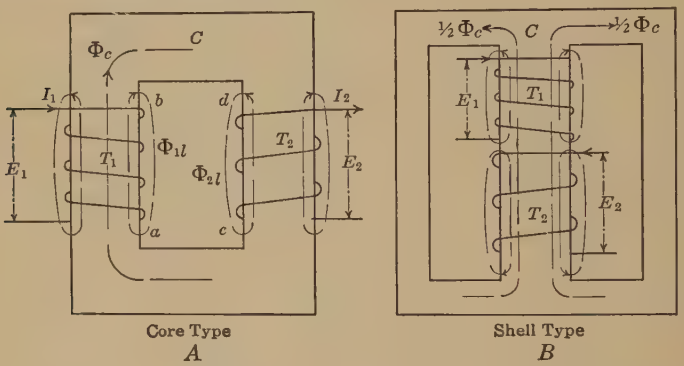

FIG. 272.—Diagrammatic representation of transformers.

An alternating voltage E_1, applied to the primary coil T_1, causes a current I_e, called the exciting current, to flow in the coil; this current produces in the core an alternating flux, ϕ_{co}. The

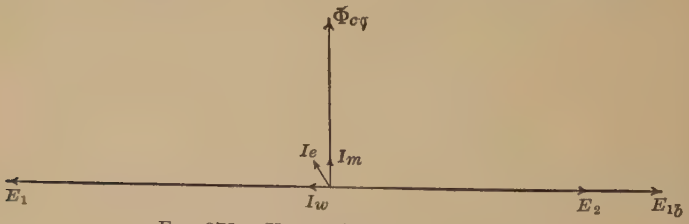

FIG. 273.—Vector diagram at no load.

flux ϕ_{co} generates an e.m.f. E_2 in the secondary winding and an e.m.f. E_{1b} in the primary winding, and to overcome this latter voltage the applied e.m.f. must have a component which is equal and opposite to E_{1b} at every instant; the other component

of the applied e.m.f. must be large enough to send the exciting current I_e through the impedance of the primary winding.

In Fig. 273, which shows the vector diagram at no load,

ϕ_{co} is the flux in the core,

I_m is the magnetizing current, or that part of I_e which is in phase with ϕ_{co},

I_w, the component of I_e which is in phase with the applied e.m.f., is required to overcome the no-load losses,

E_2, the e.m.f. generated in the secondary winding, lags ϕ_{co} by 90 deg.,

E_{1b}, the generated e.m.f. in the primary winding, also lags ϕ_{co} by 90 deg.,

E_1, the applied e.m.f., is equal and opposite to E_{1b}, since the component required to overcome the impedance of the primary winding may be neglected at no load.

Since E_2 and E_{1b} are produced by the same flux ϕ_{co}, and since $E_1 = E_{1b}$, therefore

$$\frac{E_2}{E_1} = \frac{T_2}{T_1}. \tag{62}$$

289. Full-load Conditions.—When the secondary of a transformer is connected to a load, a current I_2 flows in the secondary winding; the phase relation between E_2 and I_2 depends on the power factor of the load.

The fluxes which are present in a transformer core at full load are shown in Fig. 272. The m.m.f. between a and $b = T_1 I_1$ ampere-turns, where I_1 is the full-load current, and due to this m.m.f. a flux ϕ_{1l} is produced which threads the primary winding but does not thread the secondary; ϕ_{1l} is called the primary leakage flux and is in phase with the current I_1.

The m.m.f. between c and $d = T_2 I_2$ ampere-turns, where I_2 is the full-load secondary current, and due to this m.m.f. the secondary leakage flux ϕ_{2l} is produced which threads the secondary winding but does not thread the primary.

In Fig. 274

I_2 is the current in the secondary winding,

ϕ_{2l}, the secondary leakage flux, is in phase with I_2,

ϕ_c, the flux in the core, threads both primary and secondary windings,

ϕ_2 is the actual flux threading the secondary winding,

E_2 is the e.m.f. generated in the secondary winding by ϕ_2,

E_{2t}, the secondary terminal e.m.f., is less than E_2 by I_2R_2, the e.m.f. required to overcome the resistance of the secondary winding,

I_1 is the current in the primary winding,

ϕ_{1l}, the primary leakage flux, is in phase with I_1,

ϕ_1 is the actual flux threading the primary winding,

E_{1b} is the e.m.f. generated in the primary winding by ϕ_1,

E_1, the primary applied e.m.f., is made up of a component equal and opposite to E_{1b}, and a component I_1R_1 to overcome the primary resistance.

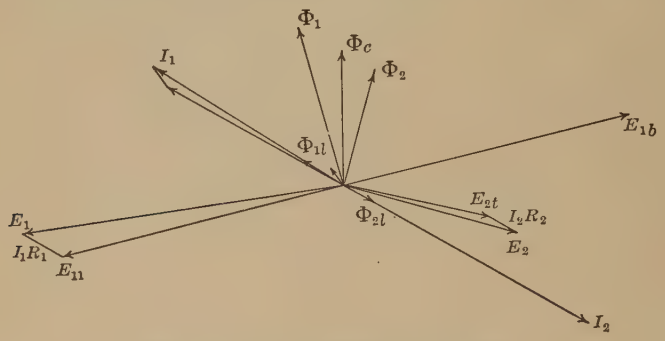

Fig. 274.—Vector diagram at full load.

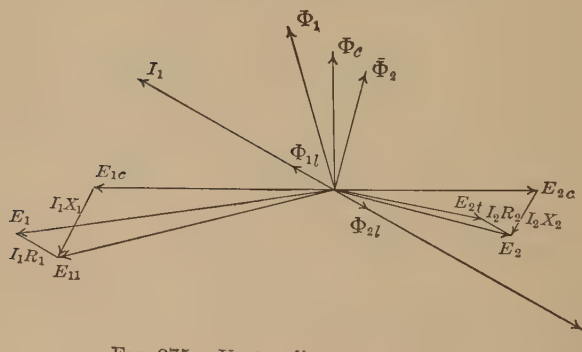

Fig. 275.—Vector diagram at full load.

The applied voltage E_1 is constant, and I_1R_1 is comparatively small even at full load, so that it may be assumed that E_{1b} is equal to E_1, and that ϕ_1, which produces E_{1b}, is approximately constant at all loads; the resultant of the m.m.fs. of the primary and secondary windings at full load must, therefore, as far as the primary is concerned, be equal in effect to the m.m.f.

of the exciting current I_e, so that the primary current may be divided up into two components, one of which has a m.m.f equal and opposite to that of the secondary winding, while the other is equal to I_e.

It is usual to consider that the primary and secondary leakage fluxes have an existence separate from that of the core flux ϕ_c, so that in Fig. 275

ϕ_2 consists of two components ϕ_c and ϕ_{2l},

E_2 consists of two components; E_{2c} due to ϕ_c, and E_{2l} due to ϕ_{2l},

E_{2l} lags ϕ_{2l} and therefore I_2 by 90 deg., it is also proportional to I_2, so that it acts exactly like a reactance and $= I_2X_2$, where X_2 is the secondary leakage reactance,

ϕ_1 consists of two components ϕ_c and ϕ_{1l},

E_{11} consists of two components E_{1c} and E_{1l} which latter $= I_1X_1$ the primary leakage-reactance drop.

290. Conditions on Short-circuit.—On short-circuit the terminal voltage of the secondary is zero; the diagram representing the operation is shown in Fig. 276 when the transformer is short-

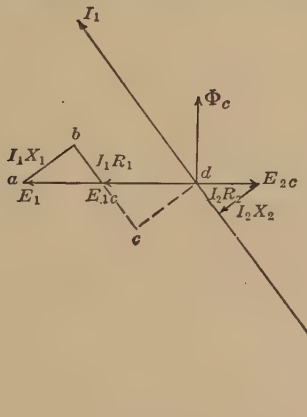

FIG. 276.—Vector diagram on short circuit.

circuited and a primary e.m.f. applied which is large enough to circulate full-load current through the transformer. Since the applied e.m.f., and therefore the primary flux, is small, the exciting current may be neglected and T_1I_1 and T_2I_2 will then be equal and opposite.

$$E_1 = \sqrt{(ab + dc)^2 + bc^2},$$

where $ab = I_1X_1$,

$$dc = \frac{T_1}{T_2}(I_2X_2) = \left(\frac{T_1}{T_2}\right)^2 I_1X_2,$$

$$bc = I_1R_1 + \left(\frac{T_1}{T_2}\right)^2 I_1R_2.$$

Therefore $$E_1 = I_1\sqrt{\left(R_1 + \left(\frac{T_1}{T_2}\right)^2 R_2\right)^2 + \left(X_1 + \left(\frac{T_1}{T_2}\right)^2 X_2\right)^2},$$

$$= I_1\sqrt{(R_{eq})^2 + (X_{eq})^2},$$

where R_{eq} and X_{eq} are the equivalent primary resistance and reactance, respectively.

291. Regulation.—Figure 277 shows the vector diagram at full load with the primary voltages expressed in terms of the secondary and the magnetizing current neglected.

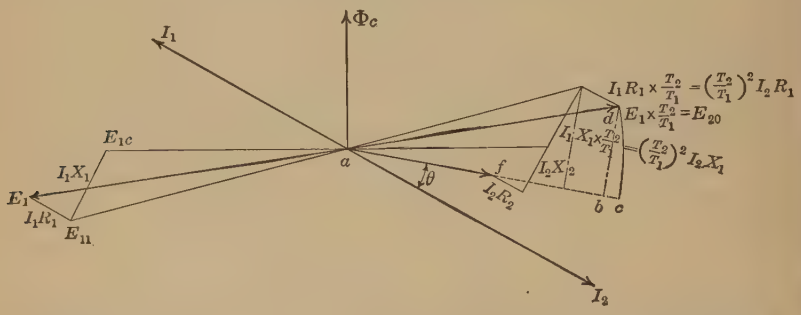

FIG. 277.—Vector diagram on full load with primary voltages expressed in terms of the secondary.

The regulation of constant potential transformers is defined as the per cent increase of secondary terminal voltage from full load to no load, the primary applied voltage being constant.

In Fig. 277 the rise in secondary voltage from full load to no load $= fc,$

$$= I_2R_e \cos\theta + I_2X_e \sin\theta + bc,$$

where R_e and X_e are the equivalent secondary resistance and reactance, respectively, and

$$bc \times 2ab = (bd)^2,$$

or

$$bc = \frac{(bd)^2}{2ab},$$

$$= \frac{(I_2X_e \cos\theta - I_2R_e \sin\theta)^2}{2(E_{20} - bc)},$$

$$= \frac{(I_2X_e \cos\theta - I_2R_e \sin\theta)^2}{2E_{20}} \text{ approximately.}$$

The per cent regulation $= 100\left(\frac{fc}{ac}\right)$,

$$= 100\,\frac{I_2R_e}{E_{2o}} + \frac{1}{2}\left(\frac{I_2X_e}{E_{2o}}\right)^2 \text{ at 100 per cent power factor,}$$

$$= 100\left(\frac{0.8I_2R_e + 0.6I_2X_e}{E_{2o}}\right) \text{ approximately at 80 per cent power factor, lagging current.} \quad (63)$$

CHAPTER XXXVI

CONSTRUCTION OF TRANSFORMERS

292. Distribution Transformers.—By the term "distribution transformers" is meant those transformers having capacity ratings from 1½ to approximately 200 k.v.a. with voltage ratings up to 46,000 volts, frequencies of 25 to 60 cycles and single-phase, two-phase or three-phase transformation. No single type of transformer design is best adapted to cover this entire range of capacity, voltage, frequency and phase. There are in

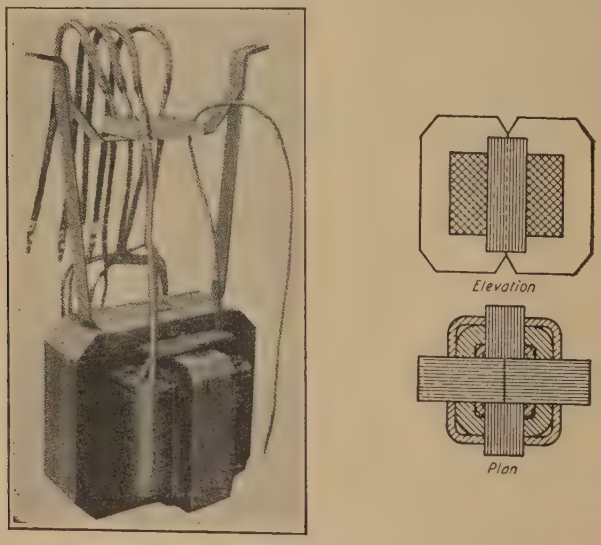

FIG. 278.—Group 1. Distributed shell type of construction.

general four types of construction employed. These four types are:

Group 1. Distributed shell type.
Group 2. Rectangular core type.
Group 3. Cruciform core type.
Group 4. Simple shell type.

These four types of construction are illustrated in Figs. 278 to 281.

In general, the selection of the type to be used is the result of some predominating characteristic of design that makes it best

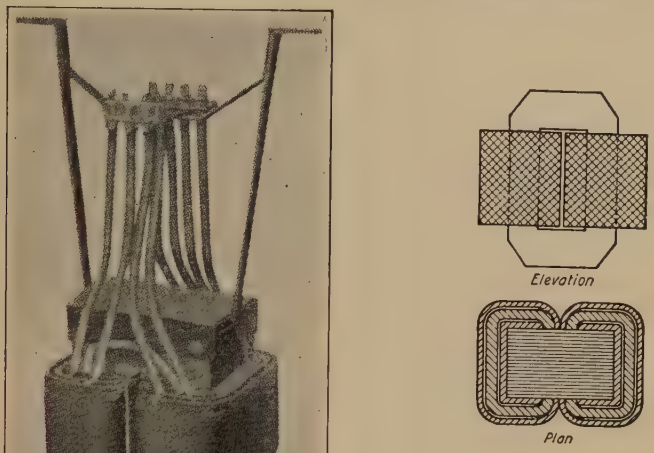

FIG. 279.—Group 2. Rectangular core type of construction.

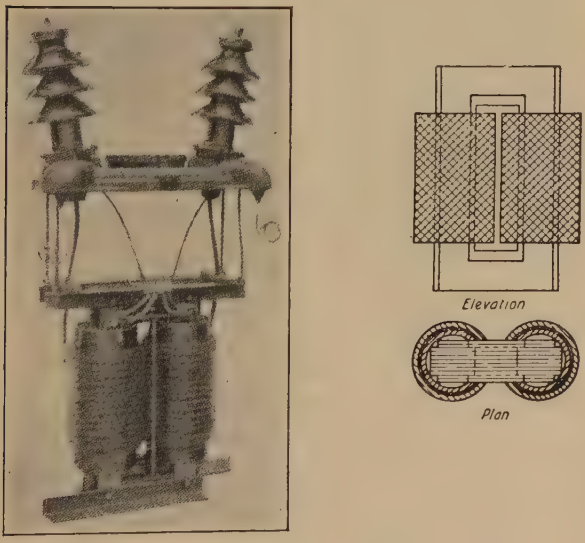

FIG. 280.—Group 3. Cruciform core type of construction.

suited for its particular field of service. Broadly speaking, the shell type of construction finds its best field of application for

relatively low voltage or large capacity ratings, that is, for transformers where the space factor is high. The core type, on the other hand, finds its best field where the voltage is relatively high or the capacity low, that is, where the space factor is low. This general consideration may be modified in actual application by other considerations such as ventilation or mechanical bracing, which may make one design better than another and thereby be a determining factor in the selection of the type of construction to be employed.

Figures 282 and 283 indicate how the product of one of the large manufacturing companies is distributed among these various types of construction.

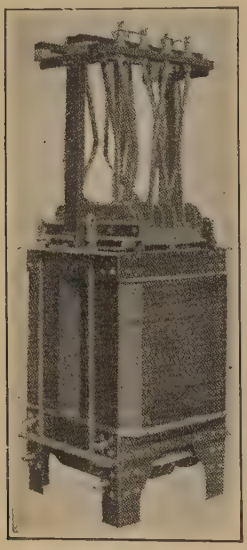

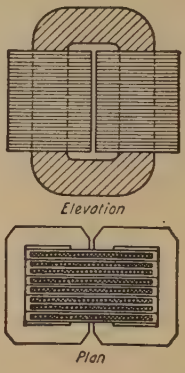

FIG. 281.—Group 4. Simple shell type of construction.

Both the distributed shell type and the rectangular core type have been selected for their field of service because of the high operating efficiency that is obtainable with these two types. On account of the poor load factor, under which distribution transformers of small capacity usually operate, very low iron and copper losses are absolutely essential. A close approximation to the ideal design for maximum electrical efficiency is obtained in the shell type of design by the distributed shell transformer and the core type of design by the rectangular core type. For transformers of relatively high voltage and small

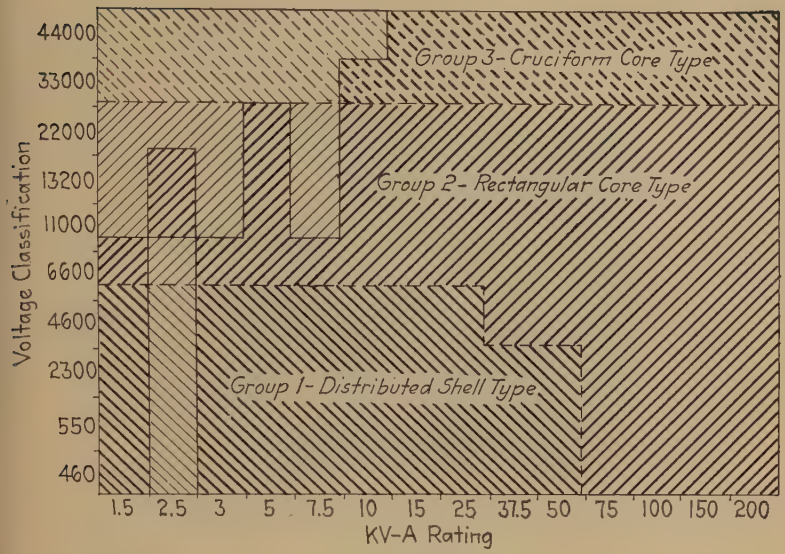

Areas lightly shaded represent capacity ratings that are not standard in the voltage classes under which they are included.

FIG. 282.—Showing the type of construction as affected by voltage and capacity —60 cycle distribution transformers.

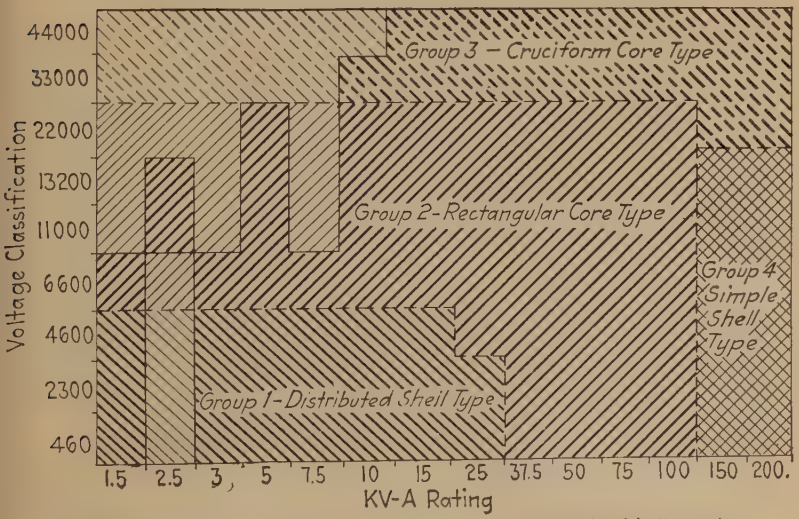

Areas lightly shaded represent capacity ratings that are not standard in the voltage classes under which they are included.

FIG. 283.—Showing the type of construction as affected by voltage and capacity —25 cycle distribution transformers.

capacity, the high-voltage coils are necessarily wound with very small wire, and, therefore, circular coils are employed to give the

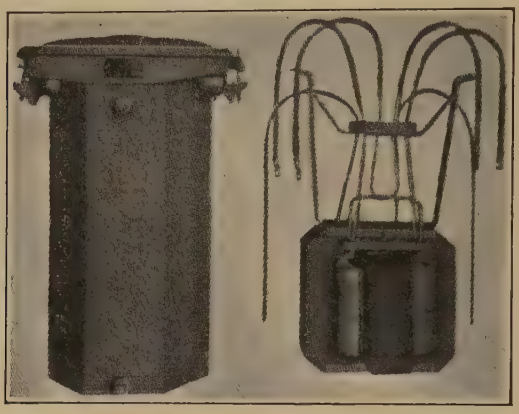

FIG. 284.—Transformer and case of the distributed shell type (group 1).

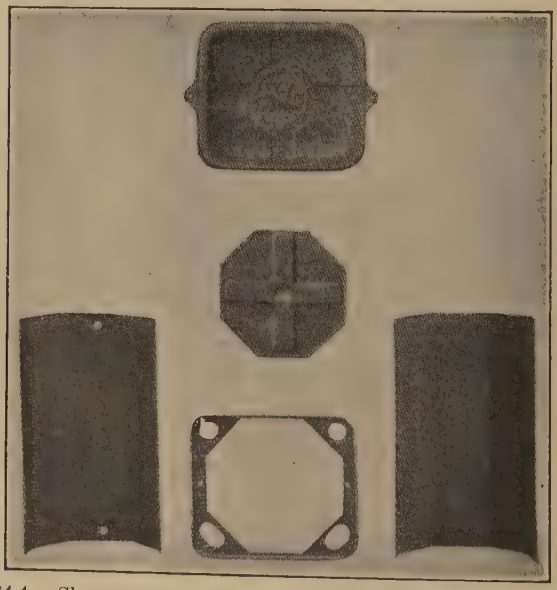

FIG 284A.—Sheet metal parts of a transformer case prior to welding.

requisite mechanical strength. This construction also permits the use of cylindrical insulating barriers on which the coils can

be thoroughly braced against mechanical stresses and leads to the selection of group 3, the cruciform core type of construction. For large capacity transformers of relatively low voltage, the two important requirements are ventilation and mechanical bracing of the ends of the winding. For these requirements the

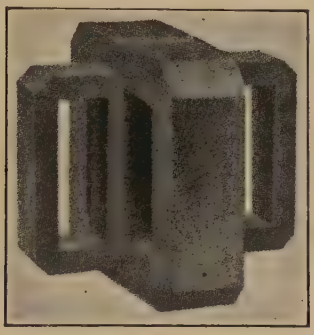

FIG. 285.—Magnetic circuit of the distributed shell type of transformer (group 1).

simple shell type of construction offers the best solution, as the vertical coils assure very thorough ventilation and the pancake coils can be thoroughly braced by clamps across the end of the winding. While the simple shell type (group 4) does not find a

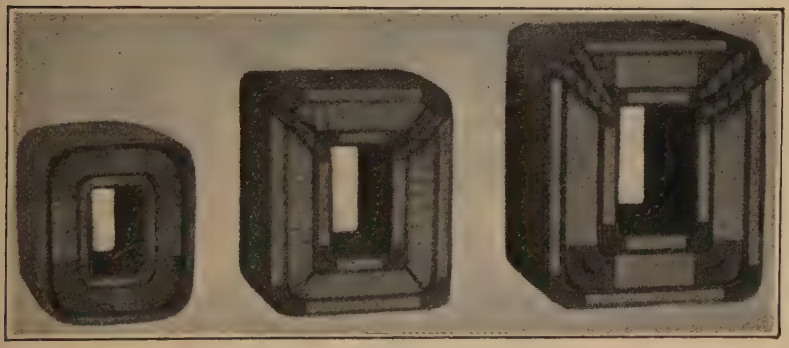

FIG. 286.—A group of coils of the distributed shell type transformer (group 1).

very large field in distributing transformers—where in general the capacity is limited—it does find a wide application in power transformers which will be discussed later.

The most widely used distributing transformers are those of the distributed shell type (group 1). Figure 284 shows a typical

transformer of this type of 15-k.v.a. capacity. It will be observed that the transformer itself occupies only about one-half the total height of the case, thereby obtaining sufficient area of case to dissipate the heat.

The case is made of sheet metal welded together. Figure 284*A* shows the five sheet-steel parts which are welded together to form the completed tank shown in Fig. 284. Figure 285 shows the form and construction of the magnetic circuit (see Fig. 278),

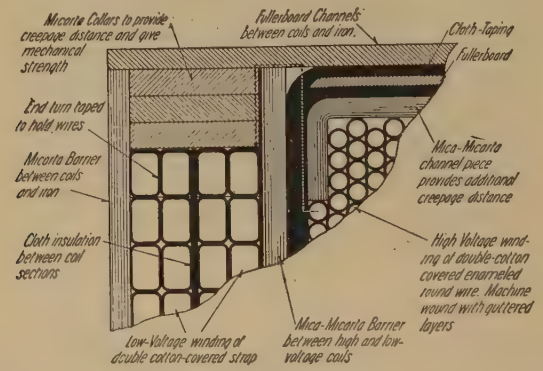
Micarta Collars to provide creepage distance and give mechanical strength
Fullerboard Channels between coils and iron
Cloth Taping
Fullerboard
End turn taped to hold wires
Micarta Barrier between coils and iron
Mica-Micarta channel piece provides additional creepage distance
Cloth insulation between coil sections
High Voltage winding of double-cotton covered enameled round wire. Machine wound with guttered layers
Low-Voltage winding of double cotton-covered strap
Mica-Micarta Barrier between high and low-voltage coils

FIG. 287.—Cross-section through coils, showing insulation, of the distributed shell type transformer (group 1).

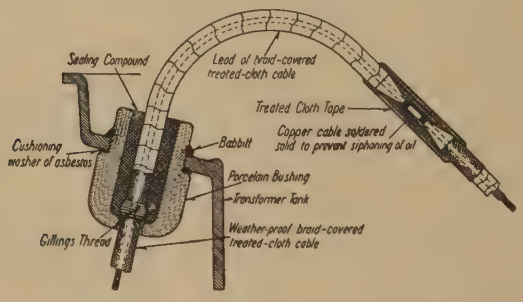

FIG. 288.—Bushing for transformer of the 2300 volt class.

and Fig. 286, a group of coils ready to receive the magnetic circuit shown in Fig. 285. Figure 287 shows a typical cross-section through the winding of one of these transformers and indicates the disposition and character of the insulation employed. Figure 288 shows the construction of the bushings in these transformers. This type of construction is used for voltages up to 4600 and capacities up to and including 25 k.v.a. (see Fig. 282); also for voltages up to 2300, up to and including 50 k.v.a.

For higher voltages and larger capacities, the rectangular core type of construction is used (see Fig. 279). Figure 289 shows a transformer of this type partially assembled and Fig. 290 is a cross-section through a part of the winding showing the method of insula-

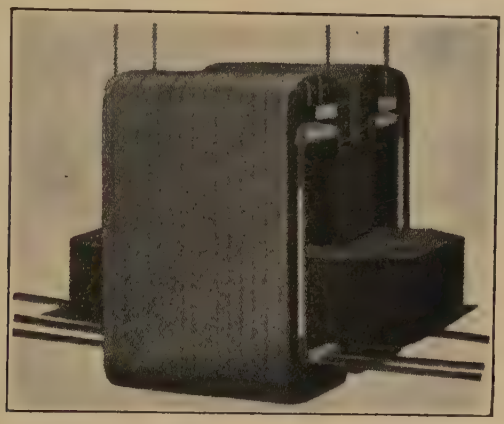

FIG. 289.—Coils and partially built up core of a rectangular core type transformer (group 2).

tion. Figure 291 shows the insulating barriers that are used between primary and secondary windings. Insulating barriers simliar to this are used on all transformers of groups 1, 2 and 3, Figs. 278, 279 and 280. These barriers are made of paper and mica

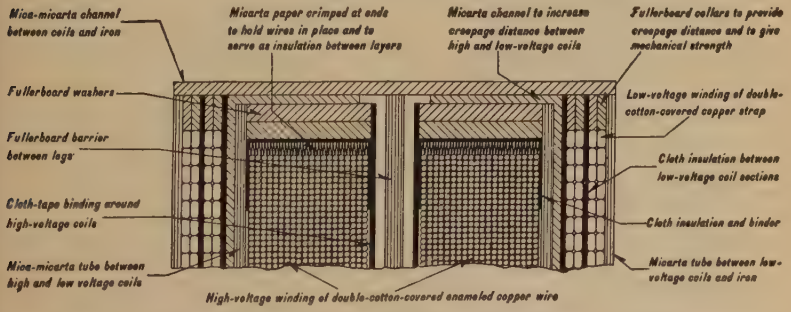
Mica-micarta channel between coils and iron
Micarta paper crimped at ends to hold wires in place and to serve as insulation between layers
Micarta channel to increase creepage distance between high and low-voltage coils
Fullerboard collars to provide creepage distance and to give mechanical strength
Fullerboard washers
Low-voltage winding of double-cotton-covered copper strap
Fullerboard barrier between legs
Cloth insulation between low-voltage coil sections
Cloth-tape binding around high-voltage coils
Cloth insulation and binder
Mica-micarta tube between high and low voltage coils
Micarta tube between low-voltage coils and iron
High-voltage winding of double-cotton-covered enameled copper wire

FIG. 290.—Cross-section through coils, showing insulation, of the rectangular core type transformer (group 2).

wound up into a cylinder of the proper length and diameter, and then, when required, formed into the rectangular shape shown in Fig. 291 under heat and pressure. Figure 292 shows the bushing used in a 6900-volt transformer. It will be noted that its construc-

tion is similar to that shown in Fig. 288, the difference simply being due to the higher voltage.

The main difference between the transformers made according to group 1 (Fig. 278) and group 2 (Fig. 279) is that the latter may be more easily insulated and is therefore better suited for a higher voltage.

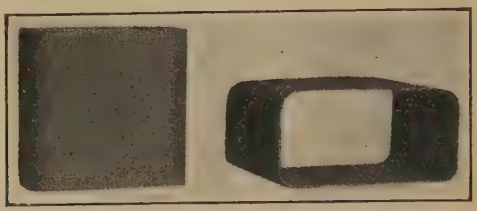

FIG. 291.—Insulating barriers formed to rectangular shape.

A construction in accordance with group 3 (Fig. 280) is suitable for still higher voltages and is the type of construction that is used on all very high voltage designs. It is similar in all particulars to the construction of group 2 except that the coils

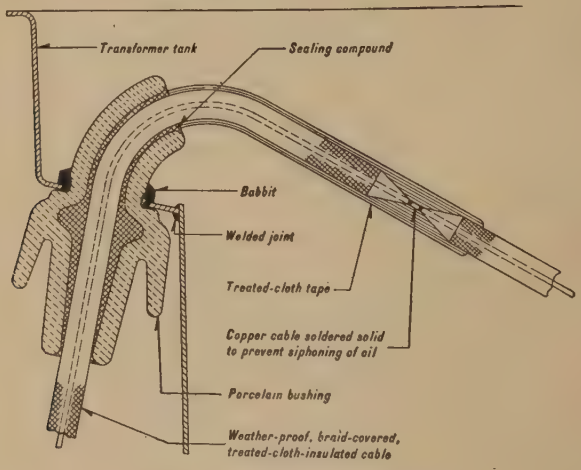

FIG. 292.—Bushing for transformer of the 6900-volt class.

are round instead of rectangular; the round coil is better suited to withstand the stresses due to short-circuit than is the rectangular coil and hence is better adapted to high voltage where the space for leakage between primary and secondary is necessarily large and to large capacities where the short-circuit currents reach a high value.

FIG. 293.—Coils and partially built up core of a simple shell type transformer (group 4).

FIG. 294.—"Pancake" coil for a simple shell type transformer (group 4).

FIG. 295.—Water cooled transformer showing relative positions of transformer and cooling coils.

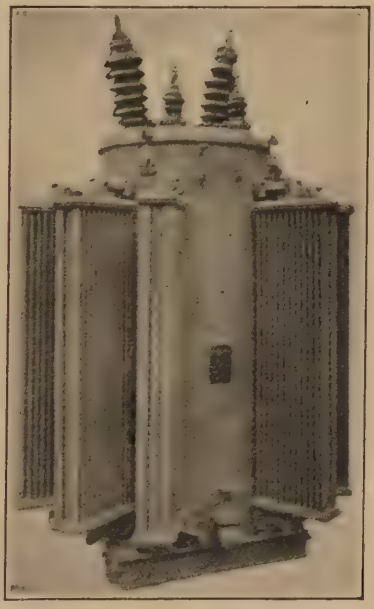

FIG. 296.—Self cooled transformer, showing radiators attached to tank.

293. Large Power Transformers.—For large-capacity transformers of moderate voltage, the shell type of construction is used. Figure 293 shows a 1500-k.v.a. transformer of this type in process of construction. Figure 294 shows one of the so-called "pancake" coils of such a transformer. The spacing strips between coils permit the circulation of oil for cooling purposes; these are made wavy as shown in Fig. 294 so that all parts of the coil will be exposed to the cooling oil flowing in the vertical ducts.

Various methods of cooling are used—water cooling, air blast and self cooling. Figure 295 shows a shell-type transformer with the cooling coils, through which water is circulated to cool the oil, in place above the body of the transformer. Figure 296 shows a typical self-cooled oil-insulated transformer; this is equipped with radiators so as to increase the surface that is exposed to the cooling air.

CHAPTER XXXVII

MAGNETIZING CURRENT AND IRON LOSS

294. The E.M.F. Equation.—If in a transformer
ϕ_a is the maximum flux threading the windings at no load,
T is the number of turns in the winding,
f is the frequency of the applied e.m.f., then the flux threading the windings changes from

$$\phi_a \text{ to } -\phi_a \text{ in the time of half a cycle,}$$

or the average rate of change of flux $= 2\phi_a \times 2f$,
and the average voltage in the coil $= 4\ T\phi_a f 10^{-8}$.
The effective voltage in the coil = average voltage × form factor,
$= 4 \times$ form factor $\times\ T\phi_a f 10^{-8}$.
For a sine wave of e.m.f., the form factor = 1.11 and

$$E_{eff} = 4.44 T\phi_a f 10^{-8} \text{ volts.} \qquad (64)$$

295. The No-load Losses.—The losses in a transformer at no load are the hysteresis and eddy-current losses in the active iron, and the small eddy-current losses due to stray flux in the iron brackets and supports; these latter losses may be neglected if care is taken to keep the brackets away from stray fields.

The hysteresis loss is usually taken $= KB^{1.6}fW$ watts, and the eddy-current loss $= K_e(Bft)^2W$ watts, where
K is the hysteresis constant and varies with the grade of iron,
K_e is a constant which is inversely proportional to the electrical resistance of the iron,
B is the maximum flux density in lines per square inch,
f is the frequency in cycles per second,
t is the thickness of the laminations in inches,
W is the weight of the iron in pounds.

Hysteresis loss up to a value of B = about 75,000 lines per square inch varies, as indicated above, approximately as $B^{1.6}$. Above this value, the exponent begins to increase.[1] As shown in Fig. 298, losses in the usual commercial grades of transformer iron

[1] See article by T. Spooner, *Elec. Jour.*, March, 1925, p. 132 *et seq.*

appear as nearly straight lines when plotted on single log paper, indicating that the losses (both hysteresis and eddy-current combined) can be closely represented by an expression of the form

$$\text{Loss} = K_l B^n W$$

where K_l is a constant
W is the weight of iron.
and B is the magnetic density.

The eddy-current loss $= i^2 r$, where r is the resistance of the eddy-current path and i, the eddy current $= \frac{e}{r}$; therefore the eddy-current loss $= \frac{e^2}{r}$, where e, the voltage producing the eddy current is proportional to the flux density, the frequency and the thickness of the iron.

The eddy-current loss may be reduced by a reduction in t, the thickness of the laminations, but this reduction cannot be carried to extreme because, for a given volume of core, the space taken up by the insulation on the laminations depends on their thickness; as they become thinner the amount of iron in the core decreases, the flux density for a given total flux increases, and finally a value is reached at which the amount of iron in the core is so small that the increase in flux density, and therefore in iron loss, more than compensates for the reduction in the eddy-current loss due to the reduction in the value of t. The iron which is used for other electrical machinery and is 0.014 in. thick is also that in most general use for transformers up to frequencies of 60 cycles.

When ordinary iron under pressure, as in the core of a transformer or other electrical machine, is subjected to a temperature of over 80° C. for a period of the order of 6 months, it will be found that the hysteresis loss has increased from 10 to 20 per cent due to what is known as ageing. This ageing causes the iron loss and the temperature of a transformer to increase and the efficiency to decrease, but is not of importance in revolving machinery, because in such machines the hysteresis loss is only a small part of the total iron loss. Special alloyed iron (high in silicon) shows very little ageing.

The hysteresis loss in a transformer is affected by the wave form of the applied e.m.f. because, as shown by the equation

$$E = 4 \times \text{form factor} \times T\phi_a f 10^{-8}$$

for a given voltage, the higher the form factor, the lower the flux,

the lower the flux density and, therefore, the lower the hysteresis loss. A wave with a high form factor is peaked, so that the advantage of low hysteresis loss is counteracted by the fact that the peaked e.m.f. has the greater tendency to puncture the insulation; a sine wave is the best for all conditions of operation.

296. The Exciting Current.—Assume first that the maximum flux density in the transformer core is below the point of satura-

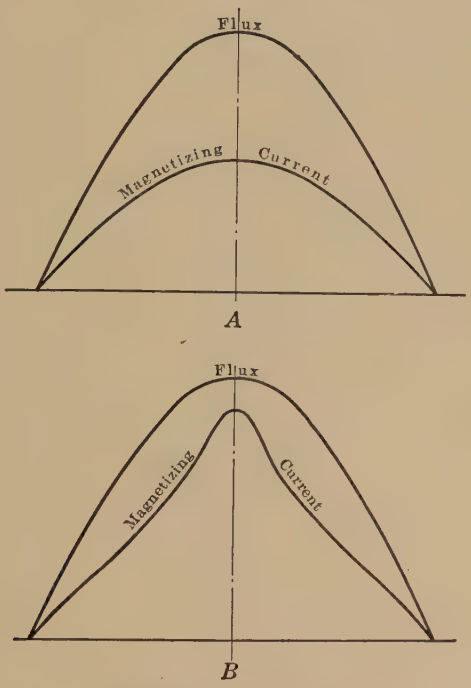

FIG. 297.—Curves of flux and magnetizing current.

tion, so that the magnetizing current is directly proportional to the flux; then, if the flux varies according to a sine law, the magnetizing current also follows a sine law, as shown in diagram *A*, Fig. 297.

For the given value of B_m, the corresponding maximum ampere-turns per inch of core may be found from Fig. 47, page 49, and the effective magnetizing current I_m

$$= \frac{\text{maximum ampere-turns per inch} \times \text{length of magnetic path}}{\sqrt{2} \times T},$$

or $\sqrt{2} I_m T$ = maximum ampere-turns per inch $\times L_m$.

Now $E = 4.44T\phi_a f10^{-8}$,

$= 4.44TB_mA_cf10^{-8}$, where A_c is the core area in square inches.

Therefore EI_m = a constant $\times B_m \times$ ampere-turns per inch $\times A_cL_m \times f$,

= a constant $\times$ function of $B_m \times$ core weight $\times f$;

since ampere-turns per inch depend on B_m and A_cL_m, the core volume, is proportional to the core weight; therefore

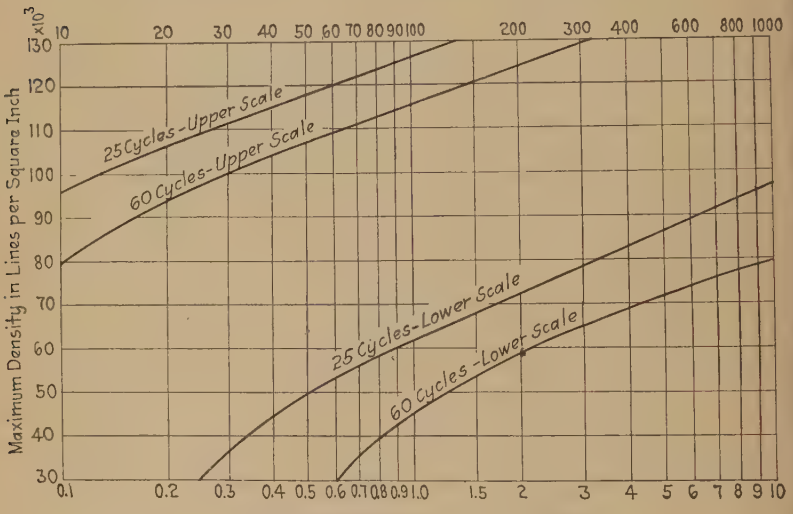

FIG. 298.—Iron loss curves for transformer design.

$\frac{EI_m}{\text{core weight}}$ = the magnetizing volt amperes per pound,

= a function of $B_m \times f$.

When the core is saturated at the higher densities, the curve of magnetizing current is no longer a sine curve but is peaked, as shown in diagram *B*, Fig. 297, because, as the points of high density are reached, the current increases faster than the flux on account of saturation, so that it is not possible to use the curves in Fig. 47 directly; a correction factor must be applied because of the form of the wave; in practice a different method is followed which allows the effect of joints, saturation and losses all to be taken into account.

It was shown that the magnetizing volt amperes per pound
= a function of $B_m \times f$,
the iron loss per pound = $KfB^{1.6} + K_e(Btf)^2$,
= a function of B_m for a given thickness and frequency;
therefore the exciting volt amperes per pound
$= \sqrt{(\text{magnetizing volt ampere per pound})^2 + (\text{iron loss per pound})^2}$,

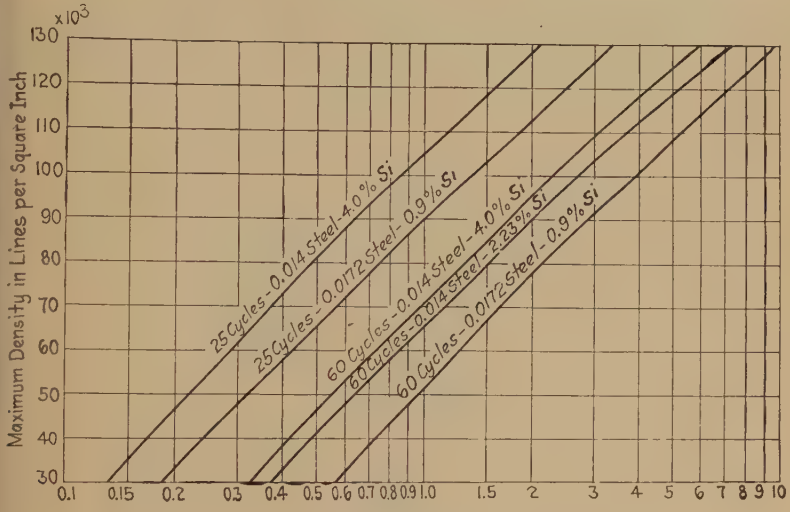

Volt-amperes of excitation per pound of iron.

FIG. 299.—Volt-amperes of excitation for transformers.

= a function of B_m for a given thickness and frequency.

If then a small test transformer be made of the material to be used for a line of transformers, and tested at no load for exciting current and iron loss, the results may be plotted against maximum flux density as shown in Figs. 298 and 299, where test results are given for iron at 25 and at 60 cycles. In using these curves, particularly Fig. 299 it should be borne in mind that there may be expected a variation of some 25 per cent most of which depends on the care used in eliminating air-gaps at the joints in the iron.

Example.—A transformer is constructed as follows:

Weight of core	1760 lb. (4 per cent silicon steel).
Turns of primary winding	526.
Output	300 k.v.a.
Primary voltage	12,000.

Frequency..... 60 cycles.
Core section..... 122 sq. in.
ϕ_a....8.6×10^6 (from formula 64, p. 439).
$B_m = \frac{8.6 \times 10^6}{122}$..... 70,000 lines per square inch.
Apparent volt amperes..... 4.4×1760 (from Fig. 299) = 2.58 per cent of output.
Iron loss..... 0.98×1760 (from Fig. 298) = 0.57 per cent of output.

In the case of transformers which have a butt joint in the magnetic circuit, it is necessary to insulate each joint with a

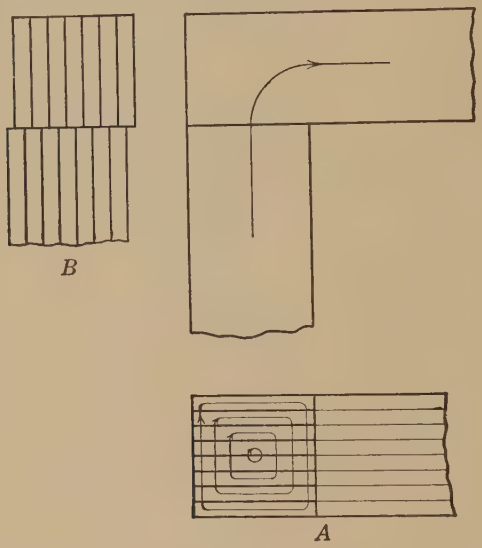

FIG. 300.—Eddy currents in transformer joints.

layer of tough paper 0.005 in. thick to keep down the eddy-current loss, otherwise the flux will send currents across the face of the joint, as shown in diagram *A*, Fig. 300, because the laminations generally lie staggered as shown in diagram *B*. In such transformers these joints must be figured as air-gaps which have a thickness of 0.005 in. and
the effective ampere-turns for each joint

$$= \frac{\text{maximum ampere-turns}}{\sqrt{2}},$$

$$= \frac{B_m \times \text{air-gap}}{\sqrt{2} \times 3.2}.$$

CHAPTER XXXVIII

LEAKAGE REACTANCE

297. Core Type with Two Coils per Leg.—Figure 301 shows the leakage paths for a core type transformer which has one primary and one secondary coil on each leg; the secondary is wound next to the core.

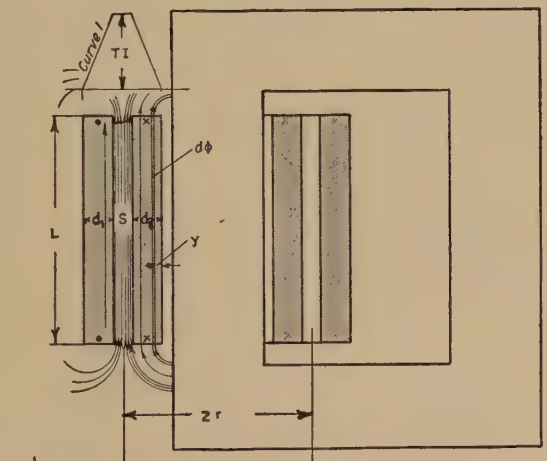

FIG. 301.

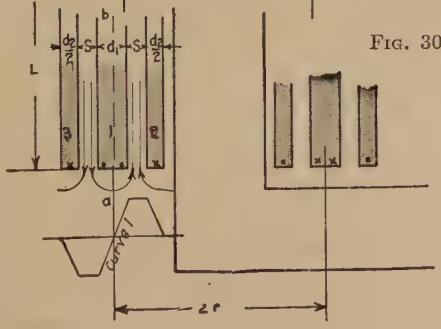

FIG. 302.

FIGS. 301 and 302.—Leakage paths in core-type transformers.

The m.m.fs. of the two coils, as shown in Fig. 274, are equal and opposite, and the currents are shown at one instant by crosses and dots. The leakage flux passes between the coils

and returns by way of the core on one side, and through the air on the other side; the space S is like the center of a long thin solenoid, and the return path of the leakage flux that links the primary coil has an infinite section so that its reluctance may be neglected; the return path for the flux that links the secondary coil is through the iron core, and its reluctance may also be neglected.

The m.m.f. between the top and bottom of the coils for different depths y is given by curve 1,

the m.m.f. at depth $y = T_2 I_2 \times \frac{y}{d_2}$ ampere-turns;

therefore the flux $d\phi = 3.2 T_2 I_2 \frac{y}{d_2} \times \frac{2\pi r \times dy}{L}$ all in inch units.

This flux links $T_2 \frac{y}{d_2}$ turns of the secondary coil, and the interlinkages per unit current $= 3.2\left(T_2 \frac{y}{d_2}\right)^2 \times \frac{2\pi r}{L} \times dy$;

the coefficient of self-induction of the secondary coil due to the leakage flux which passes through the coil

$$= 3.2 \times \frac{2\pi r}{L} \times T_2^2 \int_o^{d_2} \frac{y^2 dy}{d_2^2} \times 10^{-8},$$

$$= 3.2 \times \frac{2\pi r}{L} \times T_2^2 \times \frac{d_2}{3} \times 10^{-8} \text{ henry.}$$

The m.m.f. along the space between coils

$= T_1 I_1 = T_2 I_2$ ampere-turns; therefore the flux which passes between the coils

$= 3.2 \times \frac{2\pi r \times S}{L} \times T_2 I_2$; since half of this flux may be assumed to link the primary and the other half the secondary coil, the coefficient of self-induction of the secondary coil due to this flux

$$= 3.2 \times \frac{2\pi r}{L} \times T_2^2 \times \frac{S}{2} \times 10^{-8} \text{ henry;}$$

the total coefficient of self-induction of the secondary coil

$$= 3.2 \times \frac{2\pi r}{L} \times T_2^2 \times 10^{-8}\left(\frac{d_2}{3} + \frac{S}{2}\right) \text{ henry;}$$

the leakage reactance of each secondary coil

$$= 2\pi f \times 3.2 \times \frac{2\pi r}{L} \times T_2^2 \times 10^{-8}\left(\frac{d_2}{3} + \frac{S}{2}\right);$$

similarly the leakage reactance of each primary coil

$$= 2\pi f \times 3.2 T_1^2 \times \frac{2\pi r}{L}\left(\frac{S}{2} + \frac{d_1}{3}\right)10^{-8},$$

and X_e, the equivalent secondary reactance,

$$= X_2 + X_1\left(\frac{T_2}{T_1}\right)^2,$$

$$= 2\pi f \times 3.2 \times T_2^2 \times \frac{2\pi r}{L}\left(S + \frac{d_1}{3} + \frac{d_2}{3}\right)10^{-8}; \qquad (65)$$

also the equivalent primary reactance

$$= 2\pi f \times 3.2 \times T_1^2 \times \frac{2\pi r}{L}\left(S + \frac{d_1}{3} + \frac{d_2}{3}\right)10^{-8}.$$

If the coils on the two legs are connected in series the total reactance will have double the above value, and if connected in parallel will have half the value.

298. Core-type Transformers with Split Secondary Coils.—Figure 302 shows the leakage paths for one leg of such a transformer.

The m.m.f. between the top and bottom of the coils for different depths of winding space is given by curve 1, and the distribution of leakage flux is symmetrical about the line *ab*.

Consider coil 2 and half of coil 1, the equivalent primary reactance,

$$= 2\pi f \times 3.2 \times \left(\frac{T_1}{2}\right)^2 \frac{2\pi r}{L}\left(S + \frac{d_1}{6} + \frac{d_2}{6}\right)10^{-8},$$

and, similarly, for coil 3 and the other half of coil 1, the equivalent primary reactance has the same value; therefore the total equivalent primary reactance

$$= 4\pi f \times 3.2 \times \frac{T_1^2}{4} \times \frac{2\pi r}{L}\left(S + \frac{d_1}{6} + \frac{d_2}{6}\right)10^{-8},$$

$$= \pi f \times 3.2 \times T_1^2 \times \frac{2\pi r}{L}\left(S + \frac{d_1}{6} + \frac{d_2}{6}\right)10^{-8}, \qquad (66)$$

which is between half and quarter of the value given in formula (65), for the case where the coils are not split up.

299. Shell-type Transformer.—One coil of this type of transformer is shown in Fig. 294; these coils are nested together as shown in Fig. 293. A cross-section through a group of these coils is shown in Fig. 303, which also shows the distribution of the leakage flux. The distribution of leakage flux is symmetrical about the lines *a*, *b*, and *c*, and for one primary and one secondary coil the equivalent primary reactance

$$= 2\pi f \times 3.2 \times T_1^2 \times \frac{MT}{L}\left(S + \frac{d_1}{3} + \frac{d_2}{3}\right) 10^{-8} \text{ ohms,} \quad (67)$$

where MT is the mean turn of coil; the total equivalent primary reactance when the primary coils are all in series

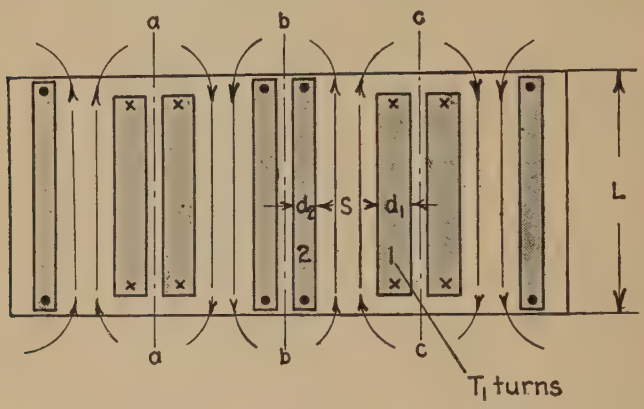

Fig. 303.—Leakage paths in shell-type transformers.

$= 2\pi f \times 3.2 \times T_1^2 \times \frac{MT}{L}\left(S + \frac{d_1}{3} + \frac{d_2}{3}\right)10^{-8} \times$ number of primary coils.

This gives a value which is low; the error, however, seldom exceeds 6 per cent.

CHAPTER XXXIX

TRANSFORMER INSULATION

The insulation of transformers differs from that of the machines previously discussed in that it is usually submerged in oil.

300. Transformer Oil.—Oil has the following properties which make it valuable for high-voltage insulation: It fills up all the spaces in the windings; it is a better insulator than air at normal pressure; it can be set in rapid circulation so as to carry heat from the small surface of the transformer to the large surface of the tank; it has a fairly high specific heat, and will allow the transformer immersed in it to carry a heavy overload for a short time without excessive temperature rise; it will quench an arc.

To be suitable for transformer insulation and cooling, the oil should be light over the range of temperature through which the transformer may have to operate, because the ability of the oil to carry heat readily from the transformer to the case or cooling coils depends on its viscosity; it must be free from moisture, acid, alkali, sulphur, or other materials which might impair the insulation of the transformer; it must have as high a flash point as is consistent with low viscosity and must evaporate very slowly up to temperatures of 100° C.

The oil largely used is a mineral oil which begins to burn at 149° C., has a flash point of 139° C., a specific gravity of 0.83, and a dielectric strength greater than 40,000 volts when tested between ½-in. spheres spaced 0.15 in. apart.

The dielectric strength is greatly reduced by the addition of moisture; 0.04 per cent of moisture will reduce the dielectric strength about 50 per cent. This moisture may be removed by filtering the oil under pressure through dry blotting paper. Suitable drying and purifying outfits are available and should be employed as soon as any deterioration of the insulating value of the oil is noted. When a transformer is in operation, the oil may be sampled by drawing some off from the bottom of the tank through a tap provided for the purpose; the bulk of the moisture settles to the bottom.

Only materials which are not attacked by nor are soluble in transformer oil should be used for transformer insulation; the materials generally used are cotton, paper, wood and special varnishes.

Wood, which is largely used for spacers, must be free from knots, and, in the case of maple, must also be free from sugar. Maple and ash are largely used, and, to insure that they are free from moisture, they are baked and then impregnated with compound, or are boiled for about 24 hours in transformer oil at 110° C.

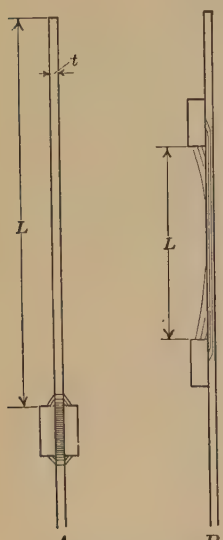

FIG. 304. — Surface leakage.

Fullerboard and pressboard are largely used for spacers in transformers; the latter material has a laminated structure, so that impurities seldom go through the total thickness of the piece; it also bends readily, so that there is no objection to its use in sheets $\frac{1}{16}$ in. thick. When baked and then allowed to soak in transformer oil $\frac{1}{16}$-in. pressboard will withstand about 30,000 volts.

Only varnishes which are specially made for transformer work should be used for impregnating coils; other varnishes may be soluble in hot transformer oil.

301. Surface Leakage.—Figure 304 shows two electrodes in air with pressboard between them. When the difference of potential between the two electrodes is increased, streamers will creep along the surface of the pressboard and finally form a short-circuit between the electrodes.

The distribution of the dielectric flux is shown in the two cases, and in diagram *A* the stress around the electrodes is much larger than in diagram *B*. The mechanism of the break-down due to surface leakage is not definitely known; creepage takes place under oil as well as in air, but the creepage distance under oil is only about one-third of that in air for the same test conditions.

The following tests[1] were made on a sheet of pressboard which was dried and then boiled in transformer oil:

Tested as in diagram A: $L = 6$ in.; $t = 0.095$ in.; creepage distance = 12.095 in.; voltage to cause arcing across the surface = 40,000 volts.

[1] A. B. Hendricks, *Trans.* A. I. E. E., Vol. 30, p. 295.

Tested as in diagram B: L = 3 in. = the creepage distance; voltage to cause arcing across the surface = 50,000 volts.

Figure 305 shows the results of similar tests made under oil, different thicknesses of pressboard being obtained by increasing the number of sheets; it may be seen from the curves that an increase in the thickness of the insulation has little effect on the creepage distance between two electrodes that are on the same side of the sheet, but has a large effect on the creepage distance around the end, the reason being that in the former case, shown in diagram B, the distribution of stress around the electrode

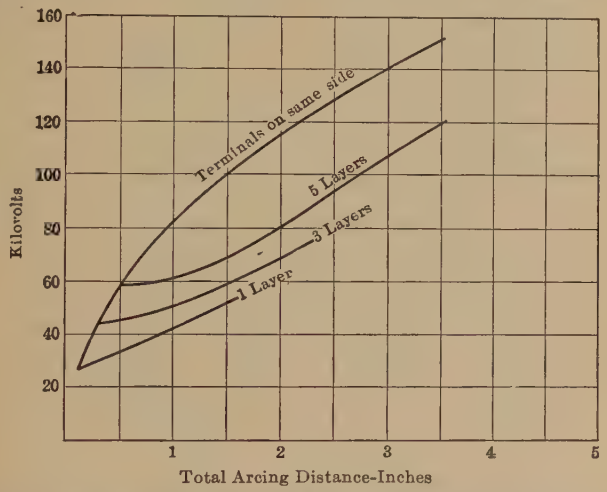

FIG. 305.—Creepage voltage on oiled pressboard. Conditions of test; Pressboard 0.095 in. thick, boiled in transformer oil, then tested under oil for creepage voltage with the electrodes first on the same side of the pressboard and then on opposite sides.

is almost independent of the thickness of the material on which the electrodes rest, while in diagram A the dielectric flux passing through the material is inversely proportional to the thickness between electrodes, so that the greater the thickness the lower the stress around the electrodes. Trouble due to surface leakage is often eliminated more economically by an increase in the thickness of the dielectric than by an increase in the creepage length.

302. Transformer Bushings.[1]—The terminals of the high- and low-voltage windings have to be brought out of the tank through bushings. For voltages up to about 25,000 above ground, bushings made of porcelain or of composition are used. These

[1] A. B. Reynders, *Trans.* A. I. E. E., Vol. 28, p. 209.

bushings extend below the surface of the oil at one end; the other end is carried above the tank to a height sufficient to prevent break-down due to surface leakage.

Figure 306 shows a bushing built to withstand a puncture test of 200,000 volts to ground for 1 minute. Diagram *B* shows the distribution of dielectric flux across a section of the bushing at *xy*, and since the strain in the material is proportional to the dielectric flux density, this strain is a maximum at the surface of the conductor and a minimum at the outer surface of the

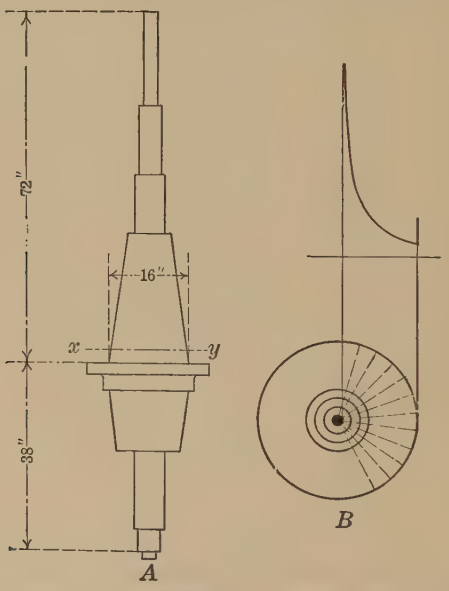

FIG. 306.—Solid bushing to withstand a puncture test of 200,000 volts for one minute.

bushing; the strain at any point is proportional to the potential gradient at the point, the curve of which is shown.

To reduce the maximum value of the potential gradient it is necessary to reduce the dielectric flux density at the surface of the conductor, which may be done by increasing the diameter of the conductor without reducing the thickness of the bushing, or by increasing the thickness of the bushing.

In order to make the outer layers of the bushing carry their proper share of the voltage, the condenser type of bushing shown in Fig. 307 was designed. It consists of a number of concentric condensers of tin-foil and paper in series between the center

conductor and the cover of the tank. When condensers are put in series, the voltage drop across each is inversely proportional to its electric capacity so that, in the condenser type of bushing, if each concentric condenser have the same thickness and the same capacity, the voltages across the different layers will all be equal and the strain will be uniform through the thickness of the bushing.

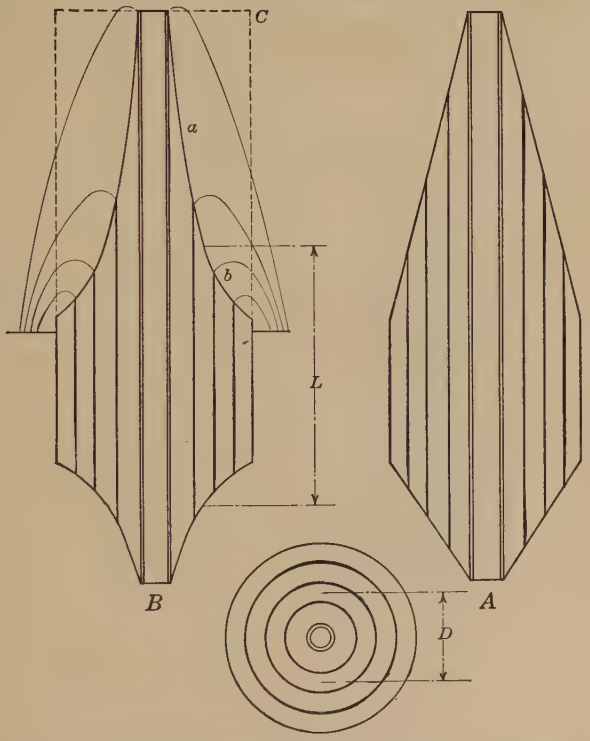

FIG. 307.—Diagrammatic representation of a condenser bushing.

The capacity of such condensers is proportional to

$$\frac{\text{area of plates}}{\text{thickness of dielectric}},$$

so that, if the thickness of the different layers of dielectric, and also the area πDL of the different layers of tin-foil, be kept constant, the voltage across each thickness of insulation will be equal to the total voltage divided by the number of layers.

A bushing built with equal areas of plate and equal thicknesses of dielectric has the shape shown in diagram B; in such a case

the voltages across the different layers are all equal, but the distance between two adjacent layers of tin-foil at *a* is greater than at *b*, so that the bushing is not economically designed for surface leakage. Condenser bushings are generally constructed as shown in diagram *A*; the surface distance between layers of tin-foil is constant, and the creepage distance under oil is considerably less than in air.

When such a bushing is in operation, lines of dielectric flux pass through the air as shown in diagram *B*, and since the edge

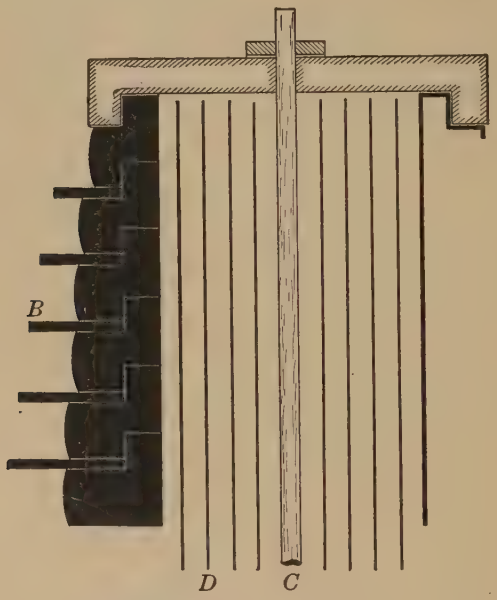

FIG. 308.—Oil-filled bushing.

of the tin-foil is thin, the stress in the air at that edge is large and the air breaks down there, forming a corona. The corona contains ozone and oxides of nitrogen which attack the adjoining insulation and finally cause break-down of the bushing. To prevent the corona from forming it is necessary to eliminate the air from around the bushing, and for this purpose the bushing is surrounded by a cylinder of fiber shown at *C*, which is then filled up with compound.

Another type of bushing which is largely used for high-voltage work is the compound or oil-filled bushing of which a section is shown in Fig. 308. This type of bushing is built up of composi-

tion rings which are carefully fitted into one another and then clamped between two metal heads by a bolt C which acts as the conductor. The creepage distance is obtained by building rings B of composition into the bushing. The whole center of the bushing is filled with compound or thick oil into which baffles of pressboard are placed as shown at D to prevent lining up of impurities in the compound along the lines of stress.

Figure 309 shows a solid bushing, a condenser bushing, and an oil-filled bushing, all able to withstand a puncture test of 200,000 volts for 1 min.

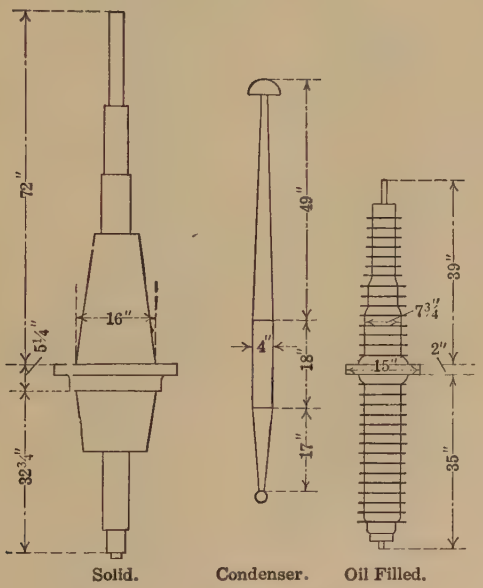

FIG. 309.—Bushings built to withstand 200,000 volts for one minute.

303. Insulation of Coils.—In most high-voltage shell-type transformers of moderate output, and in all core-type transformers, the high-voltage coils have several turns per layer, and the voltage between end turns of adjacent layers, which is equal to the volts per turn multiplied by twice the turns per layer, may become high, so that, while the cotton covering on the wire is generally sufficient for the insulation of adjacent conductors in the same layer, it is necessary to supply additional insulation between adjacent layers of the coils. It is also necessary to provide sufficient creepage distance, which is done, where the

space is available, by making the insulation between layers extend beyond the winding as shown in Fig. 312. Where the space is not available, as in the coils for shell-type transformers,

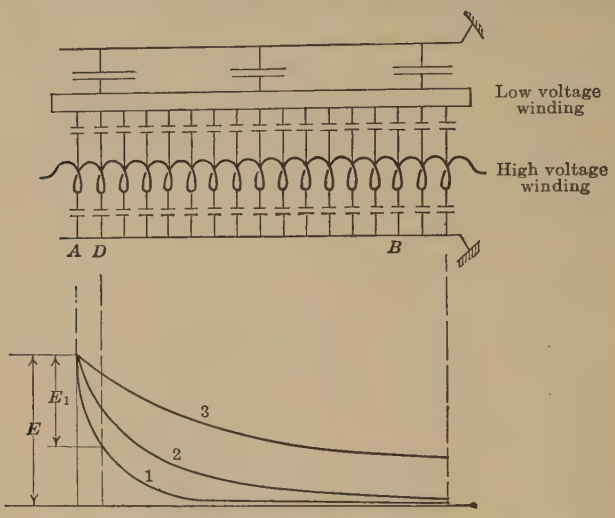

FIG. 310.—The potential of transformer coils immediately after switching.

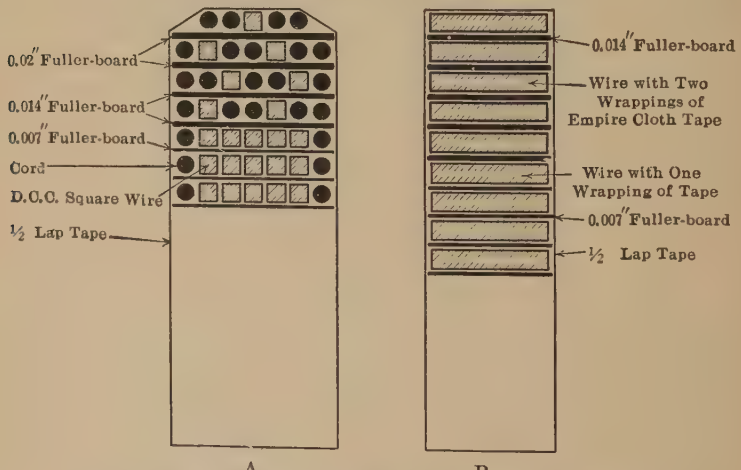

FIG. 311.—Insulation of the end turns of a 12,000-volt transformer coil.

the construction shown in diagram *A*, Fig. 311, is often adopted; one turn of cord is placed at each end of each layer and the insulation between layers is carried out to cover the cord; this construction lessens the chance of damage to the coil while being handled.

For high-voltage transformers it is advisable to make the high-voltage winding of a number of coils in series with ample creepage distance and ample insulation between them, and to limit the voltage per coil to about 5000. The voltage between layers should not, if possible, exceed 350 volts.

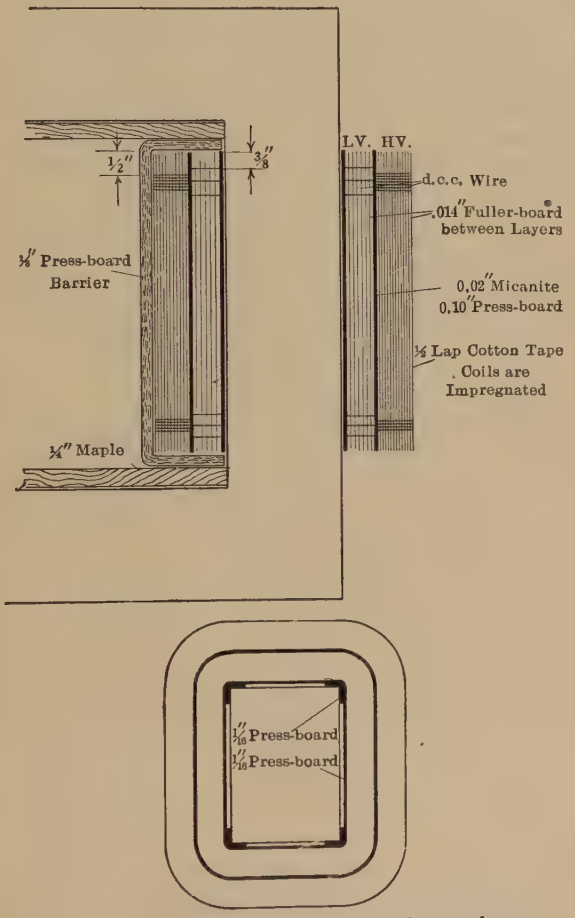

FIG. 312.—Insulation for a 2200/220 volt transformer.

304. Extra Insulation on the End Turns of the High-voltage Winding.[1]—A condenser consists of two conductors with dielectric between, so that the high- and low-voltage windings of a trans-

[1] Walter S. Moody, *Trans.* A. I. E. E., Vol. 26, p. 1173.

former, with the oil between, form a condenser; so also is th an electrostatic capacity between the high-voltage winding the tank and between the low-voltage winding and the t A transformer may therefore be represented diagrammatic by a distributed inductance and capacity as shown in Fig.

Suppose that the transformer is disconnected from the line all at the ground potential. If the potential of one end the high-voltage winding be suddenly raised to a value E, potential of the whole high-voltage winding will gradually to the same value. The potential cannot rise instantaneous the voltage at B, for example, cannot reach the value E until t condensers at that point have been charged to a value $Q = \int i dt$ CE, where C is the electro-static capacity between point B and th ground. The charging current i has to flow through the windi to B, and this takes a definite, though very short, time. The condensers near A will be charged first and the potential above ground of each point in the high-voltage winding is given by curves 1, 2 and 3 at successive instants.

At the instant after switching represented by curve 1, the difference of potential between two points A and D, that is, across the first few turns of the winding, $= E_1$, which is almost equal to the full potential E; because of this high voltage between turns, it is necessary to insulate the end turns from one another for a voltage between turns of many times the normal value.

Any sudden change in the potential of a transformer terminal, such as that due to switching or to grounding of a line, will produce this high voltage between end turns.

Diagram A, Fig. 311, shows a method of insulating the end turns of a coil for a shell-type transformer, when the coil is of wire wound in layers; and diagram B, for a coil wound with strip copper. This extra insulation is put on each end of the high-voltage winding for a distance of about 75 ft., and then any taps that are required for the purpose of changing the transformer ratio are connected to the inside of the winding, so that the extra insulation is always on the end turns.

305. Insulation between the Windings and Core.—Figure 312 shows the method of insulating a small core-type distributing transformer wound for $^{2200}/_{220}$ volts. Further details of this insulation are shown in Figs. 287 and 290. Figures 287 and 290 show particularly the insulation between the primary and secondary windings.

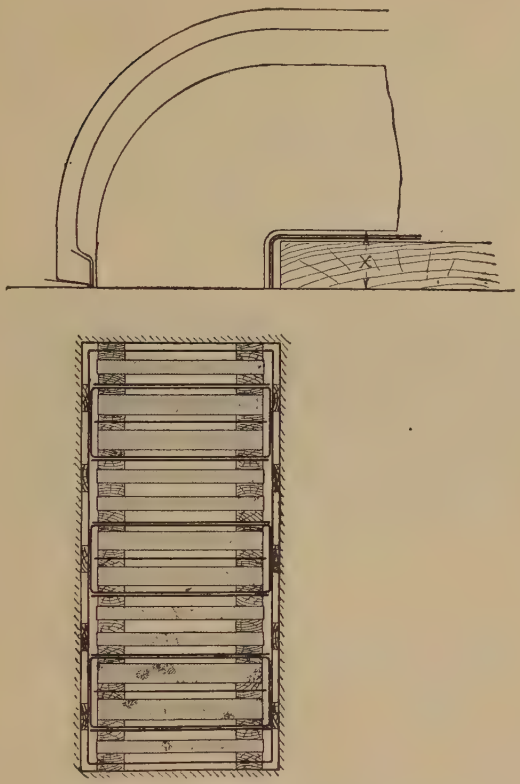

FIG. 313.—Insulation for a shell-type transformer.

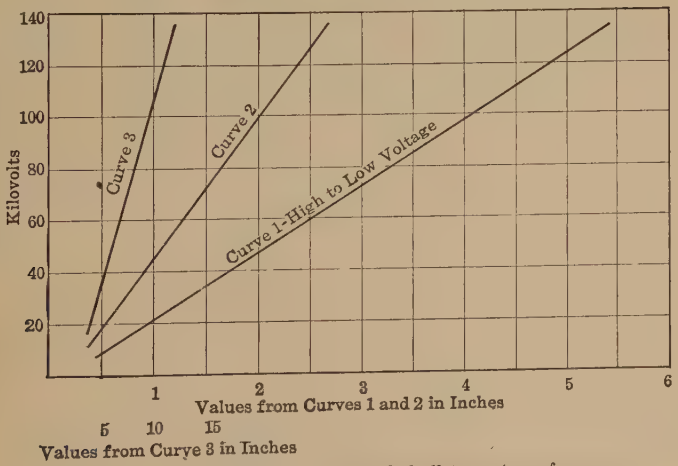

FIG. 314.—Spacings for the coils of shell-type transformers.

Figure 313 shows an example of a shell-type transformer wound for moderate voltage; an illustration of such a winding and insulation is shown in Figs. 293 and 294. The various spacings used for different voltages are given in Fig. 314, where curve 1 gives the distance between high- and low-voltage windings and also between the high-voltage winding and the core; curve 2 gives the total thickness of the pressboard in this distance; curve 3

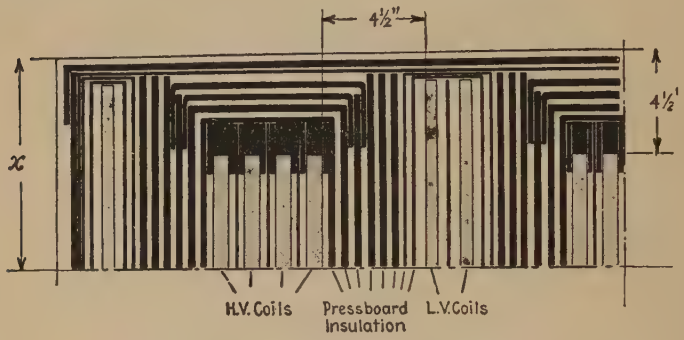

Fig. 315.—Insulation for 110,000 volts.

gives the distance X between the high-voltage coil and the iron at the top and bottom of the core.

Figure 315 shows an example of a shell-type transformer wound for $\frac{63{,}500}{13{,}200}$ volts for operation in a Y-connected bank on 110,000 volts; the insulation to ground, and also from high- to low-voltage winding, is the same as that for a 110,000-volt transformer. One-quarter of the total winding is shown in plan; there are 12 high-voltage coils, so that the voltage per coil = 5300.

CHAPTER XL

LOSSES, EFFICIENCY AND HEATING

306. The Losses.—The losses in a transformer are: the iron loss, the loss in the dielectric and the copper loss.

The iron loss has already been discussed in Art. 295, page 439.

The loss in the dielectric, about which very little is known, causes the material to heat up and its dielectric strength to decrease. The loss is kept small by the use of ample distances between points at different potential, and the heating is kept small by a liberal supply of oil ducts through the insulation; the layers of solid insulation should not be thicker than 0.25 in.

307. The Copper Loss.

If MT is the mean turn of a transformer coil in inches,

M is the section of the wire in the coil in circular mils,

I is the effective current in each turn of the coil,

then the resistance of each turn $= \frac{MT}{M}$ ohms

and the loss per coil in watts $= \frac{MT \times I^2}{M} \times$ turns. (67)

In addition to the above copper loss there is the eddy-current loss in the conductors, which may be large if the conductors are not properly laminated or arranged so that the leakage flux cuts their narrow sides. Diagram B, Fig. 316, shows part of the winding of a core-type transformer and the direction of the alternating leakage flux at one instant. If the coils are wound of strip copper on edge as shown at E, then eddy currents will flow in the direction shown by the crosses and dots, and the loss will be much larger than if the coils are wound with flat strip as shown at A.

Diagram D, Fig. 316, shows part of the winding of a shell-type transformer, and the direction of the leakage flux and the eddy currents at one instant. If such a coil is laminated in the direction of the leakage lines, it will be weakened mechanically; for that reason it is not advisable to laminate the conductors unless they are wider than 0.5 in. for 60 cycles, or 0.75 in. for 25 cycles,

for which values, and for ordinary current densities, the eddy-current loss will be about 20 per cent of the calculated I^2R loss.

Even after the conductors of a core-type transformer have been laminated, considerable eddy-current loss may under certain circumstances be found in the windings; for example, A, Fig. 316, shows part of the winding of a low-voltage large-current transformer where the coil is made up of four wires in parallel; eddy currents tend to flow in the direction represented at one instant by the crosses and dots, and since the parallel wires are all connected together at the ends, the current will flow down

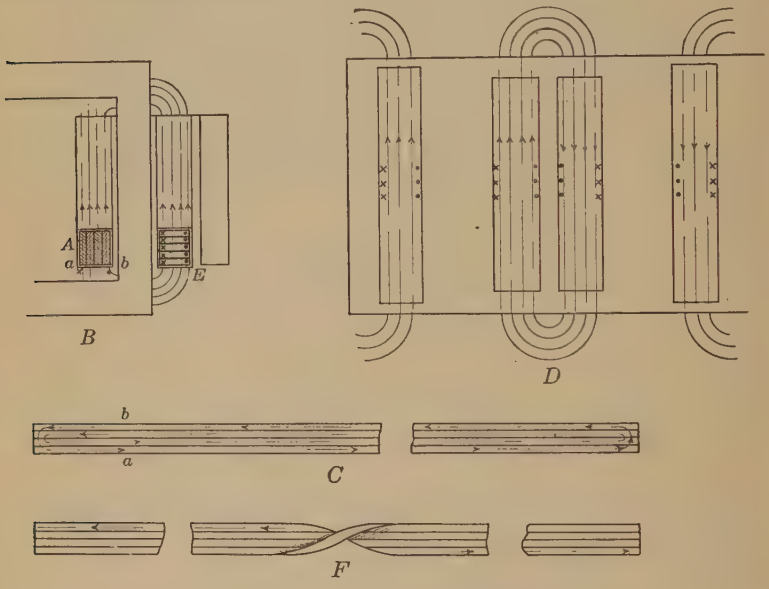

Fig. 316.—Eddy currents in transformer coils.

one wire a, cross through the soldered joint at the end to wire b, up which it will pass and then return by the other soldered joint to conductor a, so that if the coil is developed on to a plane, the currents will flow as shown in diagram C. To eliminate this circulating current the bunch of wires is given a half twist, as shown at F, so that in any one strip there are two e.m.fs., produced by the leakage flux, which are equal and opposite, the resultant e.m.f. is therefore zero and no circulating current will flow.

308. The Efficiency.

If CL is the iron or core loss in watts,

I^2R the copper loss in watts,

EI the output of the transformer in watts,

then η, the efficiency, $= \dfrac{\text{output}}{\text{output} + \text{losses}}$,

$$= \frac{EI}{EI + I^2R + CL}.$$

The efficiency is a maximum when

$$\frac{d\eta}{dI} = 0,$$

or $(EI + I^2R + CL)E - EI(E + 2IR) = 0,$

or $$I^2R = CL;$$

that is, when the copper loss is equal to the core loss.

The all-day efficiency, which is of importance in distributing transformers, is defined by the following equation:

$$\text{all-day efficiency} = \frac{EI \times X}{EI \times X + CL \times 24 + I^2R \times X},$$

where X is the number of hours during which the transformer is loaded each day, and 24 is the number of hours during which the iron loss is supplied. Distributing transformers should therefore be designed to have as small a core loss as possible, because this loss has to be supplied continuously.

309. Heating of Transformers.—When a transformer is in operation under oil, the heat generated in the core and windings has to be carried to the tank, from the external surface of which it is dissipated to the air. When the oil in contact with the transformer surface is heated, it becomes lighter and rises, and cool oil flows in from the bottom of the tank to take its place, so that a circulation of oil is set up, as shown in Fig. 317. That it may circulate freely the oil should have a low viscosity, and the lighter the oil the better it is as a cooling medium for transformers.

310. The Temperature Gradient in the Oil.—Figure 317 shows a core-type transformer and also shows the temperature of the oil at different points along its surface. At the bottom of the tank, the oil temperature is T_b; the oil moves along the circulation path and its temperature rises and reaches a maximum value T_t at the top of the transformer; it then passes to the tank and, as it moves downward, the heat is gradually given up to the tank. After a number of hours, during which the whole body of the transformer and the oil are absorbing heat and being raised in temperature, conditions become fixed, the oil circulation and

its temperature cycle become definite, and the different points of the transformer have their maximum temperature.

311. The Temperature Gradient in a Core-type Transformer. Consider the core of the transformer shown in Fig. 317. Iron is a good conductor of heat along the laminations, so that the difference in temperature between the points A and B of the core cannot be great, and the difference in temperature between the core and the adjacent oil must be greater at the bottom of the core than at the top; because of this, much of the heat

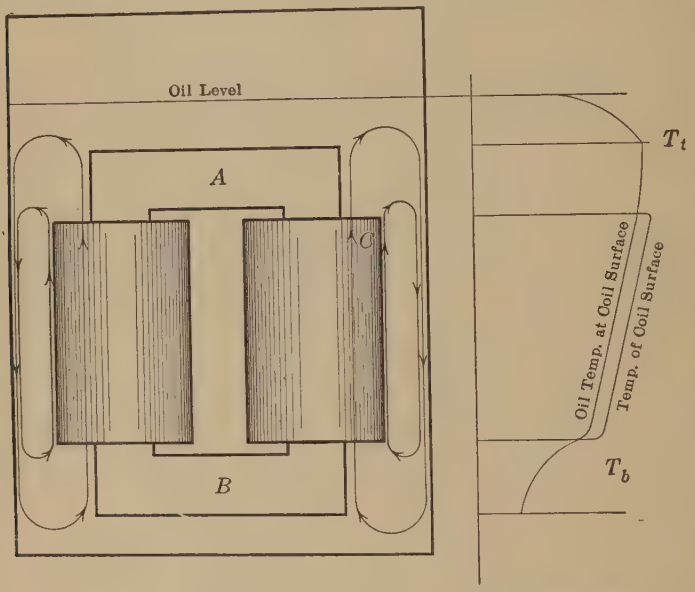

Fig. 317.—Temperature gradient in a core-type transformer.

generated in the top part of the core is conducted downward and dissipated from the surface at the bottom; that is, the bottom part of the core surface is more active than the top part in dissipating the heat due to the iron losses.

The conditions are different for the windings. These are formed of insulated wire wound in layers, and, because of the number of layers of insulation in the length of the coil, very little of the heat generated in the top turns will be conducted downward through the winding. Most of the heat generated at any point in the winding will be conducted to and dissipated from the nearest coil surface, so that the watts dissipated per unit area of coil surface, and therefore the temperature difference

between the coil surface and the adjacent oil will be approximately constant at all points, and the temperature of the surface of the coil will be a maximum at the top of the transformer. The hottest part of the whole winding will be at *C*.

Measurement of the temperature rise by resistance gives little information as to the temperature of the hottest part of the coil of a core-type transformer, because the temperature so found is the average temperature and may be less than that of the oil measured at the top of the transformer.

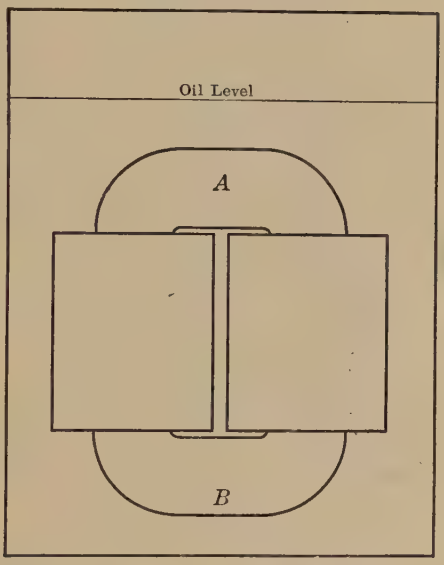

FIG. 318.—Shell-type transformer in tank.

312. The Temperature Gradient in a Shell-type Transformer. Figure 318 shows such a transformer. Since the core is laminated horizontally, and since iron is a poor conductor of heat across the laminations, most of the heat generated at any point in the core is conducted to and dissipated from the nearest core surface, so that each part of the core surface is equally active in dissipating heat, and the temperature of the core is a maximum at the top and a minimum at the bottom.

The conditions are different for the windings. These are made up of what are known as pancake coils, which are thin and have a large radiating surface. Since the top layers of the winding at *A* are connected directly to the bottom layers at *B* by a short length of copper, the temperature difference between

A and B cannot be very great, and the difference in temperature between the winding and the adjacent oil must be greater at the bottom than at the top. Because of this, much of the heat generated in the top part of the winding is conducted downward and dissipated from the winding surface at the bottom of the coil. The temperature of the winding is more uniform throughout than in a core-type transformer, and resistance measurements are of more value.

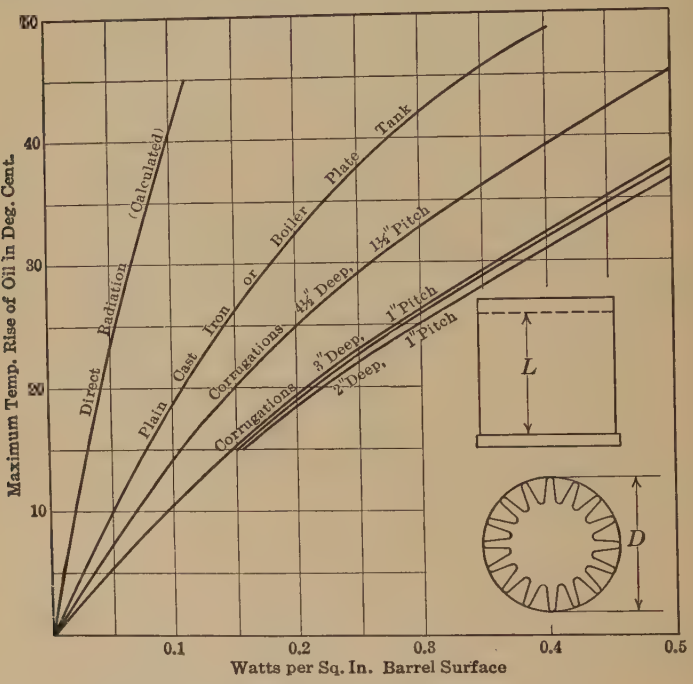

Fig. 319.—Heating curves for transformer tanks.

313. The Temperature of the Oil.—The rise in temperature of the oil over that of the external air depends principally on the loss to be dissipated, and on the external surface of the tank.

The heat in the oil is transmitted through the tank and dissipated from its external surface. A small part of this heat is dissipated by direct radiation, but most of the heat is dissipated by convection air currents which flow up the sides of the tank. For a plain boiler-plate tank, without ribs or corrugations, the highest temperature rise of the oil is plotted against watts per square inch external surface in Fig. 319, for a tank which is

round in section, and which has a height of approximately 1.5 times the diameter. This temperature rise is made up principally of the temperature difference between the air and the tank, and that between the tank and the oil; the former is about three times as large as the latter.

The temperature rise of the oil may be reduced by increasing the surface of the tank which is readily done by making it

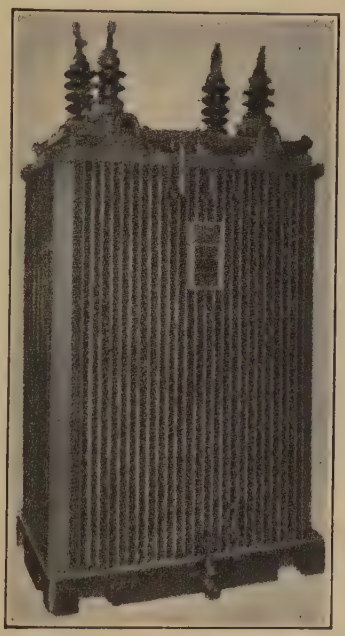

FIG. 320.—Oil insulated, self-cooled transformer with corrugations in tank surface to increase heat dissipating surface.

corrugated, as shown in Fig. 320 and also in Fig. 296. This increase in surface does not increase the direct radiation from the tank, because only that component of surface which is perpendicular to a radius is effective; for this reason and also because air does not circulate so freely in the corrugations as it does at the surface of a cylindrical or flat surface exposed directly to the air, the watts per square inch for a given temperature rise does not increase directly as the increase in surface. Consider the curve in Fig. 319 for corrugations 3 in. deep and spaced 1 in. apart; the external surface of the tank is increased about 6.5 times, while the watts per square inch for a given

temperature rise is increased only about 60 per cent over the value for a plain boiler-plate tank.

Figure 321 shows the results of tests on a boiler-plate tank with external pipes added to improve the heat dissipation. It will be seen from curves 1 and 2 that the watts per square inch of total surface for a given temperature rise is almost as large in the special tank as in the plain boiler-plate tank or, comparing curves 1 and 3, the surface of the special tank is 2.8 times that of the

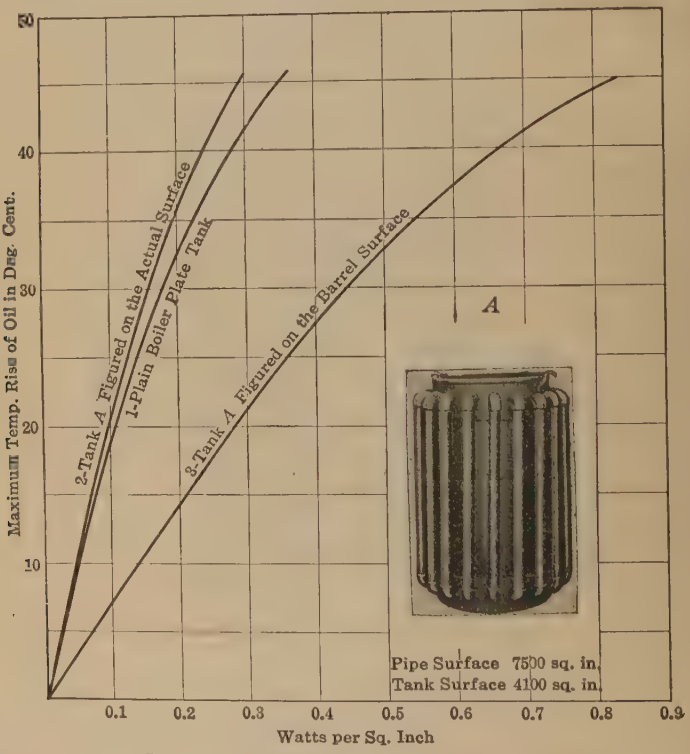

FIG. 321.—Heating curves for transformer tanks.

plain boiler-plate tank, while the watts per square inch for a given temperature rise is increased about 2.5 times.

Figure 296 shows the method of increasing radiating surface that is used in modern self-cooled transformers.

314. Air-blast Transformers.—Figures 322 and 323 show such a transformer. The problem in this case is like that discussed fully on page 283 on the heating of turbo-generators; 150 cu. ft.

of air is supplied per minute per kilowatt loss, and the average temperature of the air increases about 12° C. between the inlet and outlet. The temperature of the coils and core is kept within reasonable values by providing the necessary radiating surface, using the formula,

watts per square inch for 1° C. rise $= 0.01 + 0.025V$,

where the temperature rise is measured on the surface and V is the velocity of the air across the surface in thousands of feet per minute.

FIG. 322.—Air blast transformer of the shell type—outside case removed.

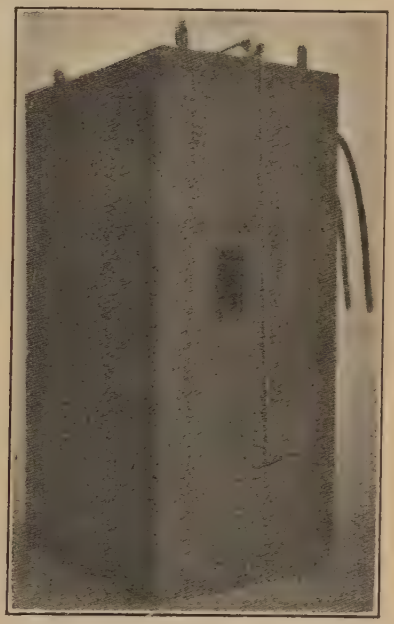

FIG. 323.—Air blast transformer—external view.

The air used should be filtered; otherwise the ducts will become clogged up with dust and the transformer will get hot. Dampers are usually supplied at the top of the case so that the distribution of the air through the core and coils may be controlled.

315. Water-cooled Transformers.—If coils of copper pipe carrying water be placed at the top of the case as shown in Fig. 295, then the oil which is heated by contact with the transformer will rise and carry the heat to the cooling coils.

If t_i is the inlet temperature of the water,

t_o is that at the outlet,

then each pound of water passing through the coils per minute takes with it $(t_o - t_i)$ lb. calories per minute,

or $32(t_o - t_i)$ watts.

With 2.5 lb. of water per minute per kilowatt loss the average temperature rise of the water will be 12.5° C.

It is advisable in water-cooled transformers to immerse the whole of the cooling coil; otherwise, due to the low temperature of the water passing through, moisture will deposit on the coil and get into the oil. The coil should be of seamless copper tube about 1¼ in. external diameter, and the drain tap should be at the bottom of the spiral so that, when not in operation, the spiral will be empty and therefore will not burst in frosty weather.

316. Heating Constants Used in Practice.—The calculation of the temperature rise of a transformer is so complicated by the oil circulation, and by the temperature gradient in the oil, coils and core that, until the results of a complete investigation of the subject are available, empirical constants will have to be used.

The necessary tank surface for a given loss is found from Fig. 319.

The watts per square inch coil surface

= 0.35 for self-cooled shell-type coils wound with small wire;

= 0.4 for self-cooled shell-type coils wound with strip copper;

= 0.35 for small core-type transformers; these figures may be increased 20 per cent for transformers which are water cooled or cooled by forced draft.

The watts per square inch iron surface

= 1.0 for both core and shell type; the area of cooling surface is taken as the edge surface and half of that part of the flat surface which is exposed to the oil circulation (see Art. 317).

The watts per square inch water pipe surface

= 1.0 for a 1.25-in. pipe, the supply being 2.5 lb. per minute per kilowatt loss.

317. Effect of Ducts.—It is difficult to determine how effective the ducts are in keeping a transformer core cool. Figure 324 shows a block of iron which is laminated vertically. The hottest part of the iron is at A and the temperature difference from A to B

$$= T_{ab},$$

$$= (\text{watts per cubic inch}) \frac{Y^2}{3} \text{ deg. Cent. (p. 124);}$$

that between A and C

$= T_{a_1}$ (assuming that the thermal resistance across the laminations is fifty-six times that along them),

$= (\text{watts per cubic inch}) \frac{56X^2}{3}$ deg. Cent.

The temperature difference between surface B and the oil

$= (\text{watts per cubic inch}) Y \times 16$,

since the temperature difference between the iron and the adjoining oil is 16° C. per watt per square inch. The temperature difference between surface C and the oil

$= (\text{watts per cubic inch}) X \times 16$.

The relative heat resistance of the two paths may be taken approximately as

$$\frac{\text{path } B}{\text{path } C} = \frac{Y\left(\frac{Y}{3} + 16\right)}{X\left(\frac{56X}{3} + 16\right)}.$$

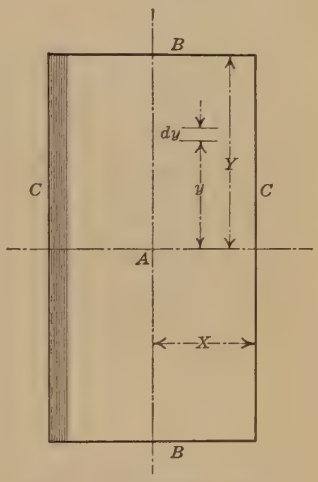

FIG. 324.—Heat paths in a transformer core.

If the ducts are spaced 2 in. apart, so that $X = 1.0$ in., then for different values of Y the relative heat resistance may be found from the following table:

RELATIVE HEAT RESISTANCE

X	Y	ALONG LAMINATIONS	ACROSS LAMINATIONS
1 in.	1 in.	0.48	1.0
1 in.	2 in.	1.0	1.0
1 in.	3 in.	1.5	1.0
1 in.	4 in.	2.0	1.0

That is, for the particular values taken, the duct surface is half as effective as that of the edge, if it is as well supplied with cool oil, that is, if the ducts are vertical and of sufficient width to allow free circulation.

Modern transformers do not use ducts in the iron, depending on the escape of heat from the edges of the iron to keep the iron at a reasonable temperature.

318. The Maximum Temperature in the Coils.—Although the maximum temperature in the coils of a transformer cannot readily

be determined, it is necessary to find out on what it depends and what its probable value may be.

In Fig. 325, which shows part of the coil of a transformer, let the thickness of the coil be small compared with the mean turn MT, and assume that the heat passes in both directions from the center line L.

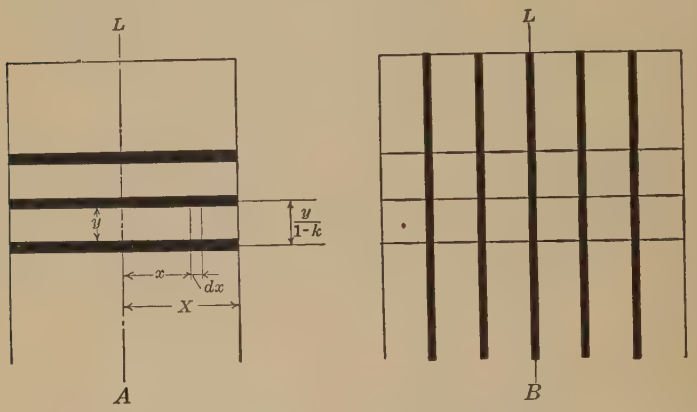

FIG. 325.—Part of a transformer coil showing insulation between layers.

If, of the thickness x, the part kx is insulation and $(1 - k)x$ is copper, then the current in the section xy

$$= xy(1 - k) \times \text{amperes per square inch},$$

$$= \frac{xy(1 - k)}{\text{square inches per ampere}},$$

$$= \frac{xy(1 - k) \times 1.27 \times 10^6}{\text{circular mils per ampere}}.$$

The resistance of a ring of length MT and section $xy(1 - k)$ sq. in.

$$= \frac{MT}{xy(1 - k) \times 1.27 \times 10^6}.$$

The loss in this ring = current^2 $\times$ resistance

$$= \frac{(xy(1 - k) \times 1.27 \times 10^6)^2 \times MT}{xy(1 - k) \times 1.27 \times 10^6 \text{ (cir. mils per ampere)}^2},$$

$$= \frac{MT \times xy(1 - k) \times 1.27 \times 10^6}{\text{(circular mils per ampere)}^2}.$$

The heat due to this loss crosses the section of thickness dx, of which $k \times dx$ is insulation, and since the specific conductivity of insulating material = 0.003, in watts per inch cube per degree

Centigrade difference in temperature, therefore the difference in temperature between the center and the surface

$$= \Theta = \int_0^{\theta} d\Theta = \int_0^{x} \frac{MT \times xy(1-k) \times 1.27 \times 10^6}{(\text{circular mils per ampere})^2} \times \frac{k \times dx}{MT \times y} \times \frac{1}{0.003}, \quad (68)$$

$$= \frac{2.1 \times 10^8 k(1-k)X^2}{(\text{circular mils per ampere})^2}. \quad (68)$$

Consider the following example: A core-type transformer, with the windings insulated as in Fig. 312, has the high-tension winding made with No. 12 square d. c. c. wire. The high-voltage winding is 1 in. thick, the current density is 1600 cir. mils per ampere, and there is one thickness of 0.007 in. fullerboard between layers; it is required to find the maximum difference in temperature between the inner and outer layers of the winding.

Thickness of wire	0.0808
Thickness of cotton covering	0.01
Thickness of fullerboard	0.007
Value of k	$\frac{0.017}{0.0978} = 0.174$
Value of $1 - k$	0.826
Temperature difference	$\frac{2.1 \times 10^8 \times 0.174 \times 0.826}{1600^2} = 12°$ C.

If round wire is used instead of square, then the contact area between adjacent layers is greatly reduced, and the temperature difference increased. It is advisable for such coils as that discussed above to use square or rectangular wire and to limit the thickness of the coil to 1 in., and the current density to about 1600 cir. mils per ampere.

319. The Section of the Wire in the Coils.—Diagram *A*, Fig. 325, shows part of a coil of a shell-type transformer, and *B* shows part of a coil of a core-type transformer.

The loss in one layer of the winding, as may be seen from the last article,

$$= \frac{MT \times 2Xy(1-k) \times 1.27 \times 10^6}{(\text{circular mils per ampere})^2} \text{ watts.}$$

The corresponding radiating surface $= MT \times \frac{2y}{1-k}$ sq. in.

Therefore the watts per square inch

$$= \frac{2X(1-k)^2 \times 1.27 \times 10^6}{2 \times (\text{circular mils per ampere})^2},$$

and circular mils per ampere $= 8 \times 100\sqrt{\dfrac{2X(1-k)^2}{\text{watts per square inch}}}$, (69)

$= 1350\sqrt{2X(1-k)^2}$ when watts per square inch $= 0.35$,

$= 1260\sqrt{2X(1-k)^2}$ when watts per square inch $= 0.4$.

CHAPTER XLI

PROCEDURE IN DESIGN

320. The Output Equation.

$E = 4.44T\phi_a f 10^{-8}$, (formula (64), p. 439),

and EI = the watts output,

$$= 4.44TI \times \phi_a \times f \times 10^{-8},$$

$$= 4.44\frac{\phi_a{}^2}{k_t} \times f \times 10^{-8} \text{ where } k_t = \frac{\phi_a}{TI} = \frac{\text{magnetic loading}}{\text{electric loading}}.$$

The volts per turn of coil $= V_t$,

$$= 4.44\phi_a f 10^{-8},$$

$$= 4.44f \times 10^{-8}\sqrt{\frac{\text{watts} \times k_t}{4.44f10^{-8}}},$$

$$= \sqrt{\text{watts}} \times \sqrt{4.44k_t f 10^{-8}}.$$

Now $E = 4.44T\phi_a f 10^{-8}$,

so that, for a given voltage, the lower the frequency the larger the product $\phi_a \times T$. If a transformer is built with a large number of turns, so that $k_t = \frac{\phi_a}{TI}$ is small, then the copper loss is large because of the large number of turns, and the core loss is small because of the relatively small amount of iron; such a transformer would therefore have its maximum efficiency at a fraction of full load (see p. 463). In order that the efficiency may be a maximum at or near full load, the full-load copper and the core loss must be approximately equal and the flux must increase as the frequency decreases; it is found in practice that the value of $k_t = \frac{\phi_a}{TI}$ is approximately inversely proportional to the frequency, or that $k_t f$ is approximately constant; therefore

volts per turn, V_t = a constant $\times \sqrt{\text{watts}}$, (70)

where the following average values of the constant are found in practice:

$\frac{1}{80}$ for core-type distributing transformers,

$\frac{1}{50}$ for core-type power transformers,

$\frac{1}{25}$ for shell-type power transformers.

The constant for the distributing transformer is less than that for the power transformer because, while in the latter the highest efficiency is desired around full load, in the former a small core loss and a high all-day efficiency is desired. To obtain a small core loss it is necessary to keep the value of $k_t = \frac{\phi_a}{TI}$ small, and therefore the constant in formula (70) must be small.

The constant is different for core- and for shell-type transformers because of the difference in construction. Figure 326 shows the ordinary proportions of a core-type transformer; the

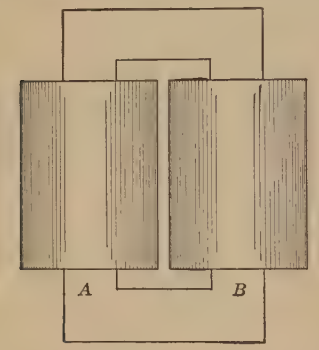

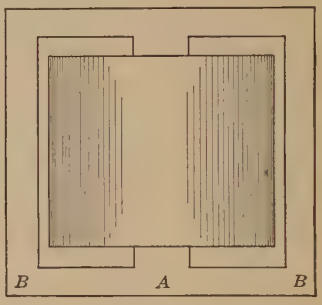

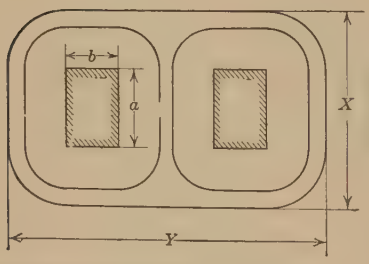

Fig. 326.—Core-type transformer.

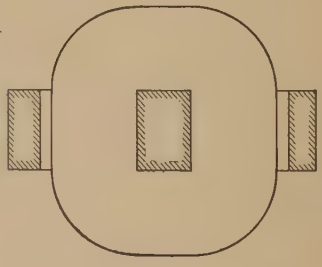

Fig. 327.—Shell-type transformer.

distance a is generally about $1.5 \times b$ so as to keep the ratio of X to Y within reasonable limits, and prevent the use of a thin wide tank.

If the coil on limb B of the transformer in Fig. 326 be placed on limb A, and limb B then split up the center and one-half bent over to give Fig. 327, a shell-type transformer is produced which has the same amount of copper and iron as the corresponding core-type transformer. The resulting shell-type transformer is flat and low, so that the tank required to hold it takes up con-

siderable floor space; the proportions are therefore changed so as to give the ordinary shape shown in Fig. 328, and for a given rating it will be found that the ratio $\frac{\phi_a}{TI}$ is about four times as large for the transformer in Fig. 328 as it is for that in Figs. 326 or 327; that is, the shell-type transformer has generally twice the flux and half the number of turns that the core-type transformer has for the same rating. The distance a is generally about $6 \times b$ to give a reasonable shape of core.

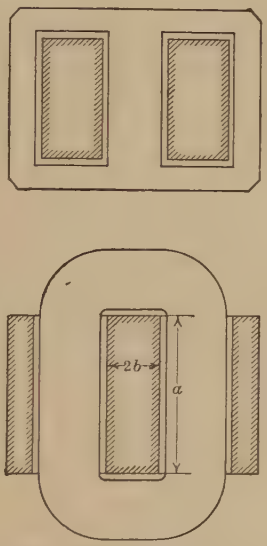

FIG. 328.—Shell-type transformer.

321. Procedure in the Design of Core-type Transformers. The volts per turn $= \frac{1}{50}\sqrt{\text{watts}}$ for power transformers,

$= \frac{1}{80}\sqrt{\text{watts}}$ for distributing transformers.

The number of coils is chosen so as to keep the voltage per coil less than 5000, but there should not be less than two high-voltage and two low-voltage coils; the number of turns per coil is equal to

$$\frac{\text{terminal voltage}}{\text{volts per turn} \times \text{number of coils}}.$$

The depth of the coil measured from the nearest oil duct should not be greater than 1.0 in., except in the case of small distributing transformers insulated as shown in Fig. 312 which have no oil

duct between the low-voltage winding and the core. In such a case the depth from the core to the oil may be 2 in., the reason being that the heat in the inner layers of the winding is conducted through the insulation into the core and dissipated by the core surface.

The section of the wire in circular mils is found from formula (69), page 474, namely,

circular mils per ampere $= 1350\sqrt{(1-k)^2 \times 2X}$ where

X = the greatest depth from the inside of the winding to the nearest oil or core surface,

$(1-k)^2$ = per cent copper in the vertical layers of the winding $\times$ that in the horizontal layers,

and the area of the wire is the product of the full-load current in the winding and the circular mils per ampere. The section of wire should be chosen so that it is not thicker than 0.125 in., and the wire should be wound flat as shown at A, Fig. 316.

The number of layers in the winding is the same as the number of wires in the assumed depth of the coil; the number of conductors per layer is the total number of turns per coil divided by the number of layers, and the height of the winding is the number of turns per layer multiplied by the width of the wire in the direction parallel to the limbs of the core.

The flux in the core is found from formula (64), page 439; namely, $E = 4.44 \times$ turns $\times$ flux $\times$ frequency $\times 10^{-8}$,

and the core area $= \dfrac{\text{flux in core}}{\text{core density}}$, where the value of the core density is taken for a first approximation,

= 65,000 lines per square inch 60-cycle distributing transformers

= 75,000 lines per square inch 25-cycle distributing transformers

= 90,000 lines per square inch 60-cycle power transformers

= 80,000 lines per square inch 25-cycle power transformers

alloyed iron being used for 60-cycle transformers, to keep down the loss in the distributing transformer so as to have a high all-day efficiency, and to keep down the heating in the power transformers. Ordinary iron is used for 25-cycle transformers, because, due to the low frequency, the loss is generally small, while the densities have to be kept low in order that the magnetizing current will not be too large a per cent of the full-load current.

The core and windings are drawn in to scale; the losses, magnetizing current, resistance and reactance drops are determined, and the size of the tank is fixed. If the transformer as

designed does not meet the guarantees, then certain changes must be made.

If the core loss is too high, either the core density must be reduced, which will increase the size of the transformer, or the total flux must be reduced, which will require an increase in the number of turns for the same voltage, and, therefore, an increase in the copper loss.

The resistance and the reactance drops may both be reduced by a reduction in the number of turns, because the resistance is directly proportional to the number of turns, while the reactance is proportional to the square of the number of turns.

Example.—Design and determine the characteristics of a 15-k.v.a., 2200- to 220-volt, 60-cycle distributing transformer.

Design of the High-voltage Winding

Volts per turn = 1.52.

Total number of turns = 1440.

Coils = 2; one on each leg.

Turns per coil = 720.

Total depth of winding = 2.0 in., assumed.

Circular mils per ampere $= 1350 \times \sqrt{2 \times 0.9 \times 0.8}$.
$= 1620$.

Full-load current = 6.8 amperes.

Section of wire = 11,000 cir. mils;
use No. 10 square B. & S.
= 0.1019 in. × 0.1019 in.
which has a section of 13,000 cir. mils, not allowing for rounding of the corners.

Insulation = 0.01 in. double cotton covering,
0.014 in. fullerboard between layers.

$(1 - k)$ vertical $= \frac{0.1019}{0.1119} = 0.91.$

$(1 - k)$ horizontal $= \frac{0.1019}{0.1259} = 0.81.$

Number of layers $= \frac{1.0}{0.1019 + 0.01 + 0.014}$.
$= 8.$

Turns per layer = 90.

Height of winding = 90 × (0.1019 + 0.01).
= 10 in.

Height of opening = 11.75 in. (see Fig. 312).

Design of the Low-voltage Winding

Total number of turns = 1440 × ratio of transformation.
= 144.

Turns per coil = 72.

Circular mils per amperes = 1620; the same as for the high-voltage coil.

Section of wire = 110,000 cir. mils.
= 0.087 sq. in.
= 0.11 in. × 0.8 in.; this will be difficult to wind on a small transformer because of its width; therefore, change the winding as follows:

Turns per coil = 72; number of coils = 4 connected two in parallel; size of wire = 0.11 in. × 0.4 in.

Insulation = 0.015 in. cotton covering.
0.014 in. fullerboard between layers.

Turns per layer $= \frac{\text{winding height}}{\text{width of wire}}$.
$= \frac{10.0}{0.415}$.
= 24.

Number of layers per coil $= \frac{72}{24}$.
= 3.

Number of layers per leg = 6, because there are two coils per leg.

Depth of winding = (0.11 in. + 0.015 in. + 0.014 in.) 6.
= 0.83 in.

Thickness of insulation between the high- and low-voltage coils = 0.12 in.

Design of Core

Flux = 5.72×10^5.
Core density, assumed = 65,000 lines per square inch.
Necessary core section = 8.8 sq. in.
Actual section adopted = 2.5 × 4 and stacking factor = 0.9.
Width of opening = 4.5 in., to allow a little clearance between coils on different legs (see Fig. 312).

Calculation of the Losses and the Magnetizing Current

Mean turn of low-voltage coil = 16.6 in.

Resistance of secondary winding $= \frac{144 \times 16.6}{2 \times 0.11 \times 0.4 \times 1.27 \times 10^6}$.
= 0.021 ohm.

Mean turn of high-voltage coil = 24 in.

Resistance of primary winding $= \frac{1440 \times 24}{13{,}000}$,
= 2.6 ohms.

Loss in primary winding $= 2.6 \times 6.8^2$,
= 120 watts.

Loss in secondary winding $= 0.021 \times 68^2$,
= 97 watts.

Weight of core = 110 lb.
Actual core density = 63,500 lines per square inch.

Core loss in watts (4 per cent silicon steel) $= 110 \times 0.81$ (from Fig. 298, p. 442).
$= 89$ watts.

Volt amperes excitation $= 110 \times 2.8$,
$= 308$ volt amperes.

Per cent exciting current $= 2.1$.

Calculation of the Regulation

Equivalent primary reactance $= 2\pi f \times 3.2\, T_1^2 \times \frac{MT}{L}\left(\frac{d_1}{3} + \frac{d_2}{3} + S\right)10^{-8} \times 2$

where $f = 60$,
$T_1 = 720$,
$MT = \frac{16.6 + 24}{2}$,
$= 20.3$ in.
$L = 10$ in.
$d_1 = 1.0$ in.
$d_2 = 0.83$ in.
$S = 0.12$ in.
coils $= 2$.

X_{eq} of primary $= 2\pi \times 60 \times 3.2 \times 720^2 \times \frac{20.4}{10}\left(\frac{1.0+0.83}{3} + 0.12\right) \times 10^{-8} \times 2$,
$= 18.6$ ohms.

The reactance drop referred to the primary $= 18.6 \times 6.8$,
$= 126$ volts,
$= 5.8$ per cent.

The primary resistance drop $= 2.6 \times 6.8$,
$= 17.6$ volts.

The secondary resistance drop $= 0.021 \times 68$,
$= 1.43$ volts.

The resistance drop referred to the primary $= 17.6 + 1.43 \times \frac{2200}{220}$,
$= 31.9$ volts,
$= 1.44$ per cent.

Design of the Tank

The total losses at full load are:

Iron loss,	89 watts.
Primary copper loss,	120 watts.
Secondary copper loss,	97 watts.
Total loss,	306 watts.

The watts per square inch for 35° C. rise of the oil $= 0.225$; therefore the tank surface in contact with the oil

$= \frac{306}{0.225}$,
$= 1400$ sq. in.

322. Procedure in the Design of a Shell-type Transformer.—The work is carried out in exactly the same way as for a core-type transformer except that the width of the coil is seldom made

greater than about 0.5 in., so as to provide ample radiating surface and allow the use of comparatively high copper densities.

The number of coils is again chosen so as to keep the voltage per coil less than 5000; still further subdivision of the winding may be required in some cases to reduce the reactance.

Example.—Design a 1500-k.v.a., 63,500- to 13,200-volt, 25-cycle power transformer for operation in a three-phase bank on a 110,000 volt line.

Design of the High-voltage Winding

Volts per turn = 49.
Total number of turns = 1300.
Coils = 12.
Turns per coil = 108 average; use 10 coils with 113 turns and 2 end coils with 85 turns.
Width of coil, assumed = 0.4 in.

Because of the high voltage the distance x, Fig. 315, will be large, and there will be little iron saved by making the strip wider than 0.4 in. with the idea of keeping the distance x small.

Circular mils per ampere $= 1260 \times \sqrt{0.4 \times 0.6}$
where $(1 - k)^2$ is assumed to be $= 0.6$,
$= 615$.
Section of wire = 14,500 cir. mils,
$= 0.0285 \times 0.4$ in.
Insulation = 0.015 in. cotton covering,
0.014 in. fullerboard,

$$(1 - k) = \frac{0.0285}{0.0575} = 0.5.$$

Under ordinary circumstances the calculation for the size of conductor would be repeated using the correct value for $(1 - k)$ to find the value of the circular mils per ampere. In a very high voltage transformer, however, the amount of copper is small compared with the amount of iron and insulation, so that it is not advisable to run the chance of high temperature rise for a small gain in the amount of copper used. The conductor chosen for this transformer is therefore 0.03×0.4 in.

Height of winding = turns × thickness of insulated wire.
$= 113 \times (0.03 + 0.015 + 0.014)$.
= 6.7 in.
= 7 in. to allow for bulging.
Space between winding and core = 4.5 in., from Fig. 314.
Width of opening $= 7 + (2 \times 4.5)$,
= 16 in.

The arrangement of the winding must now be decided on and several possible methods are shown in Fig. 329. *A* would give a very long core and take up a large floor space, it would also have a large core loss and magnetizing current because of the large amount of iron in the magnetic circuit, but of the three shown it would have the lowest reactance.

B would have a lower magnetizing current and a lower core loss than *A*; it would also be considerably cheaper, but would have a larger reactance.

C will have values of core loss, magnetizing current and reactance between these of *A* and *B*, and the design will be completed for this arrangement to find its characteristics.

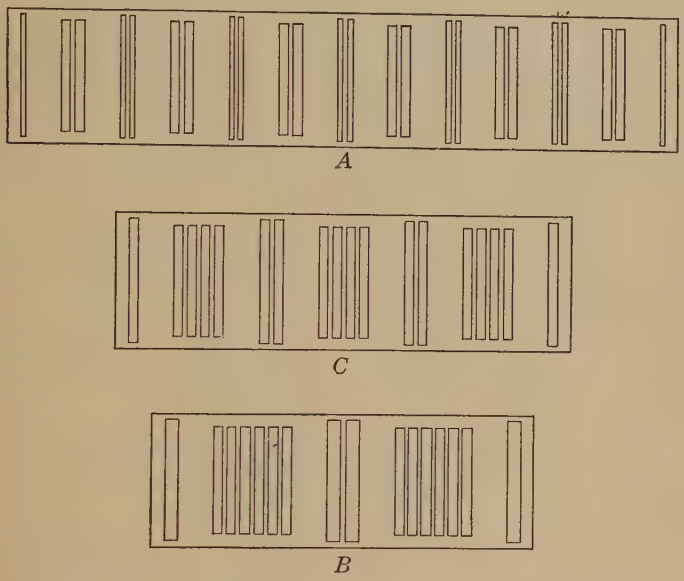

FIG. 329.—Arrangement of coils in a 110,000-volt shell-type transformer.

Design of the Low-voltage Winding

Total number of turns	= 270.
Coils	= 6.
Turns per coil	= 45.
Width of copper assumed	= 0.4 in.
Circular mils per ampere	= $1260 \times \sqrt{0.4 \times 0.9}$ where $(1 - k)^2$ is assumed to be = 0.9,
	= 755.
Section of wire	= 86,000 cir. mills.
	= 0.17 in. × 0.4 in. use 2 × (0.085 in. × 0.4 in.) with a strip of fullerboard between.
Insulation	= 0.007 fullerboard between wires, 0.024 half-lap cotton tape, 0.014 fullerboard between layers.
Thickness of insulated strip	= 0.215 in.
Height of winding	= 0.215 × 45,
	= 9.7 in.
	= 10.2 in. to allow for bulging.

This allows ample clearance between the winding and the core, in fact the winding could be made narrower and higher because 0.75 in. would be ample spacing for 13,200 volts, but it is advisable to use the larger spacing, where it is available without any sacrifice of space or material.

The coils with the insulation are now drawn to scale as shown in Fig. 315 and the length of the opening determined; this value is 43 in.

Design of the Core

Flux $= 44 \times 10^6$.
Core density, assumed = 80,000 lines per square inch.
Necessary core section = 550 sq. in.
Actual section adopted $= 14 \times 43.5$ in.

Calculation of the Losses and the Magnetizing Current

Mean turn of the low-voltage winding = 170 in.

Resistance of the low-voltage winding $= \dfrac{6 \times 45 \times 170}{0.17 \times 0.4 \times 1.27 \times 10^6}$,
$= 0.53$ ohm.

Mean turn of high-voltage winding = 190 in.

Resistance of high-voltage winding $= \dfrac{1300 \times 190}{0.03 \times 0.4 \times 1.27 \times 10^6}$,
$= 16.2$ ohms.

Loss in the high-voltage winding $= 16.2 \times 23.6^2$,
$= 9000$ watts.

Loss in the low-voltage winding $= 0.53 \times 114^2$,
$= 6900$ watts.

Weight of core = 22,000 lb.

Core loss in watts (0.9 per cent silicon steel) $= 22{,}000 \times 0.76$ (from Fig. 298),
$= 16{,}720$ watts.

Total loss at full load = 32,620 watts.
Efficiency = 97.8 per cent.
Volt amperes excitation $= 22{,}000 \times 3.3$ (from Fig. 299),
$= 72{,}600$
$= 4.8$ per cent.

The equivalent primary reactance $= 2\pi f \times 3.2 \times T_1^2 \dfrac{MT}{L}\left(\dfrac{d_1}{3} + \dfrac{d_2}{3} + S\right) \times 10^{-8} \times$ coil groups,

where $MT = 180$ in.
$L = 16$ in.
$d_1 = 1.3$ in. (see Figs. 303 and 315).
$d_2 = 0.4$ in.
$S = 4.5$ in.
coil groups = 6 (diagram *C*, Fig. 329).

Equivalent primary reactance $= 2\pi \times 25 \times 3.2 \times 216^2 \times \dfrac{180}{16}\left(\dfrac{1.7}{3} + 4.5\right) 10^{-8} \times 6$,
$= 80$ ohms.

The reactance drop referred to the primary $= 80 \times 23.6$,
$= 1900$ volts,
$= 3.0$ per cent.

The primary resistance drop = 380.

The secondary resistance drop referred to the primary $= 60 \times \frac{63{,}500}{13{,}200} = 290.$

The resistance drop referred to the primary = 670,
= 1.05 per cent.

The tank is made round in section and clears the core by 2 in. at the corners.

The total loss = 32,620 watts.

The water-pipe surface required = 35,000 sq. in.
= 750 ft. of 1¼-in. pipe.

CHAPTER XLII

SPECIAL PROBLEMS IN TRANSFORMER DESIGN

323. Comparison between Core- and Shell-type Transformers. For very high voltage service the losses are not of so much importance as reliability in operation. Figure 330 shows the relative proportions of a high-voltage core and of a high-voltage

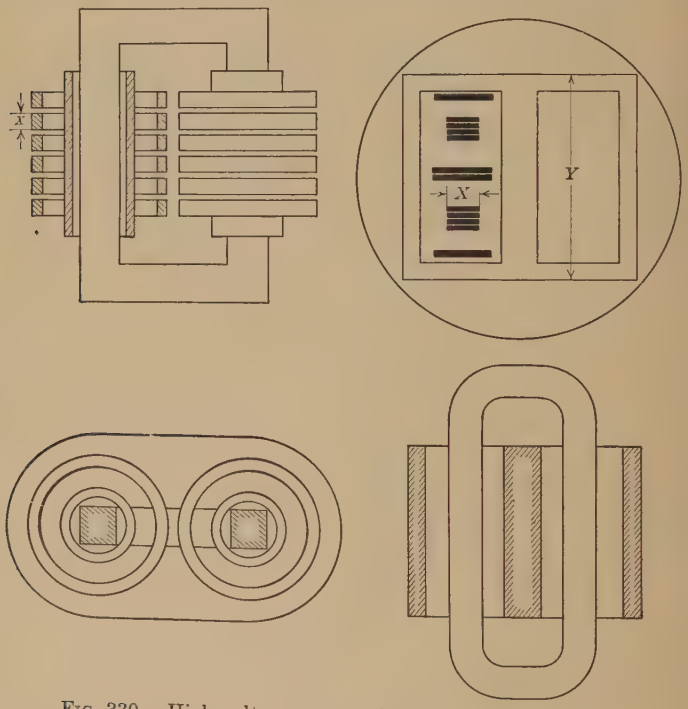

Fig. 330.—High voltage core, and shell-type transformers.

shell-type transformer; the coils of such transformers are not easily braced and supported if the core-type of construction is used, and the forces due to short-circuits are more liable to destroy the winding than in the case of shell-type transformers, in which the coils are braced in such a way that these forces cannot bend them out of shape.

The current on a dead short-circuit $= \frac{\text{terminal voltage}}{\text{impedance of winding}}$ and may reach, in power transformers, a value of twelve to twenty times full-load current. In the case of an instantaneous short-circuit the current may reach still greater values depending, as shown in Art. 203, page 288, on the point of the voltage wave at which the short-circuit takes place. Since the forces tending to separate the high- and low-voltage windings, and to pull together the turns of windings of the same coil, are proportional to the square of the current, they may reach very large values on short-circuit and may destroy the winding. Of the two types of transformers, the shell type is the better able to resist such forces.

The winding of a transformer is divided up into a number of coils in series, and the voltage per coil should not exceed about 5000 volts. It will generally be found that the distance X, over which this voltage is acting, is less in the core- than in the shell-type transformer.

The reactance of a transformer depends on the square of the number of turns, and on the way in which the winding is subdivided. Due to the large space required between the high- and low-voltage coils it is not practicable to subdivide the winding of a high-voltage core-type transformer more than is shown in Fig. 330, while the shell-type winding can be well subdivided before the length Y is greater than that required for a cylindrical tank. Because of this, and also because it has the smaller total number of turns, the reactance of a shell-type transformer can readily be kept within reasonable limits while that of a core type cannot.

So far as the coils themselves are concerned the shell type of transformer, in large sizes, has the advantage that strip copper wound in one turn per layer may be used; this gives a stiff coil and one not liable to break down.

For outputs up to 500 k.v.a. at 110,000 volts the core type is probably the cheaper, and for outputs greater than 1000 k.v.a. the shell type must be used to keep the reactance drop within reasonable limits; between these two outputs the type to be used depends largely on the previous experience of the designer.

The core-type transformer has the great advantage that it can be easily repaired, especially if built with butt joints so that the top limb may be removed and the windings and insulation lifted off.

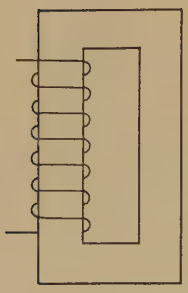

A

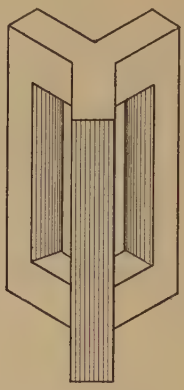

B

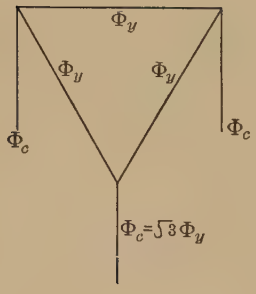

D

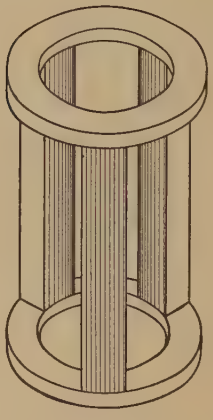

C

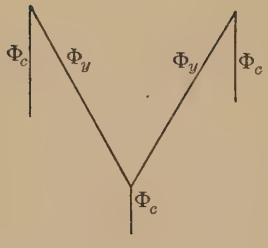

E

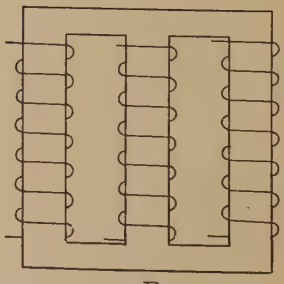

F

FIG. 331.—Development of the three-phase core-type transformer.

324. Three-phase Transformers.—Diagram *A*, Fig. 331, shows a single-phase transformer with all the windings gathered together on one leg, and diagram *B* shows three such transformers with the idle legs gathered together to form a resultant magnetic return path. The flux in that return path is the sum of three fluxes which are 120 electrical degrees out of phase with one another and is therefore zero; the center path may therefore be dispensed with.

In diagram *B* the flux in a yoke is the same as that in a core; the yoke and core have therefore the same area. If the three cores are connected together at the top and bottom as shown in

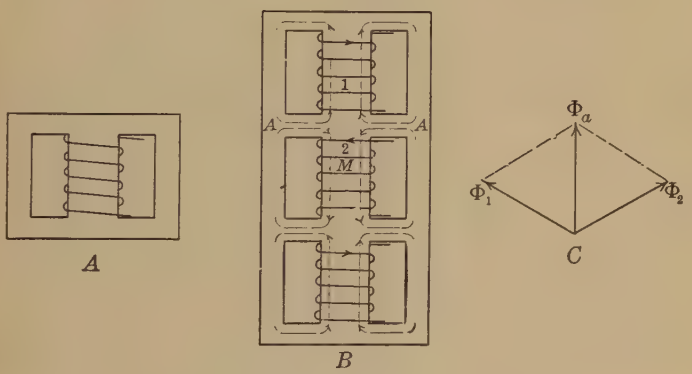

FIG. 332.—Three-phase shell-type transformer.

diagram *C*, then the three yokes form a Δ-connection, and, as shown by the vector diagram *D*, the flux in the yoke is less than that in the core in the ratio $\frac{1}{\sqrt{3}}$, and the yoke section may be less than that of the core. The bank of transformers may be still further simplified by operating it with a V or open Δ-connected magnetic circuit as shown in diagram *E*, and this latter transformer, when developed on to a plane as shown in diagram *F*, gives the three-phase core type that is generally used. There is a considerable reduction in material between three transformers, such as that in diagram *A*, and the single transformer in diagram *F*, so that the three-phase transformer is cheaper, has less material, greater efficiency, and takes up less room than three single-phase transformers of the same total output.

So far as the design is concerned there is no new problem; each leg is treated as if it belonged to a separate single-phase transformer.

Diagram *A*, Fig. 332, shows a single-phase shell-type transformer, and diagram *B* shows three such transformers set one above the other to form a three-phase bank. If the three coils were all wound and connected in the same direction, as in the case of the three-phase core-type transformer, then the flux in the core at *M* would be produced by three m.m.fs., 120 deg. out of phase with one another, and would be zero, because at any instant the m.m.f. of one phase would be equal and opposite to the sum of the m.m.fs. of the other two phases. The center coil is connected backward and the direction of the flux in the cores and cross-pieces at one instant is shown by the arrows. The total flux in one of the cross-pieces, say *A*, is the sum of the fluxes in cores 1 and 2, and the value may be found from diagram C.

A unique type of three-phase transformer—not used to any large extent in present day commercial practice—is shown in Fig. 333; it is almost circular in section and may be used in a cylindrical tank. The iron parts of this design are not made up of straight strips or L-shaped pieces and hence are not so economical of iron as some other designs.

325. Operation of a Transformer at Different Frequencies.—

The e.m.f. $= E$,

$= 4.44\ T\phi_a f 10^{-8}$,

$= 4.44\ TB_m A_c f 10^{-8}$,

$=$ a constant $\times\ B_m \times f$ for a given transformer;

the iron losses $=$ hysteresis loss $+$ eddy-current loss,

$= KB_m^{1.6} f + K_b B_m^2 f^2$ for a given transformer,

$= \text{a constant} \times \dfrac{E^{1.6}}{f^{0.6}} + \text{a constant} \times E^2$,

so that, for a given voltage, as the frequency increases the hysteresis loss decreases, while the eddy-current loss remains constant. A standard transformer, designed for a definite frequency, may operate at frequencies which are considerably higher or lower than that for which the transformer was designed; if the transformer is designed so that at normal frequency and full load the copper and iron losses are equal and the efficiency a maximum, then at lower frequencies the iron loss will be larger

than the copper loss, and at higher frequencies the copper loss will be the greater.

In order that a low-frequency transformer may have approximately the same core loss and copper loss at full load, the section of the iron in the core must be increased over that required for a transformer of the same rating but of higher frequency, in order

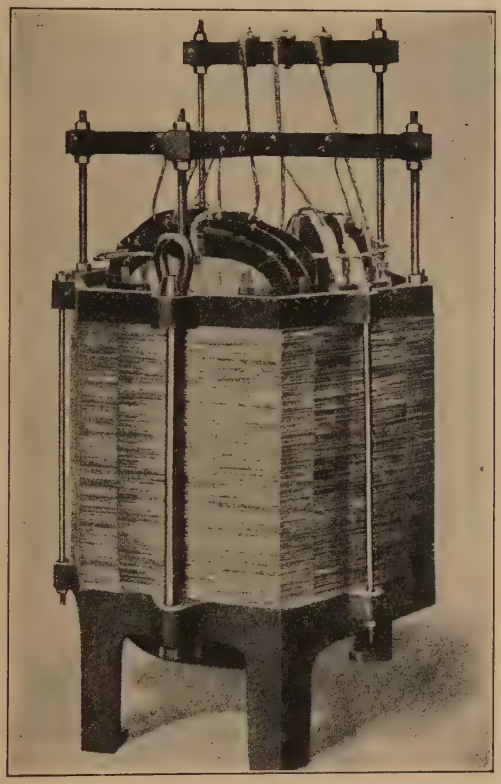

Fig. 333.—Three-phase shell-type transformer.

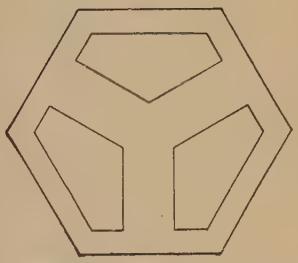

Section of the iron core.

to lower the densities and reduce the core loss, so that, for the same rating and efficiency, the lower the frequency, the larger the amount of iron, and the heavier the transformer.

326. Methods of Specifying and Testing Transformers.—The A. I. E. E. standardization committee has standardized temperature rises, testing methods, insulation tests, etc. for transformers which may be found by reference to those rules.

327. Transformer Performance.—The following tables give dimensions and performance data on a line of standard transformers. There are two classes of transformers included in these tables:

1. A line of transformers made with 4 per cent silicon steel; these give an iron loss that is as low as can be obtained with the best obtainable commercial grades of transformer steel, and give a comparatively high cost of iron.

2. A line of transformers made with a poorer and cheaper grade of steel and consequently lower in cost.

HIGH-EFFICIENCY TRANSFORMERS, 2300 TO 230–110 VOLTS
(All losses based on 75° C. temperature)

K.v.a.	Iron loss, watts	Copper loss, watts	Per cent efficiency				Per cent impedance at 75° C.	Per cent regulation	
			¼ load	½ load	¾ load	Full load		100 per cent power factor	80 per cent power factor
1.5	21	51	93.9	95.6	95.7	95.4	3.8	3.45	3.85
3	33	75	95.2	96.6	96.7	96.5	3.1	2.54	3.11
5	42	102	96.2	97.3	97.4	97.2	2.9	2.08	2.80
7.5	56	133	96.6	97.6	97.7	97.5	2.6	1.84	2.60
10	70	178	96.3	97.7	97.7	97.6	2.8	1.84	2.69
15	91	265	97.2	97.9	97.9	97.7	2.6	1.82	2.55
25	132	384	97.5	98.1	98.1	97.9	3.0	1.60	2.80
37.5	195	491	97.6	98.3	98.3	98.2	2.7	1.35	2.42
50	250	614	97.7	98.3	98.4	98.3	2.6	1.30	2.40
75	460	825	97.3	98.2	98.3	98.3	3.3	1.20	2.80
100	615	1120	97.3	98.2	98.3	98.3	3.9	1.30	3.10
150	870	1800	97.4	98.2	98.3	98.2	3.9	1.30	3.20
200	1145	2400	97.4	98.2	98.3	98.2	3.4	1.30	2.90

The dimensions of this line of transformers are given in the following table referring to Fig. 334, all dimensions in inches:

K.v.a.	*A*	*B*	*C*	*D*	*E*	*F*	*H*	Oil, gallons	Weights	
									Net	Shipping
1.5	15¼	16 3/16	11 1/16	9 7/16	9 7/16	3½	7	1¼	84	107
3	16¼	16 3/16	12 5/32	10 1 3/16	10⅜	3½	7	1¾	138	170
5	17¾	18	13 ¾	11 ¾	11⅜	3½	7	3½	195	225
7.5	21	19⅝	15 5/16	13 3/16	13 1/16	3½	11	6	277	335
10	28½	19⅝	15 5/16	13 3/16	13 1/16	3½	11	9¼	342	400
15	28½	19⅝	15 5/16	13 3/16	13 1/16	3½	11	9	383	440
25	34¾	24⅛	21 ⅞	16 1 3/16	16 9/16	8	19½	18½	665	735
37.5	44½	28 5/16	23 1 5/16	18 ¾	18 7/16	10	27	31	987	1075
50	50½	28 5/16	23 1 5/16	18 ¾	18 7/16	10	33	37	1154	1250
75	54¼	35¼	27 ⅛	28 7/8	20¾	....	....	72	1740	1900
100	66	35¼	27 ⅛	28 ⅞	20¾	....	....	93	2040	2260
150	65½	43⅛	36 ¾	35	28⅝	....	....	168	2760	3950
200	80¼	40½	34 1/16	34 ⅝	30 5/16	....	....	193	3890	4300

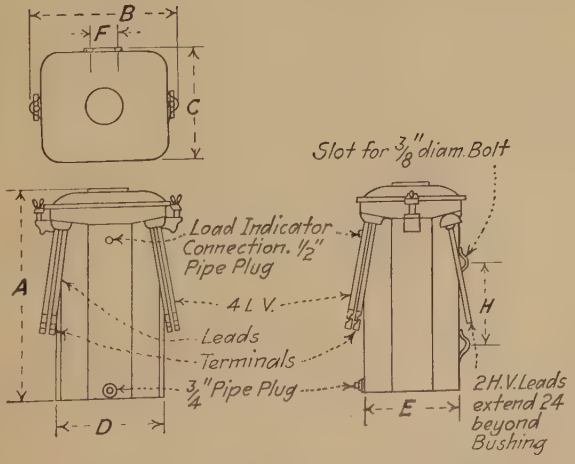

FIG. 334.—Transformer outline—for dimensions.

REDUCED-EFFICIENCY TRANSFORMERS, 2300 TO 230–110 VOLTS
(All losses based on 75° C. temperature)

K.v.a.	Iron loss, watts	Copper loss, watts	Per cent efficiency				Per cent impedance at 75° C.	Per cent regulation	
			¼ load	½ load	¾ load	Full load		100 per cent power factor	80 per cent power factor
1.5	31	49	91.6	94.5	95.0	94.9	3.8	3.31	3.85
3	56	71	92.5	95.3	95.9	95.9	2.8	2.40	2.80
5	60	120	94.9	96.5	96.7	96.5	3.0	2.44	3.05
7.5	80	171	95.4	96.8	96.9	96.7	3.0	2.31	2.96
10	104	195	95.6	97.0	97.2	97.1	2.7	1.98	2.70
15	124	269	96.3	97.5	97.6	97.4	2.5	1.85	2.58
25	181	375	96.8	97.8	97.9	97.8	2.7	1.56	2.54
37.5	238	435	97.2	98.1	98.2	98.1	2.5	1.35	2.40
50	307	604	97.3	98.1	98.3	98.2	2.9	1.28	2.53
75	550	1025	96.8	97.8	98.0	97.9	...	1.50	3.20
100	850	1250	96.4	97.7	97.9	97.9	...	1.40	3.20

The dimensions of this line of reduced efficiency transformers are given in the following table, referring also to Fig. 334:

K.v.a.	*A*	*B*	*C*	*D*	*E*	*F*	*H*	Oil, gallons	Weights	
									Net	Shipping
1.5	15¼	16 3/16	11 11/16	9 7/16	9 7/16	3½	7	1¼	72	95
3	16¼	16 3/16	12 5/32	10 13/16	10 3/8	3½	7	1¾	105	140
5	17¾	18	13 ¾	11 ¾	11 3/8	3½	7	3½	147	185
7.5	21 1/16	19 5/8	15 5/16	13 3/16	13 1/16	3½	11	6	200	258
10	28½	19 5/8	15 5/16	13 3/16	13 1/16	3½	11	10	272	320
15	27¼	22 7/8	20	15 ¾	15¼	7½	16	12	374	450
25	34¾	24 1/8	21 7/8	16 13/16	16 9/16	8	19½	18½	575	648
37.5	44½	28 5/16	23 15/16	18 ¾	18 7/16	10	27	34	838	930
50	50½	28 5/16	23 15/16	18 ¾	18 7/16	10	33	37	1087	1250
75	54¼	35¼	27 1/8	28 7/8	20¾	....	....	80	1460	1600
100	52	43 1/8	36 ¾	35	28 5/8	....	....	128	2110	2300

The insulation tests on all of these transformers are:

Primary winding to secondary winding and iron, 10,000 volts for 1 min.

Secondary winding to iron, 4000 volts for 1 minute.

Double voltage impressed across all windings for 7200 cycles at suitable frequency.

The temperature guarantees are:

Full load, 24 hours, 55° C. rise.

CHAPTER XLIII

MECHANICAL DESIGN

328. A complete discussion of the mechanical design of electrical machinery is beyond the scope of this work, but there are several points which the student is liable to overlook unless his attention is drawn to them.

The fundamental principle in the design of revolving machinery is that the frame shall be as heavy as possible, the revolving part as light as possible, and the shaft as stiff as possible.

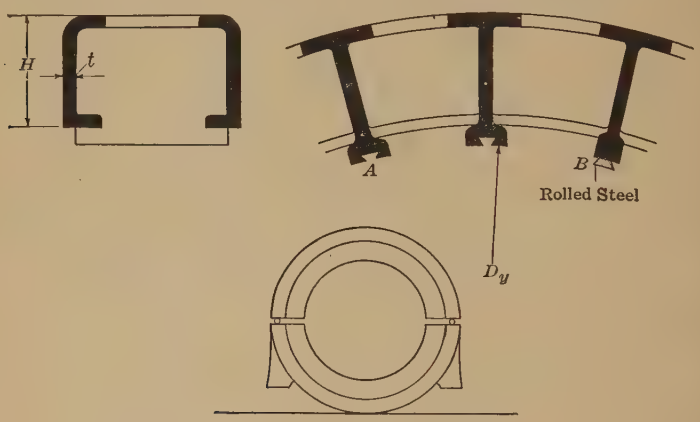

FIG. 335.—Alternator yoke.

The yokes, housings, spiders and bases should be designed so that the work in molding them shall be a minimum, and the smaller parts, when used in large quantities, should be designed for machine molding.

The yoke must be made stiff enough to prevent sagging, when built up with its poles as in the case of a D.-C. machine, or with its stator punchings as in the case of an alternator or induction motor. It must also be strong enough to stand handling in the shop as, for example, when supportd as shown in Fig. 335. If the yoke will stand this latter treatment it will generally be stiff enough for operating conditions.

The following rough rule may be used for checking a new yoke design. For yokes of the box type shown in Fig. 335,

$$H = 1.5 + \frac{D_y}{12} \text{ in.},$$

$t = 0.25 + 0.01D_y$ in., for values of D_y from 5 to 100 in.; above 100-in. bore increase the thickness by 0.375 in. for every 50-in. increase in diameter.

The distance between dovetails should be about 12 in., for which value the length of the segment used to build up the core will be 24 in. It is at present standard practice to dovetail the laminations into the yoke as shown at *A*, but the method shown at *B* has been found satisfactory and has the advantage over *A* that it is cheaper and does not block up the ventilation so much. The distance between dovetails is determined finally by the slot pitch and the number of slots per segment.

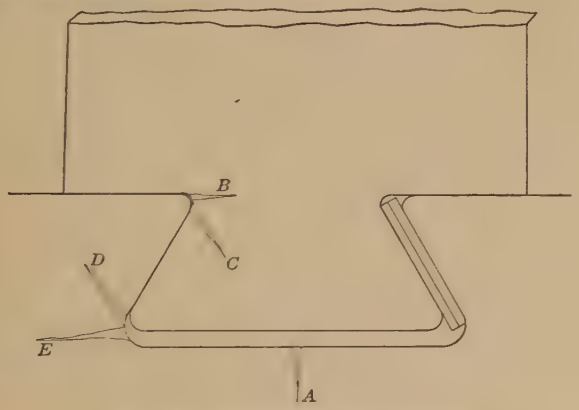

FIG. 336.—Stresses in pole dovetails.

329. Rotors and Spiders.—These must be designed so that they will stand handling in the shop.

The rotor of a revolving field alternator is usually built with the poles dovetailed in, as shown in Fig. 336, and care must be taken that it is strong enough at *A* to prevent overstress due to its own centrifugal force and to the bursting action of the pole dovetails, and also strong enough at *B*, *C*, *D*, and *E*. The stresses to be allowed at the maximum speed are:

2,500 lb. per square inch for cast iron.
12,000 lb. per square inch for cast steel.
14,000 lb. per square inch for sheet steel.
18,000 lb. per square inch for nickel steel.

The arms of the spiders should be able to transmit the full-load torque with a factor of safety of 12; then they will be strong enough to withstand sudden overloads and short-circuits.

330. Commutators.—Figure 337 shows a typical commutator. The mica between segments has parallel sides, and the segments themselves are tapered to suit. The clamping of the segments is done on the inner surface of the V so that the segments will be pulled tightly together, and the design should be strong enough to prevent the stresses at *A*, *B*, *C*, *D* and *E* from becoming dangerous. In a long commutator considerable trouble is experienced due to the expansion and contraction of the bars as the commutator is heated or cooled, and the type of construction shown is designed to take care of such expansion by the extension of the

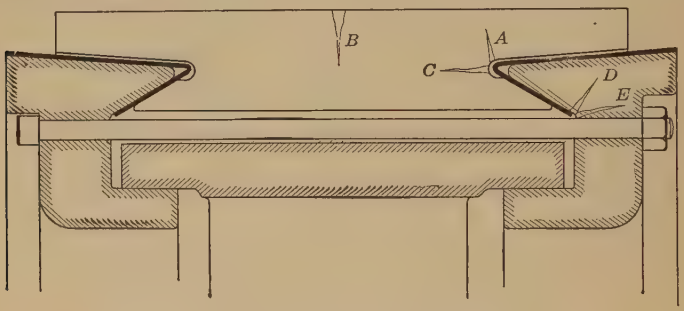

FIG. 337.—Construction of a long commutator.

bolts. If the type of construction shown in Fig. 30 were used for a long commutator, then, when the commutator is heated and expands, the shell has to burst, the bolts break or the commutator bars bend.

331. Unbalanced Magnetic Pull.[1]—If two surfaces of area S sq. cm. have a magnetic flux crossing the gap between them, and the flux density in this gap $= B$ lines per square centimeter, there will be a force of attraction between the two surfaces $= \frac{1}{8\pi} SB^2$ dynes.

Figure 338 shows part of an electrical machine of which the revolving part is out of center by a distance Δ cm. The flux density in the air-gap at C is greater than at B, so that the magnetic force acting downward is greater than that acting upward. The resultant downward pull is called the unbalanced magnetic pull of the machine.

[1] B. A. Behrend, *Trans.* A. I. E. E., Vol. 17, p. 617.

In the following discussion it is assumed that the flux density in the air-gap at any point is inversely proportional to the air-gap clearance at that point, and also that the eccentricity is not more than 10 per cent of the average air-gap clearance:

δ_a = the air-gap clearance at any point A,

$= ab - bc$,

$= \delta - \Delta \cos \theta$;

and B_a = the flux density at point A,

$$= B\frac{\delta}{\delta_a},$$

$$= B\left(\frac{\delta}{\delta - \Delta \cos \theta}\right),$$

$$= B\left(\frac{1}{1 - \frac{\Delta}{\delta} \cos \theta}\right)$$

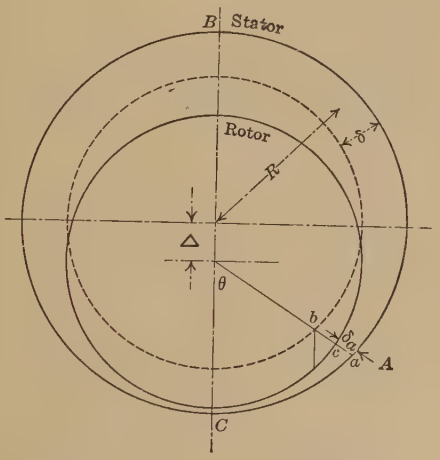

FIG. 338.—Machine with an eccentric rotor.

df = the force at A over a small arc $Rd\theta$,

$$= \frac{1}{8\pi} \times B_a^2 \times Rd\theta \times L_c \text{ dynes};$$

and the vertical component of this force

$$= df \times \cos \theta,$$

$$= \frac{1}{8\pi} B^2 \left(\frac{1}{1 - \frac{\Delta}{\delta} \cos \theta}\right)^2 RL_c \cos \theta d\theta,$$

$$= \frac{1}{8\pi} RL_c B^2 \left(1 + 2\frac{\Delta}{\delta} \cos \theta\right) \cos \theta d\theta; \text{ higher powers}$$

of $\frac{\Delta}{\delta}\cos\theta$ than the first being neglected since $\frac{\Delta}{\delta}$ is small, being less than 0.1.

The total downward force

$$= \frac{2}{8\pi} RL_c B^2 \int_0^{\frac{\pi}{2}} \left(1 + 2\frac{\Delta}{\delta}\cos\theta\right)\cos\theta d\theta,$$

$$= \frac{2}{8\pi} RL_c B^2 \left(1 + \frac{2\pi\Delta}{4\delta}\right) \text{dynes.}$$

Similarly the total upward force

$$= \frac{2}{8\pi} RL_c B^2 \left(1 - \frac{2\pi\Delta}{4\delta}\right) \text{dynes.}$$

The total unbalanced magnetic pull is the difference between the total downward and the total upward force and

$$= \frac{2}{8\pi} RL_c B^2 \times \frac{4\pi\Delta}{4\delta},$$

$$= (2\pi RL_c)\frac{1}{8\pi} B^2 \frac{\Delta}{\delta} \text{ dynes.}$$

In inch-pound units the unbalanced magnetic pull is given by the following formula:

$$\text{Pull in pounds} = \frac{1}{72} S \left(\frac{B}{1000}\right)^2 \frac{\Delta}{\delta}, \tag{71}$$

where B is the effective gap density in lines per square inch,

Δ is the displacement in inches,

δ is the average air-gap clearance in inches,

$S = 2\pi RL_c$, is the total rotor surface in square inches.

Since the flux density in the air-gap at B is less than that at C, the e.m.f. generated in the conductors at C will be greater than that generated in conductors at B. If a multiple winding is used for the rotor, such as the D.-C. multiple winding or the squirrel-cage winding of the induction motor, then the current in each conductor will be proportional to the e.m.f. generated therein and will be greater in conductors at C than in those at B. Now the armature current in a D.-C. machine tends to demagnetize the field which produces it and so also does the current in the rotor bars of an induction motor, with such multiple windings; therefore the demagnetizing effect will be greatest at C and least at B; the flux in the air-gap will not be inversely proportional to the air-gap; and the magnetic pull will be less than that given by the above formulæ.

332. Bearings, Journals and Pulleys.—The subject of bearing friction has already been discussed in Art. 89, page 110.

A useful rule for the design of self-cooled bearings with ring lubrication is that

P = 60 to 100; PV less than 90,000 for bearings up to 5 in. diameter;

P = 40 to 60; PV less than 60,000 for bearings above 5 in. diameter;

where P = the bearing pressure in pounds per square inch projected area,

V = the rubbing velocity of the journal in feet per minute.

Bearings having values within these limits will carry 50 per cent overload without injury; if the values at normal load are greater, water-cooled bearings should be used.

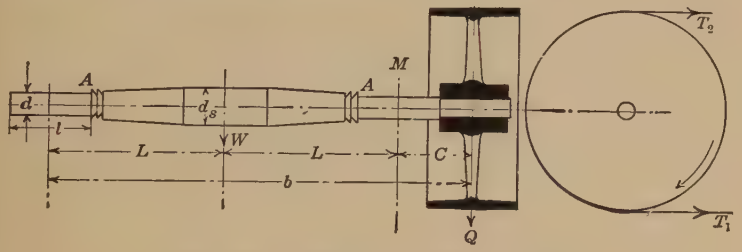

FIG. 339.—Shaft for a belted machine.

The length of the bearing will generally be from three to four times the diameter, but the stress in the neck of the journal at A, Fig. 339, must be checked to see that it is not too high;

if M_b = the bending moment at A,

M_t = the twisting moment at A;

then M_e, the equivalent bending moment at A,

$$= \frac{M_b + \sqrt{M_b + M_t}}{2},$$

$$= \text{stress} \times \frac{\pi}{32} d^3.$$

This stress should not exceed 5000 lb. per square inch.

The shaft at the center is designed principally for stiffness. The size of shaft necessary to transmit the torque is comparatively small; the actual diameter is chosen so that the rotor deflection shall not exceed 10 per cent of the air-gap clearance; this diameter should, however, be checked for strength to resist the combined effect of torsion and bending.

Figure 339 shows a loaded shaft. W, the weight between the bearings, includes the unbalanced magnetic pull, and Q is the total pull of the belt.

If, as is generally the case, the belt is in contact with the pulley over half the circumference, then

$$\begin{aligned} T_2 &= 2T_1 \text{ approximately;} \\ \text{and } Q &= T_2 + T_1, \\ &= 3T_1 \text{ approximately;} \\ T_2 - T_1 &= \frac{\text{hp.} \times 33{,}000}{\text{belt speed in feet per minute}}, \\ &= T_1. \end{aligned}$$

The total force on the bearing next the pulley, when the belt pull is vertically downward $= \frac{1}{2}W + Q \times \frac{b}{2L}$.

The lower the speed of the belt the greater is the value of $T_2 - T_1$, the effective force on the belt, and the greater the value of Q, so that, with a given bearing, there is a minimum diameter and a maximum width of pulley which may be used without overloading the bearing or overstressing the shaft.

Consider the following example. Design the shaft for a 50-hp. 900-r.p.m. induction motor.

Air-gap clearance = 0.03 in.
Deflection allowed = 0.003 in.
Rotor weight = 500 lb.
Rotor diameter = 19 in.
Frame length = 6.5 in.
Carter coefficients = 1.52.

S, in formula 71 $= \pi \times 19 \times 6.5 \times \frac{1}{1.52} = 255$ sq. in.

Maximum flux per pole $= 1.04 \times 10^6$.

Maximum flux density $= \frac{\text{flux per pole} \times \text{poles}}{S} \times \frac{\pi}{2}$.

$= \frac{1.04 \times 10^6 \times 8}{255} \times \frac{\pi}{2}$.

$= 51{,}000$ lines per square inch.

Average value of $\left(\frac{B}{1000}\right)^2 = \frac{51^2}{2} = 1300$.

Unbalanced pull $= \frac{1}{72} \times 255 \times 1300 \times 0.1$.

$= 460$ lb.

Weight between bearings $= 460 + 500 = 960$ lb.

The deflection is limited to $0.1 \times 0.03 = 0.003$ in.

and deflection $= \frac{W \times (2L)^3}{48 \times E \times I}$,

where $2L$ = the distance between bearings in inches (see Fig. 339),
E = Young's modulus = 30,000,000 in inch-pound units,
I = the moment of inertia to bending,

$$= \frac{\pi}{64} d_s^4.$$

Therefore d_s, the necessary shaft diameter $= \sqrt[4]{\frac{W \times (2L)^3}{7 \times 10^6 \times \delta}}$,

$$= \sqrt[4]{\frac{960 \times 19^3}{7 \times 10^6 \times 0.03}},$$

$$= 2.4 \text{ in. approximately.}$$

Assume now that the belt speed = 4000 ft. per minute; then the pulley diameter = 17 in.,

$$T_2 - T_1 = \frac{50 \times 33{,}000}{4000} \text{ lb.}$$

$$= 414 \text{ lb.}$$

The maximum pull in the belt $= T_2$,

$$= 2T_1,$$

$$= 828 \text{ lb.}$$

The belt width = 10 in. and the belt stress = 83 lb. per inch width.

For a single belt the stress should be less than 45 lb. per inch width and for a double belt should be less than 90 lb. per inch; a double belt should not be used on a pulley smaller than 12 in. in diameter. With a 10-in. belt and the pulley overhung, the smallest possible value for C, Fig. 339, = 10 in. The value of $Q = 3 \times 414 = 1240$ lb.

The belt pull on the bearing $= 1240 \times \frac{29}{19}$,

$$= 1900 \text{ lb.}$$

$$\tfrac{1}{2}W = 480 \text{ lb.}$$

Total bearing pressure $= 2380$ lb.

Size of bearing = 3 × 9 and the value of P = 88 lb. per square inch and PV = 62,000.

The stress in the shaft must now be determined.

The bending moment at $M = Q \times 10$,

$$= 1240 \times 10,$$

$$= \text{stress} \times \frac{\pi}{32} d^3.$$

Therefore the stress at the neck of the journal = 4700 lb. per square inch.

The shaft will be cut out of 3½ in. stock and the journals turned down to 3 in.; the deflection will be less than 10 per cent of the air-gap clearance.

BROWN AND SHARP GAGE; COPPER WIRE

Gage number B. & S.	Diameter		Cross-sectional area			Diameter double cotton covered	Insulation (mils on diameter)	Ohms per thousand feet	
	Inches	Millimeters	Square inches	Circular mils	Square millimeters			15° C.	60° C.
0000	0.46000	11.684	0.16619	211,600	107.19	0.472	12	0.048119	0.056969
000	0.40964	10.404	0.13179	167,810	85.013	0.421	12	0.060677	0.071838
00	0.36480	9.266	0.10452	133,080	67.433	0.377	12	0.076511	0.090583
0	0.32495	8.252	0.082931	105,590	53.482	0.337	12	0.096428	0.11416
1	0.28930	7.348	0.065733	83,694	42.406	0.301	12	0.12166	0.14403
2	0.25763	6.543	0.052129	66,373	33.623	0.269	12	0.15341	0.18162
3	0.22942	5.827	0.041338	52,633	26.667	0.241	12	0.19345	0.22903
4	0.20431	5.189	0.032784	41,743	21.147	0.216	12	0.24392	0.28879
5	0.18194	4.620	0.025998	33,102	16.764	0.194	12	0.30759	0.36417
6	0.16202	4.115	0.020617	26,250	13.299	0.174	12	0.38789	0.45923
7	0.14428	3.665	0.016349	20,817	10.549	0.156	12	0.48913	0.57909
8	0.12849	3.264	0.012967	16,510	8.3673	0.140	12	0.61673	0.73016
9	0.11443	2.906	0.010284	13,094	6.6325	0.126	12	0.77760	0.92061
10	0.10189	2.588	0.0081536	10,382	5.2603	0.114	12	0.98078	1.1612

BROWN AND SHARP GAGE; COPPER WIRE—*Continued*

Gage number B. & S.	Diameter		Cross-sectional area			Diameter double cotton covered	Insulation (mils on diameter)	Ohms per thousand feet	
	Inches	Millimeters	Square inches	Circular mils	Square millimeters			15° C.	60° C.
11	0.09074	2.304	0.0064637	8,233.7	4.1692	0.103	12	1.2366	1.4640
12	0.08081	2.052	0.0051288	6,530.3	3.3070	0.093	12	1.5592	1.8460
13	0.07196	1.829	0.0040669	5,178.2	2.6273	0.084	12	1.9663	2.3279
14	0.06408	1.628	0.0032250	4,106.2	2.0816	0.076	12	2.4796	2.9357
15	0.05706	1.450	0.0025571	3,255.8	1.6513	0.068	11	3.1273	3.7025
16	0.05082	1.290	0.0020284	2,582.7	1.3070	0.062	11	3.9424	4.6675
17	0.04525	1.150	0.0016081	2,047.6	1.0387	0.056	11	4.9727	5.8873
18	0.04030	1.024	0.0012755	1,624.9	0.82354	0.051	11	6.2694	7.4224
19	0.03589	0.900	0.0010117	1,288.1	0.63617	0.046	10	7.9047	9.3586
20	0.03196	0.813	0.00080223	1,021.4	0.51912	0.042	10	9.9682	11.802
21	0.02846	0.724	0.00063614	809.97	0.41168	0.038	10	12.571	14.883
22	0.02534	0.643	0.00050431	642.12	0.32472	0.035	10	15.857	18.773
23	0.02257	0.574	0.00040008	509.41	0.25877	0.032	10	19.988	23.664
24	0.02010	0.511	0.00031738	404.01	0.20508	0.030	10	25.202	29.838

LIST OF SYMBOLS

Used along with these symbols the suffix $_1$ stands for stator or primary and the suffix $_2$ for rotor or secondary.

Unless otherwise stated the dimensions are in inch units.

		Page
A	= brush contact area	111
A_{ag}	= actual gap area per pole	46
A_b	= projected area of bearing	110
A_c	= core area	46
A_g	= apparent gap area per pole	46
A_p	= pole area	46
A_r	= section of end connector	372
A_t	= tooth area per pole	46
A_y	= yoke area	46
AT	= ampere-turns.	
AT_c	= ampere-turns per pole for the core	52
AT_g	= ampere-turns per pole for the gap	51
AT_{g+t}	= ampere-turns per pole for gap and tooth	54
AT_{max}	= ampere-turns per pole, maximum excitation	238
AT_p	= ampere-turns per pole for the pole core	52
AT_t	= ampere-turns per pole for the teeth	51
AT_y	= ampere-turns per pole for the yoke	50
B	= flux density	6
B_{ag}	= actual gap density	48
B_{at}	= actual tooth density	48
B_c	= core density	48
B_g	= apparent gap density	48
B_i	= Commutating gap density	103
B_m	= maximum flux density in transformer cores	441
B_p	= pole density	48
B_t	= apparent tooth density	48
B_y	= yoke density	48
$B.\ \&\ S.$	= Browne and Sharpe gage	504
C	= Carter fringing constant	47
C_z	= width of commutating zone	100
D_a	= armature external and stator internal diameter	45
D_c	= commutator diameter	131
D_r	= mean diameter of rotor end connector	372
E	= volts per phase.	
E_{11}	= component of applied e.m.f. equal and opposite to the back-generated e.m.f	328
E_{1b}	= back-generated e.m.f. in primary	327
E_f	= volts per field coil	71

		Page
E_s	= generated voltage in the short-circuited coil	93
E_t	= terminal voltage	162
F	= commutator face	131
F	= finish of winding	156
I	= amperes per phase.	
I_{11}	= component of primary current with a m.m.f. equal and opposite to that of the secondary current	328
I_a	= armature current	116
I_c	= current per conductor	57
I_d	= maximum current in induction motors	334
I_e	= exciting current	341–422
I_f	= field current	45
I_l	= line current	162
I_m	= magnetizing current	423
I_o	= magnetizing current	327
I_{sc}	= short-circuit current	342
K	= hysteresis constant	113
K_1	= reactance constant	369
K_2	= reactance constant	369
K_e	= eddy-current constant	113
K_{Bag}	= factor in surface iron loss	353
K_{ft}	= factor in surface iron loss	353
K_q	= factor in surface iron loss	353
K_λ	= factor in surface iron loss	353
$K.V.A.$	= kilovolt amperes.	
$K.W.$	= kilowatts.	
L	= length of transformer coils	445–448
L	= coefficient of self-induction	82
L_b	= length of conductor	116
L_c	= axial length of core	45
L_e	= length of end-connections	128
L_f	= radial length of field coil	71
L_g	= gross iron in frame length	46
L_i	= axial length of commutating pole	102
L_n	= net iron in frame length	46
L_p	= axial length of pole	46
L_s	= axial length of pole shoe	55
M	= section in circular mils	71
M	= coefficient of mutual induction	82
MT	= mean turn of coil	71
MT	= mean turn of transformer coils	448
N	= number of slots	46
$P.F.$	= power factor.	
R	= reluctance.	
R	= resistance per phase.	
R	= brush-contact resistance	82
R_e	= equivalent secondary resistance	426
R_{eq}	= equivalent primary resistance	426
$R.V.$	= reactance voltage	83

		Page
S	= number of commutator segments	18
S	= space between high- and low-voltage coils	445–448
S	= start of winding	156
S	= total rotor surface	500
T	= time constant	376
T	= turns per coil.	
T_c	= time of commutation	82
T_f	= field turns per pole	45
V	= air velocity in feet per minute	125
V	= peripheral velocity of rotor in thousands of feet per minute	396
V_b	= rubbing velocity of bearing	110
V_r	= rubbing velocity of brush	111
W	= weight of iron in pounds	113
W_p	= pole waist	46
W_s	= width of pole shoe	55
W_s	= surface loss	353
X	= leakage reactance per phase	211
$\overline{X}$	= synchronous reactance	214
X_2	= rotor reactance at standstill	328
X_e	= equivalent secondary reactance	426
X_{eq}	= equivalent primary reactance	426
Z	= total face conductors in D.C. armatures	11
Z	= conductors in series per phase	184
Z_c	= total number of conductors in alternators	249
a	= slots per pole	179
b	= conductors per slot	216
c	= slots per phase per pole	216
$\cos\theta$	= power factor	162
d	= slot depth	46
d_1, d_2, d_3, d_4	= slot dimensions	218
d_1, d_2	= dimensions of transformer coils	445–448
d_a	= depth of armature core	46
d_b	= bearing diameter	110
d_f	= depth of field winding	71
d_s	= shaft diameter	281
$d.c.c.$	= double cotton covering on wires.	
e	= volts per conductor	183
f	= frequency	157
f	= constant in Carter formula	47
h_p	= height of pole	55
h_s	= height of pole shoe	55
$hp.$	= horsepower.	
i	= current in amperes.	
k	= constant in reactance voltage formula	91
k	= distribution factor	184
k	= a whole number, in winding formula	18
k_r	= end-ring resistance factor	372
k_t	$= \frac{\text{magnetic loading in transformers}}{\text{electric loading}}$	475

		Page
$(1 - k)$	= per cent of copper in a given thickness of winding	472
k.v.a.	= kilovolt amperes	183
kw.	= kilowatts.	
l_1	= length of leakage path	55
l_3	= length of leakage path	55
l_b	= length of bearing.	110
l_c	= magnetic length of core.	52
l_p	= magnetic length of pole core.	50
l_y	= magnetic length of yoke	50
lf.	= leakage factor.	54
m.m.f.	= magneto-motive force.	
n	= number of phases.	
p	= number of poles.	
p_1	= number of paths through the armature.	11
q	= ampere conductors per inch.	133–256
r.p.m.$_1$	= synchronous speed of induction motors.	330
r.p.m.$_2$	= rotor speed	327
s	= per cent slip.	326
s	= slot width	46–218
sf.	= space factor.	71
t	= thickness.	
t	= time in seconds.	
t	= tooth width.	46
v_2	= leakage constant in induction motors.	331
w	= slot width.	218
δ	= air-gap clearance.	47
η	= efficiency.	
λ	= slot pitch.	46
λ_e	= distance the end connections project	128
τ	= pole pitch.	45
ϕ	= magnetic flux.	
ϕ_a	= useful flux per pole	11, 173
ϕ_a	= flux in transformer core at no load.	439
ϕ_e	= leakage flux between poles	45
ϕ_e	= end-connection leakage constant	86, 216, 360
ϕ_m	= total flux per pole	45
ϕ_s	= slot-leakage constant	86, 216, 360
ϕ_t	= tooth-tip leakage constant	216
ϕ_{ta}	= tooth-tip leakage constant	221
ϕ_{tp}	= tooth-tip leakage constant	221
ϕ_z	= zigzag leakage constant.	360
ψ	= per cent pole enclosure.	45

INDEX

A

Ageing of iron, 439, 440
A. I. E. E., definitions of insulation, 32
rulings for temperature, 122–123, 201–202
on efficiency, 116–121
standard tests for transformers, 491
Air blast for cooling, 125, 283–285, 468–469
ducts, armature, 25, 29, 187, 347
field coils, 43, 44
films in insulation, 197, 199, 200
-gap, area, 46
clearance, 73, 75, 228, 230, 240, 243, 262, 269, 394, 403, 404
flux density in, 48, 102, 133, 257, 294, 393
distribution, 46, 57–61, 209, 295, 358
fringing constant, 47
length and diameter, 73, 75, 230, 240, 243, 262, 393, 403
Albrecht, G. M., 20
Alloyed iron, 113, 439
steel, 440
Alternating and rotating fields, 181
Alternators, armature reactions, 208–236
construction, 186–193, 274
current density, 252, 253
design procedure, 256
efficiency, 252
e.m.f., 173, 184
engine-driven, flywheel design for, 302–303
field system design, 237
flux densities, 229, 245, 252, 257–259, 285, 295
Alternators, generated e.m.f., 173
heating, 239, 252–255, 282–286
high-speed, 274–301
insulation, 188, 190, 201–207
losses, 247–252
natural frequency, 303, 308
parallel operation, 302
ratings, 183, 236
reactance of armature, 215–226, 234–236, 292
reactions of armature, 208–236, 295
regulation, 228
rotor (see *Rotor*).
short circuit test on, 224
single-phase, 231
slots, 175, 256–258, 261, 263, 265
theory of operation, 208
turbo- (see *Turbo-alternators*).
vector diagrams, 210–212
water-wheel driven, 253, 274
windings, 155–172
Amortisseur, 300, 308
Ampere conductors, 134, 258
per inch, 128, 134, 136, 257, 260, 381, 393, 395
-turns, 4
commutating pole, 95, 103
cross-magnetizing, 57–64, 104–106, 209
demagnetizing, 62, 209, 214, 233
field excitation, 49–54, 73, 237, 238
per pole, armature, 65–67, 101, 104, 230, 296
demagnetizing, 62, 103, 209, 214, 233, 295
field excitation, 50–54, 73, 237–242, 296
series field, 74
Areas, magnetic, 45, 359

Armature coils (see *Coils, armature*).
D.-C., construction, 25
current density, 128–130, 142
flux densities, 48, 127, 133
generated e.m.f., 11
heating, 122
insulation, 38–43, 201–207
losses, 110, 247, 371
procedure in design, 133–147, 256
reaction, 57–67, 208
resistance, 116, 248
slots, 25, 96, 141
strength relative to field, 65, 94, 101
windings, 7–24, 160
diameter and length, 136, 140, 259, 261, 267, 393, 405

B

Back e.m.f., 321
Bearing, construction, 28, 30
design, 110, 501–504
friction, 110, 247, 341, 357
loss, 247
housings, 27, 348
oil temperatures, 111
Belt leakage, 329, 366–368
Breakdown point, 326
Breathing of coils, 200
Brush, arc, 9, 86, 98–101
carbon, 84
circulating current in, 13, 100
contact resistance, 83
current density, 82–85, 98–99, 191
friction, 111, 247
loss, 353
number of sets, 12. 18, 19
pressure, 85
shifting, 94
width, 98
Bushings, transformer, 434, 435, 451-455

C

Carter coefficient, 47
Cast iron, magnetic properties, 49
stresses in, 497
Cast steel, magnetic properties, 49
stresses in, 497
Centrifugal force, of turbo-rotors, 274–282
Chain windings, 164–165
Characteristics, and frequency, 392, 410, 420, 490
and speed, 116, 392, 409
and voltage, 153, 420–421
Circle diagrams, 330–345
Circular mils per ampere, 128–130, 193, 253, 298, 380, 381, 474
Circulating current in brushes, 13, 100
in windings, 13, 19, 159, 166, 168, 179, 303
Closed slots, 25, 346, 411
Coils, armature, 22, 24, 39–43, 128, 201–207
length and diameter, 127
breathing of, 200
exciting, 188, 190
field (see *Field coils*).
groups, 40
pancake, 433, 438, 465
transformer, 433–438, 445–447, 455–456, 459–460
Commutating poles, 27, 94
dimensions, 95, 102
excitation, 103
saturation in, 106
Commutation, 78–109
counter e.m.f. method, 92–109
perfect, 82
resistance method, 78–91
current density in brush, 82
effect of self-induction of coil, 80
selective, 19
with duplex winding, 9
series windings, 19, 89
short pitch windings, 15, 89, 96–98
Commutators, 27
design, 139–140, 144
diameter, 139
heating, 131
insulation, 27
losses, 111, 116

Commutators, mechanical design, 498
number of segments, 18, 107
peripheral velocity, 139
ventilation, 131
voltage between segments, 107–109
wearing depth, 140
Compensating field coils, 104–106
Condenser bushings, 453
Conductors, ampere, per inch, 128, 136
current density in, 128–130, 142, 252, 269, 298, 380, 381, 473
eddy currents in, 249–251, 373, 461
in same slot, insulation, 203
lamination of, 249, 252. 461
magnetic field surrounding, 2
number of, 11, 133, 140, 149, 261, 268, 397, 407
size of, 268
Contact resistance, 83
Cooling (see also *Heating*).
by convection, 125
Copper loss, armatures, 116, 119, 248
field coils, 68, 116, 248
induction motors, 371–374
rotor, 335
stator, 335
transformers, 461–462, 480
resistance of, 116
Core, flux density in alternator, 252, 286
in D.-C. armature, 48, 127
in induction motor, 358, 381
in transformer, 478
in D.-C. armature, 48
losses, 115, 247
or iron loss, 112, 247, 353–355, 439–443
-type transformer, 430, 435
compared with shell type, 486–488
construction, 428–429, 435–436
heating, 464–465
insulation, 458–460
procedure in design, 477–481
Core-type transformer, reactance, 445, 481
three-phase, 490
Corrugated tanks, 466–467
Cotton, 32, 34
covering for wire, 34, 504
Creepage, surface, 38–39, 450–456
Cross-magnetizing ampere-turns, 57–64, 104–106, 209
Current density, in alternator windings, 252–253, 263, 265, 298
in brush contacts, 82–85, 98–99, 191
in D.-C. armatures, 128–130, 142
in field coils, 74–76, 379
in induction motors, 380, 381, 397, 407–408
in transformers, 473–474
direction of, 1
maximum in induction motors, 334, 363, 394–395
relations, in induction motors, 318, 328, 332
in transformers, 424
Curves, ampere conductor per inch, 134–135, 257–258, 393
armature heating, 135, 253, 382
efficiency, 392
field coil heating, 70, 239
full-load saturation, 62
gap density, 134, 257, 258
heating and cooling, 375–379
iron loss, 115, 354, 356, 442
magnetization, 49, 51, 443
power factor, 392
saturation, 53, 60, 63, 212, 225, 237, 300, 307, 313, 339–341
short-circuit, 225, 341–343
space factor, 71
transformer heating, 466, 468

D

D^2L, 133, 256, 259, 391
Dampers, 300, 308–311
Dead coils, 24
points at starting, 314, 388–390
Delta connection, 158, 178, 407
and harmonics, 178

Demagnetizing ampere-turns, 62, 94, 103, 209, 214, 233, 295
Density of current in alternator windings, 252–254, 263, 265, 298
in brush contacts, 81–85, 98–99, 191
in D.-C. armatures, 128–130, 142
in field coils, 74–76, 379
in induction motors, 380–381, 397, 407–408
in transformers, 473–474
of flux and m. m. f., 5
in air gap, 48, 102, 133, 257, 294, 393
in armature and stator cores, 48, 127, 252, 286, 358, 380
in pole cores, 48, 73, 229
in rotor cores, 380
in teeth, 48, 51, 127, 252, 286, 358, 380
in transformer cores, 478
in yoke, 48, 73
limiting values, 126
Design procedure, for alternators, 256
for D.-C. generators, 133
for field system, 68, 237
for induction motors, 391–408
for synchronous motors, 312–313
for transformers, 475–485
for turbo-alternators, 274, 297
Dielectric flux, 194
strength 34, 195
cotton, 34
empire, cloth, 35
micanite, 35
oil, 449
paper, 36
Dimensions and frequency, 415, 490
and output, 133, 256, 391
Direction of current, 1
of e. m. f., 2
of magnetic lines, 1, 2
Distributed windings, 165, 175, 182
Distribution factor, 184
of magnetic field, core, 113, 358
gap, 46, 57–61, 209, 294, 358
transformer, 428–437, 463, 475, 486, 492–495
Double-frequency harmonics, 232
layer winding, 13, 164, 165
Doubly re-entrant winding, 8
Dovetails, 29, 187, 189, 191, 349, 497
Drum windings, 9
Ducts in armature and stator cores, 25, 30, 187, 347
in field coils, 30–31
in transformer, 470–471
Duplex windings, 8, 20

E

Eddy currents in armature, and stator cores, 113, 353–354
in conductors, 249–252, 373, 461
in pole shoes, 114, 300
in transformer coils, 439, 444
loss, 113, 114
Efficiency, A. I. E. E. standard rules, 116–121
effect of speed, 392, 420–421
of voltage, 420–421
of alternators, 252
of D.-C. machines, 110, 117–121
calculation of, 152
of induction motors, 392
of transformers, 462–463, 492, 494
of voltage, 240
Electric loading, 136, 150, 475
Electrical degrees, 157
E. m. f., 2
direction of, 3
equation, 11
generated, 173–185
in alternators, 173, 184
in D.-C. machines, 11
in induction motors, 350
in transformers, 439
Empire cloth, 35
Enclosed machines, 348, 383
End connections, heating, 127, 253, 254, 381
insulation, 38
leakage, 218
length, 128
supports, 294, 348–349

End play for shafts, 26
rings, loss in induction motor, 372
section, 400
turns, insulation, of transformer, 457–458
Equalizer connections, 13, 20, 24
Equivalent reactance, induction motor, 337, 363
transformer, 426, 447
resistance, 426
Even harmonics, 178
Excitation, calculation of full load, 62, 227, 246
induction motor, 357
of no-load, 50, 241
of transformer, 441, 480, 484
effect of power factor, 237
for joints, 444
synchronous motor, 311
Exciter, 188, 193, 315
Exciting coils, 26, 188, 190
current, 350, 357, 394, 440, 480, 484

F

Fans, 253, 276, 284, 288, 349
Field coils, 43–44, 68–77, 187–191
compensating, 104–106
construction, 31, 43, 68, 74, 188, 190
current density, 74–76
design procedure, 68, 237
ducts in, 30–31
heating, 68, 239
insulation, 43, 188
losses, 68, 116, 152, 237, 248
sizes of wire for, 71
ventilation, 43, 68, 70, 190
distribution, in commutating pole machine, 64
magnetic, distribution in core, 115, 358
in gap, 46, 57–61, 209, 294, 358
leakage between poles, 45, 54, 213
in alternators, 216, 234
in induction motors, 360
in transformers, 445
Field, magnetic, relation between main and armature, 65, 229, 296
surrounding conductor carrying current, 2
magnets, construction, 27, 187–193
dimensions, 27, 71, 73, 238
flux density, 48, 73, 229
turbo, 276–279
revolving, in induction motors, 316–317
Flashing over, 105–106
Fleming's rule, 3
Flux density (see *Density, of flux*).
distribution in air-gap, 46, 57–61, 209, 294, 358
in armature coil, 113, 358
fringing, 47
pulsation, 179, 386
Flywheels, 302–306
Force, lines of, 1
Forced draft, 283–288, 468–469
oscillations, 303, 307
Form factor, 173, 439, 440
Fractional pitch winding, 15, 88, 176, 184, 419
Frequency and characteristics, 392, 410, 420–421, 490, 491
and dimensions, 415, 491
speed and poles, 157, 319
Friction in bearings, 110, 247, 341, 353, 359
in brush, 111, 247, 353
Fringing of flux, 47
Fullerboard, 450, 456, 457
Full-load saturation, 62, 212, 227, 237, 313
-pitch windings, 15

G

Gap (see *Air-gap*).
Generators, high-speed, 192
vertical shaft, 192
Gramme ring winding, 7, 9
Grounds, 37
Guarantees, power factor, 392

H

Harmonics, effect of Y- and Δ-connection on, 178
in e. m. f. wave, 173
trouble due to, 174
in the magnetic field, 179, 231, 301, 418
produced by armature slots, 179
Heat, effect on insulation, 35, 36, 122
Heating, 122–132 (see also *Temperature rise*).
alternator rotors, 239
and construction, 252, 383
and cooling curves, 375–381
commutator, 131
constants, application of, 132
dampers, 308–311
D.-C. armature, 122
enclosed motors, 383
field coils, 68, 239
high-voltage coils, 124–126, 252–255
induction motors, 375–384
oil in bearings, 111
rotor, induction motor, 381
semi-enclosed motors, 383–384
squirrel-cage motors, 379–380
stator, induction motor, 252, 380–383
transformers, 463–473
turbos, 276, 282, 299–301
High-speed alternators, 274–301
induction motors, 414–417
limitations in design, 417
torque ratings, 381
-voltage coils. heating, 124–126, 252–255
insultation for alternators, 203–207
due to harmonics, 174
for transformers, 459, 486
limitations in design, 487
Horn fiber, 36
Housings, 27, 348
Humming, 416
Hysteresis loss, 133, 439, 440

I

Impedance of windings (see *Reactance*).
Impregnating compound, 34, 36, 200, 450
Induction, magnetic, 1–6
motors, A.-C., 316–328
construction, 320, 346–349
current density, 380, 381
end rings, loss in, 372
excitation, 350
flux densities, 358–359, 381, 393
generated e. m. f., 350
graphical treatment, 329–338
heating, 375–384
high-speed, 414–417
leakage fields, 360–361
losses, 353, 371
noise, 385–390
peripheral velocity, 416
procedure in design, 391–408
reactance, 360
equivalent, 337, 363
revolving field in, 316–317
slots, 355, 386, 387, 389, 391, 397–398, 416
slow-speed, 409–411
starting torque, 388
theory of operation, 316
two-pole, 417–420
vector diagrams, 326–327, 330
windings, 319–321
Insulating materials, canvas, 43
cotton covering, 34
tape, 34
empire cloth, 35
fiber, 36
fullerboard, 450, 456, 457
impregnating compound, 34, 36, 200, 450
mica tape, 33, 201
micanite, 35
papers, 36
pressboard, 450
properties desired, 33
silk, 35
thickness, 36
varnish, 35, 36, 450

Insulating materials, wood, 450
wrappers, 33
Insulation, 32–44, 194–207 (see also *Insulating materials*).
air films in, 197, 200
armature, 38–43, 40–43, 201–207
chemical effects in high voltage, 200
commutators, 27
condenser type, 453
creepage across, 38, 450, 454, 455, 456
dielectric strength, 33, 34, 195
effect of heat air, 35, 36, 122
of moisture, 34, 36, 449
of time, 199
of vibration, 36
end connections, 38
field coils, 43, 190
grading of, 198, 199
potential gradient, 195, 197, 199, 452
puncture tests, 34, 38
rotor bars, 411
slot, 201
specific inductive capacity, 196, 198, 200
thickness, 36, 43, 114, 197, 459
transformers, 438, 449–460
turbo-rotors, 276
types defined, 32
volts per mil, 207
Interpoles (see *Commutating poles*).
Iron, ageing of, 440
alloyed, 113, 439, 440
laminations, thickness of, 346, 348, 440
losses, 112, 247, 353, 356–358, 439–440, 442, 443
magnetization curves, 49, 51

J

Joints in magnetic circuit, 444
Journals, design, 501–504
Jumpers, 165

K

Kilo volt amperes, 183

L

Lag of current in induction motors, 323, 324
in synchronous motors, 311, 312
Laminations of conductors, 249, 250, 461
of core bodies, 25, 30, 113, 186, 346, 348, 440
of pole faces, 26, 114
thickness of, 113, 186, 346, 348, 440
Lap windings, 20
Lead of current in synchronous motors, 311–312
Leakage factor, full-load, 213, 245
no-load, 45, 54, 56, 245
field, belt, 329, 366–368
end-connection, 216, 218
pole, 45, 54, 213
slot, 215, 218
tooth tip, 216, 220
transformer coils, 423, 445
zigzag, 361, 387
reactance in alternators, 216, 234, 291
in induction motor, 360–361
in transformers, 445–448, 481
surface, 38
Leatheroid, 36
Lenz's law, 3
Limitations in design, high voltage, 486
speed, 274, 417
Lines of force, 1
Loading, electric and magnetic, 136, 475
Locking points at starting, 314, 388
Losses, armature, 110, 247, 371
bearing friction, 353, 357
commutator, 111
constant, 334
contact resistance, 116
copper, 116, 248, 335, 371, 461–462
core, 115
due to filing of slots, 113
to leakage flux, 113
to non-uniform distribution of flux in armature core, 113

Losses, eddy-current, 113, 114
in conductors, 249, 373
field coils, 116, 248
friction, 110, 111
bearing, 247
brush, 247
hysteresis, 133
in alternators, 247
in D.-C. machine, 110
in induction motors, 353, 371
in transformers, 439–441, 461
iron, 112, 353, 356–358, 439–440
or core, 247
load, 252, 336
no-load, 353
pole-face, 114
rotor ring, 372–373
tooth pulsation, 354, 355
windage, 111, 247, 353

M

Magnet coils (see *Field coils*).
Magnetic arears, 45, 359
circuit, 45–56
design of, 68–77
field (see *Field, magnetic*).
induction, 1–6
loading, 136, 475
potential, 4
poles, in induction motor, 360
in transformers, 445
pull, unbalanced, 498–500
Magnetization curves, 49, 51, 443
Magnetizing current, in induction motors, 350–353, 357, 394
in transformers, 440, 480, 484
Magneto induction, 2
Maximum current in induction motors, 334, 363, 394, 395
output, 338, 344, 409
temperature rise, 68, 122, 464, 471–473
torque, 325, 338, 345
Mechanical design, 496–505
Mica, 205
tape, 33
wrappers, 33
Micanite, 35
M.m.f., 4
Moisture and insulation, 34, 36, 449
Motors, D.-C., calculation of efficiency, 152
procedure in design, 148
Motors, induction (see *Induction motors*).
multipolar, 317–319
synchronous (see *Synchronous motors*).
Multiple windings, 16, 23, 85
Multiplex windings, 8
Multipolar machines, 12

N

Nickel steel, 497
Noise, in induction motors, 385–390, 416
No-load current (see *Magnetizing current*).
losses, 353
saturation curve, 50, 240, 339–341

O

Oil for transformer, 449–450, 463, 466–468
temperatures, in bearings, 111
Output and dimensions, 133, 256, 391
limits, high voltage, 486
maximum, 338, 344, 409
speed, 274
of three-phase alternators, 162
Overload capacity, 84
Overspeed requirements, 274

P

Pancake coils, 433, 438, 465
Paper, 36
Peripheral velocity of rotors, 274, 276, 416
Pitch of poles, 45, 137, 259
of slots, 46, 257–258, 357, 386, 389, 391
of windings, 15
Pole arc and harmonics, 173
construction, 114, 187
enclosure, 260

Pole commutating (see *Commutating pole*).
construction, 26, 276
dimensions, 26, 71, 73, 238
enclosure, 45, 52, 261
face and wave form, 175
losses, 114
flux density, 48, 73, 229
number of, 137, 157, 259, 319
pitch, 45
and characteristics, 409, 410
Potential gradient, 195, 197, 198, 199, 452
Powell, W. H., 20
Power factor and armature reaction, 208, 226
and excitation, 237
and frequency, 392, 410, 420
and speed, 392, 409
and voltage, 420
correction by synchronous motors, 311–312
in three-phase machine, 162
Pressboard, 450
Pressure on bearings, 501
Progressive windings, 18
Pulleys, design, 501–504
Pulsations of magnetic field, 179, 386
Puncture tests, 34, 38

R

Rails, slide, 29
Ratings, high torque induction motors, 383
intermittent, 379
single and polyphase alternators, 183, 236
Reactance of alternators, 215, 216, 234, 291
of induction motors, 360
synchronous, 213
voltage, 83
formulæ, 90
machines with full-pitch multiple windings, 85
of non-interpole machines, 85
Reaction, armature, in D.-C. machines, 57
in polyphase alternators, 208, 295
in single-phase alternators, 231
Re-entrant windings, 8
Regulation, effect of air-gap on, 229
of pole saturation on, 228
of power factor on, 246
Regulation in synchronous motors, 312
of alternators, 228, 236
of transformers, 426–427, 445, 487
Resistance of alternator windings, 116, 249
of brush contacts, 83
of copper, 116
of field coils, 71
of transformers, 461
starting in induction motors, 324, 383
Resonance in electric circuits, 174
Retrogressive windings, 19
Reversing of induction motors, 316
Revolving field, design, 237–246
in induction motors, 316–317, 330
type of alternator, 186
Ring winding, 7, 9
Rocker arm, 28
Rotating and alternating fields, 181
Rotor of alternator, construction, 187, 275
current density, 238, 243
flux density, 229, 245
heating, 239, 276, 282
insulation, 190
losses, 247
peripheral velocity, 274, 276
procedure in design, 237, 297
strength relative to armature, 230, 296
turbo, 276
of induction motor, construction, 321, 348
current density, 380, 381
effect of resistance, 324, 383
flux density, 358, 380
heating, 381
insulation, 411
losses, 353, 371–372

Rotor of induction motor, peripheral velocity, 416
procedure in design, 399, 400
slip, 325
slots, 355, 386, 387, 389, 397
voltage, 401, 411
windings, 320, 324, 408
of ring losses, 372–373

S

Sandwiched coils for transformers, 483
Saturation curves, full-load, 212, 227, 237, 313
no-load, 50, 240, 339–341
Saturation in commutating poles, 106
Screen covered motors, 348, 383
Segmental punchings for armatures, 24, 29, 187, 349
Segments of commutator, number, 18
Selective commutation, 19
Self-induction of windings (see *Reactance*).
Semi-enclosed motors, 348, 383
Series field design, 74
windings, 17, 23
commutation with, 19, 89
Shafts, 281, 501
Shell-type transformer, 429, 430, 433, 447–448
compared with core type, 486–488
heating, 465–466
insulation, 459
procedure in design, 481–485
reactance, 447, 484, 487
three phase, 489
Short-circuit, 37
instantaneous, 291
on transformers, 425–426
sudden, 289, 487
test on alternators, 224
on induction motors, 341
pitch windings, 15, 89, 176, 184, 419
Silk covering for wires, 35
Simplex windings, 7
Single-phase alternators, armature reaction, 231
regulation, 236
turbos, 299
windings, 155, 172, 183
Singly re-entrant windings, 8
Size of machine and frequency, 415, 490
and output, 133, 256, 391
Skew coils, 171
Slide rails, 29
Slip, 328, 336
rings, 191, 325
Slots, dimensions, 87, 257–258, 261–262, 397, 398
effect on wave form, 175
insulation, 38, 201, 203–207, 411
number, 22, 96, 175, 182, 261, 397, 399, 416
open and closed, 25, 347, 355, 381, 411–414
Slow-speed motors, 409–411
Space factor of field coils, 71, 242
Sparking, cause, 82
criteria, 82
prevention, 82, 92
voltage, 92
Speed and characteristics, 392, 409
and efficiency, 420–421
and torque curves, 325
frequency and poles, 157, 319
limitations in design, 274, 417
of rotors, 416
peripheral, of commutators, 139
of rotors, 274, 276, 297
synchronous, 319
Spiders, 348, 497–498
Squirrel-cage dampers, 300, 308
rotors, construction, 320, 348
current density, 380, 381
flux density, 358, 381
heating at starting, 379
Starting current, 323
torque, and rotor loss, 323, 338, 373
dead points, 314, 388
in two-pole motors, 418
synchronous horsepower, 338, 343, 345
motors, 313

Stator, construction, 196, 346–348, 496
current density, 253, 263, 298, 380
diameter of, 405
end connections, 294
flux density, 252, 358, 380
generated e. m. f., 173, 350
heating, 252, 283, 380–383
losses, 247, 353, 371
procedure in design, 256, 391
reactance, 216, 234, 290, 360
resistance, 248
slots, 175, 257–258, 261, 263, 397, 399
strength relative to field, 229, 296
ventilation, 286
windings, 155, 319–321
Steel (see *Iron*).
Strength of main and armature fields, 65, 229, 296
Sub-synchronous speed, 418
Surface creepage, 450, 454, 455, 456
leakage, 38
Synchronous motors, design for, 312–313
excitation, 311
for power-factor correction, 311–312
lead of current in, 311–312
size, 312
starting torque, 313–315
reactance, 213

T

Tanks for transformers, 466, 481, 485
Tape, 34
Teeth, dimensions, 257, 262, 398
effect on wave form, 175
flux density, 48, 50, 127, 252, 286, 358, 380
Temperature, 122–132
alternator rotors, 239
maximum, 68, 464, 471
rise, A.I.E.E. rules, 122–123, 201–202
by resistance, 69, 465, 466
cause, 122
Temperature rise, commutators, 131
D.-C. armatures, 124
enclosed machines, 383
field coils, 68, 239
high-voltage coils, 128, 253
induction motors, 375–384
maximum, 122
of oil, 463, 466–468
in bearings, 111
semi-enclosed machines, 383
stators, 252
transformers, 463
turbos, 276, 282, 301
Tests for saturation, 339
for short circuit, 341
for transformers, 491
Thickness of core laminations (see *Laminations*).
of insulating materials, 36, 200, 461
of mica in commutators, 27
of slot insulation, 38, 200
Third harmonic and connection of winding, 183
Three-finger rule, 3
-phase alternators, regulation, 236
power, 162
transformers, 489–490
windings, 157
Torque and speed curves, 325, 420
in synchronous horse-power, 338, 343, 345
maximum, 325, 338, 345
starting, in induction motors, 323–325, 328, 373, 388, 418
in synchronous motors, 313–315
Transformers, air-blast, 468–469
bushings, 435, 451–455
construction, 433–438
core-type (see *Core-type transformers*).
current density, 473
distribution, 428–437, 463, 475, 486, 492–495
efficiency of, 462–463
excitation, 439, 480, 484
flux density, 478
generated e.m.f., 439

Transformer, heating of, 463
insulation, 438, 449–460
large power, 438
losses, 439–441, 461
methods of specifying, 491
of testing, 491
oil, 449–450
performance, 492–495
procedure in design, 475–486
reactance, 445–448, 481
regulation, 426–427
shell-type (see *Shell-type transformer*).
short circuit on, 425–426
tanks, 466, 481, 485
theory of operation, 422
three-phase, 489–490
vector diagrams, 422
water-cooled, 469–470
Turbo-alternators, 276
construction, 276
flux density, 286
heating, 276, 282, 301
procedure in design, 297
reactance of armature, 292
reactions of armature, 295
shaft, 278, 281
single-phase, 299
stresses, 278
Turbo-rotors, critical speed of, 281
Two-phase windings, 157
-pole motors, 417–420

V

Varnish, 35, 36, 450
Vector diagrams, alternator, 210, 211
induction motor, 326–327, 330
transformer, 422
Vent ducts, in armature cores, 25, 187, 347
in field coils, 44
in stator cores, 347
Ventilation, air-blast transformers, 468
commutators, 131
D.-C. armatures, 128
machines, 25, 30
field coils, 44
Ventilation, induction motors, 347, 383
power house, 253
stator, 286
turbo-alternators, 284
Vibration, effect on insulation, 36
Voltage, and characteristics, 153, 420, 421
and efficiency, 421–421
limitations in design, 300, 486
per bar, 107
per turn in transformers, 475
Volt-ampere rating, 183

W

Water-cooled transformers, 469–470
wheel driven alternators, 253, 274
Wave form, 173
windings, 20, 165
Windage, 111
loss, 247, 353
noise due to, 385–386
Winding, choice of, 261, 398
for different voltages, 270, 407
pitch, 15
Windings, A.-C. chain, 164, 165
distributed, 165, 175, 182
double-layer, 164, 165
odd number of coil groups, 171
several circuits, 166
short-pitch, 176, 184, 419
single-phase, 155, 172, 183
three-phase, 157
two-phase, 157
wave, 165
Y- and Δ-connection, 407
D.-C. armature, 7–24, 160
compensating, 104
dead coils, 24
double layer, 13
doubly re-entrant, 8
drum, 9
duplex, 8, 22
equalizers, 13, 19, 24
gramme ring, 7, 9
lap, 20
multiple, 16, 23, 85
progressive, 18

Windings, D.-C., re-entrant, 8
retrogressive, 19
series, 17, 19, 23, 89
short pitch, 15, 89
simplex, 7
wave, 20
Wire, size for field coils, 71
transformer coils, 473–474
table, 504
Wood, 450
Wound rotor, motor, construction, 324, 349
procedure in design, 400, 411
Wound rotor, motor, rotor voltage, 401
theory, 324, 325

Y

Y-connection, 158, 178, 261
Yoke, construction, 26, 30, 186, 348, 496
flux density, 48, 67, 73

Z

Zigzag leakage, 361, 387

Date Due

OCT 2 1946

621.3131 G77A

a39001 007324646b

59538

DIETER BINDS BETTER DENVER COLO

S0-EJK-521